IREX / French National Project PerfDuB

Performance-based approach to the durability of concrete structures

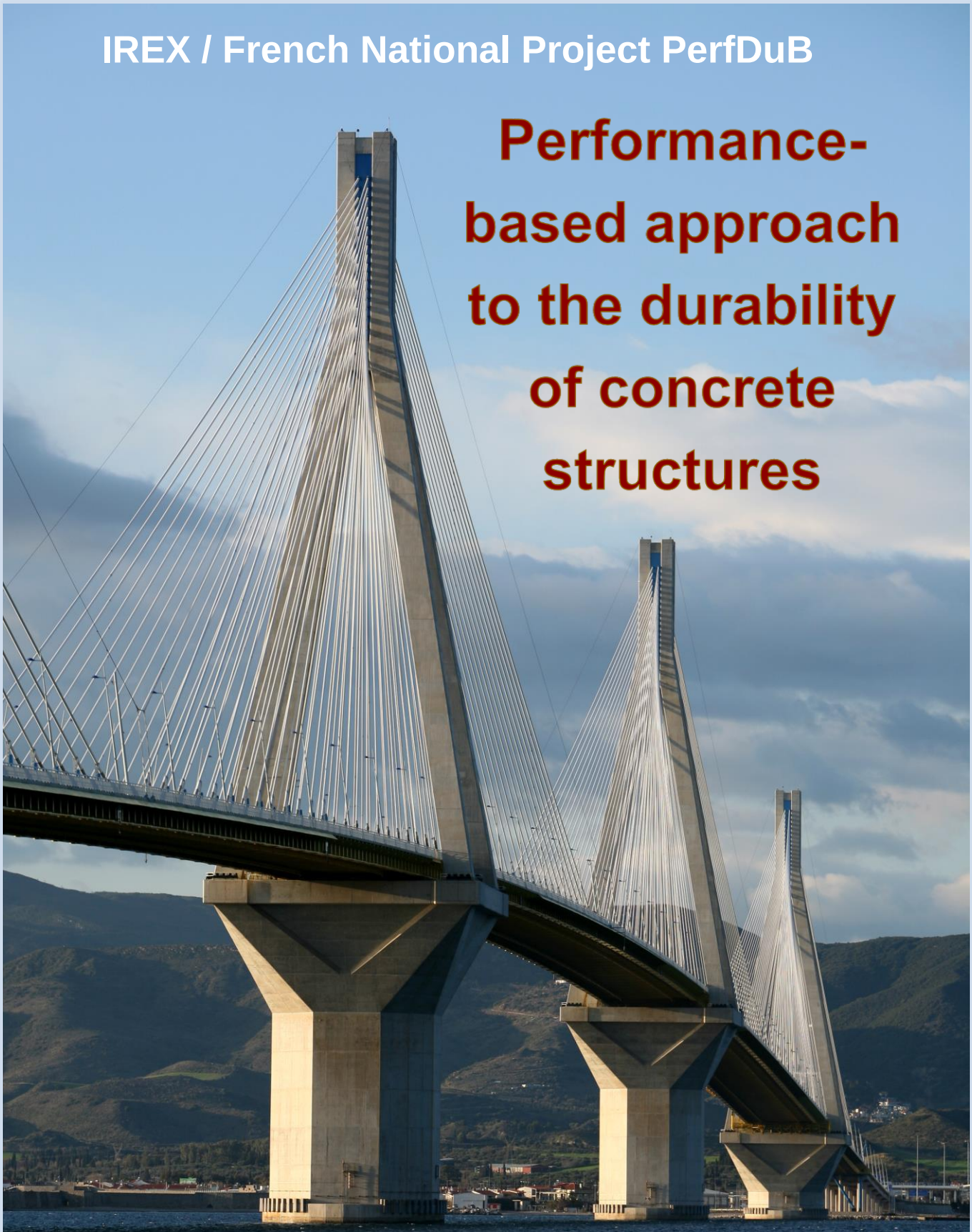

Under the direction of

Didier BRAZILLIER, François CUSSIGH, Gilles ESCADEILLAS

IREX Edition, 2024

Authors' notes

From one chapter to the next, readers may sometimes find certain differences in the choice of symbols used to write formulae and equations. The authors trust that their text will be clearly understood despite any differences in notation, and thank them in advance for their kindness.

Edition book

Page layout: Gilles Escadeillas (LMDC, Université de Toulouse)

If you notice any errors, please send your comments to the following address:
gilles.escadeillas@univ-tlse3.fr

Editor

IREX, 9 r Berri, 75008 Paris

ISBN: 978-2-9568055-4-0

Year of edition: 2024

IREX / French National Project PerfDuB

Performance-based approach to the durability of concrete structures:
From laboratory qualification to implementation monitoring

The project PerfDuB (Performance-based approach to the sustainability of concrete structures) is a French National Project, a specific mechanism for implementing collaborative research in the field of construction, approved by the Steering Committee for Applied Research in Civil Engineering.

This collective academic and professional work is the result of 6 years of research, during which the contributors challenged a national methodology for justifying the durability of concrete structures.

This methodology, including the "absolute" method and the "comparative" method, is intended for works for which a specified level of quality assurance is assured. In principle, these are civil engineering structures, certain complex building constructions or certain prefabricated factory products. The field of research concerns new structures, but also old structures, with the aim of linking pathologies or ageing observed to the type of concrete used and its durability characteristics.

To ensure a balance between theoretical and pragmatic approaches, research work is conducted by representatives from industry and academia.

Contents

General introduction, objectives of the PN - Evaluation of concrete performance: from improving existing durability tests to defining new protocols - Analysis of data obtained on existing structures - Database and its use - Definition of performance thresholds according to exposure classes.

Direction of the authors' collective

Chairman: Didier BRAZILLIER (DIR CE)

Director: François CUSSIGH (Vinci Construction France)

Scientific Director: Gilles ESCADEILLAS (LMDC, University of Toulouse)

Industrial partners and university centers

The PerfDuB National Project has mobilised 50 partners: project owners, public and private project managers, construction companies, design offices, engineering firms, materials-producing industries, public and private laboratories, universities and engineering schools.

Public

Researchers
Academics (teachers and students)
Professionals (construction engineers)

Summary

Foreword

For a very long time, compressive strength was the only characteristic measured on hardened concrete, a universal building material...

Then, in the 1980s, with the development of High-Performance Concrete, in addition to the potential savings in structural design, the argument of durability began to be put forward; since then, this quest for durability has not ceased *via* the development of appropriate tests, the study of test bodies on exposed sites, the analysis of twin structures, the development of performance approach methodologies which were still in their infancy...

So, at the dawn of 2015, we theoretically had two methods at our disposal: one based on comparison with high-performance reference concretes, and the other based on performance thresholds, i.e. concrete characteristics that had to be respected. But we still needed reproducible, rapid test procedures with low variability, and performance thresholds defined *using* simple ageing models that reflected the actual behaviour of the structures...

Motivation was therefore high, and it was not difficult to find around fifty partners ready to commit to the objective of developing a standardised method that would be operational and in common use, based on tests that were also standardised, and that would be transposable at European level... hence the launch of this PerfDuB National Project. The context of ecological transition and the drive to reduce carbon emissions reinforced, if there was any need to do so, the importance of the lifespan of new structures, as well as the requalification of existing structures to optimise their maintenance (the greater the return on construction-related emissions over time, the better the overall balance sheet will be at the end of life).

In this evolution of concrete materials, it is worth highlighting the strength of the National Projects, supported by IREX, which mobilise all the players in the construction industry around research and development projects defined according to the concrete expectations of professionals in the field. In this way, we can see the logical, continuous and coherent trace of research into the prescription of durability through the National Projects that have followed one another since "New Ways for Concrete Materials", so dear to Yves Malier, a pioneer of the National Projects, to PerfDuB via BHP 2000.

With the FD P18-480 documentation booklet, which enables the performance-based approach to be contractualised, concrete, a material that has been unfairly criticised and blamed for many ills (when it is actually its use and/or lack of maintenance that should be criticised...), is now probably the most virtuous construction product in terms of its overall environmental record.), is undoubtedly now becoming the most virtuous construction product in terms of its overall environmental balance... Moreover, the performance-based approach is also making it possible to validate innovative concrete formulas that comply with the standards and contract specifications, but also with the sometimes-unspoken expectations of the specifier, and with excellent carbon balances.

What remains to be done is to disseminate the knowledge gained from the results of this NP, to provide training in the use of the performance-based approach and to convince principals to refer to it in their specifications. This book and the various communication initiatives that have been part of the PerfDuB programme from the outset should contribute to this.

Didier Brazillier

Chairman of the PerfDuB National Project

General introduction

Authors *(organisations)*

François CUSSIGH *(Vinci Construction)*

Gilles ESCADEILLAS *(LMDC, Université de Toulouse)*

Context

Concrete is the most widely used manufactured construction product in the world. Standardised and renowned for its ease of use and durability, it is nevertheless criticised for its environmental impact. To reduce this impact, which is mainly linked to the manufacture of clinker, the development of environmentally-friendly concretes that are better suited to the exposure conditions of structures is a major social objective. Obviously, to be used without risk, these "environmental" concretes must offer guarantees at least equivalent to those of traditional concretes.

The performance-based approach, which consists in understanding the durability of concrete by considering not only the data linked to the formulation but also certain characteristics or properties of the material that are known to be of interest in predicting how it will evolve when exposed to given environmental conditions, appears to be the best solution for qualifying these concretes. The stakes associated with the performance-based approach to durability are therefore considerable, in terms of the technical and economic optimisation of concrete structures, control of construction costs, including those relating to maintenance, and sustainable development. Indeed, the use of environmentally advantageous materials (new cements, recycled materials, local products, by-products and other constituents suitable for use in accordance with standard NF EN 206/CN) cannot be developed without verifying their impact on the durability of structures. In this sense, the performance-based approach to the durability of concrete structures, based on an obligation to achieve results, represents a major technological leap forward compared with current practices based on a prescription of means approach.

However, the performance-based approach is not covered by detailed normative rules at either French or European level. Since the early 2000s, specifiers have been able to define and specify concrete according to three approaches, as set out in standard EN 206:

- the prescriptive approach, in application of the tables in appendix NA.F. of standard NF EN 206/CN, which targets a service life of 50 years, supplemented for engineering structures by the provisions of fascicule 65 of the CCTG, which targets a service life of 100 years. This approach defines specifications essentially in terms of means (nature and dosage of constituents);
- the concept of equivalent concrete performance (provided for in article 5.2.5.3 of standard EN 206). This concept makes it possible to modify the prescriptive requirements with regard to the minimum equivalent binder dosage and the maximum equivalent water/binder ratio, provided that it is proved that the concrete has equivalent performance to that of a reference concrete, in particular with regard to its behaviour in relation to environmental aggression and its durability, in accordance with the requirements of the exposure classes concerned;
- the performance-based design method (provided for in article 5.3.3 of standard EN 206). It defines stipulations in terms of results and therefore performance. The possibility of using such an approach is also provided for in fascicule 65 (article 8.1.2.2) and in standard NF EN 1992-1-1/NA table 4.3 NF note 1 clause 4.4.1.2 (5).

Thus, as indicated in this reminder of the standards, it should be remembered that concretes defined and validated by the performance approach remain above all concretes whose properties of use in the fresh and hardened states are at least preserved. However, the 2014 version of standard EN 206, like the original 2004 version, only provides information that does not make it easy for all those involved in construction to adopt and deploy this type of approach. It remains marginal and reserved for large-scale projects. What's more, at the start of the project, there was no rapid test, in particular for resistance to carbonation and chloride penetration, standardised in Europe to enable durability indicators to be measured.

The main objective of the PerfDub project is therefore to define a national methodology for justifying the durability of concrete and concrete structures using a performance-based approach, which could potentially be transposed to European level. This methodology, including the absolute method and the comparative method, is intended for structures for which a specific level of quality assurance is ensured. These may include civil engineering structures, certain complex building constructions or certain prefabricated factory products. The field of research concerns new structures, but also old structures, with the aim of linking pathologies or ageing observed to the type of concrete used and its durability characteristics.

History of the PerfDuB National Project

In France, there are two documents that already develop these types of performance-based approach:

- the FNTP/FFB/CERIB/FIB provisional professional recommendations of March 2009 entitled "Methodology for applying the concept of equivalent concrete performance" based on the concept of equivalent performance as defined in article 5.2.5.3 of standard EN 206. The principle is to modify concrete composition specifications by showing, using performance tests and durability indicators, that the concrete to be qualified has durability properties at least as good as those of a reference concrete;
- the LCPC guide "Maîtrise de la durabilité des ouvrages d'art en béton - Application de l'approche performantielle" of March 2010, based on the AFGC guide for the implementation of a performance and predictive approach based on durability indicators, of July 2004, and adapted for its application to engineering structures. This is an innovative, global and predictive approach to the durability of reinforced concrete structures, based essentially on the concept of durability indicators, which makes it possible to deal rationally and effectively with the requirements associated with the concrete material in relation to this objective of durability. In particular, it provides a relevant response in the frequent cases where the prescriptive approach leads to requirements that are difficult to reconcile, for example with regard to frost and internal sulphate reaction.

It should also be remembered that significant work had previously been carried out or initiated in France on the standardisation of tests relating to the durability of concrete, which meant that at the start of the PerfDuB project the basic tools essential to the development of the performance-based approach were available. Among the most important are the GranDuBé and Applet projects, which have made it possible to define test methods for durability indicators and to obtain data on the variability of concrete durability properties under real conditions of use. The same is true at international level, with the proposal of characterisation tests and predictive models associated with the main mechanisms conditioning the durability of concrete structures.

The performance-based approach has also been put into practice during the construction of major engineering structures such as the Rion-Antirion Bridge in Greece and the Nouvelle Route du Littoral viaduct on Reunion Island, which have enabled a large number of durability indicator results to be collected and fed into the National Project database. Durability testing is

now essential to provide the best possible guarantee of durability for structures subjected to severe stresses (in this case, mainly the risk of corrosion of reinforcement in a marine environment).

The PerfDuB National Project is an extension of, and consistent with, this earlier work, with the aim of pooling knowledge and feedback, and filling in the gaps, within a framework that brings together all the players concerned, so that the performance-based approach can finally become operational.

Description of the national project

The PerfDuB (Performantial Approach to the Durability of Concrete Structures) national project was launched in March 2015 with the aim of defining a recognised methodology for implementing the performantial approach and achieving consensus among all the players (constituent suppliers, concrete producers, specifiers and users). This initial 5-year programme, which was unfortunately disrupted by the COVID pandemic, had a budget of €3,741k from the project's fifty or so volunteer partners.

The project was structured around themes aimed at characterising the formulations selected on the basis of tests in relation to the exposure classes of standard NF EN 206/CN:

- theme 1 deals with durability testing, highlighting tests that can be used to determine a durability indicator in the case of the "absolute" method (e.g. chloride ion diffusion coefficient) and those that can be used to characterise a concrete using an accelerated method in the case of the "comparative" method (e.g. accelerated carbonation test). More specific tests related to the main classes of chemical exposure are also concerned. The aim is to be able to define one or more indicators (or accelerated tests) linked to a recognised, accepted and robust test for each exposure class in NF EN 206/CN;
- theme 2 concerns the definition of permissible thresholds for each exposure class and for different project service lives and coating values. To do this, the approach is based on identifying the compositional parameters (effective water content E_{eff} , equivalent binder content $L_{éq}$, etc.) and production parameters (maturation, curing conditions, etc.) most likely to influence the durability of the material. In addition, the characterisation of current concretes on new or old structures, coupled with ageing models (ageing factor), makes it possible to refine the various thresholds obtained. The modelling of the ageing of concrete structures is based on the results of the ANR MODEVIE project, carried out in close liaison with the PN PerfDuB, the aim of which is to define an engineering model incorporating both the period of depassivation of the reinforcement and a permissible period of corrosion propagation. The combination of modelling approaches, characterisation of concretes considered to be durable according to the standard's composition rules, and diagnosis of old structures is the originality and strength of the method used to define the relevant performance criteria according to exposure class and project service life;
- theme 3 concerns the definition of the concretes to be investigated by proposing a range of formulations that is as representative as possible (nature and properties of the aggregates, type of cement and additions, strength class of the concretes). The qualification of these concretes makes it possible to define the reference formulas for the comparative method since, in this method, the concrete to be qualified is compared with a reference formula. A range of 42 concretes (corresponding to more than 2,500 test specimens) was defined, including formulations for which there is little feedback but which are part of an overall sustainable development approach (in particular concretes with large quantities of additions). In addition, the effects of variability in the constituents and production of the concrete are also examined on test sites;

- theme 4 deals with contractual aspects. The deployment of the performance-based approach must be accompanied by a definition of the responsibilities and commitments of the various parties involved (specifier, producer, user, customer). As the main objective of this theme is to ensure that the concrete complies with the specifications, it is essential to define the control procedures for the various stages, i.e. design, suitability and production tests;
- the last theme concerns actions to exploit the results, in particular changes in standards (introduction of fidelity data in test standards, drafting of new operating procedures in relation to the exposure classes of NF EN 206/CN, elements of positioning in relation to changes in standards at European level: Eurocode 2, concrete standard and test standards related to durability). In addition, the results of the national project are intended to propose acceptable levels of durability indicators (absolute approach) and rules for optimising the choice of reference concretes (comparative approach). In order to share the methodology and concepts developed in the PerfDuB national project and to facilitate their deployment at European and international level, an international monitoring committee has also been set up, comprising some fifteen experts unanimously recognised for their work on sustainability. Many thanks for their contribution.

The results of the various research projects are presented in the following chapters, corresponding in order to themes 1, 3 and 2 (as the conclusions of theme 2 take into account the results obtained on the 42 concretes of theme 3). Theme 4, for its part, led to a methodological proposal submitted to the Concrete Standardisation Commission, which resulted in the publication of Fascicule de Documentation FD P18-480, based of course on the results presented in this work.

References

Service life of structures, performance, predictive and probabilistic approach. Recommendations from the ANR-APPLET project, IFSTTAR, 2012.

GranDuBé : grandeurs associées à la durabilité des bétons, Hugues Hornain, Ginette Arliguie, Presses des Ponts, ISBN285978425X, 9782859784256, 2007

Standard NF EN 206-1, 2004. Concrete - Part 1: specification, performance, production and conformity

Standard NF EN 206/CN, 2014. Concrete - Specification, performance, production and conformity - National supplement to standard NF EN 206.

Maîtrise de la durabilité des ouvrages d'art en béton. Application de l'approche performantielle, Laboratoire Central des Ponts et Chaussées (LCPC), 2010.

Méthodologie d'application du concept de performance équivalente des bétons : Recommandations professionnelles provisoires, Emmanuel Rozière, François Cussigh, Fédération Nationale des Travaux Publics, 2009.

CHAPTER 1

Evaluation of concrete performance: from improving existing durability tests to definition of new protocols

Authors *(Organisations)*

Franck Cassagnabère *(LMDC, Université de Toulouse)*

Marielle Guéguen Minerbe *(MAST/CPDM, Université Gustave Eiffel)*

François Jacquemot *(CERIB)*

Philippe Turcry *(LaSIE, UMR 7356 CNRS, La Rochelle Université)*

Work Group: WG1A & WG1C

Summary

1 Introduction

For more than 20 years, the scientific community has been working on the analysis of the durability of concrete. The so-called performance-based approach is now naturally anchored in discussions and in application in various standards such as EN 206 and Fascicle 65.

In 2015, the National PerfDuB Project was launched with the main objective of establishing reliable and proven methodologies and procedures on new and old structures, validated by all technical and scientific players in the field of concrete construction.

The research program was carried out by different working groups, among which the GT1 group was interested in tests of characterization. In the end, the tests should make it possible to evaluate the performance of a concrete subjected to three types of external aggressions: carbonation, ingress of chloride ions and chemical aggressions. These attacks correspond respectively to exposure classes XC, XS/XD and XA. From the tests, it is a question of determining the properties of the concrete which control both the degradation phase of the cover of the structure until the initiation of the corrosion of the reinforcements, and the phase of corrosion propagation.

Before the launching of the project, there were already test procedures, some of which were standardized or as an experimental standard at European level, in the case of classes XC and XS/XD. In the case of the XA classes, the existing operating modes were, for the most part, far from being ready for standardization. Based on this body of existing tests, new versions have been proposed following an analysis of the operating modes, round-robin tests, and parametric studies. These new or refined procedures have been used to characterize many concretes representative of current concrete mixes.

Section 2 presents the results of the working group GT1A on various tests used to assess the performance in the case of the exposure classes XC, XS and XD, i.e., accelerated carbonation tests, porosity test, permeability test, chloride migration test and resistivity test.

Sections 3 to section 0 present the results of the working group GT1C on tests used to assess the performance of concrete submitted to various attacks in the case of the exposure classes XA, i.e., external sulfate attacks, leaching, and biodegradation.

2 Carbonation and chloride ingress (WG1A)

2.1 Program

For each performance test, the objective of the working group WG1A was to propose an operating mode obtained by possible modifications of a pre-existing operating mode (from a standard, for instance). As shown in Figure 1.1, the program consisted of 3 stages. The methodology was the same for each indicator or aging test.

- **Stage 1:** An initial version of the operating mode (denoted 1) was proposed from minor modifications of a pre-existing version (clarification of some elements of the protocol). The version 1 was used for round robin tests (RRT) on five concretes in order to assess the reproducibility of the test and its possible shortcomings. In parallel, complementary studies were carried out by varying some of the parameters of the operating mode. These two approaches led to the proposal of the version 2, i.e., a "consolidated" version;
- **Stage 2:** The version 2 of the operating mode was used for the characterization campaign of the 42 concretes of PN PerfDuB. At the end of this campaign, the

operating mode was reviewed and possibly corrected on the basis of feedback from the laboratories that have carried it out (version 3);

- **Stage 3:** The 3rd version so obtained was used for an inter-laboratory test campaign on three concretes. The aim was to determine precision data and to provide a final version.

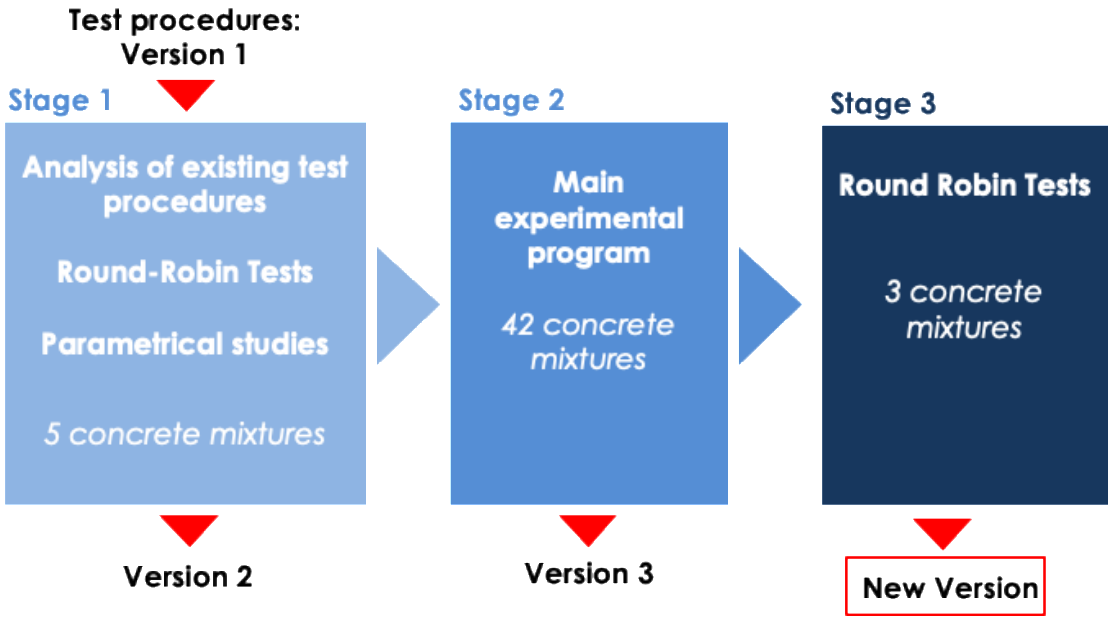

Figure 1.1. Program of the working group WG1A

2.1.1 Stage 1

For each test, 5 concrete mixtures were tested by 5 to 6 laboratories which were selected for performing the test during a round robin test (RRT) campaign. Table 1.1 gives the main characteristic of these concrete mix designs. Parametric studies were also carried with these mixtures. The results of the RRT campaign were analyzed by the statistical method from NF ISO 5725 standard.

Table 1.1. Main characteristics of the studied concrete mixtures in stage 1

Concrete	B1	B4	B7	B31	B38
Strength class	C35/45	C30/37	C35/45	C55/67	C70/85
Cement	CEM I 52.5	CEM III/A 52.5	CEM I 52.5	CEM III/A 52.5	CEM I 52.5
Cement content (kg per concrete m^3)	280	280	270	380	311
Mineral addition	Limestone filler	Limestone filler	Limestone filler	-	Silica fume
Mineral addition content (kg per concrete m^3)	50	50	190	0	35
Effective water on cement ratio (W_{eff}/C)	0.60	0.63	0.67	0.40	0.41
Concrete type	Ordinary concrete	Ordinary concrete	Self-Compacting Concrete	High-Performance Concrete	High-Performance Concrete

2.1.2 Stage 2

A large campaign was carried out on 42 concrete mixtures. The latter were characterized with the second version of the operating modes. 5 to 6 laboratories were involved in this campaign. Each laboratory was responsible for determining a given indicator for 5 to 8 concretes.

In-depth analysis of the database obtained with this campaign are proposed in another report (working group 3 synthesis report, see chapter 3).

2.1.3 Stage 3

During the final stage, an inter-labs campaign aimed at determining precision data of each operating mode, i.e., standard deviations for repeatability (s_r) and reproducibility (s_R). The method for statistical analysis was from NF ISO 5725 standard.

Almost 10 to 20 laboratories were involved in this campaign depending on the test. The concrete mixtures used for this campaign were the following: B1, B4 and B31 (Table 1.1). The concrete specimens were cured under water during 90 days before testing.

During results analysis, different criteria to eliminate laboratory results have been used:

- the operating mode was not completely followed;
- outlier variance;
- outlier mean or outside the confidence interval.

2.2 Accelerated carbonation

2.2.1 Initial operating modes

Two operating modes were studied:

- the operating mode denoted EN V1 corresponds mainly to the European one described in FprCEN/TS 12390-12:2010. Note that the relative humidity during the preconditioning period was fixed equal to 65 ± 5 % RH (while no value is given in FprCEN/TS 12390);
- the operating mode denoted NF V1 corresponds to the French procedure from XP P18-458 standard.

Table 1.2 compares both procedures. The main differences are the preconditioning method (drying at 20 °C vs. oven-drying at 45 °C) and the CO_2 concentration in the carbonation chamber (4 % vs. 50 %). In EN V1, two parallel faces of the tested specimen are protected during carbonation, while all specimen faces are carbonated in NF V1.

Table 1.2. Specifications of both procedures for accelerated carbonation (main differences are underlined)

		EN V1	NF V1
Specimen (concrete)	**Geometry**	7 cm x 7 cm x 28 cm	7 cm x 7 cm x 28 cm
	Number	3	3
Preconditioning	**Drying faces of the specimen**	All faces	all faces
	Duration	14 days	14 days
	Temperature	20 ± 2 °C	45 ± 5 °C
	Relative Humidity	65 ± 5 %	Non-controlled but measured
Carbonation	**Specimen faces in contact with CO_2**	Two parallel faces	All faces
	Total duration	70 days	28 days
	Temperature	20 ± 2 °C	20 ± 2 °C
	Relative humidity	65 ± 5 %	65 ± 5 %
	CO_2 concentration	4 ± 0,5 %	50 ± 5 %
	Testing times	28, 56, 63 and 70 days	3, 7, 14 and 28 days

2.2.2 RRT campaign and parametric studies

2.2.2.1 Round robin tests

The laboratories involved in the RRT for both carbonation methods were the following:

- EN V1: Bouygues, CERIB, LafargeHolcim, LaSIE, LGCGM, L2MGC;
- NF V1: Bouygues, CERIB, GeM, LaSIE.

In the following, the laboratories are named "Labx" with x a number between 1 and 7.

As shown in Table 1.3, laboratories used various equipment for testing.

Table 1.3. Equipment used by the laboratories for carbonation tests

	EN V1	NF V1
Protection of specimen faces against carbonation	Mortar coating Painting Paraffin Adhesive aluminium	No protection
Preconditioning equipment	Climatic chamber Tank with salt solution	Climatic chamber Oven-drying (no regulation of RH)
Carbonation equipment	Tank supplied by a 100 % CO_2 gas bottle: regulation of CO_2 concentration by a gas analyzer and regulation of RH by a salt solution Climatic chamber with regulation of CO_2 concentration Tank supplied by a 4 % CO_2 gas bottle: regulation of RH by a salt solution	Tank supplied by a 100 % CO_2 gas bottle: regulation of CO_2 concentration by a gas analyzer and regulation of RH by a salt solution Climatic chamber with regulation of CO_2 concentration Tank supplied by a 50 % CO_2 gas bottle: regulation of RH by a salt solution

Carbonation depths determined for each concrete and both procedures are given in Figure 1.2 to Figure 1.5. Results for B38 were not plotted: no carbonation depth could be determined from EN V1, while carbonation depths remained lower than 1 mm for NF V1. The studied procedures are not enough sensitive in the case of a concrete with high packing density such as B38 (concrete mixture of W/B = 0.41 made with silica fume).

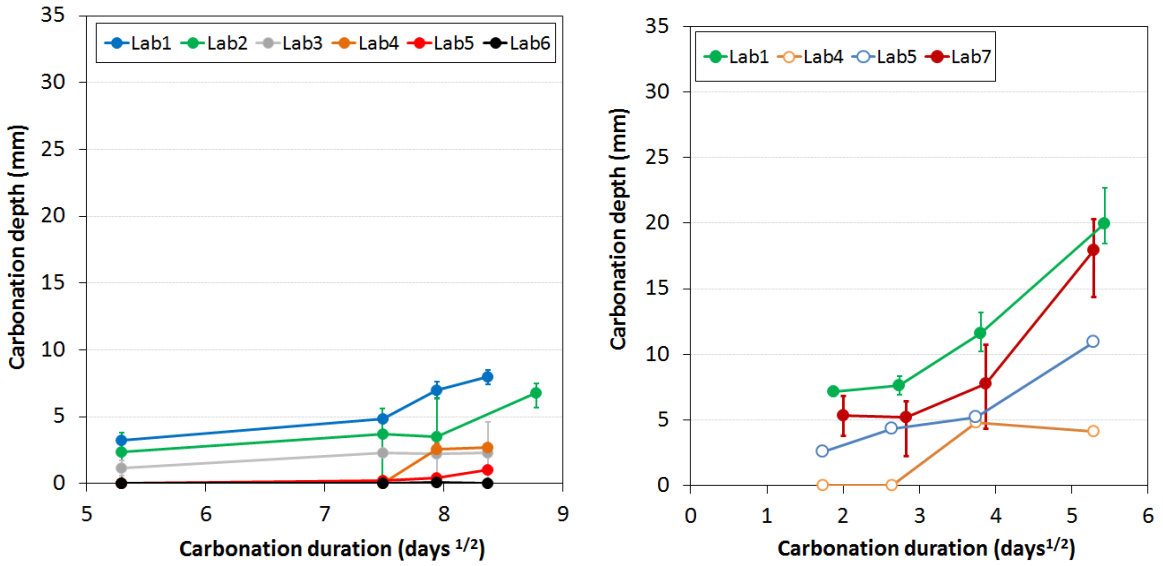

Figure 1.2. Carbonation depths of B1 concrete for EN V1 (left) and NF V1 (right) procedures

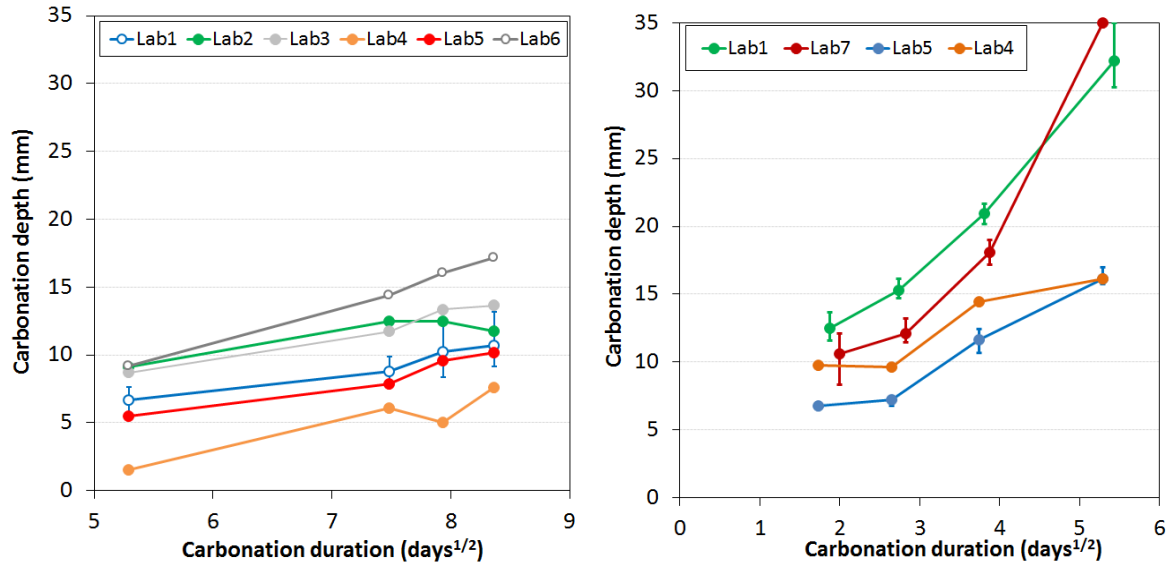

Figure 1.3. Carbonation depths of B4 concrete for EN V1 (left) and NF V1 (right) procedures

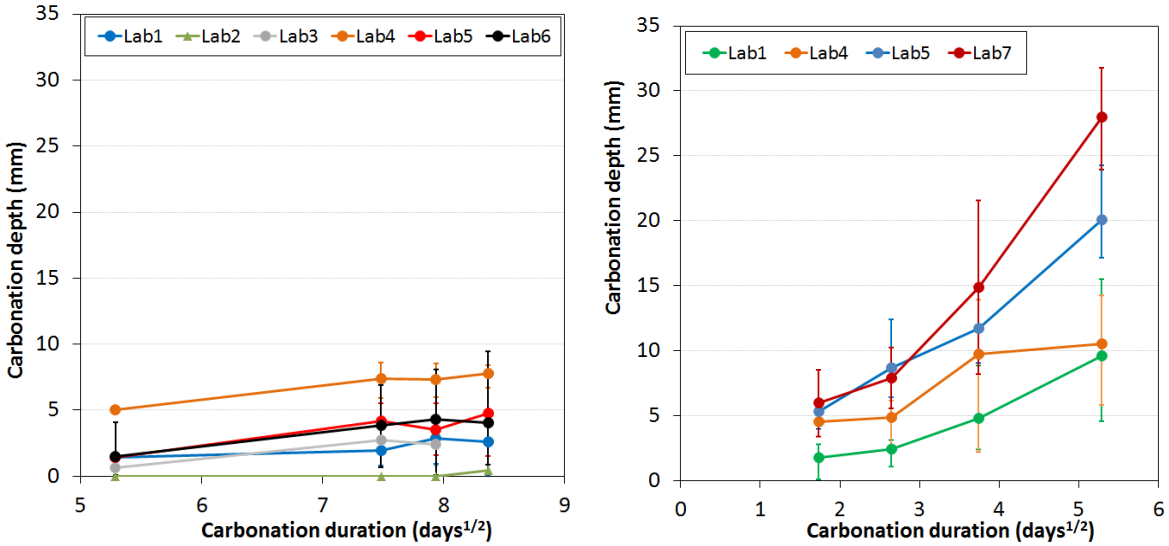

Figure 1.4. Carbonation depths of B7 concrete for EN V1 (left) and NF V1 (right) procedures

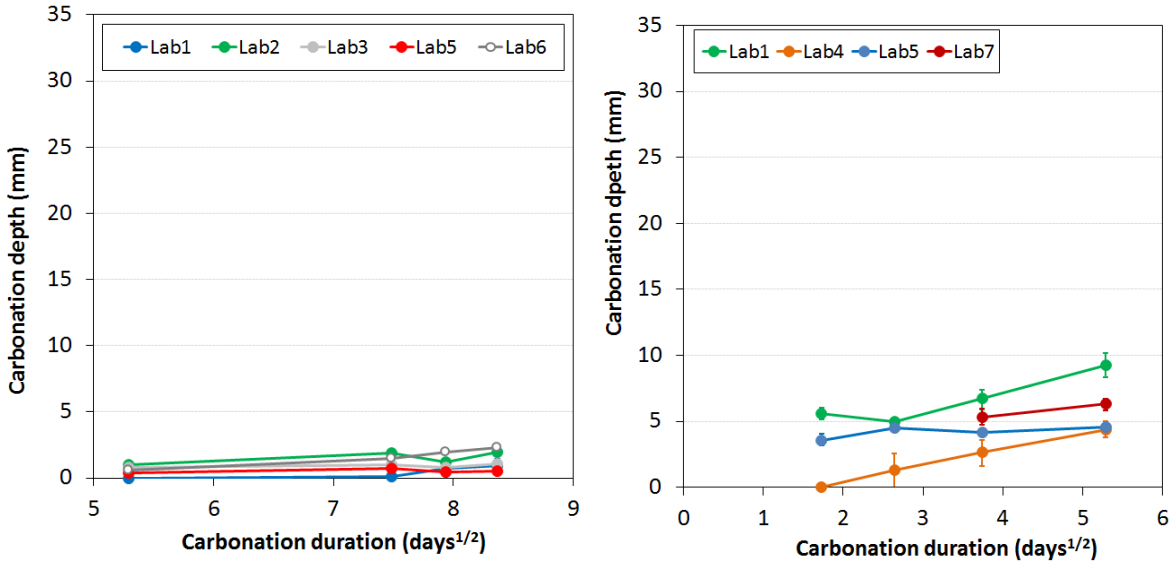

Figure 1.5. Carbonation depths of B31 concrete for EN V1 (left) and NF V1 (right) procedures

2.2.2.1.1 Repeatability

The repeatability is rather good for both operating modes. High standard deviation can be noticed only for the mixture denoted B7, i.e., a Self-Compacting Concrete (Figure 1.4). This dispersion could be explained by the inhomogeneity of the tested specimens as shown in Figure 1.6.

Figure 1.6. Views of split surfaces of specimens. Left: concrete B7 after phenolphthalein pulverization. Right: concrete B1 before phenolphthalein pulverization

2.2.2.1.2 Reproducibility

Whatever the procedure, the reproducibility is low as shown in Figure 1.2 to Figure 1.5. Many explanations can be given. Firstly, experimental set-ups are quite different from a laboratory to another, as shown in Table 1.3. Secondly, the preconditioning phase gives results that are sometimes very different from one laboratory to another.

For instance, Figure 1.7 gives the mass variations for the specimens of the concrete B7 after the preconditioning period of EN V1. Mass variations obtained by the laboratories can be very different, what could be due to the difference between preconditioning equipment. Some laboratories used oven with no RH control, while some laboratories used climatic chambers.

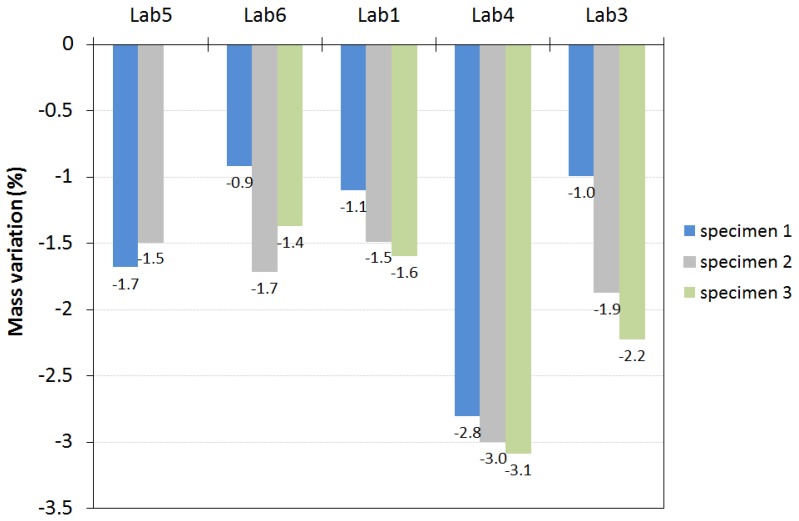

Figure 1.7. Mass variations determined by 5 laboratories after the EN V1 preconditioning for each specimen of the concrete B7

The round-robin tests also enabled us to question the size of the used specimen geometry (7 cm x 7 cm x 28 cm). The 7 cm × 7 cm section is questionable regarding the maximal aggregates size (D_{max}) which was, in the present study, between 20 and 22 mm. Figure 1.6 shows a slice of a B1 specimen which highlights the high concentration of gravels. The low carbonation depths obtained for this concrete could result especially from the alignment of coarse gravels on the specimen border. The lack of reproducibility can also be due to the material it-self. In fact, the additional campaign carried out on CEN standard mortar revealed a rather good reproducibility, as shown in section 2.2.2.4.

2.2.2.1.3 Test sensitivity

The EN V1 procedure did not permit to carbonate largely the B1 concrete, although it is an « ordinary » mixture (CEM I cement type, W_{eff}/C ratio of 0.6). This test gives significant carbonation depth or rate only in the case of a concrete mixture such as B4, i.e., a concrete made with slag cement (CEM III cement type, W_{eff}/C ratio 0.6). Of course, this limits the use of this kind of procedure.

In the case of the NF V1 procedure, measurable carbonation depths (> 5 mm) can be obtained for most of concrete mixtures (except for B38).

The NF V1 procedure is more sensitive than the EN V1 procedure. Sensitivity differences are highlighted in Figure 1.8. The latter shows carbonation rates calculated with the method in section 2.2.4.2. For a given concrete mixture, the rate is an average value calculated from the rates determined by each laboratory. The error bars give the standard deviation. The difference in carbonation rate is partly due to the difference in CO_2 concentration (50 % vs. 4 %). In addition, drying at 45 °C used as a preconditioning in the NF V1 protocol is clearly more effective in reducing the degree of water saturation in the specimens than simple drying at 20 °C and 65 % RH in the EN V1 protocol. The residual water content of the concrete has a major impact on the diffusion of CO_2: in a specimen that is too saturated with water, it will be difficult for CO_2 to diffuse and therefore carbonate the concrete in depth.

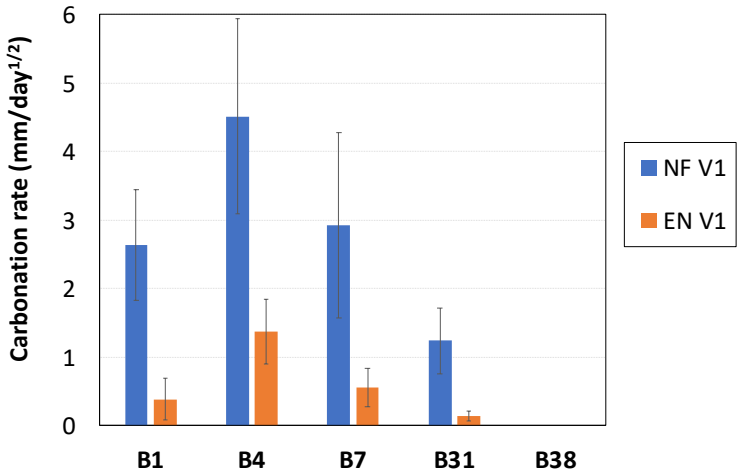

Figure 1.8. Carbonation rates deduced from NF V1 and EN V1 accelerated tests

It should be noted that the EN procedure was also addressed by the CEN/TC51/WG12. In the testing program, only very low carbonation resistance concretes were tested (namely concrete mixtures made with W/C between 0.5 and 0.6 and CEM II 32.5 and CEM II 42.5 cements). Thus, high carbonation depths could be measured at the end of the carbonation phase (between 7 and 25 mm). Our results agree with those of the WG12 but show also that the EN procedure is not relevant for concrete with higher carbonation resistance.

2.2.2.2 Parametric studies

Parametric studies aimed at investigating the impact of the following parameters: CO_2 concentration in the carbonation chamber and temperature used for preconditioning.

During a first study, the following procedures were compared:

- procedure “1 % CO_2”: preconditioning during 7 days at 65 % RH and 20 °C, then carbonation at 65 % RH, 20 °C and [CO_2] = 1 %;

- procedure “4 % CO_2”: preconditioning during 14 days at 65 % RH and 20 °C, then carbonation at 65 % RH, 20 °C and [CO_2] = 4 %.

Note that both preconditioning duration and CO_2 concentration are different. Figure 1.9 gives the main result of this first study (only one laboratory participated to this study).

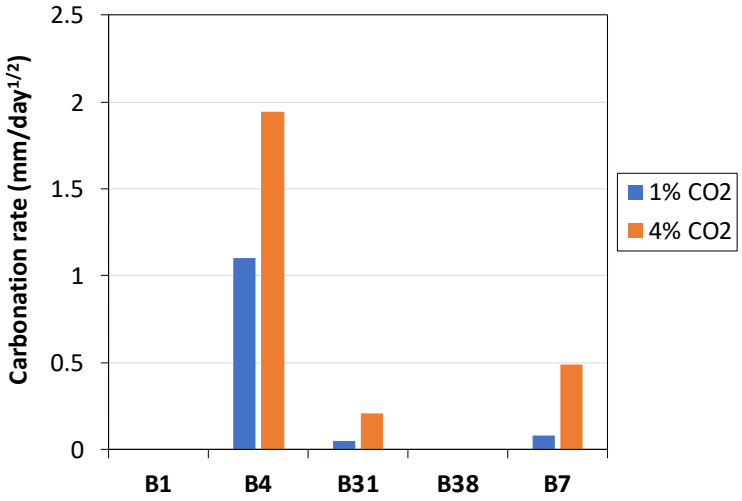

Figure 1.9. Carbonation rates for the two carbonation procedures: “1 % CO_2” (preconditioning during 7 days at 65 % RH and 20 °C, carbonation at 65 % RH, 20 °C and [CO_2] = 1 %) and “4 % CO_2” (preconditioning during 14 days at 65 % HR and 20 °C, carbonation at 65 % RH, 20 °C and [CO_2] = 4%)

No carbonation depth can be measured for concretes B1 and B38. High dispersion of the carbonation depths was obtained in the case of the self-compacting concrete B7. The change in procedure is efficient only for B4 and to a certain extent for B31. This study confirms the RRT results: carbonation is hardly accelerated by using preconditioning at 20 °C and/or at low CO_2 concentration for most of concrete mixtures.

During a second study, two procedures were compared:

- the first corresponds to EN V1 used in the round robin tests, i.e., preconditioning during 14 days at 65 % HR and 20 °C, carbonation at 65 % HR, 20 °C and [CO_2] = 4 %;
- the second corresponds to EN V1 with the preconditioning of NF V1, i.e., preconditioning during 14 days at 45 °C, carbonation at 65 % HR, 20 °C and [CO_2] = 4 %.

Figure 1.10 gives the carbonation rates for B1, B4, B31 and B7 for both procedures (average rates from results of three laboratories). Concrete B38 was also tested but no carbonation depth could be measured. Carbonation depths are higher for the preconditioning at 45 °C than for the preconditioning in “room conditions” at 20 °C. The differences between rates are more significant for concrete mixtures with lowest rates obtained after preconditioning at 20 °C (namely B1, B7 and B31). The carbonation rate increases with the preconditioning temperature because of the decrease of the water saturation degree.

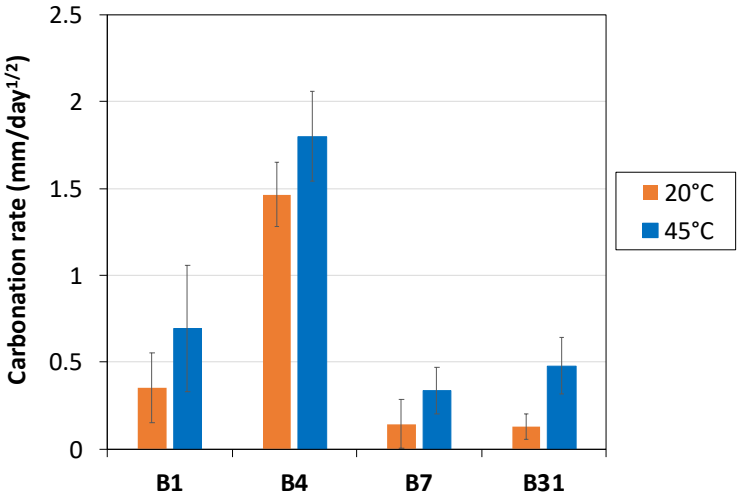

Figure 1.10. Carbonation rates for concretes carbonated at 20 °C, 65 % RH and [CO_2] = 4 % after 14-day preconditioning at 20 °C and at 45 °C

2.2.2.3 Additional study

An additional RRT campaign was also carried on a CEN standard mortar with the two carbonation procedures, NF V1 and EN V1. This mortar was made with a W/C ratio of 0.5, a cement CEM II/A-LL 42.5 R and CEN-Standard sand, according to EN196-1 standard.

A far better reproducibility was obtained than in the case of concrete mixtures. Figure 1.11 gives for example the carbonation depths for the NF V1 procedure.

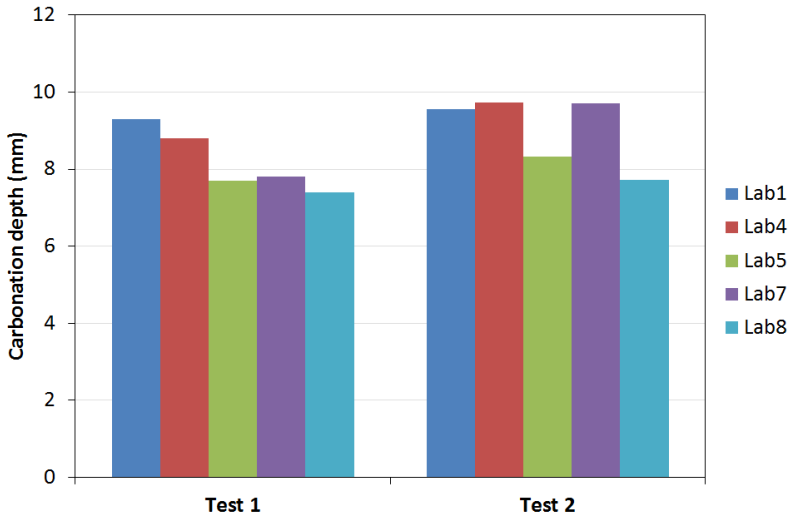

Figure 1.11. Carbonation depths after 28 days at [CO_2] = 50 % (NF V1) for CEN mortars.
Test 1: preconditioning done by each laboratory and carbonation done by Lab1.
Test 2: preconditioning done by Lab1 and carbonation by each laboratory

When the material preparation is easily reproducible, as in the case of a CEN mortar, the reproducibility of the carbonation procedures is far better. This means that the poor reproducibility observed for carbonation tests on concrete specimens are due to some extent to the material variability. The absence of too big aggregates with respect to the specimen size could also improve the reproducibility (see Figure 1.6).

Another interesting result was obtained thanks to this experimental campaign on mortars. The carbonation depth was determined after 2 days at a CO_2 of 50 % (NF V1). As shown in

Figure 1.12, a “double carbonation front” was obtained. The specimens were oven-dried 14 days at 45 °C prior to accelerated carbonation. This phenomenon is usually observed when the preconditioning results in a too low water saturation degree in the specimen perimeter. It should be recalled that carbonation depends strongly on water content.

Note that one laboratory conserved the mortar specimens 7 days in room conditions (20 °C and 65 % RH) after the 14-day oven-drying and before the accelerated carbonation. Then, after 2 days in the carbonation chamber, a classical carbonation front was observed, with a carbonated zone and a non-carbonated one (according to pH indicator). This means that the negative effect of the oven-drying used in the NF V1 procedure (i.e., excessive drying) could be partly eliminated by a 7-day cooling in room conditions.

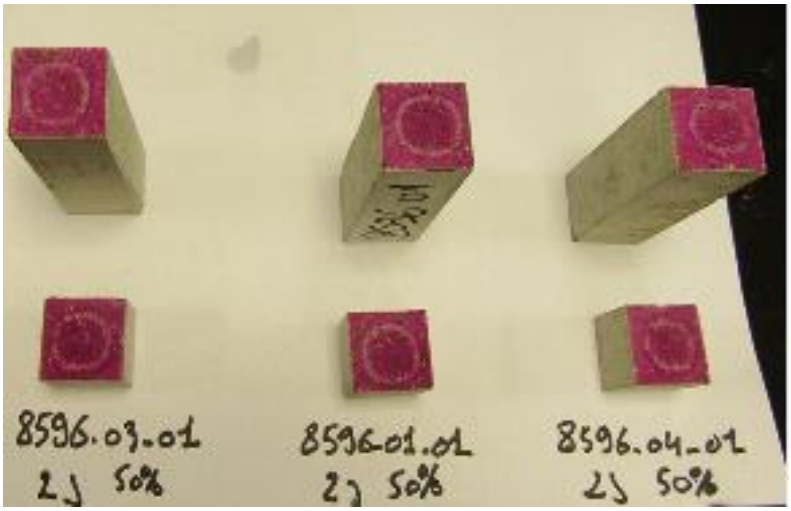

Figure 1.12. View of split mortar specimens after 2 days at a CO_2 concentration of 50 % (NF V1) and phenolphthalein pulverization

2.2.3 New operating modes

Some issues related to the studied carbonation procedures were raised by the round robin tests and the parametric studies. For each issue, solution was proposed to consolidate the procedures.

2.2.3.1 Size and geometry of the specimens

The maximum diameter of the aggregates used in the concretes studied here (D_{max} ≥ 20 mm) is too high compared to the dimensions of the 7 cm x 7 cm x 28 cm prisms. We therefore propose to use larger specimens, namely ∅ 11 cm x H 22 cm cylinders. These specimens are sawn in two to produce ∅ 11 cm x H 10 cm cylinders which will be carbonated. The carbonation of the cylinders is proposed to be radial. The determination of the carbonation depth is done after splitting of the cylinder.

2.2.3.2 Preconditioning method for NF procedure

The preconditioning of the NF procedure, i.e., 14-day oven-drying at 45 °C, leads to an excessive dryness in the perimeter of the specimen. To limit this phenomenon, we propose to extend the precondition by a 7-day cooling period at 20 °C and 65 % RH (i.e., the temperature and RH conditions in the carbonation chamber) after the oven-drying.

2.2.3.3 Preconditioning method for EN procedure:

The EN procedure was found to be too little sensitive: carbonation is accelerated only in the case of poor carbonation resistance concrete (here a W_{eff}/B = 0.6 and CEM III concrete). The

proposed solution to increase the sensitivity is to use the new preconditioning method of the NF procedure, i.e., 14 days at 45 °C followed by 7 days at 20 °C and 65 % RH.

2.2.3.4 Better control the procedure

Low reproducibility was found by means of round-robin tests. This was partly explained by the heterogeneity of concrete specimen and by the specimen geometry. However, the low reproducibility could also be due to differences in equipment between laboratories. Round robin tests carried out on CEN mortar have a far better reproducibility. We propose to test CEN mortar specimens (4 cm x 4 cm x 16 cm) in parallel to concrete specimens. This is a way to control the drying process during preconditioning (by determining the mass variation of the mortar specimens).

From the previous analysis, new operating modes were proposed (Table 1.4). Only the carbonation phase is different (CO_2 concentration, testing times). These procedures were used during the Stage 2 of the National Project for the testing of 42 concrete mixtures.

Note that the CO_2 concentration of the EN procedure is 3 % instead of 4 %. This change in concentration is in line with the evolutions of the European operating mode that were proposed by the technical committee CEN/TC 104 during the PerfDuB project.

Also note that, after the Stage 2, a slightly modified preconditioning method was proposed. The drying at 45 °C has to be stopped when both following conditions are fulfilled:

- the duration is higher than or equal to 14 days;
- mass loss of the CEN mortar is higher than or equal to 5.5 %.

The operating mode EN was the one proposed finally by the PerfDuB project, because it is much in accordance with the European procedure of the Standard EN 12390-12 completed in 2020. Thus, in the following, only results obtained with the operating mode EN are presented. The results obtained with the NF test carried on the 42 reference concretes can be found in other reports.

Table 1.4. Specifications of the proposed procedures for accelerated carbonation

		EN V2	NF V2
Specimen	**Geometry**	Ten ∅ 11 cm x 10 cm cylinders sawn from five ∅ 11 cm x 22 cm after curing)	
	Number		
Preconditioning	**Drying face of the specimen**	Lateral face of the cylinder	
	Total duration	14 days + 7 days (*)	
	First step	14 days at 45 ± 5 °C (*) RH not imposed but measured	
	Second step	7 days at 20 °C and 65 % RH	
Carbonation	**Specimen face in contact with CO_2**	Lateral face of the cylinder	
	Temperature	20 ± 2 °C	
	Relative humidity	65 ± 5 % RH	
	CO_2 concentration	3 ± 0,5 %	50 ± 5 %
	Testing times	28, 42, 56 and 70 days	3, 7, 14 and 28 days

(*) After the Stage 2, it was decided that the first step is stopped after at least 14 days and when the mass loss of the mortar specimens is higher than or equal to 5.5 %.

2.2.4 Characterization of 42 reference concretes

2.2.4.1 Experimental campaign

The carbonation resistance of 42 concretes were assessed with the operating mode of accelerated carbonation EN V2. Six laboratories participated to this experimental campaign during more than one year. The operating mode NF was also used (the results are not presented in the present report).

The concrete specimens were tested for two kinds of curing mode: wet-curing, i.e., water immersion during 90 ± 7 days, and dry-curing, i.e., demolding when the compressive strength is equal to 35 % of the 28-day strength then conservation at 65 ± 5 % RH and 20 ± 2 °C, what corresponds to the curing class 2 in the standard EN 13670 (see also the chapter of WG3).

The carbonation rate in atmospheric conditions was also determined for all concretes. The tested specimens were ∅ 11 cm x 22 cm cylinders conserved at 20 ± 2 °C and 50 ± 10 % RH. At different time, the specimens were sawn to obtain a 5 cm thick disc. The carbonation depth was determined after phenolphthalein spraying on the split disc. The testing times, expressed as the age of concrete, were the followings: 6 months, 1 and 2 years for the dry-curing mode and 1 (0.75) and 2 (1.75) years for the water-curing mode (in the case of the later, the testing times in brackets correspond to the exposure time from the beginning of carbonation to the determination of carbonation depths).

All the experimental results were analyzed by the working group WG3. A report is especially dedicated to these analyses. In the following, we present the main analyses.

2.2.4.2 How to determine the carbonation rate

The results of the experimental campaign were used to compare different methods of determining the carbonation rate. As a reminder, the latter rate is assessed by linear regression using the four carbonation depths determined at t_0 (initial depth) and at the three testing times. The two following methods were compared:

- “4 points” method: the linear regression is done with the four depths;
- “EN 12390” method: the linear regression is done with the three accelerated carbonation depths and the intercept is taken equal to the initial carbonation depth (or to 0 if the initial carbonation depth was not determined). This method is proposed in the EN 12390-12 Standard.

Figure 1.13 gives examples for both methods in the case of a concrete tested with the EN V2 operating mode.

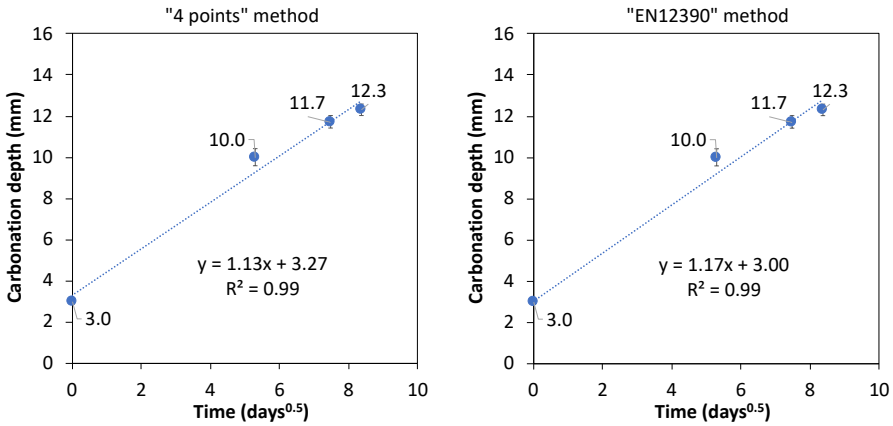

Figure 1.13. Examples of linear regression with two methods, “4 points” and “EN12390” for determining the carbonation rate (dry-cured concrete – EN V2 operating mode)

As shown in Figure 1.14, the carbonation rates obtained by both regression methods are almost equal. As a result, we decided to use the method from the EN 12390-12 Standard, for all analysis.

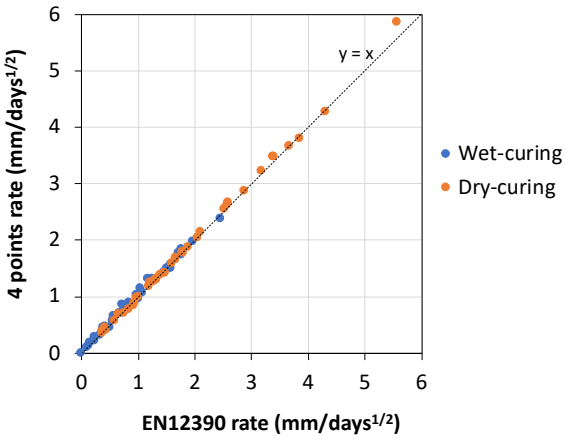

Figure 1.14. Carbonation rates determined with the "4 points" method versus rates determined with the method from EN 12390-12 Standard (EN V2 operating mode)

The coefficient of determination (R^2) is a result of the linear regression. It is usually used as an indicator to assess the relevancy of the regressions. In Figure 1.15, the coefficient R^2 of all 42 concretes is plotted as a function of the corresponding carbonation rate in the case of the EN V2 operating mode. The coefficient of determination tends to increase with the carbonation rate. In the case of concrete with high carbonation resistance, i.e., low carbonation rate, the time-evolution of the carbonation depth is not fully linear with the square root of time and the measurements are more scattered.

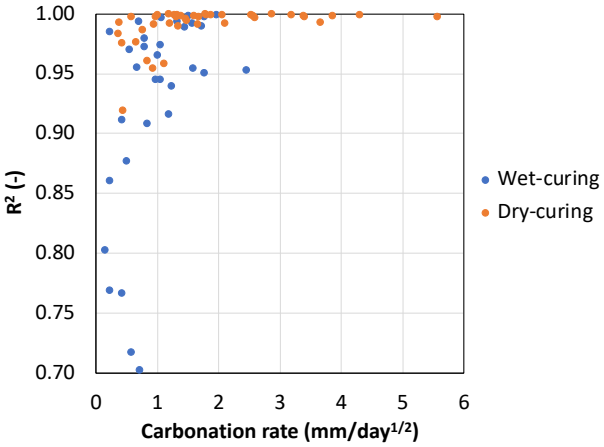

Figure 1.15. R^2 versus accelerated carbonation rates determined with the method from the EN 12390-12 Standard (EN V2 operating mode)

From these observations, two criteria based on the coefficient of determination are proposed to validate the result of a carbonation test:

- $R^2 \geq 0.95$ for carbonation rate higher than 1 mm/day$^{0.5}$
- $R^2 \geq 0.9$ for carbonation rate lower than 1 mm/day$^{0.5}$

It must be emphasized that the higher the carbonation rate is, the higher is the threshold that must be satisfied. This approach is deemed to be safe since a concrete, whose carbonation rate is difficult to determine even with an accelerated test (i.e., low and scattered carbonation depths, and so low R^2), has a priori a high resistance to carbonation.

2.2.4.3 Correlation between accelerated and natural carbonation rates

The carbonation rate of the 42 PerfDuB concretes were determined in natural conditions, i.e., 20 ± 2 °C and 50 ± 5 % RH, for 2 years. In Figure 1.16, the natural carbonation rates of 13 concretes are plotted versus the accelerated carbonation rates in the case of the wet-curing. Note that only the carbonation rates with R^2 higher or equal to 0.95 were used.

The correlation between both rates is quite good. The correlation coefficient is found equal to 3. From this linear regression, the natural carbonation rate can be estimated from the rates determined with accelerated carbonation test.

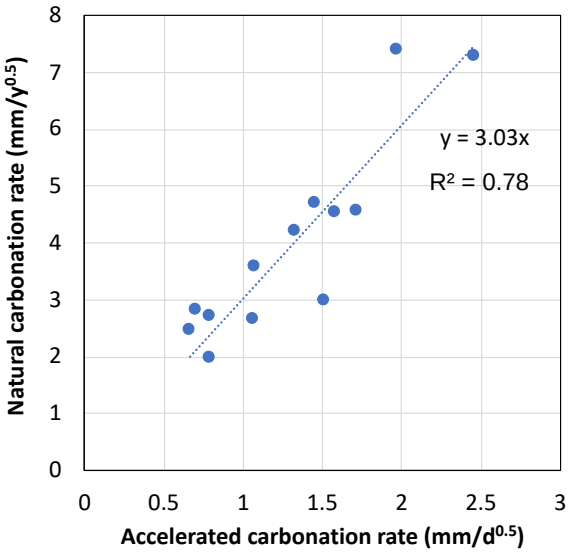

Figure 1.16. Natural carbonation rate versus EN V2 accelerated carbonation rate (wet-curing)

If the only difference between natural and accelerated carbonation was the CO_2 concentration, the natural rate v_{nat} (in mm/year$^{0.5}$) could be calculated from the accelerated rate v_{acc} (in mm/day$^{0.5}$), using the following equation:

$$v_{nat} = \sqrt{365}\sqrt{\frac{C_{nat}}{C_{acc}}}\, v_{acc} \qquad \text{(Equ. 1.1)}$$

Where: C_{nat} is the CO_2 concentration in the atmosphere (~ 0.05 %) and C_{acc} is the concentration in the accelerated test chamber (i.e., 3 %).

Thus, the theoretical ratio between v_{acc} and v_{nat} is equal to around 2.5. The latter value is not far from the correlation coefficient of 3.0 found with the PerfDuB data. Of course, the CO_2 concentration is not the only difference between the two carbonation conditions. In fact, the hydric state is not the same since the specimens are oven-dried before the accelerated carbonation while drying and carbonation are concomitant phenomena in natural condition.

One can find the same approach to convert accelerated carbonation rate into natural carbonation rate. For instance, in the Swiss standard SIA 262-1, a coefficient equal to 2.6 is used. This test is carried out with a CO_2 concentration of 4 % after a preconditioning from the age of 72 h to 28 days (drying in ambient conditions). According to Equation 1.1, the coefficient should be theoretically of around 2. In fact, the coefficient of 2.6 include a correction factor for considering the conversion from the accelerated to the natural rate. This correction factor was deduced by an empirical way.

2.2.5 Inter-laboratory campaign

Three concrete mixes (B1, B4 and B31) were tested during this campaign involving 14 laboratories. Only the operating mode EN V2 was used.

At the end of the campaign, the test results were not validated for more than 50 % of the participating laboratories. The main reasons are the followings:

- non-compliance with the operating mode: a lot of laboratories did not use the CEN mortar during the preconditioning mortar or did not comply with the criterium on the mass loss (i.e., mass loss higher than or equal to 5.5 % to stop the drying at 45 °C);
- outlier values according to the statistical tests of the ISO procedure;
- non-compliance with the R^2 criteria for the determination of the carbonation rate.

Undoubtedly, the operating mode is new and lots of laboratory would need more practice. Note also that this experimental campaign was impacted by the covid-19 crisis.

Although the number of results is low, precision data was assessed in the case of the carbonation rate. The latter is determined from four measured carbonated depths (including the initial carbonation depth after preconditioning period), as shown in Figure 1.17. The analysis was done only for concrete B4 and B31. The results for the concrete B1 are too scattered.

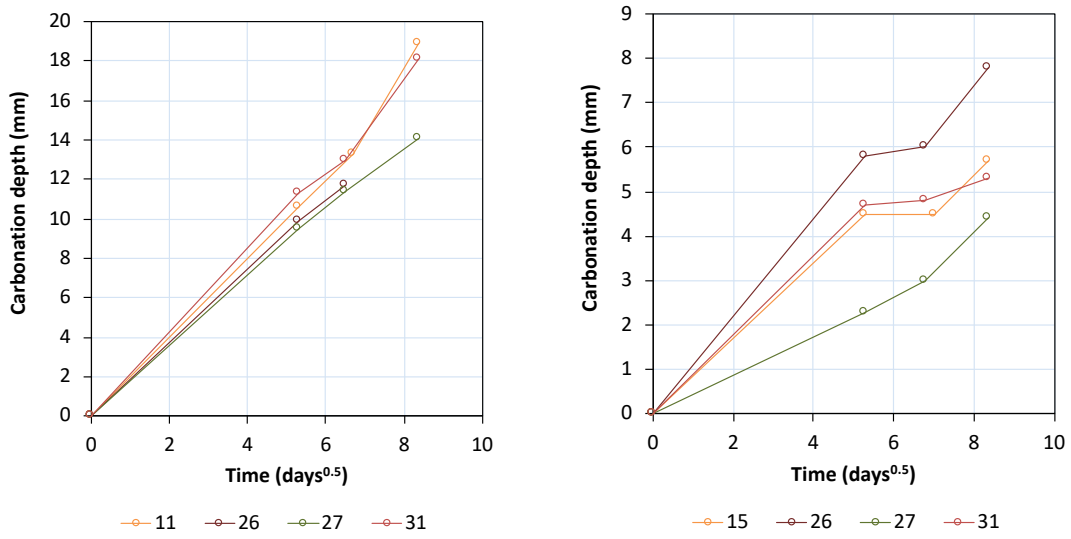

Figure 1.17. Inter-laboratory campaign: carbonation depths of concrete B4 (left) and B31 (right) determined by four laboratories complying with the operating mode

For the two concrete mixtures, the precision data for the carbonation rate are the following (with m: the mean, s_R: the standard deviation and s_R/m the coefficient of variation):

- concrete B4: m = 1.97 mm/d$^{0.5}$; s_R = 0.25; s_R/m = 13 %;
- concrete B31: m = 0.71 mm/d$^{0.5}$; s_R = 0.22; s_R/m = 31 %.

Precision data are given in the EN 12390-12 standard: the coefficient of variation for reproducibility of the carbonation rate (s_R/m) is of 10 %. Note that the latter value was obtained by testing four concrete mixes with high carbonation rate such as concrete B4. Thus, the coefficient of variation found for the PerfDuB operating mode is close to that of the EN 12390-12 standard.

2.3 Porosity and capillary absorption

2.3.1 Initial operating mode

The tests for determining porosity and water absorption by capillarity are based on the protocols described in French standards NF P 18-459 and NF EN 13057 respectively. The absorption test is carried out after the porosity test on the same specimens. Three specimens are tested: cylinders with a diameter of 11 cm and a height of 6.5 cm obtained by sawing ∅ 11 cm x 22 cm specimens. The main steps of the procedure are described here after.

- porosity test:
  - water saturation of a concrete specimen under vacuum at a pressure less than or equal to 25 mbar for 48 hours,
  - determination of the specimen mass in water by hydrostatic weighing (M_{water}) and its mass in air by hydrostatic weighing (M_{air}),
  - oven-drying at 105 °C until a mass considered constant is obtained when two successive weighing carried out 24 hours apart do not differ by more than 0.05 % between them,
  - determination of the mass of the dry specimen (M_{dry}).
- capillary absorption test:
  - sealing of the perimeter of the dry sample using a resin then placed in an oven at 105 °C for 24 hours,
  - cooling the sample at 20 °C for 3 hours then immersing the sample in 2 cm of water put on holds,
  - monitoring of mass gain due to capillary absorption for 48 hours.

After the experiments, several quantities are calculated:

- Porosity (%):

$$\varphi = 100\,\frac{M_{air} - M_{dry}}{M_{air} - M_{water}} \qquad \text{(Equ. 1.2)}$$

- Apparent volume mass (kg/m^3):

$$\rho_d = \rho_w \frac{M_{dry}}{M_{air} - M_{water}} \qquad \text{(Equ. 1.3)}$$

with: ρ_{water} volume mass of water.

- Capillary absorption coefficient at time t (kg/m^2):

$$C_{a,t} = \frac{M_t - M_0}{A} \qquad \text{(Equ. 1.4)}$$

with: M_t (kg) the specimen mass at t, M_0 (kg) the specimen mass before water absorption, A (m^2) the specimen surface in contact with water.

2.3.2 RRT campaign and parametric studies

2.3.2.1 Round robin tests

Six laboratories were involved in the RRT: EDF, Cerema Aix-en-Provence, Cerema Autun, CERIB, Bouygues Construction and LERM. Figure 1.18 gives the results of the statistical analysis from the RRT. The reproducibility of the porosity test is rather good, since the coefficient of variation (s_R/m) is lower than 9 %. The highest dispersion is observed for concretes B31 and B38 with the lowest porosity (< 11 %). The obtained porosities are well correlated with the W/C ratio since two groups are revealed: porosity lower than 11 % for concretes with $W_{eff}/C \leq 0.41$ (B31, B38) and porosity higher than 16 % for concrete with $W_{eff}/C \geq 0.6$ (B1, B4, B7).

In the case of the capillary absorption, the dispersion is higher since s_R/m is close to 40 % for 3 concretes out of 5. However, the test makes it possible to differentiate the concrete performance. Low W_{eff}/C concretes (B31, B38) have much lower absorption. The highest absorption is obtained for the concrete B1 which has a priori a coarser pore structure than concretes B4 and B7, for close porosity.

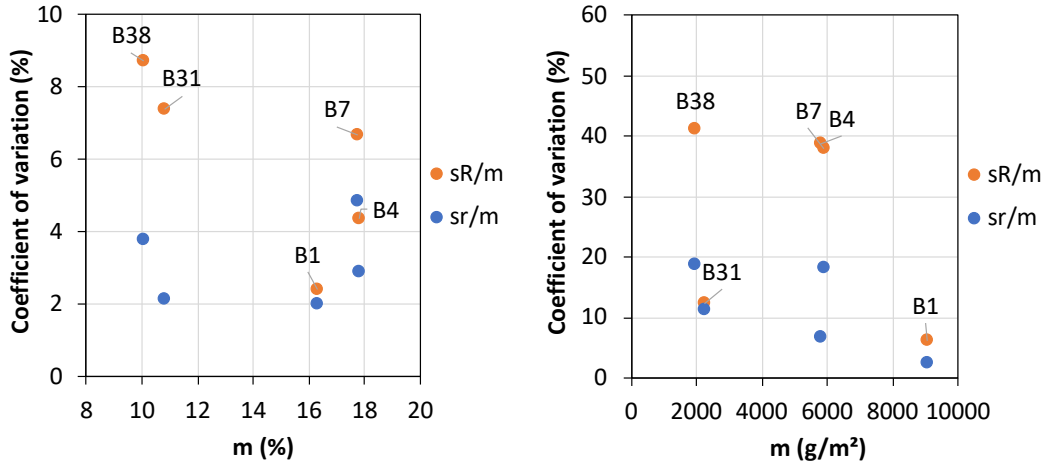

Figure 1.18. Coefficients of variation for repeatability (s_r/m) and reproducibility (s_R/m) versus the means (m) determined from RRT: porosity (left) and capillary absorption coefficient at 24 hours (right)

2.3.2.2 Parametric studies

The influence of some parameters of the porosity test was studied by two laboratories, namely CEREMA Aix-en-Provence and CEREMA Autun. The main conclusions are the followings:

- ***Influence of the vacuum pressure during the saturation step*:** The results of the tests carried out at 25, 50 and 100 mbar do not show a significant influence of the vacuum pressure on the porosity (for a saturation duration of 48 hours).
- ***Influence of the duration of vacuum exposure before adding water in the desiccator*:** A duration between 4 and 8 hours has no significant influence on the determined porosity. A duration of 4 hours is enough.
- ***Influence of the saturation duration*:** For the 5 studied concretes, the obtained porosity was identical whatever the duration of the water saturation step, 48 or 72 hours, after a 90-day water curing. A 48-hour duration allows a priori a fully saturation of water-cured specimens. This assumption was verified by the complementary study presented below.
- ***Influence of the specimen size*:** The specimen volume has an influence on the determined porosity. The increase in volume from 0.67 to 1 l leads to a reduction in the

determined porosity. The highest relative reduction (i.e. – 12 %) was obtained for the denser concrete, namely B38, whose porosity is lower than 10 %. This effect is more pronounced for concretes with porosity lower than 15 %.

- ***Influence of the specimen slenderness*:** The slenderness has a minor influence on the porosity (specimens 7 cm in diameter and 17 cm in height vs. specimens 11 cm in diameter and 7 cm in height).
- ***Influence of the oven-drying temperature*:** The temperature has a significant influence on the determined porosity, especially for the denser concretes. For the latter, an oven-drying at 80 °C minimizes the values of porosity (Figure 1.19).
- ***Influence of the stop criterion of the oven-drying*:** The determination of the dry mass by considering a relative difference between two successive weighing of 0.05 % sometimes results in higher porosity than by considering a relative difference of 0.1 % (Figure 1.19).
- ***Moulded versus cored specimens*:** The type of the specimens was found to have no influence on the value of porosity.

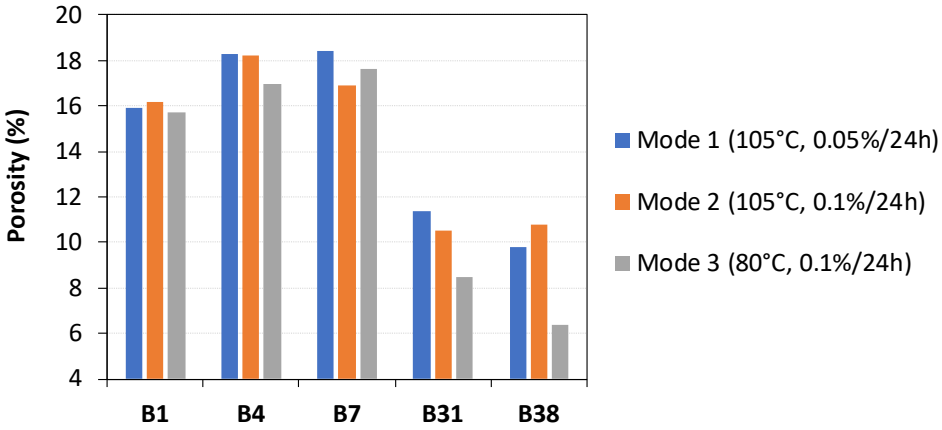

Figure 1.19. Influence of the oven-drying procedure on the obtained porosity of the five tested concretes. In brackets: oven temperature, stop criterion in relative mass variation for 24 hours

A complementary study on the rate of saturation/oven-drying was also carried out by LafargeHolcim. The aim was firstly to verify if the specimen porosity is fully filled by water after the 48-hour saturation step. Secondly, the study aimed at verifying if the criterion used to stop the oven-drying at 105 °C results in a “dry” state of the material. For that purpose, the water content was monitored using sensors embedded at different depths in specimens during the water saturation and oven-drying steps (Figure 1.20).

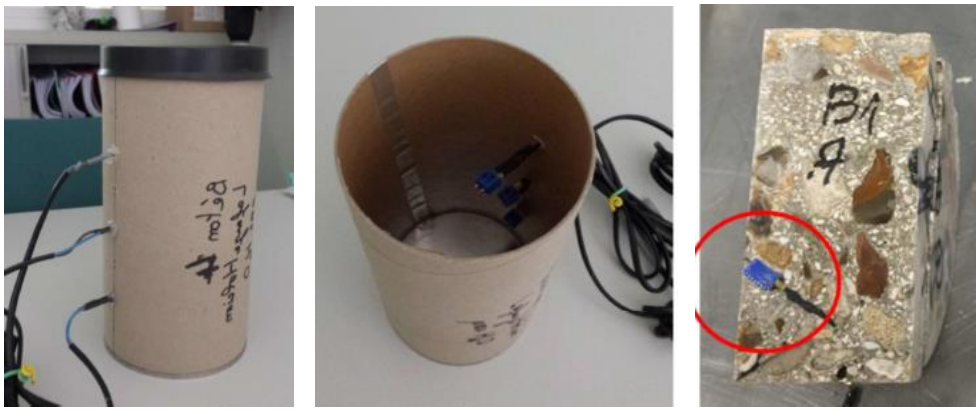

Figure 1.20. Device used for the monitoring of the water content inside a concrete specimen

The following conclusions can be drawn:

- during the 48-hour saturation step, the humidity hardly varies and is the same at different depths. This is consistent with the fact that the specimens come out of a wet cure (they are already almost saturated). On the other hand, if the specimen is dried beforehand at 105 °C, it takes at least three days to saturate it uniformly with water.
- the criterion of 0.05 % between 2 weightings makes it possible to obtain a stable and uniform "dry" state in the concrete. Figure 1.21 gives an example of the evolution of the humidity at different depth for a specimen made with the concrete B31.

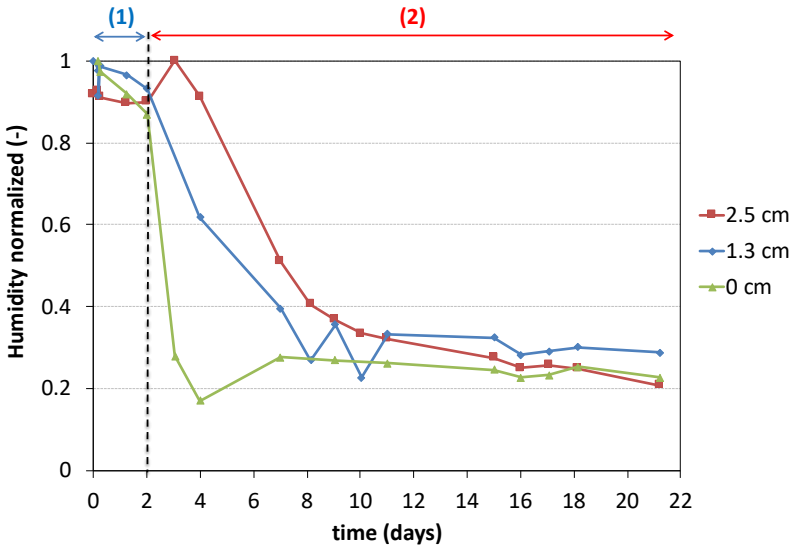

Figure 1.21. Time evolution of the humidity at different depths during the porosity test: water saturation under vacuum for 2 days (step 1) and oven-drying at 105 °C (step 2) - Concrete B31

2.3.3 Proposed modifications of the initial operating mode

From the previous results, some modifications of the initial operating modes were proposed. Note that these modifications are minor.

For the porosity test, some precisions are added regarding the geometry and the procedure to stop the oven-drying:

- each dimension of the test specimen must be higher or equal to three times the diameter of the largest aggregate (defined according to the NF EN 12620 standard) and in all cases must be higher than 40 mm;
- to obtain the dry mass (M_{dry}), the specimens must be dried at 105 °C after the water saturation step until the first constant measurable mass is obtained. The concept of “measurable mass” is used to avoid the problems of no measurement during weekends. The mass is considered constant when two successive weighings carried out 24 hours apart do not differ by more than 0.05 % from each other. Regular monitoring, i.e., without exceeding 72 hours between two measurements, is necessary to assess the loss of mass and to determine the first constant mass obtained.

Even if it is rather difficult to obtain a pressure lower than 25 mbar, this limit is maintained in the proposed operating mode. Moreover, even if the oven-drying at 105 °C is questionable (partial degradation of cement hydrates, removing of chemically bound water), this temperature remains unchanged in the modified operating mode for practical reasons. First, the duration to obtain a stable dry mass is much longer at 80 °C and at 105 °C. Second,

previously studies during the Grandubé project shows that the reproducibility of the test was much better using an oven-drying at 105 °C than at 80 °C (Arliguie et al, 2007).

Regarding the absorption test, the latter is no longer carried out after the porosity test. The temperature of the oven-drying before testing is no longer 105 °C but it is chosen equal to 80 °C.

2.3.4 Inter-labs campaign

The three concrete mixes (B1, B4 and B31) were tested during the inter-labs campaign involving 24 laboratories. Only the porosity test was carried out during this campaign. To facilitate the organization, the absorption test was not used during the inter-labs campaign. Efforts were focused on the porosity test, whose reproductivity was found much better than that of the absorption test during the RRT campaign, as shown previously).

The reproducibility of the porosity test is good, as shown for instance by the results obtained for the concrete B1 (Figure 1.22). All laboratories are inside the confidence interval, which is narrow.

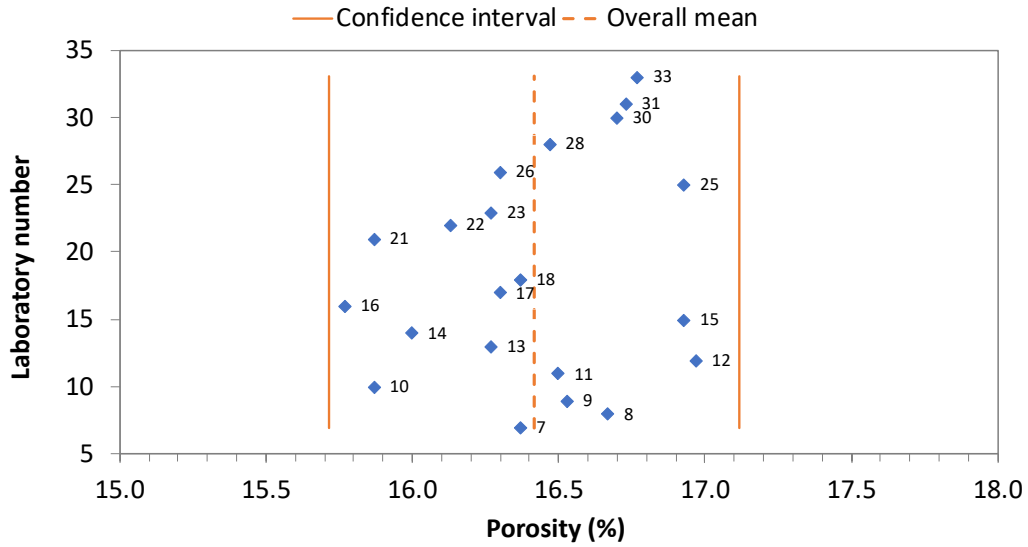

Figure 1.22. Confidence interval and porosity values obtained for the concrete B1 by 24 laboratories participating to the inter-laboratories campaign

For the three tested concretes, the standard deviations of repeatability (s_r) and reproducibility (s_R) are not dependent on the mean. Thus, constant values of s_r and s_R are proposed for the porosity range (Table 1.5). Precision data have been added to the operating mode.

Table 1.5. Precision data of the porosity test

Porosity range (%)	Standard deviation of repeatability s_r	Standard deviation of reproducibility s_R
12 - 18	0.4	0.6

2.4 Gas permeability

2.4.1 Initial operating mode

The initial operating mode is given in the French standard XP P18-463. The test consists of submitting a test specimen to a constant gas pressure gradient and to measure the volume flow rate of gas leaving the sample at steady state. These measurements make it possible to calculate the permeability (Equation 1.5).

$$k = \frac{2P_1 Q L \mu}{A(P_0^2 - P_1^2)} \qquad \text{(Equ. 1.5)}$$

With: k (m²) the gas permeability, P_0: the absolute pressure of the gas at the inlet (Pa), P_1: the absolute pressure of the gas at the outlet (Pa), μ: the viscosity of the gas used (Pa.s), Q: the flow rate which depends on the size of the flowmeter used and the time it takes for the gas to travel (m^3/s), L: the thickness of the specimen (m), A: the section of the specimen (m²).

Before testing, the specimens are oven-dried at 80 °C. A first permeability test is carried after 7 days of drying, and a second one after 28 days of drying. Two permeabilities of the concrete partially dried are so obtained, k_7 and k_{28}, respectively. The specimens are then dried at 105 °C until a constant mass is obtained. A final test is carried out on the fully dried specimens to determine a last value of permeability k_{105}.

It should be noted that the obtained permeability is an “apparent permeability” since the latter depends on the injection pressure in upstream.

2.4.2 RRT campaign and parametric studies

2.4.2.1 Round robin tests

Four laboratories were involved in the RRT: Cerema Clermont-Ferrand, CERIB, GeM and LERM. Figure 1.23 gives the results of the statistical analysis from the RRT.

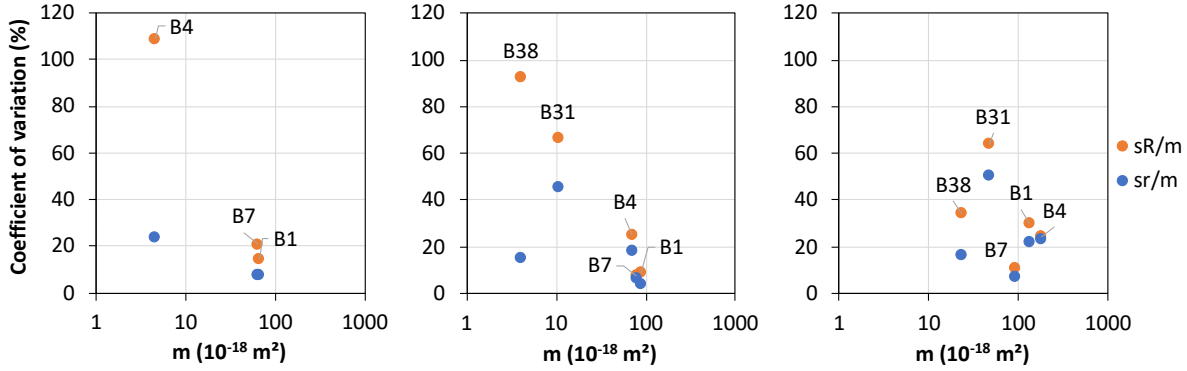

Figure 1.23. Coefficients of variation for repeatability (s_r/m) and reproducibility (s_R/m) versus the mean of permeability (m) determined from RRT: k_7 (left), k_{28} (middle) and k_{105} (right)

The permeability k_7 could not be determined for the denser concretes (B31 and B38), because the gas flows were below the detection limit of the apparatus. As expected, the permeability increases with the drying duration. The coefficients of variation of reproducibility (s_R/m) tend to increase when permeability decreases. s_R/m is lower than 35 % for most of the tested concretes. High dispersion was obtained for the concrete B31 (s_R/m > 60 %), what could be a consequence of the microcracking due to the oven-drying (even at 80 °C).

2.4.2.2 Parametric studies

The parametric studies were carried out by two laboratories: LML and GeM. The first aim was to estimate the impact of the drying temperature on the damage to the test specimens. The microcracking induced by drying was evaluated by means of permeability tests carried out under different confinement pressures. Secondly, apparent permeability of each tested concrete was compared to its intrinsic permeability. The latter was determined by means of tests carried out with different injection pressures and through a correction using the Klinkenberg coefficient (modelling the effect of gas sliding on the pore walls). The aim was to assess if all tendencies observed for apparent permeability are the same than for intrinsic permeability.

The main conclusions are as follows:

- permeabilities of specimens dried at 80 °C until a mass constant is obtained were compared to permeabilities of specimens fully dried at 105 °C. The increase in the drying temperature from 80 to 105 °C results in a variable increase in gas permeability. The self-compacting concrete B7 is hardly sensitive to it, while the high-performance concrete B38 sees its permeability multiplied by 6;
- the dispersion of the measurements varies from one concrete to another and does not appear to be linked to the heterogeneity of the specimens. The measurement deviations are of the order of 2 % for concrete B1 and reach 85 % for B38 at 80 °C. These differences also increase with increasing drying temperature. Here again, B38 undergoes the highest increase;
- a clear correlation appears between the variations in mass after drying at 80 and 105 °C and the variation in permeability. However, the increase in permeability is more related to the microcracking induced by capillary tensions generated by the drying than to the release of a higher pore volume available for the gas to percolate. In fact, the effect of confinement on the obtained permeability clearly demonstrates the effect of microcracking on gas permeability;
- the intrinsic permeability measurements lead to the same observations than those obtained for the apparent permeability ones. Heat treatment increases the intrinsic permeability because of microcracking. While it gives useful information on the transfer properties of materials, intrinsic permeability does not allow the dispersion of measurements to be reduced.

2.4.3 Proposed modifications of the initial operating mode

The parametric studies have shown that the preconditioning step before permeability test, i.e., oven-drying, could lead to microcracking of the tested specimens, especially of high-performance concrete, and therefore to permeabilities that could be higher than they are. However, no major changes to the operating mode were finally proposed. The limitations of the test for high-performance concrete should be kept in mind when analyzing the results.

Note that precision data are proposed after the inter-labs campaign only for concretes with permeability higher than 80.10^{-18} m², as shown in section 2.4.4.

Note also that it was firstly proposed to carry out the permeability test with 4 specimens and to express the result as the median of the 4 determined values for each step (k_7, k_{28} and k_{105}). This proposition aimed at increasing the repeatability. However, all the further data analyzes have shown that the median of 4 permeabilities (obtained for 4 specimens) or the average of 3 permeabilities (obtained for 3 specimens) were almost equal. Figure 1.24 gives an example of comparison of medians and averages in the case of the concrete B1 (results from the inter-labs campaign).

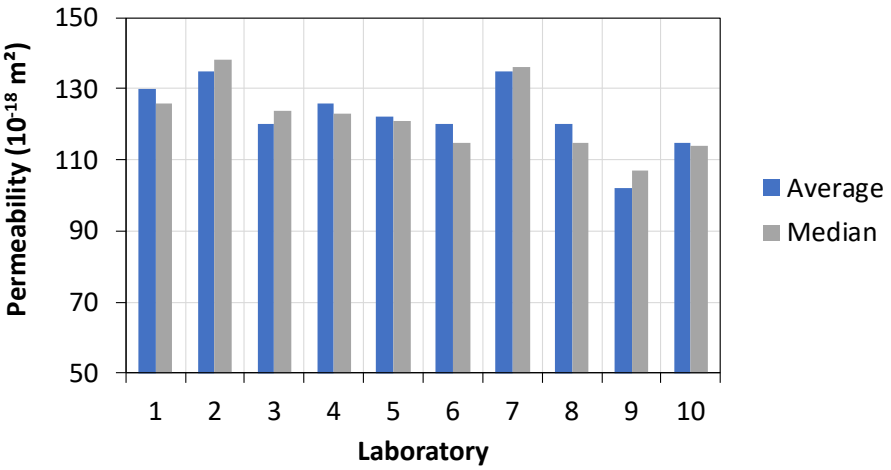

Figure 1.24. Gas permeability k_{105} of the concrete B1 determined by 10 laboratories during the inter-labs campaign. Comparison of the median values of permeabilities determined for 4 specimens and the average values calculated only with 3 permeabilities

2.4.4 Inter-labs campaign

18 laboratories were involved in the inter-labs campaign. Note that all the laboratories did not used the same gas: 39 % of laboratories carried out the test with air, 39 % with oxygen and 22 % with nitrogen. To compare all the results, the permeabilities were recalculated using the same viscosity for a given gas, i.e., $1.84.10^{-5}$ Pa.s for air, $2.05.10^{-5}$ Pa.s for oxygen, $1.77.10^{-5}$ Pa.s for nitrogen.

The results after 7 days of drying at 80 °C, i.e., k_7, were incomplete for most of laboratories, and especially for the concrete B31. As observed during the first RRT campaign, measurements of the gas flow are quite difficult. As a result, the results of k_7 were not included in the statistical analysis.

Figure 1.25 gives the coefficients of variations versus the means for repeatability and reproducibility and for permeabilities determined after 28 days of drying at 80 °C and complete drying at 105 °C. For the range of permeability between 80 and 160.10^{-18} m², the coefficient of variation is almost independent of the mean. As a result, the precision data were expressed only for this permeability range, as shown in Table 1.1.

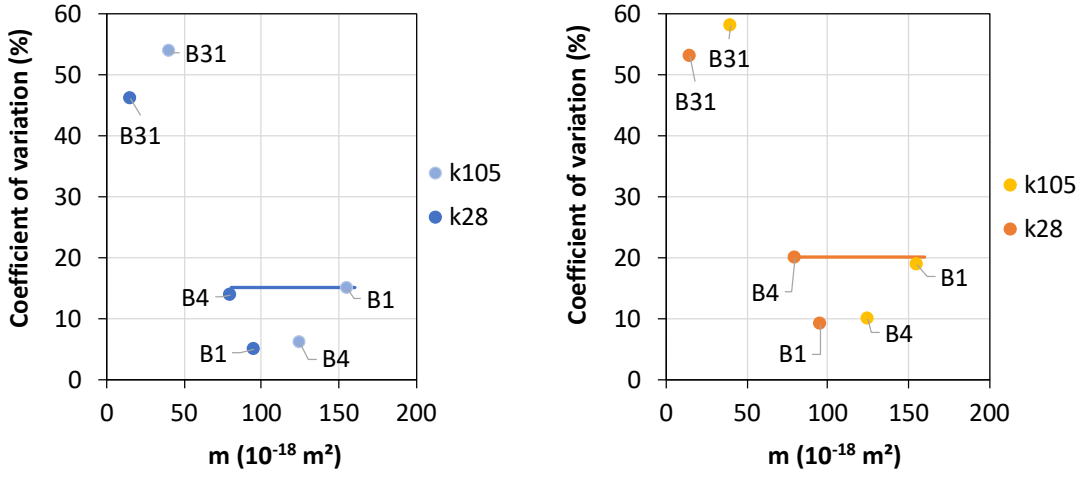

Figure 1.25. Coefficients of variation versus the mean of permeability k_{28} and k_{105} (m) from the inter-labs campaign for repeatability s_r/m (left) and reproducibility s_R/m (right) (18 laboratories)

For permeability lower than 80.10^{-18} m², it should be kept in mind that the tested specimens can be affected by microcracking during the thermal treatment.

Table 1.6. Precision data of the permeability test

Permeability range (10^{-18} m²)	Coefficient of variation for repeatability s_r/m (%)	Coefficient of variation for reproducibility s_R/m (%)
80 - 160	15	20

2.5 Chloride migration coefficient

2.5.1 Initial operating mode

The chloride migration coefficient is obtained by an accelerated electric field migration test carried out in a transient regime, derived from the procedures from XP P 18-462, NT BUILD 492 (Chlortest D2), and EN 12390-18.

After preparation, the specimen is positioned between two compartments filled upstream with a solution containing chlorides (NaCl 0.5 mol/l or 1 mol/l in the case of material with very low chloride diffusivity) and downstream with a solution free of chlorides (NaOH 0.1 mol/l). An electric field is imposed to accelerate the transfer of the chloride ions from the upstream compartment to the downstream one. The test then consists of measuring the depth of penetration of chlorides into the specimen after a given duration. The depth of penetration is detectable by spraying with an $AgNO_3$ solution the faces of the specimen after splitting. The chloride migration coefficient (D_{rcm}) is finally calculated from the depth of penetration.

2.5.2 RRT campaign and parametric studies

2.5.2.1 Round robin tests

Five laboratories were involved in the RRT: Cerema Lyon and St Brieuc, CERIB, GeM and LERM. As shown in Figure 1.26, repeatability and reproducibility are rather good for concrete with diffusivity higher than 2.10^{-12} m²/s. For concrete with lower migration coefficient, the coefficient of variation become much higher. This tendency gives an indication of the limit of the migration test.

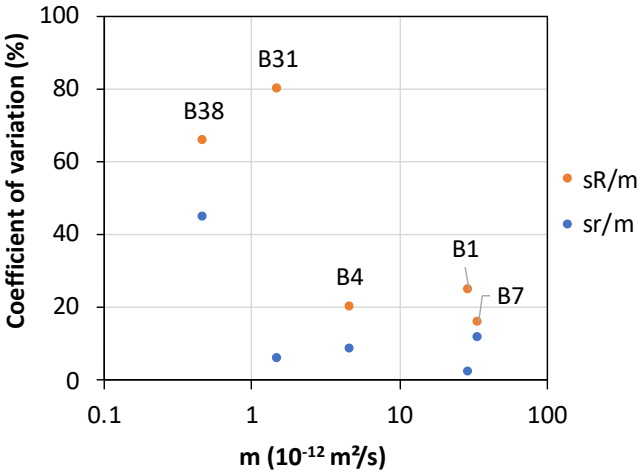

Figure 1.26. Coefficients of variation for repeatability (s_r/m) and reproducibility (s_R/m) versus the mean of chloride migration coefficient from RRT (5 laboratories)

2.5.2.2 Parametric studies

The influence of some parameters of the migration test was studied by CEREMA Saint Brieuc. The main conclusions are the followings:

- ***chloride concentration in upstream:*** between 0.5 and 2.0 mol/l, the concentration used in the upstream chamber of the migration cell has no significant effect on the obtained migration coefficient. Only the reproducibility of the test tends to increase with the chloride concentration in the case of high-performance concrete (B31 and B38);
- ***voltage:*** the increase of the voltage, from 20-30 V to 40-50 V, tends to increase the determined coefficient of migration;
- ***saturation duration:*** different durations of the water saturation step of the specimen before the migration test were investigated, from 24 to 72 hours. No significant influence on the migration coefficient was observed. Note that all the specimens were water-cured during 90 days before saturation under vacuum. Thus, they were a priori quasi saturated before testing.

2.5.3 Proposed modifications of the initial operating mode

From the RRT, parametric studies and discussions in the working group, only few modifications of the operating mode were proposed:

- the chloride concentration in upstream is fixed at 0.5 mol/l;
- for HPC, a voltage of 60 V is chosen instead of the 20-30 V for the lower strength concretes;
- different sealants for specimen lateral face are allowed: epoxy resin, paraffin, silicon;
- the chloride penetration depths must be measured on both split surfaces.

2.5.4 Characterization of 42 reference concretes

In parallel with the characterization of the 42 concretes, 5 of them, i.e., B1, B4, B7, B31 and B38, were also tested by LafargeHolcim with the natural diffusion test from NF EN 12390-11, i.e., a test protocol in line with NT Build 443. In brief, the latter consists of immersing a water-saturated specimen in a solution with a concentration of 3 % of NaCl. After a certain period, the specimen is nibbled to determine a chloride profile. The chloride diffusion coefficient is then calculated from this profile.

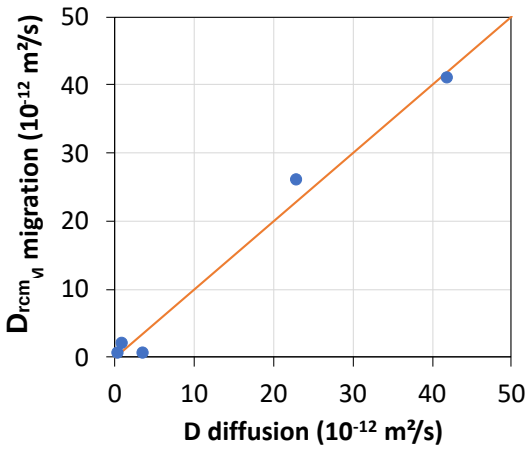

Figure 1.27. Comparison of diffusion coefficients determined by diffusion test and diffusion coefficients determined by migration test (for five concretes)

As shown in Figure 1.27, a good correlation was obtained between migration coefficient and diffusion coefficient what confirms literature results and validate the use of migration tests to assess the performance of concrete for the exposure classes XS or XD. Of course, the migration test is much faster than natural diffusion test.

2.5.5 Inter-labs campaign

Three concretes were tested during this campaign involving 21 laboratories. As shown in Figure 1.28, the coefficient of variation is constant on the range of the determined migration coefficients, for both repeatability and reproducibility.

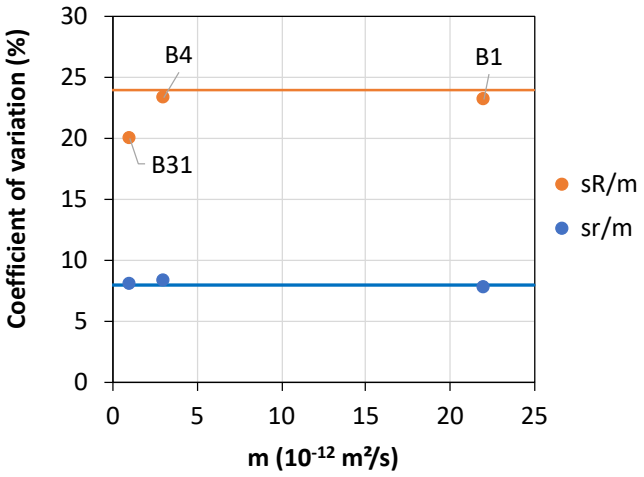

Figure 1.28. Coefficient of variation for repeatability (s_r/m) and reproducibility (s_R/m) versus the mean of chloride migration coefficient from inter-labs-campaign (21 laboratories)

The proposed precision data are given in Table 1.7.

Table 1.7. Precision data of the chloride migration test

Chloride migration coefficient (10^{-12} m²/s)	Coefficient of variation for repeatability s_r/m (%)	Coefficient of variation for reproducibility s_R/m (%)
0.5 - 25	8	24

2.6 Resistivity

2.6.1 Initial operating mode

The initial operating mode of the resistivity test was proposed by LCPC in 2010. The method is inspired by a draft operating mode written as part of the European project Chlortest (2005). This testing protocol is in line with the project of European test prEN 12390-19.

A cylindrical specimen of concrete saturated with a NaOH solution (0.1 mol/l) is placed in contact with two electrodes (conductive metal plates) via two wet sponges. The whole is connected to an electrical resistance measuring device. Knowing the specimen geometry, the resistivity is calculated after measuring the resistance of the sponges alone and the resistance of the assembly specimen/sponges. The specimen may be coated with a sealant if it is planned to also subject it to a chloride ion migration test.

2.6.2 Round robin tests

The RRT involving the same laboratories than those of migration test RRT were good since low dispersions were observed within results of a given laboratory (s_r/m) or between results of different laboratories (s_R/m), as shown in Figure 1.29. Moreover, the resistivity is an effective indicator to differentiate the concretes. The effect of both water-to-binder ratio and binder nature is clearly highlighted thanks to resistivity.

No significant modification of the operating mode was proposed at the end of the RRT.

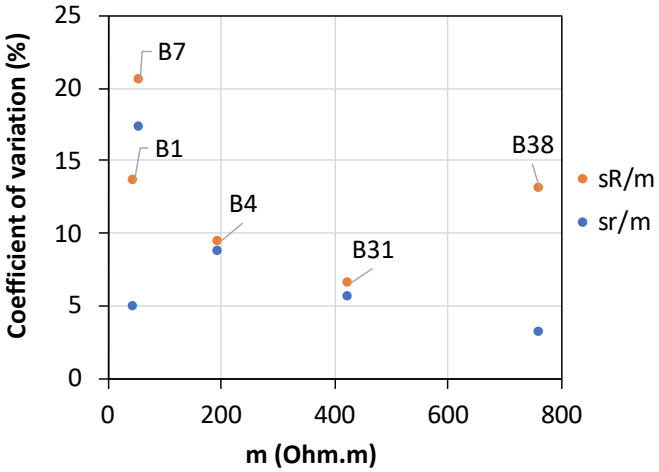

Figure 1.29. Coefficient of variation for repeatability (s_r/m) and reproducibility (s_R/m) versus the mean of resistivity (m) from RRT

2.6.3 Inter-labs campaign

Three concrete mixes (B1, B4 and B31) were tested during the inter-labs campaign involving 17 laboratories.

Based on the results shown in Figure 1.30, it was chosen to propose constant coefficients of variation for both repeatability and reproducibility within the resistivity range of 40 – 250 Ω.m as precision data (Table 1.8).

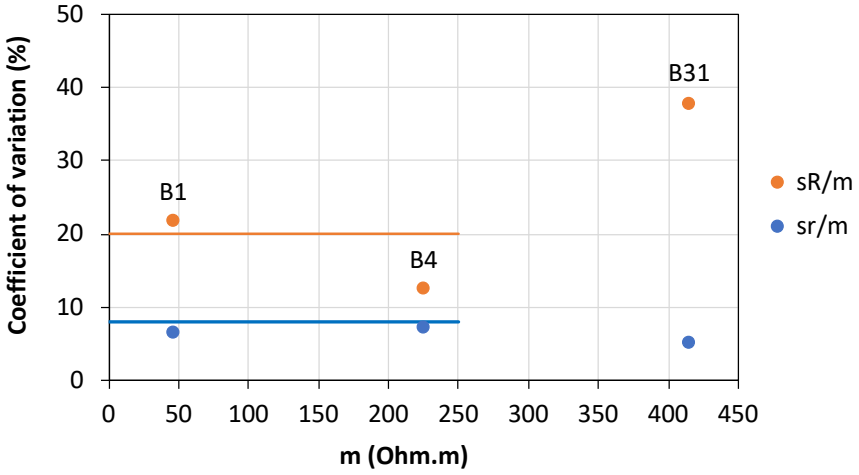

Figure 1.30. Coefficient of variation for repeatability (s_r/m) and reproducibility (s_R/m) versus the mean of resistivity from inter-labs campaign (17 laboratories)

Table 1.8. Precision data of the resistivity test

Resistivity (Ω.m)	Coefficient of variation for repeatability s_r/m (%)	Coefficient of variation for reproducibility s_R/m (%)
40 - 250	8	20

2.7 Summary

Tests used to evaluate the performance of concrete subjected to the exposure classes XC and XS/XD were the subject of a major consolidation work within the framework of the PerfDuB project. Based on existing operating modes, round robin test campaigns and parametric studies made it possible to test these operating modes and ultimately to propose modifications. The latter were the subject of many discussions, especially during meetings with the international monitoring committee. Inter-labs campaigns have made it possible to define precision data for most of the investigated tests.

The key-points of the present work are as follows.

2.7.1 Accelerated carbonation test

The French and European accelerated carbonation tests both from existing standards, NF XP P18-458 and FprCEN/TS 12390-12:2010 respectively, were compared during a round robin test campaign. The reproducibility of both tests was found low, and the European test was found little sensitive, since a significant carbonation rate was obtained only in the case of low carbonation resistant concrete.

Based on parametric studies, a new operating mode is proposed combining the two initial tests. In line with the standard EN 12390-12 completed in 2020, the test is carried out with a CO_2 concentration of 3 % for 70 days. The preconditioning period consists in an oven-drying of at least 14 days at 45 °C followed by a period of 7 days at 20 °C and 65 % RH, i.e., the exposure conditions in the carbonation chamber (while the EN 12390-12 preconditioning step is a softer drying period of 14 days at 20 °C). The oven-drying permits to increase the test sensitivity by significantly decreasing the water-saturation degree. To better control the preconditioning step, three CEN mortar prisms must be tested at the same time as the concrete specimens. The end of the oven-drying is conditioned on a minimum loss of mass of the mortar specimens.

The final inter-labs campaign, impacted by the Covid crisis, was disappointing, since the test reproducibility was low, what could be partly explained by the lack of experience of the participants. However, precision data were proposed for two types of concrete. Moreover, we propose a coefficient to convert accelerated carbonation rate into a natural carbonation rate, which can be used in prediction models (WG2 work).

Further works, such as new inter-labs campaigns, are needed to consolidate the proposed operating mode.

2.7.2 Porosity test

The round-robin test campaign involving 5 laboratories reveals the good reproducibility of the porosity test from the French standard NF P 18-459. Minor revisions of this operating mode were thus proposed from the results of parametric studies. The revisions aim mainly at enhancing the test practicality. To obtain the dry mass, the specimens must be dried at 105 °C after the water saturation step until the first constant measurable mass is obtained. The smallest dimension of the tested specimen must be higher or equal to three times the diameter of the largest aggregate and, in all cases, higher than 40 mm. A large inter-labs campaign involving more than 20 laboratories confirmed the good reproducibility of the test.

2.7.3 Absorption test

The studied absorption test was based on the standard NF EN 13057. During the experimental campaigns, the tests were carried out on specimens tested beforehand with the porosity test. The specimens had therefore been oven-dried at 105 °C before absorption. The absorption test turned out to be not very reproducible in this configuration. It was not then used during the inter-labs campaign. However, the absorption test makes it possible to differentiate the concrete performance. We suggest performing the test after curing the specimens at 80 °C.

2.7.4 Gas permeability test

The operating mode of the permeability test is given in the French standard XP-P18-463. Gas permeability is determined on specimens oven-dried successively 7 days at 80 °C, 28 days at 80 °C and finally fully dried at 105 °C. The round robin test campaign revealed a low reproducibility of the test when used for concrete of low porosity ($W_{eff}/C = 0.4$). The parametric studies showed that the oven-drying could lead to microcracking of the tested specimens, especially of high-performance concrete. However, no major changes to the operating mode were finally proposed. The limitations of the test for high-performance concrete should be kept in mind when analyzing the results. After the inter-labs campaign, precision data were proposed only for concretes with permeability higher than 80.10^{-18} m².

2.7.5 Chloride migration test

The chloride migration test is based on the procedures from XP P 18-462, NT Build 492 and EN 12390-18. Reproducibility is good for concrete with diffusivity higher than 2.10^{-12} m²/s. For concrete with lower migration coefficient, the coefficient of variation become much higher. From the parametric studies, only few revisions of the operating mode were proposed. Mainly, a voltage of 60 V must be used for high performance concrete instead of the standard voltage range of 20-30 V. Five concretes were tested with both migration test and natural diffusion test from NF EN 12390-11. A good correlation was obtained between migration coefficient and diffusion coefficient what confirms literature results. Inter-labs campaign permits to determine precision data for a large range of migration coefficients.

2.7.6 Resistivity test

An operating mode to determine the concrete resistivity in line with the project of European test prEN 12390-19 was evaluated during the project. The reproducibility obtained from both round robin test campaign and inter-labs campaign was quite good. No modification of the initial protocol was thus proposed.

At the end of the PerfDuB project, a set of tests for XC and XS/XD exposure classes are available. Their operating procedures have now been standardised or are in the process of being standardised.

3 Chemical environments - class XA (WG1C)

3.1 External sulphate attack (ESA)

3.1.1 Introduction

3.1.1.1 Context of the study

Degradation by sulfate reaction of concrete is numerous and varied (external or internal). One of the pathological constants of this type of chemical attack is the loss of cohesion and cracking of concrete, generally due to the formation of delayed (or secondary) ettringite of a massive and swelling nature in the cement matrix.

The main cause of this damage is the addition of sulfate ion from the external environment (sea water, selenitous water, etc.). It also turns out that many secondary parameters can modify the reaction kinetics involved in this complex mechanism (concentration of the external solution, associated cation, pH, temperature).

To assess the resistance to External Sulfate Attack (ESA) of a concrete, recent research (Felekoglu *et al.*, 2006; Sahmaran *et al.*, 2007a-b; Rozière *et al.*, 2009; Tosun *et al.*, 2009; Weritz *et al.*, 2009; Katsioti *et al.* 2011) focused on the relevant parameters to be considered for setting up an accelerated degradation test.

As part of the “Performance-based Approach” to design concrete (EN 206 / CN), recent work on a French scale by (Garcia and Carcassès, 2009; Messad, 2009; Cassagnabère and Carcassès, 2013; Rozière *et al.* 2013) made it possible to set up an accelerated testing protocol.

But certain aspects relating to this accelerated test need to be deepened in order to fully understand the reaction phenomena generated by this degradation for new generation concretes. This program is the continuation of a long series of studies.

3.1.1.2 Partnership

Various experienced partners (LMDC, GEM, Lafarge-Holcim) already involved in the development of this type of test naturally came together to establish this experimental program.

Other partners (IFSTTAR then Université Gustave Eiffel, Armines, LGCGM) have expressed their interest in joining this program in order to implement this test in their laboratory and to provide their skills in the analysis of the microstructure of cement matrices, healthy and degraded.

Coordination is ensured by the LMDC.

3.1.1.3 Objectives of the experimental program

This part of report presents a program initiated by PerfDuB as a continuation of a long series of studies on external sulfate attack. In this study by WG1C concerning the accelerated ESA test (or ESR for External Sulphate Reaction), two accelerated protocols were targeted:

- the improvement of the ESR test developed by (Messad, 2009);
- the alternative test described in the Swiss standard (SIA 262, 2013-2019).

The results presented in this document are the result of research from numerous academic, institutional and industrial laboratories.

3.1.1.4 Structuration of experimental campaign

This experimental campaign on the XA sulphate exposure classes was divided into 4 phases. The orientations and decisions were validated each time by the Scientific and Technical Committee (CST) of the PerfDuB National Project.

Table 1.9 summarizes this structuring: study concretes and tested protocols.

Table 1.9. Structure of the ESR experimental campaign

		Messad Protocol					SIA Protocol		Massaad Protocol
		GeM	IFSTTAR	Lafarge-Holcim	LGCgE	LMDC	Lafarge-Holcim	LMDC	GeM
Tr.1	B46	Orig	Var-sol		Var-pH		Orig		
	B47	Orig	Var-sol		Var-pH		Orig		
	B48	Orig	Var-sol		Var-pH		Orig		
	B49	Orig	Var-sol		Var-pH		Orig		
	B50					Orig			
	B51					Orig			
	B52					Orig			
	B53					Orig			
Tr.2	B15		Var-sol		Var-pH	Orig	Orig	Orig	Orig
	B17		Var-sol		Var-pH	Orig	Orig	Orig	Orig
	B18		Var-sol		Var-pH	Orig	Orig	Orig	Orig
Tr.3	B1		Orig	Orig		Orig	Orig	Orig	Orig
	B15		Orig	Orig		Orig	Orig	Orig	
	B38		Orig	Orig		Orig	Orig	Orig	Orig

Legend: *Orig: original protocol (see appendix),*
Var-sol: protocol with variant on the activity of the degradation solution,
Var-pH: protocol with variant on pH maintenance.

3.1.1.5 The organization

The organization of the ESR study is similar to that of the other two external chemical degradations (pure water and acid attacks - leaching and biodegradation) and is structured in 4 phases as follows.

- Stage 1 - Refinement of the accelerated ESR test protocol performed on 8 concretes (B46 to B53);
- Stage 2 - Reliability and repeatability tests on 3 concretes of WG3 (B15, B17 and B18);
- Stage 3 - Inter-laboratory cross-tests carried out on 3 concretes (B0, B1 and B38);
- Stage 4 - Analysis and contracting.

3.1.2 Materials

As part of the development of the accelerated ESR test, 14 concretes were tested:

- concretes made only with cement (B46, B47, B48, B49, B15 and B17 for PN references);
- Concretes made with mineral additions (B50, B51, B52, B53, B18, B0, B1 and B38 for PN references).

This paragraph presents the basic constituents used (cement, additives, aggregates, etc.) and details the preparation of the test bodies.

3.1.2.1 Raw constituents

3.1.2.1.1 Cements

Four cements (three CEM I and one CEM III) are used, coming from different production sites with different levels of sulphate resistance (mainly variation of the amount of anhydrous aluminate in the clinker). The main physical and chemical properties of the cements (according to EN197-1) are presented in Table 1.10.

Table 1.10. Compositions and properties of cements used (producer data)

	CEM I	CEM I-SR3	CEM I-SR5	CEM III
Type	CEM I	CEM I	CEM I	CEM III/A
Class/Reactivity	52.5N	52.5N	52.5N	52.5N
Sulphate resistance class	-	SR3	SR5	PM-ES
Producer/Factory	Holcim Lumbres	Lafarge Val d'Azergues	Lafarge Le Teil	Calcia Rombas
Density (g/cm^3)	3.09	3.18	3.17	2.96
Specific surface (cm^2/g)	4600	3683	3630	4150
R_{c2d} / R_{c28d}	37.0/60.0	34.6/65.0	32.0/64.6	20.0/63.0
Proportion of clinker (%)	97.0	99.0	97.0	36.0
Proportion of addition (%)	3.0(L)	1.0(L)	3.0(L)	64.0(S)
Composition of Bogue of clinker				
C_3S	61.0	66.0	67.0	68.0
C_2S	-	13.0	17.0	11.0
C_3A	8.6	1.0	4.0	10.0
C_4AF	11.1	15.0	7.0	8.0
Gypsum (% by mass)	5.0	4.0	2.5	4.0

3.1.2.1.2 Mineral additions

Four mineral additions (limestone filler L, blast furnace slag S, fly ash V and silica fume D) are used, from different producers. The main physical and chemical properties of the additions are presented in Table 1.11.

Table 1.11. Compositions and properties of mineral additions used (producer data)

	L	S	V	D
Type	Limestone filler	Slag	Fly ash	Silica Fume
Producer	Omya, Betocarb	Ecocem	Surschiste	Condensil
Density (g/cm^3)	2.70	2.90	2.22	2.24
Specific surface (cm ^{2}/g)	5960	4450	/	1.5 to 3.5.10 ^{5}
$I_{28j/90j}$	0.77 / -	- / 1.02	0.89 / 1.03	1.01 / -
D_{50}(µm)	40.0	11.0	/	/
Chemical composition (%)				
$CaCO_3$	95.0	-	-	-
CaO	-	43.7	5.1	< 0.1
SiO_2	-	37.4	83.5 (SiO_2 + Al_2O_3)	> 85 %
Al_2O_3	-	10.8		-
MgO	-	6.5	1.5	-

3.1.2.1.3 Aggregates

The granular skeleton is composed of a sand (G1-0/4) and two gravels (G1-4/11 and G1-11/22). The main characteristics of the aggregates are given in Table 1.12.

Table 1.12. Aggregate properties

	G1-0/4	G1-4/11	G1-11/22
Nature	Alluvial	Alluvial	Alluvial
Granularity (mm)	0/4	4/11	11/22
Form	Rolled	Rolled	Rolled
Density (kg/m^3)	2600	2570	2590
Absorption (%)	0.72	1.52	0.97
Fineness module	3.07	-	-

3.1.3 Concrete designs

3.1.3.1 Stage 1. Protocol development

In this paragraph, the concretes used for the first part of the ESR study, which concerns the test parameters for the development of the accelerated degradation protocol, are presented. B_{CEMI} (or B46 in the designation of the WG3 of the National Project) is the designation of the reference concrete made only with CEM I cement without specification on the resistance to sulphates. $B_{CEMI-SR3}$, $B_{CEMI-SR5}$, B_{CEMIII} (or B48, B47, B49 respectively) are the materials made with CEM I SR3, CEM I SR5 and CEM III cements respectively.

Table 1.13 summarizes the formulations of the 8 concretes for the WG1C ESR study in stage 1.

Table 1.13. Concrete mix designs for the ESR study in stage 1 (kg/m^3)

Designation WG3	B46	B48	B47	B49	B53	B50	B51	B52
	B_{CEMI}	$B_{CEMI-SR3}$	$B_{CEMI-SR5}$	B_{CEMIII}	B_{20L}	B_{20V}	B_{30V}	B_{45S}
CEM I	352				281.5	281.5	246.4	193.6
CEM I SR3		352						
CEM I SR5			352					
CEM III				352				
L					70.5			
V						70.5	105.6	
S								158.4
G1-0/4	650	650	650	650	650	650	650	650
G1-4/11	143	143	143	143	143	143	143	143
G1-11/22	1006	1006	1006	1006	1006	1006	1006	1006
Effective water	155.9	155.9	155.9	155.9	155.9	155.9	155.9	155.9
Total water	172.5	172.5	172.5	172.5	172.5	172.5	172.5	172.5

Materials B_{20V}, B_{30V}, B_{45S}, B_{20L} (or respectively B50, B51, B52, B53) are concretes incorporating 20 % and 30 % fly ash (V), 45 % blast furnace slag (S) and 20 % limestone filler (L) (replacement rate by mass). The granular skeleton of the different concretes, remaining constant, was optimized by the Dreux's method.

3.1.3.2 Stages 2 and 3. Tests on WG3 concretes and inter-laboratory cross tests

In the second and third sections of the study, 5 concretes were used. The nomenclature is identical to that used for the concretes in stage 1 (see previous paragraph, a " ' " has just been added to distinguish castings from concretes). Table 1.14 summarizes the formulations of the 5 concretes for the WG1C ESR study in stages 2 and 3.

Table 1.14. Concrete formulations for the ESR study in Sections 2 and 3 (kg/m^3)

Designation WG3	B15	B17	B18	B1* – B$_0$**	B38
	$B_{CEMI-SR3'}$	$B_{CEMIII'}$	$B_{30V'}$	B_{10L}	B_{8D}
CEM I	-	-	278	280	357
CEM I SR3	350	-	-	-	-
CEM III	-	350	-	-	-
V	-	-	119	-	-
D	-	-	-	-	30
L	-	-	-	50	-
Adjuvant	-	-	-	Ad1	Ad2
G1-0/4	832	815	781	830*	858
G1-4/11	405	303	378	906*	720
G1-11/22	625	680	590		319
Effective water	175	175	175	163	159

* for B1, the 0/4 sand and 6.3/20 gravel are different from G1
** B0 comes from B1 with a problem of water content leading to a material with very poor properties

3.1.4 Mixing and placing

For a given composition, two batches of 30 liters are made in a mixer with a maximum capacity of 50 liters. The two batches, made consecutively and according to the PerfDuB procedure, are prepared in sequence and sampled as presented in Table 1.15.

Table 1.15. Mixing and placing of concrete in the laboratory

Mixing		Implementation	
Mixer	**Mixing sequence**	**Sampling**	**Vibration**
50L capacity mixer	Laboratory preparation: Introduction phase: aggregates (G1), binder (CEM I, L, V, S), water	Cylinders (Ø 11cm × H 22cm) Prisms (7 cm × 7 cm × 28cm) Cubes (15 cm × 15 cm × 15cm)	Vibrating table (48 Hz, 1.6g)

After the mixing phase, the fresh materials are placed by vibration in cylindrical, prismatic and cubic moulds. After the demoulding of the test specimens (24 hours), the concrete samples are cured for 90 days in a conservation room in which humidity and temperature are regulated (RH = 100 %, T = 20 ± 1 °C).

The characterization tests of the concrete in its "sound" state are carried out after 90 days of curing.

3.1.5 Test protocols

This chapter is devoted to the description of the experimental protocols used in this study. Procedures for usual concrete properties such as compressive strength or water accessible porosity as well as degradation procedures by external sulphate reaction, ESR (accelerated or natural) test are described in the following lines.

3.1.5.1 Degradation protocols by ESR

3.1.5.1.1 Original protocols

For the entire study, three operating modes were used to understand the behaviour of concrete with respect to its resistance to external sulphate attack (ESA). Two accelerated ESR protocols were used in this experimental campaign:

- the protocol developed in the thesis work of (Messad, 2009);
- the protocol of the Swiss standard (SIA 262, 2013-2019) developed by (Loser and Leemann, 2015).

In parallel, a natural attack procedure was employed to obtain the acceleration kinetics of the two previously mentioned protocols. This procedure was developed during the thesis work of (Massaad, 2016).

3.1.5.1.2 Variations to the original protocol

In order to have a good appreciation of the parameters of the accelerated protocols previously mentioned, variants to the original procedure were deliberately carried out (non-maintenance of the pH and variation of the ratio $V_{concrete}$ / $V_{solution}$ and frequency of renewal of the etching solution).

3.1.5.2 Additional tests

3.1.5.2.1 Mechanical and durability properties

The hardened properties of the 8 study concretes are measured at 90 days according to the following protocols:

- compressive strength (R_c in MPa) according to the French standard (NF EN 12390-3);
- porosity accessible to water (P_w in %) according to the French standard (NF P 18-459);
- migration coefficient of Cl^- ions in a non-steady state (D_{rcm} in 10^{-12} m^2/s) according to the French standard (XP P 18-462).

3.1.5.2.2 Microstructural study

In parallel with this experimental degradation campaign, a microstructure study was conducted at LMDC. Mineralogical identification tests were carried out using X-ray diffractometry (XRD). At the same time, scanning electron microscope (SEM) observations coupled with elemental chemical analyses using energy dispersive spectroscopy (EDS) were carried out.

Healthy and degraded specimens (after the immersion phase in the sulphate solution) were compared in order to detect possible phase changes in the cement matrix.

3.1.6 Fresh and hardened state properties

The 14 concretes are characterized in the fresh (static tests) and hardened (after 90 days of maturation) states.

3.1.6.1 Fresh state properties

The static characteristics in the fresh state (consistency, density, slump, air content) were measured during the preparation of the concrete in the laboratory. Table 1.16 summarises these results.

Table 1.16. Static properties of the study concretes in the fresh state

Stage	Concrete	Wattmeter (W)	Density (kg/m^3)	Slump (cm)		Air content (%)
				T_0+5'	T_0+30'	
1	B46 (B_{CEMI})	1375	2475	8.5-9.5	8.0	1.5
	B48 ($B_{CEMI-SR3}$)	1300	2422	8.5-8.0	-	2.0
	B47 ($B_{CEMI-SR5}$)	1240	2420	10.0-10.5	-	1.6
	B49 (B_{CEMIII})	1335	2451	9.0-10.0	7.2	1.2
	B50 (B_{20V})	1420	2439	10.5	9.5	1.5
	B51 (B_{30V})	1430	2467	10.0	9.0	1.4
	B52 (B_{45S})	1340	2387	9.0	8.0	1.0
	B53 (B_{20L})	1350	2397	8.0	10.0	1.5
2	B15 ($B_{CEMI-SR3'}$)	-	2410	21.0	19.0 *	1.4
	B17 ($B_{CEMIII'}$)	-	2363	22.5	19.5 *	1.8
	B18 ($B_{30V'}$)	-	2340	21.0	19.0 *	1.5
3	B1 and B0 (B_{10L})	-	2322	21.0	-	1.3
	B38 (B_{8D})	-	2450	20.0	-	1.5

* T_0+60'

3.1.6.2 Hardened state properties

After 90 days of maturation, the study materials are characterized in the hardened and sound state on mechanical, porosity and diffusivity criteria.

3.1.6.2.1 Mechanical properties

At 90 days, the compressive strength (R_c) is measured according to the French standard (NF EN 12390-3). For each composition, the average value is calculated from 3 measurements obtained on an ∅ 11 cm × H 22 cm cylindrical specimen.

Table 1.17 shows the different values of σ_c (average values and standard deviation).

Table 1.17. Average values of compressive strength and associated standard deviation (MPa)

B46 (B_{CEMI})	**B48 ($B_{CEMI-SR3}$)**	**B47 ($B_{CEMI-SR5}$)**	**B49 (B_{CEMIII})**
53.3 ± 1.2	45.6 ± 1.1	52.5 ± 0.8	52.5 ± 0.5
B50 (B_{20V})	**B51 (B_{30V})**	**B52 (B_{45S})**	**B53 (B_{20L})**
53.3 ± 0.5	52.1 ± 1.0	49.9 ± 1.2	44.8 ± 0.8
B15 ($B_{CEMI-SR3'}$)	**B17 ($B_{CEMIII'}$)**	**B18 ($B_{30V'}$)**	**B1 / B0 ($B_{CEMI'}$)**
47.4	54.3	49.7	49.6 / 29.8 ± 1.9
B38 (B_{8D})			
81.0			

3.1.6.2.2 Durability properties

Water-accessible porosity

After 90 days of maturation, the porosity accessible to water (P_w) is measured according to the French standard (NF P 18-459). For each composition, the average porosity is calculated from 3 measurements. Table 1.18 presents the different values of P_w (average and standard deviation).

Table 1.18. Average values of water accessible porosity and associated standard deviation (%)

B46 (B_{CEMI})	**B48 ($B_{CEMI-SR3}$)**	**B47 ($B_{CEMI-SR5}$)**	**B49 (B_{CEMIII})**
13.9 ± 1.0	14.2 ± 0.8	13.7 ± 0.3	15.2 ± 0.7
B50 (B_{20V})	**B51 (B_{30V})**	**B52 (B_{45S})**	**B53 (B_{20L})**
14.2 ± 0.4	14.4 ± 0.3	14.5 ± 0.5	15.5 ± 0.5
B15 ($B_{CEMI-SR3'}$)	**B17 ($B_{CEMIII'}$)**	**B18 ($B_{30V'}$)**	**B1 / B0($B_{CEMI'}$)**
13. 6 ± 0.6	14.3 ± 0.3	14.0 ± 2.0	16.3 / 19,2 ± 1.1
B38 (B_{8D})			
9.9			

Cl^- ion migration coefficient

At the end of 90 days, the coefficient measured in non-steady state (D_{rcm}) is obtained according to the French standard XP P 18-462. For each composition, the average coefficient is calculated from 3 measurements of Cl^- penetration (silver nitrate spraying). Table 1.19 presents the different values of D_{rcm} (average and standard deviation).

Table 1.19. Mean values of Cl^- ion migration coefficient and associated standard deviation (10^{-12} m²/s)

B46 (B_{CEMI})	**B48 ($B_{CEMI-SR3}$)**	**B47 ($B_{CEMI-SR5}$)**	**B49 (B_{CEMIII})**
11,2 ± 0,7	12,8 ± 1,8	13,4 ± 0,9	1,8 ± 0,9
B50 (B_{20V})	**B51 (B_{30V})**	**B52 (B_{45S})**	**B53 (B_{20L})**
8,4 ± 0,5	7.3 ± 0.6	1,4 ± 0,6	13,8 ± 0,7
B15 ($B_{CEMI-SR3'}$)	**B17 ($B_{CEMIII'}$)**	**B18 ($B_{30V'}$)**	**B1 ($B_{CEMI'}$)**
15,0 ± 1,0	1,7 ± 1,0	2,3 ± 0,1	26,0
B38 (B_{8D})			
0,31			

3.1.7 Results

3.1.7.1 Development of the saturation test or "Messad" test

3.1.7.1.1 Test parameters

This section focuses on the advances made by WG1C on the "Messad" degradation protocol. In previous studies (Messad, 2009; Garcia and Carcassès, 2009; Cassagnabère and Carcassès, 2013; Rozière and al., 2013; Linger and al., 2014), many parameters have already been endorsed such as the concentration of the attacking solution, the pre-saturation phase or the type of measurement... In the present study, other parameters have been tested in order to refine the procedure. In particular, we are interested in:

- sampling (type of specimen and expansion measurement method);
- activity of the etching solution (volume ratio and turnover);
- maintenance of the pH during immersion in the degradation solution;
- time of the immersion test to optimize the study time.

Sampling

To test the impact of sampling on the response of the accelerated test, two aspects were evaluated:

- measurement mode with a different pin arrangement;
- geometry of the test specimen.

The main measure to evaluate the resistance to ESA is the length tracking by shrinkage measurement. Two modes of measurement are compared: an axial arrangement of "shrinkage" type studs and a lateral arrangement of flat studs. The different devices are presented in figure 1.31.

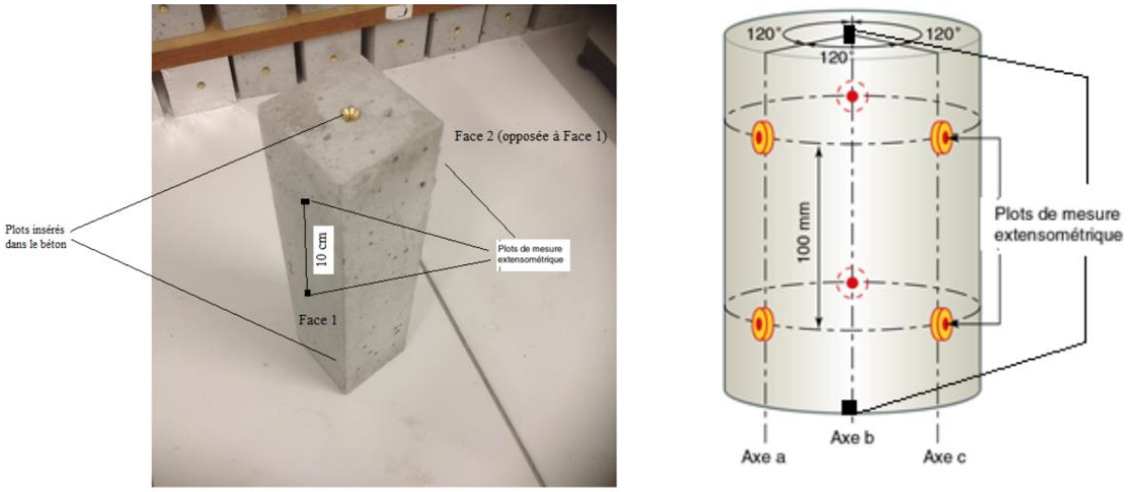

Figure 1.31. The two expansion measuring devices

The results of the experimental campaign showed that the use of lateral flat pads is more difficult to achieve. Indeed, these blocks tended to come off very easily from the specimens tested for several partner laboratories.

The solution to be retained for the measurement of length variation is therefore the "shrinkage" type stainless steel axial stud device.

Concerning the geometry of the sample, two shapes were experimented: a prismatic shape of dimensions 7 cm x 7 cm x 28 cm (original shape) and a cylindrical shape of dimensions ∅ 11 cm x H 22 cm. Figure 1.32 shows the results of the average length variation for the B51, B52 and B52 concretes measured on prismatic and cylindrical samples.

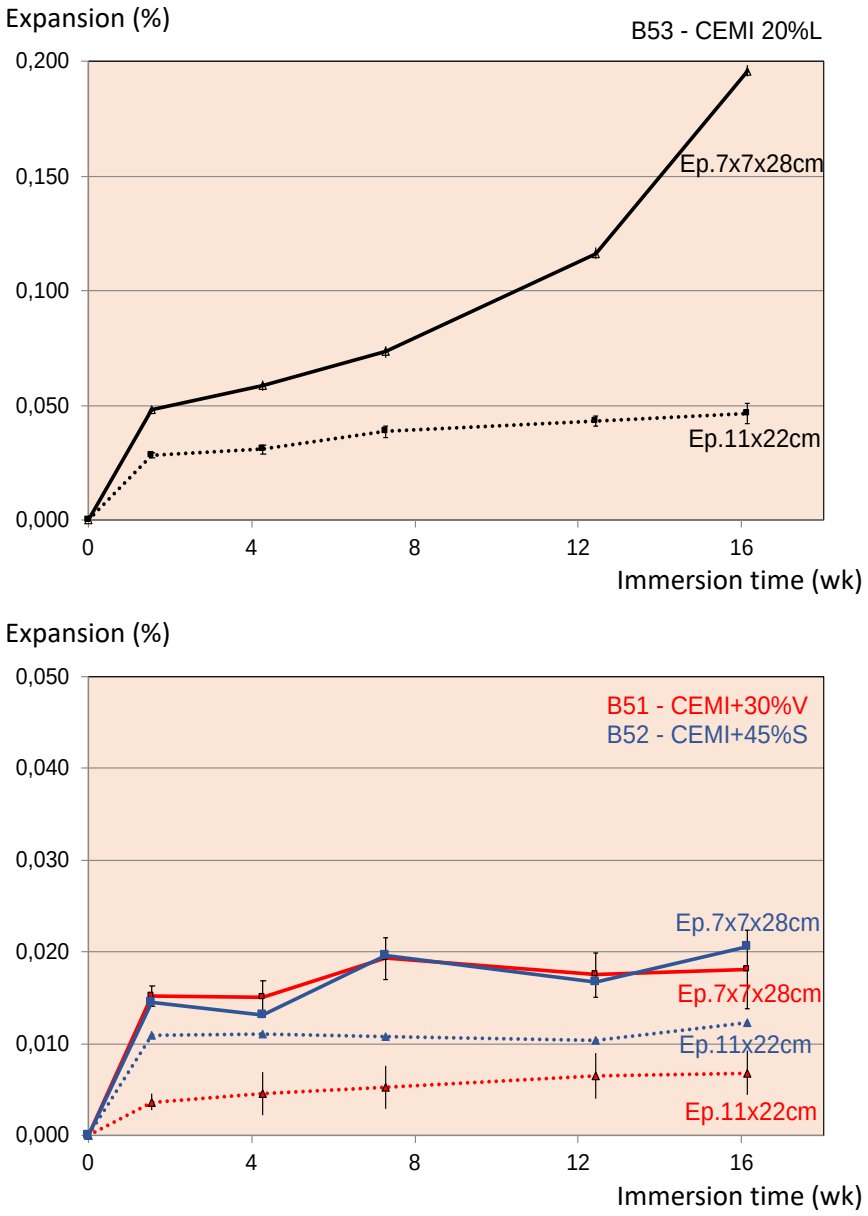

Figure 1.32. Expansion measurements for B51, B52 and B53 on prismatic and cylindrical specimens

From these two graphs, it is clear that the values collected on prisms are always higher than those obtained on cylinders, whether for a material sensitive to ESA (B53 - B_{20L}) or less swelling materials (B51 and B52 with chemically active mineral additions). It can be assumed that in the case of cylindrical test bodies, which are more voluminous, the initial pre-saturation phase is not sufficiently long, generating less efficient ettringite formations.

It is therefore recommended to use prismatic specimens of dimensions 7 cm x 7 cm x 28 cm.

Activity of the solution

Another protocol parameter to be evaluated is the activity of the Na_2SO_4. In addition to the sulphate concentration and the associated cation (in this study Na^+), the activity of the etching solution can be expressed by its renewal frequency and by the ratio between the volume of concrete and that of the solution ($V_{concrete}$ / $V_{solution}$). In order to observe the influence of these two parameters, not dissociated in this study, a concrete reactive to ESA was used (B46 - CEM I). Figure 1.33 presents these results. The black curve shows the results obtained from the original protocol with a monthly renewal of the solution and a volume ratio equal to 1. The green curve shows the results obtained with a higher activity resulting in a renewal every 15 days and a $V_{concrete}$ / $V_{solution}$ ratio equal to 0.5.

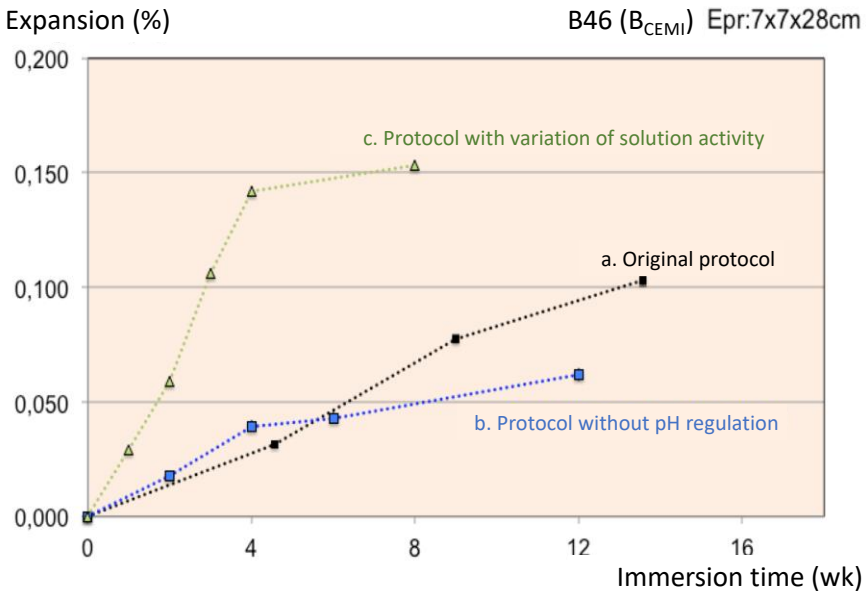

Figure 1.33. Impact of solution activity and pH maintenance on the expansion of ESA-sensitive concrete (B46)

From these results, it is clear that the volume ratio (material / solution) and the renewal will have an impact on the result obtained.

It is therefore recommended that the etching solution be renewed once a month, while maintaining a volume ratio of $V_{concrete}$ / $V_{solution}$ equal to 1. This choice is a compromise between the speed of degradation and the ease of performing the test.

Maintaining the pH

Maintaining the pH of the sodium sulphate solution is also a relatively important protocol component. Figure 1.33 shows the impact of pH maintenance on the length variation results obtained on the ESA-sensitive B46 concrete. In the original protocol, the pH is maintained at 7 (black curve) while it is not regulated for the blue curve. A regulation at a neutral pH has the consequence of favoring the development of ettringite, which results in a more important swelling.

For the saturation "Messad" protocol, it is therefore recommended to stabilize the pH of the attack solution at 7with a 5 g/L diluted sulfuric acid solution.

Test time

The test time is relatively long in order to qualify a concrete while considering the time constraints of the construction site. At the beginning of the experimental campaign for stage 1, the test was calibrated for a duration of 16 weeks (excluding preconditioning). Some industrial partners raised this organizational problem and questioned the possibility of reducing the trial from 16 to 12 weeks. Figure 1.34 presents the results over time for the "Messad" protocol. Some tests were voluntarily left until 23 weeks of immersion.

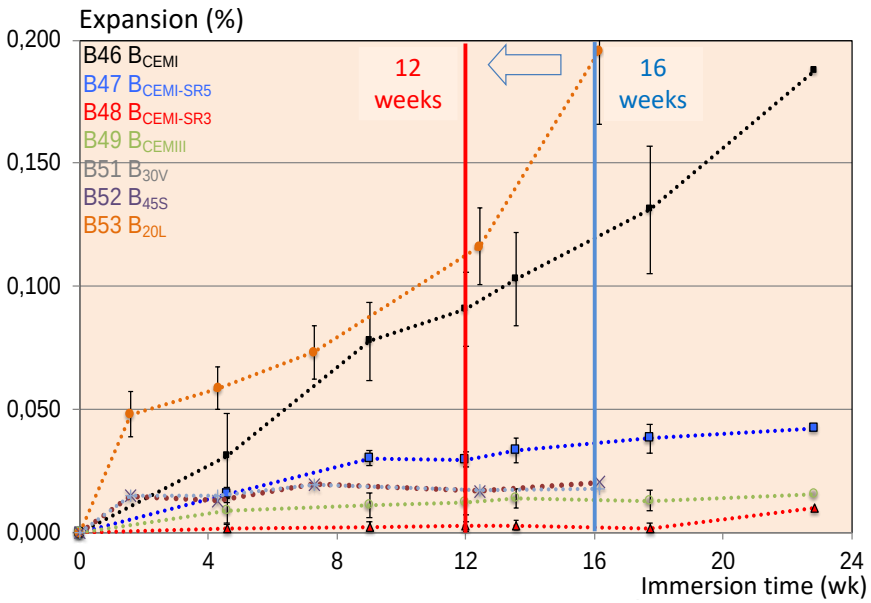

Figure 1.34. Impact of immersion time on concrete expansion

From this figure, it can be concluded that a reduction of the immersion time from 16 to 12 weeks, excluding preconditioning (drying + saturation), can be considered without fundamentally changing the conclusions resulting from the test.

This duration of 12 weeks is therefore retained for the final protocol.

Change in mass

The evolution of the mass of the specimens can be followed during the whole protocol phase. Generally, two types of trends are observed for this variation:

- **for ESA-sensible concretes** (example B53 - B_{20L} in figure 1.35), we observe an increase in mass generated by the neoformation of ettringite phases which, following the pathology, tend to fill the structural porosity of the matrix before creating damage by cracking;
- **for concretes that are not very sensitive to ESA** (B50, B51 and B52 in figure 1.35), a slight decrease in mass is visible. This decrease can be explained by a leaching of the materials (generally limestone phases) as it should be remembered that the sodium sulphate attack solution is maintained at a constant pH (7) by adding sulfuric acid.

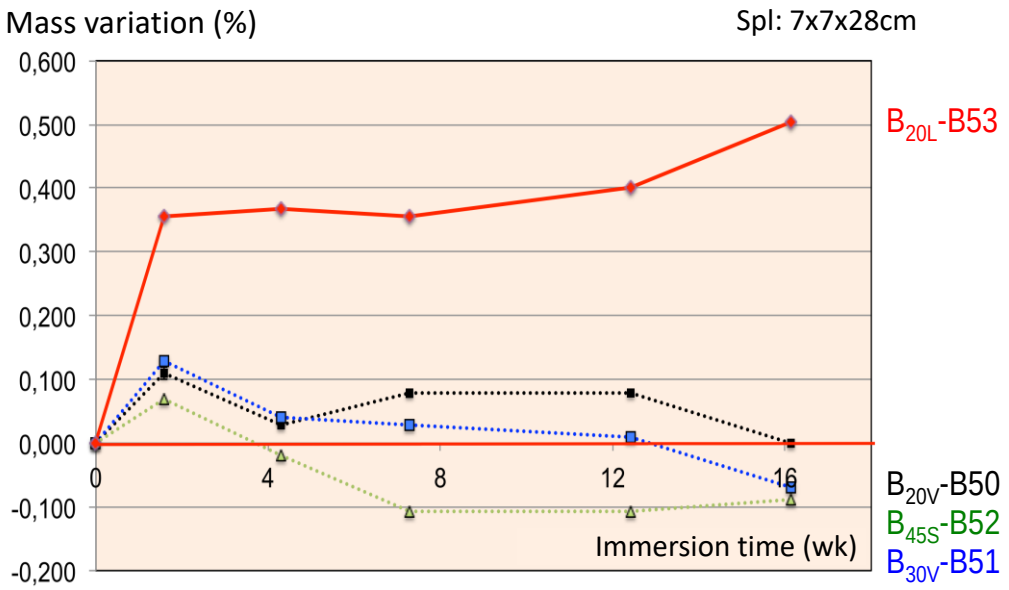

Figure 1.35. Mass variation of samples for concretes B50 to B53 (Messad protocol)

3.1.7.1.2 Verification of the formed phases

In order to ascertain the pathological mechanisms involved in this accelerated procedure, further investigations were carried out by SEM analysis. Two materials were targeted: a concrete that had reacted to the degradation with a significant level of swelling (B1 - B_{10L}) and a concrete containing silica fume and having no observable expansion (B38 - B_{8D}).

Figures 1.36 and 1.37 show the observations of fracture analysed in secondary electron mode or of polished surface analysed in backscattered electron mode as well as the chemical analyses carried out by EDS respectively on the B1 and B38 concretes.

Concrete B1- B_{10L}: ESA sensitive material with high swelling potential (ε = 0.221 % after 12 weeks of immersion).

Figures (a) and (b) show secondary electron mode observations of fractured B1 concrete (B_{10L}) after degradation (12 weeks immersion). These images show a typical morphology in a pore of massive ettringite clusters crowned with primary ettringite needles, resulting from ESA.

The following images, (c) to (g), present an analysis for the same concrete in backscattered electron mode with chemical mapping done by EDS. From images (d) and (e), it is very easy to identify siliceous (purple spots on (d)) and calcareous (light green area on image (e)) aggregates. From the aluminium analysis, we can identify the cement matrix (orange area on image (g)). By coupling images (f) and (g), revealing the respective presence of sulphur and aluminium, we can see a strong presence of massive ettringite. First, two large spots (150 μm in diameter) attract our attention (large yellow spots on (f)). These are large ettringite nests that have developed in the macro-porosity of the matrix. On the other hand, smaller ettringite phases (a few tens of μm) can also be observed very distinctly.

By doing a chemical analysis of the ettringite zone (figure 1.37), we can conclude that we are indeed in the presence of massive ettringite because the analysed mass proportions between Al, S and Ca correspond to the proportions of the chemical form of ettringite ($Ca_6Al_2(SO_4)_3(OH)_{12}26H_2O$) with Ca/Al = 4.44, Ca/S = 2.5 and Al/S = 0.56.

SEI mode picture

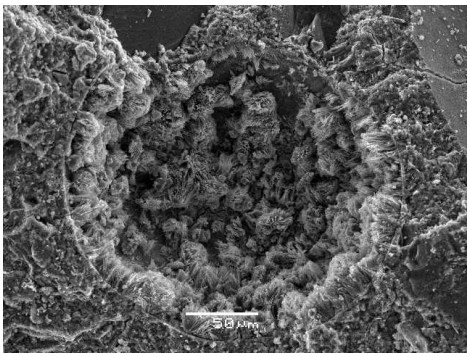

a. X400

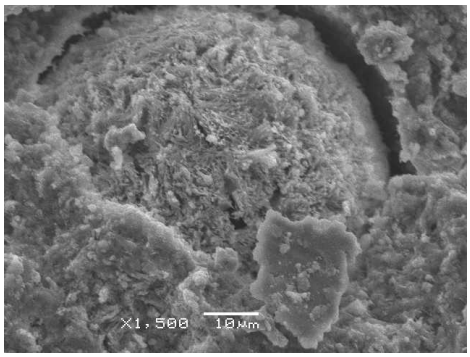

b. X1500

BSE mode picture and EDS analysis

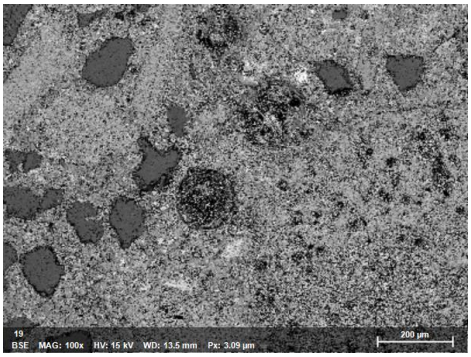

c. BSE mode picture (X100)

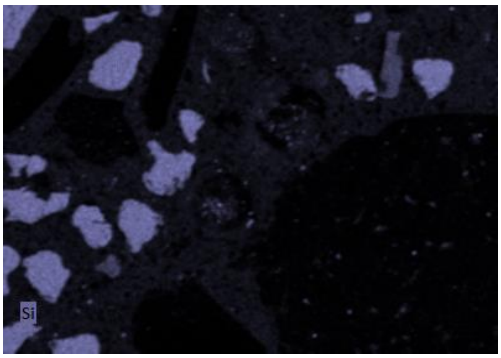

d. Si analysis

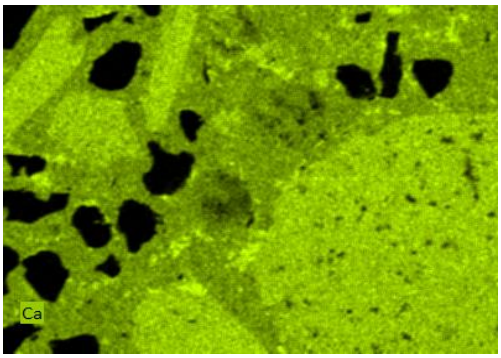

e. Ca analysis

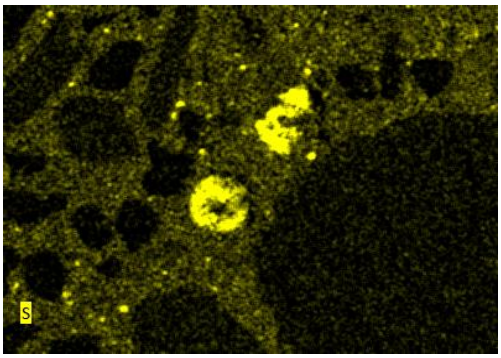

f. S analysis

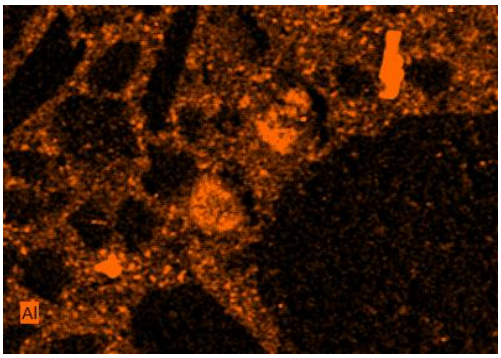

g. Al analysis

Figure 1.36. SEM investigations and EDS analyses for B1 concrete (B_{10L}) after 12 weeks of immersion in Na_2SO_4

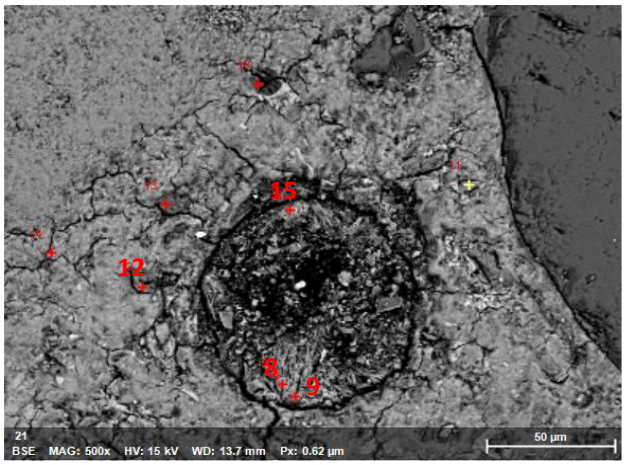

BSE mode picture (x500)

Oxide content (% mass)	Point analysis			
	8	9	12	15
Na_2O	0.22	0.73	1.29	0.21
SiO_2	1.24	3.71	9.84	2.91
SO_3	29.48	28.01	17.79	27.29
CaO	54.66	51.69	56.40	56.13
Fe_2O_3	0.42	0.88	1.70	0.66
Al_2O_3	13.28	14.30	11.08	12.26
Ca/Al	4.12	3.61	5.09	4.57
Ca/S	1.85	1.84	3.17	2.07
Al/S	0.45	0.51	0.62	0.44

Figure 1.37. Chemical point analyses in/near an ettringite zone for B1 concrete

Note on item 12. A complementary analysis was carried out on point 12. The question was to know if the cracking observed was due to the pressure of crystallization of ettringite. In the vicinity of the crack, the chemical composition of ettringite is found with elemental ratios close to the 3 ratios mentioned above.

Concrete B38 - B_{8D}: Material with low susceptibility to ESA with very low swelling potential (ε = 0.010 % after 12 weeks of immersion).

In image (a) of Figure 1.38, taken in backscatter electron mode (BSE), no area of primary or even massive ettringite is visible. In order to further investigate the presence of ettringite, a chemical analysis by EDS mapping is presented on images (b), (c), (d) and (e).

Pictures (b), (c) and (e) show that a band of cement paste is embedded between two granular inclusions (siliceous aggregate at bottom right in image (b) and limestone aggregate at top left in image (c)). From images (d) and (e), we do not observe any area of overconcentration of sulphur in the cement matrix (band between the two aggregates). In fact, we can see that the sulphur (image (d)) is homogeneously distributed on the surface of this analysis map. It can be concluded that massive ettringite, a product resulting from ESA, is not present in this concrete containing silica fume (B38 - B_{8D}). The absence of this swelling phase supports the low expansion results obtained for this material (0.01 % at 12 weeks).

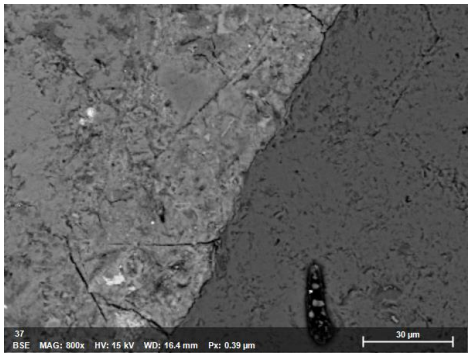

a. BSE mode picture (X800)

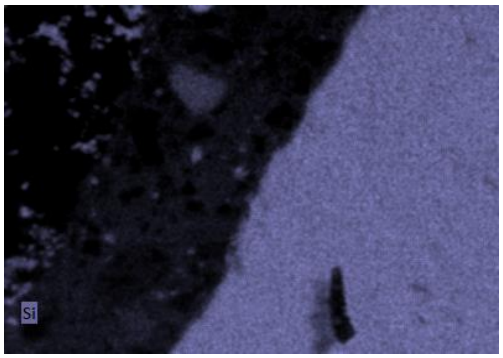

b. Si analysis

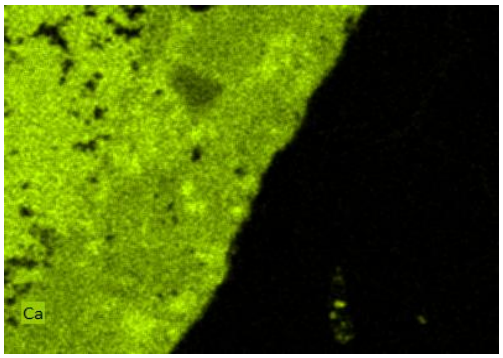

c. Ca analysis

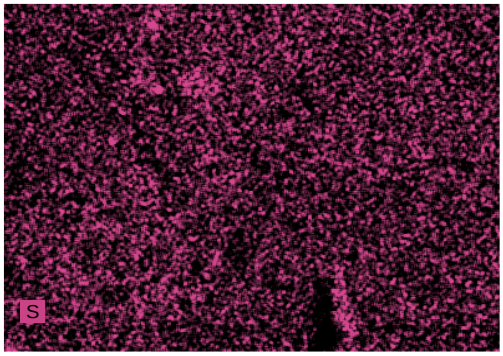

d. S analysis

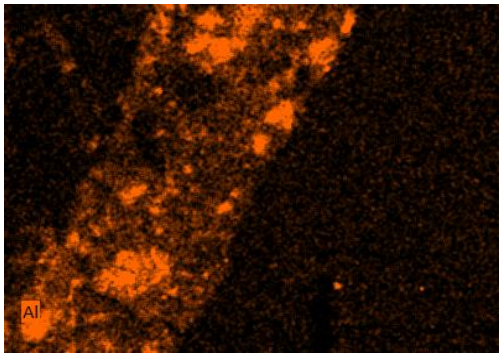

e. Al analysis

Figure 1.38. SEM investigations for B38 concrete (B_{8D}) after 16 weeks of immersion in Na_2SO_4

3.1.7.1.3 Relevance of durability indicators

Additional tests of mechanical indicators (R_c) or durability (P_w and D_{rcm}) were proposed in order to have an appreciation of the damage of the material after prolonged immersion in a sodium sulphate solution. It should be remembered that the three general performance tests are carried out on the one hand on the so-called "healthy" material before the immersion phase and on the other hand after the immersion phase. Three behaviours were observed according to the sensitivity of the material to ESA:

- reactive materials (i.e. swelling materials): B53 - B_{20L};
- low reactive materials (i.e. non-swelling materials): B48 - $B_{CEMI\text{-}SR3}$;
- moderately swelling materials: B17 - B_{CEMIII}, and B49 - B_{CEMIII}.

Figure 1.39 shows the results of the usual properties of concrete in the hardened state: compressive strength, porosity accessible to water and Cl^- ion migration coefficient. On the

one hand, they are measured after the curing phase of the material, at 90 days, i.e. before immersion in the etching solution. On the other hand, a second series of measurements is carried out after the immersion phase in the sodium sulphate solution (12 or 16 weeks).

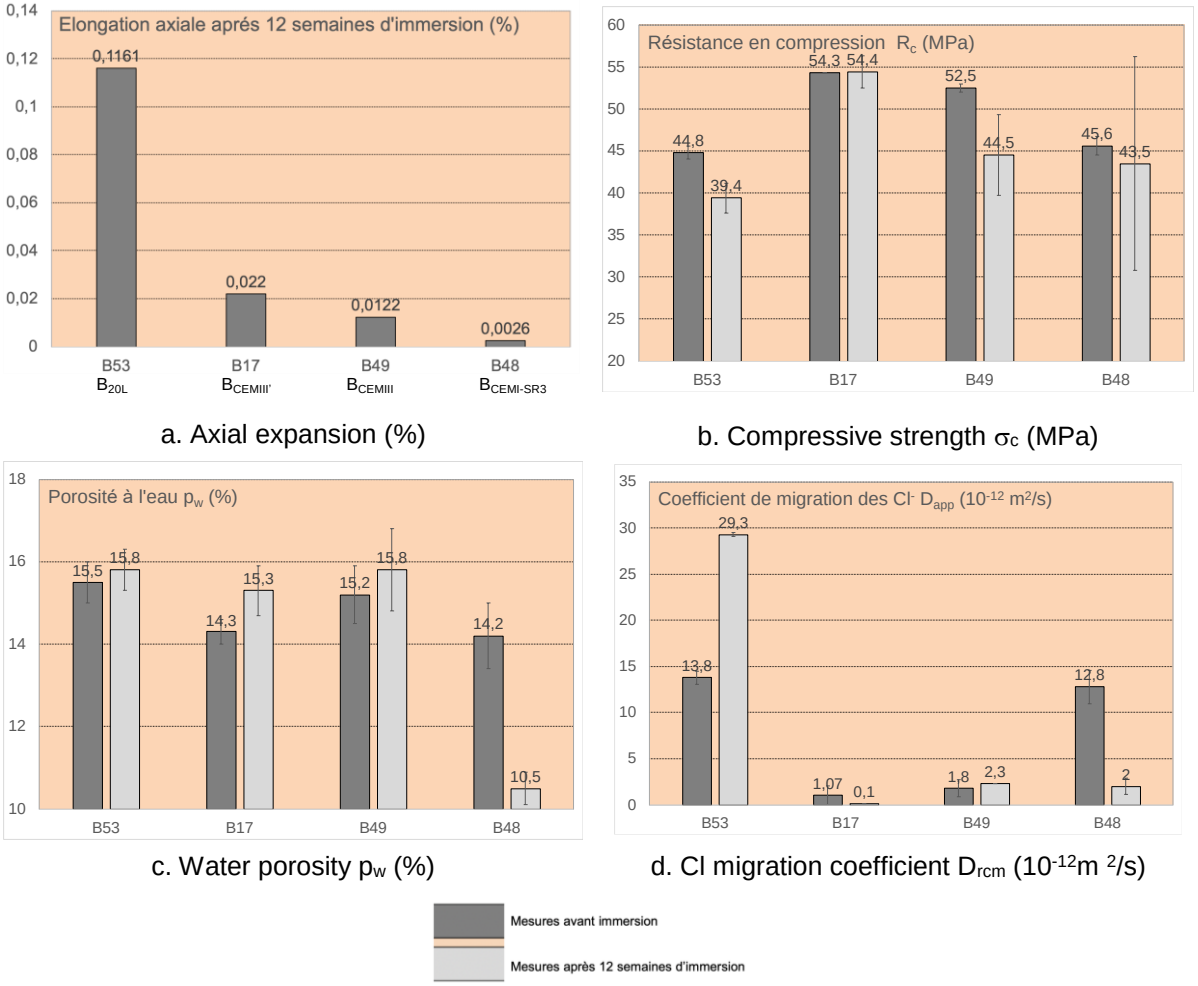

a. Axial expansion (%)

b. Compressive strength σ_c (MPa)

c. Water porosity p_w (%)

d. Cl migration coefficient D_{rcm} (10^{-12}m ^{2}/s)

Figure 1.39. Impact of ESA degradation with the "Messad" protocol on the usual properties of concrete

From this figure, three trends can be distinguished according to the reactivity of the material:

- **for a sensible concrete** (B53 - B_{20L}), a degradation of properties is observed. In this case, the damage generated by the production of massive ettringite leads to excessive cracking which is detected with these indicators;
- **for a non-sensible concrete** (B48 - $B_{CEMI-SR3}$), the opposite effect is observed with an improvement or maintenance of the properties;
- **for concretes with median behaviour** (B17 and B49), there is no clear trend on the evolution of these properties. Improvements and losses in performance can be distinguished.

Based on this analysis, it is therefore advisable to keep these complementary tests if one wishes to have a good vision of the damage of concretes sensitive to ESA, i.e. generating a significant swelling potential.

3.1.7.1.4 Summary of test parameters

Table 1.20 below summarizes all of the set measurement parameters and the measurements.

Table 1.20. Test conditions for the "Messad" protocol

Specimen	**3 prisms 7 cm x 7cm x 28 cm 6 cylinders ∅ 11 cm x H 22 cm for R_c 4 cylinders ∅ 11 cm x H 22 cm for P_w and D_{rcm}**
Saturation	48 h with attack solution
Exposure condition	Continuous immersion
pH control	Checked at 7.0 (± 1) with sulfuric acid
Concentration of the etching solution	8.9 g/L Na_2SO_4 (6 g/L of SO_4)
Temperature	Controlled at 25 °C
Renewal of the solution	Every 4 weeks
$V_{concrete}$ / $V_{solution}$	1.0
Duration of the test	12 weeks immersion
Measurements	Length variation Variation in mass Variation of indicators R_c, P_w, D_{rcm}

3.1.7.2 The protocol of the Swiss SIA standard

The protocol of the Swiss SIA standard has not been the subject of any particular development in phase 1. In fact, the procedure was taken over in its original form from the normative text already in force in Switzerland (SIA 2013-2019). A large-scale study on the validity of this method was carried out in 14 testing laboratories (Austria, Germany, Switzerland, etc.) and piloted by the EMPA (Swiss Federal Laboratories for Materials Testing and Research, in German Eidgenössische Materialprüfungs und Forschungsanstalt). The document entitled "Inter-laboratory test for sulphate resistance of concrete according to SIA 262/1, Annex D, final report" (original title: *VAB-Ringversuch Sulfatwiderstand von Beton nach SIA 262/1, Anhang D, Schlussbericht*) shows the results on 4 concretes tha are more or less reactive to ESA.

Figure 1.40 shows a synopsis of the Swiss SIA protocol (a) and the sequencing (b) of the immersion / drying cycles, the immersion phase and the measurement times.

a.

Eprouvettes (carottes) d=28 mm, 145 mm ≤ L ≤ 150 mm

Essai	4 cycles de 7 jours (28 jours)				Evaluation
	Séchage	Refroidis-sement	Immersion	Immersion supplémentaire	
			Solution de sulfate de sodium à 5% (5 g sodium anhydre + 95 g d'eau)		
	50°C, 119h	20°C, 1h	48h	56 jours	
SIA 262/1, Annexe D (ancienne)				aucun	Allongement après 4 cycles (28 jours). Limite Δl ≤ 0.5 ‰
SIA 262/1, Annexe D (nouvelle)					Allongement entre le 4e cycle et la fin de l'immersion suppl. Limite Δl ≤1.2 ‰

La durée de l'essai est désormais de 84 jours et non plus de 28 jours.
Attention, la valeur limite n'est plus la même.

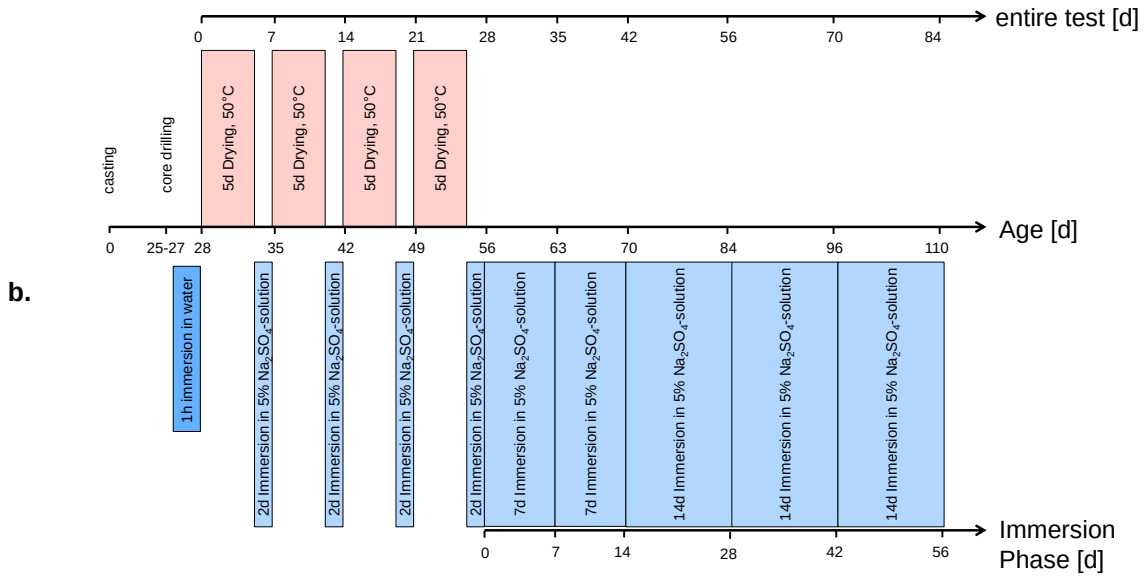

Figure 1.40. Synopsis of the Annex D Swiss SIA standard protocol

3.1.8 ESR accelerated tests on WG3

3.1.8.1 Raw expansion results

3.1.8.1.1 Variation in length for the "Messad" tests

The three graphs presented in figures 1.41 to 1.43 show the results of axial elongations obtained with the accelerated "Messad" protocol whose parameters were retained in stage 1. The graphs are presented according to the three study stages (1, 2 and 3).

In Figure 1.41, two series of ready-mixed concrete are shown:

- with cements only (a): B46 - B_{CEMI}, B47 - $B_{CEMI\ SR5}$, B48 - $B_{CEMI\ SR3}$ and B49 - B_{CEMIII};
- with a matrix incorporating chemically active (B50 - B_{20V}, B51 - B_{30V}, B52 - B_{45S}) or inert (B53 - B_{20L}) mineral additions.

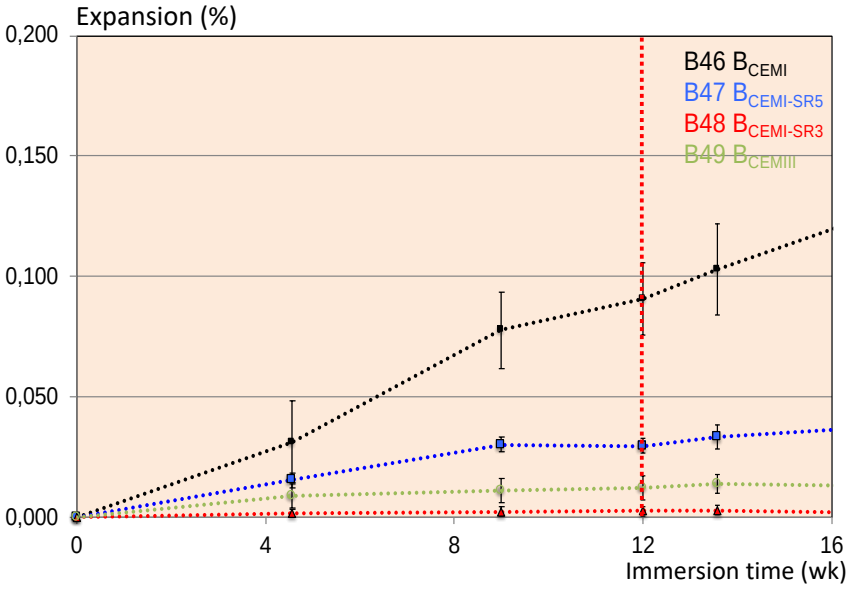

a. Concretes with cements only

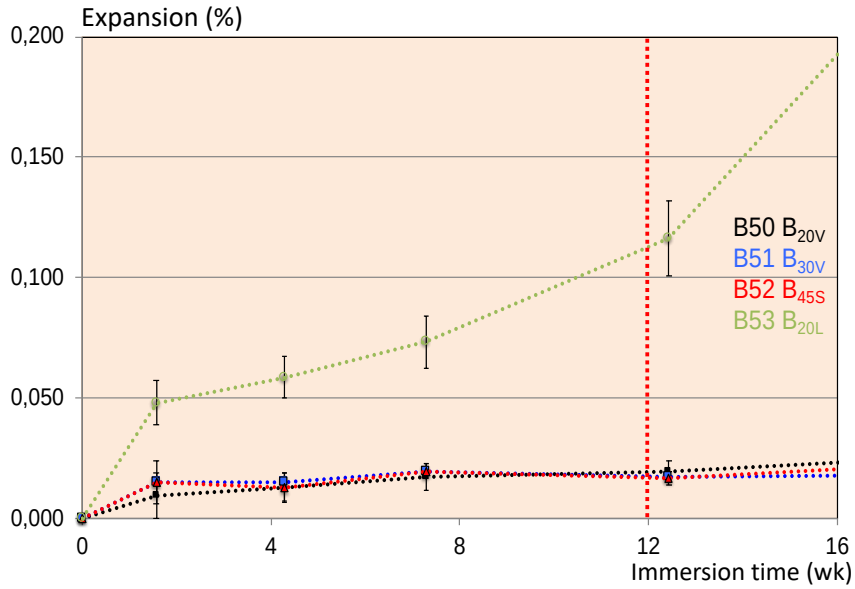

b. Concretes with cements and mineral additions

Figure 1.41. Results of axial expansion obtained for the Messad accelerated test for concrete in stage 1

Figure 1.42 presents the results of a first series of concretes of WG3A "Concrete to be studied" carried out in stage 2. Among the 42 concretes, 3 formulations were selected. These are the concretes B15 - $B_{CEMI\text{-}SR3'}$, B17 - $B_{CEMIII'}$ and B18 - $B_{30V'}$.

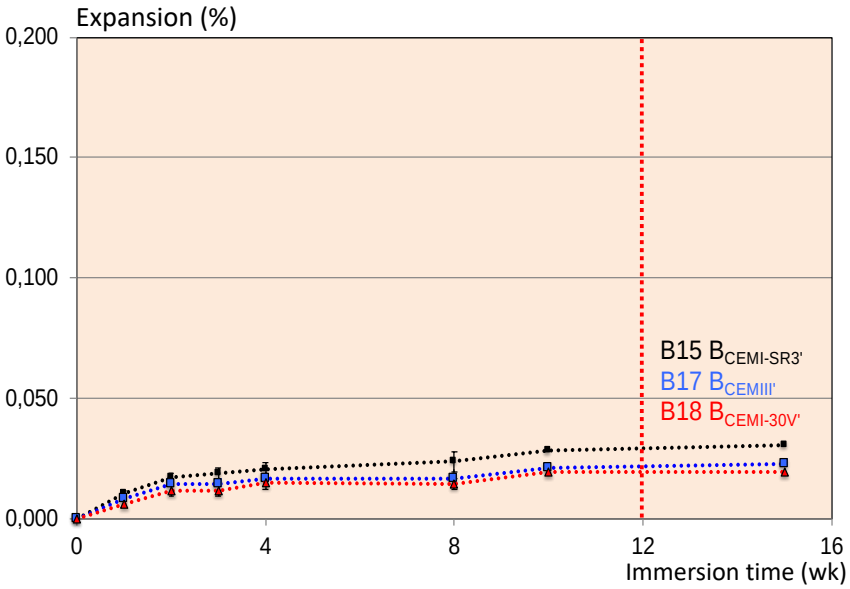

Figure 1.42. Results of axial expansions obtained for the accelerated "Messad" test for concrete in stage 2

Figure 1.43 presents the results of a second series of concretes of WG3A carried out in stage 3: B15 - $B_{CEMI\text{-}SR3'}$, B1 - B_{10L} and B38 - B_{8D}. In this campaign, concretes B1 and B38 were chosen because of their expected extreme behaviour (B1 with CEM I and high W/C ratio (0.60) and B38 with silica fume and low W/C ratio (0.38)).

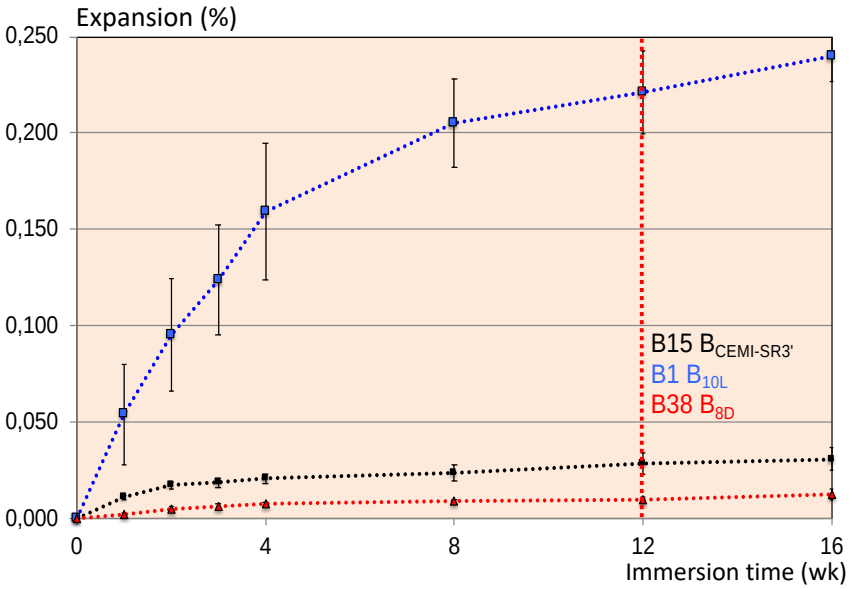

Figure 1.43. Results of axial expansions obtained for the Messad accelerated test for concrete in stage 3

All the results of the 3 figures will be used in the following development.

3.1.8.1.2 Axial length variation for SIA tests

The four graphs in figures 1.44 to 1.46 present the results of the axial elongations obtained with the accelerated SIA protocol in stages 1 to 3. The graphs are presented successively according to the three study stages (1, 2 and 3).

In Figure 1.44, the axial expansions during the 8 weeks of immersion are shown for the concretes with cements only (B46 - B_{CEMI}, B47 - $B_{CEMI\ SR5}$, B48 - $B_{CEMI\ SR3}$ and B49 - B_{CEMIII}) and with a matrix incorporating limestone filler (B53 - B_{20L}).

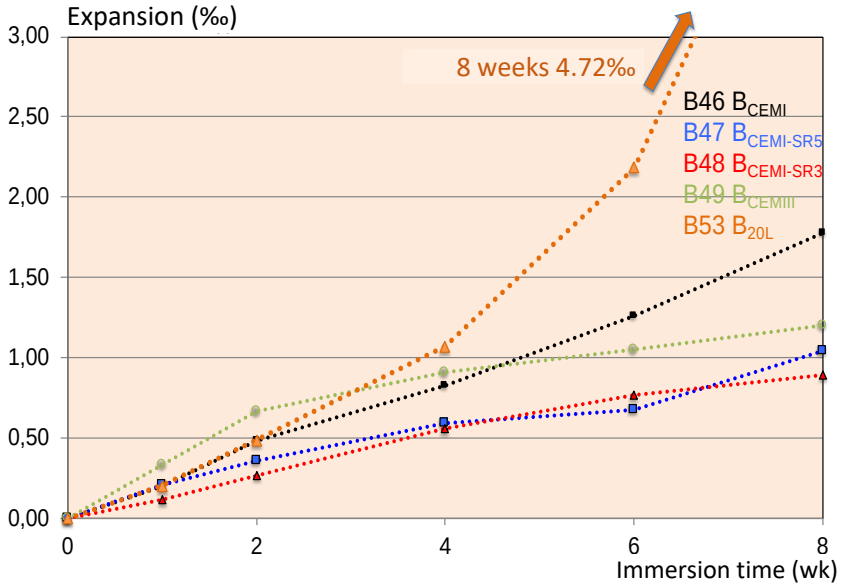

Concrete with only cements or cement and lime filler

Figure 1.44. Results of axial elongations obtained for the SIA accelerated test for concrete in stage 1

Figure 1.45 presents the results of the concretes of WG3A "Concrete to be studied" tested in stage 2. As previously, the same 3 formulations, among the 42 concretes, were selected (B15 - $B_{CEMI-SR3'}$, B17 - $B_{CEMIII'}$ and B18 - $B_{30V'}$). The results presented were measured at the Lafarge-Holcim laboratory (a) and at the LMDC (b).

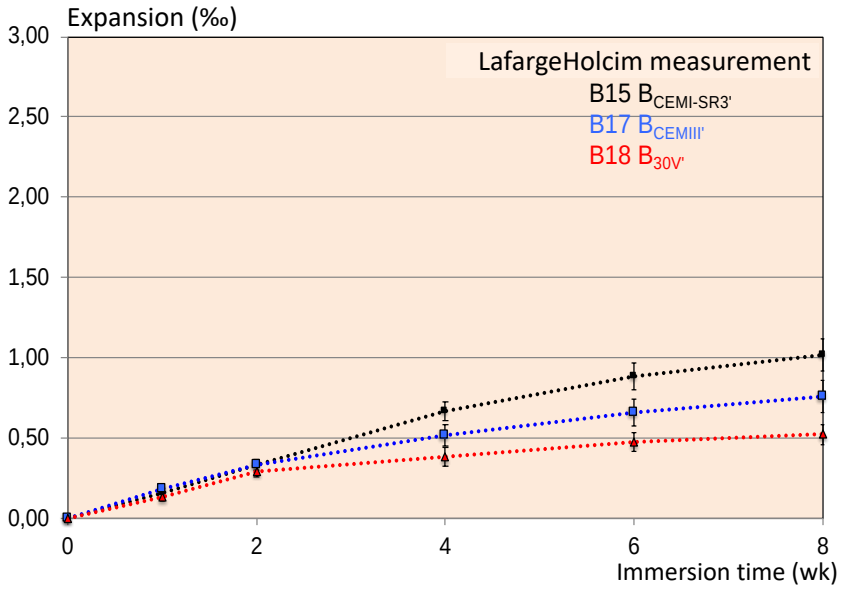

a. Concrete tested at Lafarge-Holcim cements

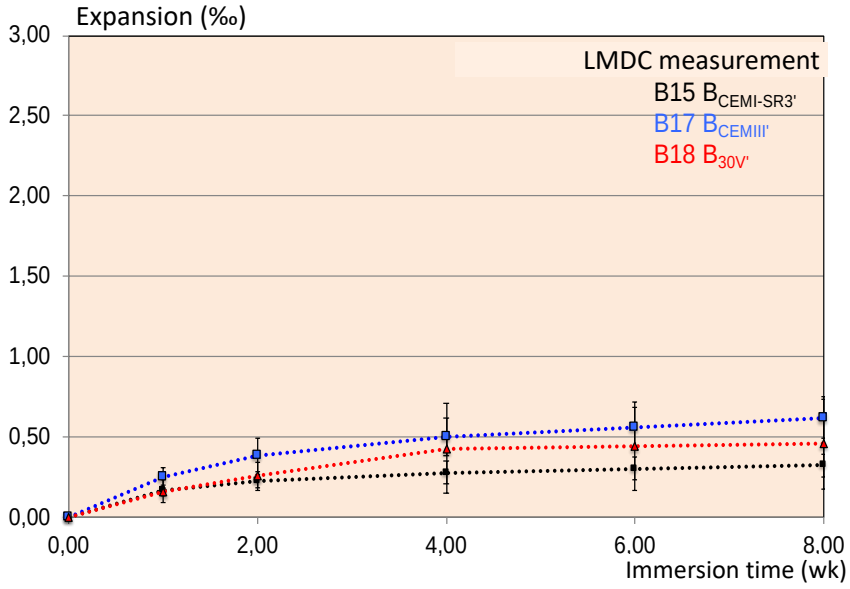

b. Concretes tested at the LMDC

Figure 1.45. Results of axial elongations obtained for the SIA accelerated test for concrete in stage 2

Figure 1.46 shows the results of a second series of GT3a concretes tested in stage 3: B15 - $B_{CEMI-SR3'}$, B1 - B_{10L} and B38 - B_{8D}.

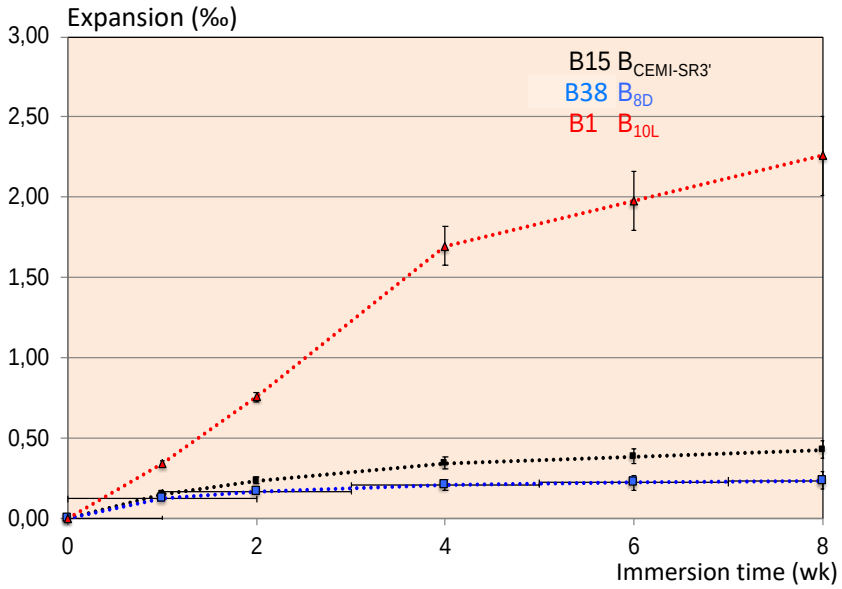

Figure 1.46. Results of axial elongations obtained for the SIA accelerated test for concrete in stage 3

3.1.8.2 Classification of concrete at the end of the protocol

Figure 1.47 shows the expansion results at the end of the protocol for both test methods.

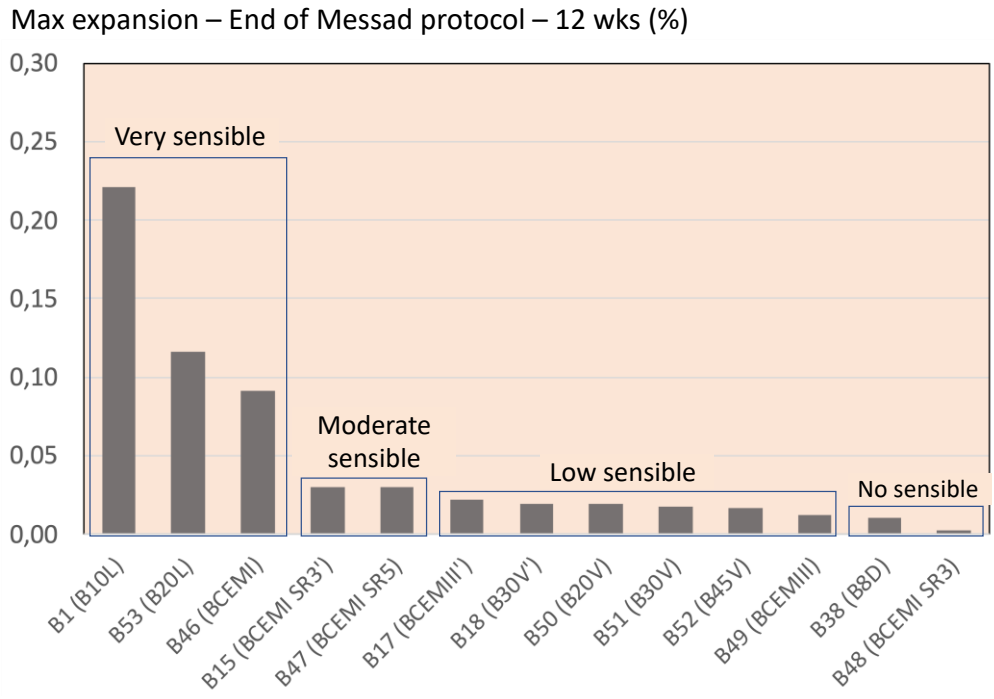

a. Messad test

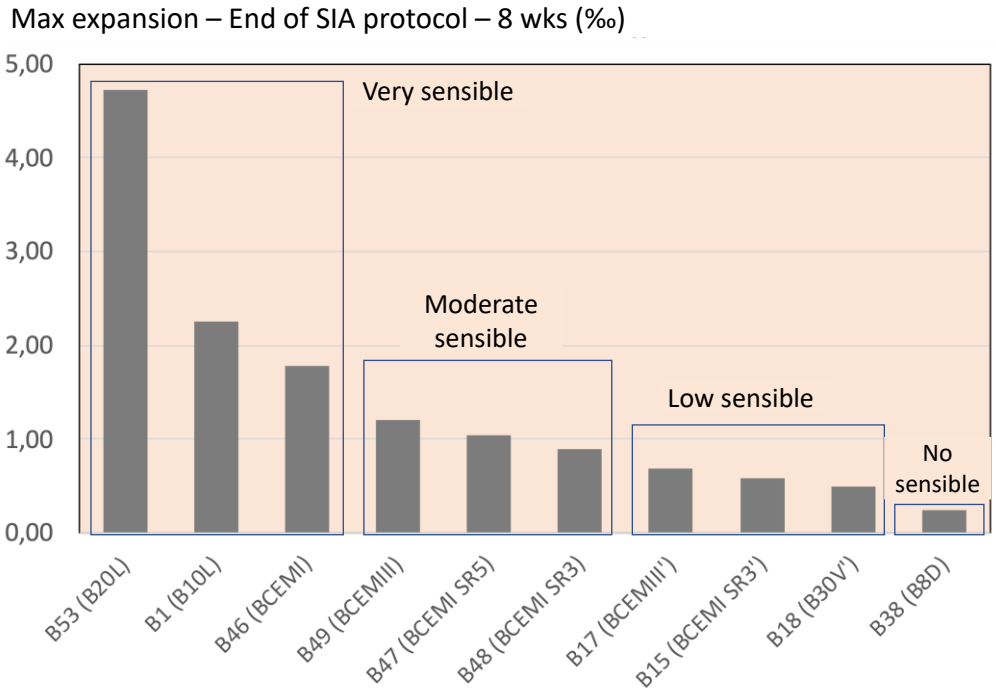

b. SIA test [1,2]

[1] *For concrete B15, the value displayed is the average of 3 distinct series (15 measurements)*
[2] *For concrete B17 and B18, the values used are from two separate experimental series*

Figure 1.47. Ranking histogram for the accelerated "Messad" and SIA tests at the end of the protocol

From these results, we can distinguish 3 to 4 types of behaviour:

- materials that are **very sensitive** to ESA with high swelling (B53, B1 and B46). In this case, dimensional variations are high regardless of the protocol used;
- **moderately responsive** concretes to ESA. For these materials, an expansion exists but it remains moderate. It should be noted that according to the two protocols a series of 4 concretes are concerned (B47, B49, B48, B15);
- concretes with **low or no reaction** to external sulphate attack. In these last two categories, the axial elongations are low to very low (B17, B18, B38, B48, B50, B51).

By analysing all of these results, it is possible to generate a ranking for resistance to sulphate attack. Table 1.21 compares the ranking made for the two test methods.

Table 1.21. ESR performance ranking

Messad protocol										
Ranking	**10**	**9**	**8**	**7**	**6**	**5**	**4**	**3**	**2**	**1**
Concretes	**B1** B_{10L}	**B53** B_{20L}	**B46** B_{CEMI}	**B15** $B_{CEMISR3'.}$	**B47** $B_{CEMISR3}$	**B17** $B_{CEMIII'}$	**B18** $B_{30V'}$	**B49** B_{CEMIII}	**B38** B_{8D}	**B48** $B_{CEMI-SR3}$
SIA protocol										
Ranking	**10**	**9**	**8**	**7**	**6**	**5**	**4**	**3**	**2**	**1**
Concretes	**B53** B_{20L}	**B1** B_{10L}	**B46** B_{CEMI}	**B49** B_{CEMIII}	**B47** $B_{CEMISR5}$	**B48** $B_{CEMISR3}$	**B17** $B_{CEMIII'.}$	**B15** $B_{CEMI\ SR3'}$	**B18** $B_{30V'}$	**B38** B_{8D}

- resistant ⇒ **+ resistant**

A good discrimination of the 10 tested materials is observed with some small modifications in the rankings. It is important to note that concretes with a matrix based on CEM I SR3 cement or chemically active additions (silica fume, fly ash and blast furnace slag) show a very good behaviour which is very often emphasized in the scientific literature (Atahan and Dikme, 2011). On the other hand, for concretes based on conventional CEM I or containing limestone filler, degradation by ettringite formation was expected at this swelling level and this behaviour is also well documented in the literature (Irassar, 2009).

3.1.9 Inter-laboratory cross-testing

3.1.9.1 Inter-lab test for Messad protocol

This paragraph presents the results of inter-laboratory cross-tests that were performed as part of PerfDuB project for the Messad accelerated test. This campaign was carried out on the basis of 3 partner laboratories (UGE, LafargeHolcim and LMDC) on a series of 12 test specimens in total for 2 study concretes (B0 and B38). For confidentiality reasons, the results have been anonymized (Lab1, Lab2 and Lab3).

Figures 1.48 and 1.49 show the results obtained respectively on concrete B0 and B38. For these 2 figures, the curves “a" are the raw results for the 12 test specimens and the curves “b” are the average curves with the standard deviations.

a.

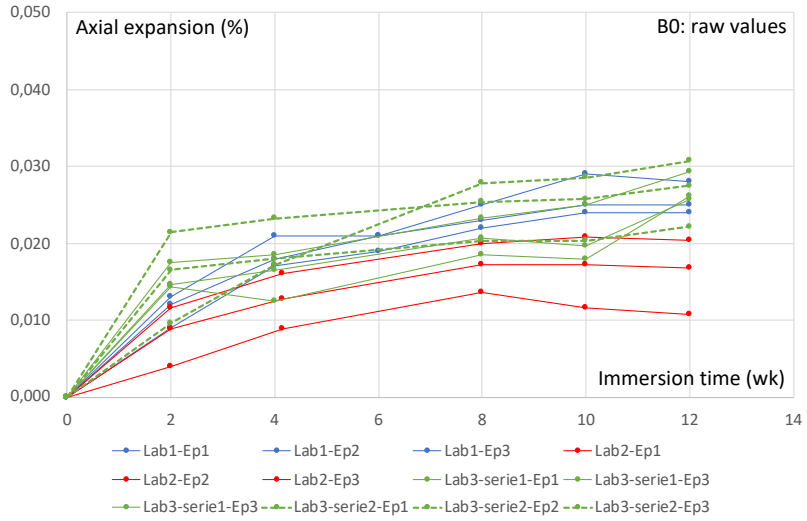

b.

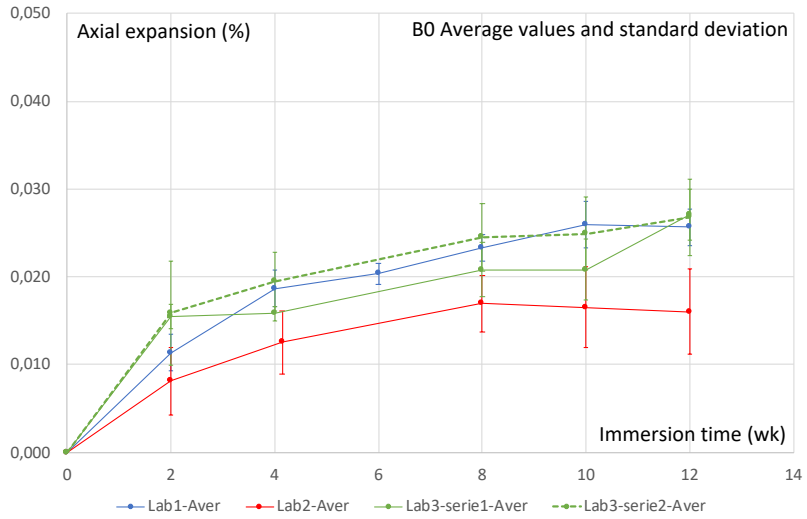

Figure 1.48. Inter-lab cross test for B0: a. Raw results b. Average curve and standard deviation

a.

b.

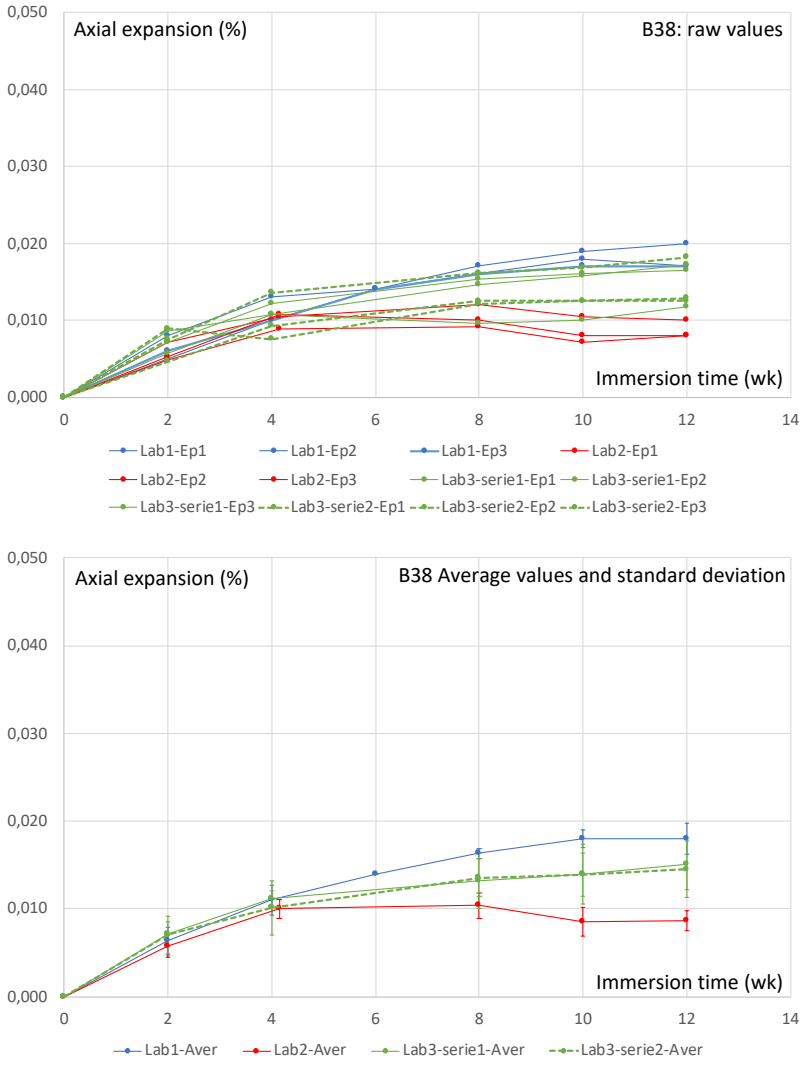

Figure 1.49. Inter-lab cross test for B38: a. Raw results b. Average curve and standard deviation

From figures 1.48 and 1.49, it is possible to draw up Table 1.22.

Table 1.22. Concrete performance value for B0 and B38 at the end of the protocol after 12 weeks of immersion

Concrete	B0	B38
Number of values	12	12
Average value (%)	0.024	0.014
Standard deviation (%)	0.006	0.004
Max value (%)	0.011	0.010
Min value (%)	0.031	0.018

3.1.9.2 Reliability for SIA method.

The test method is reliable according to:

- repeatability of 0.02 ‰;
- reproducibility depending on the level of expansion (Table 1.23).

Table 1.23. Reproducibility of the test according to the expansion level

Expansion level (‰)	Reproducibility (‰)
0.20	0.05
0.77	0.22
1.79	0.61

The reliability, reproducibility and repeatability values for the SIA test can be found in the study report "Inter-laboratory test for sulphate resistance of concrete according to SIA 262/1, Annex D, final report" (in German). (Loser, 2007)

3.1.10 Analysis and proposal of a method based on the performance approach

This section is dedicated to the analysis of all the results, which will lead to the proposal of a methodology for the performance approach of the formulation of concretes for the exposure classes XA sulphates.

3.1.10.1 Analysis of results

This paragraph will allow to evaluate the correlation that can exist between the results obtained with the "Messad" and "SIA" protocols for the same concrete and to propose a methodology based on the performance of the material according to the exposure class.

3.1.10.1.1 Correlation between "Messad" and "SIA" test results

Figure 1.50 shows the correlation between the expansions values measured with the two protocols. Two test times were chosen:

- the measurement at the end of the procedure (black point family) with 8 weeks for the SIA test and 12 weeks for the "Messad" test;
- the measurement at the halfway point of the protocol (family of red dots) with 4 weeks and 6 weeks for the SIA and "Messad" tests respectively.

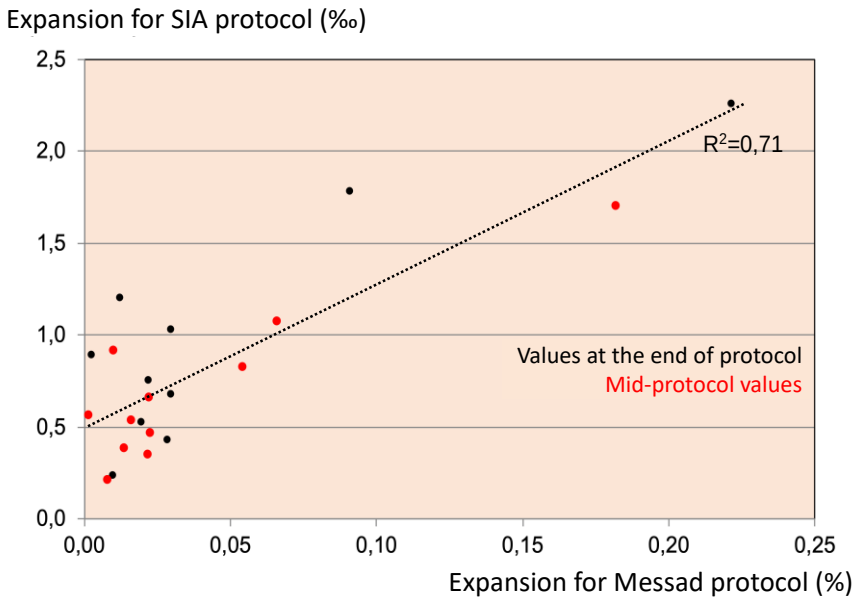

Figure 1.50. Correlation between the expansion values for the two protocols

From this figure, an average correlation is observed with an R^2 of 0.71 between the values obtained with the two protocols. It should be noted that the highly reactive concrete (B53 - B_{20L}) was removed from the population studied. Visually we note that:

- threshold of 0.012 % according to the SIA protocol corresponds to an expansion value of at least 0.08 % according to the “Messad” protocol;
- threshold of 0.05 % would correspond to an expansion of the order of 0.085 % according to the SIA protocol.

The threshold value of 0.05 % seems (legitimately) safe with the so-called "Messad" protocol for class XA3.

3.1.10.1.2 Methodology for ESA-related XA classes

There are 3 XA classes to evaluate the resistance of a concrete to an external sulphate reaction:

- XA1 - Low chemical aggression environment;
- XA2 - Environment with moderate chemical aggressiveness;
- XA3 - Environment with high chemical aggressiveness.

3.1.10.1.3 Accelerated saturation protocol (“Messad" protocol)

In order to set up a performance-based approach to the formulation of concretes for exposure classes XA sulphates, two methods are possible:

- global method using a performance threshold;
- comparative approach using a reference concrete in accordance with the normative requirements.

With the "Messad" accelerated procedure, a concrete will be qualified from the global method only for the XA3 class. To bring out this threshold, we work with two series of concretes chosen according to their conformity to the chemical exposure class (sulphate attack) XA3:

- the first series consists of concretes that comply with the requirements of class XA3. These are the materials B47 ($B_{CEMI\text{-}SR5}$), B48 ($B_{CEMI\text{-}SR3}$), B49 (B_{CEMIII}), and B50 (B_{20V});
- the second consists of materials that deviate from the requirements on the nature of the binder. These are B1 (B_{10L}), B46 (B_{CEMI}) and B53 (B_{20L}) concretes.

Figure 1.51 shows the results of the axial dimensional variations for the 7 concretes.

From this figure, a performance threshold of 0.05 % elongation after 12 weeks of immersion in the etching solution can be proposed for exposure class XA3 sulphate. It is important to note that an individual value of 0.07 % cannot be exceeded for any of the 3 specimens tested.

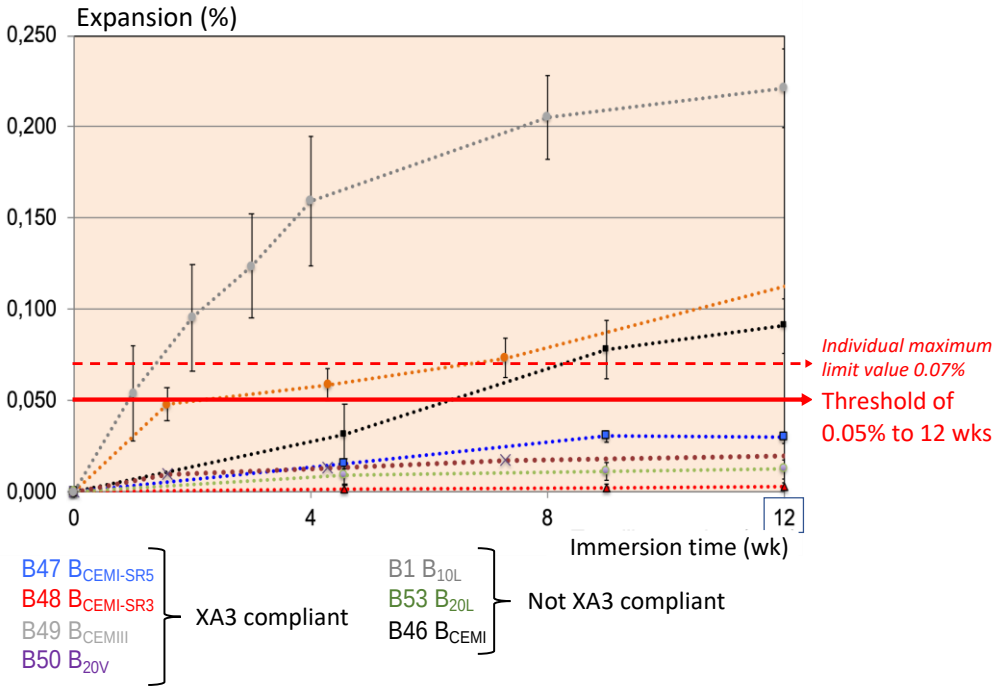

Figure 1.51. Performance threshold detection for exposure class XA3 sulphate

3.1.10.1.4 Accelerated immersion-drying protocol ("SIA" protocol)

For the SIA method used in Swiss standardization, the normative text already gives an estimated performance threshold of 1.20‰ after a complete protocol phase (4 weeks of immersion/drying + 8 weeks of total immersion). In the implemented French performance-based approach, this threshold is kept for the most severe exposure class XA3. For the two other classes, the comparative approach with a reference concrete is retained.

3.1.10.2 Methodology of the performance-based approach on XA classes

In relation to the development made previously, it appears from the WG1C-ESR study that the two accelerated protocols proposed can be retained to characterize a concrete with respect to its resistance to external sulphate reaction. The "Messad" (Option 1) and "SIA" (Option 2) accelerated tests were selected for this standardization phase. The two detailed and finalized procedures are available in the appendix.

In this methodology for evaluating a concrete mix against external sulphate attack (ESR) we can break down into two cases:

- **general case** with compliant composition criteria (L_{eq} and E_{eff}/L_{eq}) and binder not compliant with FD P18-011;
- **special case** with non-conforming composition criteria (equivalent binder B_{eq}, and W_{eff}/B_{eq} and/or non-conforming aggregates with respect to absorption) with binder conforming to FD P18-011.

It is important to note that the granular skeleton of the two concretes to be compared must be equivalent in dosage and mineralogical nature.

3.1.10.2.1 The general case

Table 1.24 presents the performance qualification criteria for the chemical attack classes XA sulphates for a DUP 50/100 years in **the general case.** It is recalled that non-compliance corresponds to the case where the binder does not comply with fascicule FD P18-011.

In the general case and for classes XA1 and XA2 sulphate, the performance approach based on the two accelerated ESR tests by comparative method to a reference concrete is retained. It is possible to choose one of the two tests (Option 1 or 2) to perform this comparison. The reference concretes must be:

- conform to the requirements of standard NF EN 206/CN or Fascicule 65;
- with a lowered W_{eff}/B_{eq} ratio of 0.05;
- with use of CEM I PM cement for class XA1 and CEM I SR3 cement for class XA2.

In the general case and for class XA3 sulphate, the performance approach based on the two accelerated ESR tests by global method with performance threshold is retained. Depending on the option chosen (one of the two tests), the axial dimensional variation of the concrete to be qualified must not exceed the threshold values given in Table 1.24 after the immersion phase in the sodium sulphate solution.

Table 1.24. Performance qualification criteria for chemical attack classes XA sulphates for a 50/100 years SLT in the general case

Exposure class	General approach (limit values)		Reference concrete
	Option 1: saturation test (Messad test	Option 2: immersion-drying test (SIA test)	
XA1	≤ Reference concrete	≤ Reference concrete	Compliant with NF EN 206/CN or F65 + W_{eff}/B_{eq} lowered by 0.05 Cement: CEM I PM
XA2	≤ Reference concrete	≤ Reference concrete	Compliant with NF EN 206/CN or F65 + W_{eff}/B_{eq} lowered by 0.05 Cement: CEM I SR3
XA3	0.05 % at 12 weeks (0.07 % max on individual values)	0.12 % to 8 weeks total immersion	

3.1.10.3 The special case

Table 1.25 presents the performance qualification criteria for the chemical attack classes XA sulphates for a SLT 50/100 years in the special case. It should be remembered that the special case represents a case where the composition criteria are not compliant (Beq and Weff/Beq, aggregate not compliant on water absorption) but with a binder compliant with Fascicule FD P18-011.

In this particular case and whatever the sulphate exposure class, the performance approach based on the Cl^- ion migration test$^-$ ($D_{rcm\ 90d}$) by a comparative method to a reference concrete is retained. The reference concrete must be:

- conform to the requirements of standard NF EN 206/CN or Fascicule 65;
- with a lowered W_{eff}/B_{eq} ratio of 0.05;
- with use of CEM I PM cement for class XA1, CEM I SR3 cement for classes XA2 and XA3.

Table 1.25. Performance qualification criteria for chemical attack classes XA sulphates for a 50/100 years SLT in the **special case**

Exposure class	Comparative approach	
	$D_{rcm\ 90d}$	Reference concrete
XA1	≤ Reference concrete	Compliant with NF EN 206/CN or F65 + W_{eff}/B_{eq} lowered by 0.05 Cement: CEM I PM
XA2	≤ Reference concrete	Compliant with NF EN 206/CN or F65 + W_{eff}/B_{eq} lowered by 0.05 Cement: CEM I SR3
XA3	≤ Reference concrete	Compliant with NF EN 206/CN or F65 + W_{eff}/B_{eq} lowered by 0.05 Cement: CEM I SR3

3.1.11 Conclusions

This "External Sulphate Attack" study (ESA) carried out within the framework of the PerfDuB National Project is part of a more global study aiming at developing accelerated aging tests (ESR, Leaching and Biodegradation). Based on the discussions within the WG1C "External Chemical Attacks", two test protocols were proposed and validated by the Scientific and Technical Committee:

- refinement of the ESR test proposed by (Messad, 2009);
- alternative test according to the Swiss standard (SIA262, 2013-2019).

This synthesis is part of a joint multi-partner study: Armines Alès and Douai, IFSTTAR then University Gustave Eiffel Champs/Marne, GEM Nantes, Lafarge-Holcim St Quentin Fallavier, LGCGM Rennes, LMDC Toulouse.

The work in stage 1 made it possible to refine the test parameters (sample sizes, maintenance of pH, test duration, activity of the solution, etc.).

Stages 2 and 3 were used to test a series of materials developed within the framework of WG3A "Concrete to be studied". This experimental campaign made it possible to widen the range of concretes tested. The inter-laboratory cross-testing phase is underway, which will allow the methodology to be completed with more complete fidelity data.

Stage 4 focused on the overall analysis of results and the contracting of a performance-based method for the XA sulphate classes:

- for class XA3, a threshold criterion was established for the two validated procedures;
- for classes XA1 and XA2, the comparative method with a reference concrete will be preferred.

3.2 Leaching

3.2.1 Abstract

The development of a leaching test provides a tool for evaluating the performance of a concrete regarding chemical attacks associated with the presence of acids whose calcium salts are soluble or weakly mineralized water, as defined in standard NF EN 206/CN and in fascicle FD P 18-011.

The works summarized in this report are those which have been conducted about leaching in the Working Group WG1C of the PerfDuB Project. The works were carried out successively in three phases: phase 1, phase 2 and phase 4 (no work in phase 3).

The work presented in this report complements that already carried out within the "leaching" working group of the French standardization expert group GEF 8. At the end of the PerfDuB project, this same GEF 8 will be able to resume its work on leaching and benefit from new results.

3.2.2 Principle of the test

The test consists of immersing a concrete test specimen in a chemically aggressive solution, monitoring the leaching of calcium over time and evaluating its degradation at the end of the test.

The concrete test specimen is immersed in a solution of demineralized water and nitric acid. The pH of the solution depends on the exposure class chosen:

- pH = 5.5 ± 0.1 for class XA1;
- pH = 4.5 ± 0.1 for class XA2;
- pH = 4.0 ± 0.1 for class XA3.

Two methods of leaching at constant pH are proposed:

- one with periodic renewals of the acid solution (also called "constant pH leaching");
- other with continuous renewal of the acid solution (also called "leachcrete").

The degraded thickness is measured from the amount of calcium leached (passed into solution). The result of the test is the indicator I_{Ca}, which is the ratio of leached calcium to the total calcium initially present in the concrete.

The following figures illustrate the two variants of the test.

Figure 1.52 Picture of the set-up of the periodic leaching test

Figure 1.53. Picture of continuous leaching test setup

3.2.3 Stage 1 - improving test protocols

The aim of the work that was carried out during phase 1 was to improve the pre-existing procedures and then to check that these improved procedures were indeed discriminating on siliceous limestone aggregate-based concretes in condition XA1 (the most moderate attack condition).

In the case of the periodic renewal procedure, the exposed concrete surface was doubled, and two study parameters were tested (reduction of the pH by half a unit and increase of the test temperature by 10 °C). Six laboratories participated in the tests on phase 1 (CEA, CERIB, EDF, LERM, LMDC, Armines).

For the continuous renewal mode, two laboratories participated in the tests (Calcia, Vicat).

3.2.3.1 Results

Table 1.26 presents the concretes B44 and B45 that were tested in phase 1. When the leaching tests were initiated, the B44 concrete was at least 28 days old and the B45 concrete was at least 90 days old.

Table 1.26. Concretes tested in phase 1

	B44	**B45**
Composition of the concrete		
Type of cement	CEM I	CEM V
Cement content (kg/m^3)	330	330
Nature of aggregates	siliceous limestone	siliceous limestone
Effective ratio water / cement	0.55	0.55
Concrete characteristics		
Compressive strength at 28 days (MPa)	39.0	46.4
Compressive strength at 90 days (MPa)	-	60.8
Porosity according to NF P 18-459 (%)	17.1	18.6
Density according to NF P 18-459 (kg/m^3)	2150	2150
Calcium content by mass Ca (%)	31.7	30.9
Initial calcium (g/m^3)	681 550	664 350
Initial calcium (mol/m^3)	17 005	16 576

Table 1.27 shows the results of the leaching tests.

Table 1.27. Results of leaching tests of phase 1

		B44	B45
Leaching periodic renewals pH = 5.5, T = 20 °C			
Lab 1.1	I_{Ca} 28 days (mm)	0.15	0.07
	I_{Ca} 60 days (mm)	0.22	0.11
	I_{Ca} 120 days (mm)	0.33	0.18
	EPDpH 120 days (mm)	0.62	0.71
	Acid volume 120 days (ml)	778	463
Lab 1.2	I_{Ca} 28 days (mm)	0.14	0.08
	I_{Ca} 60 days (mm)	0.22	0.12
	I_{Ca} 120 days (mm)	0.35	0.21
	EPDpH 120 days (mm)	0.76	0.69
	Acid volume 120 days (ml)	861	502
Leaching periodic renewals pH = 5.0, T = 20 °C			
Lab 1.3	I_{Ca} 28 days (mm)	0.11	0.08
	I_{Ca} 60 days (mm)	0.20	0.14
	I_{Ca} 120 days (mm)	0.32	0.22
	EPDpH 120 days (mm)	1.20	0.77
	Acid volume 120 days (ml)	646	403
Lab 1.4	I_{Ca} 28 days (mm)	0.15	0.08
	I_{Ca} 60 days (mm)	0.23	0.14
	I_{Ca} 120 days (mm)	0.35	0.23
	EPDpH 120 days (mm)	1.21	0.86
	Acid volume 120 days (ml)	1078	766
Leaching periodic renewals pH = 5.5, T = 30 °C			
Lab 1.5	I_{Ca} 28 days (mm)	0.20	0.12
	I_{Ca} 60 days (mm)	0.35	0.20
	I_{Ca} 120 days (mm)	0.53	0.32
	EPDpH 120 days (mm)	1.00	0.97
	Acid volume 120 days (ml)	1125	652
Lab 1.6	I_{Ca} 28 days (mm)	0.18	0.11
	I_{Ca} 60 days (mm)	0.30	0.14
	I_{Ca} 120 days (mm)	0.40	0.25
	EPDpH 120 days (mm)	1.63	1.06
	Acid volume 120 days (ml)	872	594

		B44	B45
Continuous renewal leaching pH = 5.0, T = 40 °C			
Lab 1.7	Calcium leached at 32 days (g/m²)	155.7	143.3
	Leached Ca flux 32 days (g/m²/h$^{1/2}$)	6.4	5.1
	I_{Ca} 32 days (mm)	0.23	0.22
	SEM degraded thickness 32 days (µm)	1000	500
Lab 1.8	Calcium leached at 36 days (g/m²)	147.9	108.1
	Leached Ca flux 36 days (g/m²/h$^{1/2}$)	6.3	4.4
	I_{Ca} 36 days (mm)	0.22	0.16
	SEM degraded thickness 32 days (µm)	1000	600

3.2.3.2 Conclusion of stage 1

3.2.3.2.1 Periodic leaching method

The tests consisted of a parametric study, aimed at accelerating the leaching test and making it even more precise and discriminating, especially for XA1 concretes with limestone aggregates. Six laboratories participated in the tests, which tested two concretes (one based on CEM I cement, the other on CEM V cement) and 3 variants of the test.

The main findings were as follows:

- the I_{Ca} indicator (at 60 days and 120 days), based on leached calcium dosages, is reliable and discriminating;
- the search for the best compromise for a representative, reliable, discriminating, and accelerated test led to the selection of the 60-days constant pH leaching test performed at a temperature of 30 °C with the I_{Ca} indicator.

3.2.3.2.2 Continuous leaching method

The continuous renewal test is a discriminating and reproducible accelerated test.

At this stage, it is important to note that the leaching test should be a comparative test between concretes of the same quality and with the same granular skeleton.

3.2.4 Stage 2 – Tests on WG3 concretes

The work in phase 2 consisted of carrying out the leaching tests on limestone aggregate-based concretes: one concrete was tested for exposure class XA2 and two concretes for class XA3.

In the case of the periodic renewal procedure, six laboratories participated in the tests (Armines, CEA, CERIB, EDF, LERM, LMDC). Test fidelity data could be determined.

For the continuous renewal mode, one laboratory participated in the tests (Vicat).

3.2.4.1 Results

Table 1.28 shows the concretes B20, B36 and B37 that were tested in phase 2. The concretes were at least 90 days old at the start of the tests.

Table 1.28. Concretes tested in phase 2

	B20	B36	B37
Composition of the concrete			
Type of cement	CEM II/A-S	CEM V/A	CEM V/A
Cement content (kg/m^3)	350	370	370
Nature of aggregates	Limestone G4 (WA_{24}=4 %)	Limestone G4 (WA_{24} = 4 %)	Limestone G3 (WA_{24} = 0.5 %)
Effective ratio water / cement	0.50	0.45	0.45
Characteristics of the concrete			
Compressive strength at 28 days (MPa)	58.8	49.2	55.8
Compressive strength at 90 days (MPa)	67.6	55.2	72.4
Density according to NF P 18-459 (kg/m^3)	2170	2140	2330
Mass content of calcium Ca (%)	35.5	33.6	34.6

Table 1.29 shows the leaching tests results for B20 concrete.

Table 1.29. Results obtained on B20 concrete

		B20
Leaching periodic renewals pH = 4.5, T = 30 °C		
Lab 2.1	I_{Ca} 60 days (mm)	0.53
Lab 2.2		0.37
Lab 2.3		0.35
Lab 2.4		0.42
Lab 2.5		0.31
Lab 2.6		0.54
Average		0.42
Standard deviation		0.09
Coef. of variation		23 %
Continuous renewal leaching pH = 4.5, T = 40 °C		
Lab 2.7	Calcium leached at 44 days (g/m^2)	220
	I_{Ca} 44 days (mm)	0.29
	SEM degraded thickness 44 days (mm)	0.75
	I_{Ca} extrapolated to 60 days (mm)	0.34

For the periodic leaching test, fidelity data was determined: the standard deviation under reproducibility conditions (inter-lab) was evaluated at 0.09 mm, i.e., a coefficient of variation of 23 %. It should be noted that during a previous GEF 8 test campaign, fidelity data under repeatability conditions (intra-lab) were defined: standard deviation of 0.05 mm and a coefficient of variation of 11 %.

In the case of concretes based on acid-sensible aggregates (limestone), it should be noted that the evolution of leached calcium (and therefore of the indicator I_{Ca}) as a function of the

square root of time is not entirely linear and therefore that the kinetic is not entirely diffusional (see Figure 1.54). The kinetic is the result of a diffusion (cement paste) and dissolution (limestone aggregates) component. It was observed that the limestone aggregates were slightly dug at the end of the test compared to the level of the cement matrix. The same trends were observed for the other two concretes.

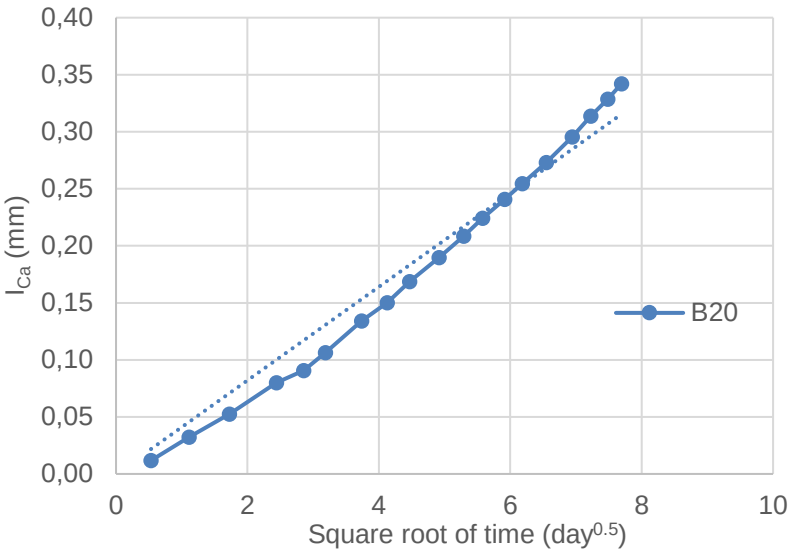

Figure 1.54. Evolution of the I_{Ca} indicator as a function of the square root of time

Table 1.30 presents the leaching test results obtained on concretes B36 and B37.

Table 1.30. Results obtained on B36 and B37 concretes

		B36	B37
Leaching periodic renewals pH = 4.0, T = 30 °C			
Lab 2.1	I_{Ca} 60 days (mm)	-	0.65
Lab 2.2		0.43	-
Lab 2.3		0.45	-
Lab 2.4		-	0.35
Lab 2.5		-	0.41
Lab 2.6		0.55	-
Average		0.47	0.47
Continuous renewal leaching pH = 4.0, T = 40 °C			
Lab 2.7	Calcium leached at 46 days (g/m^2)	189	-
	I_{Ca} 46 days (mm)	0.26	-
	Degraded paste thickness SEM 46 days (mm)	0.47	-
	I_{Ca} extrapolated to 60 days (mm)	0.31	-

The concretes B36 and B37 have very similar formulations (same cement, same dosages), only the characteristics of the limestone aggregates are different (water absorption in particular). Although no laboratory has tested both concretes simultaneously, it can be noticed that the measured performances of both concretes are very close.

3.2.4.2 Conclusion of stage 2

The work in phase 2 consisted of implementing the test procedures previously defined in phase 1 on several limestone aggregate concretes. The results of the two procedures are comparable under these conditions.

Thus, it was possible to show that the test, when used in a comparative approach, allows the performance of concretes of exposure classes XA1, XA2, XA3 to be evaluated. In addition, it was possible to measure the fidelity of the test.

3.2.5 Stage 4 - Harmonisation of the 2 protocols

The work in phase 4 consisted of carrying out leaching tests on different types of concrete: alluvial or limestone aggregates, cement-based binders CEM I, CEM III/A or CEM V/A.

The objectives of the work in phase 4 were to:

- get closer both variants of the test "periodic leaching" and "continuous leaching";
- add the results to the database.

Only one laboratory performed the periodic renewal procedure (CERIB), two laboratories participated in the tests with the continuous renewal procedure (Vicat, Technodes).

3.2.5.1 Results

Table 1.31 shows the concretes B1, B4, B35. The concretes B20 and B36 were also tested in phase 4 and have already been presented in Table 1.28. The age of the concretes was greater than 90 days when the tests were started.

For this test campaign, the operating conditions for the continuous renewal method were the same as for the periodic renewal method (same pH, same temperature of 30 °C, same duration).

Table 1.31. Concretes tested during phase 4

	B1	**B4**	**B35**
Composition of the concrete			
Nature of the binder (and dosage in kg/m^3)	CEM I (280) + limestone (50)	CEM III/A (280) + limestone (50)	CEM V/A (380)
Nature of aggregates	Alluvial Silica-limestone G2	Alluvial Silica-limestone G2	Alluvial G1
Ratio effective water / cement	0.58	0.60	0.45
Ratio effective water / total binder	0.49	0.51	0.45
Characteristics of the concrete			
Compressive strength at 28 days (MPa)	43.7	37.2	65.5
Density according to NF P 18-459 (kg/m^3)	2150	2130	2230
Mass content of calcium Ca (%)	25.2	24.7	15.5

Table 1.32 shows the leaching results obtained on B1 and B4 concretes.

For Lab 4.3, due to the covid-19 health crisis, only B1 concrete was tested, and the test had to be stopped after 20 days (instead of 60 days).

Table 1.32. Results obtained on B1 and B4 concretes

		B1	B4
Leaching periodic renewals pH = 4.0, T = 30 °C			
Lab 4.1	I_{Ca} 60 days (mm)	0.39	0.29
Leaching continuous renewal pH = 4.0, T = 30 °C			
Lab 4.2	I_{Ca} 60 days (mm)	0.11	0.10
Lab 4.3	I_{Ca} 20 days (mm)	0.23	-

Table 1.33 shows the results for B20, B35 and B36.

Table 1.33. Results obtained on B20, B35 and B36 concretes

		B20	B35	B36
Leaching periodic renewals pH = 4.0, T = 30 °C				
Lab 4.1	I_{Ca} 60 days (mm)	-	0.34	0.39
Leaching continuous renewal pH = 4.0, T = 30 °C				
Lab 4.2	I_{Ca} 60 days (mm)	-	0.14	0.09
Leaching continuous renewal pH = 4.5, T = 30 °C				
Lab 4.2	I_{Ca} 60 days (mm)	0.06	-	-

In continuous renewal with a temperature of 30 °C, the result on concrete B20 (0.06 mm) is significantly lower than with a temperature of 40 °C (0.34 mm in section 2). Similarly, the results on B1, B4, B35 and B36 in continuous renewal with a temperature of 30 °C are significantly lower than the results obtained in periodic renewals with the same temperature of 30 °C.

Regarding the results obtained in the periodic renewal tests, it can be noticed that B4 concrete (based on CEM III/A) is more resistant to acid attack than B1 concrete (based on CEM I). B35 concrete has a similar but slightly better acid attack resistance than B36 concrete.

It should also be noted that the same B36 concrete had been tested by the same laboratory in the works of phase 2 approximately 18 months earlier (Lab 2.3). The I_{Ca} indicator measured was 0.45 mm. The leaching resistance of the B36 concrete therefore seems to have improved over time (0.39 mm in phase 4).

Overall, the leaching behaviour of the different concretes is closer than expected. It seems difficult to compare the behaviour of concretes with different paste volumes, different binder types and different aggregates.

3.2.5.2 Conclusion of stage 4

The work in phase 4 consisted of carrying out leaching tests on concretes of different natures: alluvial or calcareous aggregates, cement-based binders CEM I, CEM III/A or CEM V/A.

The work led to the following conclusions:

- the best consistency of both procedures is obtained for the periodic renewal test at 30 °C and the continuous renewal test at 40 °C;
- the French standardization group GEF 8 will be able to use the results obtained to draft an experimental standard;

- at this stage, the leaching test should be used in comparison with a reference concrete. The concretes compared should have the same volume of paste and identical granular skeleton.

3.2.6 Conclusion of the experimental study

The development of a leaching test provides a tool for evaluating the performance of a concrete regarding chemical attacks associated with the presence of acids whose calcium salts are soluble or weakly mineralized water, as defined in standard NF EN 206/CN and in fascicle FD P 18-011.

The experimental work consisted of carrying out leaching tests on different types of concrete: alluvial or limestone aggregates, binder based on cement CEM I or CEM III/A or CEM V/A.

The constant pH leaching test was developed with two variants: one is performed at a temperature of 30 °C with periodic renewals of the test solution, the other is performed at 40 °C with continuous renewal of the test solution. The results of the two variants are consistent.

It has been demonstrated that the test is representative, reliable, discriminating and accelerated. When used in a comparative approach, it allows the performance of concretes of exposure class XA1, XA2, XA3 to be evaluated. In addition, test fidelity data have been determined.

The French standardization group GEF 8 will be able to use the results to draft an experimental standard.

At this stage, the leaching test should be used in comparison with a reference concrete. The compared concretes should have the same volume of paste and an identical granular skeleton.

3.2.7 Proposal for a method based on the XA leaching performance approach

In the case of validation against leaching (as in all cases), the reference concrete must comply:

- for a project service life of 50 years, with the requirements of appendix NA.F of standard NF EN 206/CN;
- for a project service life of 100 years, with the requirements of article 8.1.1.3 of fascicule 65 of the CCTG.

The reference concrete and the concrete to be qualified must be of the same consistency class. In addition, as in the case of ESA, a distinction is made between:

- the general case with compliant composition criteria (L_{eq} and E_{eff}/L_{eq}) and binder non-compliant with FD P18-011;
- the particular case with non-compliant composition criteria (L_{eq}, E_{eff}/L_{eq} and aggregates non-compliant with regard to absorption) and a binder complying with fascicule FD P18-011.

The general and specific cases are explained in paragraphs 3.2.7.1 and 3.2.7.2. In addition, it is important to specify that, in view of the sensitivity of leaching tests at constant pH, the volume of the reference concrete paste must be equivalent to that of the concrete to be qualified.

3.2.7.1 General case

For acid environments and pure water, the performance thresholds given in Table 1.34.

Table 1.34. XA Leaching Classes: criteria applicable to acid environments and pure water

Exposure class	I_{Ca}	Reference concrete	
		Cement	Paste volume fraction f_{vp} Granular skeleton (dosage and nature)
XA1	≤ I_{Ca} of the reference concrete	CEM II/B-S or CEM III/A	Equivalent to that of the concrete to be qualified
XA2	≤ I_{Ca} of the reference concrete	CEM II/B-S or CEM III/A	Equivalent to that of the concrete to be qualified
XA3	≤ I_{Ca} of the reference concrete	CEM V/A ES	Equivalent to that of the concrete to be qualified

Due to the particularity of the procedure, it is specified that the proposed comparative approach is not applicable as it stands if the binder of the concrete to be qualified includes limestone (as a limestone addition or as the main constituent of the cement) insofar as, by definition, the binder of the reference concrete does not include it.

3.2.7.2 Special case

In the case where the derogation(s) from the prescriptive approach do not concern the nature of the binder (the binder complies with the requirements of documentation fascicule FD P18-011), it is possible alternatively to justify the concrete to be qualified by complying with the criteria in Table 1.35.

Table 1.35. XA Leaching Classes: criteria applicable to acid environments and pure water

Exposure class	$D_{rcm\ 90d}$	Cement of the reference concrete
XA1	≤ $D_{rcm\ 90d}$ of the reference concrete	CEM II/B-S or CEM III/A
XA2	≤ $D_{rcm\ 90d}$ of the reference concrete	CEM II/B-S or CEM III/A
XA3	≤ $D_{rcm\ 90d}$ of the reference concrete	CEM V/A ES

3.3 Biodegradation

3.3.1 Introduction

3.3.1.1 Background of the study

In sewage networks, the deterioration of cementitious materials is mainly linked to the production of hydrogen sulphide (H_2S) in stagnant zones, its volatilisation and condensation at the top of the pipes. Different oxidation reactions of the sulphur species, first of chemical origin and then of biological origin, lead to the final formation of sulphuric acid on the surface of the cementitious material. Biological activity, developing successively on a local scale (sulfo-oxidising microorganisms), is a key factor in such deterioration.

Several studies have shown that strictly chemical tests - using sulphuric acid - are not satisfactory to qualify cementitious materials and products in sewage systems (results show differences in performance of cementitious materials between these chemical tests and *in situ* tests). In this context, various biological laboratory tests involving microbial transformations of sulphur have been developed over the last decades to quantify the resistance of these materials.

3.3.1.2 Partners

Two experienced partners participated in the biodegradation tests: the University Gustave Eiffel (UGE) and the “Laboratoire Matériaux et Durabilité des Constructions” (LMDC Toulouse).

Two tests have been developed in France in recent years:

- a system in a closed chamber with a H_2S supply, by UGE;
- a run-off system of a soluble form of reduced sulphur, called BAC Test, by INSA Toulouse (TBI and LMDC laboratories).

3.3.1.3 Objectives of the study

The objectives of the studies conducted during the 3 phases of the PerfDuB project were to:

- assess the representativeness (with regard to deterioration observed in situ, based on literature results and expected material performance) and reproducibility/repeatability of the tests;
- determine the criteria for evaluating the strength of cementitious materials;
- optimise the test parameters;
- compare the alteration kinetics induced by the two tests.

3.3.2 Structure of the experimental campaign

3.3.2.1 Partners

Two partners participated in the tests: UGE and LMDC-TBI.

UGE developed a test in the presence of H_2S and LMDC and TBI laboratories developed a test in the presence of another source of sulphur, the tetrathionate.

3.3.2.2 Organisation

The test campaigns focused on the adjustment of the test methods and their representativeness, with three test campaigns:

- Stage 1: Adjustment of test parameters for the two tests (impact of H_2S pre-treatment, H_2S content, end-of-life criteria);
- Stage 2: Impact of C_3A content and nature of aggregates;
- Stage 3: Repeatability of tests carried out in stages 1 and 2.

3.3.3 Study materials

The tests were carried out on mortars.

3.3.3.1 In stage 1

3 mortar formulations were carried out based on standardised silica sand (EN196-1) and 3 different cements:

- CEM III/ A 52.5 N, Rombas plant;
- CEM V/A (S-V) 42.5 N CE PM-ES-CP1 NF "PMF3", Airvault plant;
- Calcium aluminate cement, Calcoat® RG, Fos-sur-Mer plant.

3.3.3.2 In stage 2

Two cements with different C_3A contents were used:

- CEM I 52.5N SR 3 CE PM CP2 NF, Val d'Azergues plant, containing 1 % C_3A;
- CEM I 52.5N CE CP2 NF, Lumbres plant, containing 8.6 % C_3A.

Two different types of sand were used:

- G1 aggregates (0/4 All SC, alluvial; semi-crushed);
- G4 aggregate (Sand 0/4 Limestone, crushed).

The different mortars produced in stage 2 are shown in Table 1.36.

Table 1.36. Characteristics of the mortars studied in stage 2

	C_3A content (%)	Cement	Nature of the aggregates	Aggregates
Mortar M1	8.6	Lumbres	Siliceous	G1
Mortar M2	1.0	Val d'Azergues	Siliceous	G1
Mortar M3	1.0	Val d'Azergues	Limestone	G4

3.3.3.3 In stage 3

Five mortar formulations were made with 5 different cements (Table 1.37):

- CEM I 52.5N-SR 3 CE PM-CP2 NF, Val d'Azergues plant, containing 1 % C_3A;
- CEM I 52.5N CE CP2 NF, Lumbres plant, containing 8.6 % C_3A;
- CEM III/ A 52.5 N cement, Rombas plant;
- CEM V/A (S-V) 42.5N CE PM-ES-CP1 NF "PMF3", Airvault plant;
- Calcium aluminate cement, Calcoat® RG, Fos-sur-Mer plant.

Table 1.37. Characteristics of the mortars studied

Reference	Cement	Sand
CEM I low C_3A content	CEM I, Val d'Azergues	Siliceous G1 (0/4 All SC, alluvial; semi-crushed)
CEM I	CEM I, Lumbres	Siliceous G1 (0/4 All SC, alluvial; semi-crushed)
CEM III	CEM III/A, Rombas	Standard silica sand EN 196-1
CEM V	CEM V/A, Airvault	Standard silica sand EN 196-1
CAC	Calcoat, Fos sur Mer	Standard silica sand EN 196-1

For the 3 phases of the project, the ratios of water to cement and sand to cement are 0.4 and 3 respectively. The 4 cm x 4 cm x 16 cm specimens were made, then demoulded after 24 h and stored in sealed plastic bags at 20 ± 2 °C for 28 days. No specimens were heat cured.

The samples were then sawn into 4 cm x 2 cm x 8 cm for the LMDC-TBI tests and 2 cm x 2 cm x 2 cm for the UGE tests.

3.3.4 Biodegradation protocols

Two test methods were investigated in this study. Both methods use a bacterial consortium derived from activated sludge from wastewater treatment plants. The main difference between the two tests is the source of sulphur. The UGE test uses H_2S while the LMDC-TBI test uses tetrathionate. The physical characteristics of these two compounds differ, making the two tests distinct.

3.3.4.1 Activated sludge activity study

Activated sludge is taken directly from a sewage treatment tank and corresponds to the sludge recovered at the outlet of the clarifier during the biological treatment of wastewater (activated sludge process in an aeration tank and then in the clarifier for decantation).

This sludge is composed of microorganism's representative of the microbial population present in sewage systems, and more particularly it has several consortia of sulpho-oxidising microorganisms that produce sulphuric acid.

The concentration of activated sludge chosen for the activity test is 2.25 g per litre of nutrient medium. The tests are performed in a bioreactor.

After centrifuging 100 ml of a water + activated sludge mixture for 10 minutes at 3000 g and 5 °C, a pellet of 2.25 g of activated sludge is recovered and introduced into 1 L of a nutrient solution (0.25 g calcium chloride, 0.4 g magnesium chloride and 1.4 g ammonium chloride) at pH = 5.

The nutrient solution is used to ensure the growth of the sulpho-oxidising microorganisms in the activated sludge.

20 mL thiosulphate solution at a concentration of 4.10^{-3} molS/L is added to the reactor.

3.3.4.2 Biodegradation protocol in the presence of H_2S

3.3.4.2.1 Pre-treatment of samples with H_2S at 100 ppm

This step consists of exposing the mortars only to gaseous H_2S without the intervention of microorganisms. In particular, it allows the surface pH of the mortars to be lowered abiotically to a pH suitable for microbial development.

Hydrogen sulphide is produced chemically inside the chamber. A solution of Na_2S (0.26 mol/l) and a solution of HCl (1.4 mol/l) are simultaneously injected via two peristaltic pumps. The reaction between these two chemicals leads to the formation of aqueous hydrogen sulphide (Equ. 1.6).

$$Na_2S + 2\ HCl \rightarrow H_2S + 2\ NaCl \qquad \text{(Equ. 1.6)}$$

An air injector allows air to be blown continuously into the solution, resulting in the release of hydrogen sulphide gas throughout the cell. Moreover, this air injection provides favourable conditions for the aerobic bacteria involved in the biodeterioration mechanism.

For the pre-treatment stage, the H_2S concentration must be maintained at 100 ppm for a fortnight. The temperature maintained in the chamber is 30 ± 1 °C. The relative humidity is 100 %.

A sensor, continuously measuring the H_2S concentration and temperature, and a zinc acetate solution are placed in series at the outlet of the cell (Figure 1.55). The zinc acetate solution ensures safety in the laboratory by trapping the excess H_2S generated in the cell by the precipitation of the ZnS compound (Equ. 1.7).

$$H_2S + ZnC_4H_6O_4 \rightarrow ZnS + C_4H_8O_4 \qquad \text{(Equ. 1.7)}$$

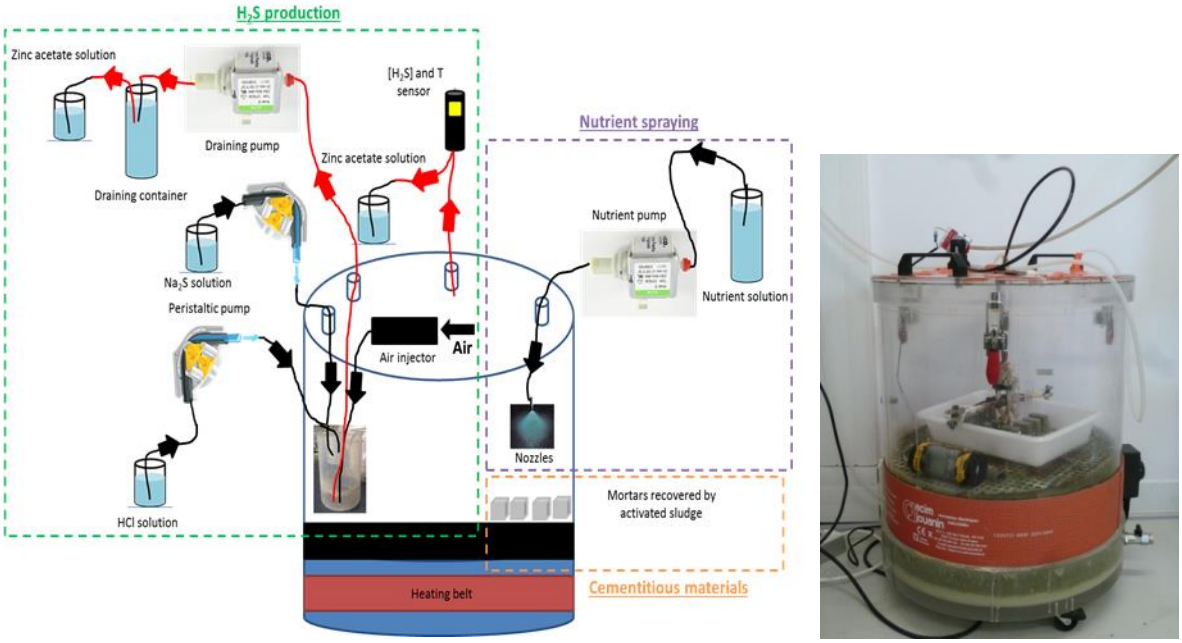

Figure 1.55. Biodeterioration chamber of UGE

3.3.4.2.2 Sludge spreading on materials

After checking the sludge, it is centrifuged at 3000 g for 20 minutes, the pellet is then spread on the surface of the mortar samples. Approximately 240 mg of slurry per 2 cm x 2 cm x 2 cm cube is spread over all the faces of the samples.

3.3.4.2.3 Biodeterioration assay

After the pre-treatment and sludge spreading phase, the mortars are placed in the chambers under controlled conditions. The temperature and relative humidity are always set at 30 °C and 100 % respectively. The H_2S concentrations are fixed.

A nutrient solution is sprayed to keep the microorganisms in the activated sludge alive. This solution contains 0,25 g/L of $CaCl_2.2H_2O$, 0,4 g/L of $MgCl_2.2H_2O$, 1,4 g/L of NH_4Cl and 5 g/L of $Na_2S_2O_3.5H_2O$.

3.3.4.2.4 Monitored parameters

Visual monitoring is carried out on the samples. The surface pH, the mass and the geometry of the samples are measured on the three cubes per formulation.

3.3.4.3 Biodegradation protocol in the presence of tetrathionate

Figure 1.56 shows a photo of the pilot (a) and a descriptive diagram (b). The pilot, consisting of a tank keeping a feed solution at 4 °C (1), allows the surface of material coupons (8 cm x 4 cm x 2 cm), previously seeded with an activated sludge taken from a wastewater treatment plant (3), to be fed at a low flow rate controlled by peristaltic pumps (25 ml/h) (2). Before the start of the test, the material coupons are coated with an epoxy resin on all sides not exposed to the test. On both edges of the exposed surface (which corresponds to a 4 cm x 2 cm x 8 cm sample box surface) a layer of epoxy resin is applied to protect the lateral zone, allowing the initial thickness of the materials to be identified on the SEM observations.

a) Photo of BAC Test pilot

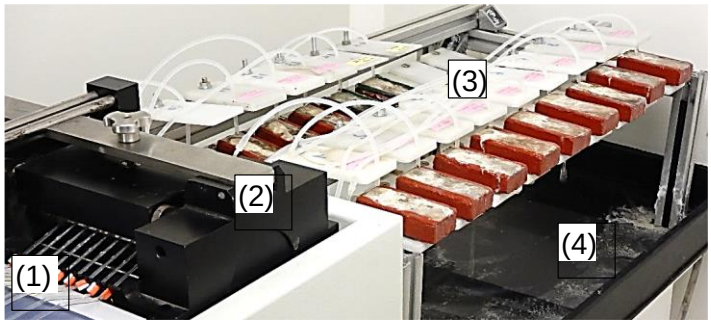

b) Descriptive diagram of BAC Test

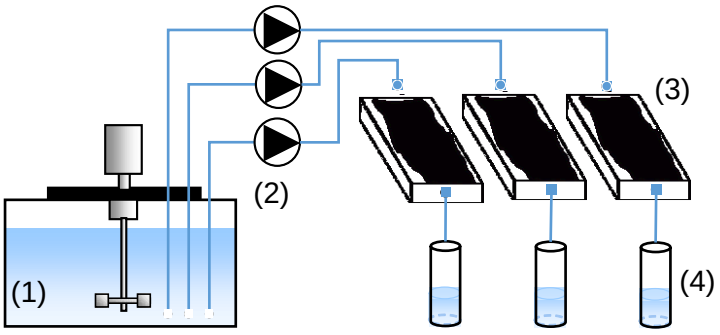

Figure 1.56. Photo and diagram describing the biodeterioration test pilot developed at INSA Toulouse

The feed solution is composed of a source of reduced sulphur (tetrathionate, an intermediate in the oxidative metabolism of reduced sulphur compounds) and sources of nitrogen, phosphorus and other mineral salts necessary for microbial growth. The leached water is collected at the outlet of the coupon (4) once a week. The flow rate of the liquid, the pH of the solution, the concentrations of calcium, sulphate, aluminium and magnesium are then measured, making it possible to evaluate the evolution of microbial activity and the reactivity

of the cement matrix. At the end of the test, SEM observations on a straight section of the material two centimetres from the edge allow the degraded depths to be assessed.

The use of a soluble source of reduced sulphur enables the work to be carried out outside the H_2S atmosphere, and to select the microorganisms on the surface of the exposed material that oxidise the reduced sulphur compounds into sulphuric acid. The pilot thus makes it possible to reproduce the microbial succession defined in a sewage network and to produce locally, by biological means, sulphuric acid in contact with a material, thus considering the influence of the microbial populations on the materials, but also the influence of the materials on the microbial populations (Peyre Lavigne *et al.*, 2015, 2016).

3.3.5 Optimisation of test method developed by UGE

3.3.5.1 H_2S content (pre-treatment and during the test)

In stage 1 of the project, the impact of H_2S content during the test, i.e. after spreading the activated slurry on the surface of the mortar samples, was tested.

Figure 1.57 shows the condition of the CEM III and CEM V based samples before exposure (t_0), and after 4 and 6 months of exposure to H_2S content of 30 or 100 ppm.

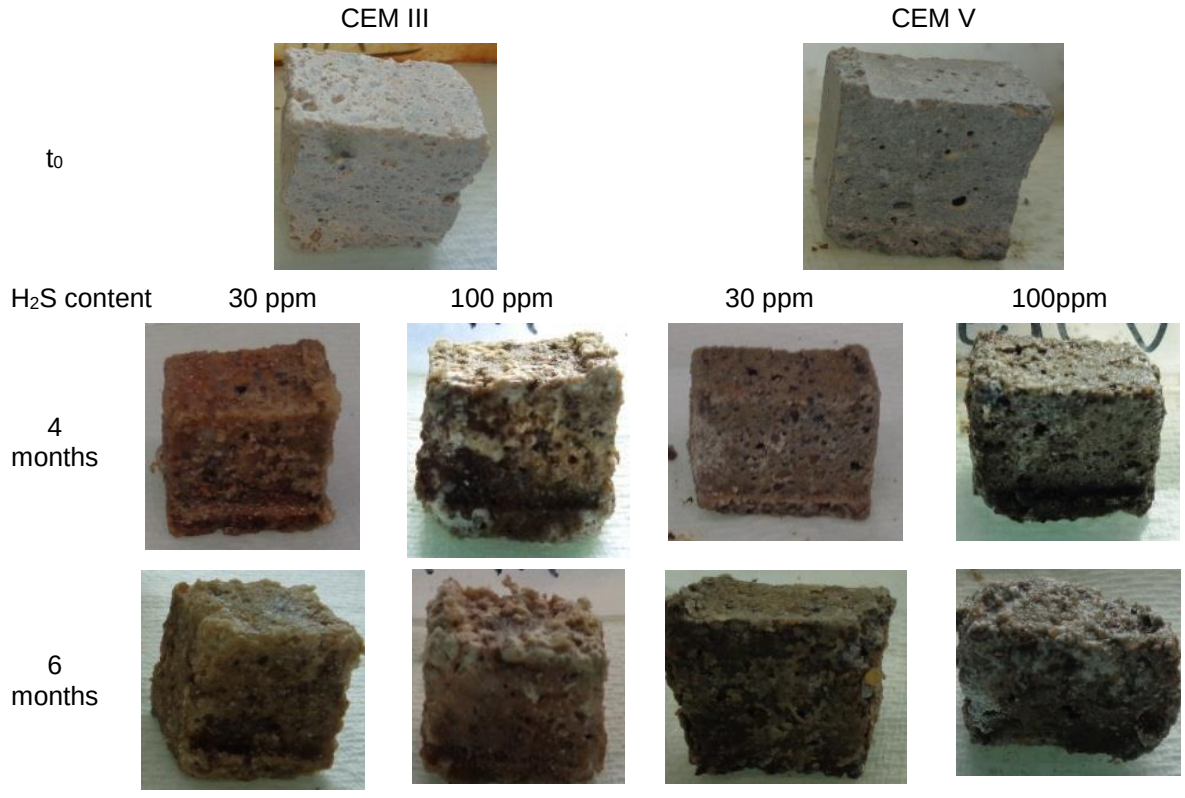

Figure 1.57. Photographs of CEM III and CEM V mortar samples exposed to 30 or 100 ppm of H_2S after 4 and 6 months of exposure

If we observe the mortar samples after 4 and 6 months of exposure in the biodegradation chamber, we can note important losses of geometry of the samples with swelling phenomena for the CEM III and CEM V samples exposed to a concentration of 100 ppm in H_2S. The degradation of samples exposed to 30 ppm is less.

Similarly, during phase 1, the impact of pre-conditioning mortars with H_2S was tested, consisting of exposing the mortar samples for 15 days to 100 ppm H_2S. After this exposure,

the activated sludge was spread on the surface of the samples and the samples were re-exposed to 30 ppm for 6 months. The samples were compared to non-pre-treated samples incubated in the same chamber with activated sludge for 6 months.

The purpose of pre-incubation is to prepare the surface of the mortars for biofilm development. One of the important parameters for a better development of the biofilm is a decrease of the surface pH. For example, if the surface pH is measured with pH paper before exposure to the pre-treatment of CEM III and CEM V samples and afterwards, it drops by 3 pH units from an initial pH of 10 to a pH of 7. This drop in pH will allow the microorganisms present in the sludge to develop better.

If we observe the state of the CEM III and CEM V samples after 4 and 6 months of exposure to 30 ppm, we can see that the pre-treated CEM V sample after 6 months of exposure is very degraded (Figure 1.58).

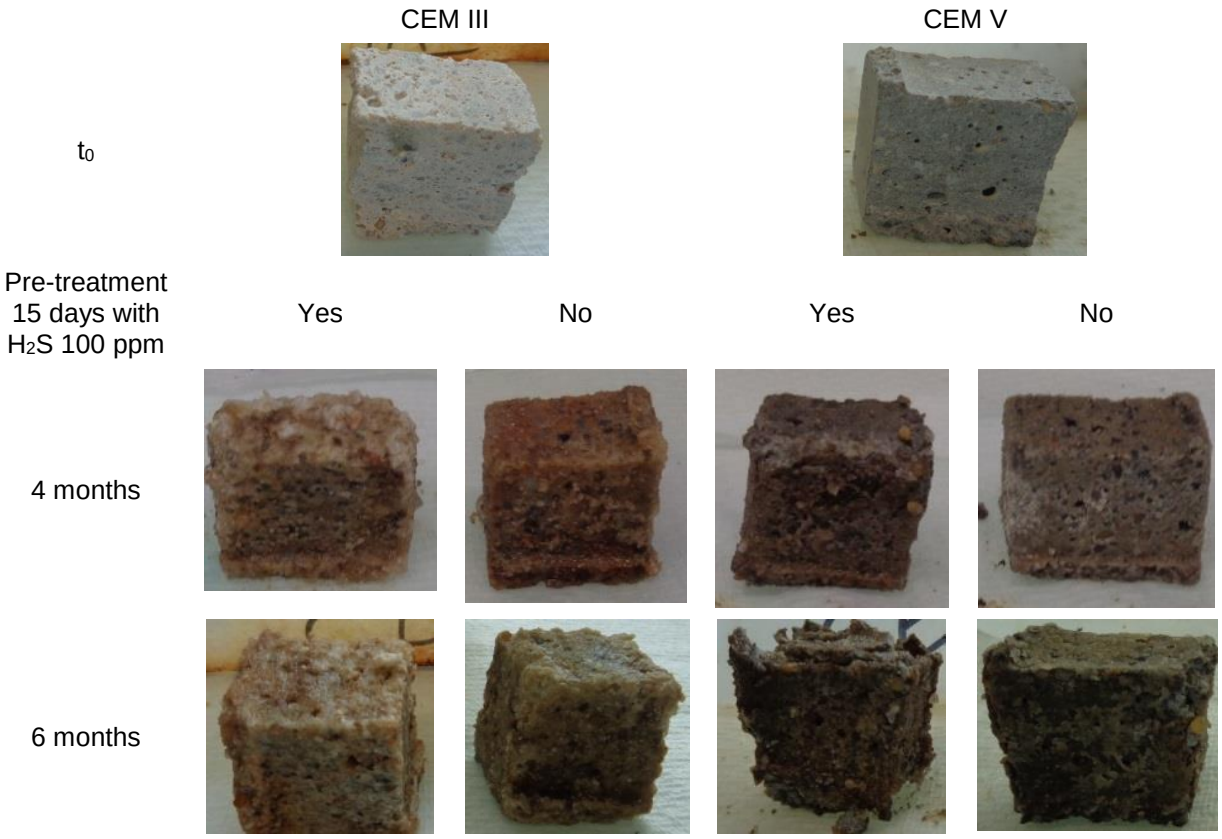

Figure 1.58. Photographs of CEM III and CEM V mortar samples pre-treated with 100 ppm of H_2S or not for 15 days and then exposed to 30 ppm for 4 and 6 months of exposure

3.3.5.2 Impact of oxygen supply

During the stage 2, a modification in the H_2S production was carried out. In order to limit the handling of the beaker inside the chamber in which the H_2S is produced, a pump to empty the beaker was installed, avoiding the need to stop the chamber for 24, 48 hours to be able to safely open the chamber. Samples incubated with activated sludge and hydrogen sulphide for 4 months showed no signs of degradation (Figure 1.59). This can be explained by the absence of oxygen inside the chamber limiting the development of aerobic microorganisms and also limiting the oxidation of sulphur elements into sulphuric acid. Furthermore, it seems important to carry out the test for 6 months.

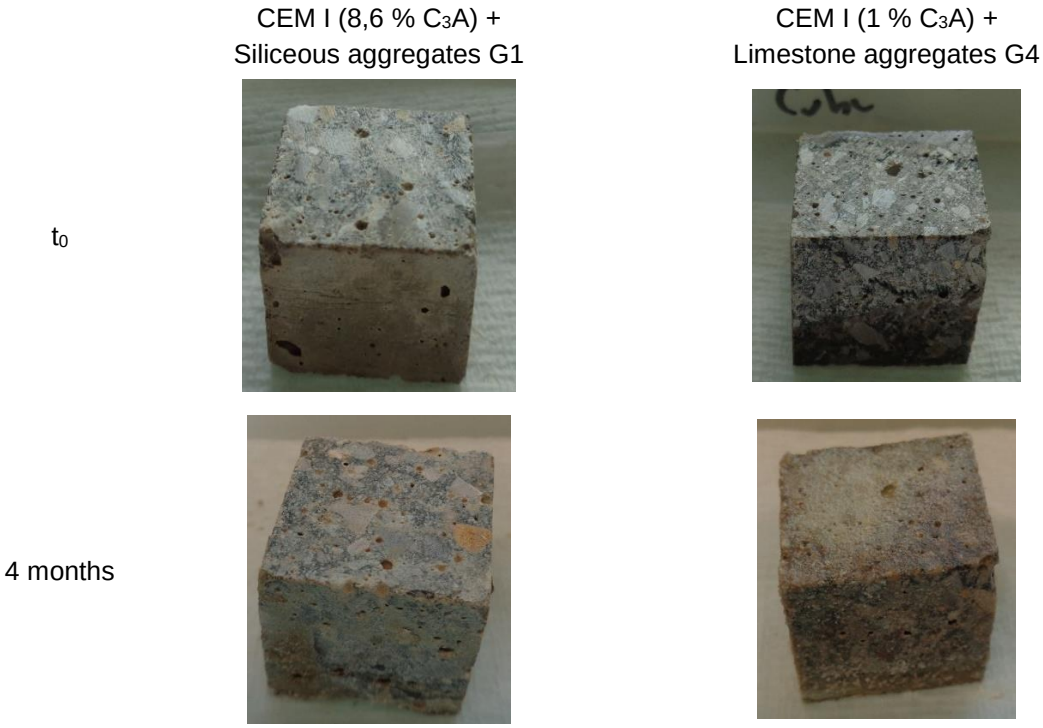

Figure 1.59. Photographs of the CEM I mortar samples after 4 months of exposure in the biodegradation chamber

3.3.5.3 Test optimisation

In order to be able to perform a test accelerating the biodegradation mechanisms, it is necessary to pre-treat the samples with a concentration of 100 ppm H_2S for 15 days. The test should be conducted with a H_2S content higher than 30 ppm and as close as possible to 100 ppm, while remaining within a reasonable range with regard to the safety of the personnel working in the test premises. The test should last 6 months to better discriminate between samples.

3.3.6 Results – End of life criteria for samples

3.3.6.1 Monitoring parameters

In phase 3, the different mortar formulations studied in phase 1 and 2 were re-analysed considering the improvements made to the test methods.

The visual aspect of the samples is a good indicator of the degradation of the samples but it is not sufficient to quantify the degradation. It is therefore important to study other parameters.

3.3.6.1.1 pH evolution

Figure1.60 shows the evolution of the surface pH of the different formulations measured with pH paper during the test conducted by UGE.

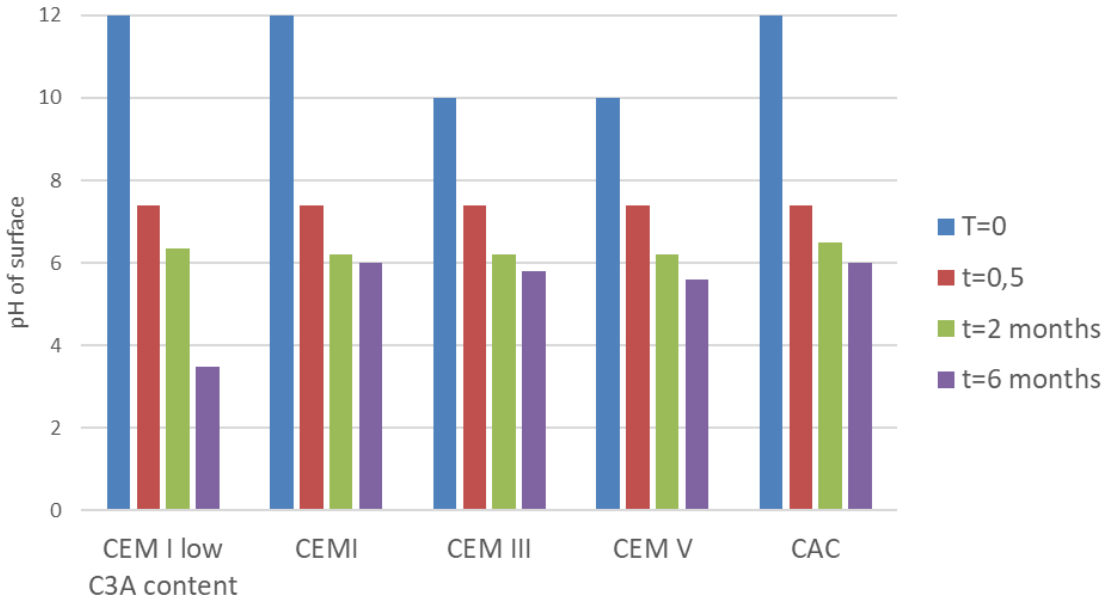

Figure 1.60. Evolution of the surface pH of different mortar formulations during exposure in a biodeterioration chamber

The impact of the pre-treatment (in red) can be noted as it reduces the surface pH of the samples from a highly alkaline pH to a pH close to neutrality. After 6 months of testing in the presence of H_2S, mortars based on CEM I, CEM III, CEM V and CAC have a surface pH of 6.

The surface pH is not a relevant criterion to discriminate between formulations but the surface pH provides information on the initial carbonation of the specimens and on the establishment of the microbial consortium during the test. Indeed, the presence of the biofilm allows the pH to be lowered to a value below 6.

Similarly, the pH of the leachate measured during the BAC Test does not allow the formulations to be distinguished, but it does allow the proper development of the biofilm to be verified (Figure 1.61).

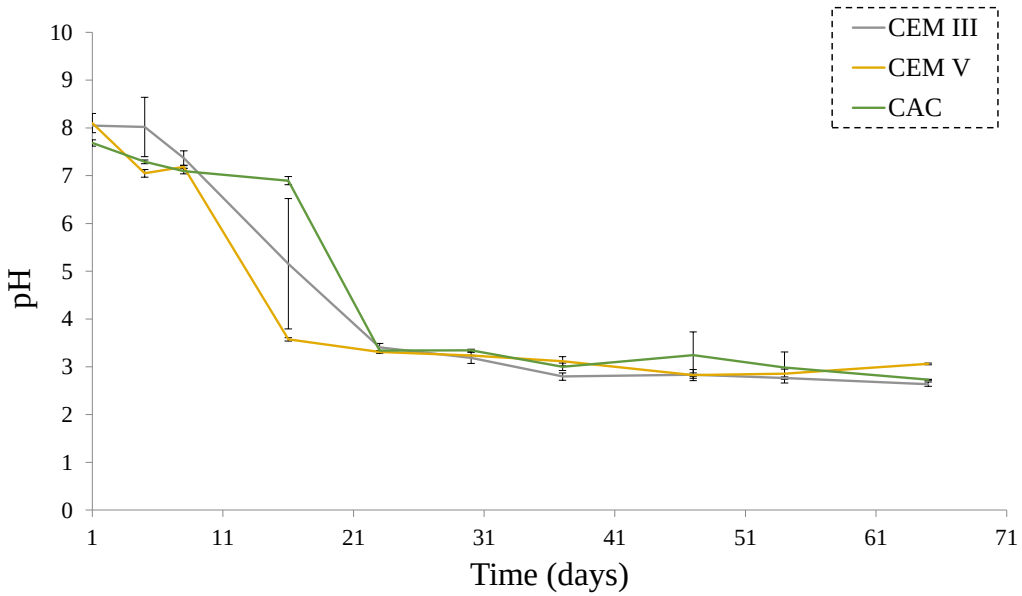

Figure1.61. Evolution of leachate pH during the BAC test for mortars based on CEM III, CEM V and CAC

3.3.6.1.2 Mass monitoring

Figure 1.62 shows the mass gain of different formulations after 4 and 6 months of incubation in the presence of H_2S in the test conducted by UGE.

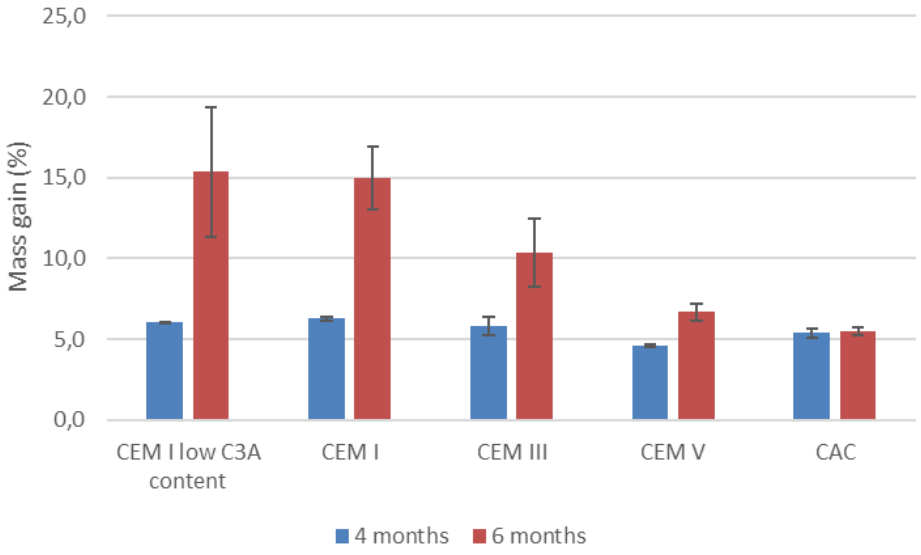

Figure 1.62. Mass evolution of CEM I, CEM III, CEM V and CAC mortar samples after 4 and 6 months of exposure in a biodegradation chamber

After 4 months, the mass gain is mainly related to moisture/porosity. After 6 months, the mass gains of the Portland-based samples are higher than those obtained after 4 months and are correlated with the formation of gypsum on the surface of the samples. This parameter makes it possible to assess the formation of gypsum, but it is difficult to assess when there is concomitance between material losses and mass gains linked to gypsum formation.

3.3.6.1.3 Monitoring of leached calcium

Figure 1.63 shows the cumulative quantities of calcium leached by the materials as a function of the cumulative quantities of sulphate produced biologically during the BAC test.

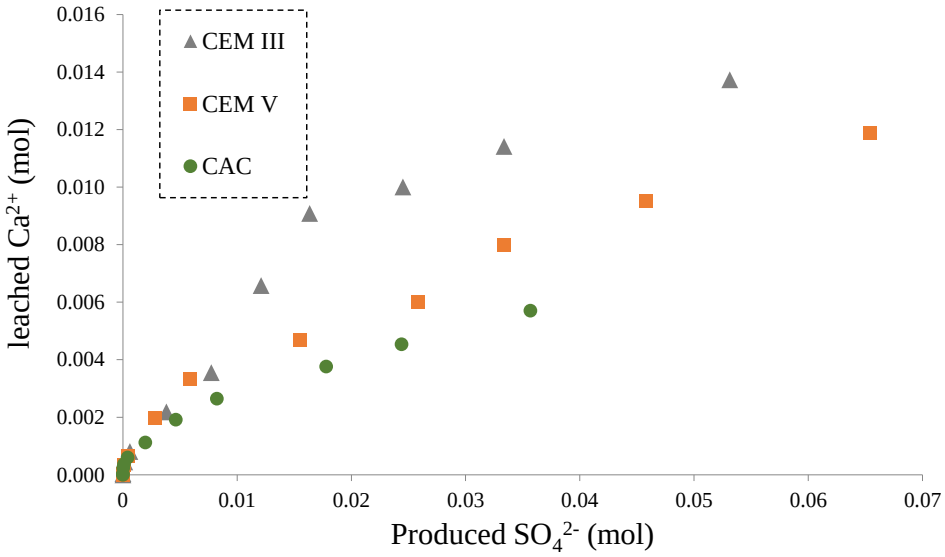

Figure 1.63. Cumulative calcium leached per material as a function of cumulative sulphate produced per material

The initial calcium contents calculated from the technical data sheets of the materials used are of the same order of magnitude for the 3 materials used (CEM III = 11 512 mol Ca/m^3; CEM V = 11 484 mol Ca/m^3; CAC = 10 156 mol Ca/m^3). The production of sulphate, for materials that initially contain little sulphur, is a good marker of the development of sulpho-oxidizing microbial activity. Figure 1.63 shows that, for equivalent amounts of biogenic acid produced, the materials behave very differently in terms of calcium leaching. CAC's leach less calcium than CEM III and CEM V.

Figure 1.64 shows the cumulative amount of calcium leached per exposed coupon over time as a function of the total amount of calcium initially contained in the materials. This figure confirms the better leaching behaviour of CAC under biogenic sulphuric acid conditions and a comparable behaviour of CEM III and CEM V.

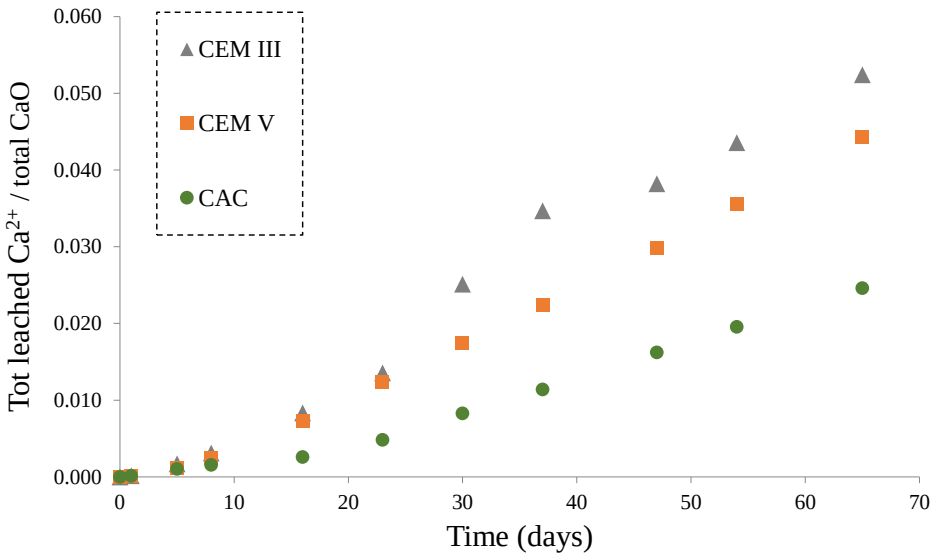

Figure 1.64. Cumulative leached calcium relative to the amount of calcium oxide initially present in the material over time

The ratio of leached calcium to sulphate produced allows the leaching of calcium to be normalized to a quantity of biogenic acid without looking at the effect of the material on biogenic acid production.

The accumulation of leached calcium over the initial amount of calcium contained in the exposed material allows the reactivity of the calcium phases (phases being the most reactive with respect to the attack) constituting the material to be evaluated.

3.3.6.2 End of life criteria

3.3.6.2.1 Loss of mass by sonication

After 6 months of exposure in the UGE biodeterioration chamber, a sample of each formulation was sonicated for 1 hour and then dried at 40 °C until its weight was equilibrated. The % loss in mass after sonication compared to the initial weight of each sample is shown in Figure 1.65.

The differences observed during sonication may be related to changes in the microstructure of CEM III. This material may have undergone more degradation at the physico-chemical level, which influences the mechanical aspect.

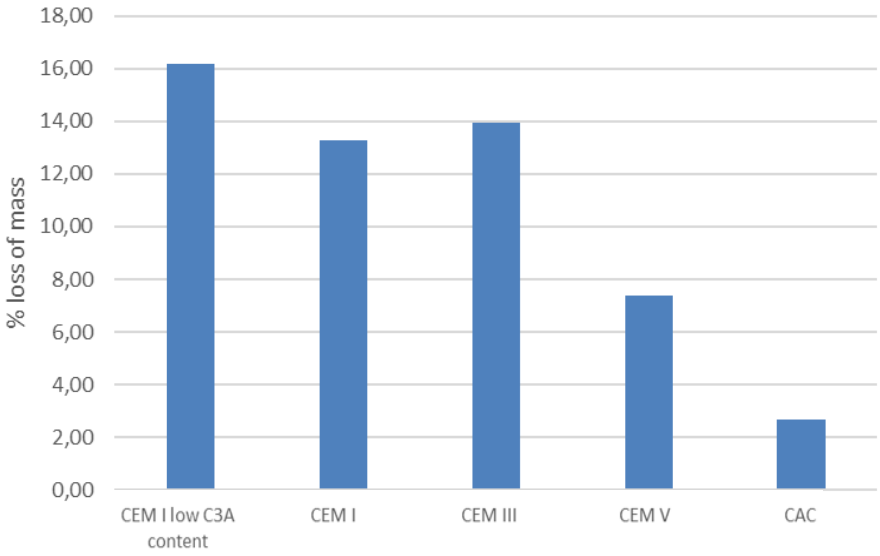

Figure 1.65. Loss of mass after sonication following 6 months incubation in the biodeterioration chamber

3.3.6.2.2 Degraded thickness

SEM observations

Figure 1.66 shows, for 3 materials exposed to the BAC test, an observation by SEM (BSE mode) of a section of the material (at the end of the test). On the right-hand side of each photo, the dark grey area corresponds to the epoxy resin application zone carried out during the preparation of the coupons. It represents the initial surface of the sample. Underneath, a matrix without any noticeable alteration can be observed, allowing the initial thickness of the coupon to be determined.

All the exposed materials have lost thickness, the cement paste being dissolved (including anhydrous) during the test by biological attack. Some of the sand grains have been loosened from the cement matrix (more pronounced for CEM III and CEM V). Concerning CEM III, the degraded zone is mostly dissolved without any notable zone of progressive decalcification, testifying to the aggressiveness of the attack. Concerning CEM V the degraded zone still contains material indicating a partial dissolution of the reactive phases. For the CAC the degraded zone is completely dissolved.

From these profiles, an approach by estimating the degraded thickness was set up. The estimated thickness losses are CAC = -590 µm, CEM V = -710 µm and CEM III = -760 µm.

The observation of the degraded areas by SEM makes it possible to compare the behaviour of the different formulations. However, it does not consider, in the current state of the measurement protocol, the possible (almost certain) loss of material before observation.

a) Profil CEM III

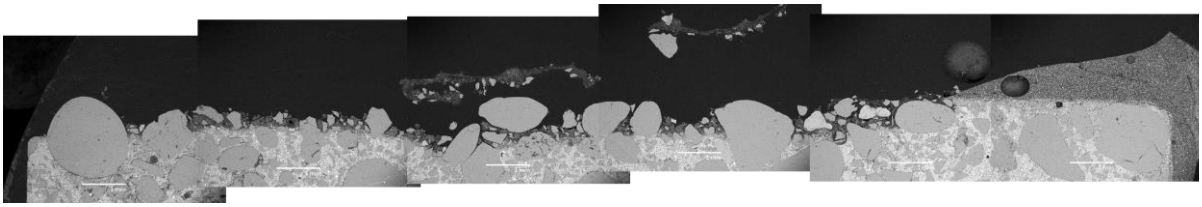

b) Profil CEM V

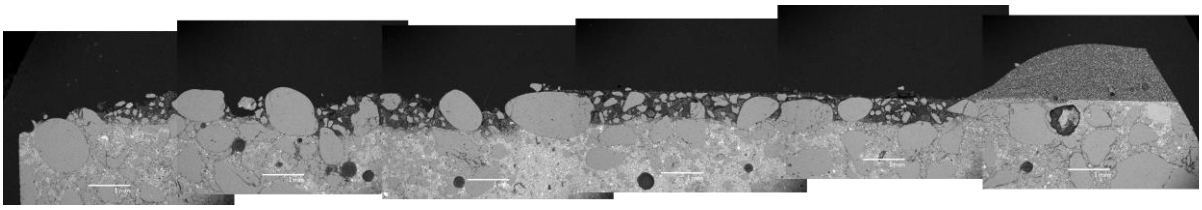

c) Profil CAC

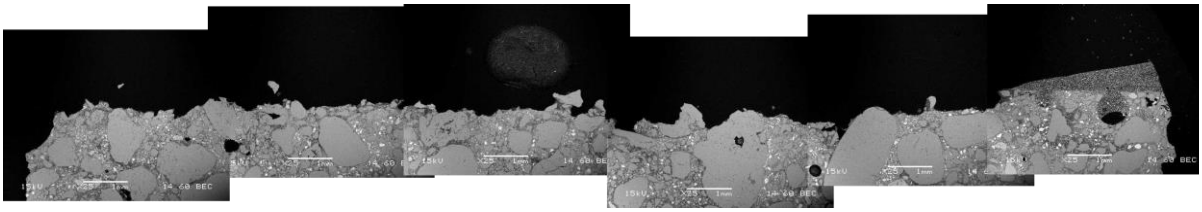

Figure 1.66. SEM observation of a section on the upper area of the exposed coupons (CEM III, CEM V and CAC)

Visual observations

After 4 and 6 months exposed in the biodegradation chamber of UGE, samples are coated with resin and then sawed in order to observe the degradation profile and to evaluate the remaining healthy part of the sample. The area of the healthy part of the samples is measured on 4 samples per formulation using the IMAGEJ software. From these areas obtained, an average sound edge size is calculated. This value is then compared to the initial measured value to determine the degraded depth per formulation. The results are presented in Figures 1.67 and 1.68.

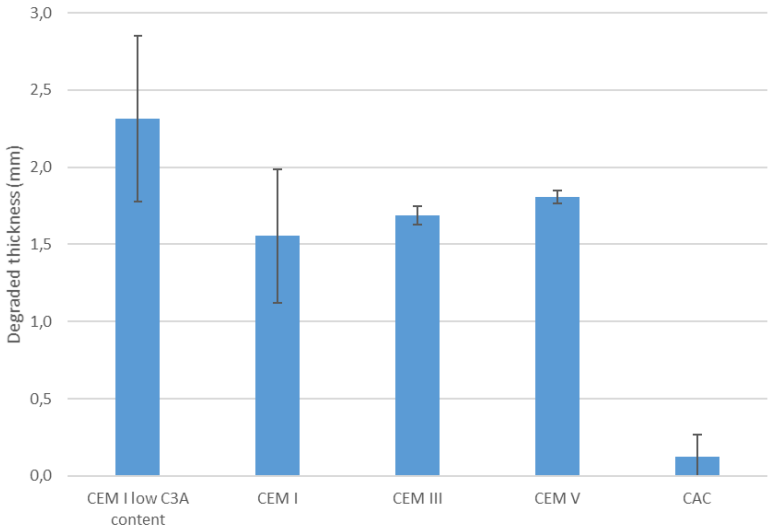

Figure 1.67. Degraded thickness in mm for the different formulations after 6 months of exposure in the biodegradation chamber

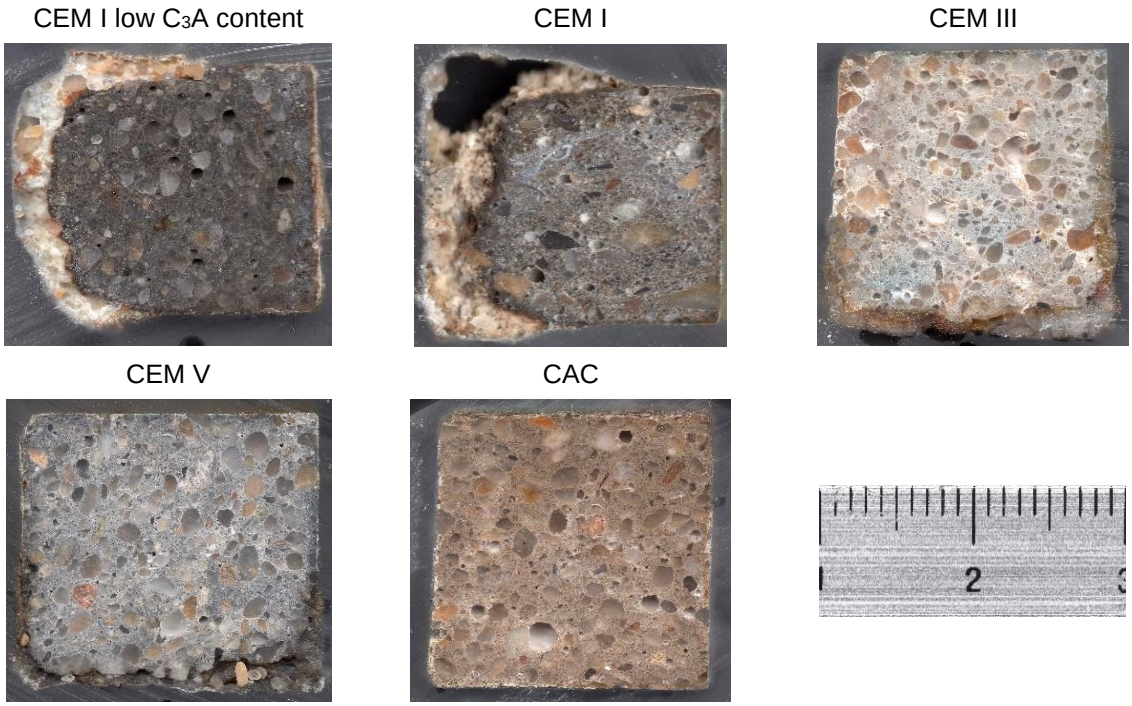

Figure 1.68. Photographs of the sections of the different formulations after 6 months of exposure in the biodeterioration chamber

Dividing the degraded thickness of the samples by the thickness of the CEM I mix with low C_3A content, we obtain a ratio called $I_{bio/tem}$.

Formulation	$I_{bio/tem}$
CEM I low C_3A content	1.00
CEM I	0.65
CEM III	0.74
CEM V	0.78
CAC	0.04

These observations show two different behaviours. On the one hand, Portland-based cements and on the other hand, calcium aluminate cement.

3.3.6.3 Conclusion

The alteration criteria are multiple in order to validate the test. Different parameters, chosen to be redundant, are considered (visual appearance, pH, mass variation, ratio of leached calcium to sulphate produced, total leached calcium to the initial quantity of calcium oxide contained in the exposed material, degraded depth on a section).

Monitoring the pH of the leached solution or the surface pH over time makes it possible to validate the implementation of the sulpho-oxidizing microbial activity necessary for the biodeterioration of exposed materials.

The visual aspect is a good indicator that should continue to be monitored despite only qualitative information.

The ratio of leached calcium to sulphate produced allows the leaching of calcium to be normalised to a quantity of biogenic acid without looking at the effect of the material on biogenic acid production.

The accumulation of leached calcium over the initial amount of calcium contained in the exposed material allows the effect of leaching on the material to be relativized with respect to the majority calcium phases (phases that are the most reactive to attack).

The estimation of the degraded thickness on a section allows to evaluate the depth of the zone really impacted by the biological attack.

At present, these different parameters are consistent and, by their redundancy, make the results of the test more reliable and ensure that the test is working properly.

A simple criterion for evaluating the performance of materials in both tests is $I_{bio/tem}$. In the case of UGE, it corresponds to the comparison of the measured degraded thickness of a sample to be qualified with that of a CEM I SR0 sample. For the BAC Test, this index is similar but the degraded thickness is assessed by the calculated value of the quantity of leached calcium over the initial quantity of calcium of the sample divided by the amount of sulphate produced.

3.3.7 Results – Recommendations

3.3.7.1 Impact of the binder: CEM I, CEM III, CEM V and CAC comparisons

The different results above show two types of behaviour: Portland cements and calcium aluminate cements, which is confirmed by the in-situ tests carried out (Figure 1.69).

The mortar samples formulated with Portland cement degraded rapidly at Site 2. Few degradations were observed at Site 1. The performance results of the formulations are similar to the results obtained from the laboratory tests.

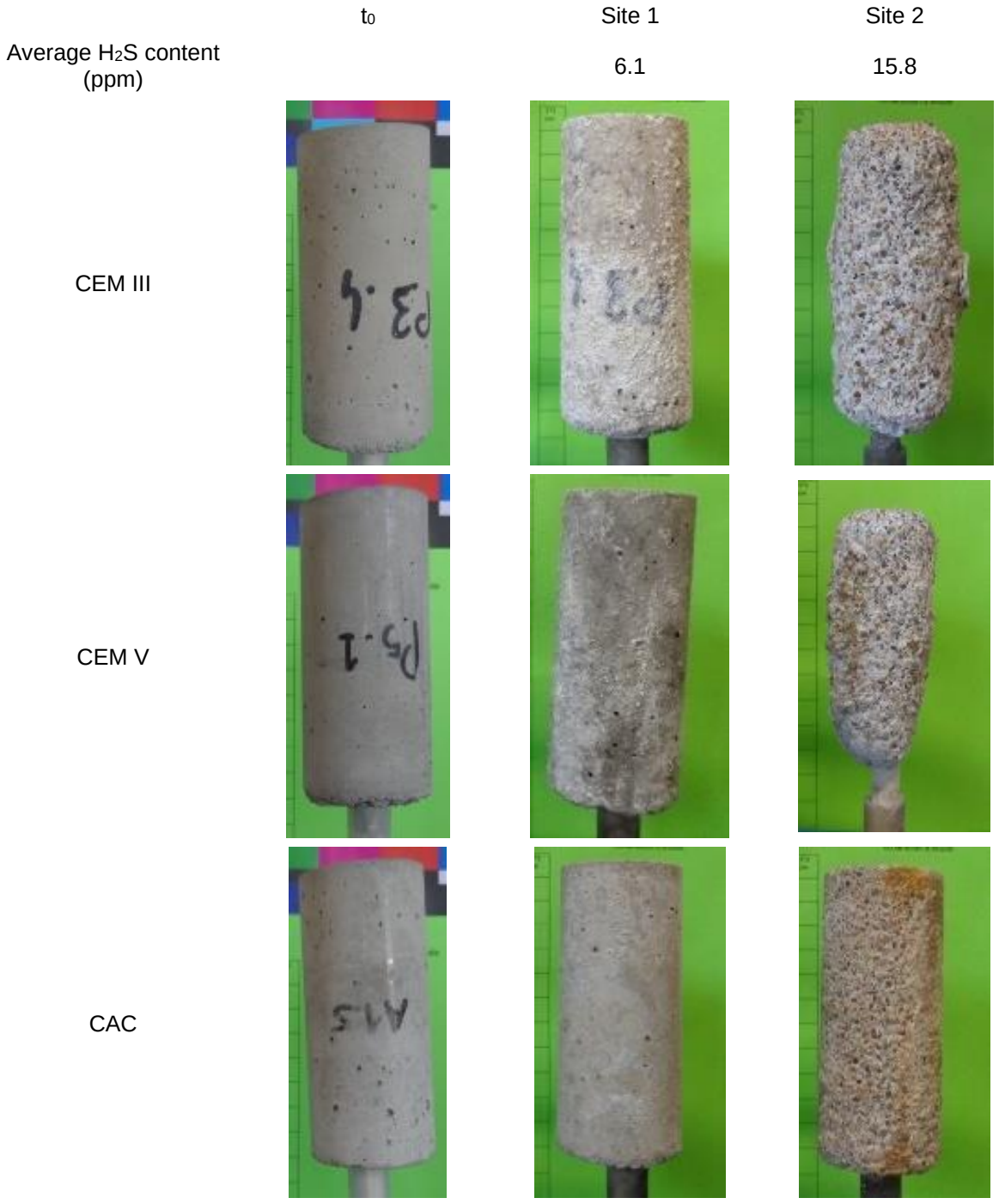

Figure 1.69. Photographs of CEM III, CEM V and CAC samples exposed for 30 months at two different sites (average H_2S content 6.1 and 15.8 ppm)

3.3.7.2 C_3A Content of CEM I

Figure 1.70 shows the cumulative amount of calcium leached as a function of the cumulative amount of sulphate produced by the microorganisms (equivalent to 1.5 moles to the amount of acid produced) for the materials with siliceous aggregates (CEM I control, M1 and M2). All Portland cement and siliceous aggregate mortars, regardless of the amount of C_3A, have equivalent behaviour, indicating that there is no difference in reactivity between these materials.

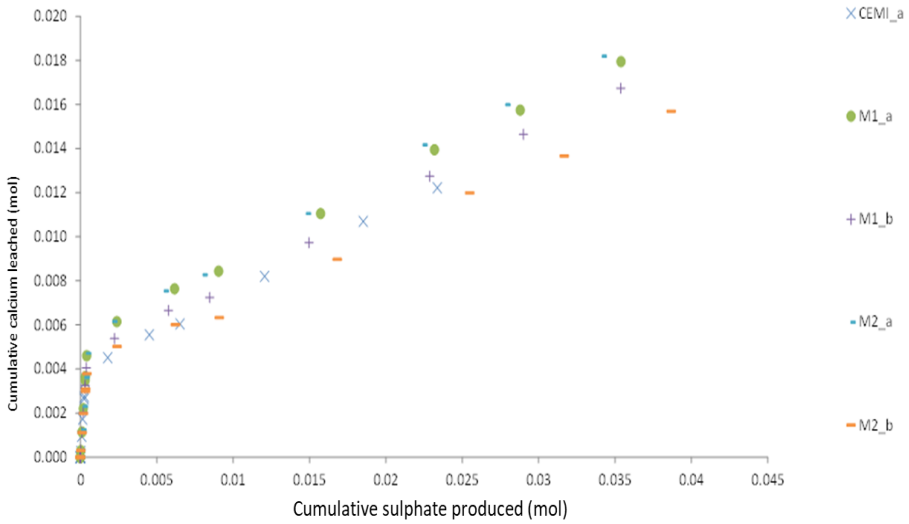

Figure 1.70. Cumulative calcium leached versus cumulative sulphate produced for materials with siliceous aggregates for the M1, M2 and M3 formulations and the CEM I control

Figure 1.71 shows the cumulative amount of calcium leached versus the cumulative amount of sulphate produced by the microorganisms for all exposed mortars. Mortars formulated with limestone aggregates (M3) show an over-leaching of calcium in relation to the acidity produced, due to the reactivity of the limestone aggregates.

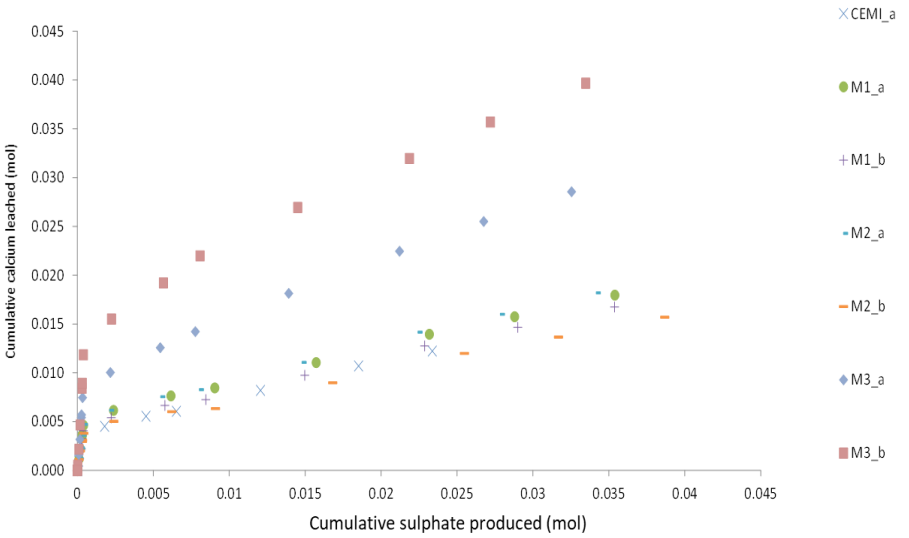

Figure 1.71. Cumulative calcium leached versus cumulative sulphate produced for the M1, M2 and M3 formulations and the CEM I control

The use of a CEM I cement with a low C_3A content did not make it possible, for mortars based on siliceous aggregates, to obtain a significantly different response in terms of the reactivity of the material in the BAC Test compared with a CEM I cement mortar with 8.6% C_3A.

3.3.7.3 Nature of aggregates

Figure 1.72 shows the cumulative amount of calcium leached as a function of the total calcium initially contained in the exposed coupon, as a function of the cumulative amount of sulphate produced.

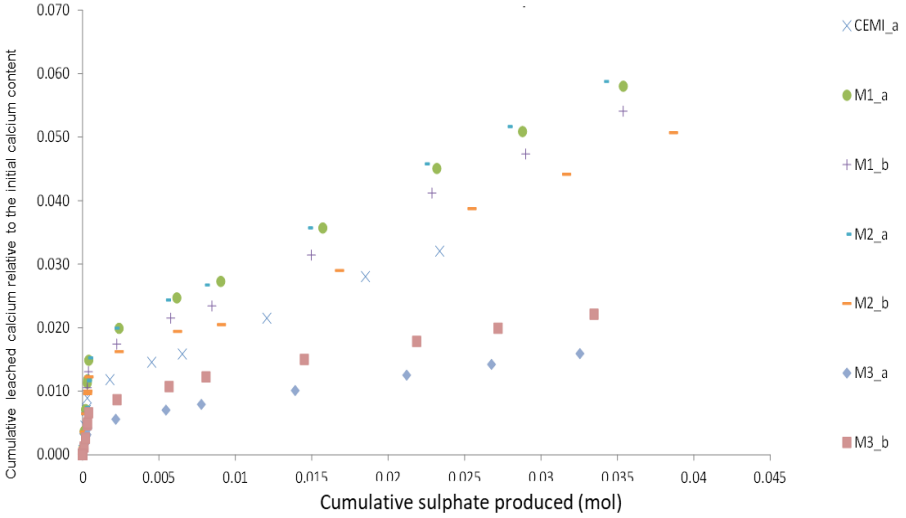

Figure 1.72. Cumulative leached calcium relative to the initial calcium content of the material per square metre of exposed surface compared to the cumulative sulphate produced for the M1, M2 and M3 formulations and the CEM I control

This representation shows that mortars with siliceous aggregates (G1) and CEM I with C_3A (M1) on the one hand, and CEM I with reduced C_3A content (M2) on the other hand, have an equivalent response to the BAC test.

Compared to the reference corresponding to a CEM I mortar with C_3A with siliceous aggregates, the tested materials with siliceous aggregates (G1) are classified in the same zone with however a slightly higher durability for the reference, related to a higher amount of calcium in the initial material due to a lower S/C ratio than for the exposed materials.

The LMDC-TBI test (BAC Test) shows a superior resistance provided by the addition of limestone aggregates (but beware of a non-linear gain in life span with the addition of acid-reactive aggregates, because of the greater reactivity of the material in relation to the acidity produced).

3.3.8 Conclusion of the experimental study

The two tests make it possible to reproduce and monitor the successive implementation of the sulpho-oxidising activities responsible for the deterioration of the materials. The operating conditions of the tests allow for the local production of biogenic sulphuric acid in contact with the materials, leading to the dissolution of the surface layers through acid attack, and to the accumulation of sulphur within the material through the penetration of sulphates.

On the basis of the different parameters currently monitored, the tests make it possible to discriminate between different cementitious matrices in relation to such environments. The two tests, in agreement with the literature, show the better resistance of CAC-based materials to sewerage areas where environmental conditions lead to strong deterioration.

Although the tests were carried out on mortar samples, it could be shown that when a CEM III/A concrete sample from a pumping station was exposed in UGE biodeterioration chamber, the degradation mechanisms were the same as those observed on the same concrete in situ and on CEM III mortar samples exposed in situ or in the biodeterioration chamber (Figure 1.73). In all cases (in situ/laboratory or mortar/concrete) a non-cohesive gypsum layer forms on the surface. The layer of cementitious material immediately below this gypsum layer is more cohesive and contains large amounts of sulphur that deepen from the surface.

Figure 1.73. Photographs of CEM III/A concrete samples exposed for 4 months in the UGE biodeterioration chamber. Both samples are from a pumping station: a) sample from non-degraded area; b) sample from a degraded area

3.3.9 Proposal for a method based on the performance approach - XA Biodegradation

In the event that the requirements of the prescriptive approach to biodegradation are not met, in particular for the choice of the nature of the constituents (binder and aggregates), it is possible to justify compliance with standard NF EN 206/CN and the specified project service life using the comparative performance approach presented in Table 1.38.

This table is based on the results obtained in phases 1, 2 and 3 of the previous study.

Table 1.38. Performance qualification criteria for H_2S media

Exposure class	$I_{bio/tem}$	Reference concrete	
		Cement	Paste volume fraction fV_p Granular skeleton (dosage and nature)
XA1	≤ $I_{bio/tem}$ of reference concrete	CEM I	Equivalent to that of the concrete to be qualified
XA2	≤ $I_{bio/tem}$ of reference concrete	CEM III/B SR	Equivalent to that of the concrete to be qualified
XA3	≤ $I_{bio/tem}$ of reference concrete	CAC	Equivalent to that of the concrete to be qualified

Note: in class XA3, a concrete formulated with a binder other than a CAC but benefiting from conclusive feedback may also be used as a basis for defining the reference concrete according to the decomposition rules given.

3.4 References

(Arliguie and Hornain, 2007) GranDuBé, Grandeurs associées à la durabilité des bétons, sous la direction de Ginette Arliguie et Hugues Hornain, 440 p., Presse des Ponts, 2007.

(Atahan and Dikme, 2011) Atahan H.N., Dikme D., Use of mineral admixtures for enhanced resistance against sulphate attack, Construction and Building Materials, 25-8, 3450-3457, 2011.

(Cassagnabère and Carcassès, 2013) Cassagnabère F., Carcassès M., Complément expérimental 2 à la thèse de S. Messad, Rapport de recherche LMDC, 2013.

(Felekoglu *et al.*, 2006) Felekoglu B., Ramyar K., Tosun K., Musal B., Sulfate resistances of different types of Turkish Portland cements by selecting the appropriate test methods. Cons. Buil. Mat. Vol.20, pp819–823, 2006.

(Garcia and Carcassès, 2009) Garcia V., Carcassés M., Complément expérimental 1 à la thèse de S. Messad, Rapport de recherche LMDC, 2009

(Irassar, 2009) Irassar E.F., Sulfate attack on cementitious materials containing limestone filler - A review, Cement and Concrete Research, 39-3, 241-254, 2009

(Katsioti *et al.*, 2011) Katsioti M., Patsikas N., Pipilikaki P., Katsiotis N. Mikedi K., Chaniotakis M., Delayed ettringite formation (DEF) in mortars of white cement. Cons. Buil. Mat. Vol.25, pp900–905, 2011.

(Linger *et al.*, 2014) Linger L., Carcasses M., Rozière E., Cassagnabere F., Cussigh F., Nicot P., Essai de vieillissement accéléré de l'attaque sulfatique externe pour l'application du concept de performance équivalente dans le cadre de la norme EN 206-1.

(Loser and Leemann, 2015) Loser R., Leemann A., An accelerated sulfate resistance test for concrete. Materials and Structures 2015, 1-13. DOI 10.1617/s11527-015-0731-2, 2015.

(Massaad, 2016) Massaad G., "Stratégie performantielle d'évaluation de la résistance des matériaux cimentaires à l'attaque sulfatique externe", Thèse de doctorat de l'École Centrale de Nantes, 2016.

(Messad, 2009) Messad S., Mise au point d'un essai de vieillissement accéléré de l'attaque sulfatique externe pour l'application du concept de performance équivalente dans le cadre de la norme NF EN 206. Thèse de Doctorat de l'Université de Toulouse, 2009.

(Peyre Lavigne *et al.*, 2015) Peyre Lavigne M., Bertron A., Auer L., Hernandez-Raquet G., Foussard J.-N., Escadeillas G., Cockx A. & Paul E., «An innovative approach to reproduce the biodeterioration of industrial cementitious products in a sewer environment. Part I: Test design », Cem. Concr. Res., vol.73, p.246–256, 2015.

(Peyre Lavigne *et al.*, 2016) Peyre Lavigne M., Bertron A., Botanch C., Auer L., Hernandez-Raquet G., Cockx A., Foussard J.-N., Escadeillas G. & Paul E., «Innovative approach to simulating the biodeterioration of industrial cementitious products in sewer environment. Part II: Validation on CAC and BFSC linings », Cem. Concr. Res., vol.79, p.409–418, 2016.

(Rozière *et al.*, 2009) Rozière E., Loukili A., El Hachem R., Grondin F., Durability of concrete exposed to leaching and external sulphate attacks. Cement and Concrete Research, Elsevier, 2009, 39 (12), pp.1188-1198

(Rozière *et al.*, 2013) Rozière E., Loukili A., El Hachem R., Etude de la durabilité des bétons par une approche performantielle (basée sur des essais de vieillissement accéléré) Compléments expérimentaux : influence du séchage à 80 °C sur le classement des performances des bétons exposés aux attaques sulfatiques externes, Rapport de recherche GEM, 2013.

(Sahmaran *et al.*, 2007a) Sahmaran M., Kasap O., Duru K., Yaman IO., Effects of mix composition and water–cement ratio on the sulfate resistance of blended cements. Cem. Conc. Comp. Vol.29, pp159–167, 2007.

(Sahmaran *et al.*, 2007b) Sahmaran M., Erdem TK., Yaman IO., Sulfate resistance of plain and blended cements exposed to wetting–drying and heating–cooling environments. Cons. Build. Mat. Vol.21 (8), pp1771-1778, 2007.

(Tosun *et al.*, 2009) Tosun K., Felekoglu B., Baradan B., Altun A., Effects of limestone replacement ratio on the sulfate resistance of Portland limestone cement mortars exposed to extraordinary high sulfate concentrations Const. Build. Mat. Vol.23, pp2534–2544, 2009.

(Weritz *et al.*, 2009) Weritz F., Taffe A., Schaurich D., Wilsch G., Detailed depth profiles of sulfate ingress into concrete measured with laser induced breakdown spectroscopy. Cons. Build. Mat. Vol.23, pp275–283, 2009.

APPENDIX A:
Accelerated external sulphate reaction (ESR) test

Introduction

The aim is to demonstrate that the concrete design that is to be used (but which deviates in certain respects from the requirements of the prescriptive approach) performs better in the performance test than a design that meets the requirements in terms of means of the prescriptive approach (standard EN 206/CN). If this requirement in terms of (better) performance (LCPC, 2010) is verified, this alternative formulation is considered to have a durability at least equivalent to that meeting the requirements from the point of view of the prescriptive approach.

As part of the performance test for the External Sulphate Reaction (ESR), two operating modes were selected. These are accelerated ageing tests on concrete specimens, involving immersion in an attack solution of sodium sulphate of the same type after a preconditioning phase (saturation or immersion/drying). The various test parameters were chosen so as to accelerate the attack sufficiently to obtain a discriminating test on concrete over a period of 12 or 13 weeks.

Two methods are available for determining the resistance of concrete to sulphate reaction:

- Method A "Accelerated protocol for ESR by saturation". It is based on S. Messad's doctoral work entitled "Development of an accelerated ageing test for external sulphate attack to apply the concept of equivalent performance within the framework of standard NF EN 206" (Messad, 2009) carried out at LMDC Toulouse and a series of complementary studies (Garcia and Carcassès, 2009; Cassagnabère and Carcassès, 2013; Rozière *et al.*, 2013; Linger *et al.*, 2014).
- Method B "Accelerated ESR protocol by immersion/drying". This method is based on the Swiss standard SIA 262 (appendix G) (SIA 262, 2013).

The choice between two protocols will depend on the equipment available in the analysis laboratory.

A.1 Field of application

This document specifies a method for determining resistance to External Sulphate Reaction by an accelerated test using two different methods. They apply to concrete elements made in the laboratory or on site, or to cores taken from structures or prefabricated elements, provided that the samples submitted for testing are not contaminated by sulphate ions (calcium, magnesium or sodium sulphate).

A.2 Normative references

The following reference documents are essential for the application of this document. For dated references, only the edition cited applies. For undated references, the latest edition of the reference document applies (including any amendments).

FD P 18-011: Concrete - Definition and classification of chemically aggressive environments - Recommendations for the formulation of concrete.

NF EN 206/CN, Concrete - Part 1: Specification, performance, production and conformity, 2012.

NF EN 12390-2, Tests for hardened concrete - Part 2: Preparation and storage of specimens for strength tests, 2012.

NF P18-427, Determination of dimensional variations between two opposite faces of hardened concrete specimens1996.

NF EN 12390-3, Tests for hardened concrete - Part 3: Compressive strength of specimens, 2019.

NF P18-459, Water porosity and density test on hardened concrete, 2010.

NF P18-462, Test on hardened concrete - Accelerated chloride ion migration test in non-stationary regime - Determination of the apparent diffusion coefficient of chloride ions, 2012.

A.3 Terms and definitions, symbols and units

For the purposes of this document, the following terms and definitions, symbols and units apply. The symbols listed below are used in this document:

R_c	compressive strength (MPa)
D_{app}	apparent chloride diffusion coefficient (m/s^2)
p_w	porosity accessible to water (%)
$V_{béton}$	volume of concrete (m^3)
$V_{Solution}$	volume of sodium sulphate solution (m^3)
sr	repeatability (%)
s_R	reproducibility (%)
τ	saturation rate (%)
M_{air}	mass of saturated test piece weighed in air (g)
M_{eau}	mass of saturated test piece weighed in water (g)
M_{sec}	mass of the dry test piece in air (g)
var	relative variation in the parameter under consideration (%)
$m_{initial}$	result obtained on sound material
m_{final}	result obtained on degraded material (after 12 weeks of immersion)
d	specimen diameter (mm)
L	Initial length of specimen at 0.1 mm (mm)
HR	relative humidity (%)
L_0	initial length, at 0.001 mm, measured after immersion of the specimen in water at 20 °C for 60 ± 10 min (mm)
t_0	start of accelerated test
m_{Ti}	mass at 0.01 g, measured after drying the i^{th} drying cycle) with *i=1 to 4 (g)*
m_{Si}	mass at 0.01 g, measured after the i^{th} drying/immersion cycle, with i = 1 to 4, drying (50 ± 5 °C for 120 ± 2 h in a ventilated chamber) and immersion (48 ± 2 h immersion in the Na_2SO_4 solution 33.8 g SO_4 /L) (g)

L_i length at 0.001 mm, measured after i^{th} drying/immersion cycle, with i = 1 to 4, drying (50 ± 5 °C for 120 ± 2 h in a ventilated chamber) and immersion (48 ± 2 h immersion in Na_2SO_4 solution 33.8 g SO_4 /L) (g) (mm)

m_{Sj} mass at 0.01 g on d^{th} measurement after permanent immersion in sodium sulphate solution at 7, 14, 28 and 56 days respectively with d = 5 to 8 (g)

L_j length at 0.001 mm on d^{th} measurement after permanent immersion in sodium sulphate solution with d = 5, 6, 8, 10 and 12 for 7, 14, 28, 42 and 56 days respectively (mm)

V_0 initial core volume (mm^3)

dL_n change in length at maturity with n = 1 to 12 mass change at maturity with n = 1 to 4

dM_{sn} mass change at maturity with n = 1 to 4

dL_s elongation after permanent storage in the sulphate solution: $dL_S = dL_{12} - dL_4$ (‰)

dm_s change in mass after permanent storage in the sulphate solution
$dm_S = (ms_{12} - ms_4) / V_0$ (kg/m^3)

A.4 Accelerated saturation ESR test (Method A)

The accelerated ageing test in the context of external sulphate attack consists of immersing pre-saturated concrete specimens in a sodium sulphate attack solution of the same nature and concentration as that used for saturation, for 12 weeks. The various test parameters were chosen so as to accelerate the attack sufficiently to obtain a discriminating test on concrete over a period of 12 weeks.

A.4.1 Materials

- Laboratory regulated at 20 ± 2 °C
- Stainless steel adhesive studs
- Scale with 0.01g resolution accurate to 0.03 g
- Caliper with 0.01 mm resolution, accurate to 0.05 mm
- Comparator with 0.001 mm resolution, accurate to 0.002 mm
- Ventilated oven, regulated at 50 ± 2 °C with good air exchange in and around the oven
- Vacuum saturation device (example of device in Figure 1) with a container of sufficient volume to allow total immersion of the test specimen during its saturation by the Na_2SO_4 solution (6.0 g of SO_4 /L) and vacuum pump enabling the pressure to be reduced and maintained at a value less than or equal to 25 mbar (2.5 kPa)
- Immersion tank with pH and temperature control (example shown in Figure 1).

A.4.2 Chemical reagents

- Sodium sulphate solution Na_2SO_4 with a concentration of 8.9 g/L (6 g/L of SO_4) for the saturation and immersion phase of the samples
- Distilled or demineralised water
- Sulphuric acid solution (H_2SO_4) diluted to 5 g/L prepared from deionised water and pure sulphuric acid

A.4.3 Test specimen

The measurements of the physical and mechanical characteristics used to assess the durability of the material in its sound state are as follows:

- chloride diffusion coefficient;
- mechanical resistance in compression;
- porosity accessible to water.

The tests used to assess the rate of degradation are mainly expansion measurements and mass monitoring.

However, it is recommended that the physical and mechanical characteristics also be measured on the specimens that have been subjected to the accelerated ageing test. The changes in these parameters between the initial state (sound) and the final state (after degradation) also reflect the damage suffered by the material and provide more details on the mechanisms responsible for the greater or lesser sensitivity of a given formulation to sulphate attack.

With the exception of expansion measurements and mass monitoring, the other measurements are carried out on two series of samples: in a sound state just after the curing period and in a degraded state after 12 weeks of immersion. For each of these tests, the measurement is carried out on three samples, and the result and uncertainty are given by the mean and standard deviation.

Table 1.A.1 gives an overview of the number and type of samples associated with each test, as well as the number and type of test specimens required per batch.

Table 1.A.1. Summary of the number and type of samples associated with each test

Test	Type of sample	Number of samples to be tested	
		In a healthy state	In a degraded state
Compressive strength (Rc)	Cylinders (x 6) ∅ 11 cm H 22 cm	3	3
Migration of Cl^- ions (D_{app})	Cylinders (x 6) ∅ 11 cm H 5 cm	3	3
Porosity accessible to water (p_w)	Cylinders (x 6) ∅ 11 cm H 5 cm	3	3
Expansion and mass tracking	Prism (x 3) 7 cm x 7 cm x 28 cm	-	3

For one batch, 3 prisms and 10 cylinders are required for the entire characterization campaign.

For classes XA1 and XA2, using the comparative method, at least two batches are required; one for the production of the reference concrete and the other for the production of the concrete to be qualified.

A.4.4 Tests on sound material

For classes XA1 and XA2, using the comparative method, the reference concrete and the concrete to be qualified are tested in a sound state by measuring the physical and mechanical properties of the material.

The measurements to be taken on sound material are carried out after 28 days of curing, in compliance with the recommendations given in the standard, guide or protocol established for each test (Table 1.A.2).

Table 1.A.2. Tests to be carried out on concrete in sound condition (before ESR protocol)

Tests	References
Compressive strength (Rc)	NF EN 12390-3
Migration of Cl^- ions (D_{app})	NF P18-462
Porosity accessible to water (p_w)	NF P18-459

In the case of concretes containing additions, it is preferable to carry out the tests after 90 days of curing, in order to take into account the evolution of the properties of the material beyond 28 days.

A.4.5. Conduct of the test

A.4.5.1 Pre-conditioning

After mixing, the specimens are placed in a wet cure for 28 days (20 °C, 100 % relative humidity). At the end of the wet cure, the specimens are sawn to obtain the desired dimension of the test specimen.

For expansion measurements (standard NF P18-427), it is necessary to use stainless steel studs (embedded or bonded), in order to avoid corrosion problems that could occur during drying or immersion of the test specimens in the etching solution.

For compressive strengths (standard NF EN 12390-3), the specimens subjected to the degradation test must be ground before the drying and saturation stages.

A.4.5.2 Drying

After curing (28 or 90 days), the samples to be degraded are placed in an oven at 60 °C until the variation in mass, between two successive weighings carried out 24 hours apart, does not exceed 0.1%.

A.4.5.3. Saturation

On leaving the oven at 60 °C, the samples must first be brought back to room temperature and then placed in an oven at 30 °C or 40 °C to prevent the absorption of water until saturation.

The samples were then saturated in a vacuum with a sodium sulphate etching solution, the concentration of which was set at 8.9 g/L. The apparatus (Figure 1.A.1) is identical to that used to measure water-accessible porosity (standard NF P18-459).

The saturation time is therefore 48 hours (4 hours vacuum, 44 hours immersion).

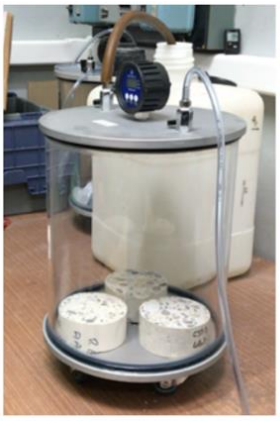

Figure 1.A.1. Vacuum saturation set up

A.4.5.4 Immersion of specimens

a. Preparation of solutions

During the test, two solutions are prepared: one to regulate the pH, the other to saturate and immerse the test specimens.

- the solution used to regulate the pH is a sulphuric acid solution (H_2SO_4) diluted to 5 g/L prepared from deionised water and pure sulphuric acid;
- the etching solution is a sodium sulphate solution with a concentration of 8.9 g/L prepared from deionised water and sodium sulphate salt.

b. Test conditions

The pre-saturated test tubes are placed in trays and then immersed in a sodium sulphate solution with a concentration of 8.9 g/L. The pH and temperature of the solution are monitored throughout the test, with the pH maintained at 7 (±1) and the temperature kept above 25 °C. The etching solution must be renewed every month. The duration of the test was set at 12 weeks.

The conditions to which the samples were subjected are summarised in Table 3.

Table 1.A.3. Test condition

Exposure conditions	Continuous immersion
pH control with sulphuric acid	Controlled at 7 ± 1
Concentration of Na_2SO_4 in the etching solution	8.9 g/L of Na_2SO_4 (6 g/L of SO_4)
Temperature	Controlled at 25 °C
Renewal of the solution	Every 4 weeks
$V_{concrete}$ / $V_{solution}$	1.0
Test duration	12 weeks

A.4.6. Experimental set-up

The device consists of a tank containing the attack solution and the test specimens, a agitator homogenizing the solution, a temperature regulator which is triggered each time the temperature falls below 25 °C, an electrode for monitoring changes in the pH of the attack solution, a pH regulator (which is triggered each time the pH rises above 7) connected to another tank containing a 5 g/L solution of sulphuric acid.

The system is shown in Figure 1.A.2.

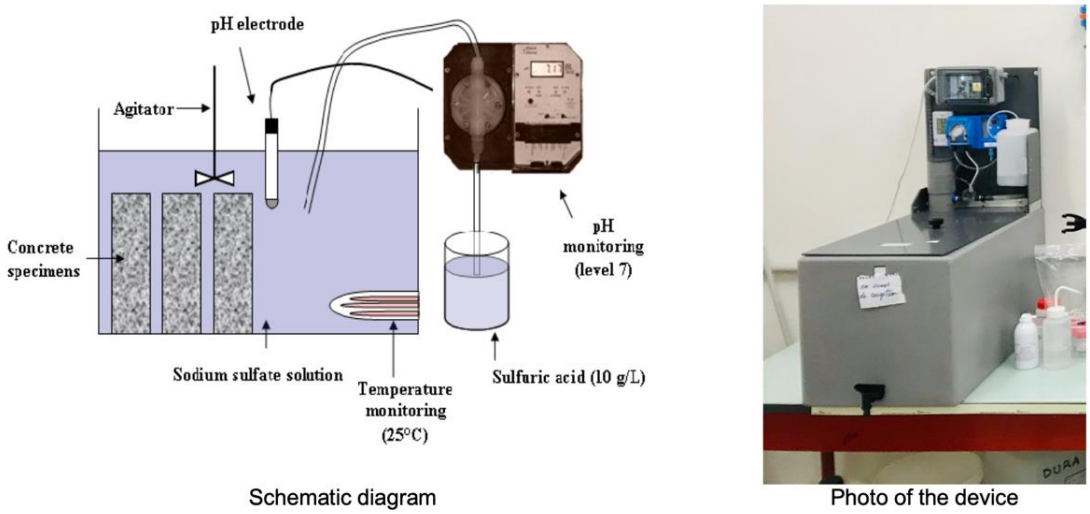

Figure 1.A.2 - Experimental set-up for the saturation test

A.4.7. Monitoring degradation and formatting results

A.4.7.1. Measurement of elongation and mass variation over time

For expansions and mass monitoring, measurements are taken every week in accordance with the recommendations of standard NF P18-427, and the initial measurement must be taken just after the saturation stage and before immersion in the tanks. For each measurement, the shrinkage plots must be cleaned to remove the water and the layer of salt that has precipitated on the surface of the pads. The measurement should not exceed 15 minutes in order to limit the evaporation of the attack solution from the surface of the sample.

A.4.7.2. Formatting the results

For each test, measurements are taken on 3 samples. The result and the uncertainty are given by the mean and the dispersion of the results (min & Max).

For expansion and mass measurements, the results are shown graphically as a function of immersion time.

A.4.8. Reliability of the method

No data is yet available on the reliability of this test.

A.4.9. Optional tests

A.4.9.1. Measurement of the saturation level of specimens

Immediately after saturation, it is possible to calculate the saturation rate of the specimens by weighing them in water and in air. The saturation rate can then be calculated using the same principle as the porosity accessible to water, with the difference that the dry mass is that obtained on leaving the oven at 80 °C.

The result is expressed as follows (Equ. 1.A.1):

$$\tau = \frac{M_{air} - M_{dry}}{M_{air} - M_{water}} . 100 \qquad \text{(Equ. 1.A.1)}$$

Where:

- τ is the saturation level in %, M_{air} is the mass, in grams, of the saturated test tube weighed in air, M_{water} is the mass, in grams, of the saturated test sample weighed in water, M_{dry} is the mass, in grams, of the dry test piece in air.
- This calculation makes it possible to ensure that a large part of the porosity is saturated by the etching solution, by comparing the saturation rates with the results for porosity accessible to water obtained on healthy material.

A.4.9.2 Measurements of mechanical and physical properties on material in a degraded state

The measurements of the physical and mechanical characteristics (Arliguie and Hornain, 2007) carried out on sound material, which were used to characterize the durability of the concrete, can also be carried out on the specimens that have undergone the accelerated ageing test, after the 12 weeks of immersion.

It is then possible to calculate the relative variation of a given parameter (Equ. 1.A.2):

$$var = \frac{m_{initial} - m_{final}}{m_{initial}} . 100 \qquad \text{(Equ. 1.A.2)}$$

Where:

- var is the relative variation in % of the parameter under consideration;
- $m_{initial}$ is the result obtained on healthy material;
- m_{final} is the result obtained on degraded material (after 12 weeks of immersion).

Two concretes with different compositions can therefore be compared in terms of the relative variation in mechanical and physical characteristics that occurred during the accelerated ageing test.

A.5. Accelerated ESR test by immersion/drying (Method B)

The second accelerated protocol is based on Appendix G of Swiss standard SIA 262 (SIA 262, 2013). In this test, concrete cores cured at 100 % RH for 90 days were subjected to 4 successive cycles of drying at 50 °C / soaking at 20 °C with a solution containing 50 g of Na_2SO_4 / L, e.g.33.8 g of SO_4/L, followed by storage in this solution for a further 56 days. The length 1 and mass of each core were measured regularly. The test lasted 25 weeks (5.8

months) with a 90-day cure[1]. The cores are taken from laboratory test samples (ideally 2 cubes 150 mm x 150 mm x 150 mm) or on site.

A.5.1. Materials

- Laboratory set at 20 ± 2 °C
- Stainless steel adhesive studs
- 0.01g resolution scale accurate to 0.03 g
- Caliper with 0.01 mm resolution, accurate to 0.05 mm.
- Comparator with 0.001 mm resolution, accurate to 0.002 mm.
- Ventilated oven, regulated at 50 ± 2 °C with good air exchange in and around the oven.

A.5.2. Test specimen

The test bodies were two 150 x 150 x 150 mm cubes cured in accordance with standard NF EN 12390-2. Between the 87 and 89eme days of curing, 6 through-cores of 28 ± 1 mm were taken from the lateral faces of two cubes (Figure 1.A.3).

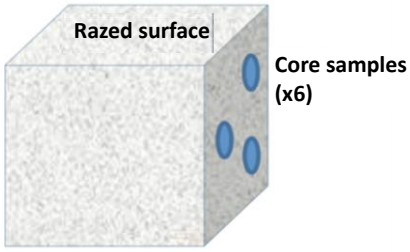

Figure 1.A.3. Taking core samples from the cubes

Before coring, sand the coring face and the opposite face so that they are parallel. Core to extract 3 cores per cube. Use a corer in good condition and a suitably powerful coring machine. Ensure that the corer is moving forward evenly, and do not "force" the corer, as this would cause micro-cracking of the cores and uneven cutting. The cores should be between 145 and 150 mm long.

Using a calliper, measure the initial length (L) in mm to the nearest 0.1 mm of the 6 cores and their diameter (d) in mm at several points to the nearest 0.1 mm. Store the cores in boxes at 20 ± 2 °C and between 70 and 90 % RH.

On day 90th, glue the stainless steel studs to both ends of the cores using epoxy resin and the centring device.

Mark the location of the stud with a pencil. The part of the surface covered by the stud and the glue must not exceed 15 mm in diameter.

[1] *The 90-day cure is prescribed for composite cement concretes or concretes containing chemically reactive mineral additions. It may be reduced to 28 days for CEM I-based concretes or concretes containing no non-reactive mineral additions*

A.5.3. Carrying out the test

One hour before starting, immerse the cores in water at 20 °C for 60 ± 10 min, then measure the initial length (L_0) in mm to the nearest 0.001 mm using the 145 mm invar bar. Check this bar and the comparator regularly with a reference bar.

At t_0 of the test, place the cores in a ventilated chamber at 50 ± 5 °C for 120 ± 2 hours (5 days). The cores should be placed on small triangular sticks 10 mm high and perforated shelves to allow even air circulation around the concrete. After this time, remove the cores from the oven, cool them to 20 ± 2 °C for 1 hour in a desiccator (RH < 5%) and then measure their mass (m_{T1}) in g to the nearest 0.01 g.

The 6 cores were then immersed for 48 ± 2 h in a 50 g/L Na_2SO_4 solution (33.8 g SO_4/L). The solution is prepared by pouring 50 g of Na_2 SO_4 into 950 g of demineralised water. The volume of solution ($V_{solution}$) should be 2.4 L. The cores must be completely immersed. The dishes must have a tight-fitting lid. The cores must be separated from the bottom of the dish, from the sides and from each other by at least 10 mm. Place only one series of 6 carrots per box. After this time, remove the cores from the solution, dry them, measure their length (L_1) in mm to the nearest 0.001 mm and weigh them (m_{s1}) in g to the nearest 0.01g.

Replace the cores in the study and carry out 3 other cycles identical to the first. Measure m_{T2}, m_{T3} and m_{T4}, L_2, L_3 and L_4, m_{s2}, m_{s3} and m_{s4}.

Following the 4th cycle, after measuring mass and length, return the cores to the sulphate solution for 56 days. At 7, 14, 28 and 56 days from the start of this permanent immersion, remove the cores, wipe them dry and measure their length and mass:

- L_5 and m_{s5} at 7 days;
- L_6 and m_{s6} at 14 days;
- L_8 and m_{s8} at 28 days;
- L_{10} and m_{s10} at 42 days;
- L_{12} and m_{s12} at 56 days with an accuracy of 0.001 mm and 0.01g.

Figure 1.A.4 - Measuring device

A.5.4. Calculations and test results

Various calculations need to be made to monitor CSR progress:

- calculation of the initial core volume: $V_0 = (d^2\pi.L) / 4.10^9$ in m, d and L in mm;
- calculation of the change in length at maturity: $dL_n = (L_n - L_0)/L$ in ‰, n = 1 to 12;

- calculation of the change in mass at maturity: $dm_{sn} = (m_{sn} - m_{Tn}) / V_0$ in kg/m^3, n = 1 to 4;
- calculation of the elongation after permanent storage in the sulphate solution: $dL_s = dL_{12} - dL_4$ in ‰;
- calculation of the change in mass after permanent storage in the sulphate solution: $dm_s = (m_{s12} - m_{s4}) / V_0$ in kg/m^3.

Note any problems or signs of degradation observed during the test (cracking of cores, detachment of aggregates, detachment of blocks, etc.).

The final result of the test is the average elongation after permanent storage in the sulphate solution (dL_s) on the 6 test specimens (or less if some specimens can no longer be measured at the end of the test).

Note: In the case of extreme values that are high and asymmetric in relation to the mean, the mean can be replaced by the median of the results.

A.5.5. Reliability of the method

The test method is reliable according to:

- a repeatability of 0.02 ‰;
- reproducibility according to the level of expansion (Table 4).

Table 1.A.4. Reproducibility of the test according to the level of expansion

Expansion level (‰)	Reproducibility (‰)
0.20	0.05
0.77	0.22
1.79	0.61

References

(Arliguie and Hornain, 2007) GranDuBé, Grandeurs associées à la durabilité des bétons, sous la direction de Ginette Arliguie et Hugues Hornain, 440 p., Presse des Ponts, 2007.

(Cassagnabère and Carcassès, 2013) Cassagnabère F., Carcassès M., Complément expérimental 2 à la thèse de S. Messad, Rapport de recherche LMDC, 2013.

(Garcia and Carcassès, 2009) Garcia V., Carcassés M., Complément expérimental 1 à la thèse de S. Messad, Rapport de recherche LMDC, 2009

(LCPC, 2010) LCPC, 2010, Maîtrise de la durabilité des ouvrages d'art en béton - Application de l'approche performantielle, Recommandations provisoires, Techniques et Méthodes des LPC, 56 p.

(Linger *et al.*, 2014) Linger L., Carcasses M., Rozière E., Cassagnabere F., Cussigh F., Nicot P., Essai de vieillissement accéléré de l'attaque sulfatique externe pour l'application du concept de performance équivalente dans le cadre de la norme EN 206-1.

(Messad, 2009) Messad S., Mise au point d'un essai de vieillissement accéléré de l'attaque sulfatique externe pour l'application du concept de performance équivalente dans le cadre de la norme NF EN 206. Thèse de Doctorat de l'Université de Toulouse, 2009.

(Rozière *et al.*, 2013) Rozière E., Loukili A., El Hachem R., Etude de la durabilité des bétons par une approche performantielle (basée sur des essais de vieillissement accéléré) Compléments expérimentaux : influence du séchage à 80 °C sur le classement des

performances des bétons exposés aux attaques sulfatiques externes, Rapport de recherche GEM, 2013.

(SIA 262, 2013) SIA, Concrete construction - Additional specifications. Swiss Standard, 2013.

APPENDIX B: Biogenic sulfuric acid attack of mortar and concrete in sewage systems

B.1 Introduction

As part of the testing of the performance of cementitious materials in a wastewater treatment environment in the presence of hydrogen sulphide, two procedures were selected. These are accelerated ageing tests on concrete specimens, involving exposure to sulpho-oxidising biological activity. The various test parameters were chosen to accelerate the attack sufficiently to obtain a discriminating test on concrete or mortar over a period of 12 or 24 weeks.

Two methods are available for determining the resistance of concrete to biodeterioration by biogenic sulphuric acid, differing in particular in the nature of the source of reduced sulphur:

- Method 1 "Accelerated biodeterioration test in the presence of hydrogen sulphide (H_2S)". This method was initiated at Fraunhofer UMSICHT Oberhausen (Holger *et al.*, 2018) and is being developed at Université Gustave Eiffel (Herisson *et al.*, 2013; Grandclerc *et al.*, 2018) (part B.2).
- Method 2 "Accelerated biodeterioration test using tetrathionate (S4O62-) as a source of reduced sulphur (BAC Test)". This method was developed at INSA Toulouse in the course of several studies (Peyre-Lavigne *et al.*, 2015a, 2015b, 2016; Aboulela *et al.* 2021), (part B.3).

The choice between two protocols depends on the equipment available in the analysis laboratory.

The protocols require the use of a microbial consortium whose sulpho-oxidising activity must be verified prior to the test (part B.4).

B.1.1 General

Biogenic sulfuric acid attack on concrete (sometimes called biogenic sulfuric acid corrosion or BSC) is a damage situation that often occurs, for instance, in sewer systems, building drainage, wastewater treatment plants and biogas plants. Biogenic sulfuric acid (BSA, H_2SO_4), which is formed in the lithotrophic metabolism of sulfur or sulfur compounds oxidizing bacteria as an end-product (mainly by conversion of sulfur), leads to a combined chemical-biological attack on the surfaces. The development of the sulfuric acid is a result of various metabolic processes in the biological sulfur cycle, which is determined by sulfate-reducing (SRB) and sulfur-oxidizing (SOB) bacteria. Figure 1.B.1 shows the mechanism of BSC in the example of a sewer system made of concrete.

Sulfide is formed aerobically from organic sulfur compounds in the sewage by methylotrophic microorganisms as well as anaerobically from anorganic compounds like sulfate in sludge deposits by sulfate-reducing bacteria, which is then transformed into hydrogen sulfide (H_2S). H_2S gas is emitted into the vapour space (stripped from the waste water with increasing temperature and pH), absorbs on the (alkaline) pipe surface and undergoes an autooxidation to intermediate such as sulfur and other reduced sulfur compounds including polythionates. SOB like thiobacilli then convert the H_2S and/or the intermediates into sulfuric acid causing the deterioration of the cement-based building material by acid and sulfate attack.

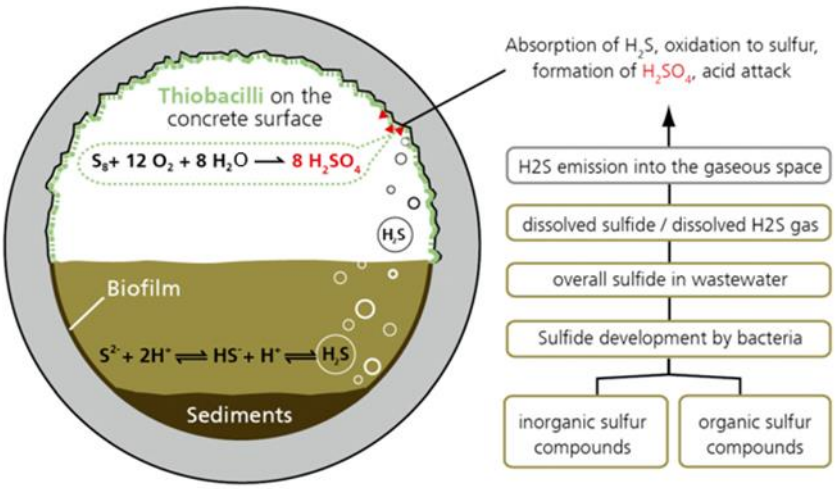

Figure 1.B.1. Mechanism of biogenic sulfuric acid corrosion presented by the example of a sewer system according to Bock *et al.*

B.1.2 Importance of biotic environmental factors for corrosion of cementitious materials

From the chemistry it is known that H_2S chemically reacts with alkaline materials to produce elemental sulfur and, derived from this, also polythionates like thiosulfate and tetrathionate. Sulfuric acid is generated by the oxidation of elemental sulfur and polythionates through the presence of sulfur oxidizing microorganisms. In doing so, interactions between the microflora and the cementitious substratum become evident which are arising from the chemical composition of this special working material.

In the course of this approach the interactions between microorganisms and materials will be included in the biological tests. The biodeterioration test is adapted to any environment where H2S is present, and specifically in this standard for the exposure class XWW4 according to DIN 19573 and is applicable to any cementitious mortar.

B.2 Test for resistance to biodeterioration with H_2S as reduced sulfur source

B.2.1 General

The biodeterioration test is carried out in a hermetic chamber. It can be operated on different types of materials simultaneously depending on the useable space. In all cases, one of the materials studied must be a mortar using a commercial available CEM I SR0 and silica sand as reference sample. This test aims (i) to validate the proper functioning of the test (material degradation) and (ii) to compare the performance of other materials with this reference.

Samples prisms are stored in the chamber and submitted to biogenic sulfuric acid produced by sulfur oxidizing bacteria in well-defined environmental conditions. The bacteria inoculum comes either from activated sludge recovered in a wastewater treatment plant or from specific selected bacteria strains. Hydrogen sulfide (H_2S) is used as sulfur source. To ensure the performance of the test, the bacteria inoculum should be validated using the procedure **"**sulfur-oxidizing potential of an environmental microbial consortium" (part B4).

The evolution of the sample biodeterioration can be evaluated each month and at least at the end of the test after 6 or 8 months of exposure. Mass change and pH values are the main measured test parameters.

The conditions of the test enable the impact of the material on the biological activity to be taken into account and thus makes it possible to test mortars with specific characteristics that lead to an alteration or inhibitation of bacterial activity including the production of sulfuric acid.

NB: This test involves the formation of H_2S inside the chamber. Safety conditions must be taken for the persons conducting this test.

B.2.2 Test method

B.2.2.1 Brief description

Studied samples are exposed in a chamber with specific environmental conditions (T = 30 °C, RH = 100 %, H_2S = 100 ppm). These parameters are monitored during the test.

They are previously inoculated with activated sludge or the bacteria inoculum containing sulfur oxidizing bacteria (verified by a method to validate the sulfur-oxidizing potential of a microbial consortium, cf. part B4).

After 6 or 8 months of exposure to the test, determinations of mass change and surface pH are measured and compared with a reference sample. The analysis allows defining a rate of degradation in the conditions of the testing methods

B.2.2.2 Sampling

Representative samples of cementitious material are used for the test. In the case of mortars, they have a size of 2 cm x 2 cm x 2 cm, extracted by sawing from a mortar cast in a 4 cm x 4 cm x16 cm or 2 cm x 2 cm x16 cm mold. In the case of concrete, they are taken from an ∅11 cm x H 22 cm concrete cylinder by sawing to obtain half-rounds 2 cm thick.

Test samples are manufactured according to the procedure specified by the applicant. The control mortar sample is formulated with CEM I SR0 cement and prepared in accordance with EN 196-1. The control concrete sample is formulated with CEM I SR0 cement dosed at 350 kg/m^3, with a water to cement ratio of 0.5 and siliceous reference aggregates complying with the requirements of standard NF EN 480-1 (a water-reducing admixture may be used if necessary).

The number of samples to be prepared is 5 for each formulation (control or test formulations).

After demolding, the mortar or concrete samples are stored in sealed bags (endogenous hydration) for 28 days. In the absence of a recommendation from the applicant, the same procedure is applied to the mortar and concrete samples to be qualified.

B.2.2.3 Reagents and test equipment

Unless otherwise specification, the chemicals used are chemical product with purity for analysis:

- distilled water, demineralized water, deionized water or water of equivalent purity (5-pH-7,5) with a conductivity of less than 0.1 (or 0.5) mS.m^{-1} in accordance with quality 2 (or 3) specified in EN ISO 3696;
- sodium sulphide Na_2S;
- hydrochloric acid;
- nutrient environment for microbial consortium: 0.25 g/L of $CaCl_2.2H_2O$, 0.4 g/L of $MgCl_2.2H_2O$, 1.4 g/L of NH_4Cl and 5 g/L of $Na_2S_2O_3.5H_2O$;

- containers (in glass or in plastic) for the reagents or such where the reactions are operated, placed in or out of the chamber;
- circulating air oven;
- sample support for each formulation. The contact surface between sample and support must be drastically limited to avoid any liquid retention;
- dosing pumps (e. g. peristaltic pump) to introduce reagents accurately;
- H_2S concentration measuring sensor linked to the H_2S production;
- temperature sensor;
- heating belt or temperature system to obtain a temperature of 30 °C inside the chamber;
- pipe connections and pipes;
- balance with an accuracy of 0.01 g;
- caliper gauge;
- camera;
- pH indicator paper or pH meter;
- shaker or ultrasonic system;
- biodeterioration chamber: it must be hermetic to avoid any risk of H_2S leaking. Its geometry may vary depending on the desired volume (number of samples to be studied). The example given on the following figure corresponds to a chamber of cylindrical or cube like geometry of volume 75 up to 300 L, closed by a cover plate with a seal. In the lower part of the chamber an evacuation system of the liquid phase is necessary. Liquid is filled up to a height of 20 cm and the temperature is maintained by a heated belt or a heat exchanger system. The cover plate is adapted to inputs (nutrients spray, H_2S supply) and outputs as gas outlet containing H_2S.

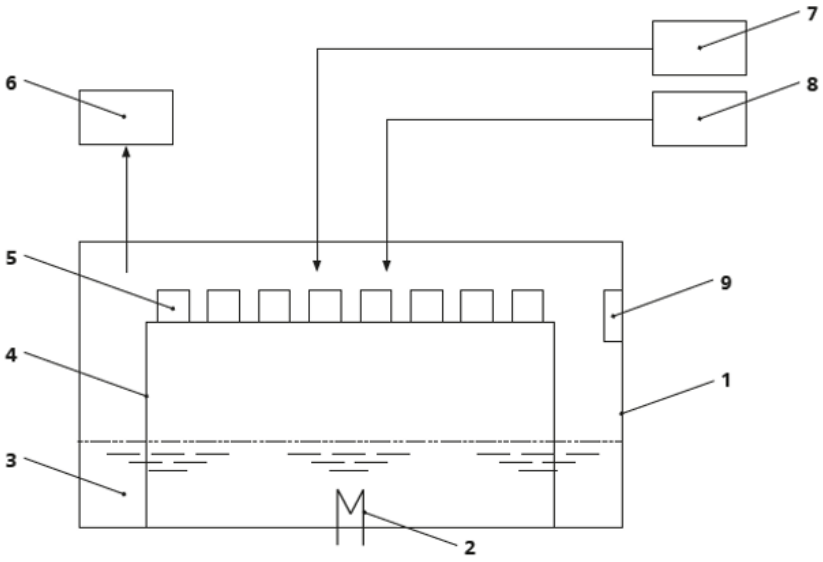

Legend

1 Chamber	**6** Exhausting system
2 Temperature system	**7** Nutrition supply and control
3 Water	**8** H_2S-gas supply and cotrol
4 Rack for samples	**9** Sensors for H_2S, Temperature, Humidity
5 Samples	

Figure 1.B.2. Scheme of the test facility

B.2.2.4 Manufacture and maintenance of samples

For all samples the mass after drying at 40 °C (3 days) is determined and taken as a reference weight.

The formulation and manufacture of the cementitious material to be studied is left to the initiative of the applicant.

B.2.2.5 Procedure

B.2.2.5.1 Sample measurements before the test

Label the studied materials sample. Since a handwriting on the samples can disappear during the test, it is recommended to take a photograph of the sample and the sample support with the index of the sample written of the sample support. Furthermore, the positions of the samples onto the rack should be recorded using a “chess field” nomenclature.

Measure the mass of all samples. Afterwards the dry mass of all samples is measured at 40 °C (3 days) in a circulation air oven. Measure the dimensions of the samples (± 0.1 mm) taking a caliper gauge.

Measure the surface pH of the sample (± 0.1 pH value) with a pH paper indicator or a pH meter with a surface electrode. In case the surfaces of the samples dry out during the opening of the chamber place a droplet of dionized water (ca. 0.1 ml) in the middle of the surface, wait 15 seconds, and carry out the measurement.

Take a photograph of each side of each sample using a scale (increment ± 1mm).

B.2.2.5.2 Pretreatment of the materials

The aim of this pre-treatment is to decrease the surface pH of the tested sample to enable the implantation of the biological activity.

Introduce water at the bottom of the chamber and start the temperature system (set temperature within the chamber at 30 °C). Adjust the humidity of the chamber at 100 %.

Arrange all samples on their support in the biodeterioration chamber.

Prepare a zinc acetate solution (2 L at 50 g/L) in a beaker (in order to neutralize H_2S at the output of the chamber) or use an exhausting system.

Prepare a sodium sulfide solution ($Na_2S.9H_2O$) (2 L at 0.08 mol/L) and a hydrochloric acid solution (2 L at 1.40 mol/L) in two separated beakers.

NB: Concentrations of $Na_2S.9H_2O$ and HCl are given as an indication for targeted H_2S concentrations. However, adjustments may be necessary to obtain these concentrations (concentration/flow correlation). H_2S production can be carried out in the chamber or outside the chamber by a separate reactor.

Close the chamber and set up the connections between the chamber and the dosing pump, the H_2S supply, the nutrition supply, and the zinc acetate solution or exhausting system. Start H_2S supply and check that bubbles appear in the zinc acetate solution or that the exhausting system is working.

Set the dosing pump that controls the injection of $Na_2S.9H_2O$ and HCl solutions for an average H_2S concentration of 100 ppm or use a pump control with the H_2S sensor to have a value of 100 ppm.

Start the dosing pump. This pre-treatment step lasts 2 weeks.

B.2.2.5.3 Inoculation of the sample surface with activated sludge or bacteria inoculum and weathering

Turn off the dosing pump after two weeks of H_2S pretreatment and wait for the H_2S concentration to reach 0 ppm. Take samples out of the chamber.

Measure the surface pH of the samples.

Centrifugate 50 mL of activated sludge into Falcon® 50 mL tubes (one tube per sample to cover); centrifugation (3000 G during 20 minutes) and remove the supernatant.

Spread the activated sludge all over the surface of each side of the mortar cubes with a brush.

Dry for an hour so that the sludge can adhere to the surface of the material.

Place the samples in the chamber using supports and start the weathering test (take care of the position defined in the first step).

B.2.2.5.4 Weathering

Set up all the connections between the spray system and the chamber.

For H_2S supply prepare 2 L of $Na_2S.9H_2O$ solution at 0.08 mol/L and 2 L of HCl solution at 1.40 mol/L and connect the containers to the dosing pump.

Start air injection and check that bubbles appear well in the zinc acetate solution. In case an exhausting system is used check that the system is working.

Set the dosing pump that controls production of H_2S, by reaction of $Na_2S.9H_2O$ and HCl solutions and achieve an average H_2S upper than 100 ppm.

Prepare 2L of nutrient solutions (0.25 g/L of $CaCl_2.2H_2O$, 0.4 g/L of $MgCl_2.2H_2O$, 1.4 g/L of NH_4Cl and 5 g/L of $Na_2S_2O_3.5H_2O$). Start the control system for nutrient spraying. During operation of the test chamber, the samples are regularly sprayed with a nutrition solution to provide the bacteria with nitrogen, phosphate, and micronutrients (trace elements). A volume of 1 L per week should be used for a sample surface of 6000 cm^2.

NB Test Maintenance of the H_2S sensor: (i) check the operation of the sensor according to the supplier's instructions and (ii) check and renew the various solutions if necessary ($Na_2S.9H_2O$, HCl, nutrients, acetate zinc) and drain the beaker inside the chamber in case H_2S is produced in the chamber.

B.2.2.6 Measurements

During the weathering a weakly inspection of samples is carried out. For this step, the opening of the chamber is necessary. Stop the supply of H_2S and wait for H_2S concentration to reach 0 ppm. Afterwards measure the pH of the sample surfaces using 3 samples and continue the weathering.

Depending on the objectives, the following analysis can be carried out at different deadlines depending on the number of samples. In all cases the final deadline (8 months or less depending on the visible evolution of the samples) will require the analysis of the samples:

- for this step, the opening of the chamber is necessary. Stop the supply of H_2S and wait for H_2S concentration to reach 0 ppm;
- open the chamber and take out the samples;
- weigh all the samples (± 0.01 g);
- measuring the dimensions (3 dimension by cubes) of samples (± 0.1 mm);
- take a photograph of all samples using a scale. (increment 1 mm);
- measuring the pH of samples (± 0.1 pH value).

At the end of the test, after carrying out the above analyses, dry the samples for 1 week at 40 °C in the oven, resinate them and cut them in 2.

Photograph or scan the samples (photographs should be scaled in 1 mm increments) and determine the healthy area of the sample. From the difference between the initial area of the sample and the measured healthy area, deduce the degraded thickness.

B.2.2.7 Expression of the results

The test report must specify:

- characteristics of the studied samples and of the reference sample documented by taking photos of each sample using a scale;
- the environmental conditions (T, H_2S, RH) in the chamber, which were monitored and logged during the test;
- remaining mass and resulting surface pH of each sample at the end of the test;
- Calculation of the average values used to determine the degradation index
- Degradation index normalized to that of a CEM I SR0-based control material for all test samples:

  Ibio/tem = Degraded thickness $_{\text{of sample}}$ / Degraded thickness $_{\text{of control}}$

B.2.2.7.1 Before the test

Table 1.B.1 shows the data collected before the start of the test for a test sample and the control material. All materials are tested in five copies, so 10 samples are exposed.

Table 1.B.1. Data to be collected for each material sample prior to testing

Samples	Mass (g)	Dimensions (mm)	pH
Control_1			
…			
Control_5			
Sample_1			
…			
Sample_5			

The activity of the sulfo-oxidant consortium was verified according to the protocol in Part B.4.2 of this document.

B.2.2.7.2 During the test

The conditions of exposure to H_2S (Table 1.B.2) in the enclosure must be indicated on a monthly basis, giving the mean value, standard deviation, median, 3rd quartile and maximum value per month. The same information should be given for the entire duration of exposure.

Table 1.B.2. Data to be collected monthly for H_2S content

	Mean	Standard deviation	Mediane	3rd quartile	Maximum
Pre-treatment					
Month 1					
…					
Month 8					
8-month report					

Table 1.B.3 shows the data and results collected for a material exposed after pre-treatment and then each month.

Table 1.B.3. Data to be collected during the test at each sampling month

	Mass (g)	Dimensions (mm)	pH
Pre-treatment			
Month 1			
…			
Month 8			

B.2.2.7.3 At the end of the test

Plot the mean variations and standard deviations of mass, dimension and pH of each formulation as a function of time.

Show photos of samples for each month of exposure for all exposed samples (Figure 1.B.3).

	6 or 8 months of incubation
Control	
Sample	

Figure 1.B.3. Cross-sections of different formulations after 6 or 8 months of incubation

Present photos/scans of samples for each resinated and sawn sample, then deduce the average degraded thickness per formulation, then deduce $I_{bio/tem}$ = degraded thickness $_{of\ sample}$ / degraded thickness $_{of\ control}$ (Table 1.B.4).

Table 1.B.4. Average degraded thickness of different formulations after 6 or 8 months incubation and $I_{bio/tem}$ index

Sample	**Average of Degraded thickness**	**$I_{bio/tem}$**
Control		
Sample		

B.3 Test for resistance to biodeterioration with tetrathionate ($S_4O_6^{2-}$) as reduced sulfur source (BAC Test)

B.3.1 General

The biodeterioration test is adapted to any environment where H_2S is present, and specifically in this standard for the exposure class XWW4 according to DIN 19573 and is applicable to any cementitious mortars, with or without admixtures (chemicals, biocide, etc.). Cementitious samples are first inoculated with an environmental microbial consortium (an activated sludge), and are then exposed to the trickling of a feeding solution containing a reduced sulfur source, tetrathionate ($S_4O_6^{2-}$), and nutrients. In presence of oxygen naturally present in the air sulfur-oxidizing microorganisms in the consortium oxidize tetrathionate ($S_4O_6^{2-}$) into biogenic sulfuric acid on the surface of the exposed cementitious samples. To ensure the performance of the test the sulfur-oxidizing activity of the activated sludge shall be validated using the procedure presented in appendix D.
A reference mortar shall be tested (CEM I mortar made with silica sand). This test aims (i) to validate the proper functioning of the test (material degradation) and (ii) to compare the performance of other materials with this reference.

The duration of exposure of the samples to the trickling solution is 3 months. The trickling solution is collected weekly downstream of each sample to analyze the concentration of calcium and sulfate ions and to measure the pH. In order to grade the mortars for corrosion resistance to biogenic sulfuric acid, the ratio of the cumulative leached calcium standardized by the calcium initially present in the exposed materials per square meter of exposed surface, to the sulfate produced is used.

B.3.2 Symbols

d_n: sampling day of the leaching solution (day)

m_0: dry mass of one sample after dry protocol, without epoxy resin (in gram)

m_1: dry mass of one sample covered with epoxy resin (in gram)

L: length of the sample (m)

w: width (m)

th: thickness (m)

S: exposed surface (m^2)

mv_0: initial mass of the empty vial dedicated to collect the leaching solution for each material sample (in gram)

mv_n: mass of the vial with the collected leaching solution for each material sample at the sampling day d_n (in gram)

$Tot(Ca)_{ini}$: initial content of calcium in the exposed material (in mol)

t_n: sampling time at the sampling day d_n (in hours)

Q_{dn}: water flow trickling at the surface of the exposed material at the sampling day d_n.

$[i]_{dn}$: concentration measured in the leaching solution at the sampling day d_n (in mol/L)

$F(SO_4^{2-})_{dn}$: punctual flux of produced sulfate for each sample at the sampling day d_n (in mol/d)

$F(SO_4^{2-})_{dn+1}$: punctual flux of produced sulfate for each sample at the sampling day d_{n+1} (in mol/d)

$Tot(SO_4^{2-})_{dn+1 - dn}$: amount of produced sulfate for each sample between the sampling day d_n and the sampling day d_{n+1} (in mol)

$Tot(SO_4^{2-})_{dn}$: total amount of produced sulfate for each sample from the start-up of the test exposure to the sampling day dn (in mol)

$F(Ca^{2+})_{dn}$: punctual flux of leaching calcium for each sample at the sampling day d_n (in mol/d)

$Tot(Ca^{2+})_{dn+1 - dn}$: amount of leaching calcium for each sample between the sampling day d_n and the sampling day d_{n+1} (in mol)

$Tot(Ca^{2+})_{dn}$: total amount of leaching calcium for each sample from the start-up of the test exposure to the sampling day dn (in mol)

$(Ca/Cam^2)_{dn}$: total amount of leaching calcium for each sample divided per the initial content of calcium in the exposed material per square meters of exposed surface.

B.3.3 Test method

B.3.3.1 Brief description

The general principle is to expose the surface of a cementitious mortar sample inoculated with a microbial consortium to a trickling solution containing a soluble form of reduced sulfur (tetrathionate) to activate a biological sulfur-oxidizing activity in contact with the exposed sample. This sulfur-oxidizing activity produces sulfuric acid on the surface of the cementitious material leading to its biodeterioration. The durability of the material is evaluated by the comparison to a reference (CEM I) mortar exposed in the same conditions. The performance criterium is the ratio of the cumulative leached calcium standardized by the calcium initially present in the exposed material per square meter of exposed surface, to the sulfate produced.

B.3.3.2 Sampling

The recommended size of mortar sample is 8 cm x 4 cm x 2 cm (typically obtained from the sawing in 4 equal parts of 4 x 4 x16 cm^3 mortar specimens).

The control mortar is a mortar made of ordinary Portland cement (CEM I[2]) prepared according to the standard EN 196-1.

The number of samples to be prepared is 3 for each mortar design (reference mortar and mortar designs to be assessed).

After removal from the moulds, the reference mortar samples are kept in sealed bags (endogenous curing) for 28 days. Without specific recommendation of the applicant, the same procedure is applied to the tested mortar samples.

After sawing of the mortar samples, all surfaces of the obtained prisms must be sanded down with 320-grade wet abrasive paper, applying even pressure to each surface for about 15 secs. Remove any abrasive dust that adheres.

B.3.3.3 Reagents and test equipment

Unless otherwise specified, the chemicals used are chemical product with purity for analysis.

[2] In this test reference is made to a benchmark mortar made with CEM I 42.5 R SR0 cement and a water/cement ratio of 0.5. Cement content is 450 g and aggregate (CEN-standard sand) 1350 g.

Distilled water, demineralized water, deionized water or water of equivalent purity (5-pH-7,5) with a conductivity of less than 0.1 (or 0.5) $mS.m^{-1}$ in accordance with quality 2 (or 3) specified in EN ISO 3696.

Nutrient environment for microbial consortium:

- $K_2S_4O_6$
- NH_4Cl
- $(Na(PO_3))_3$
- $MgCl_2$, $6H_2O$
- $MnCl_2$
- $FeCl_3$, $6H_2O$
- H_3BO_3
- $CoCl_2$, $6H_2O$
- $ZnSO_4$, $7H_2O$
- Na_2MoO_4, $2H_2O$
- $CuSO_4$, $5H_2O$
- $NiCl_2$, $6H_2O$

Biodeterioration pilot:

- Thermostated tank (4 °C) 100 L (minimum) with mixing system ((1) in the Figure 1.B.4 and (2) for the thermostated system). The composition of the feeding solution ((3) in the Figure 1.B.4) is described after.
- Peristaltic pumps (flows 20 ± 5 mL/h) ((4) in the figure 1.B.4) with tubes (PTFE Tube natural 0.50-1.00 mm) and connection tubes.
- Plastic plate with two face adhesive gel to support the samples of tested material ((5) in the Figure 1.B.4).
- Inox or plastic support for the plastic plate and designed to incline samples of tested material (5° ± 2°) (position of the sample describes in the Figure 1.B.4 (b) and (c).
- Leached disposal solutions recovery bin with liquid evacuation system by gravity ((4) in the next Figure 1.B.4)

(a)

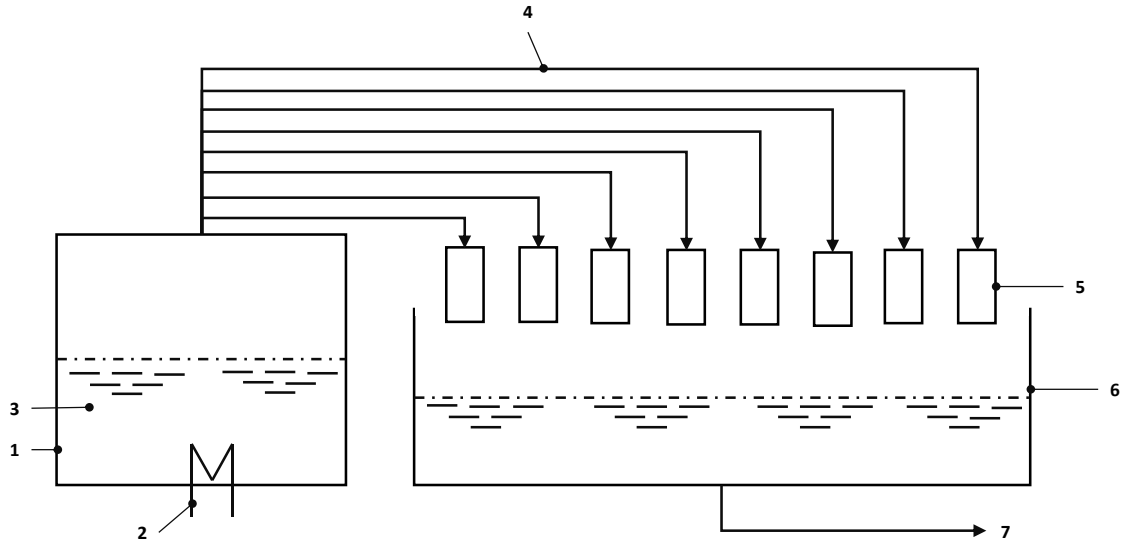

1. Feeding tank
2. Thermostated system
3. Feeding solution
4. Peristaltic pumps and connection tubes
5. Exposed sample
6. Recovery bin
7. Liquid evacuation system

(b) General view of one exposed sample (5 in the figure above)

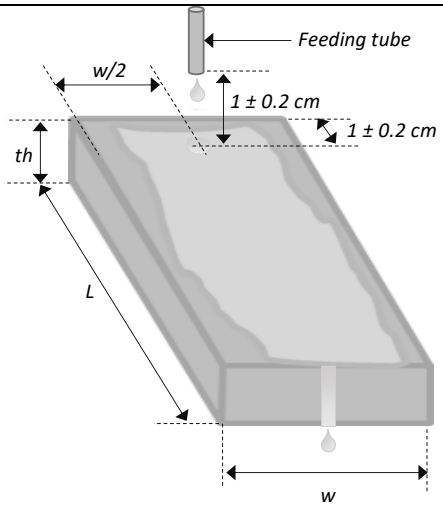

(c) Lateral view of one exposed sample (5 in figure a) with the location of the vial to collect the leaching solution

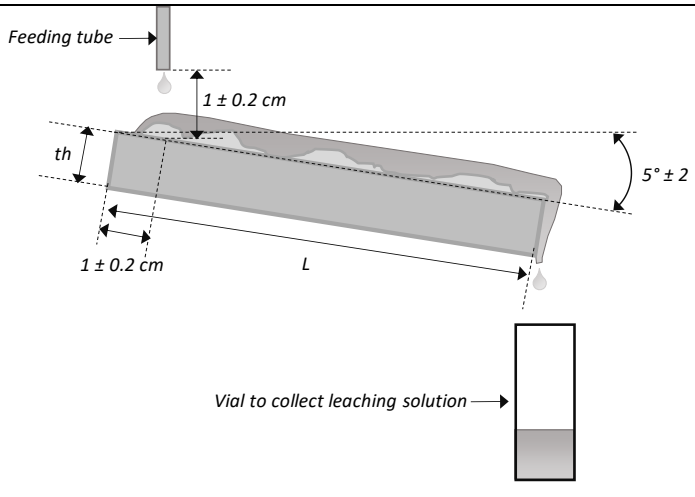

Figure 1.B.4. Scheme of the biodeterioration pilot (BACTest) (a), and of one exposed sample with the location of the feeding tubes and the vial for the sampling of the leaching solution (b) perspective view; (c) side view.

B.3.3.4 Procedure

B.3.3.4.1 Preparation of samples and measurements before the test (d0)

a. For the mortar samples

Weigh each sample → m_0 (in gram)

Measure the dimensions of the samples (length (L), width (w), thickness (th)). Use a caliper ± 0.1 mm.

To expose a set surface Keep the cast 4x8 cm2 face free and spread resin (epoxy resin resistant to acidic environment) on the 5 other surfaces as describes in the Figure 1.B.5.

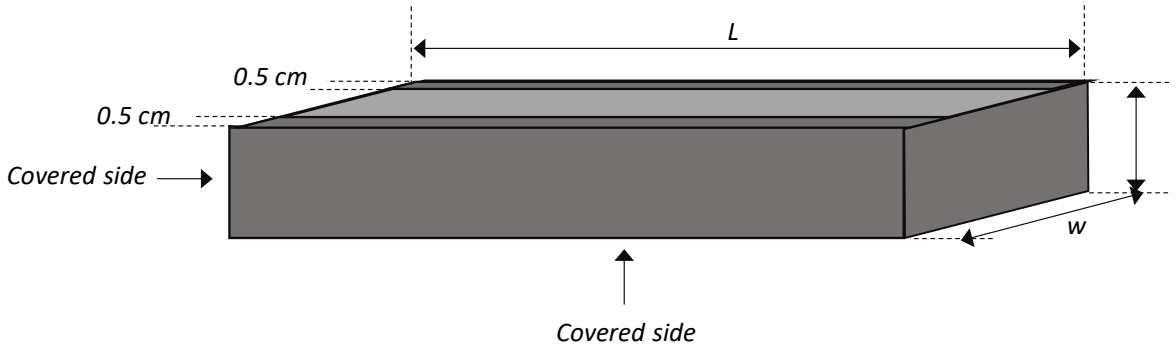

Figure 1.B.5. Scheme of the sawn mortar sample illustrating the faces covered with epoxy resin

After covering the un-exposed surface with the epoxy resin:

- weigh each sample → m_1 (in gram);
- take a photograph of each sample.

b. For the analysis of the leaching solution

- prepare one 50 mL vial per mortar sample and label it accordingly;
- weigh each closed vial → mv_0 (in gram).

B.3.3.4.2 Preparation of the feeding solution

- fill the feeding tank with deionized water;
- add nutritive salts to the deionized water. The feeding solution consists of deionized water and various dissolved salts pre-prepared and stored in separate glass bottles stored at 4 °C to prevent any microbial growth. Table 1.B.5 shows the composition of the feeding solution.

Table 1.B.5. Composition of the feeding solution

Compound	Concentration	Unit	Salt
$S_4O_6^{2-}$	158.86	mgS-S_4O_6(2-)/l	$K_2S_4O_6$
N-NH_4^+	3.93	mgN-NH_4(+)/l	NH_4Cl
P	1.71	mgP/l	$(Na(PO_3))_3$
Mg^{2+}	0.18	mgMg(2+)/l	$MgCl_2$, $6H_2O$
Mn^{2+}	0.03	mgMn(2+)/l	$MnCl_2$
Fe^{3+}	0.02	mgFe(3+)/l	$FeCl_3$, $6H_2O$

This solution is supplemented by a trace element solution (5 ml for 200 L of feeding solution). Table 1.B.6 shows the composition of this micronutrient solution.

Table 1.B.6. Composition of the solution of the trace elements

Compound	mg/L
H_3BO_3	0.3
$CoCl_2$, $6H_2O$	0.2
$ZnSO_4$, $7H_2O$	0.1
Na_2MoO_4, $2H_2O$	0.03
$CuSO_4$, $5H_2O$	0.01
$NiCl_2$, $6H_2O$	0.02

B.3.3.4.3 Inoculation of the sample surface with activated sludge

The objective is to pre-seed the surface of the material with a microbial consortium from the sanitation system. This type of microbial consortium is known to be very diverse in terms of microbial populations. Controlling the environment (feeding solution, exposed surface of the materials) allows the selection the microbial activity aimed and adapted as in sewer to the surface materials as in sewer environment.

- Centrifugate 500 mL of activated sludge at 4000 rpm.
- Remove the supernatant from all vials.
- Recovered the black-brown paste (solid phase corresponding to the suspended organic matter of the activated-sludge containing microorganisms).
- Use a brush to cover the surface of the materials to be exposed.
- Let dry for an hour so that the sludge adheres to the surface of the material.

B.3.3.4.4 Start-up

- Place the mortar sample on the support to have the feeding tube at 1 cm above the sample, and the drop fall on the exposed surface as described in figure 1.B.4 (b and c).

- Start the peristaltic pumps
- Control drop at the top of the exposed surface of the material
- Wait for the first drop to fall from the material after runoff. If the liquid film does not cover the entire surface of the material, gently spread the liquid film on the surface with a brush (the biofilm is not formed yet, thus no risk to disturb it).
- Wait for an hour and sample the leached solution for each exposed material.

B.3.3.4.5 Measurements

- At day n (d_n) stop the peristaltic pumps (sample days 1, 7, 14, 21, 28, 35, 42, 49, 56, 63, 70, 77, 84, 91)
- Put one 50 mL empty vial (previously weighed) downstream of each sample (see figure 1.B.4).
- Start the peristaltic pumps and measure the sampling time
- After 1 hour +/- 5 min., stop the peristaltic pumps. Note the exact sampling time t_n (in hours)

To calculate the exact water flow runoff to the exposed surfaces (Q_{tn} expressed for example the flow in ml/h at the day d_n). Weigh each vial with the leached solution recovered → mv_n (in gram)

Equation 1.B.1 present for one sample the calculation of Q_{dn}

$$Q_{dn} = (mv_n - mv_0) / t_n \qquad \text{(Equ. 1.B.1)}$$

Measure the pH (± 0.1) of the leached solution for each sample. Note the values pH_n (± 0.1) for each sample

Filter the solution to 0.45 µm to eliminate all microorganisms and particles. Store the liquid sample at 4 °C to limit microbial activities.

Analyze the concentration of the ionic compounds as sulfate, and calcium.

NB: the concentration of sulfate is measured by ion chromatography (anionic DIONEX-Thermofisher: IC25, IonPacTM AS19, at 30 C with eluent cartridge generator EGC III KOH), calcium and magnesium concentrations are measured by ion chromatography (DIONEX-Thermofisher: ICS 2000, IonPac CS12, at 30 C with elu generator cartridge EGC III MSA for methanesulfonic acid DX320-Dionex Thermofisher).

B.3.3.4.6 Maintenance during the test

To avoid colonization of the feeding solution and the connective tubes, thus the production of acid not in contact with the exposed material.

a. Renewing the feeding solution and cleaning the feeding tank

Every 2 weeks:

- collect 5 liters of the feeding solution in a container;
- put the feeding tubes in the newly filled container to continue to provide the exposed surface during the cleaning of the feeding tank;
- empty the feeding tank;

- clean the inside of the tank with a sponge and bleach;
- renew the feeding solution.

Changing the tubes

- stop the peristaltic pumps;
- change all the tubes between the feeding tank and the surface of the exposed samples;
- re-Start the peristaltic pumps.

B.3.3.5 Expression of results

The objective is to calculate the accumulation of the leached calcium per the initial content of calcium in the exposed sample per square meter of exposed surface and to plot this parameter as a function of the sulfate accumulation (indicator of the biogenic acid production). This presentation format documents the direct connection between the occurrence of the harmful pollutant and the appearance of the deterioration product in a quantitative way. By this means, an informative and distinguishable performance criterion is made available.

B.3.3.5.1 Initial calcium content in the materials

Data provided by the the material suppliers expressed as $Tot(Ca)_{ini}$ (mol) (mol) for the calcium.

B.3.3.5.2 Produced sulfate accumulation

The analysis of the leached solution provides weekly measurement of the sulfate concentration. At each sampling day d_n a punctual flux of produced sulfate is calculated. As an example, equation 1.B.2 shows the calculation of the sulfate flux produced at the sampling day d_n.

$$F(SO_4^{2-})_{dn} = Q_{dn} \times [SO_4^{2-}]_{dn} \qquad \text{(Equ. 1.B.2)}$$

Where $F(SO_4^{2-})_{dn}$ is the flux of the produced sulfate at date t1 (mol/d), Q_{dn} the flow of the runoff solution measured at the sampling day d_n (in L/d), and $[SO_4^{2-}]_{dn}$ is the concentration of produced sulfate measured in the leached solution at the sampling day d_n (mol/L).

The same calculation is done at the sampling day d_{n+1} to obtain $F(SO_4^{2-})_{dn+1}$. The quantity of produced sulfate between the sampling day d_n and the sampling day d_{n+1} is calculated by equation 1.B.3.

$$Tot(SO_4^{2-})_{dn+1\,-\,dn} = ((F(SO_4^{2-})_{dn+1} + F(SO_4^{2-})_{dn})/2) \times (d_{n+1} - d_n) \qquad \text{(Equ. 1.B.3)}$$

Where $Tot(SO_4^{2-})_{dn+1\,-\,dn}$ is the cumulative produced sulfate between the sampling day d_{n+1} and the sampling day d_n (mol) and $(d_{n+1} - d_n)$ the time between sampling days d_{n+1} (days) and d_n (days).

For each sampling day d_n calculate $Tot(SO_4^{2-})_{dn\,-\,dn+1)}$ and sum them during time to obtain at each sampling day d_n, $Tot(SO_4^{2-})_{dn}$.

B.3.3.5.3 Leached calcium accumulation

The analysis of the leached solution provides weekly measurement of the calcium concentration. A flux of leached calcium for each sample date must be calculated. As example, the following equation show the calculation of the calcium flux leached at day d_n (days).

$$F(Ca^{2+})_{dn} = Q_{dn} \times [Ca^{2+}]_{dn} \quad \text{(Equ. 1B.4)}$$

Where $F(Ca^{2+})_{dn}$ is the flux of the leached calcium at day d_n (mol/d), Q_{dn} the flow of the runoff solution measured at the day d_n (L/d), and $[Ca^{2+}]_{dn}$ is the concentration of leached calcium measured in the leached solution at day t_n (mol/L).

The same calculation is done at day d_{n+1} to obtain $F(Ca^{2+})_{dn+1}$. The quantity of leached calcium between day d_n and day d_{n+1} is calculated by equation 1.B.5.

$$Tot(Ca^{2+})_{dn+1 - dn} = ((F(Ca^{2+})_{dn+1} + F(Ca^{2+})_{dn})/2) \times (d_{n+1} - d_n) \quad \text{(Equ. 1.B.5)}$$

Where $Tot(Ca^{2+})_{dn+1 - dn}$ is the accumulation of leached calcium between day d_{n+1} and day d_n (mol) and $(d_{n+1} - d_n)$ the time between day d_{n+1} and day d_n (days).

For each date d_n calculate $Tot(Ca^{2+})_{dn+1 - dn}$ and sum them to obtain at each day d_n : $Tot(Ca^{2+})_{dn}$.

B.3.3.5.4 Leached calcium accumulation per the initial calcium content in the exposed material per square meter of the exposed surface

The results of the accumulation of leached calcium are standardized by the initial content of calcium in the exposed material and the exposed surface.

Calculate the exposed surface (S in m²) by equation 1.B.6.

$$S = L \times w \quad \text{(Equ. 1.B.6)}$$

Where L is the length of the sample (in m) and w is the width of the sample (in m).

Calculate for each day d_n the criteria $(Ca/Cam^2)_{dn}$ (in molCa/molCa.m²) using equation 1.B.7.

$$(Ca/Cam^2)_{dn} = (Tot(Ca^{2+})_{dn}/Tot(Ca)_{ini})/S \quad \text{(Equ. 1.B.7)}$$

B.3.3.6 Presentation of results

B.3.3.6.1 Before the test

The table 1.B.7 presents the data collected before the start of the test for two materials as an example (materials labelled Mat1 and Mat2, respectively) with the reference material (labelled Ref). All materials are tested in triplicate, thus 9 samples are exposed. As an example, for the first material (Mat1) the triplicates are labelled Mat1_a, Mat1_b and Mat1_c, respectively.

Table 1.B.7. Data to collect for each sample of materials before the test

Samples of Materials	m_0 (g)	m_1 (g)	L (m)	w (m)	th (m)	m_{v0} (g)
Ref_a						
Ref_b						
Ref_c						
Mat1_a						
Mat1_b						
Mat1_c						
Mat2_a						
Mat2_b						
Mat2_c						

B.3.3.6.2 Report during the test

Table 1.B.8 presents the data and the results collected for one exposed material for each sampling days d_n.

Table 1.B.8. Data to collect during the test at each sampling day d_n

Days	pH_{dn}	Q_{dn} (in ml/h)	$[SO_4^{(2-)}]_{dn}$	$[Ca^{(2+)}]_{dn}$	$Tot(SO_4^{(2-)})_{dn}$	$Tot(Ca^{(2+)})_{dn}$	$(Ca/Cam^2)_{dn}$
d_1							
d_2							
…							
d_{n-1}							
d_n							

B.3.3.6.3 Report after the test

Plot the pH of the leaching solution for each exposed sample according to time. To validate the test at the end, the pH of the leaching solution must inferior to 4.

Show photos at different times (day 0, day 28, day 63, and day 98) for all the exposed samples as presented in Figure 1.B.6 (two materials Mat1 and Mat2 given as an example). The observation of the development of a biofilm at the exposed surface and the observation of the production of white/yellow precipitate on the exposed surface validate the aggressive conditions of the test.

	Day 0	1 month	2 months	3 months
Ref_a				
Mat1_a				
Mat2_a				

Figure 1.B.6. Photos of the exposed samples at different times during the test

Plot $(Ca/Cam^2)_{dn}$ per $Tot(SO_4^{2-})_{dn}$ for all the exposed samples as presented in Figure 1.B.7 for one material (Mat1) and the reference as an example.

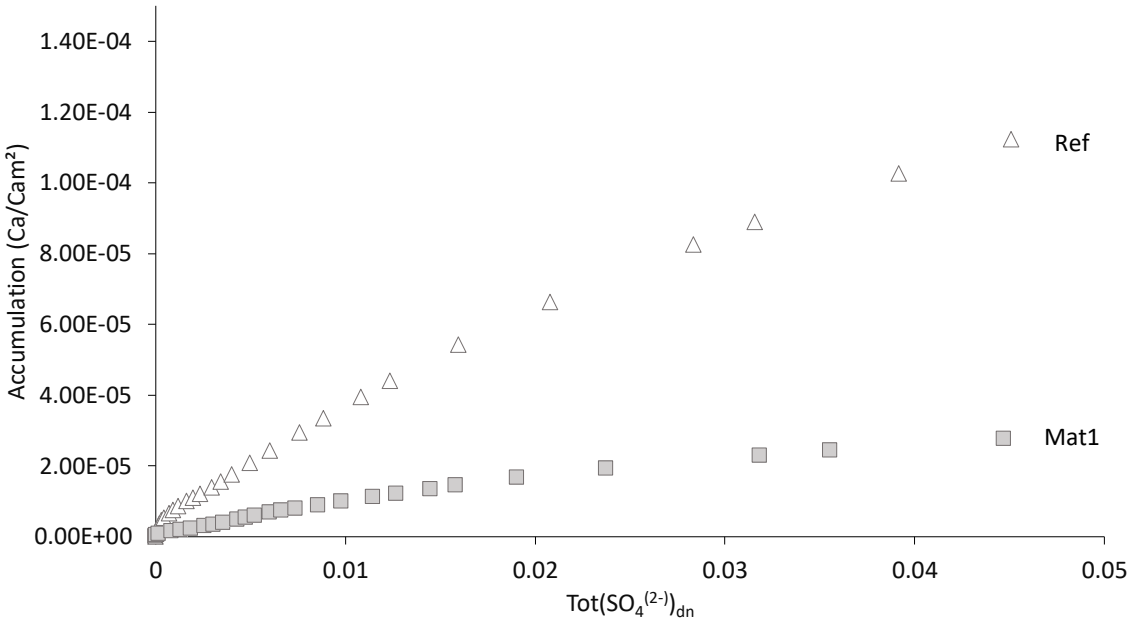

Figure 1.B.7. $(Ca/Cam^2)_{dn}$ per $Tot(SO_4^{2-})_{dn}$

B.3.3.6.4 Summary assessment

Resistance Criteria based on leaching calcium

The requirements for BAC Test for class exposure XWW4 according to DIN 19573 are satisfied if for:

- $Tot(SO_4^{2-})_{dn}$ = 0.05 mol, $(Ca/Cam^2)_{dn} < 5.10^{-5}$ molCa/molCa.m² and/or
- $Tot(SO_4^{2-})_{dn}$ = 0.1 mol, $(Ca/Cam^2)_{dn} < 8.10^{-5}$ molCa/molCa.m².

Above these values, the material is not suitable.

B.4 Test to validate the sulfur-oxidizing potential of an environmental microbial consortium

B.4.1 General

Biological testing methods to evaluate the resistance of mortars for sewers environments (class of exposure XWW4 according to DIN 19573) are based on the production of sulfuric acid by microorganisms growing at the surface of the exposed materials. This production of sulfuric is due to the succession in time of several biological activities, mainly a neutrophilic sulfur-oxidizing microbial activity in the first steps of the biodeterioration (involving several strain of microorganisms) and an acidophilic sulfur-oxidizing microbial activity in the last steps of the biodeterioration (also involving several strains of microorganisms). To provide these biological activities environmental consortia can be used. However, if this approach appears convincing and justifiable, the fact remains that all activated sludge varies from one plant to another depending on the wastewater treated, the processes implemented, but also may differ over time (depending on the seasons, rainy events, etc.). Thus to operate the biological testing methods it is necessary to validate the sulfur-oxidizing potential of the chosen environmental consortium, validate the presence of active neutrophilic and acidophilic sulfur-oxidizing microorganisms.

The objective is through successive pulses in sulfur substrate (thiosulfate ($S_2O_3^{2-}$) or tetrathionate ($S_4O_6^{2-}$)), to produce biogenic acid and by this way to validate the presence of sufur-oxidizing microorganisms. For that, only pH measurement is required due to the high acidification potential of the sulfur-oxdizing microorganisms. This acidification proves that biological oxidation has indeed taken place and therefore that the microbial consortium used has the sulfur-oxidizing potential necessary to drive the biodeterioration of cementitious materials for sewage environments.

B.4.2 Test method

B.4.2.1 Brief description

The objective is to validate the presence of a neutrophilic sulfur-oxidizing activity and an acidophilic sulfur-oxidizing activity in an environmental consortium.

The objective is to quantify the production of biogenic sulfuric acid along successive pulses of sulfur substrate (thiosulfate ($S_2O_3^{2-}$) or tetrathionate ($S_4O_6^{2-}$)) and to validate the presence of sufur-oxidizing microorganisms in the consortium. The high acidification potential of the sulfur-oxdizing microorganisms allow pH measurement only as indicator.

The tested consortium is introduced in a stirred, aerated liquid reactor. An injection of a reduced sulfur compound such as thiosulfate ($S_2O_3^{2-}$) or tetrathionate ($S_4O_6^{2-}$) is carried out. The pH of the solution is continuous or daily monitored. If neutrophilic sulfur-oxidizing microorganisms are active the biological activity produces sulfuric acid leading to a pH decrease. Subsequently a latency time is observed, and a second phase of pH lowering may be observed, linked to a slight respiration and a slight increase in the concentration of total sulfates in the culture medium. When the pH of the medium approaches 2.5, the addition of sulfur substrate leads to a rapid increase in the rate of oxygen consumption, indicating the growth of aerobic microorganisms. This increase is concomitant with a lowering of the pH and a strong evolution of the concentration of sulfates indicating at low pH the installation of an acidophilic sulfur-oxidizing activity.

B.4.2.2 Reagents

Unless otherwise specified, the chemicals used are chemical products with purity for analysis.

- distilled water, demineralized water, deionized water or water of equivalent purity (5-pH-7.5) with a conductivity of less than 0.1 (or 0.5) $mS.m^{-1}$ in accordance with quality 2 (or 3) specified in EN ISO 3696 is used;
- reagents: $K_2S_4O_6$ or $Na_2S_2O_3$.

B.4.2.3 Equipment

- Thermostated reactor (volume not defined, glass or plastic) at 20 °C with mixing system;
- Air diffuser;
- pH electrode (on line, or for punctual measurement) (range of viability pH 2 – pH 10).

B.4.2.4 Procedure

B.4.2.4.1 Preparation

It is necessary to work with diluted activated-sludge with maximum suspended solids concentration of 2 g/L (NF EN 872).

- Measure the total suspended solids of the environmental consortium (NF EN 872);
- Dissolve the chosen sulphur salt (thiosulfate or tetrathionate) in a 20 ml vial to obtain a solution at 0.4 molS/L (labelled solution 1).

B.4.2.4.2 Sulfur-oxidizing potential measurment

- Start mixing and air bubbling to ensure oxygen supply (measuring dissolved oxygen by a probe can be a plus to ensure sufficient oxygenation)[3]. Continuous dissolved oxygen concentration above 2 mg/L is sufficient to avoid oxygen limitation.
- In the case of a 1L reactor, add 10 mL of the solution 1 for an initial concentration of 4.10^{-3} molS/L in the reactor
- Monitor pH evolution[4]. If the pH decreases, the presence of neutrophilic sulfur-oxidizing microorganisms is confirmed (several examples on different sludge form different locations are presented at the end of this document)
- After pH stabilization to values below 3, perform a second injection of solution 1 (5 mL of the solution 1).
- Monitor pH evolution

14 days is the maximum duration of the test

B.4.2.5 Report and validation of sulfur oxidizing activity

Plot the pH data as a function of the time. For a solution 1 prepared with a thiosulfate salt a slight pH decrease to values around 2.3 should be observed. For a solution 1 prepared with a tetrathionate salt a pH decrease to values around 2.1 should be observed. This pH reduction may take from a few hours to to a few days. It will validate the presence of acidophilic sulfur-oxidizing microorganisms in the initial consortium.

As an example, Figure 1.B.8 illustrates pH measurements obtained for three different environmental consortia (activated sludge from different locations in France). For the three tests (labelled test 1, test 2 and test 3), the first pH decreases from 8.3 (maximal value) to 3 corresponds to the neutrophilic sulfur-oxidizing activity. 150 hours are required to reach pH 3. After this value, the pH decrease corresponds (for the three tests) to the acidophilic sulfur-oxidizing activity.

---

[3] : in the experimental conditions (with activated-sludge for example) due to the low biological needs in nutrients for the growth of the aimed microorganisms, there is no need to add supplementary nutrients to the medium as nitrogen, phosphorous or other compounds.

[4]: Considering a salt of thiosulfate of sodium ($Na_2S_2O_3$) solved in deionised water, the total oxidation of the sulfur into sulfuric acid lead theoretically to a final pH of 2.51 (the calculation is achieved considering the ionic compounds at the end of the total oxidation $Na^{(+)}$, $SO_4^{(2-)}$, $HSO_4^{(-)}$, $H^{(+)}$ and $OH^{(-)}$ and the acido-basic equilibrium concerned and the electroneutrality of the final solution. In the case of the use of a tetrathionate salt ($Na_2S_4O_6$) for the same concentration in sulfur aimed, and in the same conditions a solution with a final pH of 2.32 must be obtained.

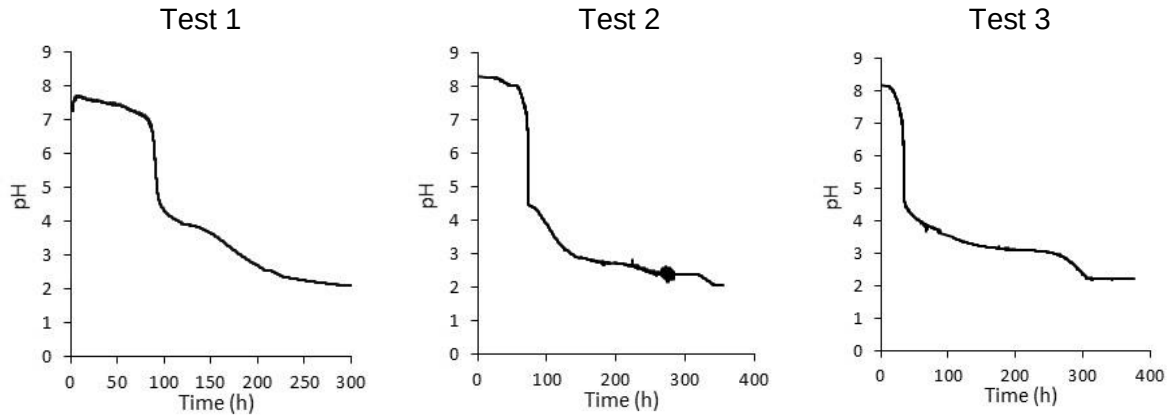

Figure 1.B.8. pH monitoring during three tests of sulfur-oxidizing activity with three different consortia from different locations

References

(Aboulela *et al.*, 2021) Aboulela A. *et al.* (2021), "Laboratory Test to Evaluate the Resistance of Cementitious Materials to Biodeterioration in Sewer Network Conditions," Materials, vol. 14, no. 3, p. 686.

(Bock *et al.*, 1983) Bock E., Sand W., Pohl A. (1983), Bedeutung der Mikroorganismen bei der Korrosion von Abwasserkanälen, TIS Tiefbau – Ingenieurbau– Straßenwesen, Sonderdruck zum 4. Statusseminar »Bauforschung und -technik, 47-49

(Grandclerc *et al.*, 2018) Grandclerc A., Guéguen-Minerbe M., and Chaussadent T. (2018), "Accelerated biodeterioration test of cementitious materials in sewer networks," in Proceedings of RILEM 253-MCI Final Conference, Toulouse, vol. PRO 123, 1, pp. 119–126.

(Herisson *et al.*, 2013), Herisson J., van Hullebusch E. D., Moletta-Denat M., Taquet P., and Chaussadent T. (2013), "Toward an accelerated biodeterioration test to understand the behavior of Portland and calcium aluminate cementitious materials in sewer networks," Int. Biodeterior. Biodegrad., vol. 84, pp. 236–243.

(Holger *et al.*, 2018) Holger W. *et al.* (2018), "Accelerated testing of materials under the influence of biogenic sulphuric acid corrosion (BSA)," in Proceedings of RILEM 253-MCI Final Conference, Toulouse, vol. PRO 123, 1, pp. 23–32.

(Peyre Lavigne *et al.*, 2015a) Peyre Lavigne M., Bertron A., Auer L., Hernandez-Raquet G., Foussard J.-N., Escadeillas G., Cockx A. & Paul E., "An innovative approach to reproduce the biodeterioration of industrial cementitious products in a sewer environment. Part I: Test design", Cem. Concr. Res., vol.73, p.246–256, 2015.

(Peyre-Lavigne *et al.*, 2015b) Peyre Lavigne M., Bertron A., Patapy C., Lefebvre X., and Paul E. (2015), "Accelerated test design for biodeterioration of cementitious materials and products in sewer environments," Matér. Tech., vol. 103, no. 2, p. 204.

(Peyre Lavigne *et al.*, 2016) Peyre Lavigne M., Bertron A., Botanch C., Auer L., Hernandez-Raquet G., Cockx A., Foussard J.-N., Escadeillas G. & Paul E., «Innovative approach to simulating the biodeterioration of industrial cementitious products in sewer environment. Part II: Validation on CAC and BFSC linings », Cem. Concr. Res., vol.79, p.409–418, 2016.

CHAPTER 2

Analysis of data obtained on existing structures

Authors *(Organisations)*

Bruno Godart *(Université Gustave Eiffel)*

Michael Dierkens *(Cerema)*

On the basis of the contributions of:

Nathalie Cordier, Benoît Thauvin, Christophe Aubagnac, Arnaud Campaner, Bruno Boulet, Bruno Berenger, Roland Queguiner et Thomas Fanget *(Cerema)*

Abdelkrim Ammouche, Alexa Bresson, Christophe Carde et Thibault Lenormand *(LERM)*

Héloïse Jourdan et Myriam Bouichou *(LRMH)*

Véronique Baroghel-Bouny, Véronique Bouteiller, Lucas Bourreau et Michael Saillio *(Université Gustave Eiffel)*

Work Group: WG2A

Summary

1 Abstract

Durability tests form the basis of the performance-based approach for the durability of concrete. The objective of the PerfDub national project is to have, for each concrete exposure class defined in standard NF EN 206 / CN, one or more indicators associated with tests and thresholds which make it possible to compare and / or assess the ability of a concrete to withstand a given deterioration and duration. But in order to set the threshold value for these durability indicators, it is important to take into account the experience feedback that can be gained on the actual behaviour of existing structures. To achieve this objective, it is necessary to study the evolution of the durability indicators of concrete structures in their environment (under the effect of concrete aging and external aggressions).

After a substantial introduction (section 2), section 3 presents a synthesis of all the results obtained on the BHP 2000 test elements and the 19 structures which were selected and appraised (bridges, wharfs, historical monuments, dam) in order to establish a database of durability indicators (water porosity, chloride diffusion, gas permeability, accelerated carbonation, etc.) and lifetime indicators (chloride penetration profiles, carbonation depths, half-cell electrode potentials, resistivity, presence of disorders, etc.). Then, sections 4 and 5 present a summary of durability and lifetime indicators respectively. Section 6 performs an in-depth analysis of the evolution of durability indicators for carbonation, in parallel with an analysis of the condition of the structures, taking into account the carbonation corrosion model developed within the ANR MODEVIE project. Section 7 performs an in-depth analysis similar to that of Section 6, but with regard to corrosion by chlorides. Section 8 presents a short analysis of the indicators of durability regarding freeze-thaw with or without de-icing salts, in the absence of established models for this phenomenon. Section 9 sets out the main conclusions of this research.

2 Introduction

2.1 Context of the research

The National Project PerfDub is a collaborative research project labeled by the RGC&U (Civil and Urban Engineering Network), scheduled for 4 years from March 2015. It is largely funded within the framework of the National PerfDub Project (managed by IREX - Institute for Experimental Research) and to a lesser extent as part of the MODEVIE research project (Modelling the aging of concrete structures) supported by the ANR (French National Research Agency).

The PerfDub research project aims at defining a methodology at the French national level to justify the durability of concretes (and concrete structures) through a performance-based approach. The objective of PerfDub project is to aggregate knowledge and feedback, to fill gaps, in a framework bringing together all the stakeholders concerned so that the performance-based approach becomes operational and commonly used on construction sites, which is not yet the case today. The application of the performance-based approach to durability is already authorized, but not defined in details, by the European standard EN 206 (and its national complement NF EN 206/CN) and a first methodology is given in the new guideline “Fascicule n°65” of the CCTG (general technical clauses for public contracts). Note that this new guideline “Fascicule 65” was finalized in 2014 and only published in 2017 (Fascicule 65, 2017), and that PerfDub has since provided numerous elements to adapt this methodology.

Durability tests are the basis of the performance-based approach for the durability of concrete. The objective of this national project is to have, for each concrete exposure class defined in

standard NF EN 206/CN, one or more indicators associated with tests which makes possible to compare and / or assess the capacity of a concrete to resist a given degradation.

One of the challenges of the national project is to set the threshold values of the durability indicators, and to validate the corrosion models, and for that it is important to take into account the experience feedback that can be acquired on the actual behaviour of existing structures. The performance-based approach must indeed lead to the use of durable concrete resisting to the aggressions for which they have been prescribed. Durability tests make it possible to ensure this, before and during construction. These tests also allow to assess the durability of the concrete of the structures in service. This is a major issue for the structure owners who need to know the condition of their structures and anticipate their degradation in order to optimize their maintenance plans. Durability tests, carried out as part of diagnostics in association with other techniques, are essential tools for evaluating and predicting the aging of structures in service; they are complementary to the lifetime indicators (chloride penetration profile, carbonation depth, degree of steel corrosion, etc.) which makes possible to follow the evolution of any pathologies affecting the structures over time, and more generally the aging of the structures.

2.2 Research done on existing structures

To achieve this objective, it is first necessary to study the evolution of the durability indicators of concrete structures in their environment (under the effect of concrete aging and external aggressions). As part of this research, 19 structures were selected. While most of these structures do not have data relating to durability indicators (water porosity, chloride diffusion, gas permeability, carbonation, etc.) obtained during their construction phase, they were subjected to measurements of these durability indicators made during the PerfDub project when investigations were carried out on the structures in service with the exception of 3 structures: Vasco de Gama and Rion-Antirion bridges, and Vezins Dam.

The constitution of the structures panel was carried out with the owners and managers (or their representatives). On those selected structures, the work consisted in particular in evaluating the degree of aging of the concrete (evaluation of lifetime indicators within the meaning of AFGC (AFGC, 2004): chloride penetration profiles, carbonation depths). Samples were also used to determine the durability indicators (porosity accessible to water, coefficient of chloride migration, gas permeability). Complementary electrochemical measurements were also carried out (free potentials, resistivity, etc.).

An in-depth analysis of the evolution of the durability indicators is carried out in parallel with an analysis of the condition of the structures. In particular, they make it possible to verify the relevance of the thresholds currently proposed for each indicator and exposure class. The main advantage of studying these ancient structures is to be able to judge these thresholds with hindsight.

Moreover, within the framework of the National Research Project "BHP 2000" (HPC 2000: High Performance Concrete 2000) that was led between 1995 and 2003, a large-scale experiment was carried out in relation to the durability properties of HPC. This study was carried out on natural aging sites, and on a range of 15 concretes whose average compressive strengths varied from 20 to 125 MPa. The behaviour of these 15 concretes was studied on the basis of a very wide range of experimental methods, not only on test elements stored in water in the laboratory, but also on structural elements exposed to natural (in situ) conditions. As part of this study, 43 test elements made of reinforced concrete were therefore installed on three natural sites in France: Paris area, La Rochelle (a city on the West Coast) and Maurienne (in the Alps) and were studied based on non-destructive measurements and on samples taken at different times. The results obtained are also considered in the present report.

2.3 Methodology applied on existing structures

2.3.1 Choice of structures

This research focuses on structures suffering from corrosion by carbonation or by attack of chlorides and on structures exposed to freeze-thaw cycles with or without de-icing salts. It therefore does not relate to structures subjected to chemical attack, nor to those whose concrete is affected by other physico-chemical degradation (alkali aggregate reaction, internal sulphate reaction, etc.) which has generated cracking or leaching. Only structures located in XC, XS and XF, XD environments are therefore studied.

The panel of structures has been divided (according to their age) among the following 3 categories:

- structures less than 20 years old: by giving priority to structures which have already been the subject of durability studies during design and execution stages (all the information sought are available without the need to carry out tests except, possibly, those relating to the evaluation of durability indicators at the present time);
- structures between 20 and 50 years old: by giving priority to structures that have been the subject of a diagnosis within less than 5 years and by measuring durability indicators and other missing information;
- structures over 50 years old: by also giving priority to structures that have been diagnosed within less than 5 years and by measuring durability indicators and other missing information.

The studied structures are listed in Table 2.1 and classified by age and exposure classes. In addition, the testing elements of the National Project "BHP 2000" (HPC 2000: High Performance Concrete 2000), are also incorporated in the study.

Table 2.1. List of the studied existing structures

Age	Exposure Class		
	XC3-XC4	**XS2-XS3**	**XF3-XF4-XD3**
Less than 20 years	BHP 2000 elements Loudéac bridge (2014) Volesvres bridge (2010-12)	BHP 2000 elements X* Marine structure (2014) Rion-Antirion bridge in Greece (1999-2004)	BHP 2000 elements
Between 20 and 50 years	--	Vasco de Gama bridge (1995-98) Piers of the Ré Island bridge (1987-1988) Chateaubriand bridge (1987-91) sur la Rance	St-Poncy bridge (1988) Vachette bridge (1984-1985) Pirou bridge (1991)
More than 50 years	Blondel bridge (1964) Bruche bridge (1947) Iena Palace à Paris (1937) Bordeaux Labor Exchange (1935-1938) Vezins dam (1929-1932) Boutiron bridge (1913)	TCD wharf (1965) X* bridge (1954)	Vallières bridge (1926)

**: X Marine structure and X bridge are structures made anonymous because of confidentiality*

2.3.2 Data obtained on structures

The data sought and obtained (as much as possible) on existing structures include data on the construction, durability indicators and lifetime indicators, as follows:

- the age of the structure
- the type (s) of past and present environment
- data already available on the structures:
  - the rules applied for design and construction,
  - the concrete composition with the origin of the constituents: quantity and type of cement, quantity and type of mineral additions, water content, nature and quantity of aggregates per granular range, possible admixtures,
  - the characterization of the fresh concrete: slump, entrained air, density,
  - the method of pouring concrete and its curing,
  - reinforcement drawings (if possible: proofing drawings) with confirmation by some profometer and radar measurements, and the grade of steels (mild, ribbed, etc.),
  - detailed inspection reports in order to see the damage history: cracking due to corrosion, spalling, visible reinforcement ...,
  - repairs carried out (patch-repair, shotcrete, cathodic protection, etc.),
  - the characterization of the concrete in its hardened state (especially the mechanical strength, durability indicators if measured during construction);
- durability indicators (at the sampling time, during the PerfDub project):
  - porosity accessible to water (according to PerfDub operating mode: NF P 18-459 completed by PerfDub WG1),
  - gas permeability (according to PerfDub operating mode: XP P 18-463 completed by WG1),
  - coefficient of chloride diffusion (migration of chloride ions) (according to PerfDub operating mode: XP P 18-462 completed by WG1),
  - electrical resistivity (according to PerfDub operating mode),
  - water absorption by capillarity (according to PerfDub operating mode),
  - accelerated carbonation (according to PerfDub operating mode),
  - and if possible (optional): the Ca $(OH)_2$ content;
- lifetime indicators:
  - carbonation depth (NF EN 14630, XP P18-458),
  - chloride profile (according to AFREM-AFPC / Grandubé operating mode) (GranDuBé, 2007),
  - sulphate profile (depending on the type of structure),
  - cover depth,
  - half-cell electrode potentials (in particular the RILEM TC154-EMC recommendations),
  - electrical resistivity (RILEM TC154-EMC recommendations),

- state of corrosion of the reinforcements (possible analysis of the steel-concrete interface).

In the absence of information on the original composition of the concrete, a complete mineralogical analysis was carried out on a sample of concrete.

For structures in XF exposure class, the following indicators have been added:

- the air bubble spacing factor according to ASTM C 457;
- the expansion according to the internal freezing test according to standard NF P18-424 or NF P18-425;
- the ratio of the squares of the resonance frequencies according to the P18-414 standard;
- scaling according to the XP P18-420 standard.

2.3.3 Investigations and sampling procedure for durability indicators

To measure the durability indicators, the cores were taken in the structure in accordance with standard NF EN 12504-1 in areas where the diagnosis of the state of corrosion had been made. The cores dedicated to determining the durability indicators were taken as deep as possible from the surface of the structure elements to avoid the effects of the external environment (carbonation, penetration of chlorides, etc.). As much as possible, 3 cores were taken per studied zone so as to be able to make averages on 3 measurements (Figure 2.1). The cores had a minimum diameter of 95 mm and a minimum length of 20 cm, except for the two monuments where cores of 50 mm in diameter were taken after having verified experimentally that the durability tests remained valid.

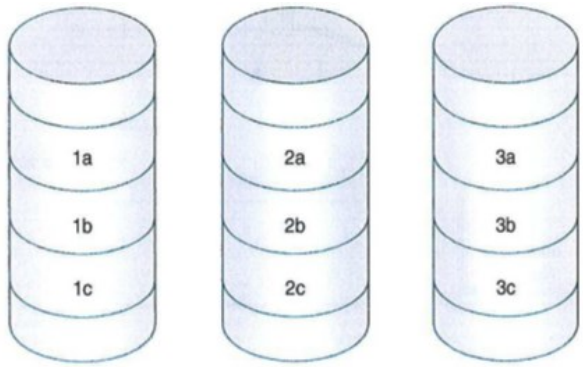

10 mm at the edge (mini) to exclude
1a, 2a and 3a: Gas permeability (50 mm)
1b, 2b and 3b: Migration coefficient of chloride ions (50 mm)
1c, 2c and 3c: Water porosity (50 mm)

10 mm at the edge (mini) to exclude
+ resistivity
+ accelerated carbonation
+ water absorption

Figure 2.1. Principle of achieving performance durability tests on cores

2.4 Consideration on the ageing factor for chlorides

The apparent coefficient of chloride diffusion is an indicator sensitive to the age of concrete. Its decrease over time is due to different causes:

- continuation of the cement hydration reaction;
- interaction with the ambient medium (ion exchanges);
- ...

The decrease over time of the apparent coefficient of chloride diffusion ("ageing factor") can be modelled as follows (*fib*, 2006):

$$D_{app}(t) = D_{rcm}(t_0).\left(\frac{t_0}{t}\right)^{\alpha} \quad \text{(Equ. 2.1)}$$

with:

- D_{rcm} (t_0): Coefficient of chloride diffusion measured by migration at time t_0 (28 days, but preferably 90 days in France);
- α: Ageing factor - Parameter governing the evolution of D_{app} over time.

The ageing factor α depends in particular on the nature of the binder and the exposure conditions of the concrete and generally varies between 0.1 and 0.8. More specifically, the feedback shows that the aging factor is more important:

- in tidal zones than in constantly submerged zones: this effect varies depending on the nature of the cement or the addition,
- when the concrete contains additions such as silica fume or fly ash or slag:
  - CEM I: α ~ 0.2 (0.3 in the fib bulletin 34 (fib, 2006)),
  - CEM I + (silica fume or fly ash or slag): α ~ 0.4 to 0.6 (variable depending on the addition content) (0.6 in the fib bulletin 34 (fib, 2006) for concrete with CEM I and a fly ash content > 20 %).

When the apparent coefficient of chloride diffusion is determined on an existing structure, this age effect shall be considered to estimate the reference apparent coefficient of chloride diffusion D_{app} (t_0) and thus be able to analyse it with regard to the thresholds defined for new structures.

2.5 Analysis of half-cell potential measurements

Data from half-cell potential measurements on reinforced concrete structures can be analysed according to three documents.

a) American standard ASTM C876 (ASTM C876, 2009)

In ASTM C876, values of corrosion potentials are associated with a probability of corrosion (Table 2.2).

Table 2.2. Three categories of probability of corrosion of reinforced concrete according to the values of corrosion potential (the colors indicate respectively a low probability in green, uncertain in yellow and high in red) according to the standard ASTM C876

Corrosion potential (mV, $Cu/CuSO_4$)	Probability of corrosion (%)
E_{corr} < -350	High (> 90 %)
-350 ≤ E_{corr} < -200	Uncertain (≈ 50 %)
-200 ≤ E_{corr}	Low (< 10 %)

b) The recommendations of the COST 509 European action (Cox *et al.*, 1997)

In these recommendations, if the half-cell potential difference between the maximum and minimum value is greater than 150-200 mV over a measurement zone (Table 2.3), then there is a risk of corrosion at the lower values. However, the surface of the measurement zone is not mentioned.

Table 2.3. Three categories of corrosion risk for reinforced concrete as a function of the corrosion potential difference values (the colors respectively indicate a low risk in green, uncertain in yellow and high in red) according to the COST 509 document

Difference of half-cell potential (DDP) (mV)	Corrosion risk
200 ≤ DDP	High
150 ≤ DDP < 200	Uncertain
DDP < 150	Low

c) The recommendations of the RILEM TC154 working group (Elsener, 2003)

Given that the values of the potential measurements are strongly influenced by the exposure and environmental conditions, the TC 154 working group of RILEM (Elsener, 2003) proposed to consider the spatial potential gradients (Table 2.4). Strong gradients should correspond to areas of corrosion. However, no gradient value is specified to characterize an active corrosion state. The value of 8mV / cm is mentioned in the Rance beam benchmark report (L'Hostis *et al.*, 2007).

Table 2.4. Two categories of corrosion activity of reinforced concrete as a function of the local gradient of corrosion potential values (the colors indicate respectively a passive activity in green and active in red) according to the recommendation of RILEM TC-154 (Elsener, 2003) and the Rance beam benchmark (L'Hostis *et al.*, 2007)

Local Gradient of half-cell potential ($mV.cm^{-1}$)	Corrosion activity
8 ≤ local gradient of potential	Active
local gradient of potential < 8	Passive

The interpretation of corrosion half-cell potential measurements according to the three documents in the literature can lead to very different, or even contradictory, evaluation results for a structure in a marine environment. The explanation lies in the altimetric gradient of humidity and oxygen which is important in a marine environment.

The complementarity of the visual inspection results, resistivities and half-cell potentials suggests that the analysis of the potentials via the RILEM document is the most relevant.

In conclusion, the analysis and interpretation of the corrosion potentials as used and validated for reinforced concrete structures in atmospheric environments must be reviewed / corrected when the structure is in a marine environment, and this is particularly true for ASTM C876.

In the present report, the preference is given to the RILEM method. The analysis of the measurements according to the RILEM TC154 documents which is relevant for atmospheric structures (on land) cannot be directly used for structures in a marine environment. In fact, in a tidal range, the values of the measurements carried out are not only relative to the corrosion phenomenon of the reinforcements but also to the environment and the climate:

- The increasing humidity from top to bottom will lead to a decrease in resistivities (see the case of the piers of the Ré Island bridge);
- The chloride ion content of the concrete facing can also be the subject of a differential over the three meters of height investigated. The higher the chloride ion content, the lower the resistivity;
- The decreasing oxygen content from top to bottom modifies the results in the sense that in a non-oxygenated zone, corrosion is unlikely even though the values of reinforcement potentials are very electronegative.

2.6 Analysis of resistivity measurements

These measures done on existing structures are analysed on the basis of the RILEM TC 154 recommendation (Polder, 2000). For CEM I concrete, this recommendation provides a table (Table 2.5) for estimating the risks of corrosion.

Table 2.5. Risk of corrosion as a function of electrical resistivity (Polder, 2000)

Electrical Resistivity (kΩ.cm)	Risk of corrosion	Pourcentage of measures
R_e > 100	Negligible	50 %
50 < R_e < 100	Low	43 %
10 < R_e < 50	Moderate	7 %
R_e < 10	High	0 %

In addition, the following Table 2.6 (extract from the RILEM TC 154 recommendations (Polder, 2000)), shows the orders of magnitude of resistivity for different conditions and different environments as an indication.

Table 2.6. Orders of magnitude of resistivity for different conditions and different exposures (Polder, 2000)

Environment	Electrical Resistivity of concrete (kΩ.cm)	
	Concrete with CEM I	Other concretes*
Very humid, submerged, splash zones (fog chamber)	5 - 20	30 - 100
Outdoor exposure	10 - 40	50 - 200
Outdoor, sheltered, coated, water-repellent (20 ° C, 80 % RH), non-carbonated	20 - 50	100 - 400
Outdoor, sheltered, coated, water-repellent (20 ° C, 80 % RH), carbonated	> 100	200 – 600 and more
Indoor environment (20 ° C, 80 % RH)	> 300	400 – 1000 and more

** Concrete made with cements other than CEM I (with blast furnace slag (> 65 % or CEM III / B), or with silica fumes (> 5 %)).*

Note that the unit used for the electrical resistivity measured at the surface on structures (kΩ.cm) is different from the unit used to measure the bulk resistivity on concrete specimen (Ω.m) and that corresponds to different testing procedures.

2.7 Analysis of corrosion rate measurements

The objective of measuring the corrosion rate is to obtain quantitative information on the instantaneous corrosion of reinforcement in concrete, in the given environment. By carrying out several measurements over time, this makes it possible to follow the evolution of the corrosion phenomenon and consequently to establish section loss behaviors and predictions.

Attempts have been made on the piers of the Île de Ré bridge; the corrosion rate measurements were carried out using a GalvaPulse™ device from Germann Instruments (Ag / AgCl reference electrode; pulsed galvanostatic method), but the results are not included in this report because their use turned out to be too uncertain. These attempts confirm the great difficulty of interpreting corrosion rate measurements which, moreover, vary according to the

devices used, and this is why this measurement method has been excluded from the set of methods applied to all the structures.

2.8 Warning

Care should be taken in analysing the results presented in this report and particularly, it is necessary to consider the following elements:

- some indicators are evolving over time (for example the “ageing effect”), and the values measured on an existing structure at a given age t are not the same as those which would have been measured at the construction time (see paragraph 2.4);
- the values given by the durability indicators are depending on the test procedures (for example, the curing of the test specimen has a great influence on the results for the water porosity test and the accelerated carbonation test). Therefore, when interpretating the potential durability classes and thresholds mentioned by reference (AFGC, 2004) or (LCPC, 2010), it should be kept in mind that these thresholds were established on the basis of slightly different test procedures, respectively in the early 2000s and in the early 2010s.

3 Brief presentation of the structures

3.1 Structures below 20 years old

3.1.1 BHP 2000 elements

3.1.1.1 Presentation of the elements

Within the framework of the National Project "BHP 2000" (HPC 2000: High Performance Concrete 2000), a large-scale experiment has been conducted with respect to the durability properties of HPC, from the year 2000. The study on natural aging sites was carried out on a range of 15 concretes whose average compressive strengths varied from 20 to 125 MPa. The behaviour of these 15 concretes has been studied on the basis of a very wide range of experimental methods, not only on test elements stored in water in the laboratory, but also on structural elements exposed to natural conditions. 43 pre-cracked elements made of reinforced concrete were therefore installed on three natural sites in France (Paris area, La Rochelle and Maurienne, respectively XC, XS and XF/XD environments) and were studied on the basis of samples taken at different times and non-destructive measurements (Baroghel-Bouny, 1999; Baroghel-Bouny *et al.,*1999; Baroghel-Bouny, 2000a; Baroghel-Bouny, 2000b; Baroghel-Bouny *et al.*, 2000, Baroghel-Bouny *et al*., 2002; Baroghel-Bouny *et al.*, 2004; Baroghel-Bouny, 2009; Baroghel-Bouny *et al.*, 2013).

The concrete compositions containing silico-aluminous fly ash are referenced CV, and those containing densified silica fumes are referenced FS. The use of an air entraining agent is indicated by EA. They are described in references (Baroghel-Bouny, 1999; Baroghel-Bouny, 2000b; Baroghel-Bouny *et al.*, 2000, Baroghel-Bouny *et al*., 2002; Baroghel-Bouiny *et al*., 2004).

The test elements are concrete prisms of trapezoidal section (thickness equal to 400 mm at the base for 200 mm at the top), of height 0.95 m and length 1 m, having a heel (800 x 200 mm) to ensure their stability (see Figure 2.2). These elements are reinforced about half of their volume, so as to leave a part available for coring. Reinforcement drawings are presented in (Baroghel-Bouny, 1999).

Figure 2.2. View of the BHP 2000 elements in the La Rochelle site

The shape of the elements and the reinforcement layout allow to obtain areas where the concrete cover of steels is variable and is between 10 mm and 100 mm. In areas where it is constant (particularly in pre-cracked areas), the concrete cover is set, according to regulatory requirements, to:

- 50 mm for the test elements of La Rochelle and Maurienne;
- 30 mm for test elements in the Paris region.

The elements are also equipped with a DIWIDAG bar (Ø 20 mm). Thanks to a specially provided notch, the tensioning of this bar caused a local pre-cracking on one face (3 transverse cracks). Based on the regulations and depending on the exposure class of the destination site, the cracks width was fixed at the following values:

- 0.1 mm for the test elements in La Rochelle;
- 0.2 mm for the test elements in Maurienne;
- 0.3 mm for the test elements in the Paris region.

The purpose of this pre-cracking was to accelerate the degradation in the concerned area of the structural element, and it was a targeted cracking since crack widths are evolving with the loads

The characteristics of the three sites are summarized in the following:

- Melun site (Department of Seine et Marne, East of Paris): this is a site with a temperate climate located in the Paris region, in a peri-urban area. On this site, the annual mean temperature and relative humidity (RH) are relatively constant: between 11.3 and 11.9 °C for the temperature, and between 77 and 80 % for the Relative Humidity;
- La Rochelle (at the foot of the Saint-Nicolas Tower): this is a marine site located in tidal zone. The elements are “dry” at low tide, and completely submerged at high tide. The annual mean relative humidity is also relatively constant between 76 and 79 % RH and the annual average temperature of the order of 13.5 °C;
- Maurienne (between Saint-Michel-de-Maurienne and Pratz, along the National Road 6): it is a mountainous site located at an altitude of 850 m, subject to freeze-thaw cycles. The site is classified as a severe frost zone. The average annual temperatures varied between 7.5 and 8.8 °C. The elements are covered with snow for about 30 days in the year, between the months of November and April. The use of de-icing salts for the

pavement takes place over a period of 6 months, also between the months of November and of April. The test elements are placed along the road 0.80 m behind the guardrail.

These test elements were not cured and were installed on the 3 sites at the age of at least 28 days.

3.1.1.2 History of works and current condition

With the objective of preventing the corrosion of the concrete reinforcements, the durability indicators: porosity accessible to water, gas permeability and coefficient of migration of chloride ions were quantified over the range of studied concretes.

The reader may refer in particular to references (Baroghel-Bouny and al., 2002, 2004) for more detailed information in relation to the experimental procedures applied or to the analysis of all the results obtained within the framework of this study.

The average values of the following indicators measured in the laboratory on the different studied concretes are reported in Table 2.7:

- the porosity accessible to water (P_{wate}) after storage in water for 28 days;
- the gas permeability K_{gas} after storage in water for 28 days and preconditioning;
- the diffusion coefficient of chlorides measured by a migration test under an electric field in non-stationary mode (D_{rcm}) at the end of 28 days after storage in water.

Table 2.7. Mean values of the durability indicators measured on cores after 28 days of curing in water and potential durability (grey boxes correspond to compositions with entrained air)

Concrete	W/C ratio	W/binder ratio	$f_{c,mean,28d}$ (MPa)	Porosity to water (%)	K_{gas} (10^{-18} m^2)	D_{rcm} (10^{-12} $m^2.s^{-1}$)	Potential Durability (global)
M25CVEA	0.84	0.67	20.5	16.4	390	5.8	
M25 CV	0.96	0.77	23.5	15.7	206	9.5	
M25	0.84	0.84	24.5	16.1	978	30.0	
M25EA	0.70	0.70	26.8	13.7	148	22.4	
M30CV	0.74	0.52	48.5	12.8	54	1.7	
M50CVEA	0.45	0.36	49.0	14.3	271	1.5	
M50EA	0.39	0.39	49.5	13.3	272	5.5	
M50CV	0.56	0.45	53.0	15.0	89	1.8	
M50	0.48	0.48	55.5	14.7	69	8.7	
M75FSEA	0.34	0.32	67.0	10.3	347	0.7	
M75EA	0.27	0.27	68.5	10.7	782	3.5	
M75	0.32	0.32	75.0	11.4	106	5.6	
M75FS	0.38	0.36	85.5	10.0	167	0.8	
M100FS	0.33	0.30	109.0	8.4	17	0.3	
M120FS	0.26	0.23	127.5	7.4	43	0.04	

CV = fly ash EA = Air entrained FS = Silica Fume

It is possible to compare the values of the indicators measured with the classes of "potential" durability (very low, low, average, high and very high) proposed in reference (AFGC, 2004).

Potential durability classes (according to AFGC, 2004)				
Very low	Low	Average	High	Very high

The overall "potential" durability of the different concretes studied within the framework of the National Project "BHP 2000", evaluated on the basis of the combination (with equivalent weight) of the three durability indicators (porosity, K_{gas} and D_{rcm}) is shown in Table 2.7. According to this qualification, it can be highlighted the excellent quality of HPC, most of them exhibiting high “potential” durability. Some C60 concretes have an average “potential” durability, while HPC with silica fumes such as $f_{c,mean,28d}$ > 90 MPa (VHPC) have a rather very high “potential” durability.

The incorporation of an air entraining agent in the composition of HPC significantly increases the connectivity of the network of pores. However, only the gas permeability is increased by this effect. The negligible effect observed on the chloride diffusion coefficient seems to indicate that the presence of entrained air bubbles will not be detrimental to the protection of reinforcements (please note the water to cement ratio of the mix-design with air entraining agent was adjusted to keep the same compressive strength). Carbonation and penetration of chlorides or oxygen in concrete are in fact governed by diffusion processes (or capillary absorption under unsaturated conditions, in the case of chlorides).

3.1.1.3 Investigations carried out during PerfDub project

Within the framework of the PerfDub National Project, measurements at the age of 19 years old were programmed on the test elements of the "BHP 2000" National Project. The measurements were carried out on the cores taken, after cutting and sampling, on a selection of materials among the 15 concretes with an average compressive strength varying between 20 and 125 MPa. Measurements relative to the porosity accessible to water, mercury porosimetry, carbonation depth and the total chloride concentration profiles have been carried out at Ifsttar and Cerema.

The porosity values accessible to water measured by hydrostatic weighing on the Paris (Melun), La Rochelle and Maurienne (Road side (E) and slope side (I)) at the 19-year maturity are reported in Figure 2.3, for M25, M30CV, M50 and M75FS concretes.

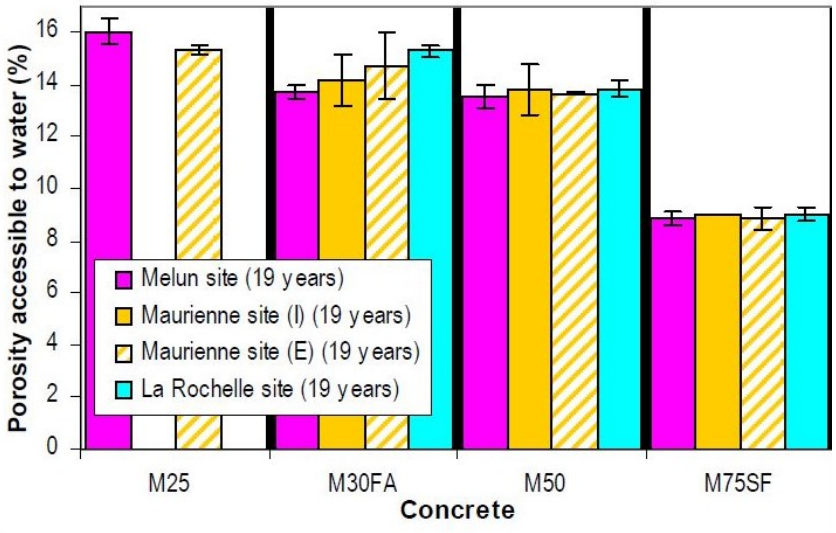

Figure 2.3. Porosity accessible to water measured by hydrostatic weighing in the internal zone of the cores (mean values and standard deviation), after 19 years of exposure at the different sites (E): road side (exposed to de-icing salts) (I): slope side

Figure 2.3 shows that very similar values of porosity (measured in the internal area) are obtained at the Paris, La Rochelle and Maurienne sites after 19 years of exposure, especially in the case of M50 and M75FS test elements, their depth affected by environmental conditions and especially by desiccation being very thin.

The results of carbonation depths obtained on the Paris (Melun), La Rochelle and Maurienne sites (sides (E) and (I)), at the 19-year maturity, are shown in Figure 2.4. For a given composition (without entrained air), the values obtained at the Melun and Maurienne sites are close, while those recorded on the La Rochelle site are systematically lower. This trend has in fact been observed at each maturity. This result is due to the fact that the tidal cycles on the sea site (and in particular the periods of submersion of test elements) reduce the time of exposure to atmospheric CO_2. They further hamper the progression of this gaseous CO_2 in the porous network of the concrete by imposing a high saturation rate. High saturation rates have indeed been systematically measured on the various concretes at the La Rochelle site.

Figure 2.4 shows also that the carbonation depth is globally well classified according to the compressive strength measured in the laboratory at 28 days (the depth decreases when the mechanical strength increases). The M25 series and the M30CV concrete are highly carbonated, while the M50 concrete and the HPC remain very low carbonated after 19 years of exposure.

The M30CV carbonates significantly on site, while it exhibits very good durability properties measured in the laboratory (cf. (Baroghel-Bouny *et al.*, 2002)). Note, however, that the carbonation of M30CV occurred very fast. There is almost no evolution after the first point of measurement, whatever the considered site (Baroghel-Bouny *et al.*, 2004). This significant and immediate carbonation is essentially the result of the absence of curing, particularly detrimental in the presence of large quantities of fly ash. The M50CV is also clearly more carbonated than other concretes of the same class but without ash (M50 and M50EA), what was foreseeable on the basis of its mechanical strength measured on the test elements at the end of one year (Baroghel-Bouny *et al.*, 2004).

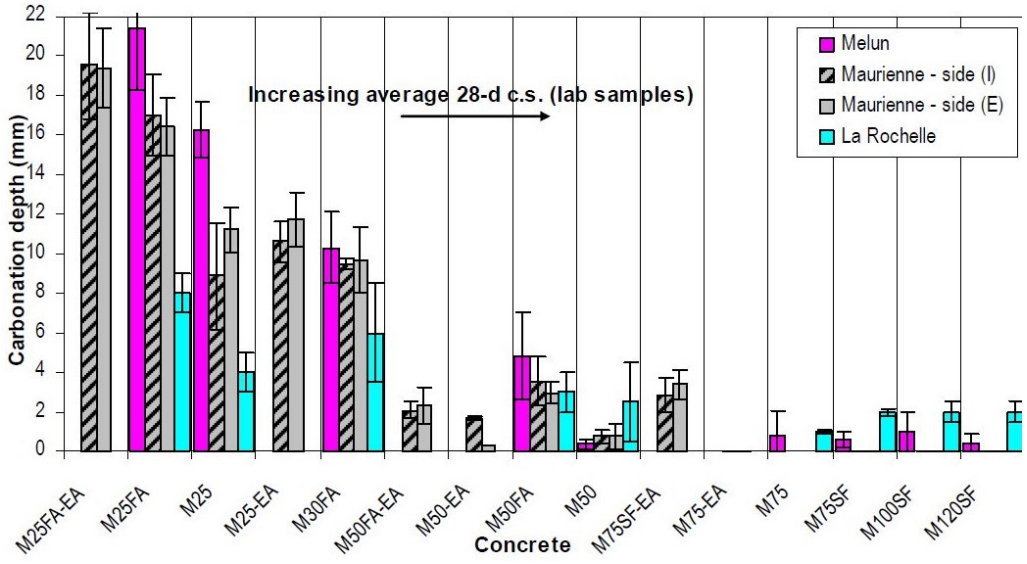

Figure 2.4: Comparison of carbonation depths (mean values and error bars) measured by phenolphthalein on the cores extracted from the test elements, after 19 years
(E): road side (exposed to de-icing salts) (I): slope side

The total chloride concentration profiles obtained on the samples taken from the test elements of the La Rochelle and Maurienne (sides (E) sites, at the end of 19 years, are presented in Figure 2.5a and Figure 2.5b, respectively. The total chlorides concentrations are expressed in g per 100 g of concrete sample.

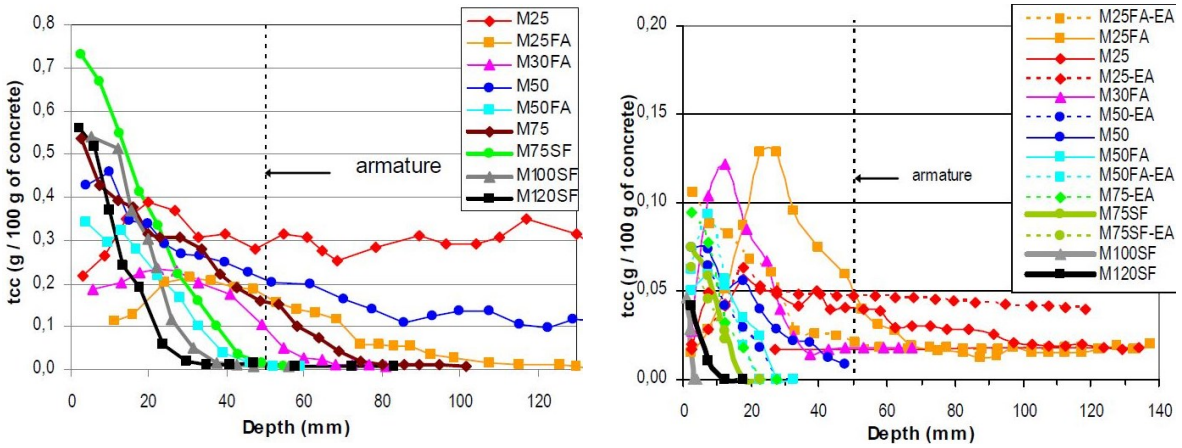

a) Site of La Rochelle b) Site of Maurienne (face E)

Figure 2.5. Total chloride concentration profiles obtained on samples taken from elements, after 19 years of exposure

At the La Rochelle site, all HPC have a decreasing monotonic profile, with a very high concentration at the surface (in fact, this indicates a peak located in the vicinity of the surface) (cf. Figure 2.5a). This results from the accumulation of chlorides at the location where evaporation occurs, after drying (at low tide). However, the penetration of chlorides remains very limited in HPC (the concentration remains below 0.01 g per 100 g of concrete beyond depth e = 50 mm).

The profiles relating to ordinary concretes at the La Rochelle site are clearly more spread out and for most of them have a maximum located at a distance from the surface (cf. Figure 2.5a), testifying of the influence of humidification-drying cycles up to this depth. Indeed, these concretes have significantly larger pore sizes (than those of HPC) allowing, at each drying cycle, a desaturation of the pores on a greater thickness and evaporation at a distance from the surface, and, during subsequent humidification, penetration of chloride ions through capillarity in the previously desaturated zone. This capillary absorption stops at the level of the drying "front". Capillary absorption allows chloride penetration much faster and much greater than in the case of a diffusion (Baroghel-Bouny *et al*., 2013).

The results obtained with the M50CV and M30CV concretes illustrate the positive impact of the compositions with fly ash to limit the penetration of ions, when the hydration of the cement and the pozzolanic reaction between the ashes and the portlandite could have taken place in good conditions (therefore beyond a certain depth). In fact, in M50CV and M30CV concretes, beyond the peak (if there is one), the chloride concentration decreases very significantly with the depth. The reader may refer to reference (Baroghel-Bouny *et al*., 2002) for the explanations relating to this observation.

On the Maurienne site, road side (E), the total chloride concentrations measured at the age of 19 years at a given depth remain significantly lower than those recorded on the La Rochelle site (cf. Figure 2.5a and Figure 2.5b). These results are consistent with the literature which still shows the tidal zones as generating the stronger penetrations of chlorides. The profiles obtained on different ordinary concretes have similar appearance, with the presence of a very marked peak, as well as those of the HPC (of decreasing monotonic type, with a very steep slope). Except for the M25 class for which the presence of chlorides is recorded beyond a depth x = 70 mm, chloride penetration is very localized (the concentration is zero beyond a depth x = 40 mm). Note the particularly low penetration of chlorides in HPC.

The concentration profiles obtained at the two sites show the lower penetration of chloride ions in HPC, in particular in M100FS concrete and M120FS.

3.1.1.4 Conclusion drawn

Numerous experimental results, obtained in the laboratory and in situ in different exposure conditions, are thus available, in particular with regard to medium-term performance of concrete of known composition (in particular HPC and concrete with fly ash).

This database, which allows in particular to follow the evolution of the microstructural characteristics and durability properties of concretes in the medium term, will be useful for future research and for modelling. In particular, these data will allow to feed and validate analytical or numerical physical models of prediction of carbonation and chloride penetration.

Likewise, the analysis of these data could provide useful elements to optimize the curing procedures for concrete structures (especially for formulas with fly ash) as a function of the set (concrete formula - geometry of the structure – conditions to the limits (i.e. environmental)), in order to obtain a good quality of the concrete in the concrete cover to provide an effective barrier against the penetration of aggressive agents.

3.1.2 Vasco de Gama Bridge

3.1.2.1 Presentation of the bridge

Built between February 1995 and March 1998, the Vasco da Gama Bridge located at Lisbon in Portugal is 17.2 km long, making it the longest bridge in Europe, 9 km of which spans the Tagus estuary (Figure 2.6).

Figure 2.6. General view of the Vasco de Gama bridge

It is made up of 8 distinct architectural bridges which are, from North to South:

- north access: two interchanges connecting the bridge to the motorway network;
- north viaduct: ribbed slab deck installed on scaffolding (488 m, 11 piers made up of columns founded on piles);
- Exhibition viaduct: deck made up of two box girders built in cantilever by assembling prefabricated segments (672 m, 13 piers made up of 2 columns founded on piles);
- main bridge: cable-stayed deck with side beams in prestressed concrete and steel braces built on site (824 m of total length with a central span of 420 m long, two pylons on caissons, 6 piers made up of 2 columns founded on piles);
- central viaduct: deck made up of two box girders prefabricated by entire spans (6531 m, 81 piers made up of 2 columns founded on driven piles);

- south viaduct: deck made up of ribbed slabs built on site by entire spans (3825 m, 84 piers made up of 4 columns founded on piles);
- south access: motorway platform and interchanges (3900 m).

The Vasco da Gama Bridge (Portugal) is an exceptional structure for which a lifespan of 120 years was required as an essential criterion of the specifications set during its construction from 1995 to 1998. It is thus one of the first structures to have been the subject of a performance-based approach for the durability of concrete (Martinet, 1999; Houdusse *et al*., 2000; Martinet et Linger, 2005; Ammouche *et al*.,2012). Due to its geographical location in the Tagus estuary, the durability of the concrete exposed to the aggressive marine environment (XS2 and XS3) was a major concern during the design of this structure; corrosion of the reinforcements induced by the penetration of chlorides being one of the main causes of possible degradation identified.

3.1.2.2 History of works and current condition

Specific studies had therefore been carried out before the construction by the Vinci Construction GP company, jointly with the LERM, in order to characterize the durability parameters of the various predefined concrete compositions and to feed the forecasting tool of chloride penetration (LERM software), in order to define the conditions for reaching the expected lifespan of 120 years, for the different exposure cases (immersion, tidal / splashing and aerial areas) (Martinet, 1999; Houdusse *et al*., 2000; Martinet et Linger, 2005; Ammouche *et al*.,2012). The lifetime indicators obtained on this structure after commissioning have made it possible to refine the input data (taking into account the actual characteristics of the concrete) and to verify the prediction of the model and to improve it.

During the studies carried out, various durability indicators were measured (porosity accessible to water, gas permeability, apparent coefficient of chloride diffusion, permeability to chloride ions). These measurements were carried out on laboratory specimens, then on site specimens and finally on concrete samples taken from the structure.

The Vasco da Gama bridge was also the subject of a durability monitoring program for several parts of the structure located in the tidal / splashing zone and in the aerial zone. This monitoring made it possible in particular to measure the durability indicators of the concrete of the structure as well as lifetime indicators between a few months and approximately 18 years after the construction of the bridge.

The cement contents (CEM I or CEM IV PM ES) were all greater than or equal to 400 kg/m^3 and the effective water / equivalent binder ratios were between 0.33 and 0.42.

The thresholds of the durability indicators selected for the project are shown in Table 2.8.

Table 2.8. Criteria for durability indicators at construction

Property	Criterion
Permeability to the oxygen (AFPC-AFREM)	< 1.10^{-17} m^2 at 90 days
Apparent coefficient of chloride diffusion (Tang-Luping method)	< 1.10^{-12} m^2/s at 90 days
Permeability to the chloride ions (AASHTO test, ASTM C1202)	< 1000 Coulombs at 90 days

Note that the test protocols selected at the time of construction differ significantly from the tests selected for the PerfDub project.

The present report provides a synthesis of the main existing data for the durability indicators of two concrete compositions: concrete of the prefabricated caissons located at the base of the piers of the central viaduct, and concrete of the columns of the south viaduct. These data

are supplemented by the chloride profiles (free and total) measured in the tidal range of these two structures (exposure class XS3).

a. Prefabricated caissons at the base of the piers of the Central viaduct (XS3 tidal zone)

The Figure 2.7 presents a photo of a part of the central viaduct and a photo of the tidal zone of a prefabricated caisson.

Figure 2.7. General view of the central viaduct (left) and view of the tidal zone of a prefabricated caisson (right)

The composition of the (GS3) concrete used for these caissons is presented in Table 2.9.

Table 2.9. Composition of the GS3 concrete

Constituents	Content (kg/m^3)
CEM I 42.5 PM (Secil)	360
Fly ashes	80
Gravels 15/25 (Galo)	578
Gravels 5/15 (Galo)	484
Rolled sand (Silva)	808
Efficient water	150
Efficient water / total binder	0.34

The measurements of the durability indicators carried out by the LERM at construction, then at 17 and 43 months on the caissons, are presented in Table 2.10.

Table 2.10. Values of the durability indicators at construction and at 17 & 43 months.

Durability indicators	Specimen during construction	First cores taken from the caissons (17 months)	Second cores taken from the caissons (43 months)
Apparent coefficient of chloride diffusion (10^{-12} m².s^{-1})	3.4	0.8	0.2
Porosity accessible to water (%)	12.4*	10.7	10.6
Gas permeability (10^{-18} m²)	58*	11	4
Permeability to chlorides ions according Aashto test (Coulomb)	5100*	-	-
Permeability to chlorides ions according Aashto test (Coulomb)	1700*	500	-

** Values measured at 28 days*

Potential durability classes (according to AFGC, 2004)				
Very low	Low	Average	High	Very high

According to the AFGC guide of 2004 (AFGC, 2004), the durability indicators measured for the concrete of the caissons of the piers of the central viaduct correspond to a high durability level, with however a downside to the water porosity which is medium to high.

Measurements of the apparent coefficient of chloride diffusion continued to be made over time on the caissons; the following Table 2.11 shows the results.

Table 2.11: Values of the apparent coefficient of chloride diffusion with the age (GS3 composition)

Age (months)	Apparent coefficient of chloride diffusion (10^{-12} m².s^{-1})
1	2.0
6	1.5
17	0.8
31	0.4
45	0.2
57	0.1
117	0.2
165	0.1

The law of evolution of the apparent coefficient of chloride diffusion as a function of time resulting from the various measurements on the concrete formula GS3 is as follows:

- D_{rcm} (t) = $2.10^{-12}.e^{-0.0527t}$ m²/s for t < 60 months
- D_{rcm} = $0.10\ 10^{-12}$ m²/s for t ≥ 60 months

This law is shown in graphical form on Figure 2.8. It allows to evaluate an “ageing coefficient” based on the law described in § 2.3; it is thus 0.7 between 1 and 60 months when it is considered to be stabilized.

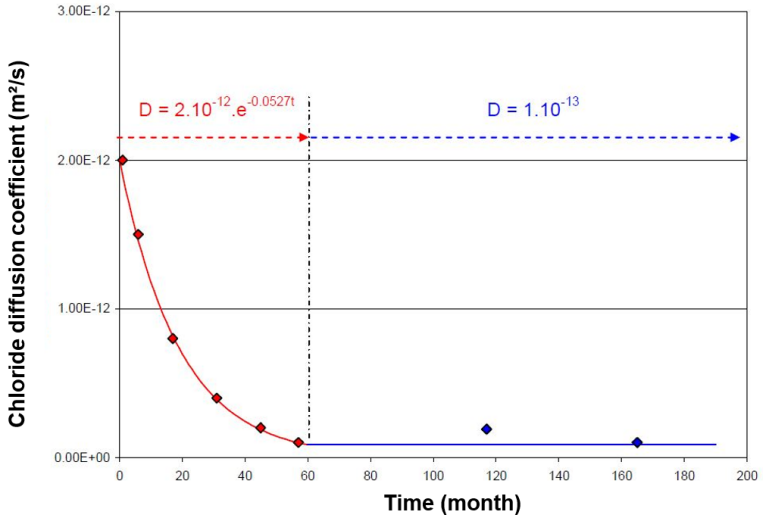

Figure 2.8. Evolution of the apparent coefficient of chloride diffusion of concrete (time in months)- Concrete law of the Central Viaduct

Measurements relating to lifetime indicators, in this case the penetration of chlorides, were also carried out by the LERM on caissons 38 and 55 in 2009 and in 2016 (at 213 months).

In 2009, chloride penetration measurements were carried out by the LERM on 3 zones Z1 to Z3 of caisson 38 and zone Z25 of caisson 55. Figures 2.9 to 2.12 show the position of the zones and photos of the zones taken in 2009.

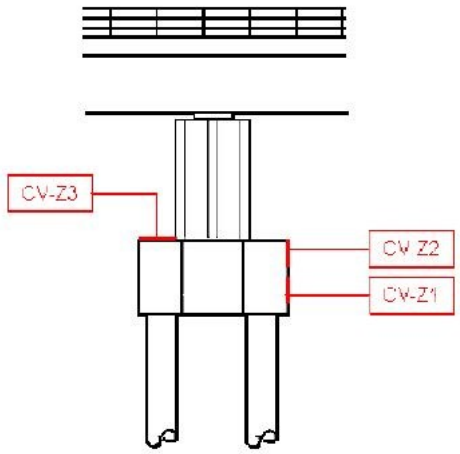

Figure 2.9. Location of zones Z1 to Z3 on the caisson 38

Figure 2.10. View of zones Z1 and Z2 in 2009

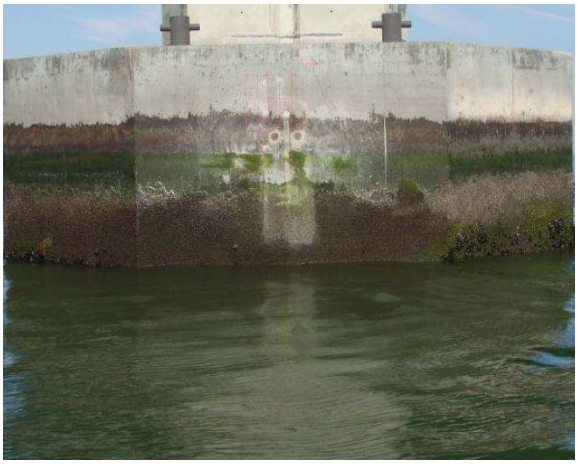

Figure 2.11. View of the Z25 zone of caisson 55 in 2009

Figure 2.12. View of the Z25 zone of caisson 55 in 2009

The results of the chloride penetration measurements (total and free) carried out in 2009 in the different zones of caissons 38 and 55 are shown in the following Figures 2.13 to 2.16.

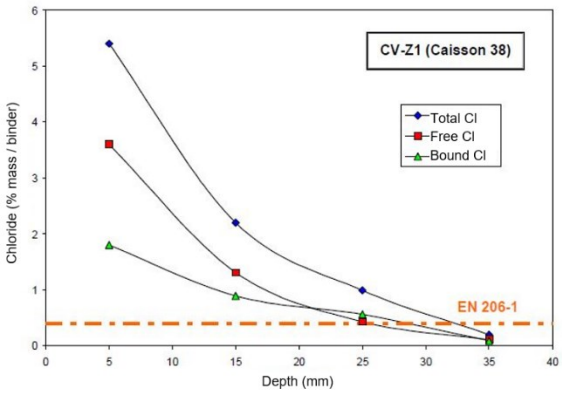

Figure 2.13. Penetration of total, free and bound chlorides measured in 2009 in the Z1 zone (caisson 38)

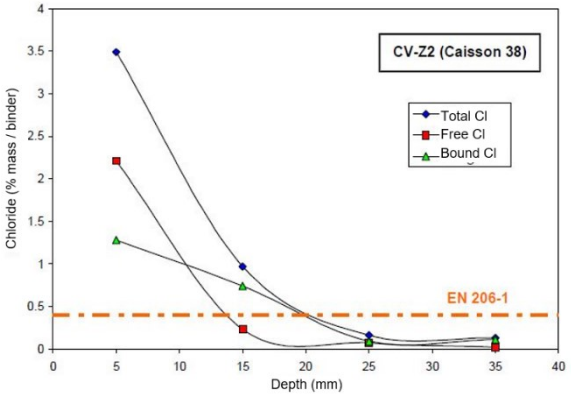

Figure 2.14. Penetration of total, free and bound chlorides measured in 2009 in the Z2 zone (caisson 38)

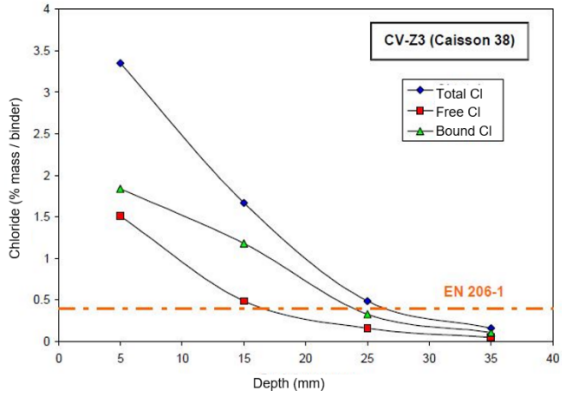

Figure 2.15. Penetration of total, free and bound chlorides measured in 2009 in the Z3 zone (caisson 38)

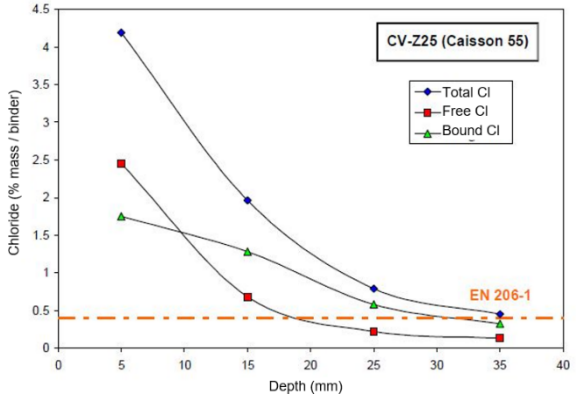

Figure 2.16. Penetration of total, free and bound chlorides measured in 2009 in the Z25 zone (caisson 55)

The results of the measurements at 213 months are reported in Table 2.12:

Table 2.12. Chloride profiles measured in the tidal range on two caissons of the central viaduct at 213 months

Depth (mm)	Caisson 38			Caisson 55		
	Chlorides (% mass / binder)					
	Total	Free	Bound	Total	Free	Bound
0 – 10	7.00	5.40	1.62	5.56	4.00	1.56
10 – 20	3.56	1.94	1.62	2.27	1.08	1.19
20 – 30	1.03	0.22	0.81	0.22	0.05	0.16
30 – 40	0.16	0.00	0.16	0.11	0.05	0.05

** Calculated considering an apparent density (AFREM) ρ_d = 2350 kg/m^3 and a binder content of 440 kg/m^3*

While chlorides progressed well in the 0-10 mm slice, the maximum chloride penetration depths have generally changed little between 2009 and 2016. The content of free chlorides (responsible for the initiation of corrosion) is greater than the 0.4 % limit (threshold given for

the total chlorides by EN 206-1 standard) up to depths of 20 to 25 mm for caisson 38 and 20 mm for caisson 55.

For the measurements carried out at 213 months, it is found that the bound chlorides which are equal to 25 % of the total chlorides in the 0-10 mm slice reach 50 % in the 10-20 mm slice, and even 75 % of the total chlorides in the 20-30 mm slice, which is significant.

Table 2.13 presents an estimate of the content of free and total chlorides at the surface of the concrete by extrapolation of the experimental chloride profiles at 213 months.

Table 2.13. Estimated total and free chloride contents at the concrete surface of caissons 38 and 55, at 213 months (limit condition)

	Caisson 38	Caisson 55
	% mass / binder	
Total chloride content estimated at the surface – Cst	8.4	7.0
Free chloride content estimated at the surface – Csf	7.0	5.3

In June 2009, the lifetime indicators measured were as follows:

- the carbonation depths were 1 mm for the two caissons;
- the minimum half-cell potentials measured ($Cu/CuSO_4$ electrode) were -270 mV for the caisson 38 and -240 mV for the caisson 55, indicating a low probability of active corrosion;
- the mean concrete covers were 45 mm for the caisson 38 and 55 mm for the caisson 55 (for a theoretical cover of 70 mm).

From an inspection point of view, and as shown on the photographs of Figures 2.10 to 2.12, there is no disorder announcing any corrosion on these 2 caissons. On all of the caissons, the rare areas of active corrosion are all located at the corners of the caissons, for which cover defects have been identified.

b. Columns of the piers of the south viaduct (XS3 tidal zone)

The Figure 2.17 presents a photo of the piers supporting the deck of the south viaduct.

Figure 2.17. View of the columns of the piers of the South viaduct

The formulation (IN3) of the concrete used for these columns is presented in Table 2.14.

Table 2.14. Composition of the IN3 concrete

Constituents	Content (kg/m^3)
CEM IV 32,5 (CIMPOR) (fly ashes content 25 %)	430
Fly ashes	---
Gravels 15/25 (Sobr.)	460
Gravels 5/15 (Sobr.)	535
Rolled sand (Sulin)	415
Crushed sand (Sobr.)	418
Efficient water	145
Efficient water / total binder	0.34

The measurements of the durability indicators carried out at construction, then at 6 months, 18 months and 29 months, on the columns of the piers of the South viaduct, are presented in Table 2.15.

Table 2.15. Values of the durability indicators at construction and at 6, 18 & 29 months

	Age (days)	Laboratory specimen	Specimen on site at construction	First cores taken from the bridge (6 months)	Second cores taken from the bridge (18 months)	Third cores taken from the bridge (29 months)
Apparent coefficient of chloride diffusion (10^{-12} m².s^{-1})	28	-	1.5	1.1	1.0	0.7
	90	0.5	0.52	-	-	-
	80	0.14	0.22	-	-	-
Porosity accessible to water (%)	28	11.9	12.9	13.6	12.8	13.9
Gas permeability (10^{-18} m²)	28	< 10	32 (*)	48	20	7
Permeability to chlorides ions according to Aashto test (Coulomb)	28	4410	3490	950	500	--
	90	1570	-	-	-	-
	180	840	-	-	-	-

Potential durability classes (according to AFGC, 2004)				
Very low	Low	Average	High	Very high

According to the AFGC guide of 2004 (AFGC, 2004), the concrete of the columns of the piers of the South viaduct is generally of high to very high durability, with however a downside to the water porosity which is average.

Measurements of the chloride apparent coefficient of chloride diffusion coefficient were pursued over time on the columns; Table 2.16 shows the results.

Table 2.16. Values of the apparent coefficient of chloride diffusion with the age (IN3 formula)

Age (months)	Apparent coefficient of chloride diffusion (10^{-12} m².s^{-1})
1	2.0
6	1.5
18	1.0
29	0.7
43	0.5
117	0.4
165	0.3

Although the law of evolution of the apparent coefficient of chloride diffusion as a function of time obtained from the various measurements on the concrete formula IN3 does not appear to have reached an asymptote at the end of the 165 months, it is approximately the following:

- $D_{rcm}(t) = 2.10^{-12}.e^{-0,0322\,t}$ for t < 60 months
- $D_{rcm} = 0.30\ 10^{-12}$ m²/s for t ≥ 60 months

This law is represented on the Figure 2.18; it allows to evaluate an “ageing coefficient” based on the law described in 2.3; it is thus 0.46 between 1 and 60 months, assuming it has stabilized.

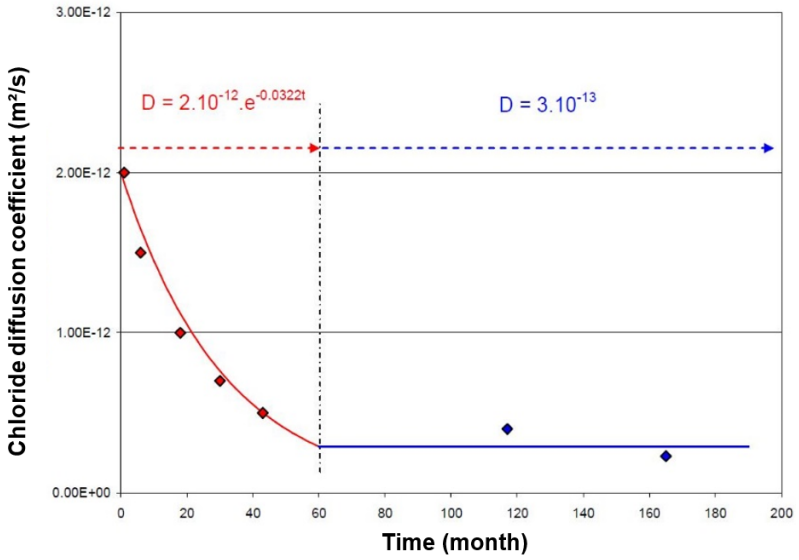

Figure 2.18. Evolution of the apparent coefficient of chloride diffusion of concrete (time in months) – South viaduct concrete law

Measurements relating to the lifetime indicators, the penetration of chlorides in this case, were also carried out by the LERM on the 45 A column in 2009 and in 2016 (at 213 months). Figures 2.19 to 2.21 show the location of the Z21 zone on column 45A, a photo of this zone taken in 2009, and the results of chloride penetration measurements done in 2009.

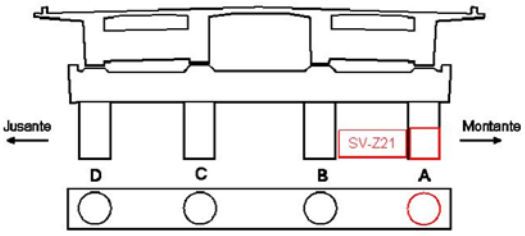

Figure 2.19. Location of the Z21 zone (Pier 45)

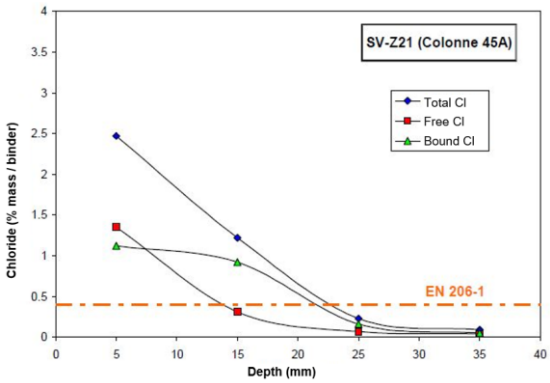

Figure 2.20. Penetration of total, free and bound chlorides measured in 2009 in the Z21 zone.

Figure 2.21. View of the Z21 zone of column 45A in 2009.

Measurements relating to the lifetime indicators, the penetration of chlorides in this case, were also carried out by the LERM on column 45A at 213 months. The results are reported in the Table 2.17.

Table 2.17. Chloride profiles measured in the tidal zone on a column of the south viaduct at 213 months.

	Column 45A		
	Chlorides (% mass / binder)*		
Depth (mm)	Total	Free	Bound
0 – 10	4.10	2.86	1.24
10 – 20	2.59	1.08	1.51
20 – 30	0.76	0.16	0.59
30 – 40	0.16	0.11	0.05

** Calculated considering an apparent density (AFREM) ρ_d = 2350 kg/m^3 and a binder content of 440 kg/m^3*

While chlorides have progressed well in the 0-10 mm and 10-20 mm slices, the maximum chloride penetration depths have generally changed little between 2009 and 2016. The content of free chlorides (responsible for the initiation of corrosion) is greater than the 0.4 % limit (threshold given for the total chlorides by EN 206 standard) up to depths of 20 to 25 mm.

At 213 months, it is found that the bound chlorides which are equal to 30 % of the total chlorides in the 0-10 mm slice reach 60 % in the 10-20 mm slice, and even 75 % of the total chlorides in the 20-30 mm slice, which is considerable.

Table 2.18 presents an estimate of the content of free and total chlorides at the surface of the concrete by extrapolation of the experimental chloride profiles at 213 months.

Table 2.18. Estimated total and free chloride contents at the concrete surface of column 45A (limit condition)

	Column 45A
	Chlorides (% mass / binder)
Total chloride content estimated at the surface – Cst	5.2
Free chloride content estimated at the surface – Csf	3.8

In June 2009, the lifetime indicators measured on column 45A were as follows:

- the carbonation depths were between 1 and 2 mm;
- the minimum half-cell potentials measured were -320 mV, indicating a low probability of active corrosion;
- the average concrete covers were 70 mm (for a theoretical cover of 70 mm).

From an inspection point of view, some columns of the South Viaduct show a microcracking with a very small opening corresponding to centimetric or decimetric mesh crazing. A mineralogical assessment carried out by the LERM concluded that the cement content of the concrete was generally in accordance with that of the theoretical formulation (cement content of the order of 430 kg/m3), but that the effective water / cement weight ratios were slightly higher than the theoretical value of 0.34, and that these concretes were not affected by any pathology of physicochemical origin (alkali aggregate reaction, sulphate reaction, etc.). As a result, it is very likely that the surface cracking affecting some of the columns, and forming crazing patterns, is the result of concrete shrinkage. No damage due to corrosion is therefore apparent.

3.1.2.3 Investigations carried out during PerfDub project

There were no additional investigations carried out within the framework of PerfDub except for the chloride contents measured on concrete samples taken at 213 months.

3.1.2.4 Conclusion drawn

The Vasco de Gama bridge is a particularly interesting case because specific studies were carried out before the construction by the Vinci Construction GP company, jointly with the LERM, with the aim of characterizing the durability parameters of the various predefined concrete compositions and to feed the chloride penetration forecasting tool (LERM software), in order to define the conditions for reaching the expected lifespan of 120 years, for the different exposure cases (immersion, tidal / splashing and aerial areas). During the studies carried out, various durability indicators were measured (porosity accessible to water, gas permeability, apparent coefficient of chloride diffusion, permeability to chloride ions). These measurements were carried out on laboratory specimens, then on site specimens and finally on concrete samples taken from the structure.

The Vasco da Gama bridge was also the subject of a durability monitoring program for several parts of the structure located in the tidal / splashing zone and in the aerial zone. This monitoring made it possible in particular to measure the durability indicators of the structure concrete as well as lifetime indicators between a few months and approximately 18 years after the construction of the structure.

This report, which focuses on caissons 38 and 55 of the central viaduct piers and on column 45A of the south viaduct, generally leads to the same conclusions for these two parts of the structure made with concrete containing 20 to 25 % fly ash (relative to the weight of cement):

- according to the AFGC guide of 2004, the concrete of the caissons of the central viaduct piers is generally of high durability and the concrete of the columns of the South viaduct of high to very high durability, with however a downside to the water porosity which corresponds to an average durability;
- from the various measurements of the apparent coefficient of chloride diffusion carried out on the GS3 concrete formula of the caissons, it was noted that this coefficient decreased according to the aging of the concrete, and it was possible to derive the law of evolution of the apparent coefficient of chloride diffusion as a function of time:
  - $D_{rcm}(t) = 2{,}10^{-12}.e^{-0{,}0527\,t}$ for t < 60 months,
  - $D_{rcm} = 0.16\ 10^{-12}\ m^2/s$ for t ≥ 60 months.
- The law of evolution of the apparent coefficient of chloride diffusion as a function of time resulting from the various measurements on the IN3 concrete formula of the columns is as follows:
  - $D_{rcm}(t) = 2.10^{-12}.e^{-0{,}0322\,t}$ for t < 60 months,
  - $D_{rcm} = 0.3\ 10^{-12}\ m^2/s$ for t ≥ 60 months.
- between 2009 and 2016, although chlorides penetrate significantly in the 0-10 mm and 10-20 mm ranges, the maximum chloride penetration depths did not change much overall. The content of free chlorides (responsible for the initiation of corrosion) is greater than the limit of 0.4 % (threshold given by standard EN 206-1) up to depths of 20 to 25 mm;
- in 2016 (at 213 months), it is observed that the bound chlorides which are equal to 30 % of the total chlorides in the 0-10 mm range reach 60 % in the 10-20 mm range, and even 75 % of the total chlorides in the 20-30 mm range, which tends to show that the percentage of bound chlorides increases with the depth in the concrete;
- In 2009, the lifespan indicators that were measured are as follows:
  - the carbonation depths are 1 to 2 mm and the risk of corrosion by carbonation is zero,
  - minimum half-cell potentials indicate a low probability of active corrosion,
  - the average cover thicknesses are 45 mm for the caissons and 70 mm for the columns (for a theoretical cover of 70 mm),
  - the inspection shows that there is no disorder announcing corrosion on the structural elements. For all caissons, the rare areas of active corrosion are all located at the corners, for which sub-covers have been identified.

Numerical simulations carried out by LERM show that after 120 years of exposure, the content of free chlorides responsible for the initiation of corrosion will be greater than 0.4 % up to a depth of about 40 to 50 mm for the caissons and 55 mm for the columns.

3.1.3 Rion-Antirion Bridge

3.1.3.1 Presentation of the bridge

The Rion-Antirion Bridge (Figure 2.22), officially called the Charilaos Trikoupis Bridge, is a cable-stayed bridge that connects the Peloponnese with mainland Greece between the two cities of Rion (near Patras) and Antirion. With a total length of 2,883 meters, the crossing consists of a main multi-cable-stayed bridge with a length of 2,252 meters (3 central spans of 560 m and 2 lateral spans of 286 m) extended by two access viaducts:

- to the south, on the Rion side, a 392 m long viaduct made of prestressed prefabricated beams;
- to the north, on the Antirion side, a 239 m long viaduct made of a two-girder composite structure.

Figure 2.22. General view of the Charilaos Trikoupis Bridge (Rion-Antirion bridge)

It was built between 1999 and 2004, and opened to traffic in August 2004, shortly before the Olympic Games.

The 4 piers of the multi-cable-stayed bridge rest at a depth of about 60 meters on a set of 200 rigid inclusions stuck in the soft soil. These inclusions consist of 200 steel tubes 2 m in diameter and 25 to 30 m long. They are covered with a gravel mat 2.75 m thick, capable of supporting the pier bases which are 90 meters in diameter and 13 meters high.

The base of the pylons is located between 25 and 45 meters (for the two central pylons) above sea level, in order to free up a navigation gauge of 52 meters in the middle of the strait. The pylons rise 115 meters and therefore reach a maximum height of 160 meters above sea level.

The top of each pier is an inverted pyramid about 15 meters high with a square base of 38 meters per side. Each pylon consists of four inclined reinforced concrete legs with a section of 4 × 4 meters, converging in the pylon head to form a monolithic structure.

The deck has a width of 27.1 m and consists of a steel concrete composite structure comprising two longitudinal girders 2.2 meters high connected every 4 meters by transverse beams. The upper slab is made of prefabricated reinforced concrete panels. The deck is suspended from the pylons by its 368 stays and looks like a giant swing equipped with shock-absorbing struts connecting the deck to the piers. This shock-absorbing strut system dampens vibrations under normal conditions, extreme wind and small earthquakes; In the event of an exceptional

earthquake, these struts act as fuses to release the movements of the deck in order to operate the viscous dampers intended to absorb the energy induced in the deck by the large-scale earthquake.

It is therefore an exceptional structure for which a lifespan of 120 years was required as an essential criterion of the specifications set during its construction between 1999 and 2004. Due to its geographical location, in the Gulf of Corinth, the durability of concrete subjected to the aggressive marine environment was a major concern during the design of this structure falling within exposure classes XS1 to XS3; corrosion of the reinforcements induced by the penetration of chlorides being one of the main causes of possible identified deterioration.

3.1.3.2 History of works and current condition

Specific studies had therefore been carried out before its construction by the company Vinci Construction GP, jointly with the LERM, in order to characterize the durability parameters of the various predefined concrete compositions and to feed the forecasting tool of chloride penetration (LERM software), in order to define the conditions for reaching the expected lifespan of 120 years, for the different exposure cases (immersion, tidal / splashing and aerial areas) (Cussigh *et al.*, 2010; Ammouche *et al.*, 2012). The lifetime indicators obtained on this structure after commissioning have made it possible to refine the input data (considering the actual characteristics of the concrete) and to verify the prediction of the model and to improve it.

As part of this bridge construction project, measurements of durability indicators (gas permeability, apparent coefficient of chloride diffusion, permeability to chloride ions) were carried out on test specimens from the site and then on samples cored on testing wall (mock-up) on the construction site (Cussigh *et al.,* 2010). In fact, as part of a monitoring program of the bridge, a sacrificial reinforced concrete wall was built near one of the structure's piers in order to acquire lifetime indicators (chloride profiles in particular) and to determine durability indicators according to the age of the concrete in-situ. Tests were carried out on samples taken from the piers of the structure in order to supplement the available data and in particular the law of evolution of the apparent coefficient of chloride diffusion as a function of time. Chloride profiles were also measured on the structure.

This section provides a summary of the main indicator data for the durability of the concrete used for the submerged parts and in the tidal zone of the structure. These data are supplemented by the chloride profiles (free and total) measured on the test wall and in the tidal zone (XS3) of two piers as well as in the submerged zone (XS2) of a pile.

The contractual specifications and the values finally retained for the construction of the bridge are summarized in the Table 2.19.

Additional contractual specifications have been requested for the tidal range and splash zone (XS3):

- water penetration depth < 20 mm;
- permeability to RCPT (Rapid Chloride Penetration Test) chloride ions at 90 days <1000 C.

Table 2.19. Contractual specifications and values finally used for the construction

Exposure	Parameters	Specifications of the tender	Values used for the project
Air conveying sea salt (XS1)	Minimum nominal concrete cover (mm)	50	50 (> MSL +10m)
	Minimal strength class (MPa)	C30/37	C45/55
	Minimal cement content (kg/m^3)	360	400
	Maximum Water/Cement ratio	0.45	0.40
Submerged zone (XS2)	Minimum nominal concrete cover (mm)	50	60 (< MSL –5m)
	Minimal strength class (MPa)	C35/45	C45/55
	Minimal cement content (kg/m^3)	400	400
	Maximum Water/Cement ratio	0.40	0.40
Tidal and splash zone (XS3)	Minimum nominal concrete cover (mm)	75	85 (MSL –5m; MSL +10m)
	Minimal strength class (MPa)	C35/45	C45/55
	Minimal cement content (kg/m^3)	400	420
	Maximum Water/Cement ratio	0.40	0.40

** MSL: mean sea level*

The four study zones are as follows:

- The durability test wall (exposure to spray and splash - XS3): A durability test wall was built in line with the pier (P2) of an access viaduct in order to minimize sampling from the structure (Figure 2.23). This wall is exposed to spray and splash;

Figure 2.23. View of the testing wall for durability study

- The submerged area of the M2 pylon (XS2);
- The tidal range of the M2 pylon (XS3);
- The tidal zone of the M3 pylon (XS3).

The composition of the class C45/55 concrete used for the entire structure in submerged areas (XS2) and in tidal / splash zones (XS3) is as follows:

- CEM III / A 42.5 PM ES (60-65 % slag);
- Cement content 420 kg/m^3;
- Weff / C = 0.39;
- Compressive strength at 28 days: average = 69 MPa; standard deviation = 4.8 MPa.

The chloride-concrete interaction isotherm was carried out as part of the preliminary study with the AFGC-GranDuBé test method on concrete aged 11.5 months during the test (Figure 2.24).

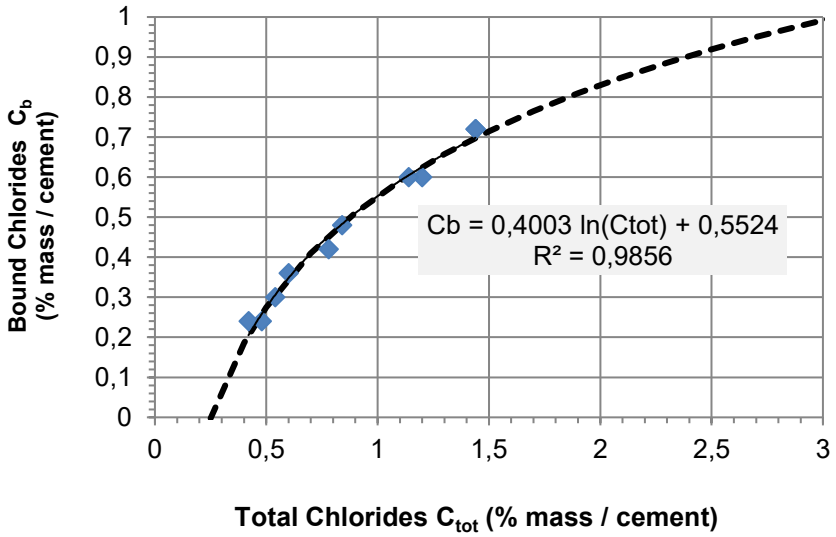

Figure 2.24. Chloride-concrete interaction isotherm (AFGC - GranDuBé test)

The results of the measurements of the apparent coefficient of chloride diffusion are summarized in the following Table 2.20.

Table 2.20. Values of the apparent coefficient of chloride diffusion with the age

Bridge part	Age (months)	D_{rcm} (10^{-12}m s^{-1})	
Preliminary Study	11.5	0.40	
Testing Wall at different times	2.5	0.86	
	11	0.44	
	24	0.50	
	62	0.43	
	169	0,50	
M1 Sampling from the interior of the pylon	24	0.63 (0.53 / 0.74)	
M2 Sampling from the interior of the pylon	33	0.24 (0.22 / 0.26)	
M3 Sampling from the interior of the pylon	36	0.34 (0.38 / 0.30)	
M4 Sampling from the interior of the pylon	33	0.61 (0.26/0.80/0.32/0.71/0.98)	
M2: On cores taken from different external faces of the pylon	45	North face: 0.63	Mean : 0.37
		South face: 0.22	
		West face: 0.28	
		East face: 0.36	

Potential durability classes (according to AFGC, 2004)				
Very low	Low	Average	High	Very high

All of the apparent coefficient of chloride diffusion measurements carried out both on the test wall and on the piers / pylons of the structure made it possible to define the following law of evolution:

- D_{rcm} (t) = 1.1 $10^{-12}.t^{-0.215}$ m^2/s for t < 120 months;
- D_{rcm} = 0.35 10^{-12} m^2/s for t ≥ 120 months.

This law is shown in blue on Figure 2.25. It allows to evaluate the ageing coefficient based on the law described in 2.3; it is thus 0.215 between 3 and 120 months when it stabilizes. This coefficient is much lower than the value of 0.45 proposed by the fib report n ° 34 for slag concretes. This is due to the fact that, from laboratory measurements of chloride diffusion coefficient at different ages, only the hydration effect is captured and interaction with the ambient marine medium is not taken into account, and also possibly because initial chloride diffusion/migration coefficient is very low and make the fitting on limit time difficult and less precise.

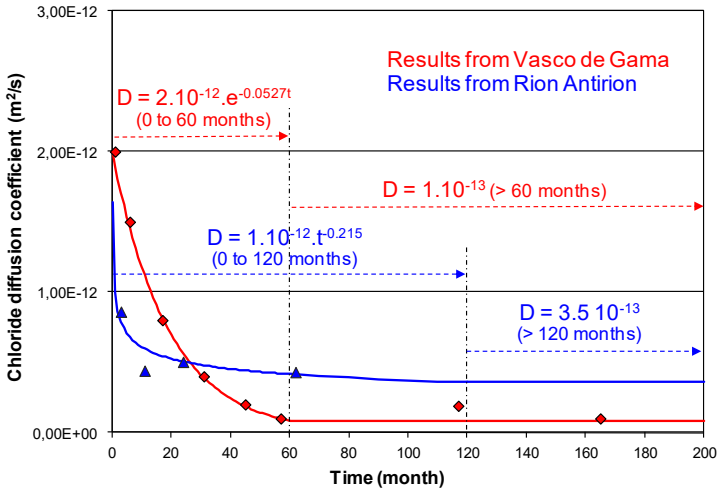

Figure 2.25. Evolution of the apparent coefficient of chloride diffusion of concrete with time

The measures of the other durability indicators are shown in the following Table 2.21.

Table 2.21. Values of durability indicators measured at construction and after 24 months

Durability Indicators	Part of structure	Concrete age	Result	
Gas Permeability	Cores of the test wall *	1 month	4.2 10^{-18} m^2	
Porosity accessible to water	Cores of the test wall *	1 month	11.3 %	
Apparent density	Cores of the test wall *	1 month	2320 kg/m^3	
Permeability to chloride ions	Control specimen	3 months	220-600 Coulombs	
Accelerated carbonation test (50 % CO2, 20 ± 2°C, 65 ± 5 % HR)	Cores of the test wall	24 months	7 days	2 mm
			14 days	3 mm
			28 days	3.2 mm
			56 days	3.4 mm

** Preliminary study*

Potential durability classes (according to AFGC, 2004)				
Very low	Low	Average	High	Very high

The concrete of the pylons and the test wall of the Rion-Antirion bridge is globally very durable according to the AFGC guide of 2004 (AFGC, 2004).

3.1.3.3 Lifetime indicators

a. Durability test wall (exposure to spray and splash - XS3)

The free chloride and total chloride profiles were measured at 2.5 months, 11 months, 24 months, 62 months and 150 months and are recorded in Table 2.22.

Table 2.22. Chloride Profiles – Concrete of the test wall – 5 durations of exposure

Ref. Sample. Age	Depth (mm)	Chlorides / concrete (%)			Chlorides / cement * (%)		
		Cl total	Cl free	Cl bound	Cl total	Cl free	Cl bound
7658-1.4 2,5 months	*0 à 10*	0.07	0.05	0.02	0.40	0.29	0.12
	10 à 20	0.02	0.02	< 0.01	0.12	0.12	< 0.06
	20 à 40	0.01	< 0.01	0.01	0.06	< 0.06	0.06
	40 à 60	0.01	< 0.01	0.01	0.06	< 0.06	0.06
	60 à 80	0.02	0.02	< 0.01	0.12	0.12	< 0.06
7658-3.4 11 months	*0 à 10*	0.25	0.15	0.10	1.44	0.86	0.58
	10 à 20	0.03	0.03	< 0.01	0.17	0.17	< 0.06
	20 à 40	0.03	0.03	< 0.01	0.17	0.17	< 0.06
	40 à 60	0.03	0.03	< 0.01	0.17	0.17	< 0.06
	60 à 80	0.03	0.03	< 0.01	0.17	0.17	< 0.06
7658-4.4 24 months	*0 à 10*	0.40	0.28	0.12	2.30	1.61	0.69
	10 à 20	0.05	0.04	0.01	0.29	0.23	0.06
	20 à 40	0.02	0.01	0.01	0.12	0.06	0.06
	40 à 60	0.02	0.02	0.00	0.12	0.12	0.00
	60 à 80	0.02	0.02	0.00	0.12	0.12	0.00
23332-5.4 62 months	*0 à 10*	0.55	0.37	0.18	3.16	2.13	1.04
	10 à 20	0.27	0.15	0.12	1.55	0.86	0.69
	20 à 40	0.03	0.02	0.01	0.17	0.12	0.06
	40 à 60	0.03	0.02	0.01	0.17	0.12	0.06
	60 à 80	0.03	0.02	0.01	0.17	0.12	0.06
43255.1 150 months	*0 à 10*	0.58	0.53	0.05	3.34	3.05	0.29
	10 à 20	0.59	0.51	0.08	3.39	2.93	0.46
	20 à 40	0.06	0.05	0.01	0.35	0.29	0.06
	40 à 60	0.02	0.02	< 0.01	0.12	0.12	< 0.06
	60 à 80	0.02	0.02	< 0.01	0.12	0.12	< 0.06

** Calculated by considering a cement content of 400 kg/m³ and an apparent density (AFREM): ρ_d= 2300 kg/m³*

From these values, it is possible to estimate the chloride contents at the surface (Table 2.23).

Table 2.23. Total and free chloride contents estimated at the concrete surface (limit condition)

	7658-1.4 2,5 months	7658-3.4 11 months	7658-4.4 24 months	23332-5.4 62 months	43255.1 150 months
	% mass / cement				
Total chloride content estimated at the surface – C_{st}	0.6	2.1	3.4	4.0	(*)
Free chloride content estimated at the surface – C_{sf}	0.4	1.2	2.3	2.8	(*)

(*) Given the shape of the profile obtained, requiring verification on a longer period, limit conditions estimated at 62 months should be considered.

It is also observed in this XS3 zone that the bound chlorides reach about 30 % of the total chlorides near the surface (between 0 and 10 mm) at 62 months and then fall to 10 % at 150 months (possibly an effect of the carbonation?), and that there are few chlorides bound after 150 months in depth (beyond 40 mm), but we are at the limit of the precision of the measurements.

b. M2 pylon - submerged zone (XS2)

The profiles of free chlorides and total chlorides were measured on samples taken under water, on three different faces of the M2 pylon (n ° 14, 16 and 19), after 9 years of exposure to -4 m below the mean level of the sea (see Table 2.24).

Table 2.24. Chlorides Profiles in the submerged zone (XS2) – pylon M2 – 108 months of exposure

Ref. 23332	Depth (mm)	Soluble silica (%)	Chlorides / concrete (%)			Chlorides / cement[(1)] (%)		
			Cl total	Cl free	Cl bound	Cl total	Cl free	Cl bound
M2 face n°14	*0 à 10*	5.19	0.36	0.29	0.07	2.05	1.65	0.40
	10 à 20	4.79	0.24	0.16	0.08	1.48	0.99	0.49
	20 à 30	5.96	0.08	0.06	0.02	0.40	0.30	0.10
	30 à 40	5.54	0.04	0.04	0.00	0.21	0.21	0.00
M2 face n°16	*0 à 10*	5.01	0.29	0.23	0.06	1.71	1.35	0.35
	10 à 20	4.25	0.17	0.12	0.05	1.18	0.83	0.35
	20 à 30	6.04	0.05	0.04	0.01	0.24	0.20	0.05
	30 à 40	6.07	0.04	0.03	0.01	0.19	0.15	0.05
M2 face n°19	*0 à 10*	5.36	0.43	0.34	0.09	2.37	1.87	0.50
	10 à 20	5.45	0.25	0.17	0.08	1.35	0.92	0.43
	20 à 30	4.80	0.05	0.04	0.01	0.31	0.25	0.06
	30 à 40	6.89	0.04	0.02	0.02	0.17	0.09	0.09
	40 à 50	5.35	0.04	0.02	0.02	0.22	0.11	0.11

(1) Calculated from the soluble silica measured in each slice and the mean content of silica in the cement (= 29,5 %)

The total chloride and free chloride contents estimated at the surface are 3.5 % and 3 % respectively with respect to the mass of cement.

It can be seen in this XS2 zone that the bound chlorides reach about 20 % of the total chlorides near the surface (between 0 and 10 mm) after 9 years, and that this percentage is maintained, or even increases with depth (50 % for face n° 19).

c. M2 pylon - tidal zone (XS3)

The profiles of free chlorides and total chlorides were measured on samples taken from four different faces of the M2 pylon, after 45 months of exposure at approximately + 1 m to +1.5 m above mean sea level (see Table 2.25).

Table 2.25. Chloride Profiles in the tidal zone (XS3) – pylon M2 – 45 months of exposure

Ref. sample	Depth (mm)	Chlorides / concrete (%)			Chlorides / cement (1) (%)		
		Cl total	Cl free	Cl bound	Cl total	Cl free	Cl bound
7878-C1 North face	*0 à 10*	0.50	0.37	0.13	2.76	2.04	0.72
	10 à 20	0.02	0.02	< 0.01	0.11	0.11	< 0.06
	20 à 30	0.02	0.02	< 0.01	0.11	0.11	< 0.06
	30 à 50	< 0.01	< 0.01	< 0.01	< 0.06	< 0.06	< 0.06
7878-C2 South face	*0 à 10*	0.68	0.51	0.17	3.76	2.82	0.94
	10 à 20	0.09	0.02	0.07	0.50	0.11	0.39
	20 à 30	0.02	0.01	0.01	0.11	0.06	0.06
	30 à 50	0.01	0.01	< 0.01	0.06	0.06	< 0.06
7878-C3 West face	*0 à 10*	0.73	0.51	0.22	4.03	2.82	1.22
	10 à 20	0.02	0.02	< 0.01	0.11	0.11	< 0.06
	20 à 30	0.02	0.01	0.01	0.11	0.06	0.06
	30 à 50	0.02	0.01	0.01	0.11	0.06	0.06
7878-C4 East face	*0 à 10*	0.91	0.64	0.27	5.03	3.54	1.49
	10 à 20	0.07	0.05	0.02	0.39	0.28	0.11
	20 à 30	0.03	0.01	0.02	0.17	0.06	0.11
	30 à 50	0.02	0.01	0.01	0.11	0.06	0.06

(1) Calculation with 420 kg/m³ of cement and an apparent density (AFREM) ρ_d = 2320 kg/m³

From these values, it is possible to estimate the chloride contents at the surface (Table 2.26).

Table 2.26. Chlorides Profiles estimated at the concrete surface (limit condition) - pylon M2 – 45 months of exposure

	7878-C1 North face	7878-C4 East face
	% mass / cement	
Total chloride content estimated at the surface – Cst	4.8	7.2
Free chloride content estimated at the surface – Csf	3.5	6.0

It is observed in this XS3 zone that the bound chlorides reach approximately 30 % of the total chlorides near the surface (between 0 and 10 mm) after 45 months.

d. M3 pylon - tidal range (XS3)

Two chloride content measurement campaigns were carried out:

- July 2010, after 114 months of exposure: a core Ø 25 mm x h 30 or 50 mm was taken from three faces (n° 14, n° 16 and n° 19), approximately +1 m above the mean sea level;
- October 2017, after 201 months of exposure: three cores Ø 25 mm x h 30 or 50 mm were taken in three zones of the face n° 19 at approximately + 0.8 m above mean sea level.

The profiles of free chlorides and total chlorides measured are shown in the following Table 2.27.

Table 2.27. Chloride Profiles in tidal zone (XS3) of pylon M3

Ref.	Exposure duration (months)	Depth (mm)	Soluble silica (%)	Chlorides / concrete (%)			Chlorides / cement(1) (%)		
				Cl total	Cl free	Cl Bound	Cl total	Cl free	Cl bound
M3 face n°14	114	0 - 10	5.72	0.59	0.44	0.15	3.04	2.27	0.77
		10 - 20	5.07	0.07	0.05	0.02	0.41	0.29	0.12
		20 - 30	4.34	0.03	0.02	0.01	0.20	0.14	0.07
M3 face n°16		0 - 10	5.58	0.46	0.31	0.15	2.43	1.64	0.79
		10 - 20	3.90	0.09	0.05	0.04	0.68	0.38	0.30
		20 - 30	5.00	0.02	0.01	0.01	0.12	0.06	0.06
M3 face n°19		0 - 10	6.07	0.78	0.64	0.14	3.79	3.11	0.68
		10 - 20	5.47	0.24	0.16	0.08	1.29	0.86	0.43
		20 - 30	5.63	0.02	0.01	0.01	0.10	0.05	0.05
		30 - 40	5.76	0.02	0.01	0.01	0.10	0.05	0.05
		40 - 50	5.61	0.02	0.01	0.01	0.11	0.05	0.05
M3 face n°19 +77 cm MSL	201	0 - 10	6.18	3.96	3.65	0.31	3.96	3.65	0.31
		10 - 20	6.13	2.06	1.68	0.38	2.06	1.68	0.38
		20 - 30	5.5	0.19	0.17	0.02	0.19	0.17	0.02
		30 - 40	5.33	0.12	0.11	<0.06	0.12	0.11	<0.06
		40 - 50	5.51	0.11	0.11	<0.06	0.11	0.11	<0.06
M3 face n°19 +72 cm MSL		0 - 10	5.4	4.4	4.03	0.36	4.4	4.03	0.36
		10 - 20	4.22	1.51	1.22	0.29	1.51	1.22	0.29
		20 - 30	5.37	0.12	0.12	<0.06	0.12	0.12	<0.06
		30 - 40	5.31	0.08	0.1	<0.06	0.08	0.1	<0.06
		40 - 50	5.12	0.12	0.12	<0.06	0.12	0.12	<0.06
M3 face n°19 +72 cm MSL		0 - 10	4.89	4.09	3.75	0.34	4.09	3.75	0.34
		10 - 20	5.06	1.83	1.43	0.4	1.83	1.43	0.40
		20 - 30	4.33	0.14	0.14	<0.06	0.14	0.14	<0.06
		30 - 40	2.40	0.12	0.12	<0.06	0.12	0.12	<0.06
		40 - 50	5.35	0.11	0.11	0.06	0.11	0.11	0.06

MSL: Mean sea level

From these values, it is possible to estimate the chloride contents at the surface (Table 2.28).

Table 2.28. Chlorides Profiles estimated at the concrete surface (limit condition) - pylon M3 – tidal zone 114 and 201 months of exposure

	M3 face n°19		
	114 months	**201 months intermediary profile**	**201 months Profil at top**
	% mass / cement		
Total chloride content estimated at the surface – Cst	5.0	5.2	5.8
Free chloride content estimated at the surface – Csf	4.2	4.8	5.4

It is observed in this XS3 zone that the bound chlorides reach about 25 % of the total chlorides near the surface (between 0 and 10 mm) after 114 months and drop to 8 % after 201 months, while chlorides have continued to penetrate by the surface, that there is 20 % of bound chlorides in the 10-20 mm slice after 201 months, and that there is little quantity of bound chlorides after 201 months in depth (beyond 40 mm) as for the test wall.

3.1.3.4 Investigations carried out during PerfDub project

There were no additional investigations carried out within the framework of PerfDub except for the chloride contents measured on concrete samples taken from the testing wall and from the tidal zone of the M3 pylon after respectively 12.3 years. and 16.75 years of exposure, and presented above.

3.1.3.5 Conclusion drawn

The concrete of the pylons and the test wall of the Rion-Antirion bridge is globally very durable according to the AFGC guide of 2004. After 20 years of age, the structure does not show any damage due to corrosion.

The measurements of the migration coefficient of the chlorides carried out over a period of 62 months make it possible to have a good evolution of this coefficient over time and to deduce therefrom a value of the ageing factor that can be estimated as 0.215 (slag concrete).

Thanks to the measurements carried out on this structure, it is possible to follow the penetration of chlorides in the form of free and total chlorides over a period of 17 years in a tidal zone (XS3). In the XS3 zones, bound chlorides are found to reach around 25 to 30 % of the total chlorides near the surface (between 0 and 10 mm) up to 62 months, dropping to around 10 % after 150 months (can it be an effect of carbonation?), and that there are few bound chlorides after 150 months in depth (beyond 40 mm), but we are at the limit of the precision of the measurements.

A comparison between the submerged (XS2) and tidal (XS3) zones of the same M2 pylon shows that the total and free chloride contents estimated at the surface are respectively 3.5 % and 3 % relative to the mass of cement after 108 months (9 years) in zone XS2, and are respectively 6 % and 4.75 % after 45 months in zone XS3.

All of these measurements can be used to calibrate the apparent coefficient of chloride diffusion models.

3.1.4 Volesvres Bridge

3.1.4.1 Presentation of the bridge

This bridge is the doubling of the Volesvres viaduct within the framework of the 2 x 2 files upgrading of the RN 79 (Figure 2.26). It is located in the town of Volesvres in the Saône et Loire department and allows the crossing of the Bourbince river, the Departmental Road n°974 and the Center canal. The structure is a steel and concrete composite bridge with a constant height, and a total length of 206 m. The deck has 5 continuous spans with a length of 32.00 - 40.00 - 50.00 - 52.00 - 32.00 meters going from Digoin to Macon.

Figure 2.26. General view of the Volesvres bridge

The abutments consist of a crossbeam which acts as a foundation footing. They are based deeply on two rows of vertical reinforced concrete piles, cast in place and 1.20 m in diameter.

The slab of the deck consists of a reinforced concrete slab approximately 30 centimeters thick. The connection of the concrete slab to the steel frame is ensured by stud type connectors. The steel frame of the deck consists of an open box, the webs of which are inclined. Transversely, the frame is stiffened by diaphragms spaced about 4 meters apart.

3.1.4.2 History of works and current condition

The Center-East Inter-Departmental Direction of Roads wishes to change the specification of the concrete used for for civil engineering structures from the current prescriptive approach (NF EN 206-1 and fascicle 65 of the CCTG) to the performance-based approach. It wished to implement the performance-based concrete approach for the construction of this structure, which took place between 2010 and 2012, on a non-contractual basis.

Four concrete formulas were chosen respectively for the piles, the supports, the slabs and the sills. The strength and exposure classes specified are as follows:

- deep foundations: C30/37 XC2 / XA1;
- footings, abutment front walls, pier shafts: C30/37 XC4 / XF1;
- deck slab: C40/50 XC4 / XF1;
- BN4 safety anchor sill, curbs, anchor beams of expansion joint: C35/45 XC4 / XF4 / XD3.

Suitability tests were carried out and the Autun Laboratory of the Cerema established a control plan "in principle", complying with the recommendations of the LCPC provisional recommendations of March 2010 "Control of the durability of concrete structures - Application of the 'performance-based approach' and based on the general provisional schedule of works (outside bad weather) made by the CBR-TP company.

The tests had to be carried out in accordance with the operating modes defined in appendix 1 of the LCPC provisional recommendations: “Simplified operating modes: Electrical resistivity and migration of chloride ions under electric field, porosity to water, CEMBUREAU Gas Permeability”.

However, during the intermediate meeting to present the results on concrete for the supports which took place on February 22, 2011, it appeared that:

- Lafarge LCR and CTG Calcia laboratories had sometimes applied internal operating procedures;
- the testing procedures of the LCPC provisional recommendations were not always sufficiently explicit.

The initial detailed inspection carried out upon receipt of the bridge did not reveal any problems, and given the date of construction, we do not have the results of further investigations; tests were nevertheless launched as part of the PerfDub project.

3.1.4.3 Investigations carried out by the Cerema

The results of the measurements of the durability indicators are as follows:

a. Deep foundation concrete (C30/37 385 kg CEM I 52.5 N CE PM ES CP2 NF; W_{eff} / B_{eq} = 0.48)

2 samples taken (06/01/2010: suitability of Gueugnon concrete plant and 09/24/2010: casting of footing P1):

- $f_{cm,28}$ from 48.3 to 56.1 MPa (compliant for a C30/37);
- $P_{water,28}$ from 14.1 to 15.5 % - results of contradictory tests: deviation of 1 % (in absolute value);
- $P_{water,90}$ from 14.2 to 15.6 % - results of contradictory tests: difference of 1.4 % (in absolute value) (acceptability threshold at 15 % for XC2, according to LCPC recommendations);
- $resistivity_{28}$ from 48 to 55 (Ω.m);
- $resistivity_{90}$ from 48 to 85 (Ω.m) - result of contradictory tests: difference of 37 Ω.m (in absolute value).

b. Concrete of supports (C30/37 330 kg CEM III / A 52.5 L CE PM ES CP1 NF; W_{eff} / B_{eq} = 0.47)

7 samples taken

- $f_{cm,28}$ from 45.3 to 61 MPa;
- $P_{water,28}$ from 12.2 to 16.9 % - 5 values: mean = 15.7 %, standard deviation = 0.3 % - contradictory test results: deviations from 0.4 to 2.5 % (in absolute value);
- $P_{water,90}$ from 14.5 to 16.5 % - 5 values of Autun laboratory: mean = 15.6 %, standard deviation = 0.6 % - contradictory test results: deviations of 0.1 to 1 % (in absolute value);

- resistivity$_{28}$ from 235 to 312 (Ω.m) - 4 values of Autun laboratory: mean = 276, standard deviation = 25;
- resistivity$_{90}$ from 287 to 369 (Ω.m) - 5 values of Autun laboratory: mean = 323, standard deviation = 31 - result of contradictory tests: deviation of 27 - 28 Ω.m (in absolute value);
- $K_{gas,90}$ from 54 to 92 (10^{-18} m^2) - 4 values of Clermont-Ferrand laboratory: mean = 76, standard deviation = 11 - contradictory test results: deviations from 3.7 to 14.1 (in absolute value).

Convenience tests (2 plants) (considered as study test)

- $f_{cm,28}$ from 45.3 to 51 MPa (compliant for a C30/37);
- $P_{water,28}$ from 16.1 to 16.9 %;
- $P_{water,90}$ from 14.5 to 16.5 % > acceptability threshold of 13 % for XC4;
- resistivity$_{28}$: 235 (Ω.m);
- resistivity$_{90}$ from 287 to 369 (Ω.m);
- $K_{gas,90}$ from 77 to 92 (10^{-18} m^2) < acceptability threshold of 150 for XC4.

Control tests (2 plants)

- $f_{cm,28}$ from 53.7 to 61 MPa (compliant for a C30/37);
- $P_{water,28}$ from 12.2 to 16 % < 1.1 $P_{water,28}$ “study”;
- $P_{water,90}$ from 15 to 15.6 % > threshold of acceptability of 13 % for XC4;
- resistivity$_{28}$ from 256 to 312 (Ω.m) > 0.8 resistivity$_{28}$ “study”;
- resistivity$_{90}$ from 310 to 338 (Ω.m);
- $K_{gas,90}$ from 53.9 to 68 (10^{-18} m^2) < acceptability threshold of 150 for XC4.

c. Concrete of slabs (C40/50, 350 kg CEM I 52.5 N CE CP2 NF; W_{eff} / B_{eq} = 0.42)

10 samples taken:

- $f_{cm,28}$ from 53 to 65.7 MPa;
- $P_{water,28}$ from 13.9 to 14.7 % - 10 values of Autun Laboratory: mean = 14.4 %, standard deviation = 0.2 % - contradictory test results: deviations of 0.2 to 0.3 % (in absolute value);
- $P_{water,90}$ from 13.6 to 14.3 % - 4 values of Autun Laboratory: mean = 14.1 %, standard deviation = 0.3 % - contradictory test result: deviations of 0.1 to 0.4 % (in absolute value);
- resistivity$_{28}$ from 52 to 81 (*) (Ω.m) - 10 values of Autun Laboratory: mean = 62, standard deviation = 6 - result of contradictory tests: deviation from 7 to 20 Ω.m (in absolute value);
- resistivity$_{90}$ from 74 to 175 (**) (Ω.m) - 4 values of Autun Laboratory: mean = 119, standard deviation = 50 - result of contradictory tests: deviation from 39 to 47 Ω.m (in absolute value);
- $K_{gas,90}$ from 64 to 93 (10^{-18} m^2) - 3 DLCF values: mean = 75, standard deviation = 16 - contradictory test result: difference of 21.2 - 21.6 (in absolute value).

Convenience tests (2 plants) (considered as study test)

- $f_{cm,28}$ from 53 to 57 MPa (compliant for a C40/50);
- $P_{water,28}$ from 13.9 to 14.6 %;
- $P_{water,90}$ from 13.7 to 14.3 % > acceptability threshold of 13 % for XC4;
- resistivity$_{28}$ from 52 to 81 (Ω.m);
- resistivity$_{90}$ from 99 to 175 (Ω.m);
- $K_{gas,90}$ from 71.4 to 93 (10^{-18} m^2) < acceptability threshold of 150 for XC4.

Control tests (2 plants)

- $f_{cm,28}$ from 57.1 to 65.7 MPa (compliant for a C40 / 50);
- $P_{water,28}$ from 14.1 to 14.7 % < 1.1 Porosity 28 days “study”;
- $P_{water,90}$ from 13.6 to 14.3 % > acceptability threshold of 13 % for XC4;
- resistivity$_{28}$ from 57 to 65 (Ω.m) > 0.8 Resistivity 28 days “study”;
- resistivity$_{90}$ from 74 to 118 (Ω.m);
- $K_{gas,90}$ from 64 to 85.2 (10^{-18} m^2) < acceptability threshold of 150 for XC4.

d. Concrete of the beam for anchoring the BN4 safety barrier (C35/45 420 kg CEM I 52.5 N CE PM ES CP2 NF; W_{eff} / B_{eq} = 0.34)

Only 2 samples taken (12/13/2010: casting of west side wall C5 and 03/05/2012: casting of the prototype element of a sill XF4 G + S): 2 different compositions tested with only 1 sample per formula

- $f_{cm,28}$: 37 - 40.2 MPa or 42.7 - 54.7 MPa (compliant for a C35/45);
- $P_{water,90}$: 15.7 % or 13.6 % (acceptability threshold at 11 % for XD3);
- resistivity$_{90}$: 47 or 61 (Ω.m);
- $K_{gas,90}$: 580 or 338 (10^{-18} m^2) (acceptability threshold at 150 for XD3);
- $D_{app,90}$: 15.3 or 11.9 (10^{-12} m^2/s) (acceptability threshold at 3 for XD3).

3.1.4.4 Investigations carried out during the PerfDub project

Given the young age of the concrete (less than 5 years in 2016), it was decided not to measure the lifetime indicators on the structure (carbonation depth and chloride content profile), but it was decided to determine the durability indicators on samples resulting from core drilling carried out in September 2016 in a support and an area of the slab, in order to be able to compare with the indicators determined on 11x22 molded specimens during construction.

In addition, it was decided to determine the apparent coefficient of chloride ions diffusion and to carry out capillary absorption tests, despite the absence of a point of comparison "during construction" for these parameters for the concretes studied.

In September 2016, three cores named I, II and III were taken from the earth retaining wall at the end of the bridge on the C5 abutment and three cores named a, b and c were taken from the slab of the deck.

The results of the various tests carried out on these cores are reported in Table 2.29.

Table 2.29. Values obtained for the durability indicators

Durability indicators		Abutment C5	Deck slab
Apparent coefficient of chloride diffusion (10^{-12} m².s^{-1})	D_{rcm}	11,2 (10,4/12,0/10,5)	7,9 (8,1/7,6/8,0)
Electrical resistivity (Ω.m)	Res	637 (680/644/588)	106 (117/101/100)
Porosity accessible to water (%)	P_{water}	14,6 (14,4/14,8/14,6)	12,1 (12,1/12,4/11,8)
Gas Permeability (10^{-18} m²)	K_{gas}	90 (70/100/100)	80 (70/90/70)
Other characteristics			
Capillary absorption coefficient at 24h (kg/m²)	C_a	4,68 (5,09/3,72/5,22)	5,68 (5 ,83/5,28/5,92)
Apparent Density (kg/m^3)	ρ_b	2230 (2234/2212/2231)	2260 (2261/2250/2263)

Potential durability classes (according to AFGC, 2004)				
Very low	Low	Average	High	Very high

First, it can be considered that there is very little difference between the procedures for the water porosity, resistivity and gas permeability tests carried out at construction and 6 years later; which makes it possible to make direct comparisons of test results and to establish the following findings.

a. For the concrete of the slab (CEM I)

Five to six years later, we can see that the tendency of the porosity accessible to water to decrease is even more marked. The porosity of 12.1 % obtained on core samples represents an average decrease of 2 % compared to the average of the tests carried out on this concrete at the term of 90 days ($P_{water,90}$ avg = 14.1 %). This decrease is far greater than the standard deviation of the tests. The threshold recommended in the LCPC guide was "$P_{water,90}$ < 13 %" for this type of concrete (XC4). If during the various convenience or control tests none of the samples made it possible to respect this value, we note that today the porosity accessible to water has fallen below this threshold, at least in our sampling zone. The potential durability of the concrete slab changes from "low" to "medium" according to the 2004 AFGC recommendations.

Five to six years later, we can see that the electrical resistivity measured on core samples (106 Ω.m), remains of the same order of magnitude as the average of the tests carried out on this concrete after 90 days (Res_{90} average = 119 Ω.m), given the importance of the standard deviation of the 90-day tests. This result therefore does not correlate directly with the observed decrease in the porosity accessible to water, despite the fact that these two values are physically linked as far as cementitious types are identical (the higher the porosity, the lower the resistivity, due to a higher large volume fraction of pores occupied by the interstitial liquid phase). In the 2013 summary report, we had already identified the relatively low resistivity of "CEM I" concretes. The measured resistivities correspond to the "average" potential durability class according to the 2004 AFGC recommendations.

Six to seven years later, we also see that the gas permeability measured on core samples (80.10^{-18} m²) remains of the same order of magnitude as the average of the tests carried out on this concrete after 90 days (75.10^{-18} m²), taking into account the standard deviation of the tests.

b. For the concrete of the supports (CEM III/A)

Six years later, we can see that this tendency of the porosity accessible to water to decrease is even more marked. The porosity of 14.6 % obtained on cored specimens represents an average drop of 1 % compared to the average of the tests carried out on this concrete after 90 days ($P_{water,90}$ avg = 15.6 %). This decrease is greater than the standard deviation of the tests. The threshold recommended in the LCPC guide was "$P_{water,90}$ < 13 %" for this type of concrete (XC4). During the various convenience or control tests, none of the samples allowed this value to be respected. We note that today the porosity accessible to water remains above this threshold. The potential durability of the concrete supports remains "low" according to the 2004 AFGC recommendations.

Six years later, we can see that the electrical resistivity measured on core samples (637 Ω.m) is significantly higher than the average of the tests carried out on this concrete after 90 days (Res_{90} avg = 323 Ω.m). This result correlates with the observed decrease in porosity accessible to water. In the 2013 summary report, we had already identified the greater resistivity of "CEM III/A" concretes. The measured resistivities correspond to the "high" potential durability class according to the 2004 AFGC recommendations.

Seven years later, we can see that the gas permeability measured on core samples (90.10^{-18} m²), remains of the same order of magnitude as the average of the tests carried out on this concrete after 90 days (76.10^{-18} m²), taking into account the standard deviation of the tests.

3.1.4.5 Conclusion drawn

The values of the porosity accessible to water exceed the thresholds of the LCPC Provisional Recommendations (up to + 0.6 and + 1.3 % in absolute value for CEM I concretes and up to + 3.5 % in absolute value for CEM III concrete; this could be explained by the testing procedure used for these measurements, with a stage 1 of saturation of the concrete under vacuum (25 mbar) lasting 72 hours instead of 48 hours or even less (phase of maintaining the vacuum in the presence of water for 68 hours instead of 44 hours or less).

This case study allows conclusions to be drawn in terms of dispersion of porosity measurements accessible to water carried out during construction:

- the dispersion of results within the same sample is low (less than 3 % in relative value in almost all cases);
- the standard deviations of the measurements carried out by the Autun Laboratory are low (0.6 % in maximum absolute value);
- the differences between laboratories on contradictory tests are most of the time less than 1 % in absolute value (and in all cases less than 10 % in relative value);
- the porosities at 90 days measured on the 4 concretes are "of the same order of magnitude", with however higher values (approximately + 1 %) measured on the "CEM III" concrete:
  - CEM I: from 13.6 % to 15.7 %,
  - CEM III: from 14.5 % to 16.5 %.

The gas permeability values meet the thresholds of the LCPC Provisional Recommendations. The standard deviations of the measurements carried out by the Clermont-Ferrand laboratory are of the order of 15 to 20 % in relative value.

For electrical resistivity measurements made at construction:

- the electrical resistivity is lower for CEM I concretes (< 200 or even < 100 Ω.m) than for CEM III concrete (rather between 200 and 400 Ω.m);
- the electrical resistivity seems to increase between 28 and 90 days (despite the significant dispersion observed for certain samples);
- the dispersion of the results within the same sample is quite large (generally less than 20 % in relative value, but sometimes more...);
- the standard deviations of the measurements carried out by the Autun laboratory are generally of the order of 10 % in relative value (but sometimes beyond...);
- the differences between laboratories on contradictory tests are of the same order of magnitude (10 % in relative value), but sometimes also beyond...

The comparison between the values of the durability indicators measured during construction on standard specimens, then 6 to 7 years later on cores, with similar procedures, shows that:

- for the slab concrete, made from CEM I cement, the porosity accessible to water has significantly decreased (from 14.1 % to 12.1 %) and falls below the threshold of 13 % defined by the LCPC guide for an XC4 concrete, while the electrical resistivity (approximately 110 Ω.m) and the gas permeability (approximately 80.10^{-18} m²) remain of the same order of magnitude as at the end of 90 days;
- for the support concrete, made from CEM III / A cement, the porosity accessible to water has decreased (from 15.6 % to 14.6 %) but remains above the threshold of 13 % defined by the LCPC guide for an XC4 concrete, while the electrical resistivity, which is greater than for the concrete of the slab, has almost doubled compared to the 90-day deadline (637 Ω.m for 323 Ω.m), and that the gas permeability (90.10^{-18} m²) remains of the same order of magnitude as after 90 days.

Finally, the apparent coefficient of chloride diffusion, measured for the first time six years after construction, is 8.10^{-12} m².s^{-1} for the slabs and 11.10^{-12} m².s^{-1} for the supports, which corresponds respectively to “medium” and “low” durability classes according to the AFGC recommendations of 2004.

The implementation of the performance-based concrete approach allowed to identify certain difficulties, in particular certain excessively restrictive values of the admissible thresholds of porosity accessible to water in application of the operating mode of the LCPC's provisional recommendations. This feedback was already taken into account in 2014 for the draft revision of the fascicle 65 of the technical specifications relating to the execution of concrete structures (porosity thresholds accessible to water revised taking into account the duration of vacuum saturation of concrete) and also within the PerfDub project. It has also made it possible to provide data on the dispersions of the measurements of the durability indicators, and, in the future, this will make it possible to move from average values to characteristic values and to set characteristic values as thresholds.

3.1.5 Loudéac Bridge

3.1.5.1 Presentation of the bridge

The bridge concerned is the underpass n ° 1 of the North detour from Loudéac carrying the RN164 and crossing the municipal road V.C.6 in Cojan (Figure 2.27).

Figure 2.27. General view of the Loudéac Bridge

It consists of a portal frame with a span of 8.50 m and a total length of 13.50 m. The piers are founded on footings (Figure 2.28).

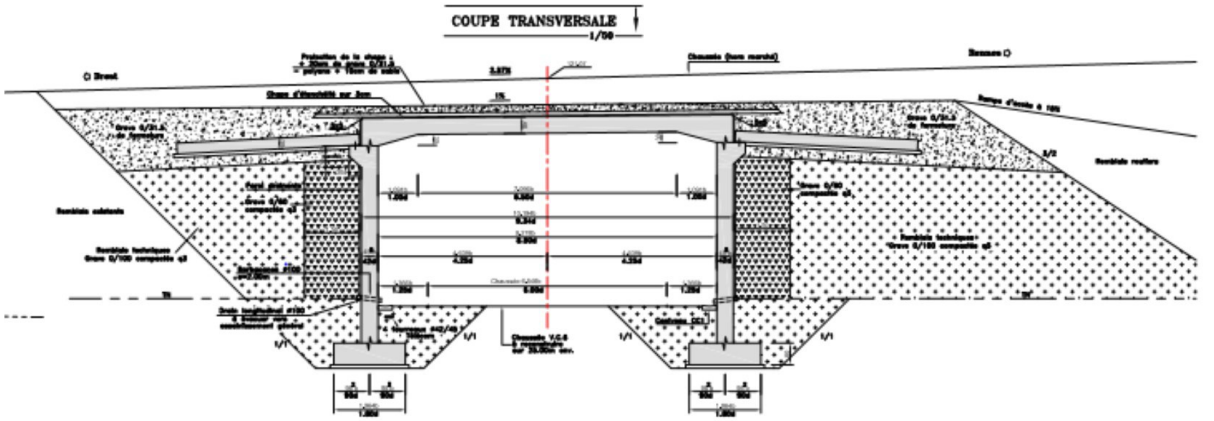

Figure 2.28. Cross section of the bridge

The west side wall was cast on the 23rd October of 2014 and investigations carried out 2 years after its construction.

The Loudéac bridge is located in an XC4 and XF1 environment; it is not exposed to deicing saltsand is in a moderate frost zone.

3.1.5.2 History of works and current condition

The technical specifications for construction included specific clauses relating to the performance-based approach to durability from the version of fascicule 65 being revised in 2013.

The concrete was poured with a container and the curing ensured by keeping the formwork in place. Its composition is presented in Table 2.30.

Table 2.30. Concrete composition of the Loudéac bridge

Composition of the concrete with origin of the constituents: C30/37 XC4(F) D_{max}10, Self-compacted concrete of category 2a (Sieve < 20%, L-box > 0,8 with 2 bars) Consistence: SF2 (660 – 750 mm)	
Cement content	350 kg/m^3
Cement type	CEM III/52.5 L PMES CP1 LAFARGE LE HAVRE
Quantity of mineral additions	170 kg/m^3
Type of mineral additions	Limestone filler Betocarb HP Erbray
Water content	Efficient Water: 183 l/m^3
Quantity of aggregates by aggregate size	
0/4 sablière d'Armorique Lafarge Aggregates (marine aggregates recomposed)	800 kg/m^3
6.3/10 St Lubin LESSARD (crushed diorite)	800 kg/m^3
Admixtures	
Optima 220 Chryso	4.95 kg/m^3
Chryso Tard	1.10 kg/m^3

The targeted slump-flow of fresh concrete is 700 mm and the theoretical density is 2350 kg/m^3. Its compressive strength fc28 is equal to 59.5 MPa (sample taken on 23/10/14 on the west side wall (check carried out during casting)).

The minimum cover required for steels is 45 mm for the side walls and 40 mm for the deck slab and the footings.

Table 2.31. Specifications for durability indicators

		Durability indicators regarding steel corrosion	
Bridge parts	**Exposure class**	**Water porosity $P_{water,90}$ (%)**	**Gas permeability $K_{gas,90}$ (10^{-18} m^2)**
Footings	XC2	< 15.5	--
Walls, deck slab and longitudinal beams supporting guardrails	XC4	< 14.5	< 200

The specifications related to the durability indicators (porosity accessible to water: Pwater and gas permeability: Kgas), with possible consideration of their variations for the modulation of the structural class, were as follows in Table 2.31.

During the concrete studies in laboratory, the producer obtained the following values of the durability indicators (average of 3 values each time) (Table 2.32).

Table 2.32. Values of the durability indicators at construction (studies)

Test for Studies		Porosity accessible to water (%)	Gas permeability (10^{-18} m^2)
At 28 days	Initial Formula	17	18
	Formula – 5 litres	15.9	19
	Formula + 5 litres	17.1	86
At 90 days	Initial Formula	16.0	24
	Formula – 5 litres	15.9	24
	Formula + 5 litres	17.0	51

During the convenience tests, the following values of the durability indicators were obtained (average of 3 values each time) (Table 2.33).

Table 2.33. Values of the durability indicators at construction (convenience)

Test for convenience		Porosity accessible to water (%)	Gas permeability (10^{-18} m^2)
At 28 days	Concrete Producer	15.3	28
	Producer Control	13.8	32
	Cerema	15.2	Outlier value
At 90 days	Concrete Producer	16.5	25
	Producer Control	15.0	37
	Cerema	17.1	Outlier value

Moreover, additional tests were carried out by Cerema on test specimens made for convenience tests, to measure the resistivity and the apparent coefficient of chloride diffusion (average of 3 values each time and standard deviation in brackets) (Table 2.34).

Table 2.34. Values of the durability indicators at construction (convenience) measured by Cerema

	Electrical resistivity (Ω.m)		Apparent coefficient of chloride diffusion D_{app} (10^{-12} m^{2}s^{-1})	
	At 28 days	At 90 days	At 28 days	At 90 days
Loudéac concrete plant	296 (2.0)	400 (17.2)	2.3 (0.1)	1.5 (0.3)
Locminé concrete plant	271 (14.5)	331 (10.6)	2.3 (0.1)	2.0 (0.1)

For each part of the structure, Cerema carried out control tests which gave the following results (average of 3 test specimens each time) presented in Table 2.35.

Table 2.35. Values of the durability indicators at construction (control) measured by Cerema

		Footing	West wall	Deck slab
Sampling date		01/10/2014	23/10/2014	02/12/2015
Testing date		08/01/2015	23/02/2015	16/03/2015
Age of concrete		99 days	123 days	104 days
Durability indicators				
Apparent coefficient of chloride diffusion (10^{-12} m².s^{-1})	D_{rcm}	1.5 (1.5/1.4/1.5)	1.4 (1.3/1.3/1.7)	1.6 (1.5/1.5/1.7)
Electrical resistivity (Ω.m)	Res	354 (340/350/371)	419 (409/426/424)	36 (31 / 41)
Porosity accessible to water (%)	P_{water}	16.1 (16.0/16.0/16.3)	15.8 (15.9/15.8/15.8)	15.5 (15.8/15.2/15.4)
Gas Permeability (10^{-18} m²)	K_{gas}	27 (29/25/28)	39 (44/35/X)	18 (16/18/19)
Other characteristics				
Pseudo permeability to liquid water (kg.m^{-2}.s$^{-0,5}$)	w	0.630 (0.627/0.606/0.658)	0.571 (0.537/0.547/0.629)	0.490 (0.484/0.454/0.531)
Capillary absorption coefficient at 24h (kg/m²)	C_a	3.12 (3.09/3.00/.3.27)	4.31 (4.66/4.59/3.68)	3.26 (3.25/3.00/3.51)
Density (kg/m^3)	ρ_b	2217 (2222/2219/2211)	2210 (2206/2211/2213)	2226 (2217/2232/2229)
Corrected compressive strength (MPa) à 28 days	$f_{cm,28}$	57.0 (58.3/56.8/55.9)	59.5 (60.6/59.6/58.4)	64.5 (63.6/64.0/63.9)

Potential durability classes (according to AFGC, 2004)				
Very low	Low	Average	High	Very high

In terms of resistance to the penetration of aggressive agents, the results show overall a concrete that is durable with regard to the corrosion of reinforcements. Except the porosity value, the set of durability indicators obtained for the concrete corresponds to a high durability level according to (AFGC, 2004).

The porosity results are singular and can be explained mainly by the high volume of the paste in a self-compacted concrete.

Concrete meets the gas permeability criterion but not the porosity criterion specified by the tender. A slight variability in the results from one control to another is observed but it is not likely to modify the classes of potential durability.

3.1.5.3 Investigations carried out during PerfDub project

The investigations were carried out in 2016 on the wall on the Rostrenen side, at man height. The investigations were carried out over an area 1.60 m high and 2.50 m long.

The Table 2.36 shows the characteristic statistical values of the cover (in mm).

Table 2.36. characteristic statistical values of the cover (in mm)

Part - Zone	Horizontal reinforcement					Vertical reinforcement				
	Mean	Min	< 45	e95+*	e95-**	Mean	Min	< 45	e95+*	e95-**
West wall	55	44	10 %	45	64	67	60	0 %	61	72

** Typical cover e_{95+}: 95 % of the covers measured are greater than e_{95+}*
*** Typical cover e_{95-}: 95 % of the measured covers are lower than e_{95-}*

10 % of the measured covers (horizontal reinforcement) have a lower cover than the expected cover (45 mm), but these measured covers (horizontal reinforcements) are greater than 44 mm. The vertical reinforcements of the wall are better covered (by design) and the measured covers are greater than 60 mm.

No carbonation was observed on the core collected from the structure.

After the preconditioning phase (drying at 45 ° C for 14 days), six samples were placed in a carbonation chamber (4 % CO_2, 20 °C, 65 % RH) for 28 and 56 days to carry out an accelerated carbonation test (these testing conditions were in effect when the tests were done). The results are as follows:

- Core Loudéac 4: 5.1 mm at 28 days and 6.0 mm at 56 days;
- Core Loudéac 5: 4.0 mm at 28 days and 5.2 mm at 56 days;
- Core Loudéac 6: 4.6 mm at 28 days and 5.3 mm at 56 days;
- Average of cores: 4.6 mm at 28 days and 5.5 mm at 56 days.

The following graph (Figure 2.29) summarizes the total chloride penetration profiles obtained in the investigation area from samples 1d, 2d and 3d.

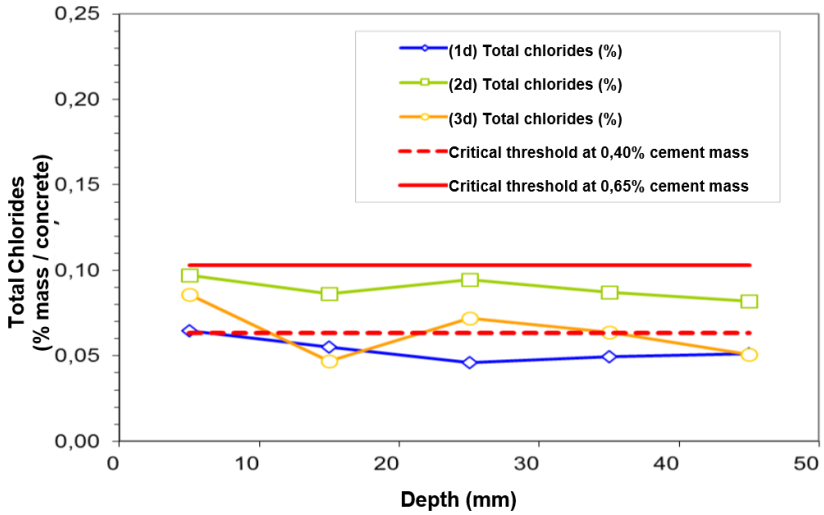

Figure 2.29. Total chloride profiles (% per concrete mass) with depth

The profiles are relatively flat. Their appearance shows that there is no penetration phenomenon from the outside, and this is consistent with the exposure of the part of the structure.

The critical corrosion initiation threshold in % of the concrete mass (0.103 %) was calculated from the cement content of the nominal formula (350 kg/m³) and the density determined during the porosity test (2203.4 kg/m³). Given the nature of the cement (CEM III), the assumption was made that the critical threshold was 0.65 % (as a % of the cement mass).

Although they remain below the critical threshold for initiation of corrosion, the total chloride contents are relatively high and can be explained by the fact that the concrete has been formulated with a CEM III which can contain up to 0.65 % of total chlorides relative to the mass of cement. The analytical balance on the nominal concrete formula carried out from the FTP had shown at the time of the concrete studies that the chloride rate was close to 0.65 %.

The concrete covers measured and the results of carbonation depth and chloride contents show that, statistically, there are no reinforcements located in carbonated or chlorinated concrete and therefore likely to be depassivated.

a. Durability indicators

A new measurement of these indicators was carried out in 2016. Table 2.37 presents the obtained results.

Table 2.37. Values of the durability indicators in 2016

Durability indicators		West wall
Apparent coefficient of chloride diffusion (10^{-12} m².s^{-1})	D_{rcm}	2.4 (2.2/2.1/3.0)
Electrical resistivity (Ω.m)	Res	377 (375/383/374)
Porosity accessible to water (%)	P_{water}	15.4 (15.4/15.5/15.2)
Gas Permeability (10^{-18} m²)	K_{gas}	23 (22/23/23)
Other characteristics		
Pseudo permeability to liquid water (kg.m^{-2}.h$^{-0,5}$)	w	0.744 (0.632/0.927/0.673)
Capillary absorption coefficient at 24 h (kg/m²)	C_a	4.95 (4.28/6.05/4.53)
Density (kg/m^3)	ρ_b	2203 (2203/2204/2204)
Compressive strength (corrected (MPa)	f_{cm}	69.5
Accelerated Carbonatation (4 %) at 28 and 56 days (mm)	X_{c28}, X_{c56}	4.6; 5.5
Accelerated Carbonatation (50 %) à x et y days (mm)	X_{cx}, X_{cy}	Not realised
Portlandite content by potentiometry (% of concrete mass)		10,5 (11,0/10,5/10,0)
Portlandite content by SAA (Atomic Absorption Spectrometry) (% of concrete mass)		13,4 (11,9/14,6/13,8)
Portlandite content by « pseudo-ATG » (% of concrete mass)		11,9 (10,6/10,6/14,5)

Potential durability classes (according to AFGC, 2004)				
Very low	Low	Average	High	Very high

The results of the durability indicators obtained on cores are consistent with those obtained on specimens within the framework of the control tests. The orders of magnitude and the trends are similar.

In terms of resistance to the penetration of aggressive agents, the results show overall a concrete that is durable with regard to the corrosion of reinforcements. Apart from the results of porosity and portlandite content, concrete is in a high durability class (AFGC 2004).

With all the caution that is required on the methods of dosage and interpretation, the contents of portlandite (measured according to three dosage modes) lead to a low to medium durability class for corrosion of reinforcements (by carbonation). These low portlandite contents can be explained by the nature of the binder (CEM III) and the composition (self-compacted concrete). These last two results (porosity, portlandite content) lead to questioning the durability of this concrete regarding the specific phenomenon of carbonation.

Within the area of investigation, there is little variability in individual results (except for the capillary absorption test and the pseudo-permeability to water (Ca, w).

b. Electrochemical evaluations

Resistivity

The mapping of resistivity measurements shows the presence of 2 singular zones with significantly lower resistivities. These areas correspond to areas where cores were taken and where patching with mortar was carried out. These low resistivities are probably explained by the water content of the recently applied mortar and possibly by the composition of this mortar.

Apart from these singular values, the resistivities measured in the investigation area vary between 86 and 126 kΩ.cm (average: 102 kΩ.cm). The resistivities are globally homogeneous (standard deviation of 10 kΩ.cm). Based on RILEM indications, these values would correspond to a non-carbonated CEM III concrete in wet outdoor exposure.

Half-cell potential

The potential measurements were carried out with a $Cu/CuSO_4$ electrode on the longitudinal and transverse reinforcements with a measurement step of 2 cm, which allows them to be used in the form of maps (see Figures 2.30 and 2.31).

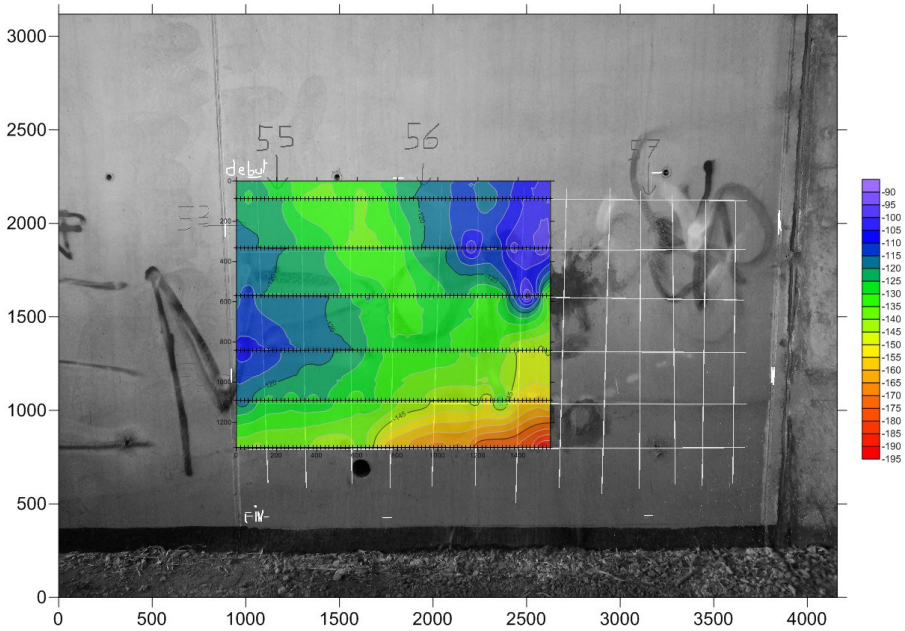

Figure 2.30. Mapping of half-cell potential measures on the horizontal rebars

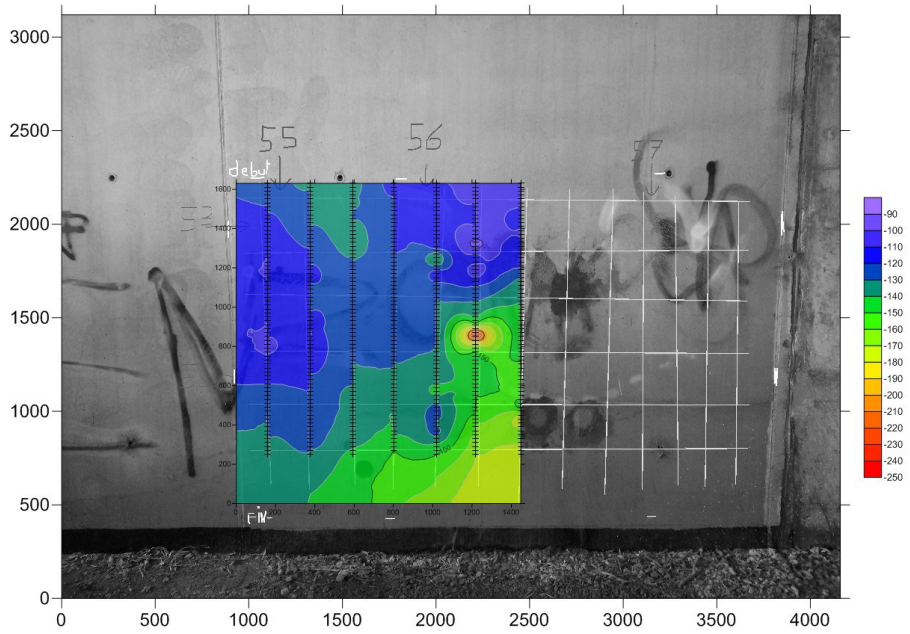

Figure 2.31. Mapping of half-cell potential measures on the vertical rebars

The Table 2.38 presents the descriptive data of the potential measurements (mV).

Table 2.38. Half-cell potential measurements

Half-cell Potential (mV)	Horizontal rebars	Vertical rebars
Minimum	- 190	- 260
Maximum	- 90	- 90
Mean	- 131	- 129
Maximum deviation	- 100	- 170

On the considered investigation zone, the maximum difference in potentials is respectively 100 and 170 mV for the horizontal and vertical rebars. Direct application of the COST 509 principles would therefore indicate that horizontal rebars do not exhibit corrosion. On the other hand, they would indicate corrosion on the vertical rebars. Indeed, the mapping of the potentials indicates a localized singular zone with significantly more electronegative potentials. This situation could be symptomatic of an anodic zone and therefore of a corrosion of the reinforcement at this location.

In order to have a finer qualitative approach, the horizontal and vertical gradients of the potentials were studied. Gradients greater than 10 mV/cm are likely to be symptomatic of anodic zones and therefore of the presence of corrosion. Regarding horizontal rebars: the analysis indicates the existence of gradients greater than 10 mV/cm (maximum: 17.5 mV/cm). The data indicates that these gradients are located on the third horizontal rebar. It is actually a localized area with less electronegative potentials. It is therefore not an anodic zone. Regarding vertical rebars: the analysis also indicates the existence of gradients greater than 10 mV/cm (maximum: 35 mV/cm). These values could indicate the localized presence of an anodic zone and therefore corrosion on this sixth rebar.

3.1.5.4 Conclusion drawn

The investigations carried out on the western side of the underpass n ° 1 of the northern detour of Loudéac on the RN164 led to the following results:

- Respectively 10 % and 0 % of the coverings measured on the horizontal and vertical reinforcements are less than the expected cover (45 mm);
- Given the environment (XC4), the main risk of degradation is corrosion due to carbonation; the carbonation depth measured is zero to date. In view of the absence of carbonation and of the concrete covers measured, the risk of corrosion due to carbonation is zero to date. However, the relatively high porosity values and the portlandite content values raise questions about the durability of this concrete regarding the specific phenomenon of carbonation over the long term;
- The total chloride contents measured in the cover concrete are high but remain below the theoretical critical threshold for corrosion initiation. Chloride penetration from the outside was not observed. The high chloride contents can only be explained by the presence of chlorides coming from the CEM III slag cement;
- The durability indicator values generally indicate concrete with a "high" potential durability class according to the criteria of the AFGC 2004, which could correspond to a foreseeable lifetime of around 100 years. However, if the concrete satisfies the gas permeability criterion, on the other hand it does not meet the porosity criterion required by the tender; the rather high value of the porosity can be explained mainly by the high volume of the paste in a self-compacted concrete;
- The values of the durability indicators measured on cores are consistent with those measured on specimens during construction;
- The electrochemical evaluations are consistent with the previous results: the results indicate a negligible to low corrosion risk to date:
  - The resistivities measured in situ are generally between 90 and 120 kOm.cm,
  - Apart from a zone located on a vertical reinforcement, the potential gradients do not show anodic zones.

3.1.6 X marine structure

3.1.6.1 Presentation of the structure

This case concerns a maritime structure X located on the Mediterranean coast. The structure is voluntarily anonymized. The investigations concern this maritime structure as well as a proof element (Figure 2.32) located on the platform next to the structure. Concreting of the structure took place from early 2014 until early 2015, and the proof element was concreted early 2014. The structure is 87.5 m long, 15 m wide and 13 m high.

The service life of the structure was planned for 50 years, and to achieve this objective, the following technical choices were made:

- Use of a C 60/75 High Performance Concrete;
- Implementation of the durability performance approach for concrete;
- Formwork fitted with a membrane with controlled permeability on the sea side;
- Electrical insulation of the prestressing tendons;
- Cathodic protection of reinforcement steels (lifespan 10 years).

The core samples taken as part of this study were carried out on the proof element. The results of tests done for design, studies and control of works are from the construction of the maritime structure.

All the accessible parts of the structure as well as the proof element fall within exposure classes XC4, XS3, according to standard NF EN 206 / CN.

Figure 2.32. View of the proof element

3.1.6.2 History of works and current condition

The recommendations of the Technical Specifications concerning the concrete are as follows:

- C60/75, exposure class XC4, XS3, minimum equivalent binder content 350 kg, W_{eff} / B_{eq} ratio less than 0.35, CEM I cement, CP, PM, Cl 0.2, D_{max} = 20 mm;
- level of prevention for alkali-silica reaction: C;
- level of prevention for the internal sulphate reaction: Ds (structure category III and exposure class XH3);
- performance-based approach to the durability of concrete - 90-day indicators:
  - porosity accessible to water, P_{water} <11 %,
  - apparent coefficient of chloride diffusion, D_{rcm} <2.5 10^{-12} m^2/s,
  - gas permeability, K_{gas} < 50 10^{-18} m^2.

The thresholds taken into account correspond to the “High” class of the AFGC 2004 guide.

The concrete composition is presented in the Table 2.39.

The characteristics of the fresh concrete are shown in the Table 2.40:

The summary Table 2.41 brings together the test results obtained during the construction (the results are those of Cerema except those specified "LE = Company Laboratory").

Table 2.39. Concrete composition

Concrete composition	BHP C60/75 XS3 XC4 S5 Dmax 20
Cement content	280 kg/m³
Cement type	CEM I 52,5 N SR3 CE PM-CP2 NF
Quantity of mineral additions	120 kg/m³
Type of mineral additions	Slag
Water content	Effective Water 132 l/m³
Water effective / Equivalent Binder Ratio	< 0,35
Aggregates	Sand 0/4 and gravel 6,3/16
Admixtures	1 superplasticizer and 1 retarder

Table 2.40. characteristics of the fresh concrete

Slump	210 ± 30 mm
Shock table	500 ± 30 mm
Theoritical Density	2 489 kg/m³

Table 2.41. Values of the durability indicators at construction

Follow-up of samples		Control 1	Control 2	Control 3	Control 4	Control 5	Control 6	Control 7
Date of sampling		17/06/14	10/07/14	05/08/14	19/08/14	04/09/14	02/10/14	
Durability indicators								
Porosity accessible to water at 28 days (%)	$P_{water,28}$	9.8 & 10 (LE 10.6)	NR (LE 10.4)	10.1 (LE 10.6)	NR	NR	NR	10.0
Porosity accessible to water at 90 days (%)	$P_{water,90}$	9.9 (LE 10.5)	NR (LE 9.5	11 (LE 10.5)	NR	NR	NR	10.2
Apparent coefficient of chloride diffusion (10^{-12} m².s^{-1})	D_{rcm}	2.5 (LE 3)	NR (LE 2.8)	2.6 (LE 2.4)	NR	NR	NR	NR
Gas Permeability (10^{-18} m²)	K_{gas}	NR (LE 27)	NR (LE 42)	31 (LE 23)	NR	NR	NR	NR
Other Characteristics								
Slump / Flow (mm)		230-255	226-590	210-565	205	215	217	200-590
Compressive strength at 7 days (MPa)	$R_{c,7}$	67 (LE 62.9)	70.6 (LE 69.3)	68.3 (LE 70.7)	76.3	68.5	73.5	69 .5 (LE 53.2)
Compressive strength at 28 days (MPa)	$R_{c,28}$	97 (LE 96.3)	100.3 (LE 90.1)	93.9 (LE 92.5)	107	93.2	98.7	94 (LE 94.7)

LE = Laboratory of the Company - NR = Not Realised

Potential durability classes (according to AFGC, 2004)				
Very low	Low	Average	High	Very high

Regarding the durability indicators, the values obtained compared to the limit values proposed according to the criteria of the AFGC 2004, reflect a concrete with a "high" potential durability class.

3.1.6.3 Investigations carried out during PerfDub project

As part of the National PerfDub Project, the Cerema defined and carried out the following program of investigations on samples taken from the proof element, a representative element of the constructed structure:

- lifetime indicator measurements: carbonation and chloride penetration;
- measures of durability indicators: porosity and capillary absorption, gas permeability, apparent coefficient of chloride diffusion and accelerated carbonation;
- concrete compressive strength measurements.

It is recalled that the works provide for the use of a membrane with controlled permeability on the formwork on the sea side of the structure. In order to qualify the interaction on the concrete of this device, the proof element has faces made with this membrane and faces without.

a. Lifetime indicators measured on the proof element

These lifetime indicators measured on such a recent structure (one to two years of age) are not useful at this time, but their objective is to obtain a reference point and may subsequently enable to verify the evolution of these aggressive agents with time.

The results show an average carbonation depth of 2 mm (minimum 1 - maximum 2.5 mm) in areas without membrane, and 0.5 mm (minimum 0 - maximum 1 mm) in areas with membrane.

The chloride profile measurements relate to 4 samples, 2 on faces with formwork fitted with the membrane and 2 on faces with unequipped formwork. The results obtained show that for all the cores, from the first slice (between 0 and 10 mm from the facing) and for the following slices tested, the chloride content is less than 0.005 % of the mass of the concrete (detection limit of the test).

b. Durability indicators measured on the proof element

These indicators are summarized in the following Table 2.42:

The results of durability indicators obtained on the cores are consistent with those obtained on the test specimens within the framework of structural construction control tests. The indicators measured on the proof element are a little better than those measured during the control of the structure.

Regarding the durability indicators, the values obtained compared to the limit values proposed according to the criteria of AFGC 2004 reflect a concrete with a "high" potential durability class.

Table 2.42. Values of the durability indicators measured on the proof element

Data synthesis		
Lifetime Indicators		
Carbonation depth (mm)	X_c	< 2.5 mm
Free chlorides content at the facing (% of the cement mass)	$[Cl^-]$	< 0.031
Durability Indicators		
Apparent coefficient of chloride diffusion (10^{-12} m².s^{-1})	D_{rcm}	1.9
Porosity accessible to water (%)	P_{water}	9.9
Gas Permeability (10^{-18} m²)	K_{gas}	20
Capillary absorption coefficient at 24h (g/m²)	C_a	811
Accelerated carbonation (3 %) at 28 and 56 days (mm)	$X_{c,28}$; $X_{c,56}$	0; 0
Accelerated carbonation (50 %) at 7 and 28 days (mm)	$X_{c,7}$; $X_{c,28}$	0; 0
Compressive strength on site (MPa) Strength Class	f_c Class	87.3 C100/115

Potential durability classes (according to AFGC, 2004)				
Very low	Low	Average	High	Very high

3.1.6.4 Conclusion drawn

The investigations carried out within the framework of the PerfDub project on the concrete of the proof element of a maritime structure X located on the Mediterranean coast, make it possible to identify that:

- the values of the durability indicators obtained on samples (coring) compared to the limit values proposed according to the criteria of the AFGC 2004 reflect a concrete with a "high" potential durability class;
- the values of durability indicators measured on sampling (core samples) are consistent with those measured on specimens during the construction of the structure;
- there is a good compliance of the measured durability indicators with the technical specifications, whether on test specimens during construction or on sampling (coring);
- the measured lifetime indicators constitute a reference point at 2 years and could subsequently make it possible to verify the progression of aggressive agents.

3.2 Structures between 20 and 50 years old

3.2.1 TCD wharf on the Scorff river

3.2.1.1 Presentation of the wharf

The TCD wharf, built in 1964 and 1965, is used for arming ships. It is a wharf on steel piles composed of three parts (see Figure 2.33):

- the main part of the structure, parallel to the Scorff channel, with a length of 180 m for docking;
- The access pier located to the South, 109.34 m long;
- the northern return of the wharf with a length of 52.11 m.

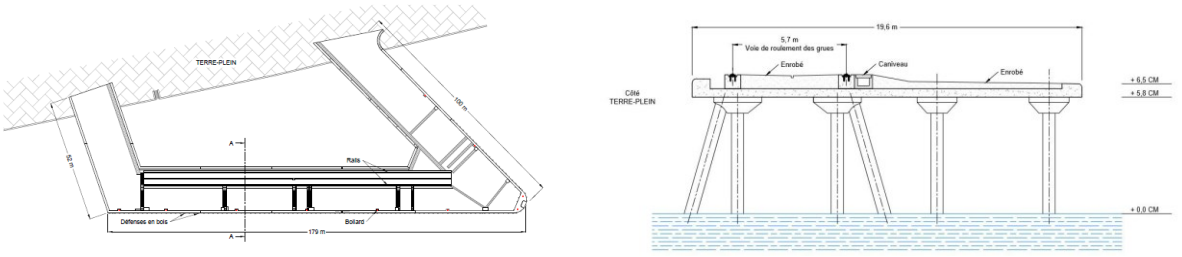

Figure 2.33. Left: Plan view of the wharf with the access pier on the right; Right: transversal cross section of the wharf

Figure 2.34. Left: View of the TCD wharf on the Scorff chanel; Right: Capitals on inclined piles

The deck consists of a reinforced concrete slab 42 cm thick, without stiffening beams; it rests on vertical and inclined steel piles by means of reinforced concrete capitals (Figure 2.34). This slab is surmounted by a pavement structure of 25 cm thick on the sea side and 50 cm thick on the land side. The deck has a width of 19.60 m in the current part and has a transverse slope of about 1.5 %.

The wharf is located in a marine environment (XS3). The lower surface of the deck is exposed to spray. By strong tidal coefficient, it can be exposed to splashing.

3.2.1.2 History of works and current condition

In 1992, a patch repair of the pile capitals was carried out. In 2010, a rehabilitation of the docking front and the construction of a crane track were done.

In 1997, the CETE's detailed inspection showed:

- defects in the patch repair of the pile capitals,
- disorders due to the aging of the reinforced concrete and not to mechanical defects in the structure,
- patching repair works of spalling caused by boat shocks.

In 2003, the technical inspection of Véritas "did not report any damage to the underside of the slab such as spalling in the concrete, visible corroded steels ...". If this inspection was carried out correctly, it can be deduced that the disorders observed on the underside of the slab during the detailed inspection in 2012 probably appeared after 2003.

In 2012, the detailed inspection carried out by Concrete company concluded that: "The structure, built in 1965, is generally in a poor condition. The distribution of disorders is relatively homogeneous and independent of their location on the structure. No structural disorder was noted. Concerning the deck, the coated upper surface of the structure is in good general condition. On the intrados, some minor short-term damage can be observed: corroded assembly ties, crazing, a few spalls of concrete without or with visible corroded reinforcements, concrete segregation areas, traces of active humidity and white efflorescence at the location of the expansion joints and storm water drains. The vast majority of capitals present numerous disorders resulting from the aging of the material and/or accompanied by rust-colored runs, concrete spalling without or with visible corroded reinforcements, and numerous cracked patch repairs areas."

3.2.1.3 Investigations carried out in 2012

In 2012, a diagnosis of the reinforced concrete durability was carried out on the structure. The investigations were made on the underside of the slab, on a capital and on the slab lateral face. On these areas, the following investigations were carried out: statistical survey of concrete covers, determination of durability indicators, chloride penetration profiles (free and total), mapping of half-cell potentials of reinforcement, mapping of electrical resistivities, density measurements of corrosion currents.

The results of the durability indicators determined on the slab lateral faces, in accordance with the LCPC 2010 guide, are presented in Table 2.43.

Table 2.43. Values of the durability indicators determined on the slab lateral faces

Durability indicators		**Slab lateral face**
Apparent coefficient of chloride diffusion (10^{-12} m².s^{-1})	D_{rcm}	2.3 (1.9 / 2.6)
Electrical resistivity (Ω.m)	Res	68.5 (81 / 56)
Porosity accessible to water (%)	P_{water}	11.3 (11.0 / 11.5)
Gas Permeability (10^{-18} m²)	K_{gas}	154 (43 / 266)
Other characteristics		
Density (kg/m^3)	ρ_b	2323 (2318 / 2327)

Potential durability classes (according to AFGC, 2004)				
Very low	Low	Average	High	Very high

The main results concerning the intrados of the slab are recalled below:

- the depths of the free chloride and total chloride front are 52 mm and 60 mm respectively;
- The measurements (carried out with Galvapulse) show potentials between -121 and +51 mV (Ag / AgCl). The report indicates that, taking into account the potential gradients (mapping), there are no anodic zones on the investigated area;
- The measurements (carried out with a Resipod) are generally between 50 and 100 kΩ.cm corresponding to a low risk of corrosion;
- The measurements (carried out with a Galvapulse) are homogeneous over the investigation zone and between 0.1 and 2.2 µA / cm². These values correspond to negligible to low corrosion activity.

3.2.1.4 Investigations carried out during PerfDub project

Investigations were carried out on the intrados PerfDub of the slab of the south access pier, at the height of a man, close to the shore. The investigations were carried out in 2016 over an area with a width of 1.40 m and a length of 1.70 m. 7 cores were taken. The main conclusions are as follows.

With regard to the carbonation phenomenon and the concrete covers measured, the risk of corrosion due to carbonation is null (carbonation depth of the order of mm).

The main risk of degradation is the corrosion due to chlorides; the average depth of the chloride front (defined as the value above the critical corrosion initiation threshold expressed in % Cl / concrete mass) is around 30 mm. Figure 2.35 illustrates these profiles for 3 cores.

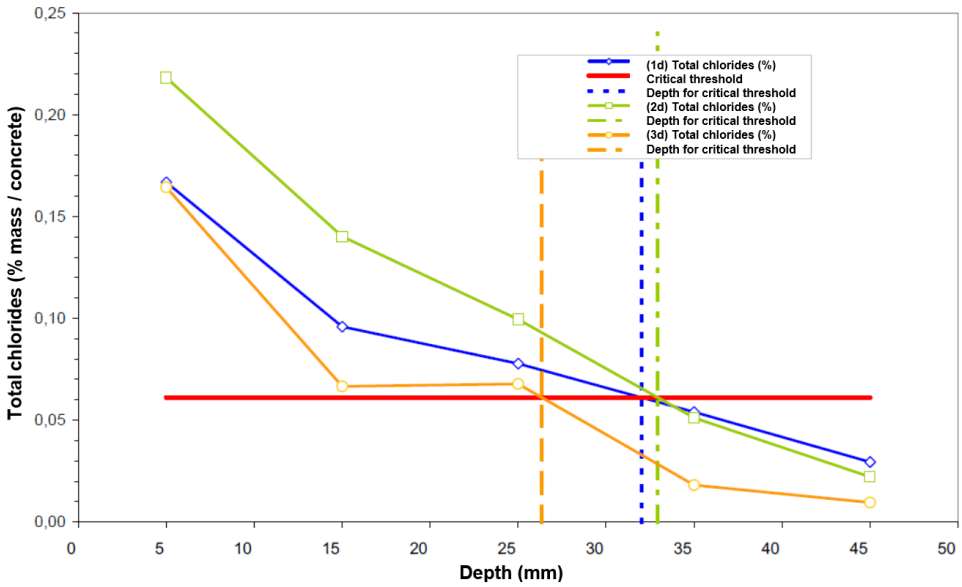

Figure 2.35. Profiles of penetration of total chlorides for cores 1d, 2d and 3d (per mass of concrete)

Almost all of the measured covers of the longitudinal reinforcements are less than 50 mm. The transverse reinforcements of the slab are better protected (by design). However, a significant proportion of them have a cover of less than 50 mm (32 %) (see Table 2.44).

Table 2.44. Data relating to cover measurements (mm)

Part / Zone	Longitudinal reinforcement					Transversal reinforcement				
	Min.	Mean	≤ 50	e_{95+} **	e_{95-} *	Min.	Mean	≤ 50	e_{95+} **	e_{95-} *
South wharf intrados	17	40	97 %	20	48	38	58	32 %	40	69

** 95 % of the measured coverings are higher than the characteristic value e95-*

*** 95 % of the coverings measured are lower than the characteristic value e95+*

The crossing of the information from the statistical study of the covers with the information from the penetration of chlorides makes it possible to estimate the proportion of reinforcement located in a chlorinated concrete cover (Figure 2.36). Respectively 18 % and 0 % of the longitudinal and transverse reinforcements are located in a concrete polluted by chlorides and therefore likely to be depassivated.

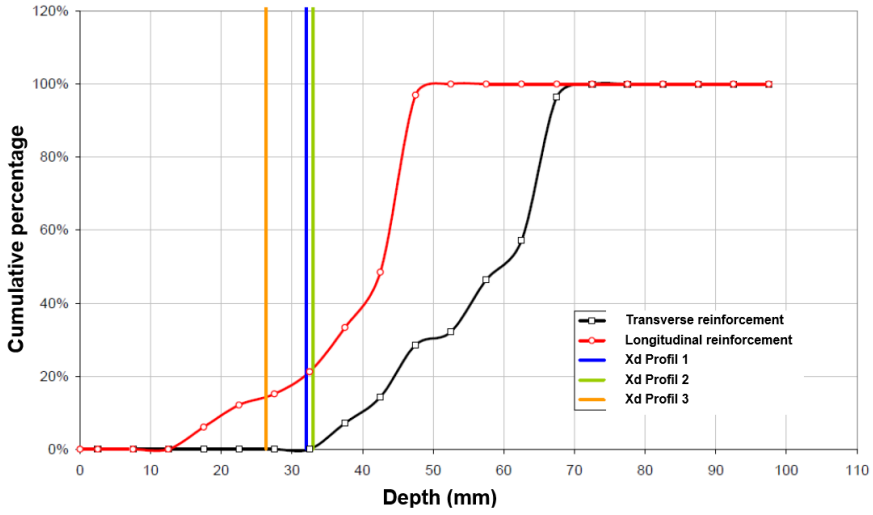

Figure 2.36. Crossing of the cumulative statistical distribution of covers and chloride depth fronts

Taking into account the age of the structure and the depth of the chloride front measured, the average service life of the estimated structure would have been of the order of 140 years if at the time of construction the concrete covers indicated by the Eurocode had been applied.

Half-cell potential measurements indicate potential gradients lower than 5.5 mV / cm and 7.5 mV / cm, respectively, for the transverse and longitudinal reinforcements. The potential gradients do not clearly identify anodic zones. The localized gradients measured on the longitudinal reinforcements are however greater than those obtained on the transverse ones and therefore seem to indicate a greater risk of corrosion. It can nevertheless be concluded from this that the reinforcements are not in an active corrosion state.

The resistivities measured in situ are between 35 and 76 kΩ.cm (58 on average). The resistivities are globally homogeneous (standard deviation of 9 kΩ.cm). Most of the values are located in the range 50-100 kΩ.cm. Given the nature of the binder (artificial Portland cement), the resistivity values measured correspond to a low risk of corrosion (according to the RILEM TC 154 recommendation).

The mineralogical analysis concludes on the absence of slags and fly ash in the binder; this latter is essentially made of clinker and the cement is similar to a CEM I type of cement. It leads to an estimated cement content of 460 kg/m^3 (+/- 40 kg/m^3), with a W/C ratio of about 0.60. It is also observed a cohesive concrete, a limited carbonation (great quantity of portlandite) and no specific anomaly.

The values of the durability indicators are given in Table 2.45.

Table 2.45. Values obtained for the durability indicators

Durability indicators		Slab intrados
Apparent coefficient of chloride diffusion (10^{-12} m².s^{-1})	D_{rcm}	4.1 (3.8 / 3.9 / 4.6)
Electrical resistivity (Ω.m)	Res	159 (170 / 150 / 157)
Porosity accessible to water (%)	P_{water}	12.8 (12.6 / 13.0 / 12.7)
Gas Permeability (10^{-18} m²)	K_{gas}	89 (78 / 73 / 115)
Other characteristics		
Pseudo permeability to liquid water (kg.m^{-2}.h$^{-0,5}$)	w	1.06 (1.02 / 1.08 / 1.07)
Capillary absorption coefficient at 24 h (kg/m²)	C_a	5.18 (5.03 / 5.30 / 5.22)
Density (kg/m^3)	ρ_b	2298.8 (2293 / 2286 / 2291)
Compressive strength (corrected) (MPa)	Rc_b, Rc_c	73
Accelerated carbonatation (4 %) at 28 and 56 days (mm)	$X_{c,28}$; $X_{c,56}$	0; 0
Accelerated carbonatation (50 %) à x et y days (mm)	$X_{c,x}$; $X_{c,y}$	Not done
Content of lime: [$Ca(OH)_2$] potentiometry / SAA / psdATG (%)	[$Ca(OH)_2$]	26.8 / 23.5 / 33.2

Potential durability classes (according to AFGC, 2004)				
Very low	Low	Average	High	Very high

The indicator values indicate a concrete with a potential durability class "medium" to "high" according to the criteria of the AFGC 2004 document (AFGC, 2004), which could correspond to a foreseeable lifespan of the order of 100 years.

As an indication, the Table 46 below recalls the thresholds of the 3 indicators * taken from fascicule 65 of the technical specifications (CCTG) for a project life of 100 years.

Table 2.46. Thresholds of durability indicators prescribed by the Fascicule 65

Exposure Class	Cover $c_{min,dur}$ Structural class S6 (mm)	P_{water}* (%)	K_{gas}* (10^{-18} m²)	D_{rcm}* (10^{-12} m².s^{-1})
XC4	40	< 14.5	< 200	--
XS3	55	< 13	< 200	< 3.5

** indicators measured on concrete samples 90 days old*

The two apparent coefficients of chloride diffusion measured are 2.3 (lateral face of the slab) and 4.1 (intrados of the slab). In the first case, it is below all the fixed thresholds, and in the second case, it is a little above the fixed thresholds. The concrete constituting the lower surface of the slab satisfies all the criteria except the criterion relating to the coefficient chloride diffusion for the XS3 exposure class. The results obtained are however very close to the threshold.

But, of course, care should be taken in analysing these results because the indicators change over time ("ageing effect"). The values obtained in 2012 and 2016 (age of the concrete: 47 & 51 years) are not the same as those which would have been measured during construction in 1965.

3.2.1.5 Conclusion drawn

The investigations carried out on the intrados underside of the TCD wharf lead to the following results:

- with regard to the carbonation phenomenon and the measured covers, the risk of corrosion due to carbonation is null;
- the main risk of deterioration is corrosion due to chlorides from the sea water; the average depth of the chloride front is 30 mm after 50 years of age. Taking into account the measured covers, respectively 18 % and 0 % of the longitudinal and transverse reinforcements would be located in a concrete polluted by chlorides and therefore likely to be depassivated;
- the durability indicator values indicate a concrete of potential durability class "Average" to "High" according to the criteria of the AFGC 2004 (AFGC, 2004), which could correspond to a foreseeable lifespan of around 100 years;
- The electrochemical evaluations seem to confirm the previous results: they indicate a low to moderate corrosion risk:
  - the resistivities measured in situ are between 50 and 100 kOm.cm and correspond to a low risk of corrosion,
  - the potential gradients do not clearly identify anodic zones.

3.2.2 Chateaubriand bridge

3.2.2.1 Presentation of the bridge

The Chateaubriand Bridge connects the municipalities of Dol de Bretagne and Dinan via the R.N. 176 on a Normandy-Brittany axis by crossing the Rance river to the south of Saint Malo. It was built between 1987 and 1991 (Figure 2.37).

Figure 2.37. General view of the Chateaubriand bridge

This structure consists of an arch supporting, by means of piers, a composite deck comprising 15 spans, for a total length of 424 m (Figure 2.38). The deck has an overall width of 11.0 m,

with a transversal slope of 2.5 % from south to north, and supports a 7.0 m two-way carriageway without central separator and two 2.0 m wide emergency lanes.

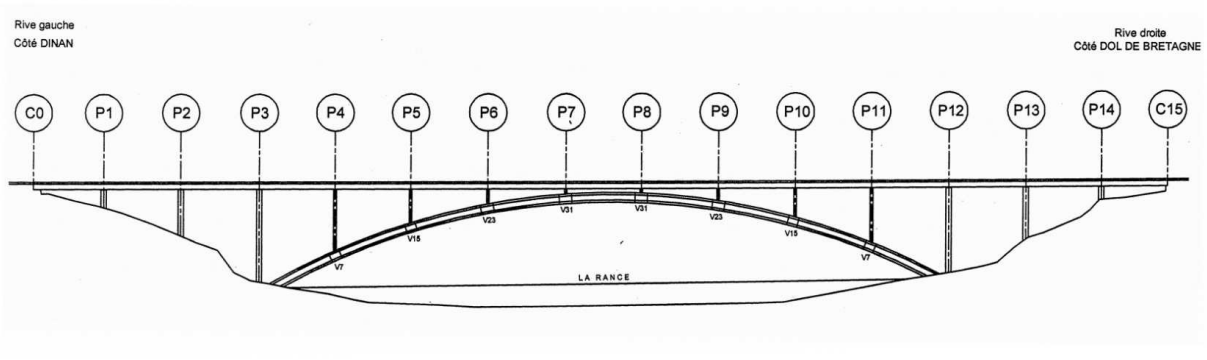

Figure 2.38. Elevation view of the bridge

The structure is located in a marine environment, and falls within classes XC4 and XS3. P3 and P12 piers are subject to the tide. The piers located on the arch (including the P11 pier) are exposed to the spray.

3.2.2.2 History of works and current condition

Piers P11 and P12 comprise in their lower part respectively HA 32 and HA 25 steels, on respective heights of 9.50 m and 23.86 m.

The composition of the concrete of the piers is shown in Table 2.47.

Table 2.47. composition of the concrete of the piers of the bridge

Composition of the concrete			
Constituent	**Class**	**Origin**	**Quantity (kg/m^3)**
Cement	CPA HP PM (CEM I)	Lafarge Saint Vigor	400
Sand	0/4	Mauron Simura	786
Gravel	8/12	Saint Guinoux	342
Gravel	12/18	Saint Guinoux	684
Water (total)		Drinking network	205

As part of monitoring the construction of the structure, the concrete in the piers was subject to regular compressive strength checks (see Table 2.48).

Table 2.48. Control of compressive strengths values at construction

	Compressive Strength (MPa)			
	Number of specimen	**Mean value**	**Minimum value**	**Maximum value**
All piers	346	46.7	35	57
P11 pier	53	47.4	40.5	53.5
P12 pier	35	44.9	37.5	48.6

The Chateaubriand Bridge was the subject of detailed inspections in 1996, 2001, 2011 and a diagnosis in 2013. The 2001 detailed inspection report mentions cracks on the piers which have changed only a little since the 1996 inspection.

In 2013, as part of the feasibility study for doubling the structure, Cerema Ouest carried out a diagnosis of the durability of the reinforced concrete. This diagnosis was focused on the arch, the piers and the slabs of the composite deck. At the time of this diagnosis, the bridge was 22 years old. The investigations focused on piles P11 upstream and P14 upstream and gave the following results.

a. Statistical record of concrete covers

Table 2.49. Statistical record of concrete covers

Zone	Horizontal reinforcement				Vertical reinforcement			
	Mean	Min	≤ 50 (%)	e_{95}*	Mean	Min	≤ 50 (%)	e_{95}*
Pier P11	51	21	52	65	71	9	4	86

** 95 % of the measured covers are lower than the characteristic value e95*

For the horizontal reinforcements, we note that approximately 50 % of the covers measured are below the cover expected for this type of exposure.

b. Durability indicators and other parameters

They were determined in accordance to the LCPC 2010 guide (LCPC, 2010) (Table 2.50).

Table 2.50. Values of durability indicators measured in 2013 (22 years of age)

Durability Indicators		Pier P14
Apparent coefficient of chloride diffusion (10^{-12} m².s^{-1})	D_{rcm}	28.3 (29.3 / 27.2)
Electrical resistivity (Ω.m)	Res	36 (31 / 41)
Porosity accessible to water (%)	P_{water}	14.8 (14.8 / 14.7)
Gas permeability (10^{-18} m²)	K_{gaz}	871 (641 / 1100)
Other characteristics		
Permeability to liquid water (kg.m^{-2}.s$^{-0,5}$)	w	1.33 (1.27 / 1.38)
Capillary absorption coefficient at 24 h (kg/m²)	C_a	6.06 (5.84 / 6.27)
Density (kg/m^3)	ρ_b	2239.5 (2242.6 / 2236.4)

Potential durability classes (according to AFGC, 2004)				
Very low	Low	Average	High	Very high

c. Free chloride and carbonation penetration profiles

Determined in accordance with the AFREM-AFPC operating mode, the shape of the profile indicates a slight penetration of free chlorides, with contents much lower than the theoretical corrosion initiation threshold, whatever the depth in the cover (Xd = 0 mm). The risk of corrosion of the reinforcements due to the penetration of chlorides is zero at the time of diagnosis (Figure 2.39).

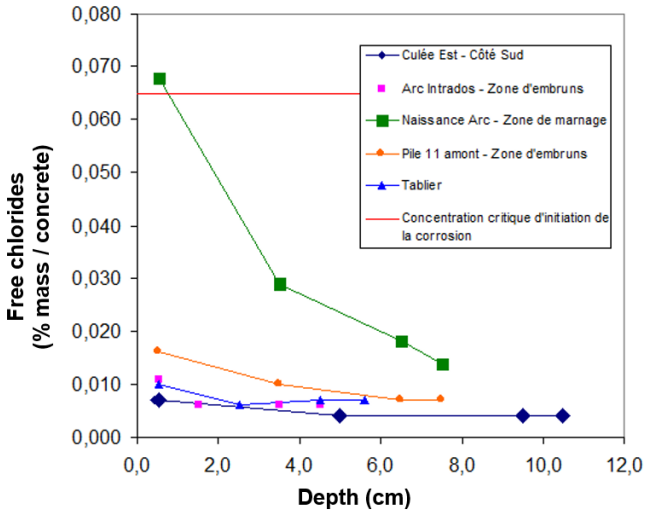

Figure 2.39. Penetration profiles of free chlorides

No carbonation phenomenon was observed (Xc = 0 mm).

3.2.2.3 Investigations carried out during the PerfDub project

The investigations were carried out on the P11 and P12 piers (see Figure 2.40 and Table 2.51).

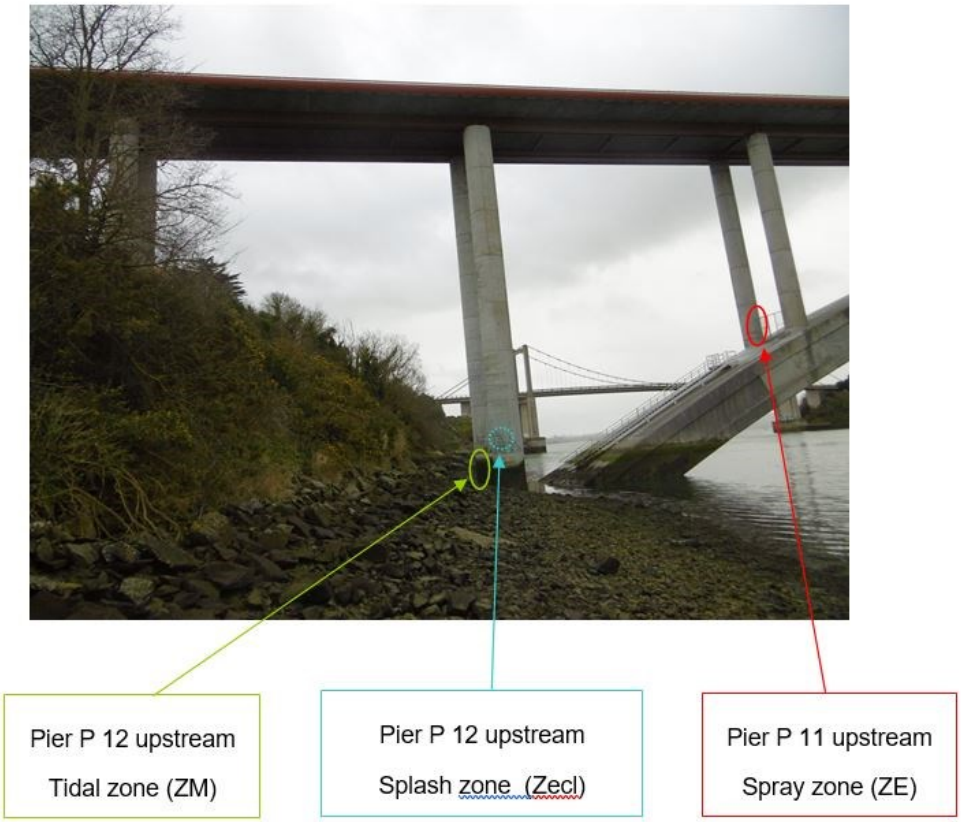

Figure 2.40. View of the investigated zones

Table 2.51. Location of the investigated zones

Pier	Localisation	Exposure	Investigation zones	Orientation	N° level	Level NGF* (m)	Area
P11	On the arch Right bank, Upstream	Sprays	ZE	North-West	1	16.50	Width: 1.60 m Height: 1.60 m
P12	In the river Right bank, Upstream	Tidal	ZM	North-East	1	3.50	Width: 1.50 m Height: 2.65 m
		Splashes	Zecl	North	2	7,50	

** Low level of the considered area.*

The results are as follows.

a. Statistical records of covers

The main statistical data on covers are given in Table 2.52. The covers are lower for P12-ZM & Zecl than for P11-ZM, and respectively 46 and 100 % of the covers (horizontal reinforcements) measured on P11 and P12 are lower than the expected cover of 50 mm for this type of environment (tidal range, spray, splash).

Table 2.52. Data relating to cover measurements (mm)

Part / Zone	Vertical reinforcement						Horizontal reinforcement					
	Nber	Min.	Mean	≤50	e_{95+} **	e_{95-} *	Nber	Min.	Mean	≤50	e_{95+} **	e_{95-} *
Pier P11 Spray Zone (ZE)	19	59	71	0 %	60	84	13	43	54	46 %	44	68
Pier P12 Tidal and Splash Zones (ZM & ZEcl)	42	33	57	2 %	53	63	42	14	35	100 %	23	40

** 95 % of the measured coverings are higher than the characteristic value e95-*
*** 95 % of the coverings measured are lower than the characteristic value e95+*

The tests show a low average carbonation of the concrete in the spray zone and in the P11 tidal zone: 2.6 mm. In the splash zone (upstream P12 pier), no carbonation phenomenon was detected. These results are consistent with those obtained during the 2013 diagnosis.

b. Profiles of chloride penetration

The three following graphs (Figure 2.41) show the total chloride penetration profiles obtained in the three investigation zones and the corresponding chloride front depths (Xd).

The profiles are strictly decreasing (except for a P12-ZM profile: singular content) and do not show any convection phenomenon linked to the humidification-drying cycles. However, the accuracy of the profile related to the thickness and distribution of the core slices can mask such a phenomenon. The results obtained on the P11-ZE pier are consistent with those obtained during the 2013 diagnostic.

The graphic analysis of the profiles makes it possible to estimate the depth of the chloride front Xd (total) (thickness of concrete for which the total chloride content is greater than the critical corrosion initiation concentration) (see Figure 2.41).

The phenomenon of chloride ion penetration decreases with altimetry. It is highest in the tidal range (P12-ZM). For this zone, the average depth of the chloride front is Xd = 43 mm. This is a significant depth for a 25-year-old structure at the time of the investigations.

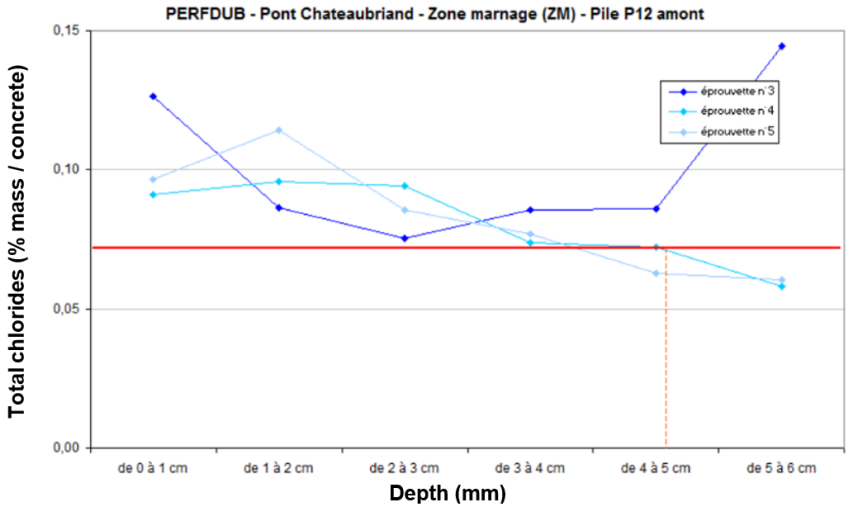

Pier P12 upstream

Tidal Zone (ZM)

Xd (core n°4) = 46 mm

Xd (core n°5) = 40 mm

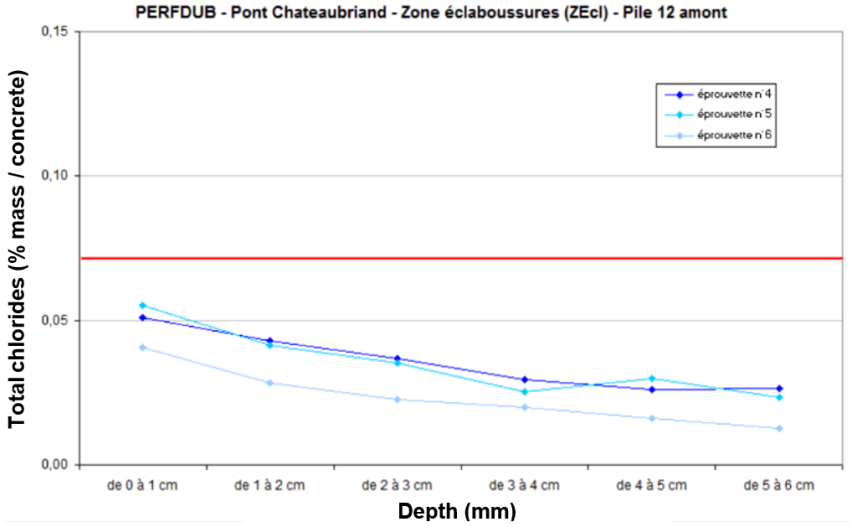

Pier P12 upstream

Splash Zone (ZEcl)

Xd < 10 mm

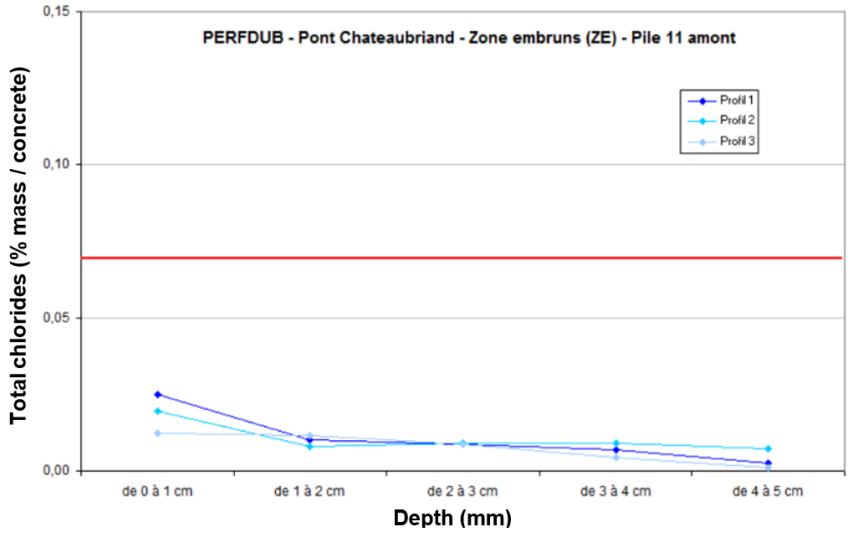

Pier P11 upstream

Spray Zone (ZE)

Xd < 10 mm

Figure 2.41. Total chloride penetration profiles obtained in the three investigation zones

The crossing of the information from the statistical survey of the covers and the chloride front depths (Xd) allows to estimate the proportion of reinforcements located in a chlorinated concrete (cover less than the depth of the chloride front) and therefore likely to be depassivated. The following graph (Figure 2.42) illustrates the principle of this analysis for zone P12.

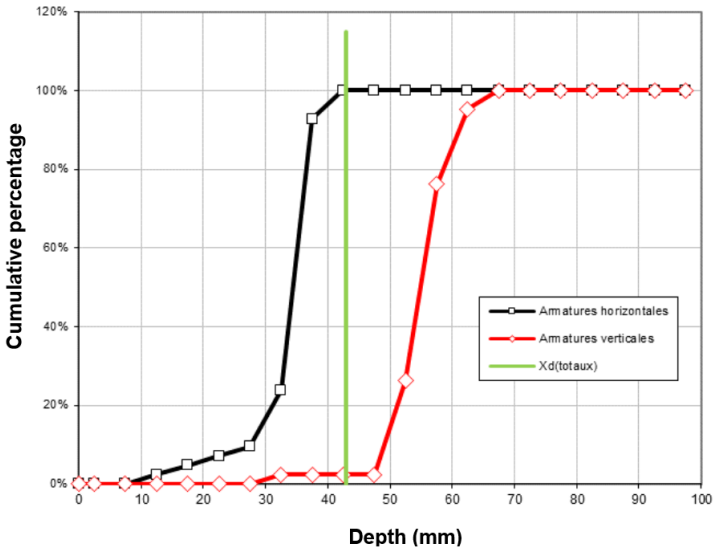

Figure 2.42. Graphical determination of the proportion of reinforcement likely to be depassivated

The Table 2.53 presents, for the investigation zones considered, the statistical percentages of reinforcements located in chlorinated concrete and therefore likely to be depassivated.

Table 2.53. Estimate of the percentage of reinforcement located in chlorinated concrete

Zone	Vertical reinforcement	Horizontal reinforcement
P11-ZE	0 %	0 %
P12-ZEcl	0 %	0 %
P12-ZM	5 %	100 %

These results show that the risk of deterioration due to corrosion is greatest in the tidal range of the P12 pier: statistically, 100 % of the horizontal reinforcements are likely to be depassivated. To a lesser extent, this risk also concerns the vertical reinforcement (5 %).

c. Durability indicators

The durability indicators were determined in accordance with the LCPC 2010 guide (LCPC, 2010) and are reported in the Table 2.54.

In terms of resistance capacity to the penetration of aggressive agents, the tests carried out on the cores extracted from the P11 pier indicate that the concrete is generally in a low potential durability class. With regard to the environment considered (spray, tidal range), this durability class corresponds to a potential lifespan (D) of the order of 30 to 50 years. These results are consistent with those obtained in 2013 for the concrete of pier P14.

Table 2.54. Values of the durability indicators for the spray zone of Pier 11

Durability indicators		P11 – Spray Zone
Apparent coefficient of chloride diffusion (10^{-12} m².s^{-1})	D_{rcm}	29.6 (30.6/33.4/24.9)
Electrical resistivity (Ω.m)	Res	38 (31/38/44)
Porosity accessible to water (%)	P_{water}	15.6 (15.8/15.0/16.0)
Gas permeability (10^{-18} m²)	K_{gas}	415 (457/373/346)
Other characteristics		
Permeability to liquid water (kg.m^{-2}.s$^{-0,5}$)	w	3.04 (3.06/2.97/3.08)
Capillary absorption coefficient at 24h (kg/m²)	Ca	6.73 (6.75/6.45/6.98)
Density (kg/m^3)	ρ_b	2258 (2243.5/2272.5/2236.1)
Compressive strength corrected (MPa)	f_c (ZM) f_c (ZEcl) f_c (ZE)	48.1 42.1 56.1
Accelerated carbonation (4 %) at 28 et 56 days (mm)	$X_{c,28}$; $X_{c,56}$	0; 0
Accelerated carbonation (50 %) at x et y days (mm)	$X_{c,x}$, $X_{c,y}$	Not realised
Content of material that can carbonate (%)	$[Ca(OH)_2]$	
Content by potentiometry		38.2 (37.4/38.3/39.0)
Content by SAA		39.9 (36.8/41.6/41.4)
Content by « pseudo-ATG »		23.0 (20.6/24.4/24.1)

Potential durability classes (according to AFGC, 2004)				
Very low	Low	Average	High	Very high

As an indication, Table 2.55 recalls the thresholds of indicators * from the fascicle 65 for a project period of 100 years.

Table 2.55. Thresholds specified by the fascicle 65 for the durability indicators

Exposure Class	Cover $c_{min,dur}$ (Structural class S6) (mm)	P_{water}* (%)	K_{gas}* (10^{-18} m²)	D_{app}* (10^{-12} m².s^{-1})
XC4	40	< 14.5	< 200	/
XS3	55	< 13	< 200	< 3.5

* indicators measured on concrete samples 90 days old

The concrete constituting the P11 pier (and P14 for the diagnosis carried out in 2013) does not meet any of the criteria for the XS3 exposure class.

The potential lifespan D, that is to say the estimated duration at the end of which the reinforcements will be depassivated in a concrete polluted by chlorides and therefore will be likely to present an initiation of corrosion, is presented. in the Table 2.56.

Table 2.56. Estimate of the potential life duration until depassivation of reinforcement

Zone	Potential service life D for conventional 50 mm cover	Vertical reinforcement		Horizontal reinforcement	
		Mean cover e_m (mm)	Potential life duration D'**	Mean cover (mm)	Potential Life duration D'**
P11 - ZE	30 to 50 years	71	60 to 100 years	54	35 to 60 years
P12 - ZM & Zecl		57	40 to 65 years	35	15 to 25 years

* Potential service life D for a conventional 50 mm cover
** Corrected potential service life D' taking onto account the measured cover

This estimated 90-day D_{rcm} value corresponds to a very low durability class (AFGC 2004), which confirms the inadequacy of this concrete composition to ensure 100-year durability.

d. Mapping of half-cell potentials of reinforcement

The half-cell potential measurements (carried out using a Canin (Proceq)) were carried out on the vertical reinforcement using an electrode wheel with a step of 2 cm and with a bar electrode every 5 cm on the horizontal reinforcement ($Cu/CuSO_4$ electrode). The Table 2.57 presents the descriptive data of the potential measurements (mV).

Table 2.57. Half-cell potential measurements (mV) on P11 and P12 piers

	Pier P11 Horizontal reinforcement	Pier P11 Vertical reinforcement	Pier P12 Horizontal reinforcement	Pier P12 Vertical reinforcement
Minimum	20	-40	-555	-530
Maximum	120	135	30	-25
Mean	74	78	-358	-357
Maximum deviation	24	39	116	107
Height of the investigated zone (m)	1.40	1.60	2.43	2.66
Width of the investigated zone (m)	1.50	1.60	1.45	1.30

For the P11 pier, the measurements show essentially positive potentials representative of dry concrete. The mapping of potentials does not highlight significant gradients. Potentially anodic areas were not detected. The probability of corrosion is therefore very low.

For the P12 pier, the mapping shows a phenomenon of potential gradients as a function of the altimetry. This phenomenon is directly linked to the exposure of the pier to the phenomenon of tidal range. The very electronegative potentials (in the lower part) are explained by a low oxygenation of the reinforcements due to the water saturation of the concrete and are therefore not significant of a corrosion phenomenon as suggested by the ASTM thresholds. Applying the principles of COST and RILEM TC154 leads to the conclusion that there are no anodic zones. The probability of corrosion is therefore low.

e. Electrical resistivity measurements.

The resistivity measurements taken in the spray zone (P11) are greater than 10 kΩ.cm, which corresponds to a moderate to low, or even negligible, risk of corrosion (according to RILEM TC 154).

The measurements taken in the tidal range are generally between 10 and 50 kΩ.cm corresponding to a moderate risk of corrosion.

3.2.2.4 Conclusions drawn

The investigations carried out on the P11 (in the spray area) and P12 (in the tidal and splash areas) piers of the Chateaubriand bridge over the Rance river led to the following results:

- The measurements indicate a heterogeneity of the concrete covers between the areas of investigation (on piers P11 and P12). A significant proportion of the horizontal reinforcements does not respect the covers that would be expected today for such an exposure class (XS3);
- With regard to the almost non-existent carbonation phenomenon, the risk of corrosion due to carbonation is zero to date;
- The main risk of degradation is corrosion due to the penetration of chlorides;
- The phenomenon of chloride ion penetration decreases with altimetry (exposure to the sea). It is highest in the tidal range (P12 - ZM) with a critical chloride front depth of 43 mm. Any critical chloride front was not detected in the spray zone (P11 - ZE) and the splash zone (P12 - ZEcl);
- A cross-analysis of the cover statistics and the position of the critical chloride front indicates that 100 % of the horizontal reinforcements in the P12 - ZM zone are likely to be depassivated;
- The durability indicators indicate that the concrete of the P11 pier has a low capacity to resist the penetration of aggressive agents (low durability class) which could correspond to a low potential life given the covers measured: from 15 to 25 years for horizontal reinforcements in zone P12 - ZM & ZEcl, from 35 to 60 years in zone P11 - ZE. These lifetimes estimated from durability indicators are consistent with those estimated from chloride penetration depths;
- The resistivity measurements are consistent with the chloride penetration results: they indicate a risk of corrosion which decreases with altimetry;
- Although the durability approach indicates a strong risk of initiation of corrosion in the P12-ZM zone, the reinforcement potential measurements do not show any corroborating signs to date (no detection of anodic zones).

3.2.3 Vachette bridge

3.2.3.1 Presentation of the bridge

The Vachette bridge (Figure 2.43) was built between 1984 and 1985, it allows the RN94 to cross over the Durance on the territory of the municipality of Val-des-Près at a location called La Vachette.

Figure 2.43. General view of the Vachette bridge, from the left bank, upstream

The crossing is ensured by a deck made up of a ribbed slab comprising three ribs in prestressed concrete and a reinforced concrete slab (Figure 2.44). This curved slab (radius of 325.00 m in the axis of the deck) has a length of 59.06 m, a slope of 4 % (downstream to upstream) and a bias of 68 grades with respect to the supports. It is made up of three spans with respective spans 16.50 m, 26.00 m and 15.00 m. The ribs are braced on supports.

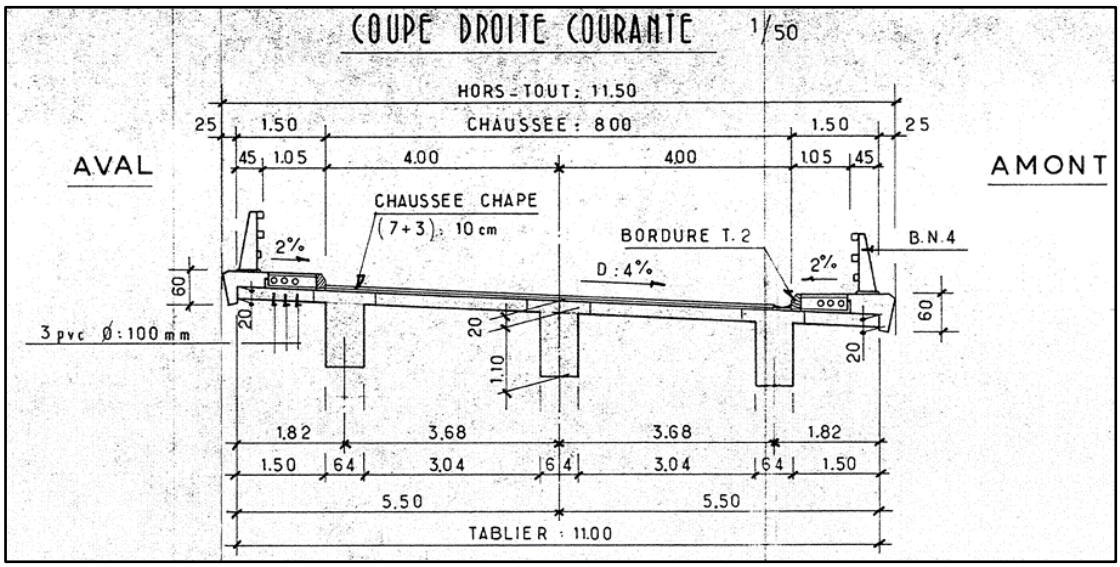

Figure 2.44. Transversal cross-section of the deck

The reinforced concrete abutments consist of a capbeam resting on a line of two piles, the two reinforced concrete piers of trapezoidal cross section rest on a footing based on two rows of piles.

The roadway on the structure is bidirectional, it is coated with a bituminous concrete spilling on the upstream side, the sidewalks are coated with gravel asphalt protected by a prefabricated border. The road joints are of the hiatus type. The retaining devices consist of a BN4 barrier on a structure connected outside the structure to crash barriers. Reinforced concrete cornices border the structure on the left and right banks.

The structure is located in a mid-mountain environment (1357 m - Canton of Briançon: Severe frost) and is subject to winter viability (very frequent application of de-icing salts). The ends of the abutments, to the right of the water collectors and the cornices are exposed to direct water inflows polluted during the winter servicing period by de-icing salts. Due to the general context of the structure and its position, the exposure class chosen for the abutment capbeams and cornices is the class XF4 / XD3.

3.2.3.2 History of works and current condition

As the deck is in good condition, the parts studied in the context of this report concern the abutments and cornices.

a. Detailed inspection in 2008

The 2008 detailed inspection indicated that:

- for the C0 abutment (right bank):
  - significant spalls of concrete and corroded visible steel at the upstream end, accompanied by traces of water flow and scour under the capbeam (Figure 2.45). Presence of a spall beginning, humidity and deposits on the capbeam, bubbles and tags on the front wall,
  - active flows on the earth retaining wall at the end of the bridge, calcite flows at the upstream end, ocher-colored facing between the downstream and central bearings,
  - the drainage of the gutter is done through a simple hole (obstructed) in the upstream hiding side wall,
  - on the side walls, presence of bubbling, honeycombs, spalls, apparent steels, some cracks and micro-crazing,
  - moisture at the sidewalk joint on the return wall and upstream hiding side wall.

Figure 2.45. Spalling of concrete of the capbeam (C0 abutment)

Figure 2.46. Exposed corroded steels, concrete spalling on the cornices

- For the C3 abutment (left bank):
  - spalls of concrete and visible corroded reinforcement steels at the upstream end, accompanied by traces of water flow on the capbeam. Presence of humidity, dry stalagmites and deposits on the capbeam,

- on the front wall, old traces of flow and peeling on the downstream side, a rust stain and tags,
- active flows on the earth retaining wall at the end of the bridge, ocher-colored facing on the downstream side, honeycomb and a rust stain at the upstream end,
- the drainage of the gutter is done through a simple hole in the upstream hiding side wall,
- a vertical crack w = 0.1 mm in the upper part to the right of the sidewalk joint and humidity to the right of the expansion joint on the return wall and the upstream hiding side wall,
- apparent bar l = 10 cm in a honeycomb at the axis of the wall and the presence of tags on the downstream side wall.

- For cornices:
  - the cornices are damaged and have numerous exposed corroded steels, concrete spalling, peeling of concrete and rust spots (Figure 2.46).

b. Detailed inspection of 2018

The detailed inspection of 2018 indicates a general worsening of the disorders with:

- for the abutments: the pathologies affecting the upstream ends of the capbeams caps are symptomatic of a physico-chemical alteration of the concrete under the effect of freeze-thaw cycles and chlorides (de-icing salts). The phenomenon has been accentuated since the previous inspection, and can only worsen since no measures have been implemented to limit the harmful effects of inflows of water polluted by de-icing salts;
- for cornices: a worsening of the physico-chemical deterioration affecting the elements of the cornice; in fact, the pathology affects more and more elements, the bare steels show significant section losses and the concrete has been deteriorated deeplier and deeplier.

c. Durability diagnosis of 2012

In 2012, the structure was the subject of a diagnosis of the durability of the reinforced concrete of the abutments and cornices by the CETE Méditerranée - LRPC of Aix-en-Provence. Regarding the abutment capbeams, it should be noted that:

- the cover of steels of the abutment capbeams is very variable (from 15 to 75 mm);
- the measured carbonation depth is between 2 and 12 mm, resulting in a carbonation front that does not reach the reinforcements;
- the chloride concentration threshold from which an initiation of corrosion is considered (about 0.06 % of the mass of concrete for an assumption of 350 kg of cement / m³ of concrete) is largely exceeded in the damaged zone and included in depth (max measured value of 0.296 % on facing and 0.128 % at 8 cm deep) and remains notable although without exceeding the threshold in healthy zone (max measured value of 0.033 %);
- the concrete of the capbeam has an average compressive strength of 48.2 MPa and a porosity accessible to water between 14.2 and 15.1 %.

Regarding the cornices, it can be observed that:

- the cover of steels of the cornices is very variable (from 5 to 90 mm);

- the carbonation depth measured on cores is low, 2mm on the facing side and 10 to 15 mm on the cornice / counter-cornice interface side; it therefore does not reach the reinforcement on the facing side (minimum cover of 5 mm at the chamfer and 9 mm on the exterior vertical facing). Regarding the cornice / counter-cornice interface, the cover could not be checked;
- the chloride concentration threshold from which an initiation of corrosion is considered (about 0.06 % of the mass of concrete for an assumption of 350 kg of cement/m³ of concrete) is never reached (max value measured 0.044 % in the damaged zone);
- the thresholds that would be set for these parts of the structure for a new structure in this type of environment in accordance with the LCPC technical guide 'Recommendations for the durability of hardened concrete subjected to frost' of 2003 (scaling less than 750 g/m² and L_{bar} less than 250 µm) are largely exceeded (7 054 g/m² and more than 466 µm);
- the concrete of the cornices has an average compressive strength of 50.9 MPa and a porosity accessible to water between 13.3 and 16.3 %.

3.2.3.3 Investigations carried out during the PerfDub project

The investigations were carried out in 2018 on the capbeam of the abutments (Figure 2.47) and on the exterior faces of the upstream cornices (Figure 2.48). The samples on the cornices were carried out on three distinct elements of prefabricated cornice, namely, elements 16, 22 and 28 and the element 1 at the end of the left bank on the upstream side.

Figure 2.47. Investigations on the left bank abutment

Figure 2.48. Coring on the upstream cornice

Three areas were chosen with apparent representative conditions.

a. Corrosion diagnosis

The corrosion diagnosis was carried out on the basis of measurement of half-cell potential, corrosion current density using a GECOR 6, and electrical resistivity. The main results are summarized in Table 2.58.

The analysis of these results shows:

- zone 1 (abutment on the left bank): corrosion of the reinforcements started and is under development;
- cornice element 28 upstream: the corrosion observed has developed, even if it was not active at the time of the measurements;

- cornice element 1 upstream: no corrosion of the reinforcements was detected, nor any short-term risk.

Table 2.58. Values obtained with various electrical investigation techniques

Zone	Half cell potentials of steel bars (mV)			Density of corrosion current (µA/cm²)		Resistivity (kΩ.cm)
Upstream and left bank abutment	-375 à -555			0.047 0.094	0.136 0.127	11 à 41
Upstream corniche element 28	6 %	28 %	66 %	0.024 et 0.060		18 à 47 (one value at 91)
Upstream corniche element 1	40 %	60 %		0.016 et 0.028		Measure non-feasible Too resistive concrete

The corrosion level scale (for current measurement) or corrosion risk level (for reinforcement potential and resistivity) is as follows:

Null or negligible	Low	Moderate	High

b. Lifetime and durability indicators

The lifetime indicators studied are the depth of carbonation and the depth of the chloride front; they are compared to concrete covers.

The results of the cover measurements are as follows:

- left bank abutment:
  - vertical steels (1st layer): average cover depth: 37 mm (max: 45 – min: 31),
  - horizontal steels (2nd layer): average cover depth: 62 mm (max: 82 – min: 43).
- upstream cornice:
  - vertical steels (1st layer): average cover depth: 40 mm (max: 64 – min: 25),
  - horizontal steels (2nd layer): average cover depth: 46 mm (max: 48 – min: 40).

The results of carbonation depth measurements are as follows:

- left bank abutment:
  - upstream of the abutment: 2 mm (2 to 3 mm measured in 2012),
  - downstream of the abutment: 26 mm (this value is not consistent with all of the other measurements).
- upstream cornice:
  - upstream face (face subjected to bad weather): 4 mm - 8 mm (2 mm measured in 2012),
  - downstream face (facing located between the cornice and the side of the deck): 15 mm - 17 mm (10 to 15 mm measured in 2012).

The carbonation front therefore did not reach the reinforcements of the various elements checked on the structure.

The free chloride penetration measurement results are all below the corrosion initialization threshold of 0.4 % by mass of cement. Nonetheless, non-negligible percentages of chlorides are observed in the first 2 centimetres of cover (from 0.20 to 0.29 % of the mass of cement).

One core per part of the structure (left bank abutment and cornice) was taken in order to do a physicochemical characterization study of the concrete in order to find its composition. The analysis carried out makes it possible to obtain the simplified mineralogical composition, for each concrete, in the following Table 2.59.

Table 2.59. Main data obtained from a mineralogical analysis

	RG1 (Left bank abutment)	CA1 (Upstream Cornice)
Total aggregates (kg/m^3 of concrete)	1710	1695
Cement content (kg/m^3 of concrete)	395 ± 40	365 ± 35
Efficient water (kg/m^3 of concrete)	195	185
Mass Ratio W_{eff} / Cement	0.49 (0.45 à 0.55)	0.51 (0.46 à 0.56)

The cement constituting the concrete corresponds to a Portland cement type CEM I.

The durability indicators that make it possible to define the potential durability of a structure were measured from cores carried out on the Left bank abutment and on the outer faces of the upstream cornices. The studied indicators are the indicators linked to the risk of reinforcement corrosion (porosity accessible to water (supplemented by capillary absorption), apparent coefficient of chloride diffusion, gas permeability and accelerated carbonation) supplemented by indicators with respect to the risk associated with the effects of freezing: spacing factor, scaling, internal freezing test and characteristic compressive strength at 28 days.

The Table 2.60 presents a summary.

Table 2.60. Values obtained for the durability indicators and lifetime indicators

Synthesis of data			
Characteristics of the bridge		**Abutment**	**Cornices**
Cover depths (values of 2018)	e_{mean} (mm)	36 (vertical steels) 61 (Horiz. Steels)	40 (Transv. steels) 46 (Long. steels)
Cement content (CEM I)	kg/m^3	395	365
Lifetime indicators		**Abutment**	**Cornices**
Carbonation depth	P_c (mm)	Left Bank: < 3 Right Bank : < 14	External Facing: < 8 Internal Facing: < 17
Content of Free chlorides at the level of the mean cover	[Cl-] % par cement mass (max value obtained)	- Damaged zone: 0.72 - Out of damaged zone: 0.19	- Damaged zone: 0.21 - Out of damaged zone:0.13
Durability indicators		**Abutment**	**Cornices**
Apparent coefficient of chloride diffusion	D_{rcm} (10^{-12} m².s^{-1})	28	19.6
Porosity accessible to water	P_{water} (%)	13.5	14
Gas Permeability	K_{gas} (10^{-18} m²)	200 (200 /300 / 2000 #)	150 (100 /200 / 6000 #)
Capillary absorption coefficient at 24 h	C_a (g/m²)	3147	1957
Accelerated Carbonation (3 %) at 28 and 56 days (mm)	$X_{c,28}$; $X_{c,56}$	6 ; 9	NR

Accelerated Carbonation (50 %) at 7 and 28 days (mm)	$X_{c,7}$; $X_{c,28}$	8 ; 10	NR
Spacing Factor (L_{bar})	L (µm)	591	466
Scaling	g/m²	10637	7054
Frost test (in water): - relative expansion - ratio of the square of resonance frequencies	ln (µm/m) $\frac{F_{Fn}^2}{F_{Fo}^2}$x100	945 38	NR
Characteristic strength of concrete on site / Strength Class	f_c (MPa) Class	46 C50/60	57.6 C60/75

**NR : non measured*
 # Value not taken into consideration

Potential durability classes (according to AFGC, 2004)				
Very low	Low	Average	High	Very high

Regarding the durability indicators, the values obtained compared to the limit values proposed according to the criteria of AFGC 2004 reflect a concrete with a potential durability class "low" to "very low". There is also a noticeable variability in the results, in particular for gas permeability.

The concrete constituting the abutment capbeams does not meet any of the criteria for exposure class XD3 / XF4 (except the strength of the concrete and the minimum cement content > 385 kg / m³).

The concrete constituting the cornices does not meet any of the criteria for exposure class XD3 / XF4 (except the strength of the concrete).

3.2.3.4 Conclusions drawn

The investigations carried out within the framework of the PerfDub project on the concrete of the abutment capbeams and the concrete of the cornices of the Vachette bridge (1984/85 structure) make it possible to identify the following points, after 33 years of life:

- the carbonation phenomenon does not reach the first layer of steels in the investigated areas;
- the measures of chloride gradients carried out show significant chloride contents but below the corrosion initiation threshold except for the 2012 samples taken in a concrete area already damaged in the abutment (water inlet area loaded with chlorides coming from the drainage system at the end of the bridge);
- regarding the durability indicators, the obtained values compared to the limit values proposed according to the criteria of AFGC 2004 reflect a concrete with a potential durability class "low" to "very low";
- the indicator thresholds from the CCTG fascicle 65 for a project period of use (DUP) of 100 years for class XD3 / XF4 are also neither verified by the abutment concrete (apart from the strength of the concrete and the minimum cement dosage), nor by the cornice concrete (apart from the strength of the concrete).

3.2.4 Piers of the Ré Island bridge

As part of a collaboration agreement signed between the IREX pilot of the National PerfDub Project and the partners of the DéCoF-Ré research project (Corrosion diagnosis and sustainability study), the latter have agreed to make available some of the data collected on 15 of the 28 piles of the Ré island bridge in the Charente-Maritime Department to the PN PerfDub, free of charge. These data relate to the results acquired on the Pb, Ph and Po piles, on the FC face of the three zones Z1, Z2 and Z3, because these 3 piles were the subject between 2014 and 2019 of complete investigations, namely the corrosion diagnostic study, the durability study (lifetime indicators and durability indicators) and visual autopsies.

3.2.4.1 Presentation of the bridge

The Ré island bridge (Figure 2.49) connects the Ré island to the mainland and spans one navigable sea pass, with a gauge of 30 m above the sea (Figure 2.50). It was commissioned in 1988 and has 2 traffic lanes, plus a pedestrian path and a cycle path. Today, with a total length of 2,928.50 m, it is the third largest bridge in France after the Nouvelle Route du Littoral viaduct in La Réunion Island (~ 5,400 m) and the Saint-Nazaire viaduct (~ 3,356 m).

Figure 2.49. General view of the bridge connecting the Ré island to the continent

It is a bridge of strategic importance, supporting the Departmental Road n ° 735, the only access to the island of Ré: the traffic is about 18,000 vehicles per day in TMJA (Mean Daily Trafic per year), with about 5 % of Heavyweight lorries and goes up in summer peak to 28,000 vehicles in a day.

It consists of:

- a box-girder prestressed concrete deck comprising 6 independent viaducts approximately 500 m long each, connected in pairs by half-joints. All of the 6 viaducts form 29 spans with a span varying between 38 and 110 m in length. The box girder bridge was made with a high performance concrete B40 FS incorporating silica fume and having a required strength of 40 MPa, which was innovative for the time;
- 29 piers numbered 1 to 29 going from the island to the mainland; Figure 2.50 shows the longitudinal profile of the bridge with the location of the navigable passage between piers P10 and P14. Piers P1 to P3 are located on the beach on the Ré island side. Piers P4 to P28 are located in the sea with a maximum height of 42 meters above sea level.

The piers of the Ré island bridge are located in a marine environment. This environment corresponds to exposure classes XS3 (parts in tidal range and in areas subject to projections or spray) and XS2 (parts permanently submerged).

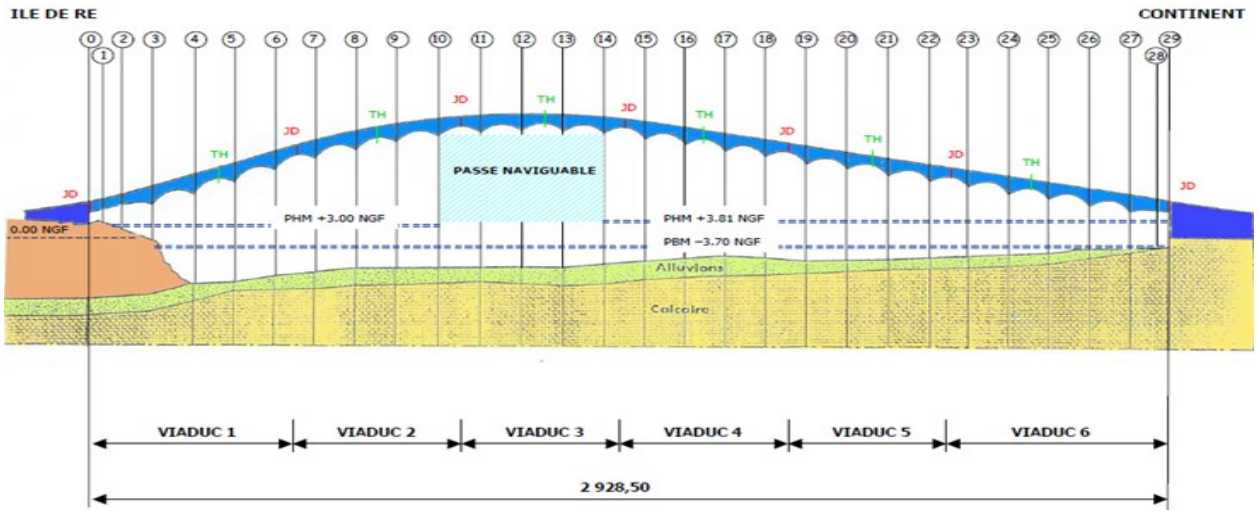

Figure 2.50. Longitudinal profile of the Ré island bridge piers with location of the navigable pass

3.2.4.2 History of works and current condition

The piles are concreted from two plants, with a B30 type concrete, by climbing formwork as the setting / drying progresses. The piles have a fluted shape. The formulation of the concrete used for the piles of the Ré bridge is given in the Table 2.61.

Table 2.61. Concrete composition of the piers of the Ré Island bridge

Composition	B 30 F
Sand 0/3	830 kg/m^3
Gravel 6/20	1 200 kg/m^3
Cement	CPJ 45 RPM (equivalent to a CEM II/A-S with 10 % of slag) (Rc=45 MPa) - content 370 kg/m^3
Water	185 kg/m^3
Admixture	Pozzolith 200N with 0,2 % of the cement mass
W/C ratio	0.5

The various concrete lifts have been subjected to compressive strength tests, with an average strength of 44 MPa for one plant and 39 MPa for the other. The first reinforcement layer of the piers consists of HA32 for vertical reinforcement and HA16 for horizontal reinforcements.

Since its construction, the structure has undergone two detailed inspections: the first in 1995 where it revealed visible steels by defective cover, the second in 2006, which showed crazing and damage caused by corrosion of the reinforcements (concrete spalling, visible corroded reinforcements).

3.2.4.3 Investigations carried out during the PerfDub project

The investigations focused on the lift N ° 2 of the piers given the need to use a boat for access to the sea and to carry out investigations subject to tides. On lift N ° 2, three zones Z1, Z2 and

Z3 (from bottom to top) of dimensions 1 m high and 1.85 m wide (i.e. the width of the pier face) were investigated (Figure 2.51).

Zones Z1 and Z2 are located in the tidal range. Zone Z3 also, but it has about 15 cm (top) which are located out of the water, except during high tides (coefficient greater than 100) and which are subject to sea spray and swashing water.

Figure 2.51. Investigations on lift N ° 2 with measurement zones Z1, Z2 and Z3 accessible by boat

Two of the eight sides of the stack were studied: the FC and FG sides (Figure 2.52). The FC side is the most exposed to the prevailing wind and daily sunshine. The FG side is the least exposed to wind and sun because most of the time it is in the shade of the deck.

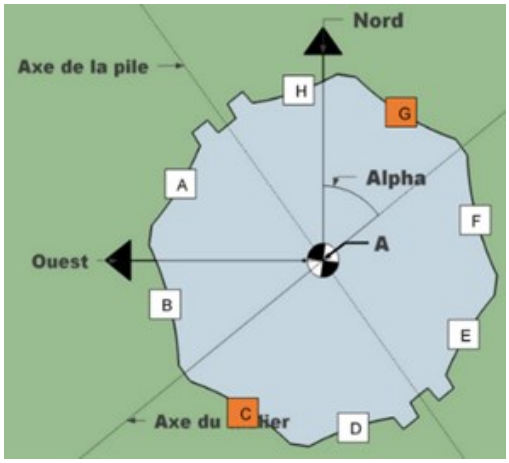

Figure 2.52. Location of the two faces studied FC and FG

Only the results of the three Pb, Ph and Po piers and only of the FC face are presented because all the diagnostic results (corrosion, durability and autopsies) are only available on these piers.

After cleaning the facing (shells, algae, etc.) and connections to the reinforcements, the following investigations were carried out: detailed inspection of visual degradations, identification of the reinforcements, electrical resistivity of the cover concrete, half-cell corrosion potential of the reinforcements, density of corrosion current in the reinforcements, autopsies of the reinforcements.

The results of the corrosion diagnostics presented were obtained during the years 2015-2017. zone Z3 is the most degraded for the three piers with the presence of several vertical cracks. Furthermore:

- the pier Pb also comprises cracks in the zones Z2 and Z1;
- the pier Ph has a spall at the top left of zone Z3 (no fault in zone Z1);
- the pier Po comprises a crack in the middle of the face from zone Z3 to zone Z2.

a. Concrete cover

The Table 2.62 presents the values of the measured concrete cover.

Table 2.62. Characteristic cover values (in cm) of piers Pb, Ph et Po

Pier - Face - Zone		Horizontal reinforcement				Vertical reinforcement			
		Mean	Min	e_{95+} *	e_{95-} **	Mean	Min	e_{95+} *	e_{95-} **
Pb-FC	Z3	7.1	4.9	4.6	8.4	8.6	5.4	5.6	10.1
	Z2	7.4	5.2	5.0	9.1	9.1	5.4	6.5	10.5
	Z1	8.4	5.3	5.1	10.5	10.4	7.1	7.2	12.4
Ph-FC	Z3	8.0	6.1	5.9	9.2	9.6	7.1	6.7	11.3
	Z2	8.1	5.7	5.1	9.5	10.1	6.3	6.8	12.8
	Z1	9.0	6.6	6.2	10.5	11.6	9.3	9.0	12.8
Po-FC	Z3	9.1	6.6	6.2	10.8	10.5	7.4	7.9	11.5
	Z2	8.4	5.4	6.2	9.8	9.7	6.6	7.0	11.2
	Z1	7.9	6.4	5.8	9.0	9.5	6.6	6.4	10.9

** 95 % of measured covers are greater than the characteristic value e95+*

*** 95 % of measured covers are smaller than the characteristic value e95-*

In Table 2.62, the average covers (between 7.1 and 9.1 cm) are greater than the nominal cover at the time of construction (4 cm in a marine environment in the 1983 revised BAEL80). However, the characteristic covers (e95 + and e95-) show that there is a proportion of horizontal reinforcements for Pb-FC-Z3 whose cover is less than 5 cm (minimum cover recommended by Eurocode 2 in a marine environment XS3).

b. Resistivity results

The average resistivity values are represented in the form of an iso-value map (Figure 2.53) with color codes that integrate the values of the RILEM TC 154 (Polder, 2000).

The analysis of the values of the measurements carried out on the three piers leads to the following conclusions:

- the resistivities of zone 3 are greater than 100 kΩ.cm and can go up to 200 kΩ.cm (for the Pb pier). They show a risk of corrosion ranging from low to negligible;
- the resistivities of zone 2 are between 50 and 100 kΩ.cm and indicate a risk of corrosion ranging from moderate to low;
- the resistivities of zone 1 are between 10 and 50 kΩ.cm and indicate a risk of corrosion ranging from moderate to high.

For the three piers, the resistivity decreases (from top to bottom) from zone Z3 towards zone Z2 towards zone Z1, which would show that the risk of corrosion is greatest in zone Z1. However, these conclusions are not in agreement with the degradations observed visually on the facings of zones Z3 (cracks and degradations) to Z1 (no or few defects). In a maritime environment, it appears in fact that the vertical gradients of the resistivity values can be mainly explained by humidity gradients and / or by chloride ion contents, and consequently that the correlation between the electrical resistivity of the concrete cover and the risk of corrosion is not a direct conclusion of the corrosion activity of the reinforcements. This encourages caution when measuring the in-situ resistivity.

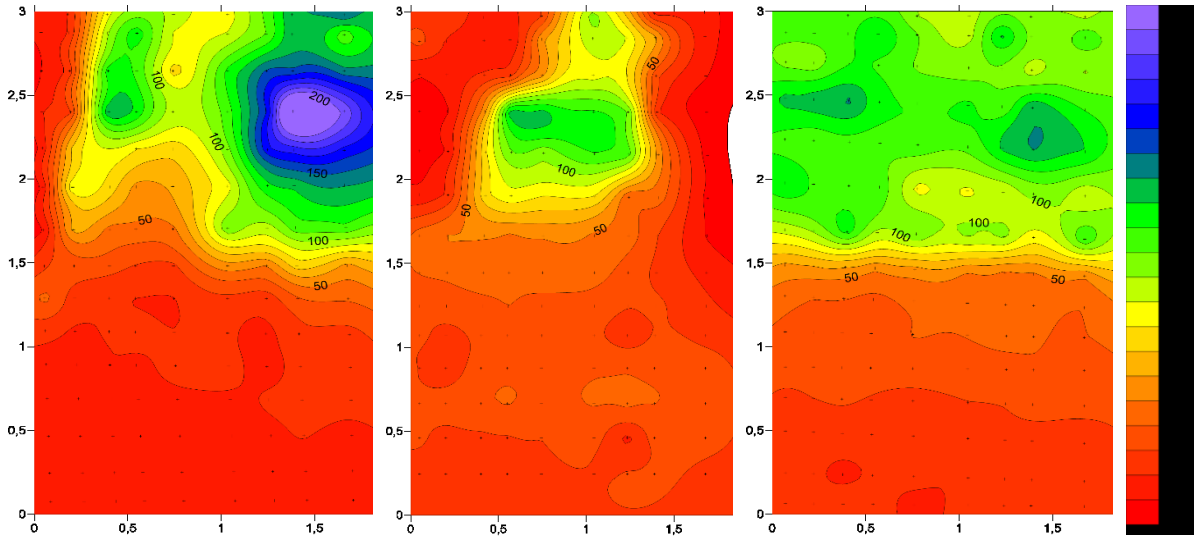

Figure 2.53. Surfermaps of iso-values of the cover concrete resistivity (in kΩ.cm) f or the piers Pb, Ph et Po

c. Half-cell potential measurements

The iso-values maps of the half-cell corrosion potentials of the horizontal reinforcements are shown in Figure 2.54.

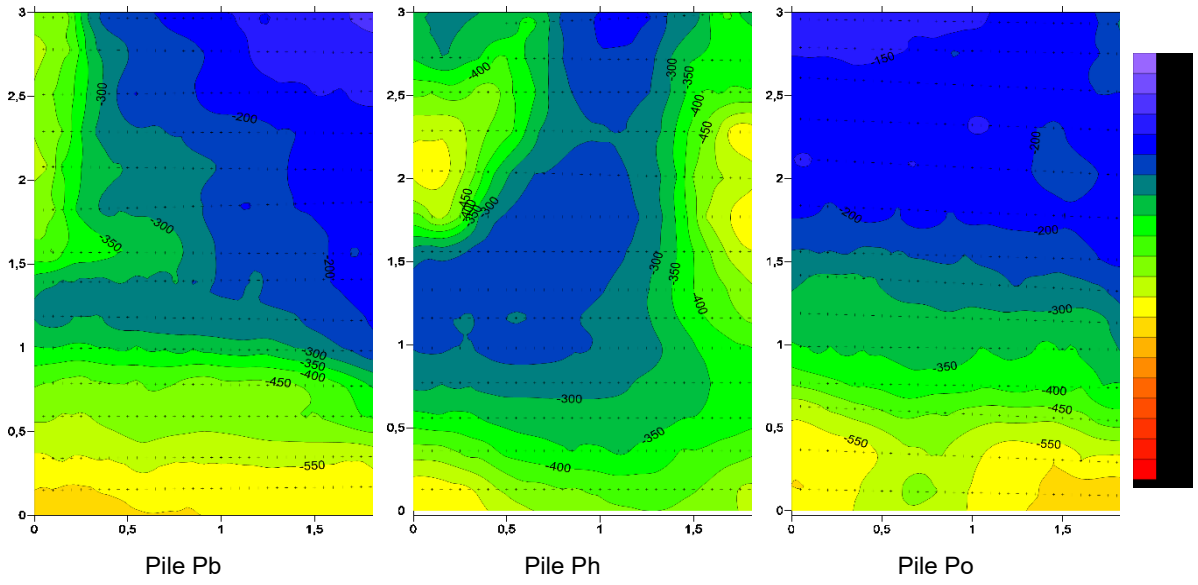

Figure 2.54. Surfer® maps of the half-cell corrosion potentials of horizontal reinforcements plotted in iso-values (mV, Cu / CuSO4) of Pb, Ph and Po piers

The results of the analysis of the half-cell potential measurements obtained on the horizontal reinforcements of the three Pb, Ph and Po piers of the Ré island bridge (Face FC, zones Z1, Z2 and Z3) according to the three documents presented in paragraph 2.5 are shown in Table 2.63.

Table 2.63. Results of the analyses of half-cell potential measurements on the Pb, Ph and Po piers (Face FC, zones Z1, Z2 and Z3) of the Ré island bridge according to the three documents

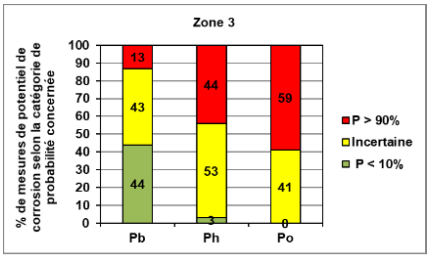

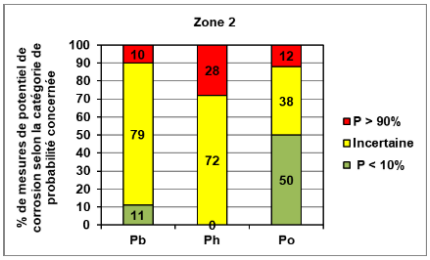

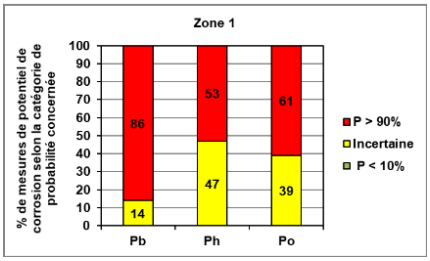

Risque de corrosion		Pb	Ph	Po
Zone 3	Fort			
	Incertain			
	Faible			
Zone 2	Fort			
	Incertain			
	Faible			
Zone 1	Fort			
	Incertain			
	Faible			

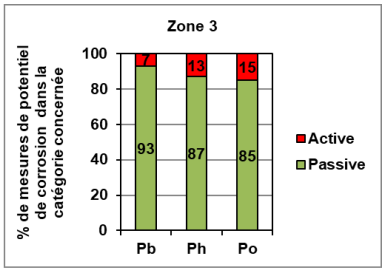

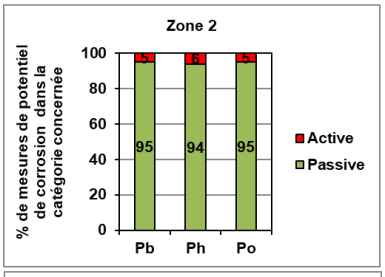

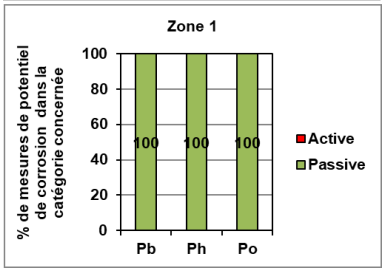

a) ASTM C876 b) COST 509 c) RILEM

In Table 2.63a, the percentages of the half-cell potential values by corrosion probability category according to the ASTM C876 standard (ASTM, 2009) show a pessimistic situation with a higher corrosion probability in zone Z1 than in zone Z3. In Table 2.63b, the distribution of the half-cell potential values according to the document COST 509 (Cox *et al.*, 1997) shows an alarmist situation with a strong risk of corrosion for all the areas investigated. In Table 2.63c, the percentage of active or passive corrosion activity according to the recommendations of RILEM shows that passive corrosion is predominant in all the areas investigated and that active corrosion concerns only the Z2 areas (5 at 6 %) and Z3 (7 to 15 %).

The complementarity of the visual inspection results, resistivities and potentials suggests that the analysis of the potentials via the RILEM document is the most relevant. By carrying out a more in-depth analysis consisting in subtracting from the raw data the effect of the tidal range phenomenon according to seasonality, the so-called "reliable" maps obtained make it possible to locate "active corrosion zones". This analysis resulted in the detection of an anodic zone at the top left for the Pb pier, two anodic zones at the left and right of the Ph pier and no suspicion of corrosion for the Po pier.

d. Lifetime indicators

The cores intended to measure the durability indicators and the lifetime indicators were taken in January 2016. The cores dedicated to the measurement of the carbonation depth were taken

from the FC faces of the Pb, Ph and Po piers and only in zone Z3. The penetration of the carbonation front is negligible.

The free and total chloride ion content profiles as a function of concrete depth are shown in Figure 2.55.

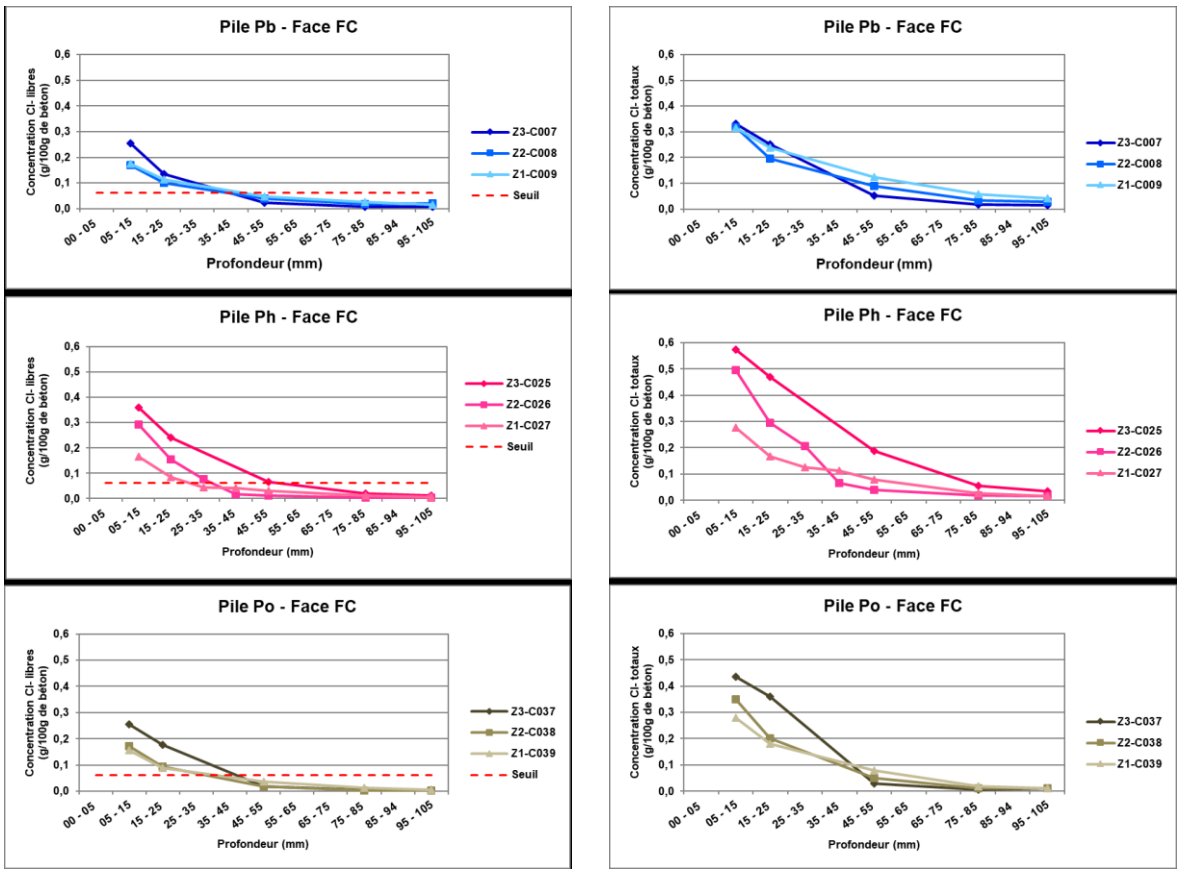

Free chlorides Total chlorides

Figure 2.55. Profiles of chloride ions contents (free and total) as a function of the concrete depth

On the basis of a critical threshold of 0.4 % of the cement mass, for the three piles Pb, Ph and Po, this critical threshold is exceeded to a depth of 15-25 mm over all the zones, with free chloride ion contents between 0.086 and 0.240 % per mass of concrete. This critical threshold is even exceeded up to 45-55 mm in zone Z3 of the Ph pier.

e. Durability indicators

Table 2.64 summarizes all the results of the durability indicators for the three Pb, Ph and Po piers on Face FC and in zone Z3 (zone for which active corrosion is most likely). The colors correspond to the durability classes according to AFGC 2004.

The obtained values correspond to a durability qualified as low to medium according to AFGC 2004. It should be noted that the values of compressive strength after 29 years are significantly higher than those indicated in the bridge documentation, without obvious explanation.

In conclusion, with regard to the environment considered (corrosion induced by chloride ions), these potential durability classes correspond globally to a potential lifespan of 30 to 50 years and less than 30 years for Ph-FC-Z3. These theoretical lifetimes are given for a conventional cover of 5 cm and must be corrected to take into account the actual covers. This correction shows that for certain pier areas the potential lifespan is relatively low; result consistent with the chloride front depths measured on this 29-year-old structure.

Table 2.64. Values of durability indicators and corresponding potential durability classes for Pb, Ph and Po piers (Face FC, Zone Z3)

Durability indicators		**Pb-FC-Z3 C067b,C068,C069**	**Ph-FC-Z3 C076,C077,C078**	**Po-FC-Z3 C070,C071,C072**
Apparent coefficient of chloride diffusion (10^{-12} m².s^{-1})	D_{rcm}	8.5 (8.5/7.2/9.9)	8.7 (10.0/4.9/11.3)	15.1 (17.7/16.2/11.3)
Electrical Résistivity (Ω.m)	Resi	139 (141/133/141)	76 (75/79/73)	72 (75/69/71)
Porosity accessible to water (%)	P_{water}	12.1 % (11.3/12.2/12.7)	15.3 % (15.5/15.3/15.2)	13.8 % (14.3/13.9 /13.2)
Gas Permeability (10^{-18} m²)	K_{gas}	109 (80/107/140)	400 (264/1709*/537)	174 (219/180/122)
Other characteristics		**Pb-FC-Z3 C067b,C068,C069**	**Ph-FC-Z3 C076,C077,C078**	**Po-FC-Z3 C070,C071,C072**
Perméability to water after capillary absorption (kg.m^{-2}.s$^{-0,5}$)	w	0.91 (0.83/0.94/0.96)	0.23 (0.22/0.29/0.19)	1.28 (1.36/1.27/1.20)
Density (kg/m^3)	ρ_b	2439.7 (2466/2430/2424)	2305.7 (2306/2300 /2312)	2363.6 (2345/2358/2388)
Capillary absorption coefficient at 24h (kg/m²)	C_a	4.80 (4.26/5.01/5.14)	1.16 (1.08/1.45/0.95)	5.94 (6.25/5.89/5.67)
Compression strength corrected (MPa)	f_c	C079 64.3	C082 70.8	C080 64.5
Compression strength at 28 days – bridge documentation (MPa)	$f_{cm,28}$	42.1 (3.8)	44.2 (0.9)	37.8 (-)

** Outlier, not taken into account in the average*

Potential durability classes (according to AFGC, 2004)				
Very low	Low	Average	High	Very high

The results of autopsies performed on reinforcements in certain areas are as follows:

- for the Pb - Face FC pier, the reliable potential mapping showed a singular zone at the top left in the Z3 zone. The autopsy shows some oxidation of the reinforcements and a pitting on the horizontal reinforcement in the foreground which confirms a state of the reinforcements in active corrosion;
- for the Po - Face FC pier, the reliable potential mapping showed that the reinforcements were sound in the three zones. The autopsy was performed on a vertical V7 bar for which the cover thicknesses are the lowest (average: 8.6 cm); the condition of the reinforcements is considered "healthy".

3.2.4.4 Conclusions drawn

The study of the durability of the cover concrete according to the durability indicators and the lifetime indicators on this 29-year-old structure showed that:

- the concrete carbonation depth is negligible for this structure in this maritime environment;
- the average covers of the horizontal reinforcements of the fluted faces of the piers are located between 71 and 91 mm (and are greater than the 50 mm which would be recommended today with Eurocode 2). Although low, there is nevertheless a percentage of linear reinforcement with covers lower than this characteristic value to the right of the edges of the faces of the piers);
- the penetration fronts of free chloride ions (between 26 and 52 mm) determined between the free chloride ion profiles (depending on the cover depth) and the critical chloride value (0.062 % of chloride ions relative to the concrete mass) are less than the cover thicknesses of the horizontal reinforcements, but they are relatively large for a 29-year-old structure;
- the values of the durability indicators obtained and compared with the limit values proposed according to the criteria of the AFGC 2004 reflect a concrete of potential durability class "low" to "medium" with a lifespan of 30 years (for 50 mm cover).

The seawater-resistant concrete formulation practices implemented in the 1980s (i.e. allowing use of CEM I or CEM II/A with limited amount of supplementary cementitious materials; slag, fly ash, silica fume) clearly show their limits. We are starting to see signs of corrosion in the tidal range and we can consider that we are starting to enter the propagation zone in zone Z3 of the piers and that we are still in the initiation phase in zones Z1 and Z2.

The results are representative of three piers of the Ré island bridge which turned out to be not degraded or only slightly degraded by corrosion of the reinforcements. They are not representative of the general condition of the piers of the Ré bridge, some of which in the tidal range have concrete spalls and visible corroded reinforcements.

3.2.5 St-Poncy Bridge

3.2.5.1 Presentation of the bridge

The St-Poncy bridge (Figure 2.56) is an overpass of the A75 motorway which supports the D 909 departmental road. It was built in 1988 and is located in the Cantal Department between Saint-Flour and Massiac.

Figure 2.56. View of the St-Poncy bridge from the South

The structure consists of a continuous reinforced concrete deck. It is made up of four spans (8.63 - 13.20 - 13.20 - 7.66 m), for a total length of 46.30 m and a width of 8.50 m. The deck rests on 3 piers and 2 abutments.

It is located in mid-mountain (altitude of 990 m), in a severe frost zone and the winter viability of the A75 presents a "very frequent" level of de-icing salts application on this section. The concrete exposure classes to be taken into account for these parts of structures are classes XF4, XD3 and XC4. In severe winter months, priority is given to the operation of the left lanes. The slow lanes (on the right side) are then used to store snow. This means that the central pier located in the middle of the highway, receives quantities of de-icing salts greater than those received by the side piers since the commissioning of the structure.

The parts investigated are two piers and more precisely:

- a pier facing not exposed to de-icing salts: west facing of the west bank pier, P2
- a pier facing exposed to de-icing salts: west facing of the central pier P3.

Each pier consists of a reinforced concrete wall on a footing. Their width is 5.80 m and their thickness 0.50 m at the level of the investigations carried out. Piers P2 and P3 have heights of 6.37 and 6.84 m, respectively, above their footing.

3.2.5.2 History of works and current condition

The composition of the concrete as checked by the Clermont-Ferrand laboratory of the Cerema is given in the following Table 2.65.

Table 2.65. Concrete composition of the St-poncy piers

Concrete composition			
Constituent	**Class**	**Origin**	**Content (kg/m^3)**
Cement	CPA 55R (CEM I)	VICAT Créchy plant (03)	350
Sand	0/5	S.A.B.L.E.S Company	756
Gravel	5/10	S.A.B.L.E.S Company	233
Gravel	10/20	S.A.B.L.E.S Company	932
Water (total)		Tapwater network	200

We note the absence of an admixture in the composition, in particular an air entraining agent.

The 28-day average compressive strength measured during construction on the walls of piers P2 and P3 were 33.6 and 35.3 MPa, respectively, which corresponds to a C30 / 37.

Only one detailed inspection had been carried out in the life of the structure in June 2001 before the one carried out in 2019 as part of PerfDub. These two inspections, carried out during 13 and then 31 years of service of the structure, revealed the following disorders (Table 2.66).

Table 2.66. Disorders observed during the detailed inspections of 2001 and 2019

Piers	Detailed Inspection 2001	Detailed inspection 2019
P3 Pier West facing	- A vertical crack of 0.1 mm opening, located at mid-width of the wall and originating at the foot. - No apparent disorder related to freezing and / or de-icing salts	- A vertical crack of 0.1 mm opening, located at mid-width of the wall and originating at the foot. - The entire foot of the pile sounds hollow when probing with a hammer, with traces of steel oxidation (Figure 2.57).
P3 Pier North facing	No apparent disorder related to freezing and / or de-icing salts	Concrete scaling (Figure 2.58)
P2 Pier West facing	No apparent disorder related to freezing and / or de-icing salts	No apparent disorder related to freezing and / or de-icing salts

Figure 2.57. Spalling of concrete with traces of oxydation

Figure 2.58. Scaling of concrete

3.2.5.3 Investigations carried out during the PerfDub project

a. Lifetime indicators

At the request of the Massif Central DIR, chloride ion penetration profiles were carried out in 2014 on the P2 and P3 piers, at different wall heights. The results of the free chloride concentrations, related to the amount of cement in the concrete formula, are given in the three following figures.

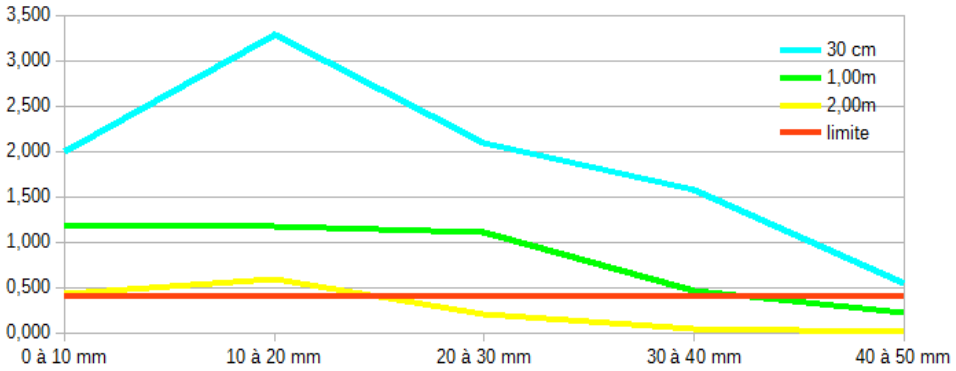

Figure 2.59. Profiles of free chlorides (% per cement mass) in the West facing of P3 pier (face exposed to salts)

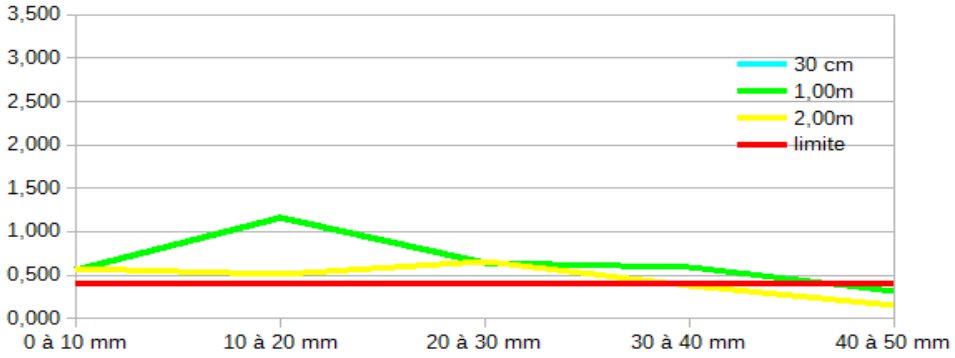

Figure 2.60. Profiles of free chlorides (% per cement mass) in the East facing of P2 pier (face exposed to salts)

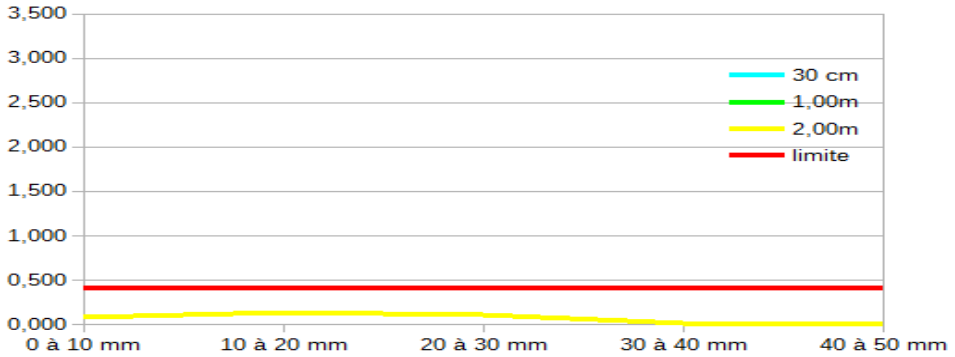

Figure 2.61. Profiles of free chlorides (% per cement mass) in the West facing of P2 pier (face not exposed to salts)

The other investigations were carried out in 2019 in the following two areas:

- the west face of the P2 pier wall (not exposed to de-icing salts);
- the west face of the P3 pier wall (exposed to de-icing salts).

b. Corrosion diagnosis (concrete cover, half-cell potential and resistivity)

The following Table 2.67 shows the characteristic statistical values of the cover (in mm) for a theoretical cover of 30 mm.

Table 2.67. Statistical values of the concrete cover (in mm)

	Horizontal reinforcement					Vertical reinforcement				
Part / Zone	**Min.**	**Mean**	**≤45**	**e_{95+} ***	**e_{95-} ****	**Min.**	**Mean**	**≤45**	**e_{95+} ***	**e_{95-} ****
West face of the P2 pier wall	21	27	100 %	22	35	14	37	81 %	25	62
West face of the P3 pier wall	12	31	95 %	14	12	33	42	62 %	35	47

** 95 % of the measured coverings are higher than the characteristic value e95+*
*** 95 % of the coverings measured are lower than the characteristic value e95-*

In the areas of investigation, the average cover of the reinforcements is respectively 30 and 40 mm for the horizontal and vertical reinforcements. Between 95 and 100 % of the measured covers of the horizontal reinforcements have a lower cover than would be expected today (45 mm). Overall, the covers measured on the P2 pier are lower than those measured on the central pier P3.

The Table 2.68 shows the proportion of resistivity measurements made on the bridge piers according to the different corrosion risk classes proposed by the RILEM TC 154 recommendation for CEMI concrete.

Table 2.68. Resistivity measurements

		Pourcentage of measures	
Electrical Resistivity (kΩ.cm)	**Risk of corrosion**	**West face of the P2 pier wall**	**West face of the P3 pier wall**
Re > 100	Negligible	100 %	40 %
50 < Re < 100	Low	0 %	18 %
10 < Re < 50	Moderate	0 %	29 %
Re < 10	High	0 %	17 %

The resistivities measured on the side pier P2 are generally high (between 108 and 268 kΩ.cm) and correspond to a compact and / or carbonated and / or sheltered concrete. A slight vertical gradient with lower resistivities is observed in the lower part, probably corresponding to a higher humidity (water projection for example). The reinforcements of this facing are located in a concrete that is not very suitable for corrosion development.

The measurements carried out on the central pier P3 clearly show a resistivity gradient with very low resistivities on the first two lines of measurement meshes to be linked with the splashing water loaded with de-icing salts. The reinforcements of this facing (lower half of the investigation area) are located in a concrete favorable to the development of corrosion.

The half-cell potentials measured on the West face of the P2 pier wall are very little electronegative (between -55 and -177 mV). They correspond to reinforcements theoretically in a passivation state. We observe a slight vertical gradient with more electronegative potentials at the bottom of the pier. This gradient is related to the humidity of the concrete and is not symptomatic of the presence of anodic areas. The study of potential gradients highlights the disruptive effects of coring, with gradients greater than 10 mV/cm which are not symptomatic of the presence of anodic zones. The removal of concrete to ensure connection of the measuring equipment shows vertical reinforcement without any sign of corrosion.

The half-cell potentials measured on the West face of the P3 pier show a classic behavior of a facing exposed to projections containing chlorides from de-icing salts. The investigation area presents high electronegative potential in the lower third. These highly electronegative values are due to humidity and the presence of chloride ions which impact the potential measurement. They are not necessarily symptomatic of reinforcement corrosion. The maximum difference of the potentials is respectively 520 and 478 mV for horizontal and vertical reinforcements. The vertical gradients of potential are generally less than 10 mV/cm. Moreover, except in the upper right corner of the zone where there are some high values (respectively 16 and 12 mV/cm on a horizontal and a vertical steel), which corresponds to a concrete spall with a visible reinforcement, the high gradient values observed occasionally are not due to "potential wells" and are therefore not symptomatic of the presence of anodic areas.

The carbonation depth measurements are summarized in the Table 2.69.

Table 2.69. Results of carbonation depth measurements

Mean / Max carbonation depth (mm)	**West facing**	**East facing**
P2 pier	16 / 20	18 / 20
P3 pier	15 / 17	15 / 17

c. Durability indicators

The summary of the measures of the durability indicators is presented in Table 2.70.

The measured values of the durability indicators with respect to the corrosion of the reinforcements, classify the concrete of the piers in a potential durability "low" to "very low", according to (AFGC, 2004).

If this bridge were to be built today, the combination of exposure classes XF4, XD3 according to NF EN 206 / CN would be retained for the piers concrete, with the additional composition requirements of fascicle 65, and those of the G + S prevention level of the “Recommendations for the durability of hardened concrete subjected to frost” released in 2003.

Table 2.70. Values of the durability indicators

Synthesis of data			
Characteristics of the bridge		**P2 pier (West) Not exposed to salts**	**P3 pier (West) Exposed to salts**
Concrete cover	e_{moy} (mm)	24	30
Cement content (CEM I)	kg/m^3	350	350
Lifetime indicators		P2 pier (West)	P3 pier (West)
Carbonation depth	P_c (mm)	16	15
Free chlorides content at the level of the mean concrete cover	[Cl^-] % per cement mass	0.113	2.09
Durability indicators		**P2 pier (West)**	**P3 pier (West)**
Apparent coefficient of chloride diffusion	D_{rcm} (10^{-12} m².s^{-1})	41.2 (46.7/33.4/43.6)	NM
Porosity accessible to water	P_{water} (%)	16.7 (16.8/17.3/17.1)	NM
Gas Permeability	K_{gas} (10^{-18} m²)	646 (438/834/667)	NM
Electrical resistivity	Ω.m	38 (31.53.31)	NM
Capillary absorption coefficient at 24h	C_a (g/m²)	5793 (5634 /5293/6453)	NM
Density (kg/m^3)	ρ_b	2250	NM
Accelerated carbonation (3 %) at 28 and 56 days (mm)	X_{c28d}; X_{c56d}	11; 16	NM
Accelerated carbonation (50 %) à 7 and 28 days (mm)	X_{c7d}; X_{c28d}	15; 28	NM
Spacing factor (L_{bar})	L (µm)	279	NM
Scaling test at 56 cycles	g/m^2	50917 (56611/61061/37999/45223)	NM
Internal Freezing test (in water): - relative expansion at 26 cycles - ratio of the square of resonance frequencies at 26 cycles	ln (µm/m) $\frac{F_Fn^2}{F_Fo^2}$ x 100	1759 (1018/2500/2180) 21 (36/10/16)	NM NM
Characteristic strength of concrete on site / Strength Class	f_c (MPa) Class	28.6 30/37	29.4 30/37

NM : Not Measured

Potential durability classes (according to AFGC, 2004)				
Very low	Low	Average	High	Very high

The Table 2.71 shows the position of the concrete of the St-Poncy bridge piers in relation to the current regulations, with the following color code:

Conform	Not conform

Table 2.71. Evaluation of the conformity of the concrete to the current regulations.

Specifications for the composition XD3, XF4 G+S		**Concrete of the St-Poncy bridge piers**
Cement type	CEM I	CEM I
Supplementary characteristics of the cement	Sea compatible or sulfate-resisting	no
Binder content	> 385 kg	350 kg
Effective Water / binder ratio	< 0,45	0,57
Class of compression strength	≥ C35/45	C30/37
Air-entrained admixture	Obligatory or freeze-thaw resistance test	no
Durability indicators specifications regarding corrosion XD3		
Porosity accessible to water (%)	< 13	16,7
Apparent coefficient of chloride diffusion (10^{-12} m².s^{-1})	< 3,5	41,2
Gas permeability (10^{-18} m²)	< 200	646
Durability indicators specifications regarding freeze-thaw with salts		
Spacing factor (µm)	< 200	279
Relative expansion (µm/m)	< 400	1759
Ratio of the square of resonance frequencies	> 75	21
Scaling (g/m²)	< 600	50917

3.2.5.4 Conclusions drawn

Except the cement type, all specifications and durability indicators for this concrete are non-conforming with respect to durability against corrosion. In addition, all performance indicators for freeze-thaw resistance are greatly exceeded, and the cover of steels does not meet the value of 50 mm set in EC2 for XD3 class.

The characteristics of the concrete used in 1988 for the construction of the piers of the St-Poncy bridge do not meet current requirements to protect against exposure to severe frost with a very frequent level of salting (XF4, XD3, G + S) and for a project life of 100 years.

30 years after its construction:

- concrete carbonation is present over 60 to 80 % of the cover depth depending on the area investigated. The first rebar bed is therefore not reached by carbonation in these areas;

- the concentration of free chlorides in relation to the mass of cement in the concrete composition (2 %), greatly exceeds the critical concentration (0.4 %) for the initiation of corrosion at the level of the first reinforcement bed of the central pier (P3);
- low concrete covers are existing whatever the zone and with a very high proportion of reinforcements with cover less than 45 mm;
- high in-situ resistivities are measured on the P2 pier. The reinforcements of this face are located in a concrete not very prone to the development of corrosion. A vertical resistivity gradient is present on the central pier P3 with very low resistivities in the lower part, to be linked to the projections of water and de-icing salts. The reinforcements located in the lower half of the investigation zone are embedded in a concrete suitable for a development of corrosion;
- half-cell electrical potentials do not show signs of the presence of anodic zones.

Globally, the non-destructive investigations indicate that, despite a weak cover and a concrete prone to the development of corrosion (P3 pier), there is no indication of a corrosion initiation in the areas studied (except for the first 10 to 20 centimetres at the base of P3 where concrete spalling, a beginning of scaling and the corrosion of the reinforcements are already visible.

3.2.6 Pirou Bridge

3.2.6.1 Presentation of the bridge

The Pirou Bridge is an overpass of the A75 motorway that supports the D4 departmental road (Figure 2.62). It was built in 1991 and gives access to the village of Pirou located in the Department of Cantal.

Figure 2.62. View of the Pirou bridge

The structure consists of a continuous prestressed concrete deck. The crossing is made up of three spans (13.40 - 24.50 - 13.40), for a total length of 55.70 m and a width of 8.80 m. It is based on 2 piers and 2 abutments.

It is located in the middle of the mountains (altitude 884 m), in a severe freezing zone and the winter viability of the A75 presents a "very frequent" level of salting in this section. The concrete

exposure classes to be taken into account for these parts of structures are XF4, XD3 and XC4 classes.

The investigated parts relate to two piers and more precisely:

- a pier face not exposed to de-icing salts: west facing of the west side pier
- a pier face exposed to de-icing salts: east facing of the west side pier.

Each pier consists of a reinforced concrete wall on a surface footing.

3.2.6.2 History of works and current condition

Table 2.72 presents the composition of the concrete of the piers based on the archives of the "Massif Central" DIR.

Table 2.72. Composition of the concrete of the Pirou bridge

Concrete composition			
Constituent	**Class**	**Origin**	**Content (kg/m³)**
Cement	CPA 55 (CEM I)	LAFARGE Teil plant	400
Sand	0/4	S. Rieutortet Company	750
Gravel	4/10	Issoire	233
Gravel	10/20	Issoire	670
Water (total)		Drinking water	182
High water reducing admixture (1.4 %)	Superplast LS		5.6
Air-entrained admixture (0.08 %)	Chryso® air		0.32

The large superplasticizer content could suggest that the amount of water displayed in the composition is the total amount of water. This would lead to a fairly low effective water / cement ratio, around 0.40, which would be compatible with the durability characteristics obtained on this concrete.

The compressive strength class is C30/37.

Only one detailed inspection had been carried out in the life of the structure in June 2001 before the one carried out in 2019 as part of PerfDub. These two inspections, carried out on the West pier after 10 then 28 years of service of the structure, did not reveal any apparent disorder which could be linked to corrosion of the reinforced concrete reinforcements, or to freezing- thaw cycles. on concrete.

3.2.6.3 Investigations carried out during the PerfDub project

a. Lifetime indicators

At the request of the DIR Massif Central, chloride ion penetration profiles were carried out in 2014 on the West pier at different wall heights. The results of free chloride concentrations, reduced to the amount of cement in the concrete formula, are given in Figures 2.63a et 2.63b.

The other investigations were carried out in 2019 in the following two areas:

- the west face of the West pier wall (not exposed to de-icing salts)
- the east face of the West pier wall (exposed to de-icing salts)

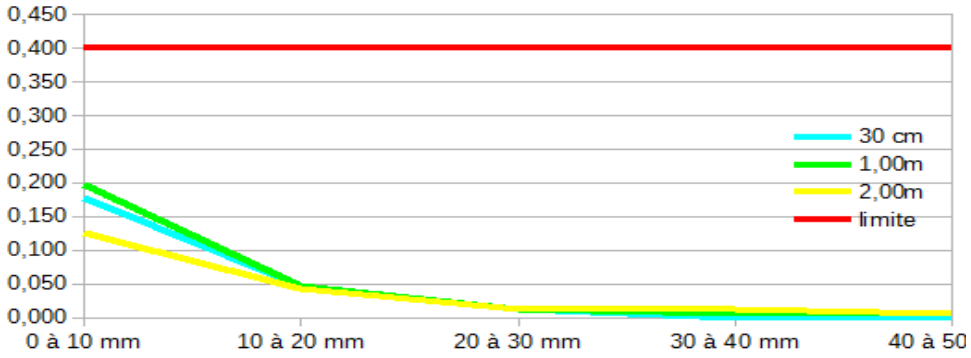

Figure 2.63a. Profiles of free chlorides in the West facing of the West pier (face not exposed to salts)

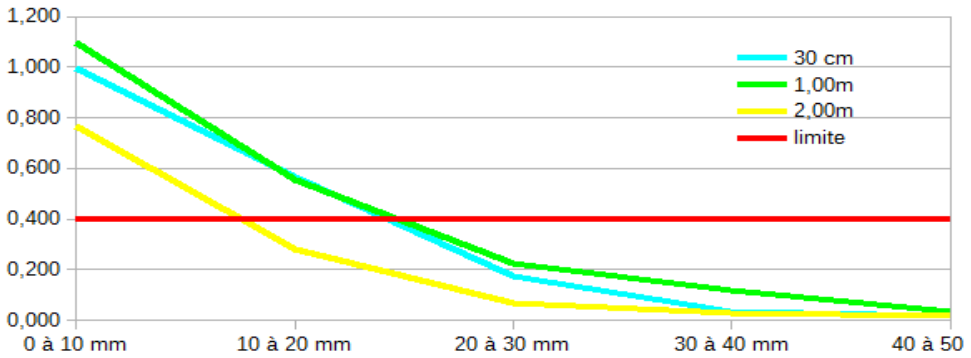

Figure 2.63b. Profiles of free chlorides in the East facing of the West pier (face exposed to salts)

b. Corrosion diagnosis (concrete cover, half-cell potential and resistivity)

The following Table 2.73 shows the characteristic statistical values of the cover (in mm) for a theoretical cover of 30 mm.

Table 2.73. Statistical values of the concrete cover (in mm)

	Horizontal reinforcement					Vertical reinforcement				
Part / Zone	**Min.**	**Mean**	**≤45**	**e_{95+} ***	**e_{95-} ****	**Min.**	**Mean**	**≤45**	**e_{95+} ***	**e_{95-} ****
West face of the West pier	18	25	100 %	18	33	27	36	100 %	30	41
East face of the West pier	23	29	100 %	24	35	37	44	57 %	38	53

** 95 % of the measured coverings are higher than the characteristic value e95+*
*** 95 % of the coverings measured are lower than the characteristic value e95-*

For the west face of the pier, the mean reinforcement cover is respectively 25 and 36 mm for the horizontal and vertical reinforcements, and 100 % of the measured covers are significantly lower than the cover that would be specified today (45 mm).

For the east face of the pier, the average reinforcement cover is respectively 29 and 44 mm for the horizontal and vertical reinforcements, and respectively 100 % and 57 % of the horizontal and vertical reinforcement measured covers are lower than the cover that would be specified today (45 mm).

The Table 2.74 shows the proportion of resistivity measurements made on the bridge piers according to the different corrosion risk classes proposed by the RILEM TC 154 recommendation for CEM I concrete.

The in-situ resistivities measured on the East and West faces of the P3 pier are globally high. A detailed analysis shows that the resistivity values on the West face (protected from sprays) are slightly higher than those of the East face (exposed to splashing water and de-icing salts). For the two faces (West and East), the measurements clearly show a vertical resistivity gradient with lower resistivities at the bottom of the pier (more exposed to humidity). The reinforcements of this face are located in a concrete that is not very prone to the development of corrosion.

On the West face, the measured half-cell potentials of the horizontal reinforcements are generally slightly more electronegative than those of the vertical ones. A slight vertical gradient with more electronegative potentials is observed at the bottom of the pier: the reinforcement exhibit more electronegative potentials in the lower 1/3 of the area of investigation; this gradient is probably linked to a greater exposure of concrete to humidity (or even chlorides from de-icing salts). The study of local gradients (local variation in potentials) shows two zones of "potential wells" for the horizontal reinforcements (- 26 mV/cm and – 8 mV/cm) and a zone (- 9 mV/cm) for the vertical reinforcements. These potential peaks could be the indication of anodic zones. At the bottom of the pier, the absence of a potential peak leads to the conclusion of an absence of anodic zones.

On the East face, the observations relative to half-cell potentials are generally similar to those formulated for the West face. However, the potentials are slightly more electronegative and the potentials of vertical reinforcements (up to – 396 mV) are more electronegative than those of the horizontal reinforcements (up to -343 mV). In addition, the more electronegative values concern a greater height than on the west face (approximately the lower two thirds of the height). The measurements show a classic behaviour of a face exposed to splashes containing chlorides from de-icing salts. The investigation area shows great electronegative potentials at the bottom of the pier. These highly electronegative values are due to humidity and the presence of chloride ions which impact the potential measurement. They are not necessarily symptomatic of corrosion of the reinforcements.

Table 2.74. Resistivity measurements

		Pourcentage of measures	
Electrical Resistivity (kΩ.cm)	**Risk of corrosion**	**West face of the west pier**	**East face of the west pier**
Re > 100	Negligible	100 %	100 %
50 < Re < 100	Low	0 %	0 %
10 < Re < 50	Moderate	0 %	0 %
Re < 10	High	0 %	0 %

The carbonation depth measurements are summarized in the following Table 2.75.

Table 2.75. Mean carbonation depth of the West pier

Mean carbonation depth (mm)	West facing	East facing
West pier	2	3

c. Durability indicators

The summary of the measures of the durability indicators is presented in the Table 2.76.

Table 2.76. Values of the durability indicators

Synthesis of data			
Characteristics of the bridge		**West pier (West face) Not exposed to salts**	**West pier (East face) Exposed to salts**
Concrete cover	e_{moy} (mm)	26	30
Cement content (CEM I)	kg/m^3	400	400
Lifetime indicators		West pier (West face)	West pier (East face)
Carbonation depth	P_c (mm)	2	3
Free chlorides content at the level of the mean concrete cover	[Cl$^-$] % per cement mass	0.012	0.226
Durability indicators		**West pier**	
Apparent coefficient of chloride diffusion	D_{rcm} (10^{-12} m².s^{-1})	9.4 (9.7/10.3/8.1)	
Porosity accessible to water	P_{water} (%)	11.9 (11.7/12.0/11.9)	
Gas Permeability	K_{gas} (10^{-18} m²)	240 (264 / 227 / 228)	
Electrical resistivity	Ω.m	104 (105/ 86 / 121)	
Capillary absorption coefficient at 24h	C_a (g/m²)	2512 (2493 /2389/2653)	
Density (kg/m^3)	ρ_b	2330	
Accelerated carbonation (3 %) at 28 and 56 days (mm)	X_{c28d}; X_{c56d}	0; 0	
Accelerated carbonation (50 %) à 7 and 28 days (mm)	X_{c7d}; X_{c28d}	0; 0	
Spacing factor (L_{bar})	L (µm)	257	
Scaling test at 56 cycles	g/m^2	103 (256 / 73 / 42 / 133)	
Internal Freezing test (in water): - relative expansion at 300 cycles - ratio of the square of resonance frequencies at 300 cycles	ln (µm/m) $\frac{F_F n^2}{F_F o^2}$x100	 289 (93 / 485 / 80) 93 (92 / 95 / 92)	
Characteristic strength of concrete on site / Strength Class	f_c (MPa) Class	64,0 70/85	

Potential durability classes (according to AFGC, 2004)				
Very low	Low	Average	High	Very high

The measured values of the durability indicators with respect to the corrosion of the reinforcements, classify the concrete of the piers in a potential durability "Average" to "High", according to (AFGC, 2004).

If this bridge were to be built today, the combination of exposure classes XF4, XD3 according to NF EN 206 / CN would be retained for the piers concrete, with the additional composition requirements of fascicle 65, and those of the G + S prevention level of the “Recommendations for the durability of hardened concrete subjected to frost” released in 2003.

The Table 2.77 below shows the position of the concrete of the Pirou bridge piers in relation to the current regulations, with the following color code:

Conform	Not conform

Table 2.77. Evaluation of the conformity of the concrete to the current regulations

Specifications for the composition XD3, XF4 G+S		**Concrete of the Pirou bridge piers**
Cement type	CEM I	CEM I
Supplementary Characteristics of the cement	Sea compatible or sulfate-resisting	Not determinated
Binder content	> 385 kg	400 kg
Effective Water / binder ratio	< 0,45	0,46
Class of compression strength	≥ C35/45	C70/85
Air-entrained admixture	Obligatory or freeze-thaw resistance test	Yes
Durability indicators specifications regarding corrosion XD3		
Porosity accessible to water (%)	< 13	11,9
Apparent coefficient of chloride diffusion (10^{-12} m².s^{-1})	< 3,5	9,4
Gas permeability (10^{-18} m²)	< 200	240
Durability indicators specifications regarding freeze-thaw with salts		
Spacing factor (µm)	< 200	257
Relative expansion (µm/m)	< 400	289
Ratio of the square of resonance frequencies	> 75	93
Scaling (g/m²)	< 600	103

The characteristics of the concrete used in 1991 for the construction of the piers of the Pirou bridge on A75, meet the current performance requirements for an exposure class XF4 supplemented by the “G + S” characteristics of the Recommendations for the frost durability of hardened concrete of 2003. The spacing factor is at the limit of conformity if we consider that in a control test, the validation criterion is to be less than 250 µm, to which we can add the commonly accepted uncertainty of 10 %, i.e. a threshold of 275 µm at most.

On the other hand, the results obtained on the durability indicators regarding corrosion of reinforcements, do not make it possible to validate an exposure class XD3 on the base of fascicle 65.

3.2.6.4 Conclusions drawn

The investigations carried out within the framework of the national PerfDub project on a pier of the Pirou bridge on the A75 motorway, allow to characterize the following elements:

- after 28 years of operation, the phenomenon of concrete carbonation is not very present. It reached a maximum of 15 % of the cover thickness in the investigated areas;
- after 23 years of operation (2014 measurements), the concentration of free chlorides, at the level of the first reinforcement layer (25 to 30 mm deep), remains below the critical concentration (0.4 %) for initiation of the corrosion. However, the critical concentration is currently exceeded (0.5 %) between 10 and 20 mm deep in the cover concrete;

- C70 / 85 concrete used in construction meets current regulatory requirements for an XF4 G + S exposure class, in terms of performance tests with respect to durability in frost, with or without salts. de-icing;
- on the other hand, concrete does not validate the performance requirements of an XD3 exposure class according to (Fascicle 65, 2017) in terms of apparent coefficient of chloride diffusion and gas permeability, and also regulatory concrete cover;
- overall low covers, more particularly on the east facing of the pile (100 % of measured covers are less than 45 mm);
- overall high resistivities values indicating that the reinforcements are located in a concrete that is not very prone to the development of corrosion;
- half-cell potential gradients which do not highlight signs of the presence of anodic areas.

The non-destructive investigations indicate that, even if the cover is insufficient, the reinforcements are located in a concrete which is not very prone to the development of corrosion. Besides, no degradation is currently visible at the foot of the pier of this structure, which is consistent with the measurements and results obtained on the lifetime indicators and concrete durability indicators.

3.3 Structures over 50 years old

3.3.1 Bridge over the Bruche river

3.3.1.1 Presentation of the bridge

The bridge of the RD 2420 over the Bruche river at La Broque is located on the Alsatian side of the Vosges mountains, in the Bruche valley (Figure 2.64). It has 2 spans with equal length of 12 m, a total length of 26 m and a width of 11.5 m. It consists of a reinforced concrete slab resting on abutments and a masonry pier. It was rebuilt in 1947.

Figure 2.64. General view of the bridge, from the upstream side

It is located at an altitude of 319 m. According to the standard document FD P 18-326 (August 2016), the town is classified in a moderate frost zone. According to standard NF EN 206/CN, the town is in a very frequent salting zone (> 30 days / year).

In the context of this study, only the deck of the structure was investigated. Due to the general context of the structure and its position, the exposure class chosen for this part of the structure is XC4. Given the low exposure to de-icing salts, except by runoff from the cornices, as well as the moderate frost, the XF1/XD3 classes can also be retained.

3.3.1.2 History of works and current condition

Detailed inspections took place in August 1988, August 1996, September 2001 and November 2011.

The detailed inspection of 1988 already showed:

- spalled concrete with visible oxidized longitudinal reinforcement over a length of 1.5 m on the downstream left bank span;
- several spallings with partially stripped and oxidized reinforcements on the side of the deck and on the cantilever of the left bank span on the downstream side and of the right bank span on the upstream side;
- A spalling of the concrete with visible reinforcements over 1.5 m in length on the right bank span on the upstream side;

- Several visible oxidized steel sections and rust spots on the intrados of the left bank span;
- a not very compact concrete with water seepage on the side of the left bank span on the downstream side and and on the right bank span on the upstream side;
- A few areas of poorly vibrated concrete in the middle of the span on the right bank span (Figure 2.65);
- an area of spalled and not very compact concrete on the cantilever.

Since the inspection carried out in 1988, many disorders have been noted. They are mainly characterized, on the deck, by concrete spallings, corrosion of the reinforcements on the lateral sides of the slab and on the intrados, as well as runoff on the lateral sides and around the gargoyles (Figure 2.66). In 2012, the recommendations for the service responsible of the management aimed at undertake on the deck, the repair of degraded areas on the intrados and on the sides of the slab, as well as the extension of the gargoyles with the creation of a drip edge in order to limit runoff on the underside of the slab.

Between 1988 and 1996, the anomalies observed on the structure did not show any notable change. Between 1996 and 2001, concrete spallings increased and new spallings appeared. Repair of the asphalt, cornices and guardrails helped limit water inflows on the structure. However, between 2001 and 2012, these disorders developed unfavorably, even if the transverse cracking noted, the opening of which is generally less than 0.2 mm, corresponds to a normal flexural behaviour of the slab.

Figure 2.65. Intrados of the deck o the right bank abutment side.

Figure 2.66. Intrados of the deck on the left bank abutment side

3.3.1.3 Investigations carried out during the PerfDub project

The average cover, close to 40mm, corresponds to a fairly standard cover for this type of part of the structure. However, whether using these readings or during detailed inspections, it is clear that these cover values are largely heterogeneous at the scale of the deck of this structure (cover varying between 13 and 73 mm, with a standard deviation of up to 12.6 mm). In fact, locally, the first reinforcement bed is well below these 40mm, thus promoting disorders linked to the corrosion of the reinforcements.

The average depth of the carbonation front is 27 mm, eliminating the value of 70 mm, which is particularly high and which may be explained by the location of the sample in an area with traces of humidity where the alternation of humidity and drying could accelerate the phenomenon of carbonation.

These values of carbonation depth are consistent for a structural part of this age with such exposure. Compared to the average cover, these values show a carbonation front that has not yet reached the first layer of reinforcement overall. However, compared to the standard deviation of these cover measurements, it appears that this carbonation front has already locally reached this first layer of reinforcement.

Whether protocol 1 (in situ sampling of powders) or protocol 2 (sampling of cores then grinding), the percentages of free chloride contents are below the critical threshold of 0.1 % with respect to the mass of the concrete. Concerning the average cover, the values are between 0.02 % and 0.05 %. This means that the chloride concentrations are insufficient to initiate corrosion, in the absence of other factors.

The average mechanical strength of concrete is 39 MPa.

Regarding durability indicators:

- the 6 values obtained are between 12.2 % and 16.1 % with an average of 14.4 % which corresponds to the porosity values of a concrete of standard quality. However, these differences reflect a fairly heterogeneous concrete at the scale of this part of the structure;
- the five obtained values for the apparent coefficient of chloride diffusion vary between $2.09.10^{-12}$ and $4.27.10^{-12}$ $m^2.s^{-1}$ with an average of about 3.10^{-12} $m^2.s^{-1}$. Relatively homogeneous between the different samples, the measured values for this durability indicator correspond to high durability values.
- the values obtained for the gas permaeability coefficient show a strong disparity in the quality of the concrete since on the three analyzed samples, the values are between $3\ 10^{-15}$ (ie $3000\ 10^{-18}$ m^2) and $3\ 10^{-16}$ (ie $300\ 10^{-18}$ m^2), i.e. a factor of 10 between the smallest and the largest value. With an average of 2000.10^{-18} m^2, the obtained values for this indicator are very low, even exceptionally abnormal.
- the capillary absorption values obtained vary between 4.99 kg/m^2 and 7.19 kg/m^2 with an average of 6.19 kg/m^2 on this part of the structure.

A core taken from the bridge (BROC A) was subjected to a detailed mineralogical analysis by the CPDM laboratory of IFSTTAR. The conclusions of this analysis show a cohesive concrete, with a high variability in its average porosity but without any particular anomaly. Concrete consists mainly of siliceous or silicate aggregates and some limestone aggregates. The dosage of active binder is 400 (+/- 40) kg / m^3 and its mineralogical composition shows that the used cement is probably a cement with a small quantity of slag.

The following Tables 2.78 and 2.79 show all the results presented previously. A distinction has been made between, on the one hand, the so-called "corroded" areas exhibiting this type of disorders (Table 2.78), and on the other hand the so-called "healthy" areas free from concrete spalls, fractures and other visible corroded steels (Table 2.79).

Table 2.78. Values of durability indicators for the so-called "corroded" areas

So-called "corroded" areas		
Lifetime indicators		**Area**
Carbonatation depth (mm) – *(samples IX, 3.1 et 3.2)*	P_c	25 (30 / 25 / 20)
Free chloride content at the level of the mean cover depth (%) – *(samples 4A et 5A)*	$[Cl^-]$	0.025 (0.02 / 0.03)
Durability indicators *(samples BROC 6, 7 et 8)*		
Apparent coefficient of chloride diffusion (10^{-12} m².s^{-1})	D_{rcm}	4.0 (3.78/4.27)
Porosity accessible to water (%)	P_{water}	14.2 (14.6/13.5/14.4)
Gas permeability (10^{-18} m²)	K_{gas}	300 (300/3000 #/2000 #)
Other characteristics		
Capillary absorption coefficient at 24 h (kg/m²)	C_a	5.48 (6.06/4.59/5.78)
Density (kg/m3)	ρ_b	2303.23 (2295/2313/2300)
Compressive strength (Mpa)	f_{cm}	39.0 (35.3/45.3/36.4)
Accelerated carbonatation (3 %) at 28 and 56 days (mm)	$X_{c,28}$; $X_{c,56}$	6.8; 11.1 (mean 8.7/13.4)
Accelerated carbonatation (50 %) à x et y days (mm)	$X_{c,x}$, $X_{c,y}$	Not Done
Content of lime (%)	$[Ca(OH)_2]$	Not done

 # Not considered

Table 2.79. Values of durability indicators for the so-called "healthy" areas

So-called "healthy" areas		
Lifetime indicators		**Area**
Carbonatation depth (mm) – *(samples VI et X)*	Pc	30 (30/30)
Free chloride content at the level of the mean cover depth (%) – *(samples ENR2 et ENR3)*	$[Cl^-]$	0.045 (0.04/0.05)
Durability indicators (samples *BROC A, B et C)*		
Apparent coefficient of chloride diffusion (10^{-12} m².s^{-1})	D_{rcm}	2.2 (2.31/2.09/2.26)
Porosity accessible to water (%)	P_{water}	14.7 (16.1/15.8/12.2)
Other characteristics		
Capillary absorption coefficient at 24 h (kg/m²)	Ca	5.42 (6.49/6.04/3.74)
Density (kg/m^3)	ρ_b	2280 (2250/2239/2349)
Corrected Compressive strength (Mpa) *(Mean of samples VII, IX et X)*	f_{cmc}	39.0 (35.3/45.3/36.4)

In the so-called corroded zone, the carbonation depth reached 25 mm and began to corrode the reinforcements which have a cover lower than this value. The measured porosity is 14.2 and therefore complies with fascicle 65. The lower retained value for the gas permeability is 300 and is higher than the threshold.

In the so-called healthy zone, the carbonation depth reached 30 mm and did not start to corrode the reinforcements, which probably have a cover greater than this value. The

measured porosity is 14.7 and therefore just conform to the threshold of fascicule 65 (14.5). There is no measured gas permeability in this zone.

Regarding the measured durability indicators in the context of these investigations, they do not show significant differences between “healthy” or “corroded” zones, when the same test could be carried out for these two cases.

However, in terms of resistance to disorders linked to the corrosion of reinforcements, these various indicators show a moderately to poorly durable concrete. The measured values of the indicators are close (Porosity) or even well below (Kgas) the threshold values currently recommended according to the fascicule 65 of the CCTG with regard to the XC4 exposure class. For the XD3 exposure class, the chloride diffusion values are close to the recommended threshold of the LCPC recommendations and of fascicle 65. But, of course, we have to keep in mind that the measured values are on a very old concrete having a priori benefited from the ageing factor (even moderate) over a long period and that the initial values at 90 days were probably significantly higher.

3.3.1.4 Conclusions drawn

The investigations carried out within the PerfDub project on the intrados of the Bruche deck allow the following points to be identified:

- from a construction point of view, the average concrete cover of the deck complies with the recommendations for exposure class XC4. However, the heterogeneity of the latter at the scale of this part of the structure, with locally concrete covers well below the value of 40 mm, favoured the occurrence of disorders linked to the corrosion of the reinforcements;
- the carbonation phenomenon is already well advanced on the intrados of the deck. The values obtained, of the order of thirty millimetres, reflect a process which, correlated with areas with a lack of cover (≤30 mm), tends to promote corrosion disorders of the reinforcements (cracking, concrete spalls, loss of steel cross-section, etc.);
- the chloride contents evaluated up to the first layer of reinforcement do not reach critical concentrations. However, locally, the combination of insufficient covers and the average carbonation front can induce disorders;
- the measured lifetime indicators do not exhibit great variability between so-called “healthy” areas and so-called “corroded” areas;
- regarding the durability indicators, the obtained values compared to the limit values proposed according to the criteria of AFGC 2004 reflect a concrete with a low to medium potential durability class.

The combination of these elements with more general structural design problems (problems related to water drainage, bad waterproofing, etc.), explains the occurrence of numerous disorders on the intrados of the structure.

3.3.2 Blondel bridge

3.3.2.1 Presentation of the bridge

The underpass PI SNCF / Blondel (Ste Musse) is located in the city of Toulon and supports the A57 motorway. It crosses the SNCF track (Marseille-Vintimille line) and the rue André Blondel (Figure 2.67). It was commissioned in 1964.

Figure 2.67. General view of the Blondel bridge, from the South

It consists of two reinforced concrete slab-type decks, each comprising two spans of 10.57 m. The total length is 22.19 m. Each deck is 13 m wide and rests on two massive reinforced concrete abutments based on footings and a central pier made up of a reinforced concrete crossbeam resting on 4 oblong reinforced concrete columns.

The exposure class retained for the deck and the structure's piles is XC4. Since the structure is located 2 km from the sea, the XS1 class could also be considered.

3.3.2.2 History of works and current condition

In 1989, a detailed inspection revealed water dripping under the deck through the joint between the two decks, and on the pile corroded reinforcements on the crossbeam (at the east-facing junction) and cracks on the stiffener (visible on the south half railway side).

In 1996, a detailed inspection revealed a water runoff at the joint between the decks, a few small damages to the concrete (spalling, existing patch repairs, patching with spalls) on the span above rue Blondel, and a slight increase of the cracking of the pile stiffener since 1989.

In 2011, a new detailed inspection still revealed the runoff at the joint between the decks, various disorders of the concrete on the span above rue Blondel (a few corroded visible reinforcements, scratches, concrete spalls, honeycombs), and a fine vertical cracking of the slab sides with a maximum opening of 0.2 mm (with dry efflorescence). It also reveals on the central pier a fragment of concrete with corroded visible reinforcements, a spall in the course of formation as well as runoff (coming from water inflows between decks) and various concrete disorders (some patch repairs, segregation zones, spallings).

In 2011, investigations were carried out and the results are as follows:

- the concrete cover of steels in the pile columns is highly variable (from 20 to 91 mm);

- the cover of the steels in the pile crossbeam varies between 50 and 76 mm, for a carbonation depth measured between 30 and 45 mm. On the crossbeam, the carbonation front therefore did not reach the reinforcements;
- the concrete of the crossbeam has an average compressive strength of 32 MPa;
- the cover of the lower layer of steels in the deck (measured on the intrados) varies from 10 to 36 mm for transverse steels and from 35 to 50 mm for longitudinal steels;
- the carbonation depth measured on the deck is around 35 mm; it therefore reaches transverse steels and begins to reach some longitudinal steels;
- the concrete of the southern deck has an average compressive strength of 35.6 MPa.

Therefore, the results obtained in 2011 show that the concrete has a moderate compressive strength and that the carbonation front has not yet reached the longitudinal reinforcements of the deck and the reinforcements of the pier crossbream. However, the transverse reinforcements of the lower surface of the deck are in the carbonated concrete zone.

3.3.2.3 Investigations carried out during the PerfDub project

Samples were taken in 2015 by coring on the crossbeam of the central pier and the intrados of the deck (Figure 2.68):

- on the crossbeam, east face, of the south deck and the north deck;
- on the intrados of the North deck, except for the H15 core carried out on the South deck.

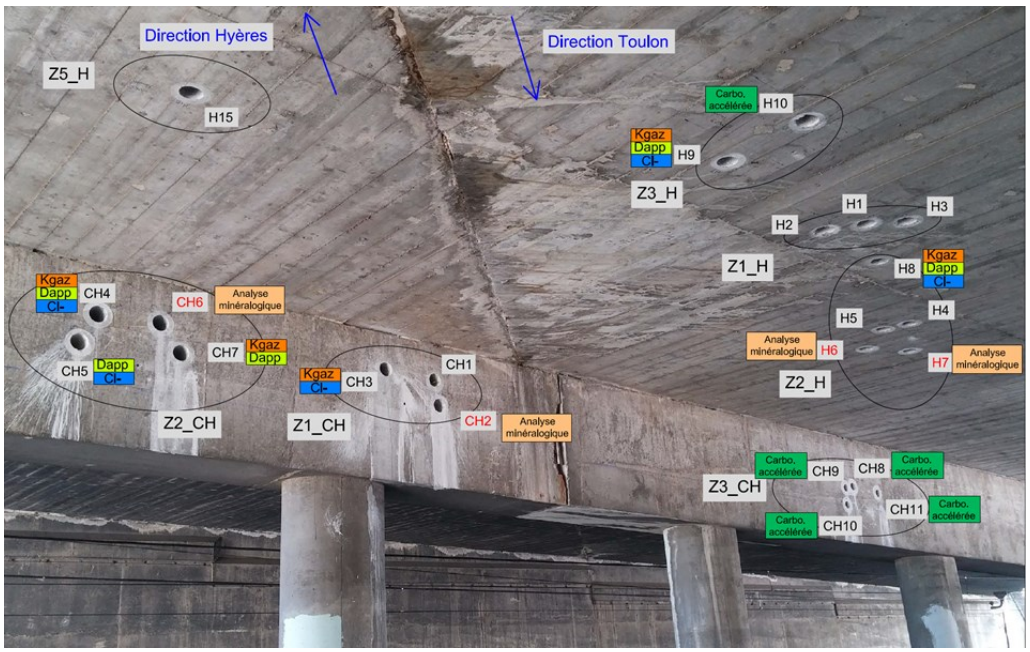

Figure 2.68. Sampling plan on the pier crossbeam and the deck (Investigations of 2015). Some of the disorders are visible (water runoff at the joint between the decks)

a. Corrosion diagnosis and investigations

The corrosion diagnosis was carried out in October 2015 on 6 distinct areas of the structure: 4 areas on the underside of the north and south decks over the Blondel street, and 2 areas on the crossbeam of the central pier; the main results are summarized in the Table 2.80.

Table 2.80. Results of the diagnosis related to corrosion

Zone	Half cell Potentials (mV)	Density of corrosion current (µA/cm²)	Resistivity (kΩ.cm)
1 – North deck	-110 à +85	0,027 et 0,120	106 à 533 (11 % of values between 46 and 96)
2 – North deck	-129 à +115	0,027 et 0,052	116 à 457 (one zone between 11 and 39 – about 17 %)
4 – South deck (« healthy »)	-112 à +95	0,003 et 0,013	116 à 478 (one zone between 11 and 39 – about 20 %)
6 – South deck	-50 à +90	0,008 et 0,014	282 à 958
3 – South crossbeam	-1 à +173	0,010 et 0,082	104 à 486
5 – South crossbeam (« healthy »)	+50 à +228	0,003 et 0,080	200 à 447

The analysis of all these results shows that the reinforcements do not show any sign of corrosion, both in the deck and in the crossbeam:

- half-cell potential less than -200 mV (low probability of corrosion);
- Current density less than 0.1 µA / cm² except for a measurement at 0.12 µA / cm² in zone 1 (negligible corrosion level);
- Resistivity greater than 100 kΩ.cm (zero risk) for the crossbeam and with values between 10 and more than 500 kΩ.cm for the deck corresponding mainly to zero risk and locally to a low or moderate risk.

The concrete cover measurements carried out in 2016 are consistent with those noted during the 2011 investigations, namely:

- deck:
  - transverse steels (1st layer) - mean depth = 26 mm (variable from 10 to 36 mm),
  - longitudinal steels (2nd layer) - mean depth = 45 mm (variable from 35 to 50 mm).
- pile crossbeam:
  - vertical steels (1st layer) - mean depth = 60 mm (variable from 50 to 76mm),
  - horizontal steels (2nd layer) - mean depth = 67 mm (variable from 62 to 72mm).

The results obtained with the chloride contents are systematically less than 0.005 % of the mass of the concrete and therefore less than 0.027 % of the mass of cement for the deck and 0.023 % for the crossbeam. These results are therefore well below the corrosion initiation threshold of 0.4 % of the cement mass.

The complete mineralogical analysis carried out on the concrete shows that the cement of the concrete is a CEM I and that the concrete does not contain slag or fly ash. The binder content is:

- 420 Kg (± 40 Kg) for the deck;
- 470 Kg (± 40 Kg) for the crossbeam.

Microscopic observations of the samples did not indicate the presence of pathology. The concretes appear to be healthy and without any particular anomaly. For the concrete of the

crossbeam, cement paste / aggregate interfaces which are slightly decohesive from time to time are noticed, and anhydrous phases are observed in greater number than for the deck concrete.

b. Durability indicators

The synthesis of the measurements of the durability indicators is as follows (Table 2.81):

Table 2.81. Values of durability indicators and lifetime indicators

Synthesis of the measurements			
Characteristics of the bridge		**Crossbeam**	**Deck**
Cover depth	e_{mean}(mm)	60 (vertical steels) 67 (horizontal steels)	26 (trans steels) 45 (long steels)
Concrete strength	f_c (MPa)	32	35,6
Cement content (CEM I)	kg/m^3	470	420
Lifetime indicators		**Crossbeam**	**Deck**
Carbonation depth	P_c (mm)	30 à 45	35
Free chlorides content at the level of the mean concrete cover	[Cl$^-$] % per cement mass	< 0,023	< 0,027
Durability indicators		**Crossbeam**	**Deck**
Apparent coefficient of chloride diffusion	D_{rcm} (10^{-12} m².s^{-1})	35,7 (29/37/41)	16,2 (9,7/21/18)
Porosity accessible to water	P_{water} (%)	17,7 (17,6/16,7/18,9)	13,2 (12,7/11,6/15,3)
Gas permeability	K_{gas} (10^{-18} m²)	600 (2000 #/3000 #/600)	200 (8000 #/200/200)
Capillary absorption coefficient at 24h	C_a (g/m²)	5 530 (5 286/5 547/5 513)	3 290 (5 905/1 831/2 135)
Density (kg/m^3)	ρ_b	2210	2290
Accelerated Carbonation (4 %) à 28 and 56 days (mm)	$X_{c,28}$; $X_{c,56}$	10; 11	0
Accelerated carbonatation (50 %) at 7 and 28 days (mm)	$X_{c,7}$; $X_{c,28}$	11; 23	0

 # Values not taken into account

Potential durability classes (according to AFGC, 2004)				
Very low	Low	Average	High	Very high

Regarding the durability indicators, the measured values compared to the limit values proposed according to the criteria of AFGC 2004 reflect a concrete with a potential durability class "low" to "very low".

There is some variability in the results, in particular this variability is very high for gas permeability. The concrete constituting the crossbeam does not meet any of the criteria of the fascicle 65 for exposure class XC4 (apart from the cover). The concrete constituting the deck only satisfies the criterion for the porosity accessible to water but largely exceeds the criterion of gas permeability and has weak covers (26 mm on average for the 1st layer of steel of the deck).

3.3.2.4 Conclusions drawn

The investigations carried out within the framework of the PerfDub project on the concrete of the deck and the pier crossbeam of the PI SNCF / Blondel (1964 bridge) make it possible to identify the following points:

- the carbonation phenomenon is already well advanced on the intrados of the deck. The values obtained, of the order of 35 millimeters, reflect a process which, correlated with areas of weaker concrete covers (≤ 36 mm for the first layer of steels), can initiate corrosion;
- regarding the crossbeam, the carbonation, which is also well advanced (30 to 45 mm), has not yet reached the reinforcements but is not far from the first steels (minimum measured cover of 50 mm);
- chloride contents measures carried out up to the first layer of reinforcement are very far from the corrosion initiation threshold;
- the risk of corrosion of the reinforcements due to the penetration of chlorides is non-existent at the time of diagnosis;
- regarding the durability indicators, the values obtained compared to the limit values proposed according to the criteria of the AFGC 2004 reflect a concrete with a potential durability class "low" to "very low";
- although the carbonation front has reached some steel layers, the corrosion diagnosis does not show any measurements corroborating a real initiation of corrosion. This seems consistent with the absence of noticeable visible disorders. Indeed, the corroded steels identified during the detailed inspection have very low to non-existent covers or are located in areas of water runoff.

3.3.3 X Bridge

3.3.3.1 Presentation of the bridge

The X bridge (Figure 2.69) is a reinforced concrete arch bridge, comprising two lateral arches with an intermediate suspended reinforced concrete deck of 1 span (+ 2 access spans). It has a total length of 179.65 m, and the arch span is 153 m long. The useful width between guardrails is 11.86 m.

Figure 2.69. General view of the X-bridge

It was built by the company "Construction Edmond Coignet" between 1952 and 1954. The structure is located in a marine environment; the base of the arches is in the tidal range and the rest of the structure is exposed to spray. It therefore falls within the XS3 / XC4 exposure classes.

According to the bridge documentation, the concrete for the arches and the deck was dosed at 400 kg of 250/315 "Flambeau prise mer" cement, coming from the Lottinghem plant located in the Pas-de-Calais department. The gravel comes from the Brestant strand located in the vicinity of the structure. The sand was taken from the nearby river bed. The composition of the concrete is therefore as follows:

- Cement 250/315 Flambeau resisting to sea water: 400 kg
- rolled sand 0/8: 500 liters
- gravel 5.3 / 25: 650 liters
- water on dry aggregates: 160 liters.

Compressive strength tests carried out at 90 days on cubes of 20 cm edge indicate results of 335 kg/cm² (33.5 MPa).

The bridge file specifies the quantities of reinforcement steels used per part of the structure, as well as their grades. For the arches, 60 chromium-copper steel and 42 steel were used. For the deck, only 42 steel was incorporated into the concrete. The file also indicates that the arch received a water-repellent on the surface by application of a "colorless silicone paint Aquellus S.1".

At the time of construction, the designers had taken into consideration the significant risk of corrosion with regard to the exposure of the structure: "In order to protect the reinforcements against extremely active corrosion in this region, the bars are placed at 3.5 cm from the concrete facing". This provision complies with the regulations in force at the time. Indeed, the circular « series A n ° 8 of July 19, 1934 » specifies a protection of 35 mm for the structures in a marine environment.

The theoretical concrete covers (extracts from the execution drawings) of the reinforcements closest to the facing are calculated taking into account the fasteners and loops fixed around the main steel bars. The main bars of the arches are Ø 32 mm steels. Their position is variable depending on the faces considered. On the vertical faces, the cover of the Ø 10 and 12 mm fasteners is a minimum of 32 mm and a maximum of 42 mm. On the horizontal and inclined faces, the cover of the Ø 10 and 12 mm fasteners is a minimum of 52 mm and a maximum of 102 mm.

3.3.3.2 History of works and current condition

We only had access to the detailed inspection report of 2011. This latter mentions damage due to corrosion mainly on the supports of the access spans and to a lesser extent on the lower surface of the deck. On the external faces of the arcs, the report mentions:

- concrete spalling on the upstream arch, located in the tidal zones
- a few 0.2 mm opening cracks, including an old one at the keystone of the downstream arch (upstream face)
- traces of efflorescence on the intrados of the downstream arch
- some rust spots due to the presence of steel ties at the bottom of the formwork
- the presence of algae on the faces exposed to the tidal range.

Taking into account the age of the concrete and the maritime environment, the X Bridge is in a fair condition and the arches have probably been the subject of special care during the casting of the concretes, as can be judged by the few disorders observed and the excellent quality of the exterior facings. The documents made available do not refer to repair actions carried out on the arches.

3.3.3.3 Investigations carried out in the frame of the PerfDub project

The diagnosis of the reinforced concrete durability (assessment of the risk of corrosion of reinforcements due to the penetration of chlorides into the concrete cover) was carried out in 2015 and was based on the investigations carried out in the following 2 zones Z2 and Z3.

a. Presentation of the two zones

Zone Z2: springing of the upstream arch, on the left bank side (tidal area) (Figure 2.70)

At the extrados of the arch, the upper edge of the band is spalled by corrosion of the reinforcements over at least 1.50 m in length and 20 cm in width. Several cracks are observed on the studied zone. On the lower band of the arch, the cracks are more numerous, continuous, rather longitudinal and sometimes with millimeter opening. They extend over the entire tidal range but are more spaced beyond. For the record, these cracks do not appear on the 2011 inspection report. After having locally cleared the algae, they also seem to be present on the other springings of the two arches.

Zone Z3: downstream arch, at sidewalk level, on the left bank side (spray) (Figure 2.71)

The studied zone concerns the internal face of the downstream arch, between the brace n° E20 and the portico n° 4, above the sidewalk. This area is subject to spray. It is distributed between the upper band of the arch and the central area. The studied zone does not show any cracks or patch repair.

Figure 2.70. Zone Z2

Figure 2.71. Zone Z3

b. Results of investigations

The following Table 2.82 shows the values of the covers measured:

They respect the covers specified in the design (35 mm). However, a large majority of covers are observed to be lower than the covers expected today for this type of environment (of the order of 50 mm in a marine environment).

Table 2.82. Measured concrete covers

		Transversal reinforcement (or horizontal)		Longitudinal reinforcement (or vertical)	
Zone - Part		Mean (mm)	Min (mm)	Mean (mm)	Min (mm)
Z2	Bands	62	46	67	58
	Web	41	38	50	40
Z3	Bands	72	40	66	46
	Web	55	51	55	46

The Table 2.83 presents the values of the durability indicators that were measured only in zone Z3.

Table 2.83. Values of durability indicators measured in zone Z3

Durability indicators		Arch (springing)
Apparent coefficient of chloride diffusion	D_{rcm} (10^{-12} m².s^{-1})	10.2 (10.6/9.7)
Electrical resistivity	Res (Ω.m)	82 (79/85)
Porosity accessible to water	P_{water} (%)	12.2 (11.9/12.4))
Gas permeability	K_{gas} (10^{-18} m²)	495 (715/274)
Other characteristics		**Arch (springing)**
Capillary absorption coefficient at 24h	C_a (g/m²)	3890 (3780/4000)
Density (kg/m^3)	ρ_b	2270
Pseudo-permeability to liquid water	w (kg.m^{-2}.s$^{-0,5}$)	0.80 (0.77/0.82)

Potential durability classes (according to AFGC, 2004)				
Very low	Low	Average	High	Very high

It is observed that the concrete constituting the arch is of an overall low to medium potential durability class (AFGC 2004 guide). With regard to the environment considered (spray, tidal range), this durability class corresponds to a potential lifespan (D) of the order of 50 to 100 years for the concrete constituting the arch. If we compare with the maximum values of the durability indicators without reduction of covers prescribed in class XS3 by the fascicle 65 (P_{water} <13; K_{gas} <200 and D_{rcm} <3.5), we observe that the porosity is respected, but that the apparent coefficient of chloride diffusion is clearly too high, as well as the gas permeability, which confirms that the durability of this structure cannot reach 100 years, especially since the concrete covers are insufficient.

The apparent coefficient of chloride ions diffusion D_{rcm} decreasing over time ("ageing effect"), it is possible to estimate the value of D_{rcm} during the construction of the structure (D_{rcm} (t_0)) by taking this effect into account. To take into account the nature of the binder and the exposure of the concrete, two ageing factors are tested here (α = 0.2 and 0.4). The Table 2.84 presents these estimates.

Table 2.84. Values of D_{rcm}, taking into account the ageing effect

Ageing factor	D_{rcm} (t)mean t = 21900 days (60 years)	D_{rcm} (t_0) t_0 = 90 days
α= 0,2	10,2	30,6
α= 0,4		91,9

Taking into account this ageing factor only confirms the excessive value of the apparent coefficient of chloride diffusion of this concrete.

The following two graphs (Figure 2.84) summarize the penetration profiles of free and total chlorides in both zones of investigation.

These profiles show that the chloride penetration is significant in the lower parts of the structure that are exposed to the tide (springing of the arch). In zone Z2, the springing of the arch presents a relatively significant depth of pollution (more than 6 cm). In the upper part of the structure (arch zone 3), chloride penetration is very low or even negligible; which is surprising given the age of the bridge and its exposure. The lower exposure to spray does not explain everything. The application of a "colorless paint with Aquellux S.1 silicones" similar to a hydrophobic impregnation, could then explain the very low penetration of chlorides in zone Z3.

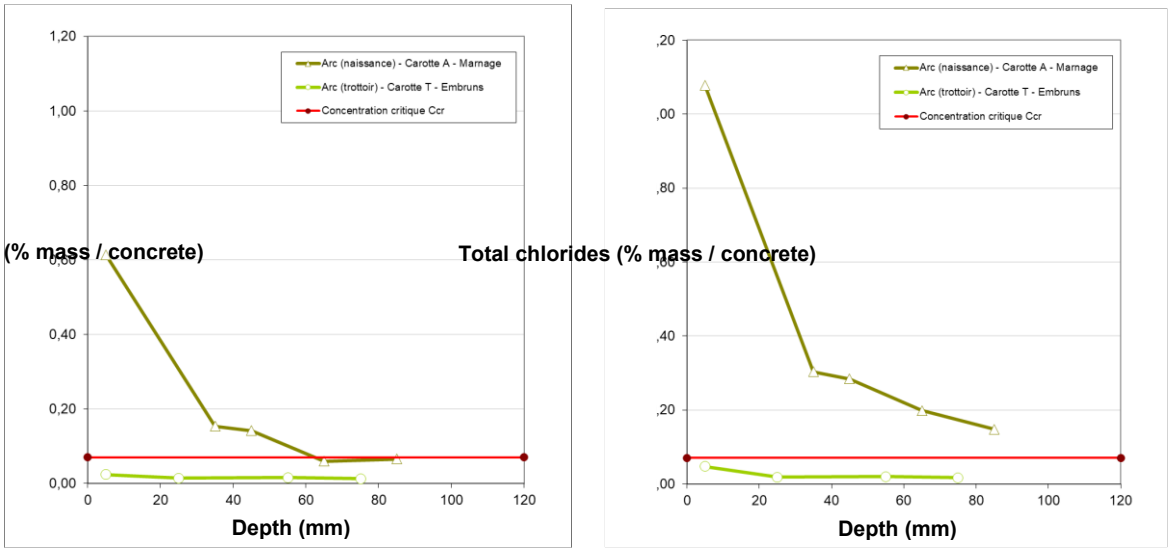

Free chlorides Total chlorides

Figure 2.84. Penetration profiles of free and total chlorides in zone Z2 (dark green Tidal zone) and Z3 (light green - spray zone)

The electrical resistivity measurements give the following results:

- Zone Z2: The resistivity mapping carried out on the arch web shows the effect of the tide (humidity and pollution of the concrete by chlorides). Two significant zones are thus observed: a zone at the bottom with resistivities of less than 30 kΩ.cm corresponding to a high risk of corrosion, a zone at the top with resistivities between 20 and 60 kΩ.cm corresponding to a lower risk of corrosion;
- Zone Z3: The resistivities are generally greater than 100 kΩ.cm. These high resistivities can be explained by a concrete that is less humid and less polluted by chlorides. The resistivities are particularly high on the lower part of the web (greater than 200 kΩ.cm).

The resistivities of the upper band are slightly lower (between 100 and 200 kΩ.cm): the band is probably wetter (more exposed to the weathering effects).

The half cell potential measurements of the reinforcement provide the following results:

- Zone Z2: The analysis of the potential gradients (recommended by RILEM) shows relatively homogeneous gradients less than 5 mV / cm for the upper band. The web has at least two zones with gradients on the order of 7 mV / cm. The lower band has homogeneous gradients less than 1 mV / cm. All of these elements lead to the conclusion that there is a moderate to high probability of corrosion for the web and the upper band, and a low probability for the lower band;
- Zone Z3: Overall, the potentials are not very electronegative (greater than -250 mV). According to ASTM, this would correspond to a low probability of corrosion. The analysis of the potential gradients (recommended by RILEM), for their part, show that the gradients are relatively homogeneous and less than 4 mV / cm. All of these elements lead to the conclusion that there is a low to negligible probability of corrosion for the upper band and the web.

3.3.3.4 Conclusions drawn

The investigations carried out on the arch of the X bridge led to the following conclusions:

- the average depth of the chloride front is of the order of 60 mm at the springing of the arch in the tidal zone (Z2) and 0 mm at the top of the arch at the level of the deck in an exposed zone spray (Z3);
- at the springing of the arch (Z2), taking into account the measured covers and the significant penetration of chlorides, statistically:
  - for the bands: respectively 65 % and 56 % of the transverse and longitudinal reinforcements are likely to be depassivated,
  - for the core: respectively 100 % and 86 % of the transverse and longitudinal reinforcements are likely to be depassivated.
- in the upper part of the arch (Z3), taking into account the measured covers and the very low penetration of chlorides, statistically, 0 % of the transverse and longitudinal reinforcements are likely to be depassivated;
- the durability indicator values indicate a concrete with a potential durability class of "low" to "medium" according to the criteria of the AFGC 2004 (AFGC, 2004), which could correspond to a foreseeable life of the order of 50 to 100 years with a 50 mm conventional cover (transverse reinforcement);
- given the age of the structure at the time of diagnosis (60 years), the measured chloride penetration depths confirm these trends and the electrochemical evaluations (resistivity and half-cell potential) confirm the previous results.

3.3.4 Vallières Bridge

3.3.4.1 Presentation of the bridge

The Vallières bridge (Figure 2.73) was built in 1926 by the Thorrand company. It allows the RD28 departmental road to cross the Vallières ravine on the territory of the town of Guillaumes in the Alpes Maritimes department.

Figure 2.73. General view of the Vallières bridge (view from the left bank, upstream)

The crossing is ensured by an arch supporting a reinforced concrete deck with a span of 45 m. The arch structure is formed by 2 arched ribs connected by a slab and embedded in 2 massive abutments 44.50m apart. The reinforced concrete deck rests on the ribbed arch by means of five piers on the left bank and four piers on the right bank (Figure 2.74).

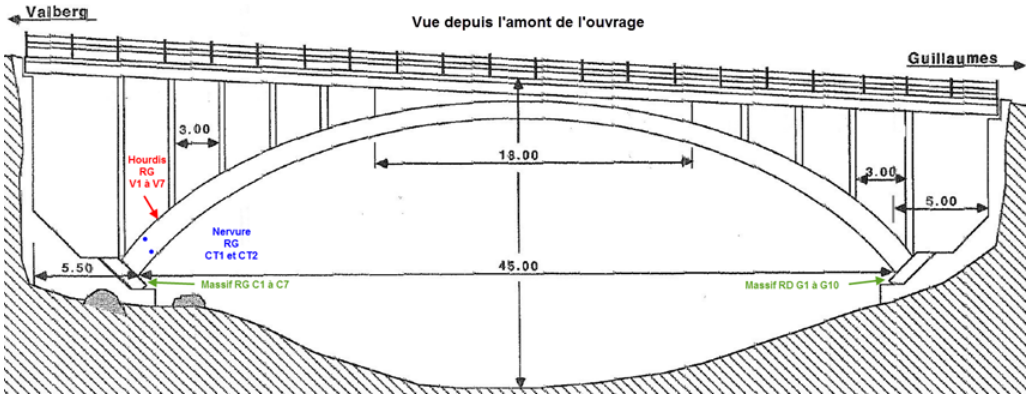

Figure 2.74. Elevation of the bridge with the locations of the samples taken in 2018

The structure is located at mean altitude in the mountains (1,100 m: Severe frost) and subject to very frequent salting (XF4), but due to the general context of the structure and its location, the exposure class retained for the arch structure is the XF3 class.

3.3.4.2 History of works and current condition

The various detailed inspections of this structure show:

- in 1968: good general condition;
- in 1974: a few fine cracks at the base of the left bank arch and a few steel loops visible on the downstream face of the arch;
- in 1980: reinforcements visible at the springing of the arch with rust estimated at 30 % and proposal made to protect the visible steels under the arch on the left bank and on the side face with a mortar;
- in 1983: bridge in fairly good condition, but existence of a transverse crack in the slab greater than 1/4 of the structure on the Left Bank with calcite, and steel angles of the sidewalk to be looked after;
- in 1988: bridge judged to be in fairly good condition. Spalls at the ends of the upstream beams of the deck on the right bank and left bank, with visible steel on the upstream beams on the right bank - Concrete spalling at the 1st and 2nd upstream piers with apparent steels - Cracks and visible steels at the foot of the 8th downstream pier. No evolutions of the transverse crack. Proposal to monitor disorders at the foot of the upstream right bank arch once a year;
- in 1993: The bearings no longer fulfill their role because they are corroded and displaced - On the pavement, a transverse crack at the joints and a longitudinal crack at the start of the corbels. Trace of humidity under the slabs on the left bank. The ground is sagging on the left bank downstream. The patch repairs deteriorate. First study requested for its replacement but no danger for the structure;
- in 1998: same conclusions as in 1993, with a continuing development of disorders;
- in 2004: Structure in fairly poor condition. A propagation of the disorders is observed on all the arcs;
- in 2011: Poor condition of the bearings, poor condition of the arches, defective waterproofing. The structure is classified as a state of emergency.

Following the identification of significant damages to the concrete of the arch during this last inspection, a concrete diagnosis was carried out by a service provider on the concretes of the deck, the arch and the pier on the right bank side. This rather imprecise diagnosis nevertheless reveals:

- a compressive strength of an average of 15.3 MPa, on the upstream face of the right bank pier;
- a carbonation depth: from 6.00 cm to 10.00 cm (5 tests) on the downstream side of the deck, on the right bank side;
- a porosity varying between 17.2 and 21.9 for the different concretes taken from the right bank side.

The department then decides to put in place a temporary bridge over the structure pending demolition / reconstruction.

3.3.4.3 Investigations made during the PerfDub project

Investigations were carried out in 2018 on the springing of the arch on the left bank of the structure and on the two massive blocks at the foot of the arch. Details of the location and diameter of the cores are illustrated in Figures 2.75 and 2.76.

Figure 2.75. Cores taken on the springing of the arch on the left bank (photo on the left) and in the arch rib on the left bank, upstream (photo on the right)

Figure 2.76. Cores taken in the massive blocks at the foot of the arch respectively on the left bank and on the right bank (respectively photo on the left and on the right)

a. Corrosion diagnosis

Firstly, for the corrosion diagnosis, four distinct zones of the structure were checked:

- zone 1: upper face of the arch slabs, at the left bank end;
- zone 2: lateral face of the upstream rib of the arch, at the left bank end;
- zone 3: upstream face of pier 1, at the left bank end;
- zone 4: upstream face of pier 1 at the right bank end.

The main results are summarized in the Table 2.85 thereafter.

The analysis of these results shows that:

- zones 1 and 2: no corrosion of the reinforcements is detected, nor any short-term risk;
- zones 3 and 4: corrosion is developed in the lower part of the zone. This corrosion was active at the time of the measurements.

Table 2.85. Results of the diagnosis for corrosion

Zone	Hal cell potential of steels (mV)			Density of corrosion current (µA/cm²)		Resistivity (kΩ.cm)	
Zone 1	89 %		11 %	0.003	0.012	113 à 214	
Zone 2	95.2 %		4.8 %	0.003		Measures not feasible - Concrete too resistive	
Zone 3	66.7 %	20 %	13.3 %	0.060	0.190	57 à 78 (spalled zone)	148 à 204
Zone 4	62.5 %	12.5 %	25 %	0.005/0.009	0.394	19	0/3/7

Corrosion level scale (for measurement of current) or corrosion risk level (for half cell potentials of reinforcement and resistivity).

Nul or negligible	Low	Moderate	High

b. Lifetime and durability indicators

Secondly, the corrosion lifetime indicators (the depth of carbonation and the chloride penetration gradient) were studied and compared to the actual concrete covers, then the durability indicators were measured on the cores taken including the indicators relating to internal freezing and scaling under the action of de-icing salts.

A core was also taken from the upstream face of the foot of the arch rib on the left bank in order to undergo a complete mineralogical analysis of the concrete to find its original composition. It follows that the cement content is estimated at 330 ± 35 kg/m^3 of concrete, that the effective mixing water is estimated at 188 kg / m^3 of concrete, which corresponds to an Weff / C ratio of 0.57 (0.52 to 0.63). The cement constituting the concrete corresponds to a Portland cement type CEM I.

The Table 2.86 shows a synthesis of all the obtained results. A distinction has been made between the different parts of the arch of the structure (slabs, rib and massive parts).

Table 2.86. Values measured for lifetime and durability indicators

Synthesis of results				
Bridge Characteristics		**Arch slabs**	**Arch ribs**	**Arch massive parts**
Cover depths (values 2018)	e_{mean} (mm)	Extrados: 45	27	NR
Cement content (CEM I)	kg/m^3	330 ± 35		NR
Lifetime indicators				
Carbonation depth	P_c (mm)	Extrados: 15 Intrados: 92	upstream 36	Right Bank 45
Free chlorides content at the level of the mean concrete cover	[Cl-] % of the cement mass (value max obtained)	Extrados: 0.69 Intrados: 0.28 (value max because unknown cover)	NR	Left Bank < 0.036
Durability indicators				

Apparent coefficient of chloride diffusion	D_{rcm} (10^{-12} m².s^{-1})	97.3	NR
Porosity accessible to water	P_{water} (%)	20.1	NR
Resistivity	(kΩ.m)	31	NR
Gas permeability	K_{gas} (10^{-18} m²)	700 (700 /3000 # / measure not feasible **)	NR
Accelerated carbonation (3 %) at 28 & 56 days (mm)	$X_{c,28}$; $X_{c,56}$	NR	28 ; 17***
Accelerated carbonation (50 %) at 7 & 28 days (mm)	$X_{c,7}$; $X_{c,28}$	NR	30.5; 17.5***
Spacing factor for air bubbles (Lbarre)	L (µm)	NR	494
Scaling	g/m²	NR	11268
Frost test (in water): - relative expansion - ratio of resonance frequency squares	ln (µm/m) $\frac{F_{Fn}^2}{F_{Fo}^2}$x100	NR	- 610 - 36
Characteristic strength of concrete on site / Strength class	f_c (MPa) Class	NR	23.6 C25/30

** NR : not measured*

*** measure not feasible: The gas permeability values obtained show a strong disparity in the quality of the concrete since on the two samples taken from the concrete of the upper surface of the arch slab (on the left bank), the values are between 700 10^{-18} and 3000 10^{-18} and for the concrete of the upstream rib in the same zone, the concrete has too high a permeability to be measured. A permeability value from the 3 samples cannot be provided, but the permeability can be considered to be greater than 700 10^{-18} m². These values obtained correspond to a "low to very low" durability class for gas permeability.*

**** The accelerated carbonation results are influenced by the presence of so-called 'cavernous' or even 'very cavernous' cores, which explains why the results at 28 days may be higher than those at 56 days for tests at 3 % CO_2 such as those at 7 days are greater than those at 28 days for the tests at 50 % CO_2.*

 # Value not taken into account

Potential durability classes (according to AFGC, 2004)				
Very low	Low	Average	High	Very high

Regarding the durability indicators related to corrosion, the obtained values compared to the limit values proposed according to the criteria of the AFGC 2004 (AFGC, 2004) reflect a concrete of the arch with a potential durability class as "very low".

From the frost point of view, the concrete of the arch massive parts has test values well above the thresholds that would be set for these parts of the structure for a new structure in this type of environment in accordance with the fascicle 65 (L_{barre} less than 250 µm for exposure class XF3, scaling less than 600 g / m², relative elongation less than 400 µm / m and resonance frequency square ratio greater than 75).

3.3.4.4 Conclusions drawn

The investigations carried out within the framework of the PerfDub project on the concrete of the ribbed arch of the Vallières bridge (built in 1926) make it possible to identify the following points:

- the chloride contents carried out on the upper surface of the arc slab are very much higher than the corrosion initiation threshold. For the intrados of the arch slab, the results show notable chloride contents but below the corrosion initiation threshold. At the level of the right bank massive part, protected from water inlets, no significant presence of chlorides was observed;
- the carbonation phenomenon is noticeable in areas not or more weakly affected by chlorides (lower surface of the arch slab, lateral face of the ribs). In these areas, when the covers have been raised, the first layer of reinforcement are reached by carbonation (side face);
- Concerning the durability indicators, the measured values compared to the limit values proposed according to the criteria of AFGC 2004 reflect a concrete with a "very low" potential durability class;
- the indicators thresholds issued from fascicle 65 of the CCTG for a project period of use of 100 years and for class XC4 / XF3 (and also XD3 / XF4) are all not verified by the concrete of the arch.

3.3.5 Boutiron Bridge

3.3.5.1 Presentation of the bridge

The Boutiron bridge is located in Creuzier-le-vieux in the Department of Allier. The Pont de Boutiron is part of the road network of the Department of Allier. It allows the departmental road RD 27 to cross the Allier River, and is located at an altitude of about 250 m (Figure 2.77).

It was built by the famous French Engineer Eugène Freyssinet known for having invented and developed the prestressed concrete in the world, and who was renowned for manufacturing quality concrete and taking great care in the construction of its bridges.

Figure 2.77. General view of the Boutiron bridge built by Eugène Freyssinet on the Allier River

The structure was commissioned in 1912. It is now restricted to vehicles with a GVW of less than 3.5 tons. The width of the bridge is 6.55 m, with a road width of 4.50 m.

The structure is made of a reinforced concrete arch and truss under a slab supporting the pavement. The 207.50 m long structure comprises three spans with 67.60 m, 72.30 m and 67.60 m length. Each span is made up of two half-arches meeting on a hinge at the middle. The height of the deck is 5.50 m on the piers and 0.50 m at mid-span.

The investigation area is located at the level of the lower slab of the edge half-arch, in the immediate vicinity of the east abutment; the depth of the lower slab is 40 cm in the investigation area.

The bridge is located in a moderate frost zone and the part of the structure investigated is not accessible to de-icing salts. The concrete exposure classes, to be taken into account for this investigated part of the structure are classes XF1 and XC4

3.3.5.2 History of works and current condition

The composition of the concrete is not known.

The arc is lightly reinforced with mild steels of small diameters. However, the arrangement of the reinforcement in the lower slab of the arch is very particular, as shown in the following extract (Figure 2.78):

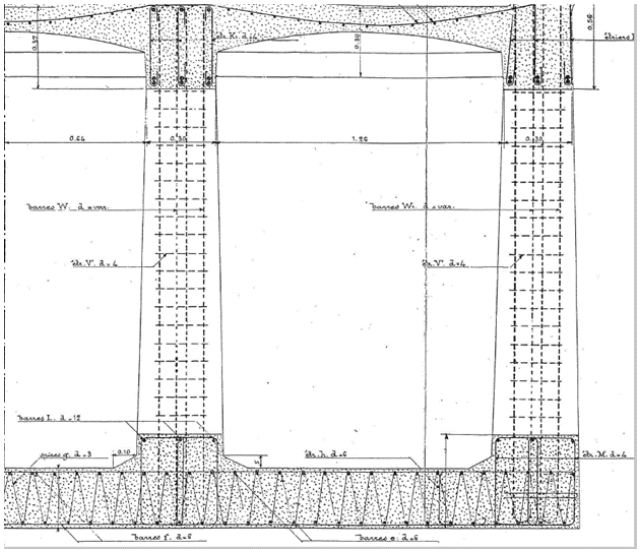

Figure 2.78. Typical reinforcement of a cross-section of the bridge

The reinforcement in the lower slab of the arch is made of inclined steels having a diameter of 4 mm; they are called “coil turn” on the plan.

In 2011, the conclusions of the detailed inspection mention:

- the bridge is in a general good condition;
- the structure is globally cracked, but the width of the cracks remains small. They are explained by the normal behaviour of the reinforced concrete of a complex structure with many built-in connections;
- as many old structures, the concrete cover of the reinforcement is too small and this produces spalls and apparent corroded steels (Figure 2.79). However, these defects are on a small scale, the concrete spalls being of small size and distributed all over the structure.

In 2018, the main conclusions of the detailed inspection are as follows:

- no significant evolution of the cracking under the upper slab (deck), in the arches and on the piers;
- slow evolution in terms of occurrence of new spalls and new corroded steels on the whole structure and due to cover defects. Some patch repairs have to be done.

Figure 2.79. Localized concrete spalling on a diagonal due to an insufficient cover

3.3.5.3 Investigations carried out during the PerfDub project

The investigation area is located on the lower slab of the side arch, near the east abutment. No disorders due to corrosion were recorded in this area where six cores were sampled.

Given the large number of through cores to be sampled in the context of these investigations, and in view of the structural slenderness of this structure, it was considered preferable to take them in the lower slab of the arch, rather than in any other part of the structure. The consequence of this choice is the presence of mild steels of small diameter in all of the concrete cores extracted.

A specific core (Figure 2.80) was taken to reconstitute the concrete formula by a complete mineralogical analysis that was carried out by the LERM laboratory. The conclusion extracted from this report presents a concrete with the following composition (Table 2.87).

The concrete core has a gray matrix. The aggregates (Dmax ≈ 20 mm), from the rolled and crushed type, are distributed homogeneously. Some voids or compaction defects are present. There is a lot of reinforcement, the smallest cover is 25mm from the internal face. On the external side and over 50 to 75 mm, a darker colored concrete is present. It can be a repair concrete because the irregular interface between the two concretes can be distinguished.

Internal Face

External Face

Figure 2.80. Photograph of the core taken for the mineralogical expertise

From a petrographic point of view, the content of reactive mineral species does not appear to be negligible and the aggregates of this concrete are likely to be classified as potentially reactive aggregate (PR). Indeed, according to this examination, the content of reactive species could exceed the limit of 4 % currently recommended in the general case by the documentation fascicle FDP 18-542. However, alkali-aggregate reaction gels were not observed. The observation with an optical microscope shows that the matrix of this concrete contains residual clinker grains of apparently large particle size as frequently encountered in the case of old cements. According to the current classification of cements (standard NF EN 197-1), the binder of this concrete would correspond to a CEM I type cement.

Table 2.87. Concrete composition of the arch of the Boutiron bridge

Composition	
Content of siliceous aggregates (kg/m^3 of concrete)	1590
Cement content (kg/m^3 of concrete)	410 (± 40)
Free water (kg/m^3 of concrete)	225
W_{eff}/C ratio	0.55 (0.50 à 0.61)

The other investigations were carried out in 2019 in the following areas:

- the bracing wall n°1 at the base of the inclined struts – South side;
- the bracing wall n°2 at the base of the inclined struts – South side (Figure 2.81);
- the bracing wall n°2 at the base of the inclined struts – in the center.

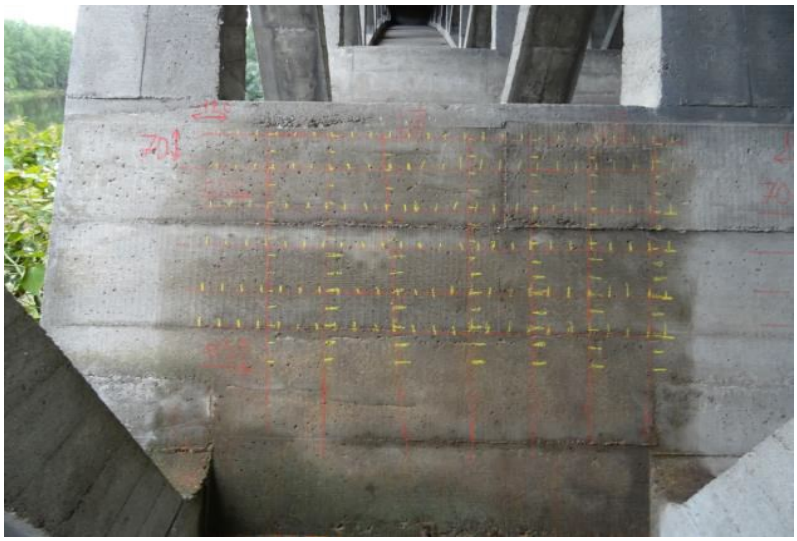

Figure 2.81. Bracing wall n°2 at the base of the inclined struts – South side

a. Corrosion diagnosis (Concrete cover, half-cell potential and resistivity)

The Table 2.88 shows the characteristic statistical values of the cover (in mm).

Table 2.88. Statistical values of the concrete cover (in mm)

	Horizontal reinforcement					Vertical reinforcement				
Part / Zone	**Min.**	**Mean**	**≤ 45**	**e_{95+}***	**e_{95-}****	**Min.**	**Mean**	**≤ 45**	**e_{95+}***	**e_{95-}****
Bracing wall n°1 South	42	56	9 %	45	68	49	58	0 %	51	67
Bracing wall n°2 South	51	55	0 %	51	60	40	54	20 %	42	67
Bracing wall n°2 Center	48	56	48 %	48	65	41	53	13 %	42	66

** 95 % of the measured coverings are higher than the characteristic value e95+*

*** 95 % of the coverings measured are lower than the characteristic value e95-*

The mean concrete cover is of the order of 55 mm for the 3 areas of investigation; the minimum measured cover is 40 mm. This is a rather surprising result when we know that at that time of construction, there was no rule for the cover, and that this cover was generally of the order of 20 mm for most of the constructions.

The Table 2.89 shows the proportion of resistivity measurements made on the bridge piers according to the different corrosion risk classes proposed by the RILEM TC 154 recommendation for CEM I concrete.

Table 2.89. Resistivity measurements

		Pourcentage of measures		
Electrical Resistivity (kΩ.cm)	**Risk of corrosion**	**Bracing wall n°1 South**	**Bracing wall n°2 South**	**Bracing wall n°2 Center**
Re > 100	Negligible	88 %	100 %	100 %
50 < Re < 100	Low	10 %	0 %	0 %
10 < Re < 50	Moderate	2 %	0 %	0 %
Re < 10	High	0 %	0 %	0 %

The in-situ resistivities measured on the three zones are generally very high (up to 1000 kΩ.cm) for zone 3 (bracing n°2 - centre). Regardless of the sheltered exposure, it is likely that the concrete has been made with a special binder. A difference of behaviour is observed between the three areas of investigation with a mean resistivity increasing from the South (zones 1 and 2) to the North (zone 3). This transverse resistivity gradient is probably due to the exposure of the bridge. Finally, in zone 1 (Bracing wall n°1 South), lower resistivities are locally measured corresponding to a less compact concrete zone (a priori a concreting defect leading to segregation). A beginning of concrete spall due to the expansion of the reinforcement is also observable.

The half-cell potential values measured are all positive and generally between 0 and 200 mV. These rather atypical values could be explained by a very dry concrete or a concrete made with a particular binder. Everything seems to indicate that the reinforcements are in a state of passivation.

In the three investigation zones considered, the maximum difference in potentials is:

- zone 1: 186 and 190 mV respectively for the horizontal and vertical reinforcements;
- zone 2: 65 and 107 mV respectively for horizontal and vertical reinforcements;
- zone 3: 123 and 91 mV respectively for horizontal and vertical reinforcements.

According to COST 509 indications, only zone 1 is likely to show areas of corrosion. However, taking into account the positive values of the potentials, the risk of corrosion is unlikely.

The study of potential gradients shows the presence of some specific and localized areas with gradients greater than 10 mV/cm which could be an indication of anodic zones (given the positive values of potentials, the risk of corrosion is however unlikely):

- zone 1: horizontal reinforcements (28 mV/cm), vertical reinforcements (33 mV/cm);
- zone 2: vertical reinforcements (16 mV/cm);
- zone 3: all values below 9.2 mV/cm.

At the level of the concrete removal necessary for the connection of the measuring equipment (CANIN) to the steel, no signs of corrosion of the reinforcement were observed.

b. Lifetime and durability indicators

Based on the six cores, the carbonation is lower than 1 mm on both sides of the cores (intrados and extrados) as shown on the Figure 2.82. The mean concrete cover is difficult to assess given the distribution of the reinforcement, but we can admit in the first approximation a cover of 20 mm.

Figure 2.82. Lack of carbonation on all six cores

A synthesis of the durability indicators is presented in Table 2.90.

Table 2.90. Values measured for durability indicators

Durability indicators		
Apparent coefficient of chloride diffusion	D_{rcm} (10^{-12} m².s^{-1})	34.3 (24.1 / 37 / 41.8)
Porosity accessible to water	P_{water} (%)	16.4 (16.1 / 17.5 / 15.7)
Resistivity	(kΩ.m)	37** (36 / 32 / 42)
Gas permeability	K_{gas} (10^{-18} m²)	> 200 (200 / 2000 # / 2000 #)
Capillary absorption at 24 hours	g/m²	3950 (3691 / 4512 / 3648)
Accelerated carbonation (3 %) at 28 & 56 days	$X_{c,28} - X_{c,56}$ (mm)	NM*
Accelerated carbonation (50 %) at 7 & 28 days	$X_{c,7} - X_{c,28}$ (mm)	NM*
Spacing factor for air bubbles (Lbar)	L (µm)	NM*
Scaling	g/m²	NM*
Frost test (in water): - Relative expansion - ratio of resonance frequency squares	ln (µm/m) $\frac{F_{Fn}^2}{F_{Fo}^2}$x100	NM*
Characteristic strength of concrete on site / Strength class	f_c (MPa) Class	42 C45/55

* *NM: not measured*
** *The conclusions of this test should be moderate, because the presence of reinforcements in the cores may have promoted electrical conduction, and thus degraded the quality of the test.*
\# *Value not taken into account*

Potential durability classes (according to AFGC, 2004)				
Very low	Low	Average	High	Very high

3.3.5.4 Conclusions drawn

The investigations carried out within the framework of the national PerfDub project on the lower slab of the arch of the Boutiron bridge in the Allier were difficult to manage; the arrangement of the reinforcement in the slab prevents any removal of concrete core free of reinforcement. Indeed, certain reinforcements called “coil turns” (loops) are neither perpendicular nor parallel to the facings of the slab. It is therefore impossible to avoid them when coring.

The presence of these reinforcements in the samples affects the quality of the durability tests carried out as part of the performance approach to the durability of reinforced concrete. Nevertheless, if we consider the results, the potential durability of the concrete appears very low, despite the fact that the bridge is in a global good condition for such an old bridge more than 100 years old. Some spalls and apparent corroded steels exist in some points distributed all over the structure, and this is due to a defective concrete cover (less than 20 mm).

The compressive strength class of the concrete of the lower arch slab, assessed in accordance with standard NF EN 13791 / CN, is C45/55, which is a very good value for such an old concrete that comprises 410 kg of CEM I type cement per cubic meter of concrete. The most surprising is the measured carbonation depth that is less than 1 mm on the studied area of the slab, located in the immediate vicinity of the east abutment.

The investigations carried out on the three bracing zones of the Boutiron bridge show concrete covers greater than 45 mm, very high resistivities, except for a localized zone corresponding to a segregated concrete, and positive electrical potentials indicating that the reinforcements are passivated. The non-destructive investigations indicate that the reinforcements are well protected, located in a concrete that is not very prone to corrosion and essentially passivated.

3.3.6 Iena Palace

3.3.6.1 Presentation of the building

The Iena Palace (Jena Palace), also known as the Musée des Travaux Publics (Public Works Museum), was designed by Auguste Perret as part of the urban plan for the International Exhibition “Arts and Techniques in Modern Life” in Paris in 1937. In 1959, the Economic and Social Council moved to the Iena Palace (Figure 2.83).

Figure 2.83. General view of the Iena Palace

Therefore, the construction of the Iena Palace began in 1937 and was completed in 1995 after four stages. The south wing of the Iena Palace is the first phase of construction, built between 1937 and 1938 by the "Société des Grands Travaux en béton armé", a Gustave Perret company. It is classified as a Monument. This monument has already been partially or totally restored, and presents fairly complete and recent diagnostic documents. The two-storey south wing of the Iena Palace is a building 80 meters long, 20 meters wide and 20 meters high (Figure 2.84).

Figure 2.84. View of the South wing of the Iena Palace

The facade of the south wing is made up of twelve bays, nine of which have monumental columns 13 meters high, spaced every 6 meters. Their diameter is 0.80 meter at the base and

1.03 meter at the top. In addition, to each column corresponds, on the rear face of the building structure, courtyard side, a pillar of square cross section. These pillars do not support the floors of the building but only the roof. Each column is joined to the corresponding pillar by a beam of 18 meters span. All of these three elements form a rigid frame. These frames are joined to the facade by a band forming the architrave of the colonnade bordered by a wide cornice. This set only bears the terrace forming the roof of the building and is independent of the interior structure of the building.

The facade of the south wing of the Iena Palace is located in an XC4 environment.

3.3.6.2 History of works and current condition

First of all, two types of manufacturing elements are to be distinguished:

- the structural elements built on site (columns, pilasters, etc.);
- the prefabricated elements such as the claustra and infill panels (bases between large windows).

Some elements contain a water repellent which was added during processing.

According to the work descriptions left by Auguste Perret, the cement used for the structural elements is an ordinary Portland cement dosed at 300 kg for 400 litres of sand and 800 litres of gravels. A first series of analyses in 2015 (BPE/studiolo 2015) did not reveal the presence of fly ash, silica fumes and slag. This would therefore indicate that the cement used could be of a CEM I type.

The concrete of the structural elements has Water / Cement (W / C) ratios varying between 0.58 and 0.63 (Table 2.91) according to samples taken by the BPE Engineering and Studiolo expert offices.

Table 2.91. Characteristics of the concrete of the South facade (BPE/Studiolo, 2015)

Zone	Element	Cement content (%)	Cement content (kg/m^3)	Aggregate content (%)	W/C Ratio
SC7	Pilaster	17.8	390	71.0	0.63
SC8	Column	20.4	460	67.8	0.58
SC9	Base	19.2	420	69.2	0.60

The load-bearing elements (columns and pilasters) have a lower open porosity than the basement (Table 2.92).

Table 2.92. Porosity and density of the South façade concrete (BPE/Studiolo, 2015)

Zone	Element	Open Porosity (%)	Apparent density (kg/m^3)
SC7	Pilaster	14.2	2160
SC8	Column	14.2	2170
SC9	Base	17.1	2200

According to the compressive strength tests, the columns, load-bearing elements of the roof, are more resistant compared to the other elements, and in particular the basement (Table 2.93).

Table 2.93. Compressive strength of the South façade concrete (BPE/Studiolo, 2015)

Zone	Element	Compressive strength (MPa)	Strength Class
SC7	Pilaster	26.4	C25/30
SC8	Column	34.9	C30/35
SC9	Base	24.1	C20/25

Having a carbon content between 0.05 and 2 %, and a tensile strength of around 400 MPa, the steel used to reinforce the concrete is a mild steel

In the early 2000s, the facade was cleaned by spraying fine abrasives in a dry process (Thomas-Hanry System). In 2009, a purge operation was carried out. A passivation treatment on the visible reinforcements was also carried out. In 2014, a major restoration project, lasting two years, was set up, during which a diagnosis of the condition of the reinforced concrete was carried out.

Diagnosis carried out as part of the 2014-2016 restoration

As part of the restoration work, an analytical diagnosis with samples and investigations was carried out by three different professionals. It was a question of measuring the depth of coating and carbonation as well as the concentrations of salts (sulphates, chlorides). On the south facade (Figure 2.85):

- three core samples were taken by BPE and Studiolo;
- seventeen cores and two samples were taken by Ginger CEBTP;
- ten cores were taken out by the LRMH.

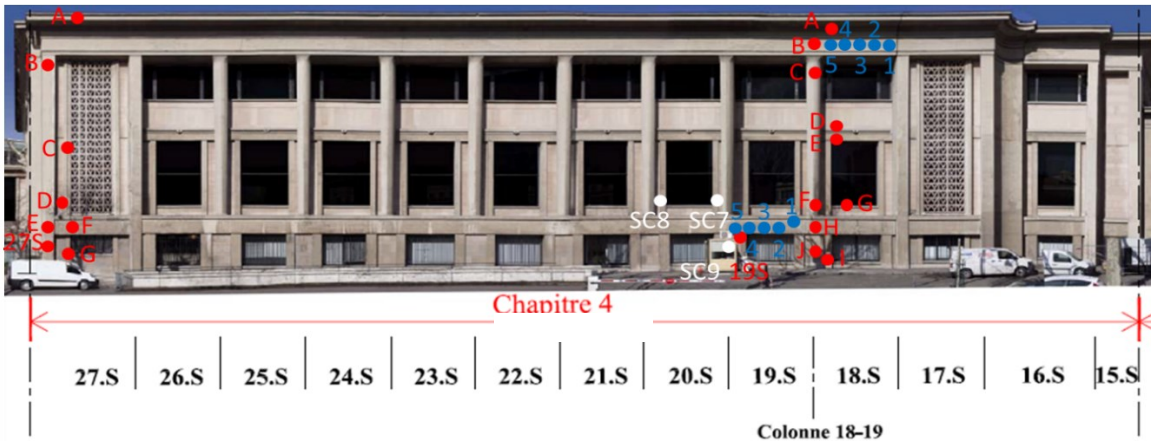

Ginger CEBTP, 2013 BPE/Studiolo, 2015 LRMH, 2016

Figure 2.85. Location of samples and cores

The concrete cover depth generally varies between 2.2 and 9.5 cm (Tables 2.94, 2.95, 2.96). The cover can also vary in the same element: from 3.5 to 9.5 cm for a cornice, from 5 to 9.5 cm for the same pillar or from 2.6 to 7.5 cm for a column.

Carbonation is present to a depth of 4cm, with an average of 1.4 cm. With the exception of a band (Table 2.94), carbonation never reaches the steel reinforcement.

Table 2.94. Cover thickness of the reinforcements and carbonation depth of the concretes of Span 18S of the south facade (Ginger CEBTP, 2013)

Ref.	Element	Cover (pachometer) (cm)	Cover (coring) (cm)	Carbonation (coring) (cm)	Carbonation/ Cover (coring)
A	Cornice	9	9.5	4	0.42
B	Frieze	-	>15	3	< 0.20
C	Column	4	4.5	2	0.44
D	Band	5.5	5	0	0
E	Band	3.5	3.5	2.5	0.71
F	Column	7	7.5	1.7	0.23
G	Spandrel	2.5	2.5	0.4	0.16
H	Band	2.5	2.2	3.1	1.42
I	Pilaster	5.5	5	2.1	0.42
J	Moldings	-	Lack of steel	0.2	

Table 2.95. Cover thickness of the reinforcements and carbonation depth of the concretes of Span 27S of the south facade (Ginger CEBTP, 2013)

Ref.	Element	Cover (pachometer) (cm)	Cover (coring) (cm)	Carbonation (coring) (cm)	Carbonation/ Cover (coring)
A	Cornice	3.5	3.5	2.4	0.69
B	Pillar	4.5	5	0	0
C	Pilaster	3.5	3.5	2.2	0.63
D	Moldings	-	Lack of steel	0.2	-
E	Pillar	9	9.5	0.5	0.05
F	Band	-	Lack of steel	0.3	-
G	Pilaster	3.5	3.5	2.7	0.77

Table 2.96. Cover thickness and carbonation depth of the concretes of Span 20S of the south facade (BPE / Studiolo, 2015)

Ref.	Element	Cover (pachometer) (cm)	Cover (coring) (cm)	Carbonation (coring) (cm)	Carbonation/ Cover (coring)
SC7	Pilaster	6.6	4.7	0.3	0.06
SC8	Column	6.7	2.6	<0.1	< 0.04
SC9	Basement	8.8	7.5	0.3	0.04

Concentration profiles of silica, chlorides and sulphates were established over depths varying from 0 to 4 centimeters. The thresholds considered as pathologic are respectively 0.4 % relative to the mass of cement for chlorides and 4 % relative to the mass of cement for sulphates. They are exceeded from the first centimeter for chlorides (0.53 and 0.57 %) and sulphates (5.28 and 6.92 %) (Table 2.97). Sulphates are present in large quantities up to 2 cm in the basement (Powder 19S).

Table 2.97. Concentration of silicas, chlorides and sulphates present between 0 and 5 cm deep in the concrete of the south facade (BPE / Studiolo, 2015) (Ginger CEBTP, 2013)

Reference	% silica	% cement	% Cl	% Cl / cement	% SO_3	% SO_3 / cement
Powder 19S (0-1cm)	42.95	14.8	0.078	0.53	1.02	6.92
Powder 19S (1-2cm)	2.47	12.4	0.016	0.13	0.50	4.05
Powder 19S (2-3cm)	2.35	11.8	0.004	0.03	0.34	2.89
Powder 27S (0-1cm)	2.99	15.0	0.085	0.57	0.79	5.28
Powder 27S (1-2cm)	3.05	15.3	0.031	0.21	0.45	2.95
Powder 27S (2-3cm)	3.80	19.0	0.006	0.03	0.41	2.16
Powder 27S (3-4cm)	3.86	19.3	0.006	0.03	0.4	2.07
SC7 (1-3cm)	-	17.8	0.031	0.17	0.45	2.49
SC8 (1-3cm)	-	20.4	0.031	0.15	0.42	1.98
SC9 (1-3cm)	-	19.2	0.031	0.16	0.41	2.15

Half-cell potential maps established by Ginger CEBTP were carried out on areas where the risk of corrosion was deemed to be significant after a visual diagnosis: no active corrosion area was observed on spans 18S and 27S.

The southern facade is the dirtiest with very large weathered areas. The monumental columns are washed out and light on the west side and very gray and dirty on the east side, unlike the exposed columns on the north side.

The bases of some columns are also very weathered, sometimes exposing the reinforcement (Figure 2.86). Some spalling is visible on the gray concrete structural elements (Figure 2.87), sometimes at the location of old repairs (Figure 2.88). In most cases, a cover defect is observed (localized spalling at the edges of the beams).

Figure 2.86. Spalling on a horizontal surface revealing the corroded reinforcements

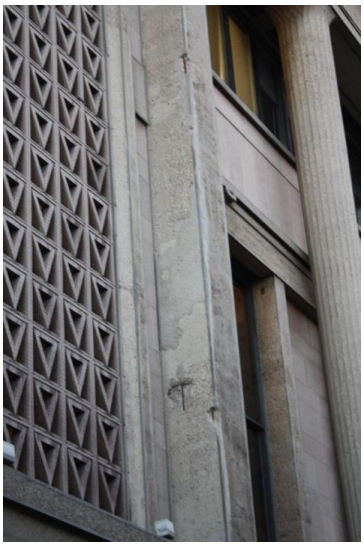

Figure 2.87. Spalling at the edges with apparent steels

Figure 2.88. Localized spalling on a corner at the location of an old repair

Traces of drips due to rain, coming from the first floor, cause white calcified efflorescence on the basement.

3.3.6.3 Investigations carried out during the PerfDub project

The Iena Palace being in the restoration phase, scaffolding provided access to the high areas of the facades for the extraction of cores which was carried out on the south facade, on spans 18 and 19 in July 2016. Two areas were chosen for the core drilling:

- a so-called "uncorroded" zone, where no alteration had been identified, located on span 18S;
- a so-called “corroded” area, repaired many times, located on span 19S.

Five 51 mm diameter cores were taken out in each of these two zones, named Cnc1 to Cnc5 for the so-called uncorroded zone and named Cc1 to Cc5 for the so-called corroded zone.

Carbonation tests were carried out on the Cnc4 and Cc5 cores: the average carbonation depths measured are 38 mm for Cnc4 and 30 mm for Cc5

The measurements of the durability indicators were carried out on these 51 mm cores after verifying by a specific study conducted within the national PerfDub project, that it was valid to conduct durability tests on cores of such small diameter. The tests relate to water porosity, gas permeability, accelerated carbonation test, and reconstruction of the concrete formula with petrography. The results are reported in the Table 2.98.

Table 2.98. Results of measurements of durability indicators

Core	Measure of the carbonation depth (mm)	Composition: Cement content (kg/m³) and W/C Ratio	Apparent density (kg/m³)	Porosity (%)	Oxygen Permeability (x 10^{-18}m²)
Cnc1	33	-	2175	18.1	-
Cnc2	30	280 (± 30) 0.75	2190	17.6	650
Cnc3	> 30	-	-	-	981
Cnc5	37	-	2150	19.0	1008
Cc1	0 (bottom of core)	-	2155	18.4	1154
Cc2	29	280 (± 30) 0.80	2135	18.6	-
Cc3	31	-	-	-	637
Cc4	29	-	2125	19.3	402
Moyenne	32	-	2155	18.5	805

* *Optical microscopic observations realized by the LERM on Cc3 and Cnc2 cores show the indisputable presence of slag in the concrete, which would correspond to the current classification of a CEM II/B-S cement type.*

Moreover, the results obtained call for the following comments:

- the chloride contents are lower than the limit of 0.4 % (expressed in relation to the mass of cement) recommended by standard NF EN 206/CN in the case of reinforced concrete;
- the sulphate contents are lower than the maximum values of 3.5 or 4 % fixed by the current cement standard (NF EN 197-1), depending on the strength class of the cement;
- the contents of the equivalent accessible alkalis in the long term are below the threshold of 3 kg of alkalis (expressed in Na_2O_{eq}) per m^3 of concrete, recommended for the prevention of disorders due to the alkali-reaction (LCPC, June 1994), in the case of use of potentially reactive aggregates.

3.3.6.4 Conclusions drawn

The concrete used at the Iena Palace is composed of a Portland cement with slag, which would correspond to a CEM II/B-S type cement with the current classification, a granular load mainly of the flint type and a varied sand load of a silica-calcareous nature. The concretes of the two zones present similar compositions, with a total aggregate load of approximately 1750 kg/m³, a cement content of 280 kg/m³, and an average Wefficient / C ratio between 0.75 (uncorroded zone NC) and 0.8 (corroded zone C).

The results of the LERM concerning the nature and the content of cement used in these two zones (NC and C) are different from those of a first diagnosis carried out in 2015 where a Portland CEM I cement type and higher cement contents (390 and 460 kg/m³) were found for a pilaster and a column of the 20.S span. This difference in the nature of the cement can be attributed either to human error in the microscopy observation in 2015, or to heterogeneity in the cement used for the concretes of the facade, even if the areas investigated in both cases are very close. However, the presence of observed slag in the concretes of the NC and C zones in the PerfDub analyses is indisputable.

The carbonation depths are slightly higher and more heterogeneous for the NC zone, with an average carbonation depth of 35 mm ± 4 mm, than for the so-called C zone, with an average depth of 30 mm ± 1 mm.

The durability indicators are also close for the two zones. The water porosity is equal to 18.3 ± 0.6 % for the NC zone, and to 19 ± 0.6 % for the C zone. The values of oxygen permeabilities show a strong disparity, included for the NC zone between 650.10^{-18} m^2 and 1008.10^{-18} m^2 (average 879.10^{-18} m^2 ± 199), and for the C zone C between 402.10^{-18} m^2 and 1154.10^{-18} m^2 (average 731.10^{-18} m^2 ± 385).

Accelerated carbonation tests are not conclusive. Indeed, the carbonation depths measured at 70 days are very disparate. A probable explanation would be linked to the conditioning of the cores, and in particular the drying at 45 °C for 14 days, which would not lead to optimal carbonation conditions, in connection with the small dimensions of the cores (51 mm in diameter and variable height).

Therefore the concretes in the two studied zones have similar compositions and similar durability indicators and lifetime indicators. If the cement content complies with the limits currently set by standard NF EN 206/CN for exposure classes XC1 to XC4 (corrosion by carbonation), on the other hand, the Weff / C ratio significantly exceeds the threshold of 0.65 or 0.60 fixed for these same classes, and the porosity and gas permeability values correspond to a concrete of very low durability class.

The damage observed on the so-called “corroded” part is probably due to the weak concrete cover of the reinforcements in this area (found at 2.2 cm by the CEBTP in 2013), compared to the cover of the so-called “uncorroded” area, with more than 12.5 cm (LRMH core drilling).

3.3.7 Bordeaux Labor Exchange

3.3.7.1 Presentation of the building

In 1935, the mayor of Bordeaux entrusted the city’s chief architect, Jacques Boistel d'Welles, with the design of the Labor Exchange hall. Begun in 1935, the building, located at 44 Cours Aristide Briand, was inaugurated on May 1, 1938. It is managed by the CGT Workers Union. The building, in Art Deco style, is listed as a Historic Monument by decree of June 25, 1998. In the 2000s, a concrete diagnosis was carried out in order to rehabilitate the building (Figure 2.89).

Figure 2.89. View of the Bordeaux Labor Exchange after restauration. (©flickr.Yvette G.)

The Labor Exchange is an irregular quadrilateral divided into two trapezoids opening onto five carved doors on the Cours Aristide Briand. The building has four facades, each 45 meters long, is four storeys high and ending in a roof terrace. The concrete on the facade is bush hammered. Very homogeneous, the building has been little transformed.

3.3.7.2 History of works and current condition

Following the collapse of the roof in 1991, a first phase of work was carried out in 2002 in order to save the building. On this occasion, the 3rd and 4th floors were renovated. The last phase of the work was launched in 2006. Elements of the 4th floor were deposited and kept at the LRMH in Champs-sur-Marne near Paris.

In prospect of the restoration of the Labor Exchange, a diagnosis was carried out from January 25, 2000 by the CEBTP. This diagnosis was based on non-destructive tests and laboratory analyses on core samples (Figure 2.90).

Figure 2.90. Plan of the 4th floor and location of the samples (CEBTP, 2000)

The diagnosis carried out on the C1 core taken from a pole on the 4th floor resulted in a cement content of 20.3 %; the aggregates are probably of alluvial origin and are mainly siliceous. Table 2.99 shows the chemical nature of the C1 core.

Table 2.99. Chemical nature (in %) of C1 core (CEBTP, 2000)

Test	Result (%)	Test	Result (%)
Fire loss	6.6	Calcium oxide	12.88
Of which loss at 80 °C	0.8	Sulfuric anhydride	0.17
Of which loss at 550 °C	4.3	Sulfide	Lack
Insoluble	73.1	Magnesia	0.25
Soluble silica	4.54	Sodium oxide	0.02
Iron oxide	0.78	Potassium oxide	0.04
Alumina	0.88	Chloride	0.029

The porosity tests were carried out by hydrostatic weighing in accordance with AFREM recommendations. The porosity of the cores taken from the columns facing the outside is lower

than that of the cores taken from the columns inside: between 11 and 13 % against 19 and 21 % (Table 2.100). Core C3 and C4 were taken from walls and core C5 to C9 from poles.

Table 2.100. Porosity of the concretes of the 4th floor (CEBTP, 2000)

Core	Density (kg/m^3)		Porosity (%)
	Apparent	Real	
C_3 (external wall)	2305	2605	11.5
C_4 (internal courtyard wall)	2170	2635	21.5
C_5 (internal pole)	2280	2575	11.4
C_6 (internal pole)	2030	2570	21.0
C_7 (external pole)	2275	2630	13.5
C_8 (external pole)	2310	2605	11.2
C_9(internal pole)	2140	2650	19.2

The simple compressive strength tests carried out on C1, C5 and C8 cores gave the respective values of 15.9 - 24.7 and 29.3 MPa.

The concrete cover of the reinforcement of the 4th floor walls varies between 9 and 71 mm and is 30 ± 6 mm on average (Table 2.101).

Table 2.101. Concrete covers of the 4th floor walls (CEBTP, 2000)

Minimum cover (mm)	Maximum cover (mm)	Mean cover (mm)	Standard deviation (mm)
24	57	40	6
29	46	37	5
16	25	19	2
16	64	30	15
18	54	24	11
13	27	18	4
14	18	16	2
21	26	23	3
15	70	28	17
17	36	27	6
14	39	28	6
13	36	23	7
21	51	37	15
44	71	51	10
16	57	27	20
16	33	27	4
9	19	14	3
9	59	21	12

The cover of the reinforcement of the 4th floor poles varies between 0 and 79 mm and is 46 ± 10 mm on average (Table 2.102).

Table 2.102. Concrete covers of the columns of the 4th floor (CEBTP, 2000)

Minimum cover (mm)	Maximum cover (mm)	Mean cover (mm)	Standard deviation (mm)
20	72	51	17
23	74	51	12
32	49	40	5
0	57	26	14
13	60	30	16
17	30	22	4
35	52	44	6
25	69	38	14
34	71	52	10
13	74	44	18
57	76	67	8
70	79	74	3
61	78	67	5

The percentage of steels reached by carbonation was deduced from the study of the cover of the reinforcements and relates to 1375 measurements. The carbonation depths were determined using phenolphthalein dosed at 1 %, either directly on the building or on the samples taken (Table 2.103).

Table 2.103. Carbonation depths of the 4th floor concretes (CEBTP, 2000)

Location	Denomination	Carbonation (mm)	Estimation of the number of steels affected by carbonation (%)
Poles	1	25	25.5
	2	2-35	
	3	30-35	
	9	20-50	
	12	0	
	13	>50	
	20	20	
	$P_{15'}$	10-25	
Walls	Core C_3	47	92.5
	Core C_4	48	
	Wall V_1	>50	
	Wall V_2	>50	
	Wall V_3	20	

The measurement of the corrosion half-cell potential on the wall of the 4th floor was carried out on a mesh of 200 × 200mm. Exposed steel has a corroded or even severely corroded appearance. The bars have a diameter of 10 mm, the cover is approximately 20mm and the carbonation depth is approximately 50 mm. The corrosive activity is considered significant (average potentials of -260 mV).

The measurement of the corrosion half-cell potential carried out on the column of the 4th floor was carried out on a mesh of 150 × 150mm. The exposed steel is healthy in appearance. The bars have a diameter of 12 mm, the cover is 45 mm and the carbonation depth is 15 mm. The corrosion activity is zero (average potentials of + 80 mV).

During the diagnosis made in the 2000s, in the upper part of the building, spalling from the bush-hammered surface were observed. Locally, concrete walls have become non-existent. Structural cracks were also noticed in the walls. Corrosion of the reinforcements caused severe spalling.

Inside the 4th floor, the ceiling collapsed in one of the conference rooms. As well as outside, there were many cracks and spalling.

Water seepage has been observed due to a lack of weather caulking between the buildings. The repairs carried out during a previous restoration did not limit the corrosion of the reinforcements.

3.3.7.3 Investigations carried out during the PerfDub project

The first step in this task was to choose the areas to be analysed and to take the 51 mm diameter cores from the wall elements (slabs) deposited and kept in a garden, under a canopy of trees, at the LRMH. There is no information on the orientation and location of these wall elements (slabs) on the building before they were sent to LRMH.

The walls do not present different facies of alteration, a single series of cores was therefore taken in August 2018 from two different slabs A and B (Figures 2.91 & 2.92). The internal face of the walls has a formed surface, while the external face has a bush-hammered surface with visible aggregates.

Figure 2.91. Slab A with drilling area of cores 1 and 2. Internal face

Figure 2.92. Slab B with drilling areas of cores 3, 4, 5, 9, 10 11, 12, 13, 14. Internal face

The first observations as well as the carbonation depths measurement were carried out by the LRMH. The analyses of water porosity, gas permeability, and identification of the formulation were carried out by LERM SETEC and accelerated carbonation tests were carried out by the LCR laboratory of LAFARGE FRANCE according to the PerfDub operating mode at 3 % CO_2, on several cores taken from the investigated walls.

Table 2.104 gives the values of the phenolphthalein measurements of the average carbonation depth carried out on the C1 and C3 cores.

Table 2.104. Carbonation depths measured on cores C1 and C3

	C1 (slab A)	C3 (slab B)
Surface in contact with the exterior	18	8
Surface in contact with the interior	23	4

The measurements of the durability indicators were carried out on these 51 mm cores after verifying by a specific study carried out within the national PerfDub project, that it was valid to conduct durability tests on cores of such small diameter. The tests relate to water porosity, gas permeability, accelerated carbonation test, and reconstruction of the concrete formula with petrography. The results are reported in the table 2.105.

Table 2.105. Results of measurements of durability indicators

Core	Measure of the carbonation depth (mm)	Composition*: Cement content (kg/m^3) and W/C Ratio	Apparent density (kg/m^3)	Porosity (%)	Oxygen Permeability (x 10^{-18}m^2)
C1	Face Int: 22 Face Ext:15	X	2245	14.5	-
C3	Face Int: 0 Face Ext:0		2300	12.2	1721 #
C5	Face Int: 2 Face Ext:1		2325	11.0	547
C9	Face Int: 7 Face Ext: 0	X	2270	13.4	-
C10	Face Int: > 21 Face Ext: 11		2260	13.6	1500 #
C13	Face Int: > 20 Face Ext: 9		2275	13.2	667
C14	Face Int: 0 Face Ext: 0	X	2300	13.1	-
Mean	-	-	2280	13.0	607

** Binder close to a Portland cement of the CEM I type*
X Measurements made only on C1, C9 and C14 cores
 # Values not taken into account

The results of the accelerated carbonation test remain inconclusive given the disparity in the observations made. Drying at 45 ° C for 14 days on samples of small dimensions (diameter 5 cm and height less than 3 cm) is probably too severe, thus allowing the samples to be thoroughly dried. Setting humidity to 65 % thereafter will not allow for a uniform water content within the sample (even after 70 days?) to achieve optimal carbonation.

The chemical analyses were carried out on an average sample which includes the 3 samples of C1, C9 and C14, with the aim of having an average sample that is as representative as possible; the results are as follows:

- The average cement content is 280 (± 30) kg/m^3 of concrete;
- The effective mixing water is 155 kg/m^3 of concrete;

- Effective Water / Cement Ratio - Average is 0.55.

In addition, the results obtained call for the following comments:

- the chloride content of 0.08 % by mass of cement is less than the limit of 0.4 % recommended by standard NF EN 206/CN in the case of reinforced concrete;
- the sulphate content of 1.95 % by mass of cement is lower than the maximum values of 3.5 or 4 % set by the current cement standard (NF EN 197-1), depending on the strength class of the cement;
- the long-term accessible equivalent alkali content of 1.35 kg/m^3 of concrete is much lower than the threshold of 3 kg of alkali, recommended for the prevention of disorders due to alkali-reaction (LCPC June 1994), when using potentially reactive aggregates.

3.3.7.4 Conclusions drawn

The elements of the 4th floor walls of the Bordeaux Labor Exchange, built between 1935 and 1938, and partly deposited at the LRMH since 2006, were investigated as part of the PerfDub project. Two slabs (cut walls) underwent a total of eleven 51 mm diameter cores in August 2018.

The concrete used for the walls of the Bordeaux Labor Exchange is composed of a Portland cement CEMI, and a siliceous type gravel and sand filler (mainly of the flint and quartzite type).

The concrete composition for the walls has a total aggregate of approximately 1870 kg/m^3, a cement content of 280 kg/m^3, and an average $W_{effective}$ / C ratio of 0.55.

The carbonation depths are variable, whether between slabs A and B or on the same slab. Two carbonation depths were measured on each core, corresponding to carbonation from the outer face (outward) and from the inner face of the wall. The carbonation front measurements by the phenolphthalein test show significant differences in terms of carbonate thickness:

- the samples C3 and C14 are not carbonated (from the internal face and the external face);
- the samples C5 and C9 have low carbonate content: between 3 and 8 mm from the internal face and between 0 and 5 mm from the external face;
- the sample C1 has an average carbonation depth of 22 on the inside and 15 mm on the outside;
- the C10 and C13 samples have a carbonation depth greater than 20 mm on the internal face and 14 and 12 mm respectively from the external face.

The average water porosity of the concrete is 13 % and the oxygen permeability values measured on the cores of slab B show a strong scatter, ranging between 547.10^{-18} m^2 and 1721.10^{-18} m^2 (average of 1109. 10^{-18} m^2).

Accelerated carbonation tests are inconclusive, probably because of the small diameter of the cores (51 mm).

The strong disparities in terms of carbonation measured between the two slabs and on the same slab could first of all be linked to different exposure conditions (rain, wind, etc.), which corroborates the measurements of 2000 on the carbonation of walls. (from 20 mm to 50 mm of carbonation). The surface treatment of the bush-hammered making aggregate visible on the external surface may also have introduced biases in the progress of the carbonation reaction, on the penetration of CO_2 and water.

The cement content and the estimated effective water / cement ratio would respect the limits currently set by standard NF EN 206/CN for exposure classes XC1 to XC4 (corrosion by

carbonation) for a service life of 50 years. The water porosity largely respects the threshold of 15 % of fascicule 65 for a lifespan of 100 years, which is absolutely not the case of the gas permeability, for walls of age 80 years which do not show any corrosion and have a carbonation depth between 0 and 22 mm, which tends to show the limits of the gas permeability indicator compared the porosity one.

3.3.8 Vezins dam

3.3.8.1 Presentation of the dam

The Vezins dam, which is under an EDF concession, is a multiple vault structure made of reinforced concrete and built between 1929 and 1932 (Figure 2.93). It was erected to block the course of the Sélune river and harness the hydroelectric power of the waterfall thus created. It is associated downstream with another dam of the same design, the “Roche Qui Boit” dam.

Figure 2.93: General view of the Vezins Dam before its demolition.

The Vezins dam is a curved multiple-arch reinforced concrete dam. Its closure on the right bank is ensured by a concrete abutment. On the left bank, the closure is ensured by the spillway structure and by a concrete abutment. The dam was designed by the consultancy firm “Pelnard, Consider and Caquot”.

The dam is made up of 40 reinforced concrete vaults with a span of 5.4 m (marked from 1 to 40 from the right bank). The inclination of the vaults is 45 ° below the 50.56 m NGF level. Above, the facings gradually straighten out to achieve verticality at the crest. The vaults are very thin. Their thickness is 0.17 m above the 60.56 m NGF level (French General Levelling). Below, the thickness is governed by the formula $e = 0.17 + 0.00014.h^2$ (where e is the thickness (in m) and h the depth (in m) with respect to the 60.56 m NGF level).

Each vault rests on solid reinforced concrete buttresses. These buttresses are directed along radiuses of 370 m. Their thickness varies according to the level. Above the 60.00 m NGF level, it is equal to 0.15 m. Below, it grows linearly with depth with respect to this same level according to the formula $e = 0.15 + 0.015.h$.

The buttresses, which are also very thin, have stiffeners made up of vertical reinforced concrete ribs spaced every 5 m. Additional bracing consists of horizontal crossbeams (struts)

spaced 5 m apart in all directions resting on the ribs. Between the 8 buttresses which surround the water pipes, a bracing by means of St-André crosses was built (vaults 20 to 26). The ribs have extra thicknesses on each side of the buttress. These extra thicknesses have a section of 0.30 by 0.25 m. The crossbeams have a section which varies from 0.25 x 0.40 to 0.25 x 0.45 m, taking into account the curvature of their lower surface.

The structure of the crown can be compared to a deck made of continuous spans of reinforced concrete girder bridges without crossbeams and made up of three longitudinal beams. The beams are of varying heights. The deck rests (a priori as built in) on the head of the buttresses.

The dam was demolished in 2019 for environmental reasons.

The Vezins dam falls under environmental classes XC1 (permanently immersed in water) for the submerged parts and XC4 for the above-ground parts.

At the request of the DREAL Bretagne, owner of the dam, a diagnosis on the durability and integrity of the reinforced concrete material was carried out by the Saint-Brieuc laboratory of the Cerema, in 2016, on the vault no. 30.

3.3.8.2 History of works and current condition

a. History of maintenance and surveillance

The history of maintenance actions is as follows:

- 1943: Bombing of the structure during the second world war;
- 1945: Repair of holes in buttresses 22 and 24 and vaults 18/20 and 20/22;
- 1952: First ten-year dam emptying and patch repair of the upstream facing;
- 1967: Ten-yearly emptying and occasional repair of the surface cement coating;
- 1977: Ten-year emptying and patch repair of the upstream facing only at 48.56 m NGF;
- 1979: Patch repair of the downstream facing;
- 1981: Patch repair of the upstream facing from 55.56 to 61.56 m NGF;
- 1982: Ten-yearly emptying and patch repair of the upstream facing from 48.56 to 55.56 m NGF;
- 1993: Ten-yearly emptying and patch repair of the upstream facing: partial surface recovery;
- 1995: Treatment of leaks at the buttress 17/18;
- 1997 - 1998: Repair of leaks at the buttresses 21/22, 23/24, 24/25 and 25/26;
- 2000: Repair of the downstream raft of the spillway.

The history of the main surveillance actions is as follows:

- 1948: Record of cracking of the buttresses;
- 1994: Record of cracking of the buttresses (update of the 1948 survey);
- 1997: Boat tour for inspecting the upstream face after lowering the water level from 59.60 to 55.50 m NGF, visit by foot (and by binoculars) of the downstream face (by SEISO company);
- 2004: Underwater visit of the upstream facing using an ROV (by SASA company) + Regulatory annual In-depth Technical Visits (by CIH).

b. Locations of investigations

The investigations carried out as part of the 2016 diagnosis were carried out on areas representative of buttresses, vault springs and keys on the intrados (downstream) and extrados (upstream). The investigations were mainly carried out on vault n ° 30 and the two adjacent buttresses (29-30 and 30-31). In addition, investigations were also carried out on the beams and intrados of three spans of the deck above the dam (above vaults 2, 12 and 30).

These investigations include visual inspections, statistical records of concrete covers, maps of reinforcement half-cell potentials, resistivity maps, Radar investigations, as well as compressive strength, carbonation, chloride content profiles, sulphate contents, durability indicators, the whole being completed by a complete mineralogical analysis of the concrete carried out by IFSTTAR.

The investigations were carried out in 4 main areas of the dam:

- upstream zone (ZA): This zone concerns the upstream facing on the reservoir side. This zone includes a constantly emerged facing zone and a usually submerged facing zone. This area is broken down into three sub-areas depending on whether they concern the key or the two grooves (interfaces between 2 successive vaults) (see Figure 2.94):
  - ZA 30: area of the key of vault n° 30 (1.2 x 1.2 m),
  - ZA 30-31: groove between vaults 30 and 31 (1.2 x 2.4 m),
  - ZA 29-30: groove between vaults 29 and 30 (1.2 x 2.4m).

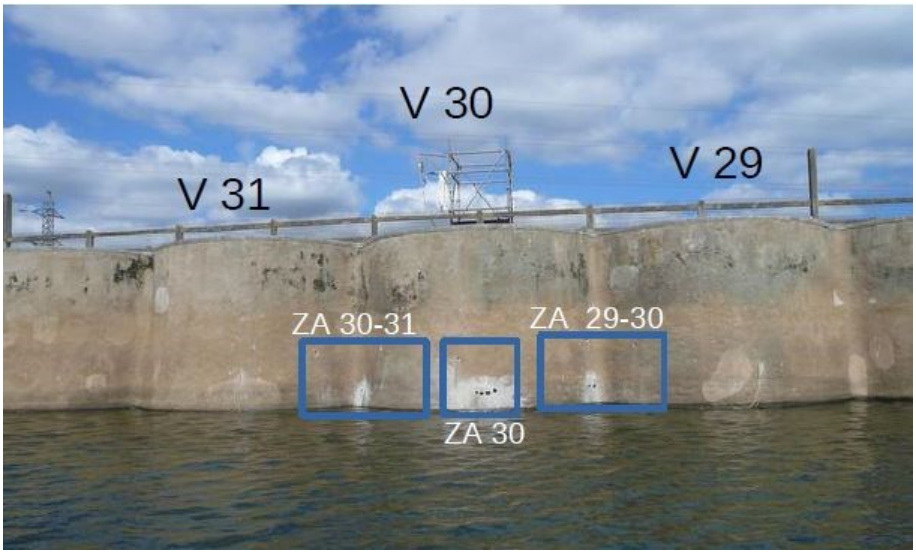

Figure 2.94. View of the 3 sub-areas of the upstream zone ZA 30

- upper Interior Zone (ZIH): Zone located on the downstream side in the upper part of the vault. This area is broken down into 3 sub-areas as follows (Figure 2.95):
  - ZIH 30: Key area of the vault n ° 30 (1 x 1 m),
  - ZIH 29-30: Spring of vault n° 30 at the junction with vault n° 29 (1 x 2 m),
  - ZIH 30-31: Spring of vault n° 30 at the junction with vault n° 31 (1 x 1 m).
- median Interior Zone (ZIM): Zone located on the downstream side at mid-height of the vault. This area is broken down into 3 sub-areas as follows:

- ZIM 30: Key zone of the vault n° 30 (1 x 1 m),
- ZIM 29-30: Vault / Buttress connection on the side of vault n° 29 (1 x 2 m),
- ZIM 30-31: Vault / Buttress connection on the side of vault n° 31 (1 x 2 m).

- lower Interior Zone (ZIB): Zone located on the downstream side in the lower part of the vault. This area is broken down into 3 sub-areas as follows:
  - ZIB 30: Key area of the vault n° 30 (1 x 1 m),
  - ZIB 29-30: buttress on the side of vault n° 29 (1 x 2 m),
  - ZIB 30-31: buttress on the side of vault n° 31 (1 x 2 m).

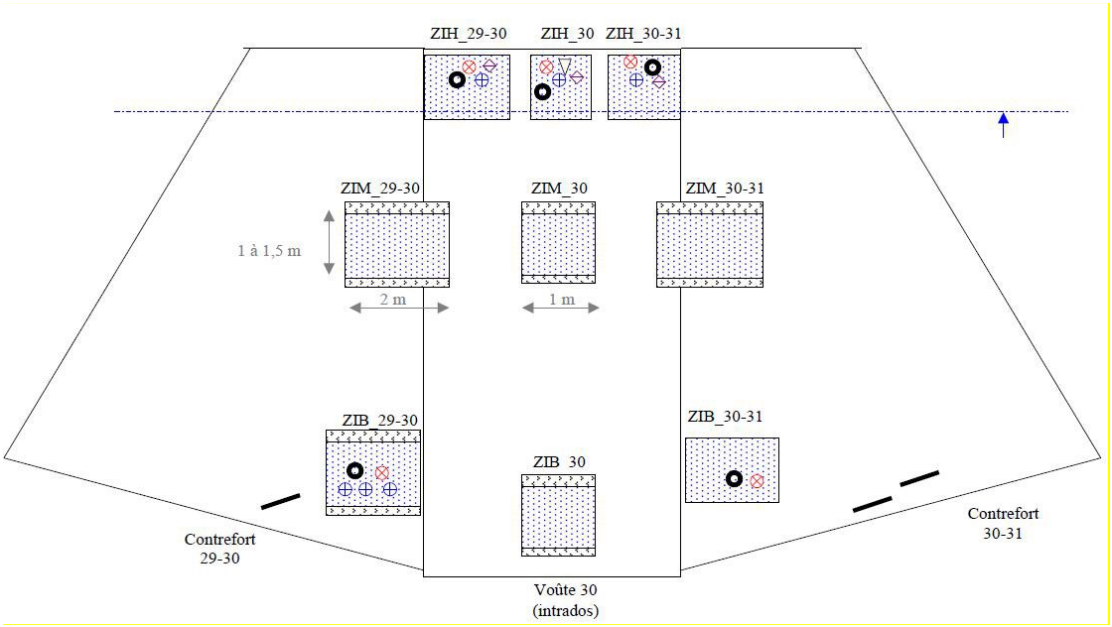

Figure 2.95: Location of the investigation zones on the downstream side

In addition, investigations were also carried out on the lower surface of the spans of the deck above vaults 2, 12 and 30, on the beam webs and soffits.

c. Results of investigations

Inspection

On the lower surface of the vault (downstream facing), there is a coating of the mortar or grout type. Occasionally this coating has disappeared following detachments. In the lower part of the vault, the facing is very wet or even dripping. Many deposits are present there (calcite, moss). The presence of the coating and these deposits hinders the examination of the facing and can mask the possible presence of cracks and defects in the concrete. The presence of active calcite is generalized throughout the facing. The exudations are mainly localized at the level of the concreting cold joints (Figure 2.96). In the lower part, mainly on the buttress 29-30, the exudates are tinged with rust. There are many localized repairs of small dimensions (< 1m) of the patch repair type mainly located at the concreting cold joints.

On the upper surface of the vault (upstream facing), the reinforced waterproofing mortar does not show any damage. Spot repairs of the patch repair type appear healthy.

Only few damages were observed on the current facing of the buttresses (Figure 2.97). The main disorders (concrete spalls with visible oxidized reinforcements) concern the stiffeners and crossbeams.

The beams of the deck show mainly a cracking of the webs with a horizontal tendency. Some cracks are filled with calcite (Figure 2.98). Occasionally, vertical cracks are present right on the steel stirrups. For one of the spans, water infiltration and runoff led to the formation of stalactites on the edge beam. Concrete spalls, mainly at the heel of a beam, reveal some reinforcements. A beam heel was autopsied locally. It shows longitudinal and transverse reinforcements exhibiting surface oxidation (Figure 2.99). The intrados of the slabs systematically shows cracking in both directions and spot repairs. In several places, the slabs show concrete spalls with visible oxidized reinforcements. Occasionally, water infiltration on the intrados was observed. Finally, the surface coating (a two-layer surface coating it seems) exhibits advanced wear with occasional blisters.

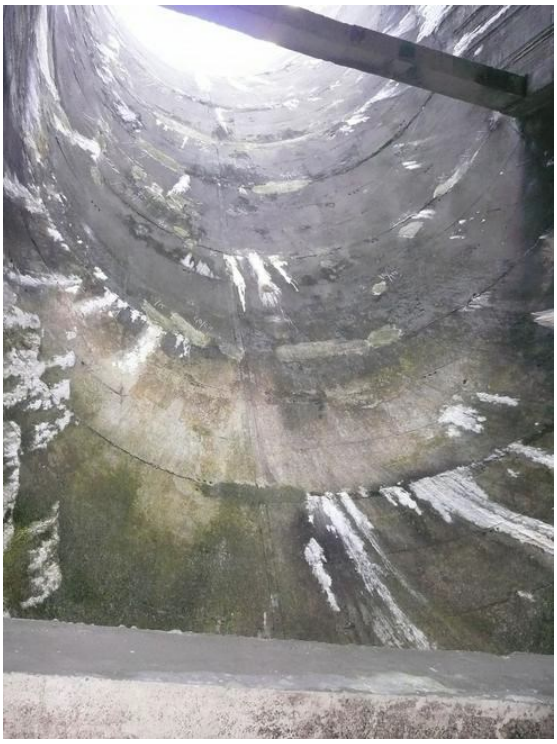

Figure 2.96. Presence of leakage with calcite in the vault between the cold joints

Figure 2.97. Concrete spalls on a buttress

Figure 2.98. Longitudinal cracking (with calcite) of an edge beam (upstream web) of the deck

Figure 2.99. Autopsy of a beam heel showing a surface oxidation of the longitudinal and transverse reinforcement

Concrete cover statistics

The cover measurements were processed statistically, and to facilitate analysis and interpretation, two characteristic covers are defined, in addition to the average cover:

- e_{95+}: 95 % of the covers measured are inferior to the e_{95+} cover;
- e_{95-}: 95 % of the covers measured are superior to the cover e_{95-}.

Table 2.106 presents the characteristic statistical values of the cover (in mm) in the different investigation zones.

Table 2.106. Statistical values of the cover (in mm) in the different investigation zones

Part-Zone		Horizontal (or longitudinal) Reinforcement					Vertical (or transversal) Reinforcement				
		Mean	Min	< 30 mm	e_{95+}	e_{95-}	Mean	Min	< 30 mm	e_{95+}	e_{95-}
ZIH	Spring Vault 30-31	47	12	9 %	23	61	57	48	0 %	49	67
	Spring Vault 29-30	36	11	6 %	16	47	58	33	0 %	43	66
	Vault Key	34	23	29 %	23	53	56	48	0 %	49	66
ZIM	Buttress V30-V31	48	25	8 %	28	66	56	37	0 %	39	71
	Buttress V29-V30	29	13	71 %	15	54	39	16	31 %	19	58
	Vault Key	42	23	11 %	29	54	51	28	14 %	33	58
ZIB	Buttress V30-V31	38	29	13 %	30	56	44	11	25 %	11	61
	Buttress V29-V30	43	18	22 %	21	56	60	29	9 %	31	75
	Vault Key	45	34	0 %	36	57	62	20	7 %	44	75

Figure 2.100 summarizes the cover values found.

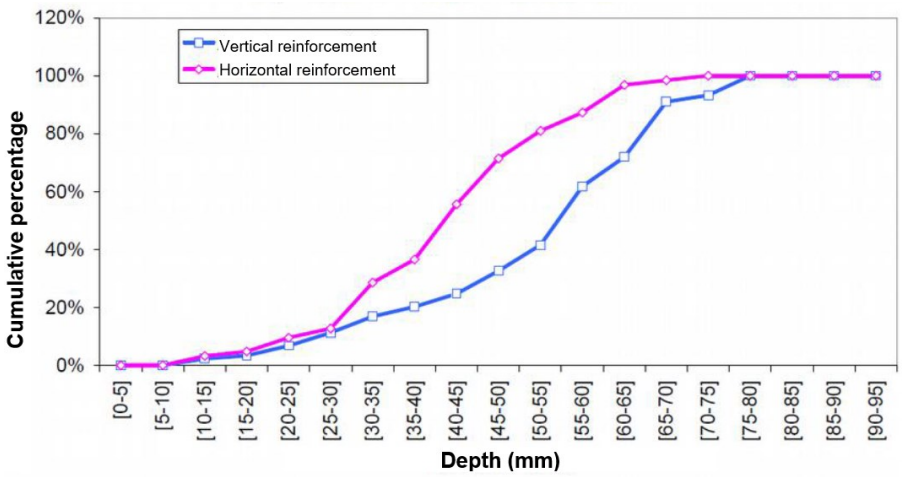

Figure 2.100. Statistical distribution of concrete covers for the vault 30 and the buttresses

On average, the measured covers are greater than the nominal covers indicated in the project file: 32 to 36 mm for the "horizontal" reinforcements of the vault underside and 20 mm for the "horizontal" reinforcements of the buttresses.

However, a significant proportion of the measured covers are lower than the covers expected today for this type of environment. Some covers can be very weak (on the order of a centimetre). These are logically the most affected horizontal reinforcements (the closest to the facing by design). Overall, between 10 and 20 % of the covers of these reinforcements are less than 30 mm.

In general, there is great variability in the measured covers and it seems difficult to identify behavioural trends depending on the position on the facing (top part, middle part, bottom part).

In the areas of the deck that have been the subject of measurements, we can overall see that a large proportion of transverse reinforcements of the beams and the slabs have a cover less than 30 mm (from 38 to 100 % for 9 areas considered). For 4 measurement zones, the measured covers are all greater than 30 mm. The longitudinal reinforcements of the slabs are better covered (by design). However, a significant proportion of them have a coating of less than 30 mm (up to 25 % for the slab upstream of span 2).

While the covers seem homogeneous in the different areas of the slabs, the same is not true on beams where the measured covers vary greatly from one area to another. In these areas where the reinforcements are less well protected (low covers), the risk of corrosion is greater. This analysis is corroborated by the general observation of longitudinal and transverse cracking of the soffit of the slabs and the occasional presence of concrete spalls and corroded visible reinforcement.

The following graph (Figure 2.101) shows the statistical distributions of the coverings measured on the crowning platform (deck) of vaults 2, 12 and 30.

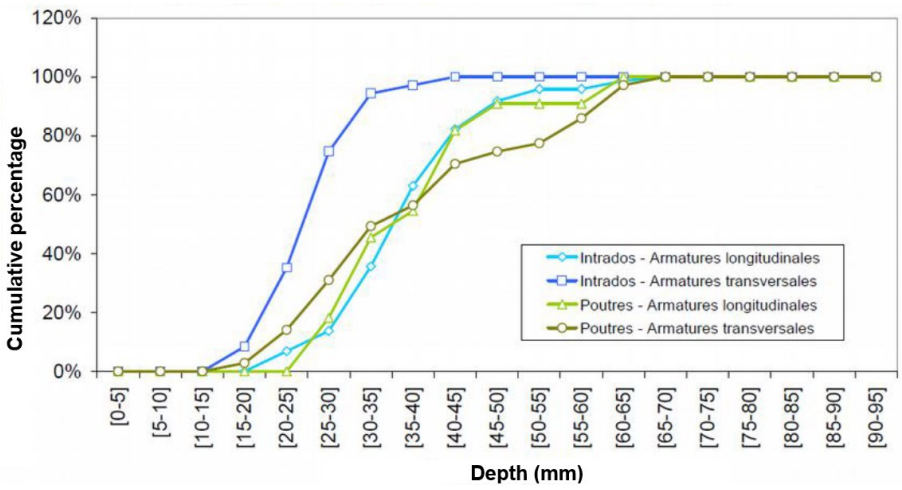

Figure 2.101. Statistical distribution of concrete covers for the deck over vaults 2, 12 and 30

Durability indicators

The table 2.107 summarizes all the results obtained with the durability indicators.

For the vault n°30 and its buttresses, globally the results show a concrete that is not very durable with regard to the corrosion of the reinforcements. The tests carried out on the concrete taken from the buttress in the lower part indicate a relatively better durability (very low to low potential durability class) than that obtained on the concrete of the vault in the upper part (very low durability class). None of the indicators meet the criteria of fascicule 65. Within the same area, there is a slight variability in the results. However, this variability remains insignificant overall, except for the indicator "apparent coefficient of chloride diffusion" for which the individual results may lead to a better class of potential durability, and to a lesser extent for the "water permeability" indicator.

Table 2.107. Values of the measured durability indicators

Durability Indicators		Vault ZIH 30 (C12/C16/C21)	Buttress ZIB 30-31 (C25/C26/C27)	V30 Central beam (C3/C4)	V2 Central beam (C8/C9)	V12 Central beam (C15/C16)
Apparent coefficient of chloride diffusion (10^{-12} m².s^{-1})	D_{rcm}	64.6 (78.9/66.0/48.9)	15.9 (9.2/12.6/26)	76.5 (71/82)	42.0 (60.0/24.1)	26.5 (16.6/36.4)
Electrical resistivity (Ω.m)	Res	25 (23/20/32)	32 (33/35/28)	26.5 (28/25)	42 (40/44)	50 (61/39)
Porosity accessible to water (%)	P_{water}	21.2 (21.1/22.4/20.1)	18.5 (17.6/18.3/19.7)	20.9 (20.7/21.1)	15.9 (16.6/15.3)	18.4 (17.4/19.5)
Gas Permeability (10^{-18} m²)	K_{gas}	3408 # (XX*/3408/XX*)	520 (312/322/925)	4824 # (3355/6287)	XX (XX*/XX*)	1277 # (1434/1121)
Other characteristics						
Permeability to liquid water (kg.m^{-2}.s$^{-0,5}$)	w	2.37 (2.69/2.59/1.85)	1.04 (1.36/0.85/0.91)	2.74 (2.68/2.81)	1.93 (2.19/1.68)	1.36 (1.28/1.44)
Density (kg/m^3)	ρ_b	2127.1 (2142.9/2111.3/ 2167.2)	2130.8 (2137.4/2124.2 /2124.7)	2141.2 (2147.0 / 2135.4)	2267.7 (2253.7/ 2281.7)	2195.2 (2221.5 / 2168.9)
Coefficient of capillary absorption at 24h (kg/m²)	C_a	9.10 (8.91/9.10/7.75)	5.36 (7.40/4.10/4.56)	9.63 (9.54/9.73)	6.87 (7.19/6.55)	6.96 (6.52/7.41)

** Not measurable due to too much flow* *# Values not considered in the following sections*

Potential durability classes (according to AFGC, 2004)				
Very low	Low	Average	High	Very high

For the crown platform (deck), the results are very close to those obtained on the vault and the buttress. Overall, the results show a concrete that is not very durable with regard to the corrosion of the reinforcements. The worst results are obtained on the concrete taken from the beam of the deck above the vault n°30.

With regard to the considered exposure (corrosion induced by carbonation), these durability classes correspond to a very low to low potential durability class (according to the AFGC 2004 guide) and to a potential lifespan (initiation of corrosion) of the order of 30 years, which is confirmed by the appearance of cracks in the 1950s and the patch repair in the 1970s.

Porosity

In its 1998 study, the CEBTP determined the porosity from 20 samples distributed over the entire structure on the downstream side. At the time, these measures had not been exploited. The Figure 2.102 shows the porosity values obtained on the structure and located accordingly to the altimetric range and the vault numbers.

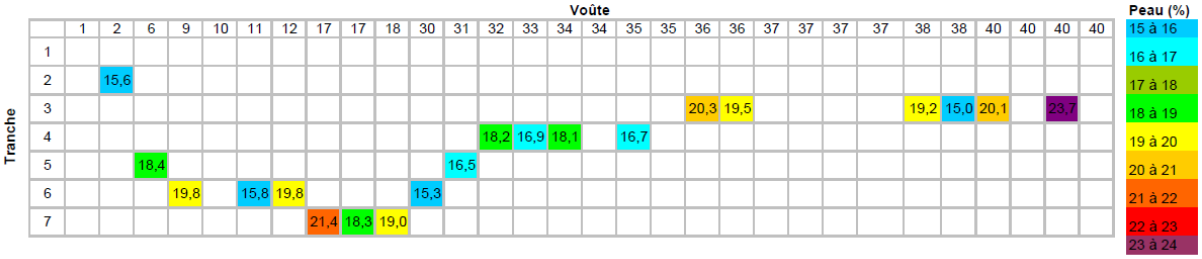

Figure 2.102. Porosities measured in 1998 by CEBTP on most of the vaults

There is a very significant variability in the porosity (from 15 to 23.7 %) without being able to identify any particular trend (depending on the altimetry or the vault numbers). The results obtained in 2016 confirm this finding. They also show significant variability within a single vault and within a single vault elevation section.

Regarding chloride penetration, the shape of the profiles does not indicate a process of chloride penetration from the reservoir water. The measured concentrations are very clearly below the critical corrosion initiation concentration regardless of the depth in the concrete. Given the covering of the reinforcements on the upstream facing, the risk of corrosion of the reinforcements due to the penetration of chlorides can be excluded.

Regarding sulphate penetration, the shape of the profiles does not indicate a process of sulphate penetration from the reservoir water. As an indication, it is observed that the measured concentrations are mostly close to the threshold concentration of standard NF EN197-1 (4 %, by % of the cement mass). It therefore seems reasonable to exclude a process of deterioration of the concrete due to a pollution by sulphates from the reservoir.

Carbonation depth

On the upstream facing of the dam (with waterproofing mortar), the carbonation depths are low, between 1 and 9 mm. Note that this phenomenon of carbonation is present in areas usually submerged.

On the downstream facing of the dam:

- at the top of the vaults (ZIH), the carbonation depths are between 10 and 37 mm (19 mm on average);
- in the lower part, on the buttresses (ZIB), the carbonation depths are low, between 0 and 5 mm.

On the downstream side, the carbonation depths are therefore very variable (from 0 to 37 mm). Lower carbonation depths (less than 5 mm) are observed in the lower part where humidity is greater.

Regarding the crown platform, there is overall a significant variability in the carbonation depth: from 0 to 31 mm (11 mm on average). The results do not allow the identification of specific behaviour between the spans, nor between the beams of the same span.

In its 1998 study, the CEBTP determined the carbonation depth from 32 samples distributed over the entire structure on the downstream side. At the time, these measures had not been exploited. The Figure 2.103 shows the carbonation depth values obtained on the structure and positioned according to the altimetric range and the vault numbers.

This Figure 2.103 shows a significant variability in the depth of carbonation (from 0 to 45 mm) without being able to identify any particular trend (depending on the altimetry or the vault numbers).

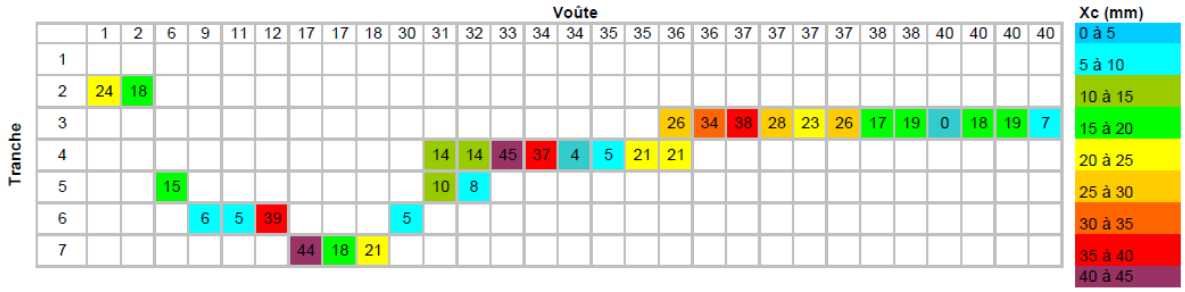

Figure 2.103. Carbonation depths measured in 1998 by the CEBTP on all the vaults

An analysis of the CEBTP data does not show a correlation between carbonation depths and porosity values (see Figure 2.104).

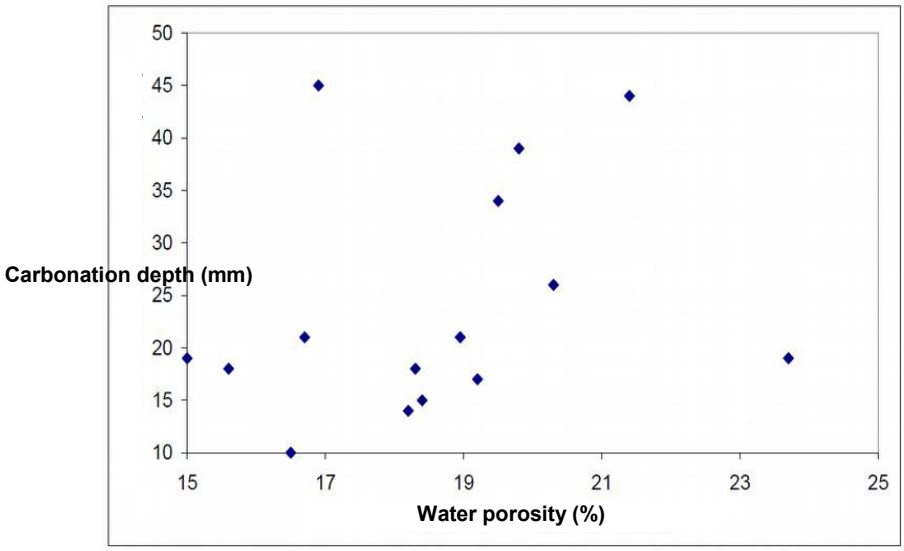

Figure 2.104. Evolution of the carbonation depth as a function of the porosity

Concerning the risk of depassivation of the reinforcements, the analysis based on the crossing of information from the statistical record of the covers and the carbonation front depths, is difficult to carry out because the cover and the carbonation depth are both significantly variable parameters. The analysis is nevertheless attempted with the carbonation depths measured by the Cerema on the downstream facing of the vault n° 30 and its associated buttresses. The carbonation process has been shown to differ between the upper vault zone (ZIH) and the lower vault zone (ZIB). In the ZIH zone, the average carbonation depth is 19 mm. In the ZIB zone, the carbonation depths are less than 5 mm. The following Table 2.108 gives estimates of the percentage of reinforcement located in carbonated concrete.

Table 2.108. Estimation of the percentage of reinforcement located in a carbonated concrete

Part of the dam		Horizontal reinforcement	Vertical reinforcement
Vault V30	ZIH	9.5 %	1 %
Buttresses V30	ZIH	11.5 %	10.5 %
	ZIB	0 %	0 %
All zones together (vault and buttresses) V30	ZIH	7.5 %	5 %

For the crown platform, the Table 2.109 presents, for the different parts considered, the statistical percentage of reinforcements located in carbonated concrete and therefore likely to be exceeded; and this with three cases of carbonation depth: 11 mm (average value measured), 20 and 30 mm (values measured in certain areas).

This table shows that given the statistical distribution of the covers, depending on the zones considered, the statistical percentage of reinforcements located in carbonated concrete can be significant (up to 40 % for transverse reinforcements). The probability of corrosion is higher for reinforcements located on the soffit of slabs.

Table 2.109: Estimate of the percentage of reinforcement located in a carbonated concrete according to the depth of carbonation.

Part of the dam	Horizontal reinforcement			Vertical reinforcement		
	Xc = 11 mm	Xc = 20 mm	Xc = 30 mm	Xc = 11 mm	Xc =20 mm	Xc = 30 mm
Intrados of the slab	0 %	3,5 %	25 %	0 %	21.5 %	42 %
Beams	0 %	0 %	16 %	0 %	8.5 %	40 %

Compressive strength

One observes a relative homogeneity of the concrete strengths on the upper part of the vault V30 (between 23.3 and 28.3 MPa). On the lower part (concrete of the buttresses), the strengths are higher and more heterogeneous (from 33.8 to 53 MPa). These results (concrete strengths of the buttresses higher than those of the vault) are also in line with the results of the durability indicators.

The compressive strength results measured on spans 2, 12 and 30 of the crowning platform (deck) show significant variability (from 19.9 to 39.1 MPa - 30.8 MPa on average) without being able to identify any particular trend.

In its 1998 study, the CEBTP determined the compressive strength from 19 samples distributed over the entire structure on the downstream side. The Figure 2.105 shows the compressive strength values obtained on the structure and positioned according to the altimetric range and the vault numbers.

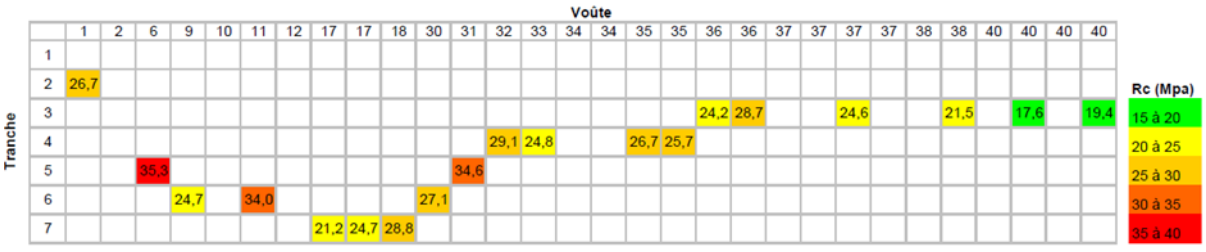

Figure 2.105: Compressive strengths measured in 1998 by the CEBTP on most of the vaults.

There is a relative variability of the compressive strength (from 17.6 to 35.3 MPa) without being able to identify any particular trend (depending on the altimetry or the vault number).

Resistivity

In the upper part (ZIH), the resistivities vary between 10 and 800 kΩ.cm. These high resistivities measured in certain areas could be explained by a concrete containing a slag cement (type CEM III). In this part, the low resistivities could then correspond to a more humid or weakly compact concrete. Note that carbonation can also lead to higher resistivities of the concrete (of the order of 1000 kΩ.cm for a CEM I type concrete).

In the middle and lower part (ZIM and ZIB), the resistivities are significantly lower (on average of the order of 30 to 50 kΩ.cm). In the hypothesis of a concrete made with a slag cement, these low resistivities are the indication of a wet and / or weakly compacted concrete.

The lowest resistivities are obtained in the lower part (ZIB). Note that the facings of the lower part of the vault n° 30 are very wet or even runny in places, which can explain these low resistivities.

Furthermore, the resistivities are very dispersed within each of the zones; which could be linked to a material heterogeneity. Finally, within the reinforcement meshes of most of the investigation areas, the measurements are hardly repeatable. This poor repeatability can have several origins: local heterogeneity of the material, facing defects disturbing the measurement, excessive reinforcement density, presence of a cement coating for example.

On the beams of the crowning platform, the resistivity values are mainly between 20 and 30 kΩ.cm, corresponding to a concrete conducive to corrosion (low compactness and / or wet). Certain zones have very low values (< 20): central beams of spans 12 and 30. Conversely, certain zones have relatively high values (> 100): span 30 (downstream beam, upstream beam), span 12 (downstream beam).

Half-cell potential measurements

On the downstream facing of the V30 vault, and for horizontal reinforcements, overall, the lower the investigation area, the more electronegative the potentials. The most electronegative potentials were measured in the lower part (ZIB) and more particularly in the ZIB_29-30 zone. This general trend is probably due to the higher concrete humidity at the bottom. Some areas show significant gradients (ZIH_29-30, ZIM_30-31 and ZIB_30-31). These strong gradients could be symptomatic of anodic zones and therefore of the presence of corroded reinforcements.

On the downstream facing of the V30 vault, and for the vertical reinforcements, the same trends are found as for the horizontal reinforcements. The gradients previously observed in zones ZIH_29-30 and ZIM_30-31 are however less marked. In the zone ZIB_30-31, a second zone of important gradients is observed.

Mineralogical analysis of concrete

Three cores were taken from the following areas:

- Key of vault n°30 upstream: on key of V30, upstream side, in a normally submerged area, with a 4 cm waterproofing coating;
- Downstream beam of the deck on the vault n°2: on the upstream face of the downstream beam of the crown platform above the vault 2;
- ZIH 30: in the upper interior area of the key of vault V30, downstream side.

The results are presented in Table 2.110.

Table 2.110. Various contents obtained from the mineralogical analysis

	Porosity accessible to water (%)	Cement content (kg/m^3)	Chlorides content (%/cement mass)	Na_2O_{eq} (kg/m^3 of concrete)	Slag content of cement (%)
Key of the vault 30 upstream	-	290	0,4	3,2	38
Downstream beam above vault V2	17,6	360	0,4	3,2	25
ZIH 30	20,7	400	0,2	3,8	33

The cement used is therefore a cement composed with blast furnace slag. The cementitious binder has strong micro-porosities, a lack of cohesion and traces of dissolution of the cement paste. The cores of the beam and of the ZIH are affected by a sulphate reaction of strong magnitude (presence of ettringite in compressed form and in the form of needles) and show the presence of chlorides and sulphates in depth, which can be explained by water circulations within the concrete which also cause leaching and dissolution / recrystallization phenomena.

3.3.8.3 Investigations carried out during the PerfDub project

No additional investigation was carried out as part of the PerfDuB project.

3.3.8.4 Conclusions drawn

The diagnostic test carried out on the vault n° 30 and its buttresses shows that the dam is in a good structural condition given its age (84 years).

On the downstream facing, the visual findings mainly relate to the signs of water infiltration observed on the lower surface of the vault at the level of the concrete cold joints (the latter have also been the subject of repairs in the past and appear to indicate original workmanship defects). In the lower part, these infiltrations are accompanied in places by rust-colored stains, suggesting corrosion of the reinforcements. In addition, very few signs of corrosion of the reinforcements were observed (cracks, concrete spalls with visible oxidized reinforcements). These latter are mainly present on stiffeners and crossbeams. On the upstream facing, no degradation was observed. In the examined areas, the waterproofing mortar appears sound and intact.

The investigations show that the main risk of deterioration is the corrosion of the reinforcements due to the corrosion process. On the upstream side, this risk is very low (even negligible), even in the long term. On the downstream side, given the covers and carbonation depths measured, the risk of medium-term corrosion cannot be excluded. In areas with weak covers and / or greater carbonation depths, the risk of short-term corrosion exists. In certain areas, it is now estimated at ~ 10 % the proportion of reinforcement likely to be depassivated and thus to initiate corrosion.

The durability properties of the concrete constituting the vault and the buttresses (low to very low potential durability) point in the same direction, as do the measurements of resistivity and reinforcement half-cell potential. As the phenomenon of carbonation and corrosion is progressive, we should therefore expect the regular appearance of disorders such as cracks and spalls of concrete in the years to come.

The spans of the crowning platform (beams and soffit of slabs) are generally in poor condition. This is mainly damage due to the corrosion of the reinforcements (cracking, spalling of the concrete visible, oxidized reinforcements). These deteriorations are generalized. In addition, the failure (or absence) of the waterproofing on the upper surface of the span is unfavorable to the durability of the structure. The deteriorations observed are due to corrosion of the reinforcements induced by the carbonation of the concrete. In some areas, the progress of the process is such that an estimated 40 % of the reinforcement is likely to be depassivated.

4 Synthesis of durability indicators

4.1 Operating mode

Various operating modes for measuring the durability indicators have been used for this study, due to the improvements provided during the PerfDub National Project and the incorporation of former studies. A synthesis of operating modes used for each structure are exposed in Tables 2.111 and 2.112.

Table 2.111. Synthesis of operating modes used for investigations

Investigated structure	Operating modes
Vasco de Gama	D_{rcm}: Tang & Nilsson (1992) ; P_{water}: AFREM (1997); K_{gas}: AFREM (1997, with O_2); RCPT: AASHTO T277-3 (1993)
Rion Antirion	D_{rcm}: Tang Luping (same principle than NT BUILD 492); P_{water} and K_{gas}: AFPC-AFREM (1997); P_{water}; RCPT: no specified; accelerated carbonation: 50 % CO_2.
Bruche	K_{gas}: XP P18-463; $P_{Ifsttar}$: NF P18-459; P_{water} and D_{rcm}: Mod.Op. PerfDub; C_{a24h}: $Xc_{j,\ 3\%}$: Mod.Op. PerfDub V2 with a 3 % CO_2 content.
Chateaubriand	2013 measurements: LCPC (2010) requirements: D_{rcm}, Res, K_{gas}, P_{water} 2016 measurements: Res, D_{rcm}, K_{gas}, P_{water}: LCPC (2010) requirements, completed by XP P18-462, XP P18-463, NF P18-459 and Grandubé (2007) operating modes. Accelerated carbonation: Mod.Op. PerfDub V2 with a 3 % CO_2 content.
TCD wharf	2012 measurements: LCPC (2010) requirements: D_{rcm}, Res, K_{gas}, P_{water} 2016 measurements: D_{rcm}, K_{gas}, P_{water}: LCPC (2010) requirements, completed by XP P18-462, XP P18-463, NF P18-459 and Grandubé (2007) operating modes. $P_{Ifsttar}$: NF P18-459. Accelerated carbonation: Mod.Op. PerfDub V2 with a 3 % CO_2 content.
PI Blondel	P_{water} and C_a: Mod.Op. PerfDub ind 1 (31/01/2016); D_{rcm} and K_{gas}: Mod.Op. PerfDub ind 1 du 2/10/2015; Accelerated carbonation: NF EN 14630, XP P18-458 with a 50 % CO_2 content.
Volesvre	Buiding phase: LCPC (2010) requirements. Diagnostic phase: Mod.Op. PerfDub
Loudéac	Buiding phase: P_{water}: NF P18-459; D_{rcm}: XP P18-462; K_{gas}: XP P18-463; Res: Mod.Op. LCPC. Diagnostic: Res, D_{rcm}, K_{gas}, P_{water}: LCPC (2010) requirements, completed by XP P18-462, XP P18-463, NF P18-459 and Grandubé (2007) operating modes. Accelerated carbonation: Mod.Op. PerfDub V2 with a 3 % CO_2 content.
Bordeaux Labor Exchange	Measurements performed in 51 mm diameter cores. P_{water}: NF P18-459; K_{gas}: Mod.Op. PerfDub V2 (O_2, saturation in accordance with NF P18-459).
Iena Palace	Measurements performed in 51 mm diameter cores. P_{water}: NF P18-459; K_{gas}: Mod.Op. PerfDub V2 (O_2, saturation in accordance with NF P18-459).
Vachette	P_{water} and C_a: Mod.Op. PerfDub ind 2 du 26/06/2017; D_{rcm}: Mod.Op. PerfDub ind 2 du 21/06/2017; K_{gas}: Mod.Op. PerfDub ind 2 du 28/06/2017; $Xc_{j,3/50\%}$: Mod.Op. PerfDub NF et EN ind 2; L_{barre}: ASTM C457-08; E: XP P18-420; gel: NF P18-424.
X bridge	D_{rcm}, K_{gas}, P_{water}: LCPC (2010) requirements, completed by XP P18-462, XP P18-463, NF P18-459 and Grandubé (2007) operating modes.
St Poncy	D_{rcm}: XP P 18-462; Res: Mod.Op. PerfDub; P_{water}: NF P 18-459; K_{gas}: XP P18-463; C_{a24h}: AFPC-AFREM; E: XP P 18-420; freeze/thaw: NF P 18-424; L_{barre}: ASTM C457-08. Accelerated carbonation: Mod.Op. PerfDub with 3 % and 50 % CO_2 content.

Pirou	D_{rcm}: XP P 18-462; Res: Mod.Op. PerfDub; P_{water}: NF P 18-459; K_{gas}: XP P18-463; C_{a24h}: AFPC-AFREM; E: XP P 18-420; freeze/thaw: NF P 18-424; L_{barre}: ASTM C457-08. Accelerated carbonation: Mod.Op. PerfDub with 3 % and 50 % CO_2.
Boutiron	D_{rcm}: XP P 18-462; Res: Mod.Op. PerfDub; P_{water}: NF P 18-459; K_{gas}: XP P18-463; C_{a48h}: AFPC-AFREM.
Ré	D_{rcm}: XP P18-462; Res: LCPC (2010) requirements; P_{water}: NF P18-459; K_{gas}: XP P18-463; C_{a24h} and w: Grandubé 2007.
Vallières	D_{rcm}; Res; P_{water}; K_{gas}: Mode opératoire PerfDub ind3 du 11/12/2018; E: XP P18-420; freeze/thaw: NF P 18-424; L_{barre}: ASTM C 457-08. Accelerated carbonation: Mod.Op. PerfDub ind3 with 3 % and 50 % CO_2 content.
X Marine structure	P_{water} and C_{a24h}: Mod.Op. PerfDub ind1 du 31/01/2016; D_{rcm} and K_{gas}: Mod.Op. PerfDub ind1 du 2/10/2015. Accelerated carbonation: Mod.Op. PerfDub ind3 with 3 % and 50 % CO_2 content.
BHP2000	P_{water}: AFPC-AFREM. D_{rcm}: Tang & Nilsson (1992); K_{gas}: CEMBUREAU.

P_{water} and $P_{Ifsttar}$: water porosity; C_{a24h}: capillary water absorption at 24 hours; D_{rcm}: rapid chloride migration; K_{gas}: gas permeability; Res: electrical resistivity; $Xc_{j,x/\,y\%}$: accelerated carbonation at x days and y % of CO_2; L_{barre}: spacing factor of air bubbles; E: scaling; w=water permeability

Table 2.112. Synthesis of operating modes used for each measurement of durability indicators

Measure	Operating modes
Rapid chloride migration (D_{rcm})	XP P18-462 Tang & Nilsson (1992), Tang Luping (principle of NT BUILD 492) Mod.Op. PerfDub LCPC (2010) requirements, completed by XP P18-462, XP P18-463, NF P18-459 and operating mode Grandubé (2007)
RCPT	AASHTO T277-3 (1993)
Water porosity (P_{water}) saturation duration: AFREM (1997): 24h LCPC (2010): 72h Others: 48h	AFREM, 1997 NF P18-459 NF P18-459 in 51 mm diameter cores Mod.Op. PerfDub LCPC (2010) requirements, completed by XP P18-462, XP P18-463, NF P18-459 and operating mode Grandubé (2007)
Gas permeability (K_{gas})	CEMBUREAU; AFREM, 1997; XP P18-463 LCPC (2010) requirements, completed by XP P18-462, XP P18-463, NF P18-459 and operating mode Grandubé (2007) Mod.Op. PerfDub, Mod.Op. PerfDub V2 with saturation according to NF P18-459, measure with O_2 on 51 mm diameter cores
Accelerated carbonation	NF EN 14630, XP P18-458 with a 4 % and 50 % CO_2 content Mod.Op. PerfDub (3 % and 50 %)
Electrical resistivity (Res)	LCPC (2010) requirements, completed by XP P18-462, XP P18-463, NF P18-459 and operating mode Grandubé (2007) Mod.Op. PerfDub
Capillary absorption coefficient (Ca)	Mod.Op. PerfDub Grandubé (2007)
Water permeability	Grandubé (2007)
Air bubbles spacing factor (L_{barre})	ASTM C457-08
Scaling	XP P18-420
Freeze/thaw	NF P18-424

A comparison of operating modes for accelerated carbonation tests gives the following results:

- Mod.Op. PerfDub V2 with a 3 % CO_2 content is equivalent to Mod.Op. PerfDub V3/V4 with a 3 % CO_2 content;
- XP P18-458 with a 50 % CO_2 content is close to Mod.Op. PerfDub with a 50 % CO_2 content. In the last one, a week of cooling at 20°C is added after the 45°C heat curing;
- NF EN 14630 with 4 % CO_2 content has no equivalence (4 % CO_2 content and no heat curing);
- Mod.Op. PerfDub (V2, V3 and V4) with a 3 % and 50 % CO_2 content have the same preconditioning but different CO_2 content. Thus, they are not equivalent. Nevertheless, a linear relation has been obtained in the PerfDub National Project.

4.2 Main results

A synthesis of the main measurements of the durability indicators is exposed in the following Tables 2.113 to 2.131.

4.2.1 Structures below 20 years old

Table 2.113. Synthesis of the main results of the durability indicators for Vasco de Gama bridge

Structure Building Date	Investigated element Exposure class	Age	fc	Durability indicator at the age t of investigations)	Core orientation (H/V)
Vasco de Gama (central viaduct) 1995-1998	Caissons of piers XS3	17 m	-	D_{rcm} = 0.8.10^{-12} m²/s P_{water} = 10.7 % K_{gas} = 11.10^{-18} m² Aashto = 500 C	
	Caissons of piers XS3	43 m	-	D_{rcm} = 0.2.10^{-12} m²/s P_{water} = 10.6 % K_{gas} = 4.10^{-18} m²	
	Durability indicators at construction phase				
	$D_{rcm,90}$ = 3.4.10^{-12} m²/s; $P_{water28j}$ = 12,4 % K_{gas28j} = 58.10^{-18} m² $Aashto_{28}$ = 5100 C; $Aashto_{90}$ = 1700 C			*Ageing factor* on D_{rcm}: D_{rcm} (t) = 2.10^{-12}.e$^{-0,0527t}$ for t < 60 months D_{rcm} = 0.16 10^{-12} m²/s for t ≥ 60 months	
Vasco de Gama (South viaduct) 1995-1998	columns XS3	6 m	-	D_{rcm} = 1.1.10^{-12} m²/s P_{water} = 13.6 % K_{gas} = 48.10^{-18} m² Aashto = 950 C	H
	columns XS3	18 m	-	D_{rcm} = 1.0.10^{-12} m²/s P_{water} = 12.8 % K_{gas} = 20.10^{-18} m² Aashto = 500 C	H
	columns XS3	29 m	-	D_{rcm} = 0.7.10^{-12} m²/s P_{water} = 13.9 % K_{gas} = 7.10^{-18} m²	H

Vasco de Gama (South viaduct) 1995-1998	**Durability indicators at construction phase**	
	Laboratory: $D_{rcm,90}$ = 0.5.10^{-12} m²/s; $D_{rcm,180}$ = 0.14.10^{-12} m²/s $P_{water,28}$ = 12.2 %; $P_{water,90}$ = 11.9 % $K_{gas,28,90,80}$ < 10.10^{-18} m² $Aashto_{28}$ = 4410 C; $Aashto_{90}$ = 1570 C; $Aashto_{180}$ = 840 C	Construction phase: $D_{rcm,28}$ = 1.5.10^{-12} m²/s; $D_{rcm,90}$ = 0.52.10^{-12} m²/s; $D_{rcm,180}$ = 0.22.10^{-12} m²/s $P_{water,28}$ = 12.9 % $K_{gas,28}$ = 32.10^{-18} m² $Aashto_{28}$ = 3490 C
	Ageing factor on D_{rcm} D_{rcm} (t) = 2.10^{-12}.e$^{-0,0322\ t}$ for t < 60 months D_{rcm} = 3.0 10^{-13} m²/s for t ≥ 60 months	

Table 2.114. Synthesis of the main results of the durability indicators for Rion-Antirion bridge

Structure Building Date	Investigated element Exposure class	Age	fc	Durability indicator at the age t of investigations)	Core orientation (H/V)
Rion Antirion 1999-2004	Piers and testing wall XS2 (immersed area) XS3 (tidal)	12.3 to 16.5 y	69 MPa (cylinders)	$D_{rcm,115}$ = 0.86.10^{-12} m²/s $P_{water,28}$ = 11.3 % $K_{gas,28}$ = 4.2.10^{-18} m² $RCPT_{90}$ = 220-660 C Control wall (2 years): $X_{c7/14/28/56\ 50\%}$ = 2.0 / 3.0 / 3.2 / 3.4 mm	H
	Durability indicators at construction phase				
	Ageing factor on D_{rcm} D_{rcm} (t) = 1.1 10^{-12}.t$^{-0.215}$ for t < 120 months D_{rcm} = 0.35 10^{-12} m²/s for t ≥ 120 months				

Table 2.115: Synthesis of the main results of the durability indicators for Volesvre bridge.

Structure Building Date	Investigated element Exposure class	Age	fc	Durability indicator at the age t of investigations)	Core orientation (H/V)
Volesvre 2010-2012	C5 abutment XC4	5 y	45.3 - 61.0 MPa (cylinders)	D_{rcm} = 11.2.10^{-12} m²/s Res = 637 Ω.m P_{water} = 14.6 % K_{gas} = 90.10^{-18} m² $C_{a,48h}$ = 4.68 kg/m²	H
	Deck slab XC4	5 y	53.0 - 65.7 MPa (cylinders)	D_{rcm} = 7.9.10^{-12} m²/s Res = 106 Ω.m P_{water} = 12.1 % K_{gas} = 80.10^{-18} m² $C_{a,48h}$ = 5.68 kg/m²	H
	Durability indicators at construction phase				
	Bridge piers: $P_{water,28}$ = 15.7 %; $P_{water,90}$ = 15.6 % $Res_{,28}$ = 276 Ω.m; $Res_{,90}$ = 323 Ω.m $K_{gas,90}$ = 76.10^{-18} m²			Deck: $P_{water,28}$ = 14.4 %; $P_{water,90}$ = 14.1 % Res_{28} = 62 Ω.m; Res_{90} = 119 Ω.m $K_{gas,90}$ = 75.10^{-18} m²	

Table 2.116: Synthesis of the main results of the durability indicators for Loudéac bridge.

Structure Building Date	Investigated element Exposure class	Age	fc	Durability indicator at the age t of investigations)	Core orientation (H/V)
Loudéac 2014	Wall XC4	2 y	69.5 MPa (cores, corrected values) 59.9 MPa (cylinders)	D_{rcm} = 2.4.10^{-12} m²/s Res = 377 Ω.m P_{water} = 15.4 % K_{gas} = 23.10^{-18} m² C_a = 4.95 kg/m² w = 0.744 kg.m^{-2}.s$^{-0,5}$ $X_{c,28/56,3\%}$ = 4.5 / 5.5 mm [Ca(OH)$_2$] pot / SAA / psd ATG = 10.5 / 13.4 / 11.9 %	H
Loudéac 2014	**Durability indicators at construction phase**				
	Initial tests: $P_{water,28}$ = 17 % $P_{water,90}$ = 16 % $K_{gas,28}$ = 18.10^{-18} m² $K_{gas,90}$ = 24.10^{-18} m²		Convenience: $D_{rcm,28}$ = 2.3.10^{-12} m²/s $D_{rcm,90}$ = 1.8.10^{-12} m²/s Res_{28} = 284 Ω.m Res_{90j} = 367 Ω.m $P_{water,90}$ = 14.4 % $K_{gas,90}$ = 35.10^{-18} m²	Controls: $D_{rcm,123}$ = 1.4.10^{-12} m²/s Res_{123} = 419 Ω.m $P_{water,123}$ = 15.8 % $K_{gas,123}$ = 39.10^{-18} m² $C_{a,24h,123}$ = 4.31 kg/m² w_{123} = 0.571 kg.m^{-2}.s$^{-0,5}$

Table 2.117: Synthesis of the main results of the durability indicators for the X Marine structure.

Structure Building Date	Investigated element Exposure class	Age	fc	Durability indicator at the age t of investigations)	Core orientation (H/V)
X Marine Structure 2014	control element XS3	2 y	87.3 MPa (cores, corrected values)	D_{rcm} = 1.9.10^{-12} m²/s P_{water} = 9.9 % K_{gas} = 20.10^{-18} m² C_{a24h} = 0.811 kg/m² $Xc_{28/56j,3\%}$ = 0 / 0 mm $Xc_{7/28j,50\%}$ = 0 / 0 mm	H
	Durability indicators at construction phase				
	Initial tests (firm): $P_{water,28}$ = 10.1 % $P_{water,90}$ = 10.4 % $D_{rcm,28}$ = 3.2.10^{-12} m²/s $D_{rcm,90}$ = 1.7.10^{-12} m²/s $K_{gas,28}$ = 29.10^{-18} m² $K_{gas,90}$ = 40.10^{-18} m²		Convenience (firm): $P_{water,28}$ = 10.5 % $P_{water,90}$ = 10.9 % $D_{rcm,28}$ = 3.4.10^{-12} m²/s $D_{rcm,90}$ = 2.0.10^{-12} m²/s $K_{gas,28}$ = 30.10^{-18} m² $K_{gas,90}$ = 64.10^{-18} m²	Convenience (independent control): $P_{water,28}$ = 11.3 % $P_{water,90}$ = 11.1 % $D_{rcm,28}$ = 4.8.10^{-12} m²/s $D_{rcm,90}$ = 2.9.10^{-12} m²/s $K_{gas,28}$ = 37.10^{-18} m² $K_{gas,90}$ = 28.10^{-18} m²
	Controls (firm): $P_{water,90}$ = 10.2 % $D_{rcm,90}$ = 2.7.10^{-12} m²/s $K_{gas,90}$ = 31.10^{-18} m²			Controls (independent): $P_{water,90}$ = 10.4 % $D_{rcm,90}$ = 2.6.10^{-12} m²/s $K_{gas,90}$ = 31.10^{-18} m²	

4.2.2 Structures between 20 and 50 years old

Table 2.118. Synthesis of the main results of the durability indicators for the TCD wharf

Structure Building Date	Investigated element Exposure class	Age	fc	Durability indicator at the age t of investigations)	Core orientation (H/V)
TCD wharf 1964-1965	Slab lateral face XS3	47 y	-	D_{rcm} = 2.3.10^{-12} m²/s Res = 68.5 Ω.m P_{water} = 11.3 % K_{gas} = 154.10^{-18} m²	H
	Intrados of the slab XS3 (sea spray)	51 y	73,0 MPa (cores, corrected values)	D_{rcm} = 4.1.10^{-12} m²/s Res = 159 Ω.m P_{water} = 12.8 % $P_{lfsttar}$ = 14.7 % K_{gas} = 89.10^{-18} m² C_a = 5.18 kg/m² w = 1.06 kg.m^{-2}.s$^{-0,5}$ $Xc_{28/56j,3\%}$ = 0 / 0 mm [Ca(OH)$_2$] pot / SAA / psdATG = 26.8 / 23.5 / 33.2 %	V

Table 2.119: Synthesis of the main results of the durability indicators for Chateaubriand bridge.

Structure Building Date	Investigated element Exposure class	Age	fc	Durability indicator at the age t of investigations)	Core orientation (H/V)
Chateaubriand 1987-1991	P14 pier XS3	22 y	46.7 MPa (cylinders)	D_{rcm} = 28.3.10^{-12} m²/s Res = 36 Ω.m P_{water} = 14.8 % $C_{a,24h}$ = 6.06 kg/m² K_{gas} = 871.10^{-18} m² w = 1.33 kg.m^{-2}.s$^{-0,5}$	H
	P11 (sea spray) and P12 tidal/splashes) piers XS3	25 y	46.7 MPa (cylinders)	D_{rcm} = 29.6.10^{-12} m²/s Res = 38 Ω.m P_{water} = 15.6 % $C_{a,24h}$ = 6.73 kg/m² K_{gas} = 415.10^{-18} m² w = 3.04 kg.m^{-2}.s$^{-0,5}$ $Xc_{,28/56,3\%}$ = 0 / 0 mm [$CaOH_2$] pot / SAA / psdATG = 38.2 / 39.9 / 23.0 %	H

Table 2.120. Synthesis of the main results of the durability indicators for the Vachette bridge

Structure Building Date	Investigated element Exposure class	Age	fc	Durability indicator at the age t of investigations)	Core orientation (H/V)
Vachette 1984-1985	Cornice XF4	34 y	57.6 MPa (cores, corrected values)	D_{rcm} = 19.6.10^{-12} m²/s P_{water} = 14 % K_{gas} = 150.10^{-18} m² [100, 200, 6000] $C_{a,\ 24h}$ = 1.96 kg/m² L_{barre} = 466 µm (2012) E = 7054 g/m² (2012)	H
	Abutment XF4	34 y	46 MPa (cores, corrected values)	D_{rcm} = 28.10^{-12} m²/s P_{water} = 13.5 % K_{gas} = 250.10^{-18} m² [200, 300, 2000] C_a = 3.15 kg/m² $Xc_{28/56,3\%}$ = 6 / 9 mm $Xc_{7/28,50\%}$ = 8 / 10 mm L_{barre} = 591 µm E = 10637 g/m² $\Delta l/l$ = 945 µm/m 100.Fn²/F0² = 38	H

Table 2.121. Synthesis of the main results of the durability indicators for the piers of the Ré bridge

Structure Building Date	Investigated element Exposure class	Age	fc	Durability indicator at the age t of investigations)	Core orientation (H/V)
Ré 1987-1988	Pb pier XS3	30 y	64.3 MPa (cores) 42.1 MPa (cylinders)	D_{rcm} = 8.5.10^{-12} m²/s Res = 139 Ω.m P_{water} = 12.1 % K_{gas} = 109.10^{-18} m² C_{a24h} = 4.80 kg/m² w = 0.91 kg.m^{-2}.s$^{-0,5}$	H
	Ph pier XS3	30 y	70.8 MPa (cores) 44.2 MPa (cores)	D_{rcm} = 8.7.10^{-12} m²/s Res = 76 Ω.m P_{water} = 15.3 % K_{gas} = 400.10^{-18} m² [264 - 1709 - 537] C_{a24h} = 1.16 kg/m² w = 0,23 kg.m^{-2}.s$^{-0,5}$	H
	Po pier XS3	30 y	64.5 MPa (cores) 37.8 MPa (cylinders)	D_{rcm} = 15.1.10^{-12} m²/s Res = 72 Ω.m P_{water} = 13.8 % K_{gas} = 174.10^{-18} m² C_{a24h} = 5.94 kg/m² w = 1.28 kg.m^{-2}.s$^{-0,5}$	H

Table 2.122: Synthesis of the main results of the durability indicators for the St-Poncy bridge.

Structure Building Date	Investigated element Exposure class	Age	fc	Durability indicator at the age t of investigations)	Core orientation (H/V)
St Poncy 1988	West pier XF4, XD3, XC4 severe frost & very frequent salting	31 y	C30/37 (cores, corrected values) 34.5 MPa (cylinders)	D_{rcm} = 41.2.10^{-12} m²/s Res = 38 Ω.m P_{water} = 16.7 % K_{gas} = 646.10^{-18} m² C_{a24h} = 5.79 kg/m² E = 50917 g/m² Δl/l = 1759 µm/m (26 cycles) 100.F_n^2/F_0^2 = 21 (26 cycles) L_{barre} = 373 µm $L_{barre, gb}$* = 279 µm $X_{c\ 28/56,3\%}$ = 11 / 16 mm $X_{c\ 7/28,50\%}$ = 15 / 28 mm	H

** Correction done by taking into account large bubbles*

Table 2.123. Synthesis of the main results of the durability indicators for the Pirou bridge

Structure Building Date	Investigated element Exposure class	Age	fc	Durability indicator at the age t of investigations)	Core orientation (H/V)
Pirou 1981	Pier XF4, XD3, XC4 Severe frost & very frequent salting	28 y	C70/85 (cores, corrected values)	D_{rcm} = 9.4.10^{-12} m²/s Res = 104 Ω.m P_{water} = 11.9 % K_{gas} = 240.10^{-18} m² C_{a24h} = 2.51 kg/m² E = 103 g/m² Δl/l = 289 µm/m 100.Fn²/F0² = 93 L_{barre} = 289 µm $L_{barre, gb}$ * = 257 µm $X_{c\ 28/56,3\%}$ = 0 / 0 mm $X_{c\ 7/28,50\%}$ = 0 / 0 mm	H

** Correction done by taking into account large bubbles*

4.2.3 Structures over 50 years old

Table 2.124. Synthesis of the main results of the durability indicators for the Bruche bridge

Structure Building Date	Investigated element Exposure class	Age	fc	Durability indicator at the age t of investigations)	Core orientation (H/V)
Bruche 1947	deck (corroded) XC4	70 y	39.0 MPa	D_{rcm} = 4.0.0^{-12} m²/s P_{water} = 14.2 % $C_{a,24h}$ = 5.48 kg/m² $C_{a,48h}$ = 6.06 kg/m² K_{gas} = 300.10^{-18} m² [2000, 3000, 300] $X_{c28/56,3\%}$ = 6.8 / 11.1 mm	V
	deck (healthy) XC4	70 y	39.0 MPa (cores)	D_{rcm} = 2.2.10^{-12} m²/s P_{water} = 14.7 % $P_{Ifsttar}$ = 12.8 % $C_{a,24h}$ = 5.42 kg/m² $C_{a,48h}$ = 6.33 kg/m²	V

Table 2.125. Synthesis of the main results of the durability indicators for the Blondel bridge

Structure Building Date	Investigated element Exposure class	Age	fc	Durability indicator at the age t of investigations)	Core orientation (H/V)
Pl Blondel 1964	Crossbeam XC4	51 y	32.0 MPa (cores)	D_{rcm} = 35.7.10^{-12} m²/s P_{water} = 17.7 % $P_{Ifsttar}$ = 17.1 % K_{gas} = 600.10^{-18} m² [2000, 3000, 600] C_{a24h} = 5.53 kg/m² $X_{c28/56j,4\%}$ = 10 / 11 mm $X_{c7/28j,50\%}$ = 11 / 23 mm	H
	Slabs XC4	51 y	35.6 MPa (cores)	D_{rcm} = 16.2.10^{-12} m²/s P_{water} = 13.2 % $P_{Ifsttar}$ = 12.5 % K_{gas} = 200.10^{-18} m² [8000, 200, 200] C_a = 3.29 kg/m² $X_{c28/56j,4\%}$ = 0 / 0 mm $X_{c7/28j,50\%}$ = 0 / 0 mm	V

Table 2.126. Synthesis of the main results of the durability indicators for the X bridge

Structure Building Date	Investigated element Exposure class	Age	fc	Durability indicator at the age t of investigations)	Core orientation (H/V)
X bridge 1952-1954	Arch (springing, tidal) XS3	60 y	C70/85 (cores, corrected values)	D_{rcm} = 10.2.10^{-12} m²/s Res = 82 Ω.m P_{water} = 12.2 % K_{gas} = 495.10^{-18} m² C_a = 3.89 kg/m² w = 0.80 kg.m^{-2}.s$^{-0,5}$	H

Table 2.127. Synthesis of the main results of the durability indicators for the Vallières bridge

Structure Building Date	Investigated element Exposure class	Age	fc	Durability indicator at the age t of investigations)	Core orientation (H/V)
Vallières Bridge 1926	Arch XF3 Severe frost	92 y	C25/30 (cores, corrected values)	D_{rcm} = 97.3 10^{-12} m²/s Res = 31 Ω.m P_{water} = 20,1 % K_{gas} = 700.10^{-18} m² (*) [700, 3000, not measurable] E = 11268 g/m² Δl/l = 610 µm/m [29 cycles] 100.F_{Fn}²/F_{F0}² = 36 [29 cycles] L_{barre} = 494 µm	H

(*): numerous microcracks in the cement matrix

Table 2.128. Synthesis of the main results of the durability indicators for the Boutiron bridge

Structure Building Date	Investigated element Exposure class	Age	fc	Durability indicator at the age t of investigations)	Core orientation (H/V)
Boutiron 1913	Arch XC4, XF1	107 y	43,6 to 52,4 MPa (cores, including reinforcements)	D_{rcm} = 34.3.10^{-12} m²/s (cores with reinforcements) Res = 37 Ω.m P_{water} = 16.4 % K_{gas} = 200.10^{-18} m² (cores with reinforcements) [224, 1830, 2080] $C_{a,24h}$ = 3.07 kg/m² $C_{a,48h}$ = 3.95 kg/m²	V

Table 2.129. Synthesis of the main results of the durability indicators for the Iena Palace

Structure Building Date	Investigated element Exposure class	Age	fc	Durability indicator at the age t of investigations)	Core orientation (H/V)
Iena Palace 1937	Facade beams XC4	80 y	-	P_{water} = 18.5 % K_{gas} = 805.10^{-18} m²	H

Table 2.130. Synthesis of the main results of the durability indicators for the Bordeaux Labor Exchange

Structure Building Date	Investigated element Exposure class	Age	fc	Durability indicator at the age t of investigations)	Core orientation (H/V)
Bordeaux Labor Exchange 1935-1938	Facade panels XC4	80 y	23 MPa	P_{water} = 13.0 % K_{gas} = 607 10^{-18} m²	-

Table 2.131. Synthesis of the main results of the durability indicators for the Vezins dam

Structure Building Date	Investigated element Exposure class	Age	fc	Durability indicator at the age t of investigations)	Core orientation (H/V)
Vezins Dam 1929-1932	ZIH 30 vault XC4	84 y	-	D_{rcm} = 64.6.10^{-12} m²/s Res = 25 Ω.m P_{water} = 21.2 % K_{gas} = irrelevant value $C_{a,24h}$ = 9.10 kg/m² w = 2.37 kg.m^{-2}.s$^{-0,5}$	-------
	ZIB 30-31 buttress XC4	84 y	-	D_{rcm} = 15.9.10^{-12} m²/s Res = 32 Ω.m P_{water} = 18.5 % K_{gas} = 520.10^{-18} m² C_{a24h} = 5.36 kg/m² w = 1.04 kg.m^{-2}.s$^{-0,5}$	-------
	V30 central beam XC4	84 y	-	D_{rcm} = 76.5.10^{-12} m²/s Res = 26.5 Ω.m P_{water} = 20.9 % K_{gas} = irrelevant value $C_{a,24h}$ = 9.63 kg/m² w = 2.74 kg.m^{-2}.s$^{-0,5}$	-------
	V2 central beam XC4	84 y	-	D_{rcm} = 42.0.10^{-12} m²/s Res = 42 Ω.m P_{water} = 15.9 % K_{gas}: not measurable $C_{a,24h}$ = 6.87 kg/m² w = 1.93 kg.m^{-2}.s$^{-0,5}$	-------
	V12 central beam XC4	84 y	-	D_{rcm} = 26.5.10^{-12} m²/s Res = 50 Ω.m P_{water} = 18.4 % K_{gas} = 1277.10^{-18} m² $C_{a,24h}$ = 6.96 kg/m² w = 1.36 kg.m^{-2}.s$^{-0,5}$	-------

(Age of investigations: m = months, y = years. Core orientation: H = horizontal, V = vertical)
P_{water} and $P_{Ifsttar}$: water porosity; $C_{a,24h}$: capillary water absorption at 24 hours; D_{rcm}: rapid chloride migration; K_{gas}: gas permeability; Res: electrical resistivity; $X_{c,x/y\%}$: accelerated carbonation at x days and y % of CO_2; L_{barre}: spacing factor of air bubbles; E: scaling; w=water permeability

5 Synthesis of lifetime indicators

5.1 Operating mode

The operating modes used to obtain chloride profiles are exposed in Table 2.132.

Table 2.132. Operating mode used for chloride content

Ouvrage	Operating modes
Vasco de Gama	Free and total chlorides: AFPC-AFREM
Rion Antirion	Free and total chlorides: AFPC-AFREM
Loudéac	Total chlorides: AFPC-AFREM
Quai des TCD	2012 measurements: free and total chlorides: AFPC-AFREM 2016 measurements: total chloride: AFPC-AFREM
Chateaubriand	2013 measurements: total chlorides: AFPC-AFREM 2016 measurements: total chlorides: AFPC-AFREM
Vachette	Free chlorides: AFPC-AFREM
Ré	Free chlorides: AFPC-AFREM (1997) and RILEM TC 178 TMC 2001, B1 procédure Total chlorides: RILEM TC 178 TMC 2002, A3-C4 procedure
Bruche	2012 measurements (healthy area): free and total chlorides: LCPC (2002) 2016 measurements (corroded area): free and total chlorides: AFPC-AFREM
PI Blondel	Free chlorides: AFPC-AFREM
X Bridge	Free an total chlorides: AFPC-AFREM

5.2 Main results

The lifetime indicators are exposed for each investigated structure in Table 2.133. Values obtained from chloride measurements are presented in section 7. Observations performed on investigated structures and results of electrochemical measurements are presented in Table 2.134.

Table 2.133. Carbonation depth and concrete cover of reinforcements measured on investigated structures

Structure Building	Investigated element (Exposure class)	Age (month / year)	Carbonation depth (mm)	Mean concrete cover e_{moy} (mm)
Structures below 20 years old				
Vasco de Gama (central)	Precast box (XS3: tidal, base of piers)	213 months	-	-
Vasco de Gama (Sud)	Piers (XS3: tidal)	213 months	-	-
Rion Antirion	Piers (element 19) (XS2: submerged area)	9 y	-	$C_{nom,\ min,\ théorique}$ = 60
	M2 pier (XS3: tidal)	45 months	-	$C_{nom,\ min,\ théorique}$ = 85

	M3 pier (element 19) (XS3: tidal)	114 months 201 months	-	$C_{nom,\ min,\ théorique}$ = 85
	Wall test (XS3: salt sprays and splash area)	2,5; 11; 24; 62; 150 months	-	-
Volesvre	Piers and deck (XC4)	5 y	-	-
Loudéac	Pier (XC4)	2 y	0	55
X Marine structure	Testing element (XS3: salt spray)	2 y	< 2,5	55 (on plans)
Structures between 20 and 50 years old				
TCD wharf	Slab lateral side (XS3)	47 y	< 1	39
	Intrados of slab (XS3)	51 y	-	40
Chateaubriand	Piers P11 (XS3: salt sprays)	22 y	P11: 0 mm	P11: 51 mm
	Piers P11 (salt spray) and P12 (tidal and splash area) (XS3)	25 y	P12 (tidal): 2,1 P12 (splash): 0 P11 (salt spray): 2,6	P11: 54 P12: 35
Vachette	Cornice (XF4)	34 y	External: < 8 Internal: < 17	40
	Abutment (XF4)	34 y	Left bank side: < 3 Right bank side: < 14	36
Ré	Pb pier (XS3: tidal) FC face, exposed to main winds and sunshine	30 y	0 in Z3	Horizontal reinforcements: 76 (e_{95}^{+} = 49 mm) Vertical reinforcements: 94 ($e_{95\%}^{+}$ = 64 mm)
	Ph pier (XS3: tidal) FC face, exposed to main winds and sunshine	30 y	0 in Z3	Horizontal reinforcements: 84 (e_{95}^{+} = 57 mm) Vertical reinforcements: 104 ($e_{95\%}^{+}$ = 57 mm)
	Po pier (XS3: tidal) FC face, exposed to main winds and sunshine	30 y	0 in Z3	Horizontal reinforcements: 85 (e_{95}^{+} = 61 mm) Vertical reinforcements: 99 (e_{95}^{+} = 71 mm)
St Poncy	Piers (XF4)	31 y	20	P3 pier, west face, exposed to salts: 30 P2 pier, west face, without salt exposure: 27 P3 pier, east face, exposed to salt: 31
Pirou	Piers (XF4)	28 y	4	West pier, without salt exposure: 25 West pier, exposed to salt: 29

Structures over 50 years old				
Bruche	Deck (XC4: corroded area)	66 y (part of carbonation) 70 y (others)	25	41
	Deck (XC4: healthy area)	66 y (chlorides and part of carbonation) 70 y (others)	30	41
PI Blondel	Crossbeam (XC4)	51 y	30-45 (about 35) (47 years)	60 Cover reinforcement of crossbeam from 50 to 76.
	Deck (XC4)	51 y	35 (47 years)	26 Cover from 0 to 36 mm for transversal reinforcement, 35 to 50 for longitudinal reinforcement.
X Bridge	Arch (springing) XS3	60 y	-	Web: 41 Band (lateral side): 62
Vallières	Arch (XF3) De-icing salt from deck (very frequent salting)	92 y	Deck: Upper: 15; Lower: 92 Upstream rib: 36 Massive part of the arch: 45 (right bank side)	Upperside of the deck: 45 Rib: 27
Boutiron	Arch (XC4, XF1)	107 y	< 1 (upper and lower surfaces)	55 (on the bracing wall), but closer to 20 or 40
Iena Palace	(XC4)	80 y	14 (mean) (from 0,2 to 2,7) PerfDub: 30 - 35 (40 Max)	e_{moy} = 57 (from 35 to 90)
Bordeaux Labor Exchange	(XC4)	80 y	Walls: 50 Columns: 25 (from 0 to 50) PerfDub: Outside: 19 Inside: 26	Walls of the 4th floor: 30 (from 9 to 71) Columns of the 4th floor: 46 (from 0 to 79)
Vezins Dam	ZIH 30 vault (XC4)	84 y	27	39
	ZIB 30-31 buttress (XC4)	84 y	2	38
	V30 central beam (XC4)	84 y	12	28
	V2 central beam (XC4)	84 y	9 (upstream and downstream beams)	29
	V12 central beam (XC4)	84 y	7 (upstream beam)	62

e_{moy}: mean cover value for first reinforcements
e95+ : value above which 95 % of cover values are present
e95- : value below which 95 % of cover values are present

Table 2.134. Characterisation of the state of corrosion of investigated structures

Structure Building	Investigated element Exposure class	Age of investi-gations	Initiation or propagation phase of corrosion	State of corrosion
Structures below 20 years old				
Vasco de Gama (central viaduct)	Precast box (XS3: tidal, base of piers)	213 months	Initiation	No cracking visible on LERM photography. No measurement of electrochemical potential.
Vasco de Gama (South viaduct)	Piers (XS3: tidal)	213 months	Initiation	Vertical cracking visible in LERM photography. No measurement of electrochemical potential.
Rion Antirion	Piers (element 19) (XS2: submerged area)	9 y	Initiation	No apparent disorder due to corrosion. No measurement of electrochemical potential.
	M2 pier (XS32: tidal)	45 months	Initiation	No apparent disorder due to corrosion. No measurement of electrochemical potential.
	M3 pile (element 19) (XS3: tidal)	114 months	Initiation	No apparent disorder due to corrosion. No measurement of electrochemical potential.
	M3 pile (element 19) (XS3: tidal)	201 months	Initiation	No apparent disorder due to corrosion. No measurement of electrochemical potential.
	Testing wall (XS3: salt spray and splash)	2,5 months	Initiation	No apparent disorder due to corrosion. No measurement of electrochemical potential.
	Testing wall (XS3: salt spray and splash)	11 months	Initiation	No apparent disorder due to corrosion. No measurement of electrochemical potential.
	Testing wall (XS3: salt spray and splash)	24 months	Initiation	No apparent disorder due to corrosion. No measurement of electrochemical potential.
	Testing wall (XS3: salt spray and splash)	62 months	Initiation	No apparent disorder due to corrosion. No measurement of electrochemical potential.
	Testing wall (XS3: salt spray and splash)	150 months	Initiation	No apparent disorder due to corrosion. No measurement of electrochemical potential.
Volesvre	Piers (XC4)	5 y	Initiation	No disorder due to corrosion.
	Deck (XC4)	5 y	Initiation	No disorder due to corrosion.
Loudéac	Pier (XC4)	2 y	Initiation	Electrochemical analysis: from negligible to weak risk of corrosion. Resistivity: usual values for an uncarbonated CEM III cement in humid exposure.

				Electrochemical potential: only one anodic localised area, not in the first reinforcement layer. No disorder due to corrosion.
X Marine structure	Testing element (XS3: tidal)	2 y	Initiation	No disorder due to corrosion
Structures between 20 and 50 years old				
TCD wharf	Slab lateral side (XS3)	47 y	Initiation	Healthy area. Electrochemical potential: no anodic area. Current density: negligible to weak risk. Resistivity: weak risk (RILEM).
	underside south wharf slab (XS3)	51 y	Initiation	Electrochemical analysis: weak to moderate risk. Electrochemical potentials do not clearly identify anodic areas. The localized gradients measured on the longitudinal reinforcements are however greater than those obtained on the transverse ones and therefore seem to indicate a greater risk of corrosion. Resistivity measurements *in situ* evolve from 50 to 100 kΩ.cm: weak risk of corrosion. $e_{95\%}^{-}$ = 20 mm; $e_{95\%}^{+}$ = 48 mm A few concrete spalls with or without visible corroded reinforcements that occurred between 2003 and 2012
Chateau-briand	P11 pier (XS3: salt spray)	22 y	Initiation	P11: $e_{95\%}^{-}$= 65 mm 2011: “Cracking of piers has changed little since the previous inspection.” Absence of corrosion cracks in the investigated areas.
	P11 pier (salt spray) and P12 (tidal and splash) (XS3)	25 y	Initiation	P11 (salt sprays): Electrochemical potential: very weak risk. Resistivity: weak to moderate risk, if not negligible. e_{95}^{+} = 44 mm ; e_{95}^{-} = 68 mm P12 (tidal): Electrochemical potential: no significant gradient (except one area). Resistivity: moderate risk. e_{95}^{+} = 23 mm ; e_{95}^{-} = 40 mm
Vachette	Cornice (XF4)	34 y	Propagation From 1996	2008: numerous corroded visible reinforcements, concrete spalling, scaling and rust spots. Causes: freeze / thaw cycles + salt penetration. 2018: the pathology affects more and more elements, the bare reinforcements show significant section losses and the concrete deteriorates more and more deeply.
	Abutment (XF4)	34 y	Propagation	Potentials / current density / resistivity: - left side bank abutment: corrosion in phase of propagation

			Left bank side: from 1987 Right bank side: from 1996	- upstream cornice 28: developed corrosion - extremity of upstream cornice: no corrosion, no risk in the short-term. 2008: C0: large spalls of concrete and corroded visible reinforcements at the upstream extremity; C3: concrete spalls and corroded visible reinforcements at the upstream extremity. 2018: strong deterioration, bare reinforcements. Cause: freezing.
Ré	Pb pier (XS3: tidal) FC, exposed to main winds and sunshine	30 y	Propagation in Z3 from 2019 Initiation in Z1 and Z2	Z3 resistivity are higher than 100 kΩ.cm and can reach 200 kΩ.cm (Pb pier): negligible to weak risk of corrosion. Z2 resistivity are between 50 and 100 kΩ.cm: weak to moderate risk of corrosion. Z1 resistivity are between 10 and 50 kΩ.cm: moderate to high risk of corrosion. Electrochemical potentials cartography shows a potential anodic zone at the top left of Z3. Singular zone in zone Z3: some corrosion of the reinforcements and a pitting on the horizontal reinforcement (active corrosion). Zone Z3 (the highest in tidal range) is the most degraded. 1 or 2 vertical cracks on the 3 areas. No visible reinforcements.
	Pile Ph (XS3: tidal) FC face, exposed to main winds and sunshine	30 y	Propagation in Z3 from 2019 Initiation in Z1 and Z2	Z3 resistivity are higher than 100 kΩ.cm and can reach 200 kΩ.cm (Pb pier): negligible to weak risk of corrosion. Z2 resistivity are between 50 and 100 kΩ.cm: weak to moderate risk of corrosion. Z1 resistivity are between 10 and 50 kΩ.cm: moderate to high risk of corrosion. Electrochemical potentials cartography shows two potential anodic zones (left and right part). No autopsy performed. Zone Z3 (the highest in tidal range) is the most degraded. About ten vertical cracks in zone Z3. Spall at the top left of the Z3 zone. No disorder in Z1 and Z2
Ré	Pile Po (XS3: tidal) FC face, exposed to main winds and sunshine	30 y	Propagation in Z3 from 2019 Initiation in Z1 and Z2	Z3 resistivity are higher than 100 kΩ.cm and can reach 200 kΩ.cm (Pb pier): negligible to weak risk of corrosion. Z2 resistivity are between 50 and 100 kΩ.cm: weak to moderate risk of corrosion. Z1 resistivity are between 10 and 50 kΩ.cm: moderate to high risk of corrosion. Electrochemical potentials cartography shows three potential anodic zones. The cracking examination shows healthy reinforcement. Z3 zone (the highest in tidal range) is the most degraded. Seven vertical cracks in Z3 zone.

				No disorder in Z1 and Z2
St Poncy	Piers (XF4)	31 y	Propagation in P3 from a date before 2019	2001: P2 and P3 piers: no apparent disorder linked to frost and / or de-icing salts. 2019: foot of P3 pier: the entire foot of the pier sounds hollow when probed with a hammer, with traces of corrosion / scaling of the concrete. Foot of P2 pier: no apparent disorder linked to frost and / or de-icing salts.
Pirou	Piers (XF4)	28 y	Initiation	No apparent damage, which could be related to corrosion of the reinforcements, or to freeze-thaw cycles.
Structures over 50 years old				
Bruche	Deck (XC4: corroded)	66 y (carbo *partial*) 70 y (rest)	Propagation from 2000 T_{ini} = 53 ans	1988: several visible sections of corroded reinforcements and rust spots on the underside of the slab; several spalls with partially corroded reinforcements on the sides of the slab where water continuously flows. Between 1988 and 1996, the anomalies observed on the structure did not show any notable change. Between 1996 and 2001, concrete spalls increased and new ones appeared. Corrosion is due to insufficient cover.
	Deck (XC4 : healthy)	66 y (Cl ; carbo *partial*) 70 y (rest)	Initiation	Since the inspection carried out in 1988, numerous disorders have been noted. In the deck, they are mainly characterized by concrete spalls, corrosion of the reinforcements on the sides of the slab and on the intrados, and runoff on the sides. The slab is overall little corroded, due to an average cover of 40 mm (between 20 and 70 mm!). Corrosion of reinforcements appears before 1988. e_{95} = 38,3 mm
PI Blondel	Crossbeam (XC4)	51 y	Initiation	Electrochemical potentials, current density, resistivity: no sign of corrosion. Resistivity higher than 100 kΩ.cm 1989: some corroded reinforcements on crossbeam.
	Deck (XC4)	51 y	Initiation	Electrochemical potentials, current density, resistivity: no sign of corrosion. Electrochemical potential lower than -200 mV Current density lower than 0.1 µA/cm² Resistivity between 10 and more than 500 kΩ.cm 1996: spalling, existing patch repairs, patch repairs with spalls… No significant disorder. 2011: some corroded visible reinforcements, steels mainly with little or no cover, some concrete spalls. The transverse reinforcements

				of the lower surface of the deck are located in the carbonated area.
X Bridge	arch (springing) (XS3)	60 y	Propagation	Resistivity: moderate risk of corrosion; values corresponding to a wet concrete and / or rich in chlorides. Electrochemical potentials: moderate to high probability of corrosion for the web and the top band, low for the bottom band. Web: e_{95}^{+} = 39 mm ; e_{95}^{-} = 43 mm Bands: e_{95}^{+} = 52 mm ; e_{95}^{-} = 69 mm 2011: concrete spalls on the upstream arch, located in the tidal range. 2015: at the upper surface of the arch, the upper edge of the band is spalled by corrosion of the reinforcements over at least 1.50 m in length and 20 cm in width. Several cracks are noted on the studied area. The cracks are more numerous, longitudinal and sometimes millimeter opening on the lower strip of the arch and extend over the entire tidal zone.
Vallières	Arch (XF3) De-icing salt from deck (very frequent salting)	92 y	Initiation in investigated areas	1974: “uprights with fine cracks at the base on the left bank. Arch with a few frames visible on the downstream side "- No previous Inspection report 1983: work in fairly good condition - protection by shotcrete of the arch on the left bank 1988: Spalls with visible steels on some beams and pillars 1993: structure is deteriorating 1998: spalls on the right bank 2004: structure in fairly poor condition – extension of disorders on the arches 2011: structure in poor condition - works classified as urgent Electrochemical potentials / current densities / resistivity: • upper face of the arch slab, on the left bank end. No corrosion of the reinforcements is detected, nor any short-term risk. • side face of the upstream arch rib, end on left bank. No corrosion of the reinforcements was detected, nor any short-term risk. • upstream face of pier 1 at the left bank end. Corrosion is developed in the lower part of the area. This corrosion was active at the time of the measurements. • upstream face of pier 1 at the right bank end. Corrosion is developed in the lower part of the area. This corrosion was active at the time of the measurements. Partly cavernous concrete.
Boutiron	Arch (XC4, XF1)	107 y	Initiation	No apparent disorder at the springing of the arch, site of the investigations.

Iena Palace	(XC4)	80 y	Initiation and Propagation	The bases of certain columns are very damaged, sometimes exposing the reinforcements. Some scars are visible on the grey concrete structural elements, sometimes at the location of old repairs. In most cases, an insufficient cover is observed (localized spalling at the edges of the beams). Carbonation does not reach reinforcements.
Bordeaux Labor Exchange	(XC4)	80 y	Initiation	2000: inside the 4th floor, the ceiling collapsed in one of the conference rooms. As well as outside, there are many cracks and spalls. Corrosion of the reinforcements caused severe spalling. The repairs carried out during a previous restoration did not limit the corrosion of the reinforcements.
Vezins Dam	Vault ZIH 30 (XC4)	84 y	Propagation	2016: presence of a cement coating on the surface. Occasional observation of concrete spalls and visible corroded reinforcement (where the covers are weakest) + occasional repairs carried out in the past. Resistivity: 326 kΩ.cm
	Buttress ZIB 30-31 (XC4)	84 y	Initiation	2016: no damage observed on the buttresses - Occasional observation and in greater number than for the vault of concrete spalls and corroded reinforcements visible on the stiffeners and struts. Resistivity: 21 kΩ.cm Occasionally, strong gradients of electrochemical potential.
	V30 central beam (XC4)	84 y	Propagation	2016: mainly horizontal cracking of the webs with calcite and stalactites - Vertical cracks along some stirrups. Concrete spalling at the heel of a beam with visible reinforcement. Resistivity: between 20 and 30 kΩ.cm
	V2 central beam (XC4)	84 y	Propagation	2016: mainly horizontal cracking of the webs with calcite and stalactites - Vertical cracks along some stirrups. Concrete spalling at the heel of a beam with visible reinforcement. Resistivity: between 20 and 70 kΩ.cm
	V12 central beam (XC4)	84 y	Initiation	Resistivity: < 20 kΩ.cm

6 Carbonation analysis

6.1 Remind on the carbonation model

This analysis is based on the carbonation modelling developed within the PerfDuB project and the associated MODEVIE ANR project supported by the French National Research Agency (ANR) (Carcassès *et al.*, 2018).

The carbonation depth is modelled by the following equation:

$$Xc(t) = v_{nat} \cdot k_c \cdot k_{RH} \cdot (t_{eff})^p \qquad \text{(Equ. 2.2)}$$

Where:

- $X_c(t)$ is the carbonation depth at time t (mm)
- v_{nat} is the carbonation rate in natural conditions (mm/year$^{1/2}$)
- k_c is the curing factor. We adopt $k_c = 1$ (This value of 1 means that the curing is supposed to be optimal)
- k_{RH} is a climatic factor linked to the relative humidity

$$k_{RH} = 1.1 \left[1 - \left(\frac{RH - RH_{crit}}{RH_{crit}}\right)^2\right] \qquad \text{(Equ. 2.3)}$$

  with RH_{crit} = critical relative humidity: taken equal to 50 %

  RH = average relative humidity on the site of the structure (%). Equation (2.3) enables to consider that the carbonation rate decreases when RH decreases below RH_{crit}, which is more realistic than the hypothesis of the fib model. The optimum value of RH to develop carbonation is comprised between 50 % and 70 %. A safe value of 50 % is considered for the beginning of the decrease.

- t_{eff} is the effective time (year)

$$t_{eff} = k_{teff} \cdot t \quad \text{(year)} \qquad \text{(Equ. 2.4)}$$

$$k_{teff} = 1 - (1 + \beta_w) \cdot ToW \qquad \text{(Equ. 2.5)}$$

  with $\beta_w = 1.5$

  ToW = time of wetness = (number of days with rain > x mm) / 365, with x assumed to be equal to 10 mm (considered as a reasonable value for wetness)

- p is the power parameter (generally assumed to be 0.5)

6.2 Predictive evolution of the carbonation depth

This section deals with the prediction of the value of the carbonation depth at a given age for existing structures.

Using equation (2.2), the value of the carbonation rate in natural conditions V_{NAT} can be obtained by reverse analysis:

$$v_{nat} = \frac{X_c(t)}{k_c \cdot k_{RH} \cdot (t_{eff})^p} \qquad \text{(Equ. 2.6)}$$

where $X_c(t)$ is the carbonation depth measured at age t in a given existing concrete structure.

Then, by reintroducing this calculated value of v_{nat} in equation (2.2), one can predict the value of penetration of the carbonation depth in this given structure at later ages:

- at 50 years (EN206 requirements):

$$x_c(50\ y) = v_{nat}.k_c.k_{RH}\ (50\ .\ k_{teff})^p \qquad \text{(Equ. 2.7)}$$

- at 100 years (fasc.65 requirements):

$$x_c(100\ y) = v_{nat}.k_c.k_{RH}\ (100\ .\ k_{teff})^p \qquad \text{(Equ. 2.8)}$$

Climatic data and parameters used in the carbonation law are summarised in Table 2.135 for some of the investigated structures.

From those values, the values of v_{nat} obtained by reverse analysis from carbonation measurements at time t are presented in Table 2.136. They evolve from 0.12 to 9.9 mm/year$^{0.5}$.

The depth of carbonation at 50 and 100 years can then be obtained from equations (2.7) and (2.8). The values are exposed in Table 2.137. The attention is drawn to the fact that those measurements are linked only to the initiation phase.

Table 2.135. Climatic data and parameters of the carbonation law

Structure	Exposure class	Climatic data			Parameters of the law of carbonation				
		RH (%)	Number of days of rain per year (R_r 10 mm)	ToW (-)	k_{HR} (-)	k_c (-)	P	β_w (-)	k_{teff} (-)
TCD wharf 1964-1965	XC4/XS3	85	40	0.11	0.561	1	0.5	1.5	0.726
Chateaubriand 1987-1991	XC4/XS3	85	40	0.11	0.561	1	0.5	1.5	0.726
Vachette 1984-85 cornice	XF4	70	25	0.07	0.924	1	0.5	1.5	0.829
Vachette 84-85 abutment	XF4	70	25	0.07	0.924	1	0.5	1.5	0.829
St Poncy 1988	XF4	73	15	0.04	0.867	1	0.5	1.5	0.897
Pirou 1991	XF4	73	15	0.04	0.867	1	0.5	1.5	0.897
Bruche 1947 (corroded)	XC4	79	16	0.04	0.730	1	0.5	1.5	0.890
Bruche 1947 (healthy)	XC4	79	16	0.04	0.730	1	0.5	1.5	0.890
Blondel 1964 crossbeam	XC4	56	19	0.05	1.084	1	0.5	1.5	0.870
Blondel 1964 deck	XC4	56	19	0.05	1.084	1	0.5	1.5	0.870
Vallières 1926 arch ribs	XF3	72	34	0.09	0.887	1	0.5	1.5	0.767
Vallières 1926 arch massive part	XF3	72	34	0.09	0.887	1	0.5	1.5	0.767
Boutiron	XC4	73	20	0.05	0.867	1	0.5	1.5	0.863
Palais d'Iena 1937	XC4	76	16	0.04	0.803	1	0.5	1.5	0.890
Bordeaux Labor Exchange 1935-38	XC4	81	31	0.08	0.677	1	0.5	1.5	0.788

Vezins dam 1929-1932 upper vault	XC4	80	20	0.05	0.704	1	0.5	1.5	0.863
BHP 2000 Melun M25CV – 4 years	XC4	76	16	0.04	0.803	1	0.5	1.5	0.890
BHP 2000 Melun M25 – 4 years	XC4	76	16	0.04	0.803	1	0.5	1.5	0.890
BHP 2000 Melun M30CV - 4 years	XC4	76	16	0.04	0.803	1	0.5	1.5	0.890
BHP 2000 Melun M50CV - 4 years	XC4	76	16	0.04	0.803	1	0.5	1.5	0.890
BHP 2000 Melun M50 - 4 years	XC4	76	16	0.04	0.803	1	0.5	1.5	0.890
BHP 2000 Melun M75FS - 4 years	XC4	76	16	0.04	0.803	1	0.5	1.5	0.890
BHP 2000 Melun M25CV - 19 years	XC4	76	16	0.04	0.803	1	0.5	1.5	0.890
BHP 2000 Melun M25 - 19 years	XC4	76	16	0.04	0.803	1	0.5	1.5	0.890
BHP 2000 Melun M30CV - 19 years	XC4	76	16	0.04	0.803	1	0.5	1.5	0.890
BHP 2000 Melun M50CV - 19 years	XC4	76	16	0.04	0.803	1	0.5	1.5	0.890
BHP 2000 Melun M50 - 19 years	XC4	76	16	0.04	0.803	1	0.5	1.5	0.890
BHP 2000 Melun M75FS - 19 years	XC4	76	16	0.04	0.803	1	0.5	1.5	0.890

RH: annual average value or Relative Humidity
Rr = height of minimal rain taken into consideration on the weather station closest to the structure

Table 2.136. Calculation of V_{NAT} for the investigated structures

Structure	Exposure class	Time of investigations and effective time		Carbonation measurements	Reverse analysis
		t (year)	t_{eff} (year)	X_c (t) (mm)	v_{nat} (mm/year$^{0.5}$)
TCD wharf 1964-1965	XC4 / XS3	51	37	1	0.29
Chateaubriand 1987-1991	XC4 / XS3	25	18	2.6	1.09
Vachette 1984-85 cornice	XF4	34	28	17	3.47
Vachette 1984-85 abutment	XF4	34	28	14	2.85
St Poncy 1988	XF4	31	28	20	4.37
Pirou 1991	XF4	28	25	4	0.92
Bruche 1947 (corroded)	XC4	66	59	25	4.47
Bruche 1947 (healthy)	XC4	70	62	30	5.21
Blondel 1964 crossbeam	XC4	51	44	35	4.85
Blondel 1964 deck	XC4	51	44	35	4.85
Vallières 1926 arch ribs	XF3	92	71	36	4.83

Vallières 1926 arch massive parts	XF3	92	71	45	6.04
Boutiron 1913	XC4	107	92	1	0.12
Palais d'Iena 1937	XC4	80	71	32	4.72
Bordeaux Labor Exchange 1935-1938 wall	XC4	80	63	50	9.30
Bordeaux Labor Exchange 1935-1938 columns	XC4	80	63	15	2.79
Vezins dam 1929-1932 upper vault	XC4	86	72	19	3.17
BHP 2000 Melun M25CV – 4 years	XC4	4	4	15	9.90
BHP 2000 Melun M25 – 4 years	XC4	4	4	10	6.60
BHP 2000 Melun M30CV - 4 years	XC4	4	4	7	4.62
BHP 2000 Melun M50CV - 4 years	XC4	4	4	2.5	1.65
BHP 2000 Melun M50 - 4 years	XC4	4	4	0.5	0.33
BHP 2000 Melun M75FS - 4 years	XC4	4	4	1	0.66
BHP 2000 Melun M25CV - 19 years	XC4	19	17	21	6.36
BHP 2000 Melun M25 - 19 years	XC4	19	17	16	4.85
BHP 2000 Melun M30CV - 19 years	XC4	19	17	10	3.03
BHP 2000 Melun M50CV - 19 years	XC4	19	17	5	1.51
BHP 2000 Melun M50 - 19 years	XC4	19	17	1	0.30
BHP 2000 Melun M75FS - 19 years	XC4	19	17	1	0.30

Name of structure in blue: structure in initiation phase of corrosion
name of structure in red: structure in propagation phase of corrosion

Table 2.137. Predictive values of carbonation depth for various ages

Structure	Exp. class	Age of investigations t	X_c measured	X_c predicted 50y	X_c predicted 100y
		year	mm	(mm)	(mm)
Vachette cornice 1985	XF4	34	17	21	29
Vachette abutment 1984	XF4	34	14	17	24
St Poncy 1988	XF4	31	20	25	36
Pirou 1991	XF4	28	4	5	8
Bruche 1947 (corroded)	XC4	66	25	22	31
Bruche 1947 (healthy)	XC4	70	30	25	36
Blondel 1964 crossbeam	XC4	51	35	35	49
Blondel1964 deck	XC4	51	35	35	49
Vallières 1926 arch ribs	XF3	92	36	27	38
Vallières 1926 arch massive parts	XF3	92	45	33	47
Boutiron 1913	XC4	107	1	1	1
Palais d'Iena 1937	XC4	80	32	25	36
Bordeaux Labor Exchange 1937 wall	XC4	80	50	40	56

Bordeaux Labor Exchange 1937 columns	XC4	80	15	12	17
Vezins dam 1929-1932 upper vault	XC4	86	19	15	21
BHP 2000 Melun M25CV-19y	XC4	19	21	34	48
BHP 2000 Melun M25 - 19y	XC4	19	16	26	37
BHP 2000 Melun M30CV-19y	XC4	19	10	16	23
BHP 2000 Melun M50CV-19y	XC4	19	5	8	11
BHP 2000 Melun M50-19y	XC4	19	1	2	2
BHP 2000 Melun M75FS-19y	XC4	19	1	2	2

Xc measured: measurement at the age of investigations
Xc predicted 50y: carbonation depth calculated for an age of 50 years
Xc predicted 100y: carbonation depth calculated for an age of 100 years
The Xc calculated values are linked to the initiation phase
Name of structure in blue: structure in initiation phase of corrosion
Name of structure in red: structure in propagation phase of corrosion

Note that the Boutiron bridge has a surprisingly very low carbonation depth.

6.3 Comparison of initition times for theoritical cover versus real mean cover

By inversing equation (2.2), and by using the value of V_{NAT} obtained from equation (2.4), one can calculate:

- the time t needed for carbonation to obtain a given depth X_c (equation 2.9);
- the time t_{ini} needed for carbonation to reach the reinforcements, which corresponds to the initiation time (equation 2.10, where $C_{min,dur}$ is the theoretical cover of reinforcement for a given age of duration of project).

$$t = \frac{1}{k_{teff}} . \left(\frac{X_c(t)}{k_c . k_{RH} . V_{nat}}\right)^{1/p} \quad \text{(Equ. 2.9)}$$

$$t_{ini} = \frac{1}{k_{teff}} . \left(\frac{c_{min.dur}}{k_c \, k_{RH} \, v_{nat}}\right)^{1/p} \quad \text{(Equ. 2.10)}$$

The values calculated for t_{ini} are exposed in Table 2.138.

Some values of t_{ini} appear to be very low in relation to the level of corrosion of the structure. This point is linked to the fact that the propagation time is not taken into account in this approach.

The disparities of values obtained for the Bordeaux Labor Exchange could be linked to differences in exposure conditions.

Other values (yellow cases) of t_{ini} are very high and are quoted "> 500". They come from weak values of carbonation measured on structures, that induce bias in modelling.

One can then estimate various safety level based on initiation time of corrosion:

- t_{ini} (at real mean cover) > age of the studied structure (for structures whose age is lower than the project duration life);
- t_{ini} (50 years Project Duration Life) > 50 years;
- t_{ini} (100 years Project Duration Life) > 100 years.

Table 2.138. Initiation time of corrosion for a project duration life of 50 years, 100 years and the one linked to the real mean cover

Structure	Exp. class	Theoretical cover for 50 years		Theoretical cover for 100 years		Real mean cover	X_c mea-sured	Calculation				
								X_c 50y	X_c 100y	t_{ini} ($C_{min, dur}$)		t_{ini} (real mean cover)
		$C_{min, dur}$ (mm)	Struct. class	$C_{min, dur}$ (mm)	Struct. class	mm	mm	mm	mm	For a 50y PDL (year)	for a 100y PDL (year)	year
Vachette cornice	XF4	45	S4	55	S6	40	17	21	29	238	356	188
Vachette abutment	XF4	45	S4	55	S6	36	14	17	24	351	525	225
St Poncy	XF4	45	S4	55	S6	30	20	25	36	157	234	70
Pirou	XF4	35	S2	45	S4	30	4	5	8	> 500	> 500	> 500
Bruche (corroded)	XC4	25	S3	35	S5	41	25	22	31	66	129	178
Bruche (healthy)	XC4	25	S3	35	S5	41	30	25	36	49	95	131
Blondel crossbeam	XC4	30	S4	40	S6	60	35	35	49	37	67	150
Blondel deck	XC4	30	S4	40	S6	26	35	35	49	37	67	28
Vallières arch ribs	XF3	30	S4	40	S6	27	36	27	38	64	114	52
Vallières arch massive parts	XF3	30	S4	40	S6	-	45	33	47	41	73	-
Boutiron	XC4	25	S3	35	S5	40	1	1	1	> 500	> 500	
Palais d'Iena	XC4	30	S4	40	S6	35	32	25	36	70	125	96
Bordeaux Labor Exchange wall	XC4	30	S4	40	S6	20	50	40	56	29	51	13
Bordeaux Labor Exchange columns	XC4	30	S4	40	S6	45	15	12	17	320	> 500	> 500
Vezins dam upper	XC4	30	S4	40	S6	39	19	15	21	209	372	354
BHP 2000 Melun M25CV-19y	XC4	30	S4	40	S6	30	21	34	48	39	69	39
BHP 2000 Melun M25 - 19y	XC4	30	S4	40	S6	30	16	26	37	67	119	67
BHP 2000 Melun M30CV-19y	XC4	30	S4	40	S6	30	10	16	23	171	304	171
BHP 2000 Melun M50CV-19y	XC4	25	S3	35	S5	30	5	8	11	475	> 500	> 500
BHP 2000 Melun M50-19y	XC4	20	S2	30	S4	30	1	2	2	> 500	> 500	> 500
BHP 2000 Melun M75FS-19y	XC4	20	S2	30	S4	30	1	2	2	> 500	> 500	> 500

Struc. class: structural class according to eurocodes, obtained by considering the real compressive stress
y = years
PDL: Project Duration Life
Yellow case: irrelevant value due to a too low value of measured carbonation Xc
t_{ini} ($C_{min, dur}$) is the time needed for carbonatation to reach the theoritical cover linked to a Project Duration Life, it corresponds to the initiation time
t_{ini} (real mean cover) is the time needed for carbonatation to reach the mean cover of the real structure

Those criteria correspond to the fact that the depth of carbonation is lower than the cover linked to the age of duration of project, for structures whose age is lower than the age of duration of project. The red case in the Table 2.139 are linked to structures with unsafe criteria.

Table 2.139. Safety levels

			Modelling			Safety level		
Structure	**Exp. class**	**Age (year)**	**t_{ini} (real cover)**	**t_{ini} (50y PDL)**	**t_{ini} (100y PDL)**	**t_{ini} (real mean cover) > age of structure**	**t_{ini} (50y PDL) > 50y**	**t_{ini} (100y PDL) > 100y**
Vachette cornice	XF4	34	188	238	356	Yes	Yes	Yes
Vachette abutment	XF4	34	225	351	525	Yes	Yes	Yes
St Poncy	XF4	31	70	157	234	Yes	Yes	Yes
Pirou	XF4	28	> 500	> 500	> 500	Yes	Yes	Yes
Bruche (corroded)	XC4	66	178	66	129	Yes	Yes (1)	Yes (1)
Bruche (healthy)	XC4	70	131	49	95	Yes	No	No
Blondel crossbeam	XC4	51	150	37	67	Yes	No	No
Blondel deck	XC4	51	28	37	67	No (3)	No (2)	No (2)
Vallières arch ribs	XF3	92	52	64	114	No (3)	Yes	Yes
Vallières arch massive parts	XF3	92	-	41	73	-	No	No
Boutiron	XC4	107	-	> 500	> 500	-	Yes	Yes
Palais d'Iena	XC4	80	96	70	125	Yes	Yes	Yes
Bordeaux Labor Exc. wall	XC4	80	13	29	51	No	No	No
Bordeaux Labor Exc. columns	XC4	80	720	320	569	Yes	Yes	Yes
Vezins dam upper	XC4	86	354	209	372	Yes	Yes	Yes
BHP 2000 Melun M25CV-19y	XC4	19	39	39	69	Yes	No	No
BHP 2000 Melun M25-19y	XC4	19	67	67	119	Yes	Yes	Yes
BHP 2000 Melun M30CV-19y	XC4	19	171	171	304	Yes	Yes	Yes
BHP 2000 Melun M50CV-19y	XC4	19	684	475	931	Yes	Yes	Yes
BHP 2000 Melun M50-19y	XC4	19	> 500	> 500	> 500	Yes	Yes	Yes
BHP 2000 Melun M75FS-19y	XC4	19	> 500	> 500	> 500	Yes	Yes	Yes

y = years
Yellow boxes: irrelevant value due to a very low value of the measured carbonation Xc which prevents from leading a good prediction of t_{ini} with the model; Orange boxes: quasi safety; Red boxes: unsafe
PDL: Project Duration Life; t_{ini} (50y PDL) is the time needed for carbonation to reach the theoretical cover linked to a PDL of 50 years
Name of structure in blue: structure in initiation phase of corrosion; Name of structure in red: structure in propagation phase of corrosion)
(1): some localised lacks of cover
(2): intermediate state of development of corrosion: the corrosion is not sufficiently advanced to generate visible disorders on the structure
(3): initiation time too low versus the Project Duration Life of the structure

6.4 Link with durability indicators

Table 2.140 sumarizes the values obtained for the durability indicators at the age of investigations of the studied structures. Red cases are linked to unsecured values based on the current rules of the fascicle 65.

Table 2.140. Durability indicators

			Modelling	Indicators measured at time t			
Structure	**Exp. class**	**t (year)**	**v_{nat} (mm/y$^{0.5}$)**	**v_{acc} (mm/d$^{0.5}$)**	**K_{gas} (10^{-18} m²)**	**Porosity (%)**	**Resistivity (Ω.m)**
Vachette cornice	XF4	34	3.47		150	14.0	
Vachette abutment	XF4	34	2.85	1.19	250	13.5	
St Poncy	XF4	31	4.37	2.13	646	16.7	38
Bruche (corroded)	XC4	66	4.47	1.44	300	14.2	
Bruche (healthy)	XC4	70	5.21			14.7	
Blondel crossbeam	XC4	51	4.85	1.55	600	17.7	
Blondel deck	XC4	51	4.85		200	13.2	
Vallières arch ribs	XF3	92	4.83		700	20.1	31
Boutiron	XC4	107	0.12		224	16.4	37
Palais d'Iena	XC4	80	4.72		805	18.5	
Bordeaux Labor Exc. wall	XC4	80	9.30		607	13.0	
Bordeaux Labor Exc. column	XC4	80	2.79		607	13.0	
Vezins dam upper vault	XC4	86	3.17			21.2	25
Melun M25CV-19y	XC4	19	6.36		206	15.7	
Melun M25-19y	XC4	19	4.85		978	16.1	
Melun M30CV-19y	XC4	19	3.03		54	12.8	
Melun M50CV-19y	XC4	19	1.51		89	15.0	
Melun M50-19y	XC4	19	0.30		69	14.7	
Melun M75FS-19y	XC4	19	0.30		167	10.0	

Name of structure in blue: structure in real and present initiation phase of corrosion; Name of structure in red: structure in real and present propagation phase of corrosion
Orange boxes: value near the threshold value of fasc. 65 ; Red boxes: value overpassing the threshold value of fasc. 65.

The rules specified by the fascicle 65 (at 100 years, and for a structural class S6) are recalled in the Table 2.141.

Table 2.141. Durability indicators thresholds fixed by the fascicle 65

	XC1	**XC2**	**XC3**	**XC4**	**XD1/XS1**	**XD2/XS2**	**XD3/XS3**
Porosity (%)	15.5	15.5	15	14.5	14	14	13
K_{gas} (10^{-18} m²)	-	-	200	200	-	-	200
D_{rcm} (10^{-12} m²/s)	-	-	-	-	7	7	3.5

From the values of carbonation rate exposed in Table 2.140, one can calculate the ratio between natural and accelerated carbonation (Table 2.142) for some of the existing structures, because it is not possible to analyse structures with a very small depth of carbonation or with zero carbonation of the concrete at the end of the accelerated test. The mean ratio obtained of 2.7 is consistent with the 3.0 ratio obtained from the study of the 42 laboratory concretes (see GT3 results).

Table 2.142. Values of V_{NAT} / V_{ACC} ratio obtained from investigated structures

Structure	v_{nat} (mm/year$^{0.5}$) calculated	v_{acc} (mm/day$^{0.5}$) measured	Ratio v_{nat} / v_{acc} (day/year)^p
Vachette abutment	2.85	1.19	2.4
St Poncy	4.37	2.13	2.1
Bruche (corroded)	4.47	1.44	3.1
Blondel crossbeam	4.85	1.55	3.1
		mean	2.7

The data obtained from structures in a propagation phase of corrosion are exposed in Table 2.143.

Table 2.143. Durability indicators linked to structures in a propagation phase of corrosion

		50 years PDL scope		100 years PDL scope		Cause of corrosion
Structure	Age (years)	Porosity (%)	K_{gas} (10^{-18} m²)	Porosity (%)	K_{gas} (10^{-18} m²)	
Vachette cornice	34	< 14.0	< 150			Freeze-thaw cycles with salts
Vachette abutment	34	< 13.5	< 250			
St Poncy	31	< 16.7	< 646			
Bruche (corroded)	66	< 14.2	< 300			Insufficient cover
Vallières arch ribs	92			< 20.1	< 700	High porosity value
Iena Palace	80	< 18.7	< 805	< 18.5	< 805	Insufficient cover
Vezins dam	86	< 21.2		< 21.2		

The values of the durability indicators linked to corroded structures are reported in the column “50 years Project Duration Life (PDL) scope” when the age of the structure in lower than 50 years or near 50 years (see Bruche, corroded). The values of Vallières arch ribs, 92 age old, are considered to be relevant for the 100 years PDL scope. Iena Palace and Vézins dam, with 80 and 86 years old, are considered to be intermediate between the two PDL scopes so values are reported in the two columns.

The corrosion observed on the Vallières Bridge is linked to a high value of porosity. For other structures, corrosion is mainly due to insufficient cover of reinforcement or presence of freeze-thaw cycles with salts. Thus, it is difficult to conclude about the values of the measured durability indicators.

The values of the durability indicators obtained from healthy structures are exposed in Table 2.144. Those values are to be considered as sufficient values (but not necessary) to obtain healthy structures for the concerned covers.

Table 2.144. Durability indicators linked to healthy structures

		50 years PDL scope		100 years PDL scope	
Structure	**Age (year)**	**Porosity (%)**	**K_{gas} (10^{-18} m²)**	**Porosity (%)**	**K_{gas} (10^{-18} m²)**
Bruche (healthy)	70	> 14.7		> 14.7	
Blondel crossbeam	51	> 17.7	> 600		
Blondel deck	51	> 13.2	> 200		
Boutiron	107	> 16.4	> 224	> 16.4	> 224
Bordeaux Labor Exchange	80	> 13.0	> 607	> 13.0	> 607

The values of the durability indicators linked to healthy structures are reported in the column "50 years Project Duration Life (PDL) scope" when the age of the structure in higher than 50 years. If the age is near 100 years, the column 100 years PDL scope is also completed. Bruche (healthy part) has been taken in consideration for 100 years PDL scope because the calculation of its t_{ini} show a quasi safety level of security (based on initiation phase only, see Table 2.133).

Those values are to be considered as sufficient values (but not necessary) to obtain healthy structures for the concerned covers.

It was observed on many old structures that the gas permeability indicator could reach very high values such as 2000 or 3000 10^{-18} m^2. This can be explained by the fact that old concrete may contain micro-cracks or a single thin crack that act as air leaks through the tested concrete and the test is no longer representative of a measure of the air permeability of the material. Moreover, when three cores are taken close in the same area of a structure for a measurement of the permeability, there is a great scatter among the three results. Therefore, this indicator seems difficult to interpret on old concretes, and there is a doubt on the existence of a relation between Kgas indicators measured on a young concrete and the same ageing concrete.

6.5 About the power used for the carbonation law

From measurements performed on existing structure, one can test the value of the power parameter p, which is generally assumed to be 0.5.

From equation (2.2), one can obtain the value of the p power parameter:

$$p = \frac{\ln\left(\frac{Xc(t)}{k_c\, k_{RH}\, v_{nat}}\right)}{\ln t_{eff}} \qquad \text{(Equ. 2.11)}$$

By using the structures whose accelerated rate of carbonation (v_{acc}) has been measured at the age of investigations, the linked natural speed of carbonation (v_{nat}) can be calculated using the relation obtained from the 42 laboratory concretes (see Figure 2.106).

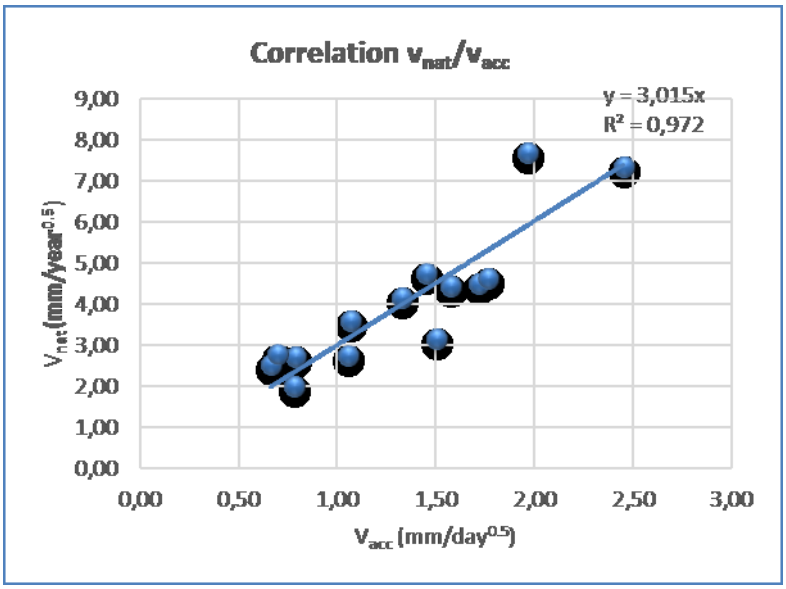

Figure 2.106. Experimental relation between v_{nat} and v_{acc}

Then, using equation (2.11), one can calculate the value of p (see Table 2.145). The obtained values evolve between 0.38 and 0.55, with a mean value of 0.48, which is consistent with the value of 0.50 generally considered.

If the theoretical value of depth of carbonation obtained with p = 0.5 at the age of investigations (last column) is calculated, the values then obtained are consistent with measurements (fifth column Xc).

Table 2.145. Calculation of the power parameter p
(measured values: v_{acc}, X_C (t); calculated values: v_{nat}, p, X_C (t) for p=0.5)

	Carbonation rate		Carbonation measurements		Parameters for modelling			Law of power	Calculation with p = 0.5
	V_{acc} (mm/d$^{0.5}$)	V_{nat} (mm/y$^{0.5}$)	Age (y)	X_c (t) (mm)	k_{RH}	k_c	k_{teff}	p	X_c (t)
Vachette crossbeam	1.19	3.65	34	17	0.92	1	0.83	0.48	18
Vachette abutment	1.19	3.65	34	14	0.92	1	0.83	0.43	18
St Poncy	2.13	6.53	31	20	0.87	1	0.90	0.38	30
Bruche (corroded)	1.44	4.42	66	25	0.73	1	0.89	0.50	25
Bruche (healthy)	1.44	4.42	66	30	0.73	1	0.89	0.55	25
Blondel	1.55	4.75	47	35	1.08	1	0.87	0.52	33

Another approach could be tested from equation (2.2). By assuming v_{nat} to be constant, the power parameter can be obtain with the following equation, knowing the carbonation depth at two ages of the structure t_1 and t_2:

$$p_1 = \frac{\ln\left(\frac{Xc(t_1)}{Xc(t_2)}\right)}{\ln\left(\frac{t_1}{t_2}\right)} \qquad \text{(Equ. 2.12)}$$

The calculated values of p_1 are exposed in Table 2.146. They evolve from 0.22 to 0.44, with a mean value of 0.33, which is inconsistent with the generally admitted value of 0.50. This

approach has only been tested on the BHP 2000 elements of the Melun site because it needs the measurements of carbonation depths at two different dates.

Table 2.146. Calculation of the power parameter p1

BHP 2000 Melun site	Carbonation measurements				Law of power
	Age (year)	X_c (t) (mm)	Age (year)	X_c (t) (mm)	p_1
Melun M25CV	4	15	19	21	0.22
Melun M25	4	10	19	16	0.30
Melun M30CV	4	7	19	10	0.23
Melun M50CV	4	2.5	19	5	0.44
Melun M50	4	0.5	19	1	0.44
Melun M75FS	4	1	19	1	~~0.00~~
				mean	0.33

If we consider an additive parameter k'_c linked to the impact of the curing of the surface layer of concrete, the equation (2.2) could be rewritten as follow:

$$X_c(t) = k'_c + v'_{nat}.k_{RH}.(t_{eff})^p \qquad \text{(Equ. 2.13)}$$

From this relation, one can then obtained:

$$k'_c = \frac{Xc(t_1) - Xc(t_2).\left(\frac{t_1}{t_2}\right)^p}{1-\left(\frac{t_1}{t_2}\right)^p} \qquad \text{(Equ. 2.14)}$$

The values of k'_c obtained for p=0.50 are presented in the last column of Table 2.147.

Table 2.147. Calculation of the cure parameter k'_c

BHP 2000 Melun site	Carbonation measurements				Cure parameter
	Age (year)	X_c (t) (mm)	Age (year)	X_c (t) (mm)	k'_c (mm)
Melun M25CV	4	15	19	21	9.9
Melun M25	4	10	19	16	4.9
Melun M30CV	4	7	19	10	4.5
Melun M50CV	4	2.5	19	5	0.4
Melun M50	4	0.5	19	1	0.1

The values of k'_c are comprised between 0 and 10 mm. In this case, V'_{NAT} would be lower than the V_{NAT} value estimated from the last carbonation depth measurement.

6.6 Main results about carbonation

This study of carbonation in existing structures provide the following main conclusions.

The following set of values (Table 2.148) could be considered as sufficient values (but not necessary) to obtain healthy structures for the concerned concrete covers.

Table 2.148. Durability indicators measured in healthy structures *(v_{acc} is obtained from measurement of v_{nat} and modelling: v_{acc} = v_{nat} / 3.0147, see §6.5 and values of Table 2.140)*

50 years Project Duration Life scope				100 years Project Duration Life scope			
Porosity (%)	**K_{gas} (10^{-18} m²)**	**v_{nat} (mm/y^p)**	**v_{acc} (mm/d^p)**	**Porosity (%)**	**K_{gas} (10^{-18} m²)**	**v_{nat} (mm/y^p)**	**v_{acc} (mm/d^p)**
13.0 - 17.7	200 - 607	0.12 – 9.30	0.04 – 3.08	13.0 - 16.4	224 - 607	0.12 – 9.30	0.04 – 3.08

The ratio between natural rate and accelerated rate (v_{nat}/ v_{acc}) obtained from existing structures evolves from 2.1 to 3.1, with a mean value of 2.7. It is consistent with the value obtained from the laboratory study with the 42 concretes (mean value of 3.0).

Experimental data support a carbonation law with a 0.5 power factor p.

The use of k_c as a multiplicative factor is not supported by a part of the measurements. An additive term, linked to the impact of the curing on the surface layer of concrete, could be more appropriate. But in this case, the power factor p should be decreased.

7 Chloride analysis

7.1 Remind on the Chloride Model

This analysis is based on the modelling of chloride penetration developed within the PerfDub project and the associated MODEVIE ANR project supported by the French National Research Agency (ANR) (Carcassès *et al.*, 2018), this modelling being based on the following equation issued from the fib bulletin n°34:

$$C(x,t) = C_0 + (C_{S,\Delta x} - C_0)\left[1 - \mathrm{erf}\left(\frac{c - \Delta x}{2.\sqrt{D_{app}(t)\,.\,t}}\right)\right] \qquad \text{(Equ. 2.15)}$$

Where:

- C_0 is the initial chloride content
- $C_{S,\Delta x}$ is the equivalent surface chloride content at the depth Δx
- erf is the error function
- Δx is the depth of the convective zone
- D_{app} is the apparent coefficient of chloride diffusion

7.2 Determination of D_{app} from chloride profiles measured

The value of the apparent coefficient of chloride diffusion D_{app} is derived from the chloride profiles obtained for the existing structures at the age of investigation (free and total chlorides when available). The values are fit to a theoretical diffusion law (see for example Figure 2.107 relative to BHP2000, La Rochelle, M75FS concrete, for total chlorides). The best fitting curve (not taking into consideration the convective zone), enables obtaining the parameters Cs (chloride surface concentration) and D_{app}.

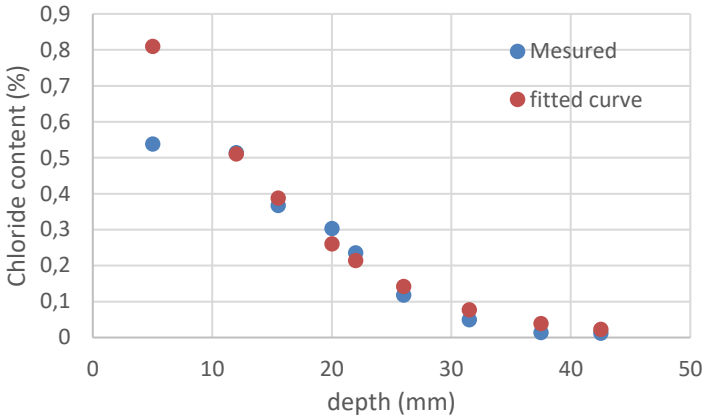

Figure 2.107. Fitting of data to a chloride diffusion law (BHP2000, La Rochelle, M75FS - total chlorides)

7.3 Comparison between D_{app} and D_{rcm}

At first, it should be remembered that D_{app} and D_{rcm} do not have the same meaning:

- D_{app} is an apparent diffusion coefficient, "averaged" over a given period resulting from the calibration of a chloride penetration curve;
- D_{rcm} is an instantaneous coefficient of migration of concrete measured at a given age.

Therefore, the word “comparison” is somewhat inappropriate, and the present article is dealing with a synthesis of the data collected on the ranges of D_{app} (t) and D_{rcm} (t).

Table 2.149. Surface chloride content and diffusion coefficients of chlorides

	Age (year)	Exp. class	Binder	Chlorides	C_s (% c)	C_s (% b)	D_{app}	D_{rcm} (t0) (10^{-12} m²/s)	D_{rcm} (t)
BHP2000 Rochelle	19	XS3, tidal		Mode Op LCPC	0.50	-	4.8	30	-
			CV		0.31	-	4.2	9.5	-
			CV		0.44	-	1.1	1.7	-
					0.51	-	2.0	8.7 [2]	-
			CV		0.60	-	0.39	1.8	-
					0.56	-	1.4	5.6	-
			FS		1.05	-	0.24	0.8	-
			FS		1.20	-	0.21	0.3	-
			FS		0.80	-	0.15	0.04	-
Ré	30	XS3, tidal	CEM II/B (10 % Slag)	free	0.41	-	0.23	-	8.5
					0.25	-	0.29	-	
					0.23	-	0.37	-	
					0.47	-	0.54	-	8.7
					0.46	-	0.23	-	
					0.24	-	0.31	-	

					0.36	-	0.41	-	15
					0.26	-	0.27 [2]	-	
					0.18	-	0.63	-	
Pirou	28	XF4	CEM I	free	-	1.30	0.17	-	9.4
					-	1.40	0.18	-	
					-	1.10	0.095	-	
Saint Poncy	31	XF4	CEM I	free	-	5.80	0.41	-	41
					-	4.10	0.25	-	
					-	1.50	0.15	-	
Chateaubriand	25	XS3, tidal	CEM I PM	total	0.14	-	1.8	-	29
		XS3, splash			0.053	-	1.4	-	
		XS3, salt spray					-	-	
	22	XS3, tidal		free	0.07		1.1 10^{-12}		-

c: concrete; b: binder;
blue text: structure in initiation phase of corrosion; red text: structure in propagation phase of corrosion

The Tables 2.149 and 2.150 present a synthesis of the main data obtained from the existing structures:

- type of chloride (free or total);
- surface chloride content C_s, obtained by fitting of profile curves;
- apparent coefficient of chloride diffusion D_{app}, obtained by fitting of profiles curves without taking into account the convective zone, thus the calculated values may be underestimated in some cases;
- apparent migration coefficient D_{rcm}, obtained by Rapid Chloride Migration test.

Table 2.150. Surface chloride content and diffusion coefficients of chlorides

	Age (year)	Exp. class	Binder	Chlorides	C_s (% c)	C_s (% b)	D_{app} (10^{-12} m²/s)	D_{rcm} (t_0) (10^{-12} m²/s)	D_{rcm} (t) (10^{-12} m²/s)
X Bridge	60	XS3	-	free	0.70	-	0.19	-	10
			-	total	1.20	-	0.13	-	
Vachette	34	XF4	CEM I	free	0.05	-	0.2	-	28
						-	-	-	
					0.05	-	0.3	-	-
					0.03	-	0.8	-	
Vallières	92	XF3	CEM I	free		-	-	-	97
					0.21	-	0.44	-	
					0.18	-	0.21	-	
					0.32	-	0.25	-	
TCD wharf	51	XS3	CEM I	total	0.26	-	0.19	-	2.3
					0.19	-	0.21	-	
Vasco de Gama	17.75	XS3	CEM I + CV (18 %)	free		8.00	0.13	3.4	0.16
						6.00	0.11		
				total		9.30	0.23		
						7.50	0.17		
			CEM IV (25 % CV)	free		4.20	0.15	0.52	0.3
				total		5.20	0.32		
Rion-Antirion	12.5	XS3	CEM III/A PM ES	free	1.10	-	0.42	0.86	0.37
				total	1.20	-	0.46		
	9	XS2		free	0.28	-	0.59	0.86	0.4
				total	0.36	-	0.59		
	3.75	XS3		free	1.40	-	0.12	0.86	0.49
					1.20	-	0.10		
				total	1.25	-	0.28	0.86	
					1.20	-	0.11		

c: concrete; b: binder
Blue text: structure in initiation phase of corrosion; red text: structure in propagation phase of corrosion

For these existing structures (without BHP 2000), the 2 tables show that the D_{app} coefficient is between 0.1 10^{-12} and 1.8 10^{-12}, while D_{rcm} (t) is much more scattered (from 0.16 10^{-12} to 97 10^{-12}). There is no correlation between these two coefficients.

7.4 Surface chloride content

A synthesis of the values of surface chloride content (Cs) derived from the chloride profiles obtained for the existing structures at the age of investigation, are presented for all investigated structures in Tables 2.151 to 2.154 for exposures classes XS1, XS2 and XD3. Concerning Table 2.151, the piers of the Chateaubriand bridge initially classified in XS3 (according to EC2) are rather exposed to the sea salt spray, and are considered as “equivalent” XS1 exposure class because of their elevation above the sea level (+ 4 m and + 13 m).

Table 2.151. Surface chloride content obtained for “equivalent” XS1 exposure class

Structure	Age (year)	Part of structure	Exp. class	Binder	Chloride type	C_s (% c)	Binder content (kg/m³)	Density (kg/m³)	C_s (% b)	Elevation *vs* sea level (m)
Chateaubriand	25	P12 Zecl	XS3 (splash zone)	CEM I PM	total	0.053	400	2417	0.32	4.00
		P11 ZE	XS3 (salt spray)			0.025	400	2417	0.15	13.00

C_s (% c): surface chloride content, expressed in concrete weight percent
C_s (% b): surface chloride content, expressed in binder weight percent

Table 2.152. Surface chloride content obtained for XS2 and XS3 exposure classes

Structure	Age (year)	Part of structure	Exp. class	Binder	Chloride type	C_s (% c)	Binder content (kg/m³)	Density (kg/m³)	C_s (% b)	Elevation *vs* sea level (m)
Rion-Antirion	9	M2 pile, immersed area 16	XS2	CEM III/A PMES	Free	0.28	420	2430	1.62	-4.00
					total	0.36			2.08	-4.00
Ré	30	PbF CZ 1C009	XS3, tidal	CEM II/B	Free	0.23	370	2390	1.49	0.40
		PhF CZ 1C027				0.24			1.55	0.40
		PoF CZ 1C039				0.18			1.16	0.40

C_s (% c): surface chloride content, expressed in concrete weight percent
C_s (% b): surface chloride content, expressed in binder weight percent

As expected, It is confirmed that the surface chloride content is the greatest for the immersed parts of structures, and decreases for the parts in tidal zone, and finally is the lowest for the parts in a splash zone and a spray zone.

The surface chloride content of the parts exposed to deicing salts (XD3) is less than the one of the parts exposed to sea water (XS3), except where the quality of the concrete is very bad.

Table 2.153. Surface chloride content obtained for XD3 exposure class (BHP 2000 elements)

Structure	Age (year)	Part of structure	C_s (% c)	$C_{s,\Delta x}$ (% c)	Binder content (kg/m^3)	Density (kg/m^3)	C_s (% b)	$C_{s,\Delta x}$ (% b)
BHP 2000 elements Maurienne	19	M25	0.10	0.06	230	2329	1.01	0.58
		M25CV	0.36	0.13	243	2327	3.45	1.24
		M30CV	0.21	0.12	318	2353	1.55	0.89
		M50	0.18	0.11	410	2351	1.03	0.63
		M50CV	0.16	0.10	404	2351	0.93	0.58
		M75	0.13	0.13	461	2456	0.69	0.69
		M75FS	0.13	0.13	382	2454	0.84	0.84
		M100FS	0.08	0.08	453	2435	0.43	0.43
		M120FS	0.15	0.15	516	2481	0.72	0.72
					mean		1.18	0.73

C_s (% c): surface chloride content, expressed in concrete weight percent
C_s (% b): surface chloride content, expressed in binder weight percent
Orange cases: doubtfull values
$C_{s,\Delta x}$ (% c): chloride content at the convective zone depth, expressed in concrete weight percent
$C_{s,\Delta x}$ (% b): chloride content at the convective zone depth, expressed in binder weight percent

Table 2.154: Surface chloride content obtained for XD3 exposure class (other structures)

Structure	Age (year)	Part of structure	Exp. class	Binder	Chloride type	Binder content (kg/m^3)	Density (kg/m^3)	C_s (% b)	$C_{s,\Delta x}$ (% b)
Vallières	92	arch, left bank, V2	XF3	CEM I	free	330	2370	1.51	1.06
		arch, left bank, V3	XF3	CEM I	free	330	2370	1.29	0.92
		arch, left bank, V4	XF3	CEM I	free	330	2370	2.30	0.75
Pirou	28	0.3 m	XF4	CEM I	free	400	2240	1.30	1.00
		1 m	XF4	CEM I	free	400	2240	1.40	1.10
		2 m	XF4	CEM I	free	460	2240	1.10	0.77
Saint Poncy	31	0.3 m	XF4	CEM I	free	350	2250	5.80	3.30
		1 m	XF4	CEM I	free	350	2250	4.10	1.20
		2 m	XF4	CEM I	free	350	2250	1.50	0.60

C_s (% b): surface chloride content, expressed in binder weight percent
$C_{s,\Delta x}$ (% b): chloride content at the convective zone depth, expressed in binder weight percent

7.5 About the ageing factor

Using the following fib evolutive law of D_{app}:

$$D_{app}(t) = k_t * k_e * (D_{rcm,\,to}) * [t_o/(age*365)]^{\alpha} \qquad \text{(Equ. 2.16)}$$

with $k_e = 1$ and $k_t = 1$, and to the age of D_{rcm} measurement, the ageing factor value can be obtained by the following relation:

$$\alpha = \ln(D_{app,\,t} / D_{rcm,\,to}) / \ln (t_o/(age*365)) \qquad \text{(Equ. 2.17)}$$

The values of the ageing factor a obtained by this approach are presented in Table 2.155. The values obtained for CEM I (orange boxes) are consistent with the usual tabulated value (0.30), when the values gathered with blended cementitious materials are broadly dispersed and not correlated (mostly significantly lower) that the tabulated values.

It should again be remembered that the D_{rcm} value taken into account in the fib model is for a term of 28 days. Taking initial values at 90 days can induce a bias in the analysis insofar as the value of D_{rcm} is (often significantly) reduced. Of course, it is clearly less the case for the concrete compositions with CEM I, and that could possibly explain the fact that one finds values of ageing factors more "aligned" with the value tabulated by the *fib* model.

Table 2.155. Values of ageing factor obtained from existing structures

Structure	Exposure class	Binder	Age (years)	t_o (days)	α tabulated	α calculated
Vasco de Gama	XS3 (box pear)	CEM I + CV (18 %)	17.75	90	0.60	0.78
						0.66
	XS3 (central pier)	CEM IV (25 % CV)			0.60	0.29
						0.11
Rion Antirion	XS3 (wall test)	CEM III/A PM ES	12.5	75	0.45	0.17
						0.15
	XS2 (M2 pier)		9		0.45	0.10
						0.10
	XS3 (M2 M3 piers)		3.75		0.45	0.71
						0.71
						0.51
						0.51
BHP2000 la Rochelle	XS3	M25 CV	19	28	0.60	0.15
		M50			0.30	0.27
		M50 CV			0.60	0.28
		M75			0.30	0.25
		M75 FS			0.40	0.22
		M100 FS				0.06
		M120 FS				-0.24*

Green box: concrete with fly ash; blue box: concretes with slag; purple box: concrete with silica fume; orange box: concrete with CEM I
t_o: age for initial measurement of D_{rcm}
** Value linked to a too low value of D_{rcm}*

7.6 Calculation of the initiation time of corrosion

From the equation (2.15), it is possible to obtain by reverse analysis the time t needed to obtained a given chloride content at a given depth by the following relation:

$$t = \frac{\left[\frac{c - \Delta x}{2.\,\mathrm{inverf}\left(1 - \frac{C(x,t) - C_0}{C_{S,\Delta x} - C_0}\right)}\right]^2}{D_{app}(t)} \qquad \text{(Equ. 2.18)}$$

Where:

- inverf is the reciprocal of the error function
- $D_{app}(t)$ is the apparent coefficient of chloride diffusion (issued from a calibration of a chloride profile) at the age of investigation
- C_0 is the initial chloride content of concrete
- $C_{S,\Delta x}$ is the equivalent surface chloride content at the depth Dx
- Δx is the depth of the convective zone
- c is the cover depth
- C(x, t) is the chloride content at the depth x
- t is the time needed to obtained the chloride content C(x, t) at the depth x

By considering:

- x as the depth of reinforcement cover measured on the structure
- C(x, t) = 0,60 % as the critical value of chloride content (free or total according to the case) to initiate corrosion at the depth of reinforcement (this value was decided within the PerfDub project)
- C_0 = 0,01 % (relative to binder)

it is therefore possible to obtain the value of t_{ini} the initiation time of corrosion for each structure on site.

A synthesis of the data needed for this calculation is exposed in Table 2.156. This calculation requires to consider that the coefficient Dapp is constant. Thus, only structures whose age is higher than 50 years are considered.

Table 2.156. Data needed for the calculation of t_{ini} for chloride corrosion

Structure, age, exposure class	Investigated area	Chloride nature	C_s (% c)	Density (kg/m³)	Binder (kg)	C_s (% b)	f_c (MPa)
Bridge X 60 y, XS3	arch	free	0.70	2274	400	4.0	
	arch	total	1.20	2274	400	6.8	
TCD wharf 51 y, XS3	slab lateral side, 2d	total	0.26	2300	235	2.5	73
	slab lateral side, 1d		0.19	2300	235	1.9	73

Structure, age, exposure class	Investigated area	Structural class 50 y	Structural class 100 y	$C_{min, dur}$ 50 y	$C_{min, dur}$ 100 y	C at cover	Δ x (mm)	$C_{s, \Delta x}$ (% c)	$C_{s, \Delta x}$ (% b)	C_0 (% b)
Bridge X 60 y, XS3	Arch	S4	S6	45	55	0.60	0.0	0.70	4.0	0.01
	Arch	S4	S6	45	55	0.60	0.0	1.20	6.8	0.01
TCD wharf 51 y, XS3	Slab lateral side, 2d	S2	S4	35	45	0.60	0.0	0.26	2.5	0.01
	Slab lateral side, 1d	S2	S4	35	45	0.60	0.0	0.19	1.9	0.01

C_s (% c): surface chloride content, expressed in concrete weight percent
C_s (% b): surface chloride content, expressed in binder weight percent
$C_{s, \Delta x}$ (% c): chloride content at the convective zone depth, expressed in concrete weight percent
$C_{s, \Delta x}$ (% b): chloride content at the convective zone depth, expressed in binder weight percent

The values calculated for t_{ini} are exposed in Table 2.157.

Table 2.157: Initiation time of corrosion for a project duration life of 50 years, 100 years

Structure, age, exposure class	Investigated area	Chloride nature	D_{app} (10^{-12} m²/s)	t_{ini}, 50y (PDL)	t_{ini}, 100y (PDL)
X Bridge 60 y, XS3	Arch	free	0.19	81	121
	Arch	total	0.13	84	126
TCD wharf 51 y, XS3	Slab lateral side, 2d	total	0.19	72	119
	Slab lateral side, 1d		0.21	93	154

PDL: Project Duration Life
t_{ini} (50y PDL / 100y PDL): initiation time of corrosion for a cover linked to a PDL of 50 years / 100 years
blue text: structure in initiation phase of corrosion; red text: structure in propagation phase of corrosion

For the X Bridge, and its mean cover from 41 to 62 mm, its condition at 60 years old does not fulfil the 50 and 100 years project duration life.

For the TCD wharf and its mean cover of 39 mm, its condition at 51 years old is, for the present time, in agreement with the predicted initiation time for a 50 years and 100 years project duration life.

7.7 Main results about chlorides

The study of chlorides in the existing structures provide the following conclusions.

The values of D_{rcm} linked to healthy structures are exposed in Table 2.158. These structures are too young to be able to draw a conclusion. Nevertheless, the value of 2.3 10^{-12} m²/s appears to be consistent with a 50 years Project Duration Life scope for the XS3 and XD3 exposure classes.

Table 2.158. Values of $D_{rcm,\ t0}$ and $D_{rcm,\ t}$ measured for healthy structures

	Age (year)	Exposure class	Binder	D_{rcm} (t_0) (10^{-12} m²/s)	D_{rcm} (t) (10^{-12} m²/s)
Vasco de Gama	17.75	XS3	CEM I + CV (18 %)	3.4	0.16
			CEM IV (25 % CV)	0.52	0.3
Rion-Antirion	12.5	XS2 - XS3	CEM III/A PM ES	0.86	0.37 to 0.49
TCD wharf	51	XS3	CEM I	-	2.3
Chateaubriand	25	XS3	CEM I PM	-	29
Vachette	34	XF4 / XD3	CEM I	-	28
Ré	30	XS3, tidal	CEM II/A	-	8.6
Saint Poncy	31	XF4 / XD3	CEM I	-	41
Pirou	28	XF4 / XD3	CEM I	-	9.4

Blue text: structure in initiation phase of corrosion

The values of D_{rcm} linked to damaged structures are exposed in Table 2.159. Values higher than 8.6 x 10^{-12} are inconsistent with a 50 years Project Duration Life scope for the XS3 exposure class.

Table 2.159: Values of D_{rcm} (t) measured for damaged structures

	Age (year)	Exposure class	Binder	D_{rcm} (t) (10^{-12} m²/s)
X Bridge	60	XS3	-	10

Red text: structure in propagation phase of corrosion

The values of the ageing factor obtained for CEM I concretes are between 0.25 and 0.27, which is consistent with the tabulated value of 0.30 in the fib bulletin 34.

8 Frost analysis

In the absence of models of the behavior of a concrete in freeze-thaw conditions, whether from internal freezing or scaling, it is not possible to make simulations of the life of structures from the data collected in order to validate thresholds of durability indicators. All we can do is to examine the current thresholds for the durability indicators and relate them to the behavior of the structures to date.

The case of the St-Poncy bridge shows that failure to comply with current thresholds on freeze-thaw with salts leads to disorders after only 30 years.

The case of the Pirou bridge shows that its C70/85 concrete used in construction meets current regulatory requirements for an XF4 G + S exposure class, in terms of performance tests with respect to durability in frost, with or without de-icing salts, but on the other hand, its concrete does not validate the performance requirements of an XD3 exposure class according to (Fascicle 65, 2017) in terms of chloride diffusion and gas permeability. Our opinion is that the PIROU pier should corrode in the areas exposed to salts where the concrete covers are not sufficient. In severe conditions, it is not possible to protect a concrete element both against corrosion and frost / spalling, and it is necessary to target the main risk. In such cases, it is advised to formulate a concrete composition suitable to resist XF4 G+S when this requirement is essential, and then to cope with corrosion.

The case of the Vallières bridge shows that 85 years after its construction, it is in a very poor condition. Regarding the durability indicators related to corrosion, the concrete of the arch has a potential durability class considered as "very low". From the frost point of view, the concrete of the arch massive parts has test values well above the thresholds that would be set for these parts of the structure for a new structure, but the disorders cannot be attributed to frost-freeze action.

9 Conclusions

These important investigations made on around twenty existing structures of various ages show the great importance of having feedback from old existing structures and bring a lot of data that help to validate the corrosion models developed within the PerfDub project and MODEVIE research project and to better calibrate the threshold values of the durability indicators.

This study made it possible to generate, at the end of the report, a rich database on the aging of structures subject to carbonation and chloride penetration, with examples of typical values of durability indicators for various concretes used in civil engineering structures, mainly bridges.

The measurements of durability indicators on existing structures show a rather strong dispersion, and this justifies a statistical approach for setting the thresholds values of the durability indicators. The maximum dispersion is observed on the gas permeability coefficient, some of the measured values of this coefficient could not be taken into account due to microcracking of the concrete.

Concerning the lifetime indicators, the corrosion density measurements are difficult to implement for existing structures and their results are difficult to interpret and transpose. A higher scatter is observed on lifetime indicators, depending on the location of the structural element and even on the location of an area within the element. The worst scatter is observed for the concrete cover of the reinforcement. It is therefore essential that the measurements of the durability indicators be made in the same areas as those where the lifetime indicators are assessed. It also means that one must conduct an intelligent analysis of the investigations carried out on the structure in order to draw valid conclusions. It appeared difficult to decide whether an existing structure is globally in an initiation phase or in a propagation phase of corrosion, and above all to decide when a corroded structure switched from the initiation phase to the propagation one.

In terms of carbonation, the study confirms the existence of a relationship between natural carbonation rate (v_{nat}) and accelerated carbonation rate (v_{acc}), which justifies the interest to use the accelerated carbonation test in a performance approach of the durability. This ratio v_{nat} / v_{acc} lies between 2.1 and 3.1 and is consistent with data obtained on the 42 laboratory concretes tested in the present project. We were able to confirm the validity of the square root of time law and the importance of the correct choice of the curing and hygrometry coefficients

in the model resulting from MODEVIE. The investigations show the importance of respecting the duration of curing before exposure, in particular for concretes with mineral additions, as well as the cover thicknesses. The values of the durability indicators for carbonation obtained on healthy structures can be considered as sufficient values but not necessary to obtain an absence of corrosion, for project service lives of 50 or 100 years.

For chloride attack, a D_{rcm} value of 2.3 10^{-12} m²/s is consistent with a project life of 50 years and values of D_{rcm} greater than 8.6 10^{-12} m²/s are incompatible with a project life of 50 years for XS3 exposure class. If we note strong dispersions of the ageing factor with concrete formulations incorporating additions, we see that the values obtained with CEM I are consistent with the value of 0.3 usually taken into account. A panel of values for chloride surface content has also been provided.

A synthesis paper presenting the main results of this study obtained on structures older than 50 years has been published (Godart *et al*., 2024).

For frost attack, in the absence of models of the behaviour of a concrete in freeze-thaw conditions, whether from internal freezing or scaling, it was not possible to make simulations of the life of structures from the data collected in order to validate the thresholds of the durability indicators. The main conclusion drawn from structures built in the 1980's and located in a severe cold zone, is the importance of respecting the current thresholds of the durability indicators set in the French recommendations for the composition of concretes subject to freeze-thaw with or without de-icing salts.

References

(AFGC, 2004) AFGC (2004) (Baroghel-Bouny V., dir.) "Conception des bétons pour une durée de vie donnée des ouvrages - Maîtrise de la durabilité vis-à-vis de la corrosion des armatures et de l'alcali-réaction - Etat de l'art et guide pour la mise en oeuvre d'une approche performantielle et prédictive sur la base d'indicateurs de durabilité", Documents Scientifiques et Techniques de l'Association Française de Génie Civil (AFGC), 252 p.

(AFPC-AFREM, 1998) LMDC (1998), "Modes opératoires recommandés par l'AFPC-AFREM", Compte rendu des journées techniques AFPC-AFREM « Durabilité des bétons », décembre 1997, Toulouse, 283p.

(Ammouche *et al.*,2012) Ammouche A., Carde C., Rafaï N., Linger L. (2012), "Overview of a two decades durability follow-up for two major bridges: Vasco de Gama (Portugal) and Rion-Antirion (Greece)", 11th fib Symposium, Proceedings No. 35. Concrete Structures for Sustainable Community, Stockholm.

(Baroghel-Bouny, 1999) Baroghel-Bouny V. (1999), "Etude expérimentale sur sites de vieillissement - Programme de suivi des corps d'épreuve en béton armé - Résultats obtenus sur prélèvements aux premières échéances de mesure - Comparaison avec les résultats obtenus sur éprouvettes, Projet National BHP 2000 - Thème 1 : Durabilité - Sous-thème : Etude expérimentale sur sites de vieillissement", Rapport LCPC, 47p.

(Baroghel-Bouny, 2009) Baroghel-Bouny V. (2009), "Projet National BHP 2000 - Etude expérimentale sur sites de vieillissement - Résultats obtenus à l'échéance de 10 ans et comparaisons", Rapport d'étude, LCPC, 22 p.

(Baroghel-Bouny *et al.,* 1999) Baroghel-Bouny V., Carcasses M., Quenard D., Arnaud S. (1999), "Durability of concretes ranging from 20 to 120 MPa - Mix-parameter influence", *Proceedings of 5th International Symposium on Utilization of High Strength / High Performance Concrete*, june 20-24, 1999, Sandefjord, Norway, (Ed. by I. Holand & E.J. Sellevold), vol. 2, pp 1377-1386.

(Baroghel-Bouny and De Larrard, 2000a) Baroghel-Bouny V., De Larrard F. (2000), “In place durability assessment for the next millenium - Long-term study”, *Proceedings of the 5th CANMET/ACI International Conference on Durability of Concrete*, June 4-9, 2000, Barcelona, Spain, SP-192 (Ed. by V.M. Malhotra, ACI), vol. I, SP 192-20, pp 319-338.

(Baroghel-Bouny and De Larrard, 2000b) Baroghel-Bouny V., De Larrard F. (2000), "Vieillissement des bétons en milieu naturel : une expérimentation pour le XXIe siècle. I - Généralités et caractéristiques mécaniques initiales des bétons", *Bulletin des Laboratoires des Ponts et Chaussées*, n° 225, pp 51-65.

(Baroghel-Bouny *et al.,* 2000) Baroghel-Bouny V., Ammouche A., Hornain H., Gawsewitch J. (2000), "Vieillissement des bétons en milieu naturel : une expérimentation pour le XXIe siècle. II - Caractérisation microstructurale sur éprouvettes de bétons de résistance 25 à 120 MPa", *Bulletin des Laboratoires des Ponts et Chaussées*, n° 228, sept.-oct. 2000, pp 71-86.

(Baroghel-Bouny *et al.*, 2002) Baroghel-Bouny V., Arnaud S., Henry D., Carcasses M., Quenard D. (2002), "Vieillissement des bétons en milieu naturel : une expérimentation pour le XXI° siècle. III - Propriétés de durabilité des bétons mesurées sur éprouvettes conservées en laboratoire", *Bulletin des Laboratoires des Ponts et Chaussées*, n° 241, nov.-déc. 2002, pp 13-59.

(Baroghel-Bouny *et al.*, 2004) Baroghel-Bouny V., Gawsewitch J., Belin P., Ounoughi K., Arnaud S., Olivier G., Bissonnette B.(2004), "Vieillissement des bétons en milieu naturel : une expérimentation pour le XXI° siècle. IV - Résultats issus des prélèvements effectués sur les corps d'épreuve de différents sites aux premières échéances de mesure", *Bulletin des Laboratoires des Ponts et Chaussées*, n° 249, mars-avril 2004, pp 49-100.

(Baroghel-Bouny *et al.*, 2013) Baroghel-Bouny V., Dierkens M., Wang X., Soive A., Saillio M., Thiery M., Thauvin B. (2013), “Ageing and durability of concrete in lab and in field conditions - Investigation of chloride penetration”, *Journal of sustainable cement-based materials*, vol. 2, n° 2, pp 67-110.

(Carcassès *et al*., 2018) Carcasses M. *et al*. (2018), “Toward an engineer-type model for the prediction of the durability of reinforced concrete structures in the framework of a performance-based approach - Corrosion risk due to carbonation or chloride ingress”, Rapport interne du projet ANR MODEVIE.

(Cox *et al*., 1997) Cox R.N., Cigna R., Vennesland O., Valente T. (1997), COST 509 – “Corrosion and protection of metals in contact with concrete - Final Report”, European Commission, Directorate General Science, Research and Development, Brussels, EUR 17608 EN1997.

(Cussigh *et al*., 2010) Cussigh F., Carde C., Papanikolas P., Stathopoulos-Vlamis A. (2010), “Rion-Antirion bridge project – concrete durability towards corrosion risk”, 3rd fib international Congress, Washington.

(Dierkens *et al*., 2019) Dierkens M., Godart B., MAI-NHU J., Rougeau P., Linger L., Cussigh F. (2019), “French national project “PERFDUB” on performance-based approach: interest of old structures analysis for the definition of durability indicators criteria”, 16th fib Symposium, *Proceedings No. 47*. Concrete Innovations in Materials, Design and Structures, Krakow, 27-29 May 2019.

(Elsener, 2003) Elsener B. (2003), “RILEM TC 154-EMC: Electrochemical Techniques for Measuring Metallic Corrosion - Recommendations - Half-cell potential measurements - Potential mapping on reinforced concrete structures”, *Materials and Structures*, RILEM, vol.36, n°261, p.461-471.

(Fasciule 65, 2017) Ministère de la Transition écologique et solidaire (2017), "Exécution des ouvrages de génie civil en béton", Cahier des clausses techniques générales applicables aux marchés publics de travaux de génie civil, Fasicule 65, Version 1.0, 171p.

(*fib,* 2006) *fib* (2006), “Model code for service life design”, *fib Bulletin* n°34.

(GranDuBé, 2007) Collectif Presses de l'Ecole Nationale des Ponts et chaussées (ENPC) (2007), "GranDuBé. Grandeurs associées à la durabilité des bétons", 438 p.

(Godart *et al.*, 2024) Godart B., Dierkens M., Cordier N., Thauvin B., Bouichou M., Marie-Victoire E. (2024), “Data acquired on some old reinforced concrete structures to validate the threshold levels of the French performance-based method for the durability of concrete structures”, Structural Concrete, Volume 25, Issue 1, pp 677-695.

(Houdusse *et al*., 2000) Houdusse O., Hornain H., Martinet G. (2000), “Prediction of Long-term durability of Vasco Da Gama bridge in Lisbon”, 5th CANMET/ACI *International Conference on Durability of Concrete*, Barcelona.

(Kollek, 1989) Kollek J.J. (1989), “The determination of the permeability of concrete to oxygen by the CEMBUREAU method, a Recommendation”, *Materials and Structures*, vol. 22, pp 225-230.

(LCPC, 2010) LCPC (2010), “Maîtrise de la durabilité des ouvrages d'art en béton - Application de l'approche performantielle, Recommandations provisoires”, Techniques et méthodes des laboratoires des ponts et chaussées, 59p.

(L’Hostis *et al*., 2007) L'Hostis V. *et al*. (2007), “Benchmark des poutres de la Rance” - *Revue européenne de génie civil* - Volume 11 - n° 1-2.

(Martinet, 1999) Martinet G. (1999), “Le Pont Vasco de Gama – La démarche durabilité”, *Bulletin of Engineering Geology and the Environment*, Spriner-Verlag, vol. 58, p.61-70.

(Martinet *et al.,* 2005) Martinet G., Linger L. (2005), “Pont Vasco de Gama à Lisbonne – Bilan de dix ans de démarche durabilité”, GC’2005, Journées Techniques de l’Association Française de Génie Civil, AFGC, 5-6, Octobre 2005.

(Moro *et al*., 2017) Moro F., Godart B., Guillot X. (2017), “PERFDUB: a four-years research project to make a performance-based approach operational in France”, International Conference on Advances in Construction Materials and Systems, ICACMS 2017, September 3 - 8, 2017, Chennai, India, *RILEM Proc*., vol. 3, pp 451-458.

(Polder, 2000) Polder R. (2000), “RILEM TC 154-EMC: Electrochemical Techniques for Measuring Metallic Corrosion - Recommendations - Test methods for on-site measurements of resistivity of concrete”, *Materials and Structures*, vol. 33, p. 603-611.

(Tang & Nilsson, 1992) Tang L., Nilsson L.O. (1992), “Rapid determination of the chloride diffusivity in concrete by applying an electrical field”, *ACI Materials Journal*, vol. 89, n° 1, pp 49-53.

(Tang & Sorensen, 2001) Tang L., Sorensen H.E. (2001), “Precision of the Nordic test methods for measuring the chloride diffusion / migration coefficients of concrete”, *Materials and Structures*, vol. 34, n° 242, pp 479-485.

Test Methods

(AASHTO T277-3, 1993) AASHTO T277-3 (1993), “Standard Method of Test for Electrical Indication of Concrete’s Ability to Resist Chloride Ion Penetration”.

(ASTM C 457, 2008) ASTM C 457 (2008), “Standard Test Method for Microscopical Determination of Parameters of the Air-Void System in Hardened Concrete”.

(ASTM C 876-09, 2009) ASTM, C 876-09 (2009), “Standard test method for half-cell potentials of uncoated reinforcing steel in concrete”.

(NF EN 14630, 2007) NF EN 14630 (2007), “Produits et systèmes pour la protection et la réparation des structures en béton - Méthodes d'essais - Mesurage de la profondeur de carbonatation d'un béton armé par la méthode phénolphtaléine (Products and systems for the protection and repair of concrete structures. Test methods. Determination of carbonation depth in hardened concrete by the phenolphthalein method)”.

(NF P18-414, 2017) NF P18-414 (2017). “Essai des bétons - Essais non destructifs - Mesure de la fréquence de résonance fondamentale ».

(NF P18-424, 2008) NF P18-424 (2008), “Bétons - Essai de gel sur béton durci - Gel dans l'eau - Dégel dans l'eau”.

(NF P18-425, 2008) NF P18-425 (2008), “Bétons - Essai de gel sur béton durci - Gel dans l'air - Dégel dans l'eau”.

(NF P18-459, 2010) NF P18-459 (2010), “Béton - Essai pour béton durci - Essai de porosité et de masse volumique”.

(NT Build 492, 1999) NT Build 492 (1999), “Nordtest method, Concrete, mortar and cement-based repair materials: Chloride migration coefficient from non-steady-state migration experiments”, Espoo, Finland.

(XP P18-420, 2012) XP P18-420 (2012), “Béton - Essai d'écaillage des surfaces de béton durci exposées au gel en présence d'une solution saline”.

(XP P18-458, 2008) XP P18-458 (2008), “Essai pour béton durci - Essai de carbonatation accélérée - Mesure de l'épaisseur de béton carbonaté”.

(XP P18-462, 2012) XP P18-462 (2012), “Essai sur béton durci - Essai accéléré de migration des ions chlorure en régime non-stationnaire - Détermination du coefficient de diffusion apparent des ions chlorure”.

(XP P18-463, 2011) XP P18-463 (2011), “Bétons - Essai de perméabilité aux gaz sur béton durci”.

Appendix A: Indications given by the AFGC 2004 guide on the concrete durability (AFGC, 2004)

Table 2.A.1. Potential durability classes

		Classes et valeurs limites				
	Durabilité potentielle →	**Très faible**	**Faible**	**Moyenne**	**Elevée**	**Très élevée**
G	Porosité accessible à l'eau (%) P_{eau}	> 16	14 à 16	12 à 14	9 à 12	6 à 9
S	Porosité mesurée par intrusion de mercure ($P_{Hg\ max}$ = 400 MPa et prétraitement par étuvage à T = 45 °C pendant 14 jours en présence de gel de silice) (%) P_{Hg}		13 à 16	9 à 13	6 à 9	3 à 6
S	Résistivité électrique (Ω.m) ρ	< 50	50 à 100	100 à 250	250 à 1000	> 1000
G	Coefficient de diffusion *effectif* des chlorures (10^{-12} m².s^{-1}) D_{eff}	> 8	2 à 8	1 à 2	0,1 à 1	< 0,1
G	Coefficient de diffusion *apparent* des chlorures (mesuré par essai de migration) (10^{-12} m².s^{-1}) $D_{app(mig)}$	> 50	10 à 50	5 à 10	1 à 5	< 1
G	Coefficient de diffusion *apparent* des chlorures (mesuré par essai de diffusion) (10^{-12} m².s^{-1}) $D_{app(dif)}$				< 5	
G	Perméabilité apparente aux gaz (à $P_{entrée}$ = 0,2 MPa et après étuvage à T = 105 °C) (10^{-18} m²) K_{gaz}	> 1000	300 à 1000	100 à 300	10 à 100	< 10
G	Perméabilité à l'eau liquide (à P_{max}, par mesure directe du flux, après saturation, cf. § 7.2.4.1 et 7.2.4.2) (10^{-18} m²) k_{liq}(*)	> 10	1 à 10	0,1 à 1	0,01 à 0,1	< 0,01
	Type de béton (indicatif et pour des formules simples)		*B25 à B40*	*B30 à B60*	*B55 à B80*	*> B80*

Table 2.A.2. Thresholds of the durability indicators as a function of project life duration and exposures

		Corrosion induite par carbonatation (e = 30 mm)				Corrosion induite par les chlorures (e = 50 mm)			
Type d'environnement →		1	2	3	4	5		6	7
Durée de vie exigée / *Catégorie d'ouvrage* / ← Niveau d'exigence		Sec et très sec (HR<65%) ou humide en permanence	Humide (HR>80%)	Modérément humide (65<HR<80%)	Cycles fréquents d'humidification-séchage	Exposition aux sels marins ou de déverglaçage		Immersion dans l'eau contenant des chlorures	Zone de marnage
						5.1 [Cl⁻] faible (1)	5.2 [Cl⁻] forte (2)		
< 30 ans *Bâtiment*	Niveau 1	$\cdot P_{eau} < 16$	$\cdot P_{eau} < 16$	$\cdot P_{eau} < 15$	$\cdot P_{eau} < 16$	$\cdot P_{eau} < 16$	$\cdot P_{eau} < 14$	$\cdot P_{eau} < 15$	$\cdot P_{eau} < 14$
de 30 à 50 ans *Bâtiment*	Niveau 2	$\cdot P_{eau} < 16$	$\cdot P_{eau} < 16$	$\cdot P_{eau} < 14$ (5)	$\cdot P_{eau} < 14$ (6)	$\cdot P_{eau} < 15$	$\cdot P_{eau} < 11$	$\cdot P_{eau} < 13$	$\cdot P_{eau} < 11$
de 50 à 100 ans *Bâtiment et Ouvrages de génie civil*	Niveau 3	$\cdot P_{eau} < 14$ (6)	$\cdot P_{eau} < 14$ (6)	$\cdot P_{eau} < 12$ (7) $\cdot K_{gaz} < 100$ (8)	$\cdot P_{eau} < 12$ (7) $\cdot K_{liq} < 0,1$ (9)	$\cdot P_{eau} < 14$	$\cdot P_{eau} < 11$ $\cdot D_{app(mig)} < 2$ $\cdot K_{liq} < 0,1$ (3)	$\cdot P_{eau} < 13$ $\cdot D_{app(mig)} < 7$	$\cdot P_{eau} < 11$ $\cdot D_{app(mig)} < 3$ $\cdot K_{liq} < 0,1$ (3)
de 100 à 120 ans *Grands ouvrages*	Niveau 4	$\cdot P_{eau} < 12$ $\cdot K_{gaz} < 100$	$\cdot P_{eau} < 12$ $\cdot K_{gaz} < 100$	$\cdot P_{eau} < 9$ $\cdot K_{gaz} < 10$ (4)	$\cdot P_{eau} < 9$ $\cdot K_{gaz} < 10$ $\cdot k_{liq} < 0,01$	$\cdot P_{eau} < 12$ $\cdot D_{app(mig)} < 20$ $\cdot K_{liq} < 0,1$ (3)	$\cdot P_{eau} < 9$ $\cdot D_{app(mig)} < 1$ $\cdot K_{gaz} < 10$ $\cdot k_{liq} < 0,01$	$\cdot P_{eau} < 12$ $\cdot D_{app(mig)} < 5$	$\cdot P_{eau} < 10$ $\cdot D_{app(mig)} < 2$ $\cdot K_{gaz} < 100$ $\cdot k_{liq} < 0,05$
> 120 ans *Ouvrages dits exceptionnels*	Niveau 5	$\cdot P_{eau} < 9$ $\cdot K_{gaz} < 10$	$\cdot P_{eau} < 9$ $\cdot k_{liq} < 0,01$	$\cdot P_{eau} < 9$ $\cdot K_{gaz} < 10$ $\cdot k_{liq} < 0,01$	$\cdot P_{eau} < 9$ $\cdot D_{app(mig)} < 1$ $\cdot K_{gaz} < 10$ $\cdot k_{liq} < 0,01$	$\cdot P_{eau} < 9$ $\cdot D_{app(mig)} < 10$ $\cdot K_{gaz} < 10$ $\cdot k_{liq} < 0,01$	$\cdot P_{eau} < 9$ $\cdot D_{app(mig)} < 1$ $\cdot K_{gaz} < 10$ $\cdot k_{liq} < 0,01$	$\cdot P_{eau} < 9$ $\cdot D_{app(mig)} < 1$	$\cdot P_{eau} < 9$ $\cdot D_{app(mig)} < 1$ $\cdot K_{gaz} < 10$ $\cdot k_{liq} < 0,01$

Appendix B: Criteria adopted for the durability indicators in the LCPC Recommendations of 2010 and the Fascicle 65 of 2017

The criteria adopted for the durability indicators in the LCPC recommendations of 2010 (LCPC, 2010) are, for average values measured on a 90-day old concrete, for structures with a design life of 100 years, for class XS3 and for a concrete cover of 50 mm:

- Porosity accessible to water: $P_{water,90} \leq 11$ %
- Gas permeability: $K_{gas,90} \leq 150\ 10^{-18}$ m²
- Migration of chloride Coefficient: $D_{rcm,90} \leq 3\ 10^{-12}$ m².s^{-1}

These criteria are replaced by the requirements of Table 8.D in the latest version of fascicle 65 of the CCTG (Fascicule 65, 2017). The values in this table correspond, for a design period of use of 100 years, for a class XS3, for covers corresponding to the structural class S6 before any reduction linked to the nature of the binder or to a compact cover (no reduction linked to the resistance class is then not possible).

Extract from Table 8.D of fascicle 65: Maximum values of durability indicators without cover reduction:

- Porosity accessible to water: $P_{water,90} \leq 13$ %
- Gas permeability: $K_{gas,90} \leq 200\ 10^{-18}$ m²
- Migration of chloride Coefficient: $D_{rcm,90} \leq 3.5\ 10^{-12}$ m².s^{-1}

The fascicle 65 also provides another Table 8E allowing modulation of the structural classes to take into account covers different from those of class S6.

Extract from Table 8.E - Maximum values of durability indicators allowing cover reductions (for exposure class XS3):

Minoration of a class	$P_{water;90} \leq 12.5$ % $K_{gas,90} \leq 150\ 10^{-18}$ m² $D_{rcm,90} \leq 3\ 10^{-12}$ m².s^{-1}
Minoration of two classes	P_{water} 90d ≤ 12 % $K_{gas,90} \leq 100\ 10^{-18}$ m² $D_{rcm,90} \leq 2.5\ 10^{-12}$ m².s^{-1}

CHAPTER 3

Data Base and its exploitation

Authors *(Organisations)*:

Sandrine Chanut *(Eiffage Génie Civil)*
Olivier Collin *(Lafarge Bétons)*,
François Cussigh *(Vinci Construction France)*
Michaël Dierkens *(Cerema)*
Faber Fabbris *(Eqiom)*
Lionel Linger *(Vinci Construction Grands Projets)*
Jonathan Mai-Nhu *(CERIB)*
Fabrizio Moro *(LafargeHolcim)*
Thomas Pernin *(CERIB)*
Gabriel Pham *(LafargeHolcim)*
Jean-Marc Potier *(SNBPE)*
Patrick Rougeau *(CERIB)*
Emmanuel Rozière *(GeM)*
François Toutlemonde *(Université Gustave-Eiffel)*
Philippe Turcry *(LaSie)*

Work Group: WG3

Summary

1 Abstract

The PerfDuB research project aims at defining a methodology to justify the durability of concretes (and concrete structures) through a performance-based approach.

A part of PerfDuB's work consists in characterizing durability properties of 42 concretes made with several standardized common cements and additions (Portland cement, Portland-limestone cement, Portland-slag cement, Blast furnace cement, composite cement, slag, fly ash, silica fume, limestone filler, siliceous filler, metakaolin), several aggregates (rounded, crushed, semi-crushed) with different porosities, and considering different packing densities (water to binder ratio varying from 0.35 to 0.60) to link the evolution of the durability indicators with changes in concrete composition. For each exposure class, most of the concrete mixes comply with prescriptive provisions of NF EN 206/CN (2014) standard. Some concretes differ relatively to their equivalent binder content, water on equivalent binder ratio, type of aggregates.

To achieve this objective, PerfDuB has carried studies to obtain four sets of data and tools:

- part 1: durability properties of 42 current concretes;
- part 2: statistical data on the in-situ variability of durability indicators in order to define mean and fractile values as for the compressive strength;
- part 3: durability models including migration, depassivation and corrosion mechanisms;
- part 4: evolution of the durability indicators of concrete structures in their environment (due to the aging of concrete and external aggressions).

The present report deals with parts 1 and 2 and detailed the characterization of durability properties of the 42 concretes. In particular, the report explains in detail how the data base is used to determine links between the mix characteristics and the durability properties and to contribute to determine the threshold values of durability properties to apply the performance based- approach. The analysis of the data base is one of the three methodologies used to determine these threshold values in the FD P 18-480, the French standard for performance-based approach in the field of NF EN 206/CN.

The Perfdub National Project database therefore makes a major contribution to the concrete industry in France, and also at European level, by providing input for work on the inclusion of ERCs (Exposure Resistance Classes) in Eurocode 2 and EN 206.

2 Introduction

The PerfDuB research project aims at defining a methodology at the French national level to justify the durability of concretes (and concrete structures) through a performance-based approach.

A part of PerfDuB's work consists in characterizing durability properties of 42 concretes made with several standardized common cements and additions (Portland cement, Portland-limestone cement, Portland-slag cement, Blast furnace cement, composite cement , slag, fly ash, silica fume, limestone filler, siliceous filler, metakaolin), several aggregates (rounded, crushed, semi-crushed) with different mineralogies and porosities, and considering different packing densities (water to binder ratio varying from 0.35 to 0.60) to link the evolution of the durability indicators with changes in concrete composition. For each exposure class, most of the concrete mixes comply with prescriptive provisions of NF EN 206/CN (2014) standard. Some concretes differ relatively to their equivalent binder content, water on equivalent binder ratio, type of aggregates.

The objective of PERFDUB project is to produce knowledge and field experience, to fill gaps, in a framework bringing together all the stakeholders concerned so that the performance-based approach becomes operational and commonly used on construction sites, which is not yet the case today. The application of the performance-based approach to durability is already authorized by the European standard EN 206 (and its national complement NF EN 206/CN) and a first methodology is given in the new guideline “Fascicule n°65” of the CCTG (general technical clauses for public contracts).

To achieve this objective, an experimental study was carried out in order to obtain four sets of data and tools:

- part 1: durability properties of 42 current concretes;
- part 2: statistical data on the in-situ variability of durability indicators in order to define mean and fractile values as for the compressive strength;
- part 3: durability models including migration, depassivation and corrosion mechanisms;
- part 4: evolution of the durability indicators of concrete structures in their environment (due to the aging of concrete and external aggressions).

The present report deals with parts 1 and 2. Note also that the precision of measurements are not described in this report and they are dealt with in the GT1A reports.

Section 3 describes the methodology used to build the data base including the choice and the characterization of the 42 concretes. This section explains also how the data base is exploited in order to determine links between the mix characteristics and the durability properties.

Then sections 4 to 8 present the results obtain for the durability properties: porosity, water absorption and resistivity (section 4), gas permeability (section 5), oxygen diffusivity (section 6), resistance to carbonation (section 7), chloride migration (section 8).

Section 9 deals with the variability (temporal and in-situ) of durability properties which are key points for the applicability of the performance-based approach.

Section 10 presents how the data base can be useful for the construction of ERC (Exposure Resistance Class) concept.

The conclusion presents the main contribution of this Perfdub National Project data base.

Note that, throughout the report, the word “binder” means “total binder”. When "equivalent binder" according to NF EN 206/CN is used, it is clearly specified "equivalent binder".

3 Database presentation

Authors: Olivier Collin, Jonathan Mai-Nhu, Patrick Rougeau

3.1 Presentation of the database and its representativeness

3.1.1 Characteristics of the 42 concrete mix design

In order to set up a performance-based approach in normative standards for concrete civil engineering and building constructions, PerfDuB National Project achieved and characterized a large panel of 42 concretes. These 42 concretes cover all exposure classes. Most of them are designed according to the prescriptive requirements of NF EN 206/CN, some concrete differ voluntarily according to their equivalent binder content, water-to-equivalent binder ratio, type of aggregates. Compressive strength varies from C20/25 to C70/85. The objective of this

set of concretes is to obtain a representative database in terms of the levels of durability performance.

The experimental design consisted in using different sources of the most different constituents possible:

- binders: wide spectrum of cements (CEM I, CEM II, CEM III and CEM V) and additions (blast furnace slag, metakaolin, fly ash, silica fume, silica addition and limestone filler). The Addition / Addition + Cement ratios were deliberately between 0 and 65 %;
- aggregates: broad spectrum of mineralogical origin with very different physical-chemical qualities, especially on water absorption. Five typologies of aggregates are studied (Table 3.1): semi crushed alluvial with an absorption of about 1 % (named G1), natural alluvial with an absorption of about 2.7 % (G2), crushed hard limestone with an absorption of about 0.6 % (G3), crushed limestone with an absorption of about 4 % (G4) and a mixture of marine sand with an absorption of 0.8 % and crushed gneiss with an absorption of 0.5 % (G5);

Table 3.1. Aggregates used in all the 42 concrete mixtures

	G1	G2	G3	G4	G5
Mineralogy	Silica-limestone Alluvial	Silica-limestone Alluvial	Dense limestone	Limestone	Fine: marine Coarse: gneiss
Shape	Mixed rounded-crushed	Round + mixed	Crushed	Crushed	Fine: rounded Coarse: crushed
Water absorption	0/4 – 0.7 % 4/11 – 1.0 % 11/22 – 1.3 %	2.7 %	0.6 %	0/4 – 4.0 % 4/10 – 4.4 % 10/20 – 4.0 %	0/4 – 0.8 % 4/11 – 0.4 % 11/22 – 0.5 %
D_{max} (mm)	22	20	20	20	22

- admixtures: products adapted to the binders and aggregates and selected to guarantee the specifications in terms of practical use duration (workability over time);
- effective water: wide variation of the Water/Binder ratio (0.60 to 0.35).

3.1.2 Sets of concretes

3.1.2.1 According to the clinker content of the binder

To compare the durability properties of the 42 concretes, the concretes are grouped into 3 sets based on the clinker content of the binder (Figure 3.1):

- the first set (“Set 1” in the following section of the document) includes concretes with clinker content between 78 % and 99 %, in red on the Figure 3.1. It corresponds to concretes made with CEM I with or without limestone addition, CEM II/A-LL, CEM II/A-S with or without limestone addition, CEM I + silica fume addition, CEM I + metakaolin addition. It has been decided to put concrete 7 which is a SCC with a high paste volume and high proportion of clinker in set 1;
- the second set (“Set 2” in the following section of the document) includes concretes with clinker content between 60 % and 70 %, in green on the Figure 3.1. It corresponds to concretes made with CEM I + fly ashes, CEM I + limestone, CEM I + siliceous addition;
- the third set (“Set 3” in the following section of the document) includes concretes with clinker content between 30 % and 60 %, in blue on the Figure 3.1. It corresponds to

concretes made with CEM I + limestone, CEM I + slag, CEM III/A, CEM V, CEM II/A-LL + fly ashes, CEM II/A-LL + slag.

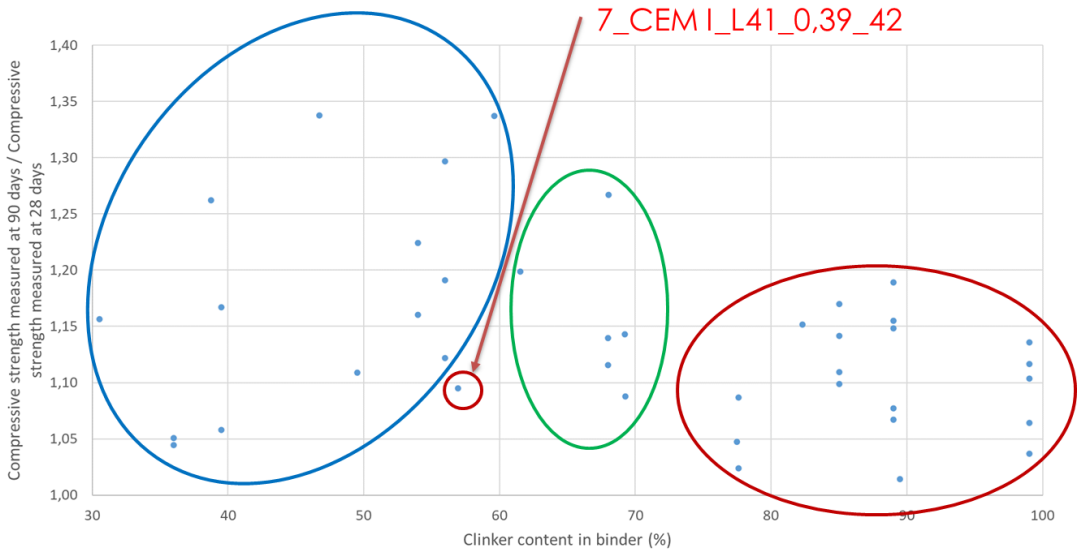

Figure 3.1. Schematic representation of the choice of concrete sets for the study of durability properties – the sets are based on the evolution of the compressive strength and the clinker content in the binder

3.1.2.2 According to concrete compressive strength classes

In the same way, and still in order to compare the durability properties of the 42 concretes, 3 groups of concretes based on the compressive strength classes, determined from the results obtained in the laboratory, are defined:

- Group A" includes compressive strength classes C20/25, C25/30 and C30/37;
- Group B" includes compressive strength classes C35/45, C40/50, C45/55;
- Group C" includes the highest compressive strength classes C50/60, C55/67, C70/85.

3.1.3 Nomenclature of concretes

Concretes are named as follow: Concrete number – Cement type – Addition type – Addition content in the binder – W/B – Mean compressive strength at 28 days measured on 3 samples (Φ110 mm x H 220 mm).

For example, “5_CEM I_S60_0.58_26” corresponds to the concrete n°5 which is made with CEM I and slag (60 % of the binder). Its W_{eff}/B is equal to 0.58 and $f_{cm,cyl,28}$ = 26 MPa.

The nomenclature of the 42 concretes tested as part of the project, and their classification by group, are summarised in Table 3.2. The concrete compositions are given in Appendix A.

Table 3.2. Nomenclature of concrete and their classification by group

N° of concrete	Nomenclature	Aggregates	Group based on the clinker content of the binder	Group based on the compressive strength of the concrete
1	1_CEM I_ 0,5_43	G2	1	B
2	2_CEM I_V30_0,52_33	G2	2	A
3	3_CEM II/A-LL_0,6_41	G2	1	A

4	4_CEM III/A_ 0,53_37	G2	3	A
5	5_CEM I_S60_0,58_26	G2	3	A
6	6_CEM I_L30_0,46_34	G2	2	A
7	7_CEM I_L41_0,39_42	G2	1	B
8	8_CEM II/A-LL_V30_0,53_31	G2	3	A
9	9_CEM II/A-LL_S45_0,57_31	G2	3	A
10	10_CEM II/A-LL_0,61_32	G2	1	A
11	11_CEM II/A-LL_0,54_50	G1	1	B
12	12_CEM I_S60_0,55_46	G1	3	B
13	13_CEM I_L30_0,42_39	G1	2	A
14	14_CEM I_0,55_38	G1	1	A
15	15_CEM I_0,48_58	G1	1	C
16	16_CEM II/A-S_0,5_51	G1	1	B
17	17_CEM III/A_0,5_47	G1	3	B
18	18_CEM I_V37_0,53_56	G1	2	B
19	19_CEM II/A-S_0,5_60	G3	1	C
20	20_CEM II/A-S_0,5_59	G4	1	B
21	21_CEM I_L30_0,39_57	G1	2	B
22	22_CEM II/A-LL_0,49_53	G1	1	B
23	23_CEM II/A-S_0,49_46	G2	1	B
24	24_CEM II/A-S_0,5_44	G5	1	B
25	25_CEM I_0,5_39	G1	1	B
26	26_CEM I_0,45_39	G1	1	B
27	27_CEM I_S50_0,43_68	G1	3	C
28	28_CEM I_0,45_NM	G1	1	C
29	29_CEM I_S60_0,42_NM	G1	3	C
30	30_CEM I_V30_0,35_64	G1	2	C
31	31_CEM III/A_0,4_67	G1	3	C
32	32_CEM I_S50_0,33_90	G1	3	C
33	33_CEM III/A_0,45_52	G1	3	B
34	34_CEM III/A_0,45_59	G1	3	B
35	35_CEM V/A (S-V)_0,45_66	G1	3	C
36	36_CEM V/A (S-V)_0,45_49	G4	3	B
37	37_CEM V/A (S-V)_0,45_56	G3	3	B
38	38_CEM I_D8_0,38_94	G1	1	C
39	39_CEM I_M20_0,43_62	G2	1	C
39b	39b_CEM I_M20_0,42_66	G2	1	C
40	40_CEM I_Qz30_0,49_28	G2	2	A
41	41_CEM I_M20_0,35_93	G1	1	C

3.1.4 Mix design, manufacture, and cure

The manufacturing of the concretes was divided between 4 laboratories (Vinci Construction France, Bouygues, Cerib and Lafarge Holcim) following the same methodology. The objective was to define a framework so that all the selected laboratories could use the same testing methodologies: preparation of aggregates, characterization of constituents, concrete formulation, mixing, curing, traceability of specimens, synthesis of laboratory results, etc.

Each composition was adjusted in a pre-study phase with an adjustment on the type and dosage of admixture. Targeted consistency of the concretes according to the NF EN 12350-2 standard is 180 ± 30 mm at 1 hour in order to comply with standard building site applications.

The preparation of the specimens was carried out according to the NF EN 12390-2 standard: consolidation of the concrete by vibration, until achieving a smooth and shiny concrete surface, without large bubbles.

Two types of curing conditions were carried out:

- wet curing: standard wet curing (under water or wet room RH > 95 %);
- dry curing: drying exposure class 2 of the standard NF EN 13670 consisting of wet curing until strength achieve 35 % of compressive strength class then drying exposure (20 °C and relative humidity of laboratories).

3.1.5 Measurements and testing

Concrete and laboratory temperatures were measured at $T_{5\ minutes}$, T_{30} and T_{60}. The relative humidity of the laboratories was also measured. All the concretes were characterized as follows:

- fresh state:
  - slump test according 12350-2 at $T_{5\ minutes}$, T_{30}, T_{60} and T_{90},
  - for SCC: flow table state according 12350-5 and sieve stability at T_5 and T_{60},
  - density according to NF EN 12350-6,
  - air content according to NF EN 12350-7.
- hardened state:
  - compressive strength according to NF EN 12390-3 at 24 hours, 7 days, 28 days and 90 days. 3 cylinders (110x220 mm) were measured for each time,
  - durability properties according to Table 3.3.

Table 3.3. Durability measurements on the 42 concretes studied in PN PerfDuB database

	Property	Wet curing	Dry curing	Age of testing (day)
For all concretes	Gas permeability Cembureau	X		28, 90
	Water porosity	X		28, 90
	Capillary absorption	X	X	28, 90
	Water absorption	X		28, 90
	Oxygen Diffusivity	X		28, 90
	Chloride migration	X		28, 90
	Electrical resistivity	X		28, 90
	Natural carbonation	X	X	90
	Accelerated carbonation according to XP P 18-458	X	X	90
	Accelerated carbonation according to prNF EN 12390-12 (including alternative preconditioning part)	X	X	90
For some concretes	Gas permeability Torrent	X		28, 90
	Permeability on 50 mm diameter cores	X		
	Biodegradation	X		
	Leaching	X		
	External sulphate attack	X		
	Natural chloride diffusion	x		90

3.1.6 Cartography of mechanical strength and durability properties

3.1.6.1 Compressive strength class

The Figure 3.2 shows the characteristic strength classes of the 42 concretes.

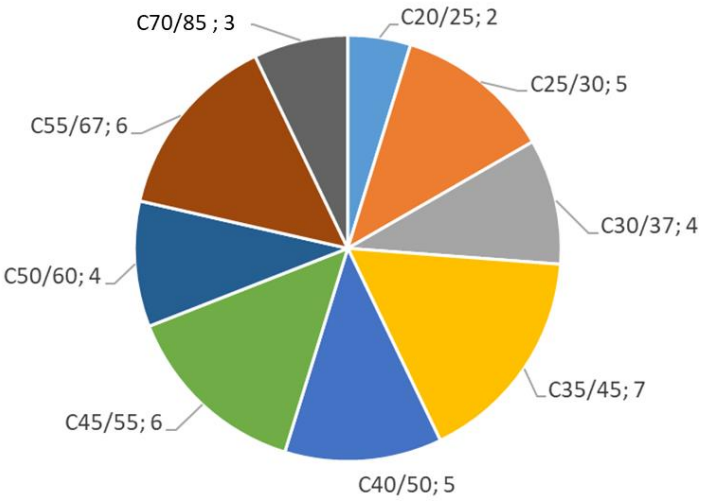

Figure 3.2. Distribution of 42 concretes by compressive strength classes

3.1.6.2 Span values of durability properties

The followings figures (3.3 – 3.10) show the span values of the durability properties for each strength class and highlight the representativeness of the database studied in PerfDuB. The lowest point is the minimum of the data set, and the highest point is the maximum of the data set. The box is drawn from the first quartile to the third quartile with a horizontal line drawn in the middle to denote the median. The cross indicates the mean value.

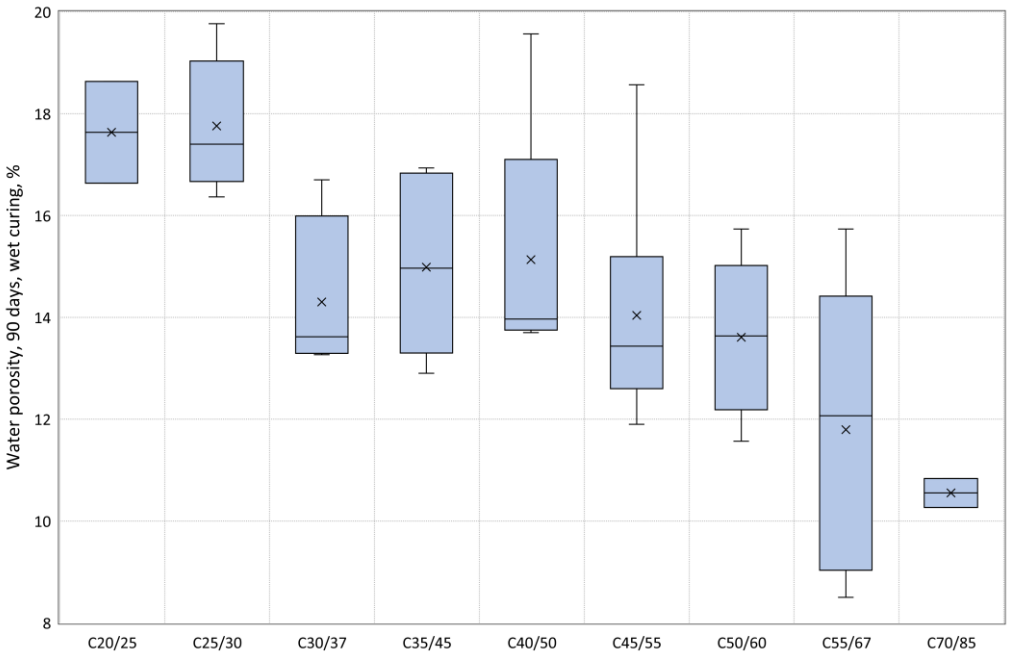

Figure 3.3. Cartography of the 42 concretes – water porosity – mean values

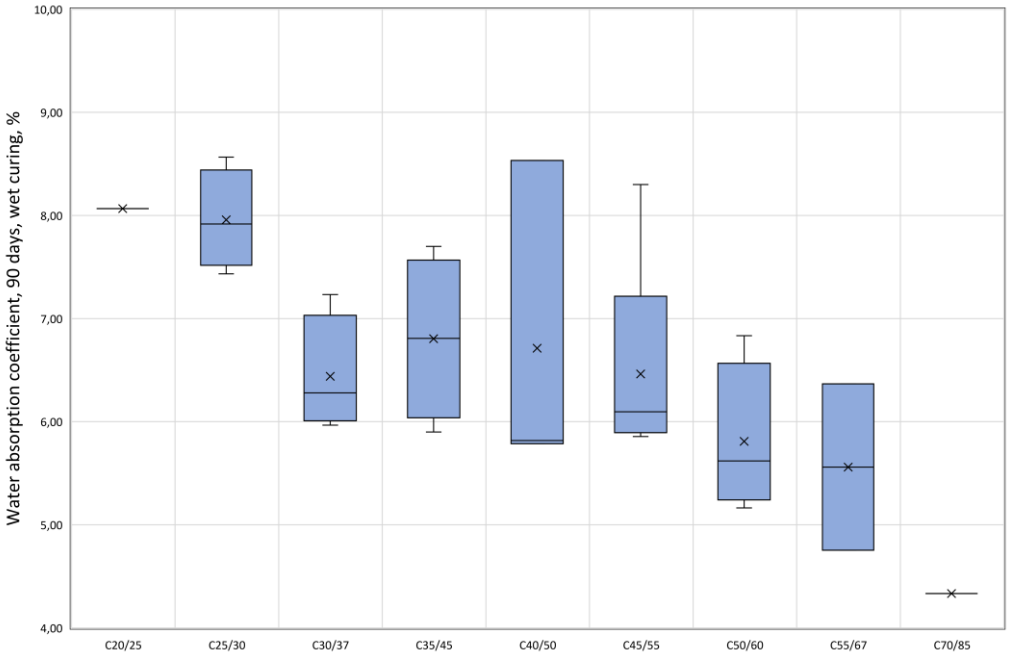

Figure 3.4. Cartography of the 42 concretes – water absorption coefficient – mean values

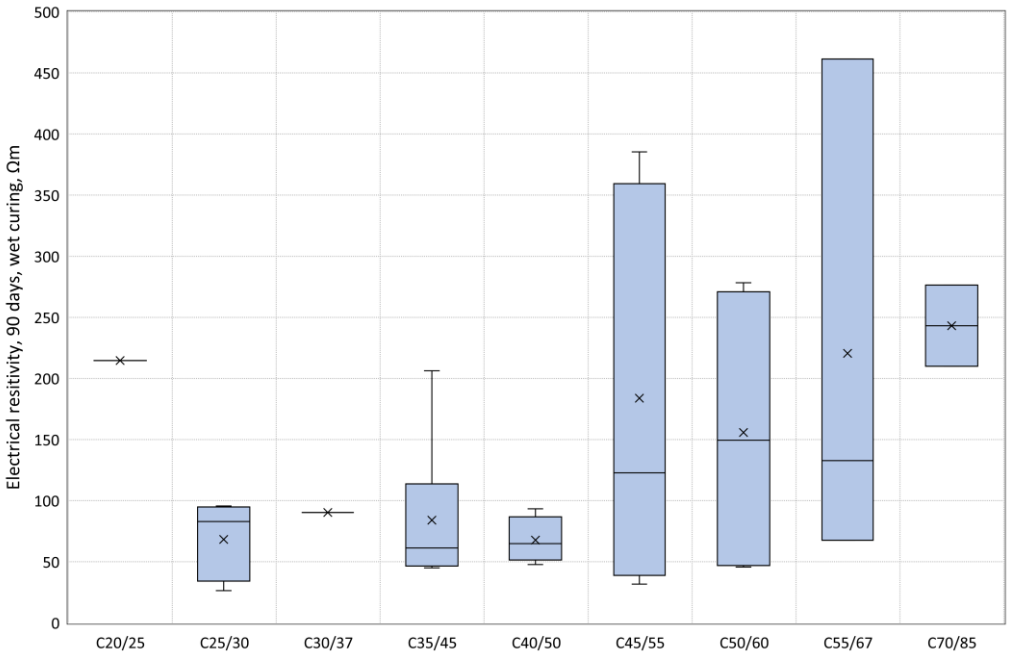

Figure 3.5. Cartography of the 42 concretes – electrical resistivity – mean values

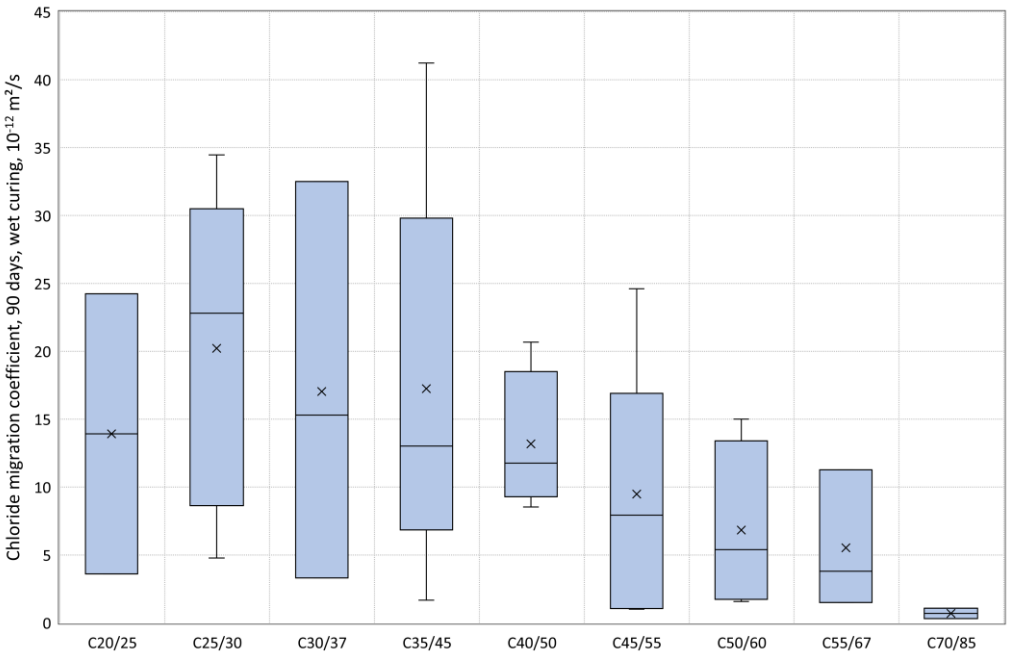

Figure 3.6. Cartography of the 42 concretes – chloride migration – mean values

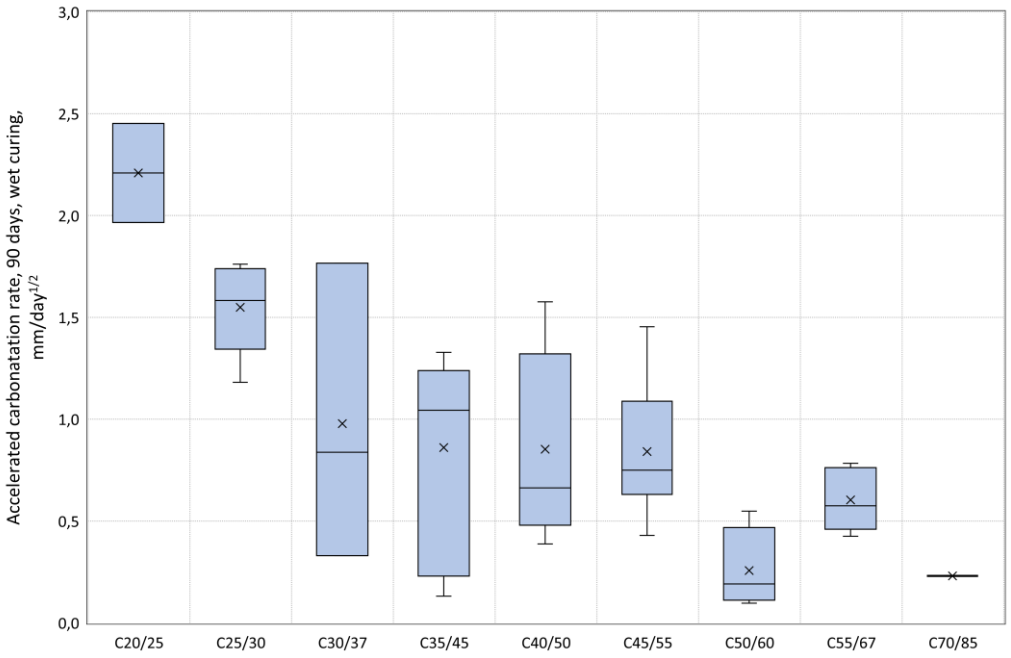

Figure 3.7. Cartography of the 42 concretes – accelerated carbonation according to EN 12390-12 (including alternative preconditioning part) – mean values

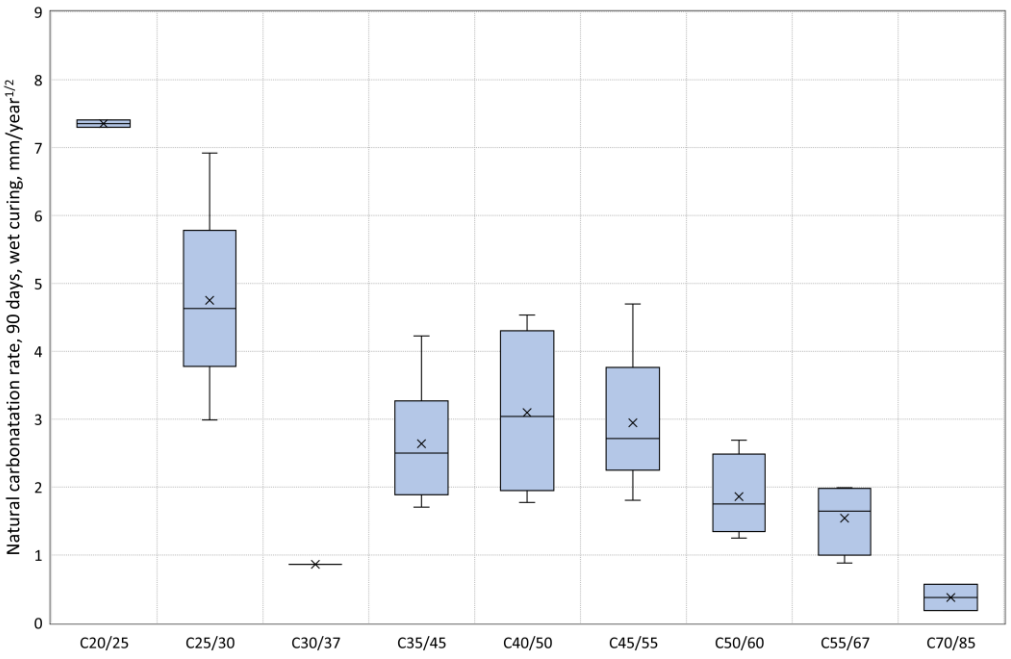

Figure 3.8. Cartography of the 42 concretes – natural carbonation – mean values

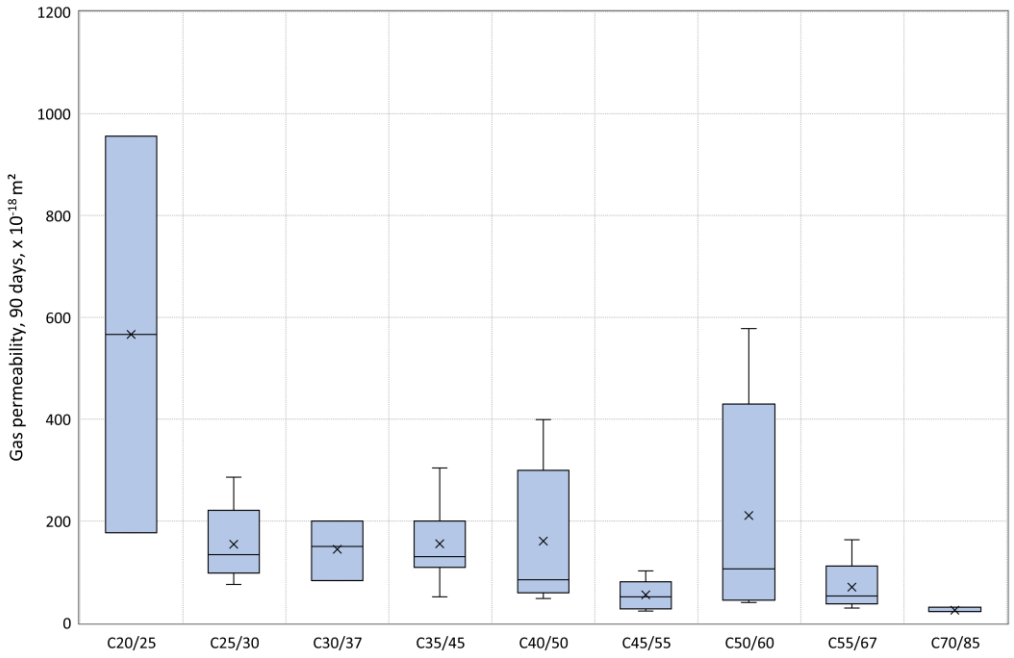

Figure 3.9. Cartography of the 42 concretes – Cembureau gas permeability, dry state – mean values

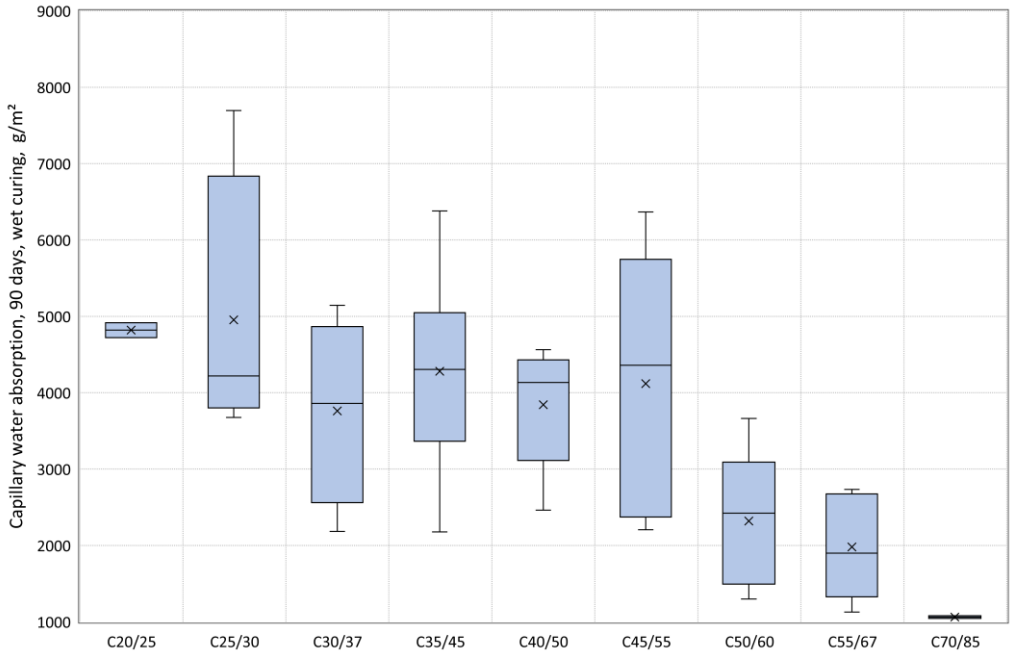

Figure 3.10. Cartography of the 42 concretes – capillary water absorption – mean values

3.2 Conclusions

The large and representative data base of PerfDuB National Project, is a necessary determinant tool in the methodology to determine threshold values for durability.

The manufacturing, characterising, and analysing of the 42 concretes contribute to determine robust threshold values for each durability indicator. These results combined with those given by modelling (GT2B) and those given by feedback from old structures (GT2A) are the basis for the implementation of the performance-based approach in NF EN 206/CN.

4 Porosity, water absorption and resistivity

Authors: François Cussigh, Jonathan Mai-Nhu, Thomas Pernin

4.1 Operating modes

The operating mode for the porosity is based on the modified French standard NF P 18-459 (2010). The operating mode for the Immersion absorption is based on the annex F of the common rules for precast concrete products NF EN 13369.

4.2 Porosity and water absorption

The results obtained from the 42 concretes tested are summarised in Table 3.4.

Table 3.4. Synthesis of experimental results

N° conc.	ε (%)		Water absorption (%)		N° conc.	ε (%)		Water absorption (%)	
	28 days	90 days	28 days	90 days		28 days	90 days	28 days	90 days
1	16.3	16.9	7.3	7.2	22	13.5	13.4	5.9	5.9
2	17.0	17.4	7.1	7.8	23	16.2	15.3	-	-
3	-	13.3	-	6.0	24	13.3	13.3	6.0	5.9
4	-	16.7	-	7.2	25	13.0	13.8	-	-
5	19.0	18.6	7.9	8.1	26	12.9	12.9	-	-
6	16.1	17.0	7.1	7.4	27	11.6	13.1	5.0	4.8
7	15.8	16.8	8.3	7.7	28	11.9	8.5	-	-
8	18.0	19.8	-	-	29	10.3	9.6	-	-
9	16.2	16.4	7.9	8.1	30	11.5	11.6	4.6	5.2
10	17.7	18.3	8.9	8.6	31	11.7	12.1	-	-
11	14.8	14.6	-	-	32	12.2	-	-	-
12	14.5	14.7	6.5	6.5	33	14.2	14.0	6.1	5.8
13	14.8	13.4	6.1	6.1	34	13.8	13.4	5.9	-
14	13.6	13.9	6.1	6.4	35	13.8	14.3	-	-
15	13.4	13.6	5.7	5.5	36	19.3	19.6	8.7	8.5
16	13.8	13.7	5.8	5.8	37	13.0	12.8	5.5	6.1
17	14.3	15.0	-	-	38	9.9	10.3	-	-
18	13.6	14.1	6.2	5.9	39	15.4	15.7	6.7	6.8
19	13.5	12.8	5.6	5.8	39b	15.2	15.7	6.1	6.4
20	18.2	18.6	8.5	8.3	40	16.0	16.6	7.6	8.1
21	-	11.9	-	6.1	41	10.6	10.8	4.4	4.3

Nomenclature: concrete number_cement type_addition type and content_effective water / binder ratio compressive strength
Binder = total binder = cement + addition

4.2.1 Impact of the aggregate porosity on the water porosity

The aggregates used for the fabrication of the 42 concretes have different water absorption coefficients. Aggregates G2 have a water absorption coefficient of 2.5 % and aggregates G4 have a water absorption coefficient of 4 %. For the aggregates G1, G3, G5, the water absorption coefficient is equal or less than 1 %.

The sets of concrete defined in the 3.1.2.1 are linked to the clinker content in the concrete and are not relevant to fully analyse the water absorption porosity which is a more physical property.

The sets used hereafter to analyse the distribution of the water porosity are based on the compressive strength classes defined in 3.2.2.2. The following sets are proposed to analyse the distribution of the water porosity with the coefficient of immersion absorption (CIA) (Figure 3.11) and with the compressive strength classes (Figure 3.12).

Results presented in Figures 3.11 and 3.12 highlight the influence of the water absorption of aggregates on the water porosity of the concrete. For concrete with compressive strength classes higher than C50/60, the water porosity of concretes is less than 14 %, whatever the other composition parameters, except when using aggregates with 2.5 % and 4 % of water absorption. For these concretes, the water porosity values on concrete vary between 15.8 % (aggregates with 2.5 % of water absorption) and 18.6 % (aggregates with 4 % of water absorption).

More than 90 % of concretes with high absorption aggregates have a measured water porosity higher than 15 %, whatever the compressive strength class. All the concrete made with aggregates G1, G3 and G5 have a water absorption porosity less than 15.5 %, whatever the compressive strength class.

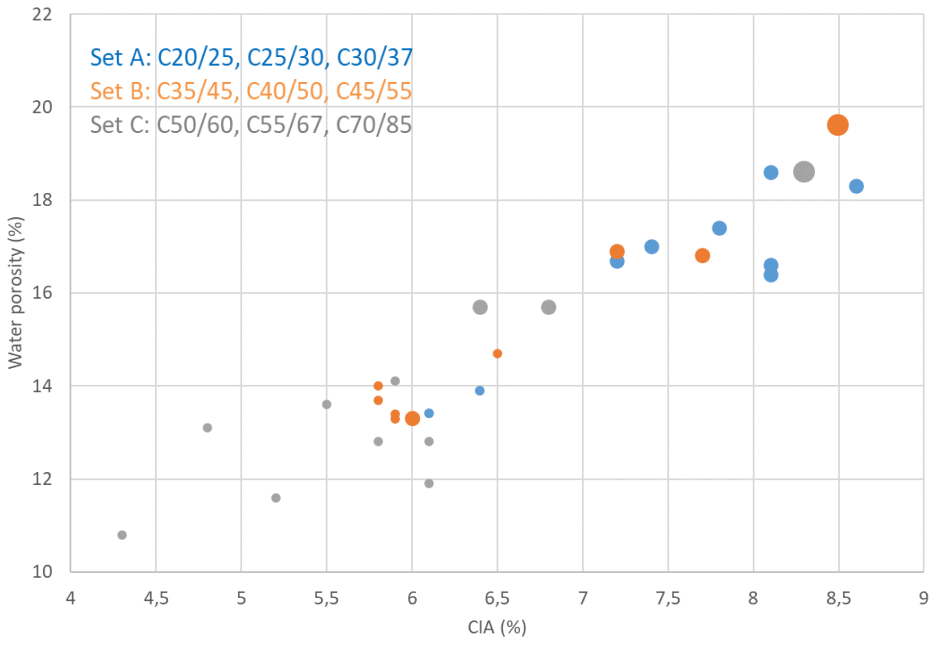

- Represents 15 concretes including aggregates with low water absorption of aggregates (< 1 %)
- Represents 12 concretes including aggregates with medium water absorption (around 2.5 %)
- Represents 2 concretes including aggregates with high water absorption (around 4 %)

Figure 3.11. Water porosity according to the coefficient of immersion absorption at 90 days

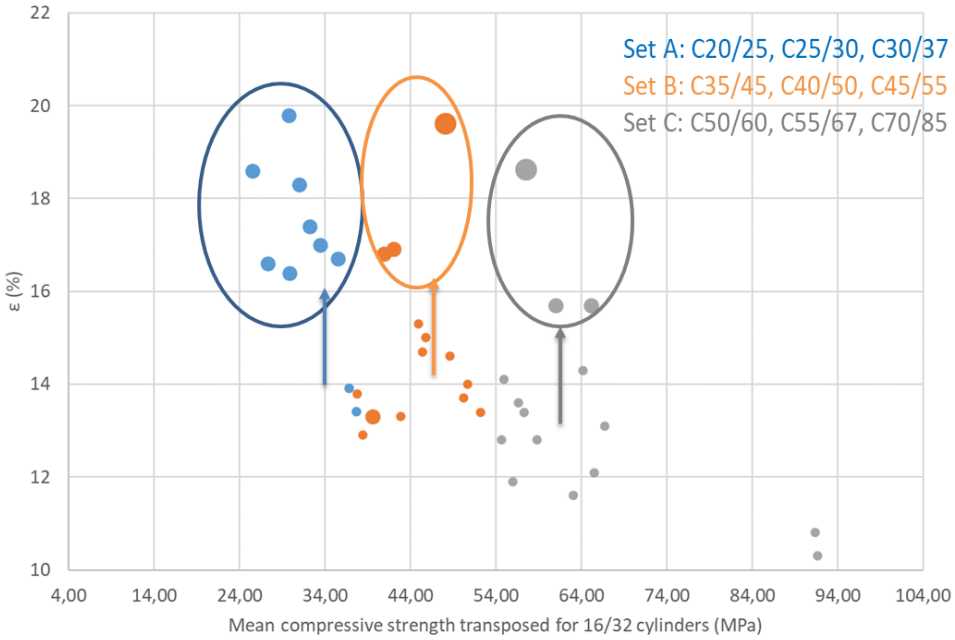

- Represents 24 concretes including aggregates with low water absorption of aggregates (< 1 %)
- Represents 13 concretes including aggregates with medium water absorption (around 2.5 %)
- Represents 2 concretes including aggregates with high water absorption (around 4 %)

Figure 3.12. Distribution of water porosity values according to compressive strength classes – Influence of water absorption of aggregates

4.2.2 Introduction of the ratio Water porosity/Paste volume

The literature shows that using concrete with medium water absorption of aggregates might increase the water porosity of the considered concrete. But an increase in this porosity would not necessarily be correlated with a degradation of the durability properties.

To focus on the porosity of the paste, using the water porosity linked to paste volume shows several interesting results, as seen in (Rozière, 2007) (Figure 3.13).

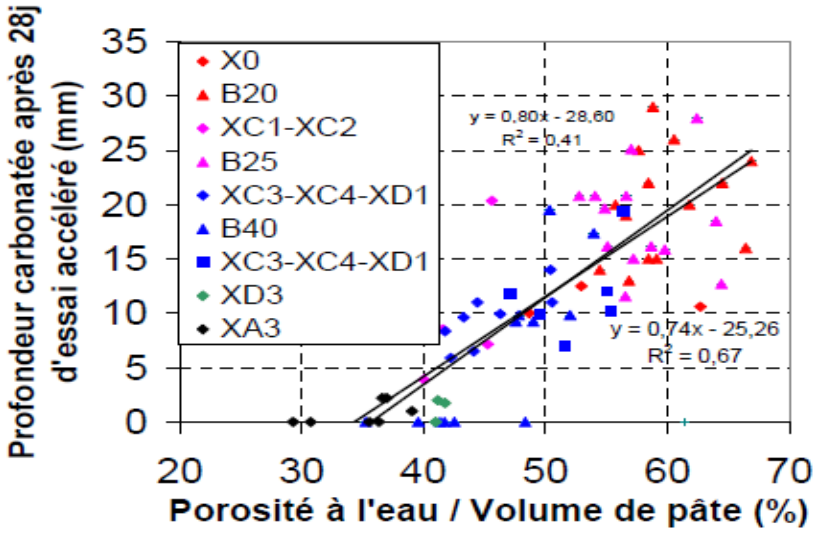

Figure 3.13. Carbonated depth depending on the porosity of the paste, the granular mixture, and the specifications of the standard according to the exposure classes (Rozière, 2007)

In his thesis, (Roziere, 2007) studied several concretes depending on specifications of the standard with several aggregates. The author mentions that several "water porosity/paste volume" ratios were studied to observe an influence of the porosity of the paste on carbonation depth (obtained with the French standard XP P 18-458).

The paste volume fraction (in %) considered is composed of the fraction of the binder and the fraction of the sand under 0.063 mm in the composition, as shown in the equation 3.1.

$$\text{Paste volume fraction (\%)} = 100 - \text{Aggregates volume fraction} > 0{,}063\ \text{mm (\%)} \qquad \text{(Equ. 3.1)}$$

The results in Figure 3.13 show no significant differences in behaviour between concretes from the same exposure classes but made with different aggregates.

With significant differences in porosities (overall or of the paste), which would be indirect consequences of variations on aggregates, the deviations do not necessarily lead to corresponding variations of carbonation depths.

However, general tendency is to increase carbonate depth with porosity, but for a given porosity value, a high dispersion of carbonation depth values occurs.

4.2.3 Link between porosity values and other durability properties

Table 3.5 presents the durability results obtained from the tests on the 42 concretes. The results are expressed in characteristic values: water absorption, carbonation rate, resistivity, apparent migration coefficient and gas permeability.

Table 3.5. Characteristic values for every 42 concretes

N° concrete	Water porosity $P_{water,k,90\ d}$ (%)	Carbonation rate $V_{acc,k,90d}$ (mm/day$^{1/2}$)	Resistivity ρ_k (Ωm)	App. Migration Coeff. $D_{rcm,k}$ (10^{-12} m²/s)	Gaz perm. $k_{sec,k}$ (10^{-18} m²)
1	18.2	1.38	69	34.3	168.8
2	18.7	2.26	120	16.5	166.1
3	14.3	1.11	113	20.2	114.9
4	18.0	2.33	-	-	276.8
5	20.0	3.24	270	4.8	1323.1
6	17.3	1.56	53	35.0	215.9
7	18.1	1.63	57	54.4	70.6
8	21.3	1.99	104	30.1	104.1
9	17.7	2.09	118	6.3	395.8
10	19.7	2.32	33	45.5	185.5
11	15.7	1.41	60	27.3	66.2
12	15.6	1.32	-	-	276.8
13	15.9	0.00	-	-	207.6
14	14.6	0.44	-	42.9	-
15	14.6	0.72	63	19.8	67.5
16	14.8	0.87	84	11.3	117.2
17	16.2	1.75	259	2.2	179.9
18	15.2	1.04	154	3.0	101.7

N° concrete	Water porosity $P_{water,k,90\ d}$ (%)	Carbonation rate $V_{acc,k,90d}$ (mm/day$^{1/2}$)	Resistivity ρ_k (Ωm)	App. Migration Coeff. $D_{rcm,k}$ (10^{-12} m²/s)	Gaz perm. $k_{sec,k}$ (10^{-18} m²)
19	13.8	0.13	57	11.3	388.9
20	20.0	0.57	40	32.5	40.1
21	12.8	0.94	-	18.0	96.9
22	14.4	0.92	58	18.9	44.7
23	16.5	0.30	84	14.1	420.7
24	14.3	1.39	59	20.2	236.7
25	14.9	0.75	79	15.8	96.9
26	13.9	0.17	104	11.3	150.9
27	14.1	0.98	-	-	83.0
28	9.2	0.56	85	14.9	40.1
29	10.3	0.65	-	-	63.0
30	12.5	0.00	-	-	55.4
31	13.0	1.03	579	2.0	72.7
32	13.1	0.30	-	-	30.4
33	15.1	0.51	-	-	276.8
34	14.4	1.92	484	1.3	141.2
35	15.4	0.21	312	2.1	146.7
36	21.1	2.08	117	15.2	552.2
37	13.8	1.28	419	1.4	31.8
38	11.1	-	-	0.4	42.2
39	16.9	0.30	350	2.9	800.0
39b	16.9	0.31	167	5.0	225.6
40	17.9	0.76	-	32.0	245.0
41	11.4	2.59	264	1.4	30.4

Calculation of characteristic values given in section 10

4.2.3.1 Link between porosity and gas permeability

The gas permeability measurement was carried on most of the 42 concretes. The evolution of gas permeability as a function of the ratio of Water porosity/Paste volume ratio is shown in Figure 3.14.

The Figure 3.14 shows that gas permeability is not correlated with the porosity accessible to water in concrete, whatever the set of concrete or the aggregates water absorption. No robust link can be determined to define some criteria with this indicator. The exploitation of the gas permeability results is detailed in the section 5.

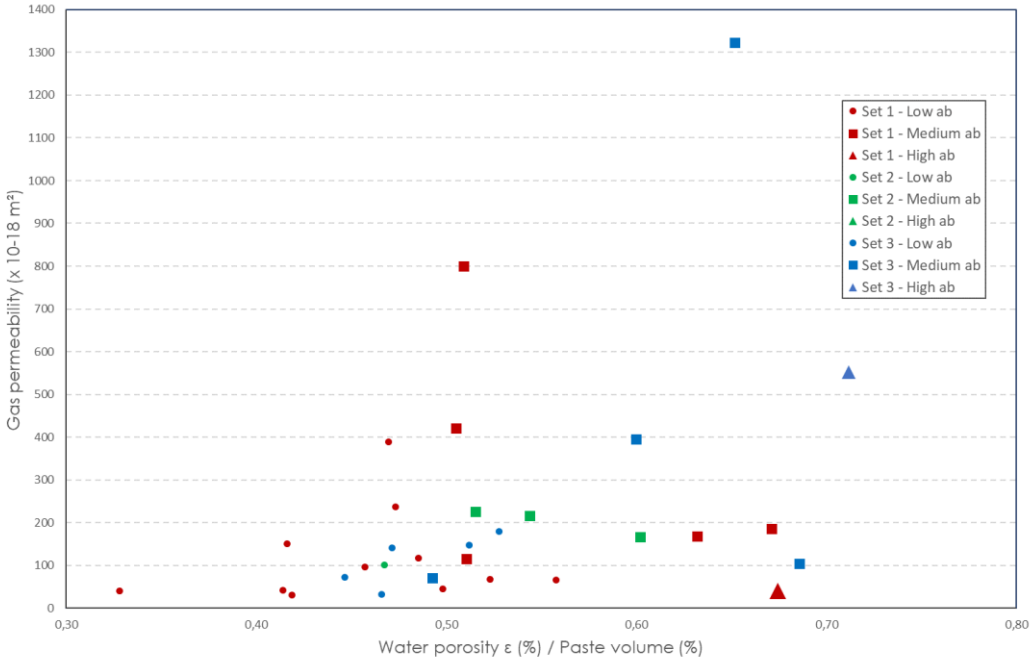

Figure 3.14. Evolution of the gas permeability as function of the Water porosity/Paste volume– Influence of water absorption of aggregates and the paste volume

4.2.3.2 Link between porosity and accelerated carbonation rate measured according EN 12390-12 (including alternative preconditioning part) – wet curing

In Figure 3.15, results present the influence of the water porosity on the accelerated carbonation rate of the concrete (the numbers associated to each concrete correspond to the number of the concrete indicated en Table 3.2).

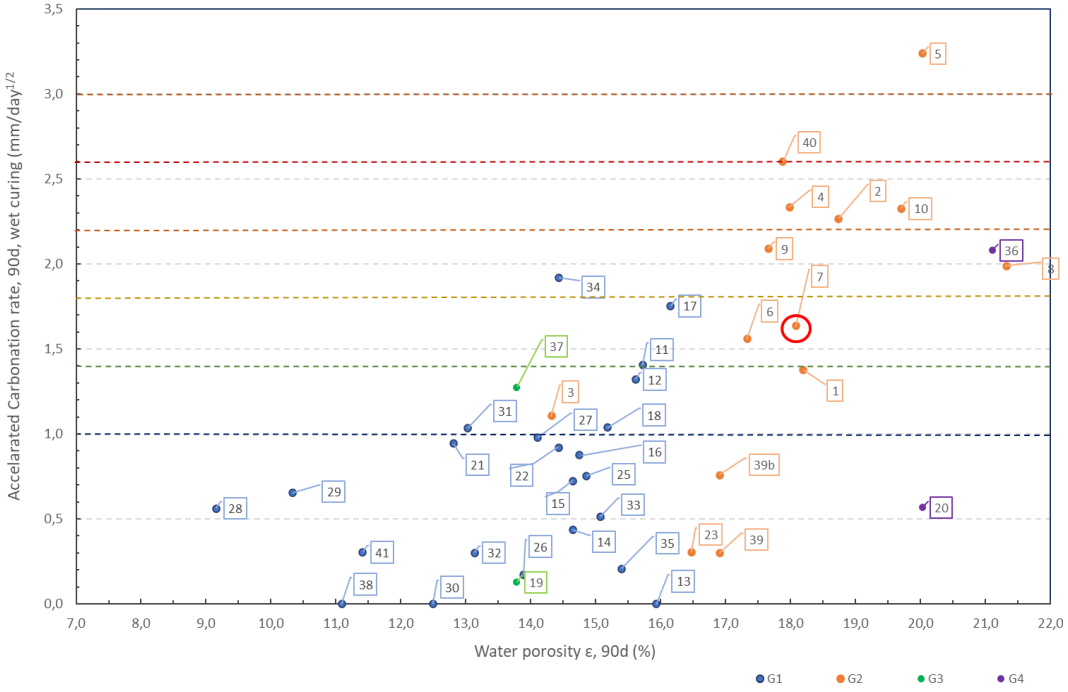

Figure 3.15. Link between accelerated carbonation rate and water porosity – characteristic values

The water absorption of the aggregates, which have, as seen in previous part, a significant impact on the water porosity of the concrete is visible with the distribution of the results (colour of the points linked to the aggregate type, Table 3.2).

In PerfDuB Project, it was decided to use a criterion based on indicators making it possible a better consideration of the concretes with high volumes of paste. The Figure 3.16 shows the distribution of accelerated carbonation rate according to the “water porosity/paste volume”.

This method allows self-compacting concrete to be valorised although its relatively high paste volume, as shown by the concrete 7 pointed in the Figure 3.16.

The wide dispersion of the results shows in the Figure 3.16 leads to adopt an approach on the safe side in the definition of thresholds values of the “water porosity/paste volume” as an alternative criterion for XC exposure classes.

The choice of the threshold values is represented by the dashed line in Figure 3.16. The choice of the slope of the black dotted line is made in such a way that the use of this alternative criterion does not make it possible to validate concretes whose accelerated carbonation rates are higher than the threshold values represented by the horizontal dotted lines.

As an example, by retaining a criterion “water porosity/paste volume” lower than 55 %, it is ensured that the corresponding validated concretes do not exhibit a carbonation rate higher than 2.2 mm/day$^{1/2}$.

With this approach, only three concretes do not fulfil the criterion “Water porosity/Paste volume” compared to the accelerated carbonation rate, but it has to be noticed that two of the three concretes are fulfilling the specifications of prescriptive approach of NF EN 206/CN.

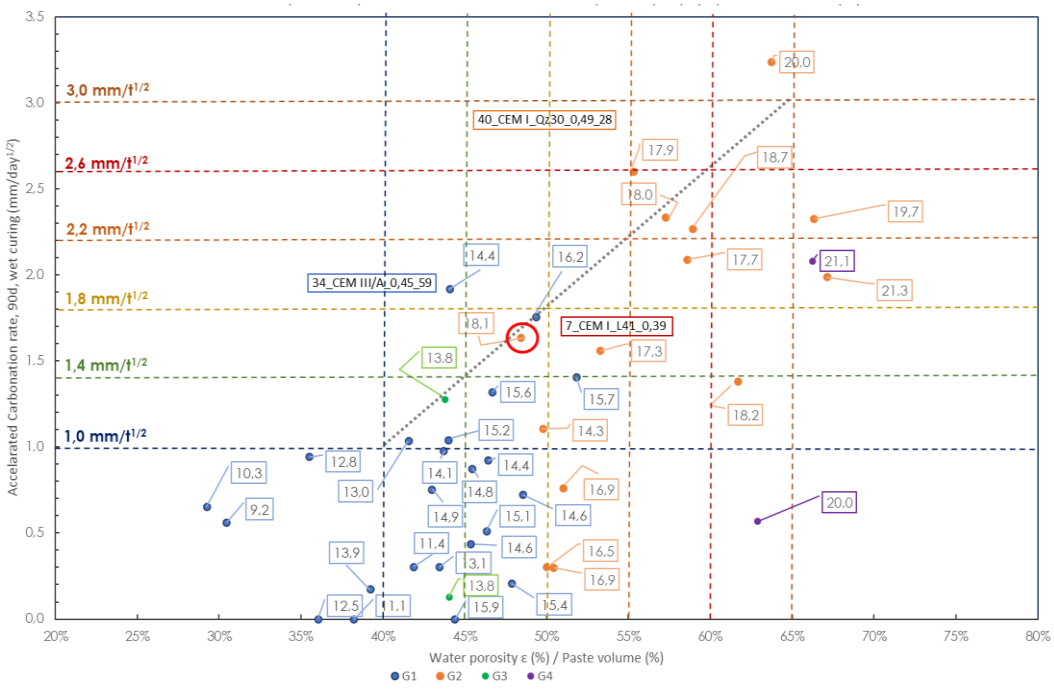

Figure 3.16. Distribution of accelerated carbonation rate according to the “water porosity/paste volume” – characteristic values* - Characteristic water porosity (%) are indicated for each concrete

The Table 3.6 presents the performances criteria on the acceleration carbonation rate and the ratio water absorption/paste volume.

The wide dispersion of the results required to adopt an important security approach in the definition of these thresholds and to allow the use of one of the properties considered as a substitute option for the other (with exception of concretes 34 and 40).

Table 3.6. Performance criteria considering the concretes complying with the prescriptive approach on the acceleration carbonation rate and the ratio water absorption/paste volume

Performance criteria (90 % characteristic values)		
Option 1	**Option 2**	**For information**
Accelerated carbonation rate according the PerfDuB Procedure, wet curing during 90 days ($mm/day^{0.5}$)	**Water porosity/paste volume (%)**	**Water porosity for a standard concrete with 30 % paste volume (%)**
1.0	40	12.0
1.4	45	13.5
1.8	50	15.0
2.2	55	16.5
2.6	60	18.0
3.0	65	19.5

4.2.3.3 Link with observations on old structures (WG2A work)

Some of the porosity values may seem high compared to the expected performance. However, the porosity limit values proposed should be compared with the water porosity measurements carried out on old structures (GT2a work, in exposure class XC4, which vary between 13.2 % and 18.7 %). The corrosion problems encountered are systematically linked to cover defects. For structures that are not affected by corrosion, and whose ages vary between 51 years and 107 years, the porosity values are between 13.2 % and 17.7 %.

4.3 Link between resistivity and other durability properties

4.3.1 Link between resistivity and chloride migration coefficient (D_{rcm})

Figure 3.17 presents the values of the chloride migration coefficient (D_{rcm}) and the resistivity (ρ) expressed as a function of effective water / binder ratio. It shows no strong influence of the ratio on the D_{rcm} of the concretes while the nature of the binder seems to be underlined. Concretes with less clinker from the Set 3 show low D_{rcm} values and globally higher resistivity compared to the other sets (see 3.2.2.1 for the definition of the different sets depending on clinker content).

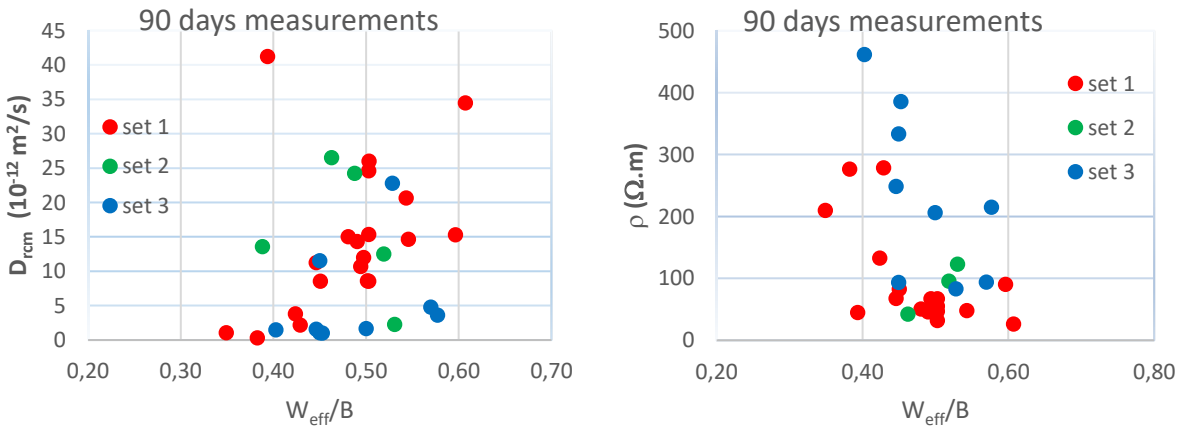

Figure 3.17a and 3.17b. Values of the chloride migration coefficient (D_{rcm}) and the resistivity (ρ) expressed as a function of content effective water / binder ratio. Measurements at 90 days

Figures 3.18 and 3.19 show that most of the concretes from Set 3 (less clinker in the binder) lead to a higher resistivity value. Reducing the amount of clinker by substitution with reactive mineral additions seems to be linked to the resistivity of the concrete.

This result was shown previously in the literature (Liu et al., 2015) (Figure 3.20). Also (Denis et al., 2018) carried out electrical resistivity and chloride diffusion coefficient test during a completion of major project such as the New Coastal Road in Reunion Island. The authors confirmed that resistivity could be a quick and reliable quality control indicator and performance assessment tool for concrete materials.

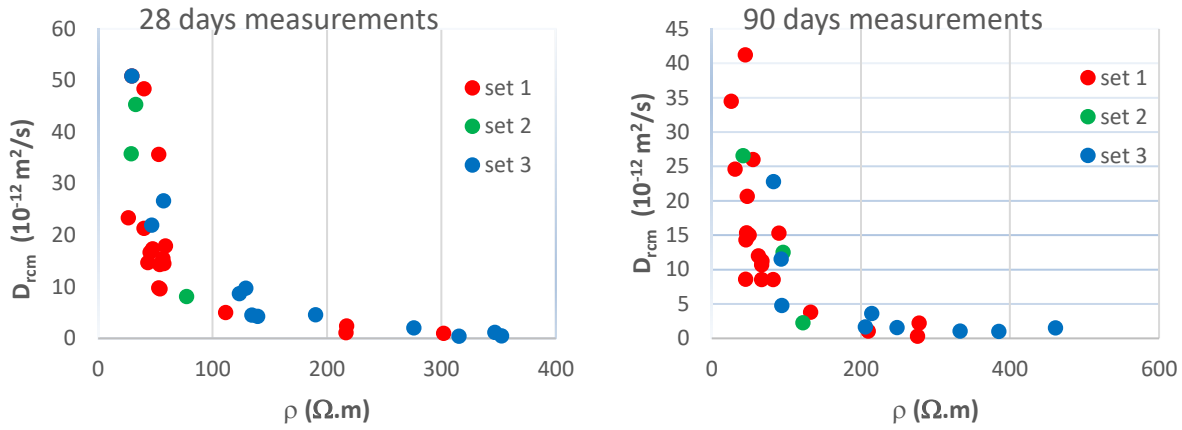

Figure 3.18a and 3.18b. Values of the chloride migration coefficient (D_{rcm}) at 28 and 90 days expressed as a function of resistivity (ρ)

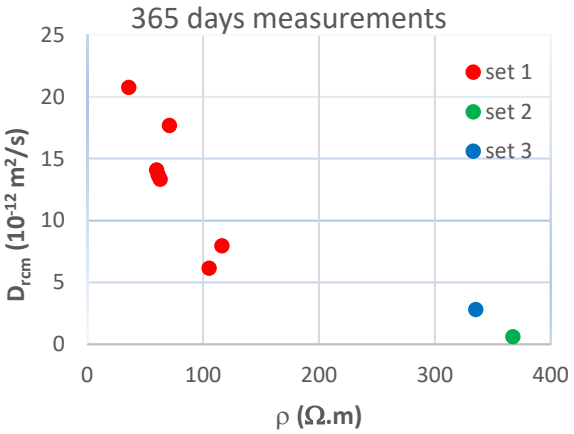

Figure 3.19. Values of the chloride migration coefficient (D_{rcm}) at 365 days expressed as a function of the resistivity (ρ)

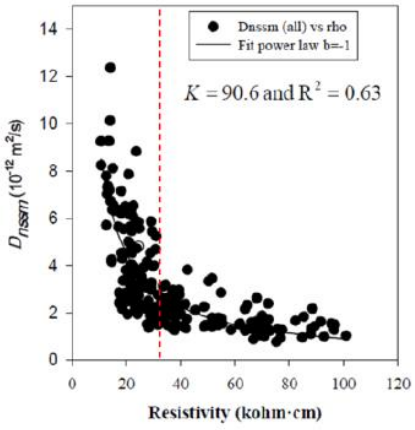

Figure 3.20. Chloride migration coefficient (D_{rcm}) expressed as a function of the resistivity (ρ)
(Liu et al, 2015)

The results with the 42 concretes of the project confirm that there is an interest in further exploiting this indicator easy to measure.

The Figure 3.21 presents the same results but in a logarithmic scale, showing a strong relation between the chloride migration coefficient (D_{rcm}) and the resistivity (ρ), and for all the sets of concrete and different types of binders. These results also confirmed other results in the literature such as (Andrade et al., 2014) (Figure 3.22).

Reducing the amount of clinker increases for most of the concretes of Set 3 the value of the resistivity, linked to a decrease the chloride migration coefficient.

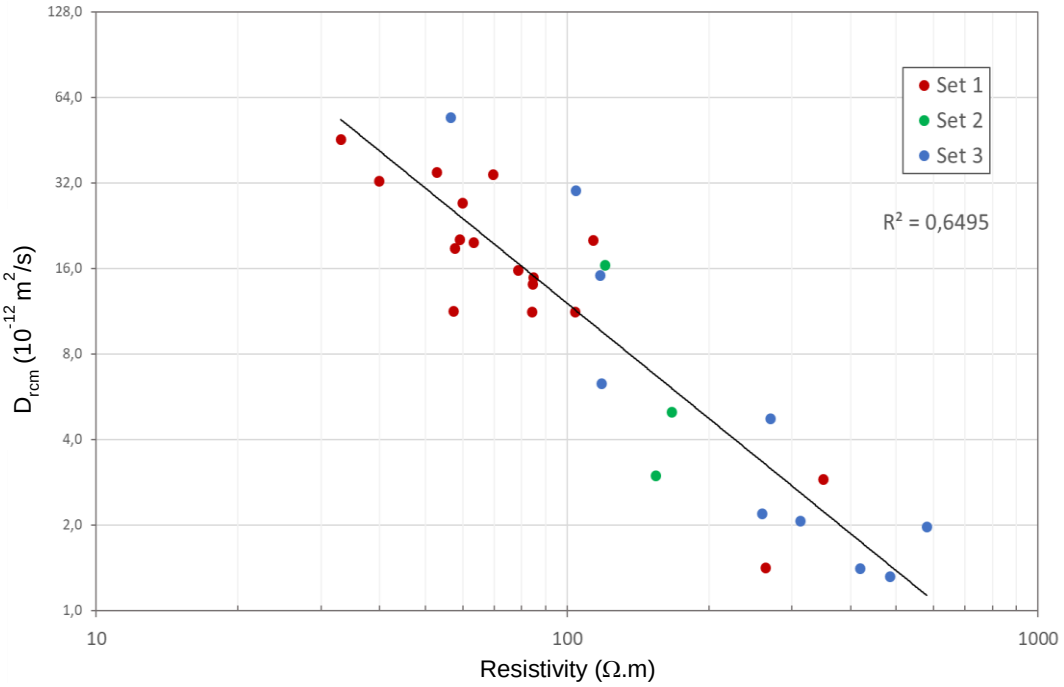

Figure 3.21. Chloride migration coefficient (D_{rcm}) as a function of the resistivity (ρ) at 90 days

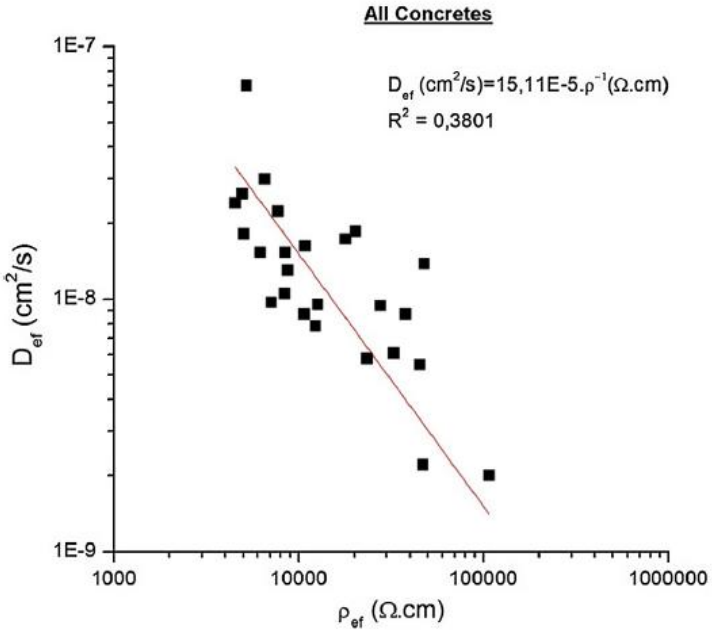

Figure 3.22. Representation of relation between effective diffusion coefficient and effective resistivity (Andrade *et al*, 2014)

4.3.2 Link between resistivity and accelerated carbonation

The relation between the resistivity and the carbonation rate is presented in Figure 3.23.

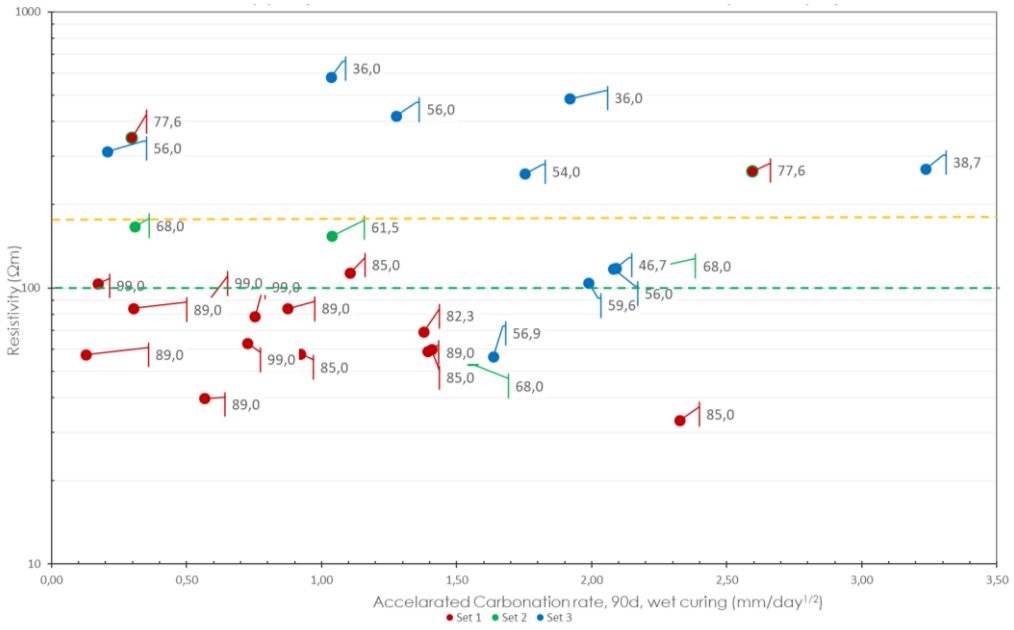

Figure 3.23. Resistivity (ρ) at 90 days function of the accelerated carbonation rate. Colours are related to the concrete set defined previously (see section 3). The dotted lines correspond to the threshold values of electrical resistivity allowing a modulation of threshold values for the accelerated carbonation rate in the performance-based approach. The clinker content in the binder appears for each concrete.

The Figure 3.23 shows that there is no such correlation between the results of the two tests.

However, as detailed in the PerfDuB-GT2B report, the resistivity of the concrete is involved in the corrosion propagation phase of the corrosion process. A modulation of the thresholds values for carbonation rate for the different exposure classes is introduced based on PerfDuB modelling (PerfDuB GT2b) to consider the good performance of high resistivity concretes towards corrosion development, in particular the concrete with mineral additions (see section 3 for the different sets of concrete depending on the clinker proportion in the binder).

The modulation proposed in Figure 3.23 (first class: mean resistivity lower than 100 Ω.m; second class: mean resistivity between 100 Ω.m and 175 Ω.m; third class: mean resistivity higher than 175 Ω.m) makes it possible to enhance the concrete with mineral additions which are efficient with regard to the corrosion propagation phase because their electrical resistivities are high.

4.4 Conclusions

With the study of the porosity and resistivity in correlation with other properties of durability, the following conclusions could be given:

- porosity and carbonation: the correlation observed between these two properties allowing the definition of a criteria between carbonation rate and “Porosity/Paste volume”, with an approach on the safe side in the definition of the thresholds values;
- porosity and gas permeability: there is no correlation between these general indicators. Generally speaking, it has been observed no correlation between gas permeability and other durability properties and composition parameters. The relevance of this general indicator and the use of the results of the database are detailed in section 5;
- resistivity and chloride diffusion coefficient: a link is observed, resistivity is a relevant test and easy to carry to estimate a magnitude of D_{rcm}. To illustrate, it has not been

observed concrete having chloride diffusion coefficients higher than 5.10^{-12} m²/s when the electrical resistivity of the concrete is higher than 175 Ω.m;

- resistivity and carbonation: as detailed in the PerfDuB-GT2B report, the resistivity of the concrete is involved in the corrosion propagation phase of the corrosion process. A modulation of the thresholds values for carbonation rate for the different exposure classes is introduced to take into account the good performance of high resistivity concretes towards corrosion development, in particular the concrete with mineral additions.

5 Gas permeability (CEMBUREAU and Torrent)

Authors: Fabrizio Moro, Emmanuel Roziere

5.1 Introduction

This section is focused on gas permeability, determined through CEMBUREAU and Torrent's derived procedures on 42 and 7 concretes respectively. The data are analysed with regard to concrete compositions and prescriptive provisions, general durability indicators, and performance testing. The CEMBUREAU type procedure requires 80 °C then 105 °C drying until constant mass. The changes induced at the microstructural scale affected the tested materials with a detrimental effect, so that extended curing time or higher compressive strength did not result in expected improvement of performances. The correlations between the gas permeability at dry state and concrete composition or any other property are discussed.

5.2 Operating modes

5.2.1 CEMBUREAU based procedure

The purpose of the test procedure is to measure the apparent gas permeability of a hardened concrete specimen at different water saturations. The test consists to expose the test specimen to a constant pressure gradient. The gas permeability is then determined by measuring the steady state volume flow rate of gas Q going through the specimen using soap bubble or mass flow meters. The result is the apparent permeability k (m^2). Four test specimens are taken from two ∅ 11 cm x H 22 cm cylinders for each measurement (at 28 and 90 days). The apparent permeability is determined at three water saturation states: after oven-drying at 80 °C for 7 days and 28 days (k_7 and k_{28} respectively) and drying of test specimen at 105 °C up to constant mass (k_{dry}).

5.2.2 Torrent based procedure

Non-destructive testing allows assessing the durability of concrete structures without systematically drilling cores. Torrent's permeability test has been developed to determine the air permeability from the surface. The method consists in applying a vacuum inside a cell placed on the concrete surface and measuring the rate at which the pressure returns to the atmospheric value (Torrent, 1992). A two-chamber cell allows creating a unidirectional airflow into the inner chamber. A model is used to calculate the coefficient of permeability (Equ 3.2). The air permeability kT was first calculated assuming a 15 % porosity, then the permeability $k_{T,cor}$ was deduced from the actual porosity of studied concretes when available (see section 4).

$$k_T = \left(\frac{V_c}{A}\right)^2 \frac{\mu}{2.\varepsilon.P_a} \left(\frac{\ln\left(\frac{P_a+\Delta P_i(t_f)}{P_a-\Delta P_i(t_f)}\right)}{\sqrt{t_f}-\sqrt{t_0}} \right)^2 \qquad \text{(Equ. 3.2)}$$

With:

- k_T: air permeability (m^2)
- V_c: volume of inner cell (m^3)
- A: area of inner cell (m^2)
- μ: viscosity of air ($2.0.10^{-5}$ $N.s.m^{-2}$)
- ε: porosity of concrete, initial value (0.15)

- Pa: atmospheric pressure ($N.m^{-2}$)
- ΔP_i: variation of pressure in the inner cell at the end of test ($N.m^{-2}$)
- t_f: time at the end of test (s)
- t_0: time at the test (60 s)

Torrent's permeability test was performed on 7 out of 42 concretes (B2, B5, B6, B7, B23, B32, B39) according to Swiss standard SIA 262-1/E:2013. Three 15x15x15 cm cubes were tested after 28 and 90 days of moist curing. The preconditioning stage consisted in 7-day oven drying at 50 °C. First the moisture content at the surface of specimen was measured with a capacitive hygrometer then the air permeability test was performed under a pressure of 30 mbar. The measurements took place on lateral faces.

5.3 Cartography

First CEMBUREAU permeabilities are presented, then Torrent ones. The results obtained from the 42 concretes tested are given in Table 3.7.

Table 3.7. Synthesis of experimental results obtained with CEMBUREAU

N° conc.	CEMBUREAU gaz permeability (x 10^{-18} m²)					
	28 days			90 days		
	k_7	k_{28}	K_{dry}	K_7	K_{28}	K_{dry}
1	84	96	135	68	86	122
2	102	129	165	37	75	120
3	81	-	102	56	65	83
4	60	200	300	40	100	200
5	204	556	811	262	700	956
6	133	142	160	122	125	156
7	66	68	75	49	50	51
8	43	64	87	26	51	75
9	0	6	164	0	0	286
10	0	0	0	102	115	134
11	33	46	55	27	36	48
12	400	400	400	30	100	200
13	80	100	100	65	100	150
14	70	100	200	-	-	-
15	23	36	55	25	40	49
16	-	-	-	-	44	85
17	39	-	87	8	39	130
18	-	-	-	-	23	74
19	0	177	345	0	128	281
20	0	0	41	0	0	29
21	40	60	70	30	50	70

N° conc.	CEMBUREAU gaz permeability (x 10^{-18} m²)					
	28 days			90 days		
	k_7	k_{28}	K_{dry}	K_7	K_{28}	K_{dry}
22	28	35	43	23	29	32
23	80	139	192	129	204	304
24	57	138	206	0	88	171
25	-	34	56	25	52	70
26	34	70	109	26	67	109
27	1	20	50	1	30	60
28	8	24	42	6	21	29
29	5	12	40	4	22	46
30	2	10	30	1	7	40
31	4	17	58	6	21	53
32	4	8	17	4	10	22
33	20	60	200	6	40	200
34	9	31	76	10	37	102
35	-	-	-	-	19	106
36	22	92	184	0	208	399
37	0	0	0	0	0	23
38	-	-	-	-	6	31
39	58	206	498	61	271	578
39b	30	78	142	32	91	163
40	194	206	231	139	140	177
41	3	12	21	3	11	22

Figure 3.24 shows the influence of drying on apparent permeability, taking into account the influence of binder type and aggregates water absorption coefficient. Oven-drying induced an increase in permeability for all types of concretes. After 7-day drying, most of permeability values were relatively low (Figures 3.24 and 3.25). For several concretes, drying at 105 °C was necessary to measure significant values. This trend is consistent with existing studies on the influence of water saturation on gas permeability.

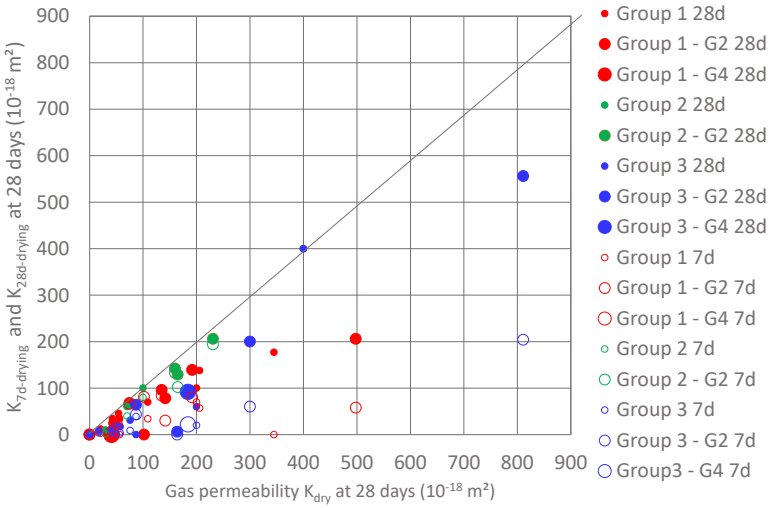

Figure 3.24. Apparent permeability after 7-day and 28-day drying as a function of permeability k_{dry}

The apparent permeability decreased with the increase of compressive strength (Figure 3.25). This can be attributed to lower porosity and a refinement of porous network. It is noteworthy that aggregates with the highest water absorption coefficients did not necessarily result in the highest permeability. The dotted lines on the graphs represent the highest measured permeability for each set of concrete mixtures, excluding the two highest values. After drying at 105 °C up to constant mass, the differences between the three sets were relatively lower. Drying at 80 and 105 °C actually induce several types of damage in hydrated cement paste, such as micro-cracking due to drying shrinkage restrained by aggregates, decomposition of monosulfoaluminates and ettringite, loss of water by C-S-H, etc. The concrete mixtures leading to the highest compressive strengths were also characterized by higher volume of paste, thus they were likely to be more severely affected by oven-drying. Consequently, drying at 105 °C resulted in lower relative variations of the maximum permeability between the three sets of concretes.

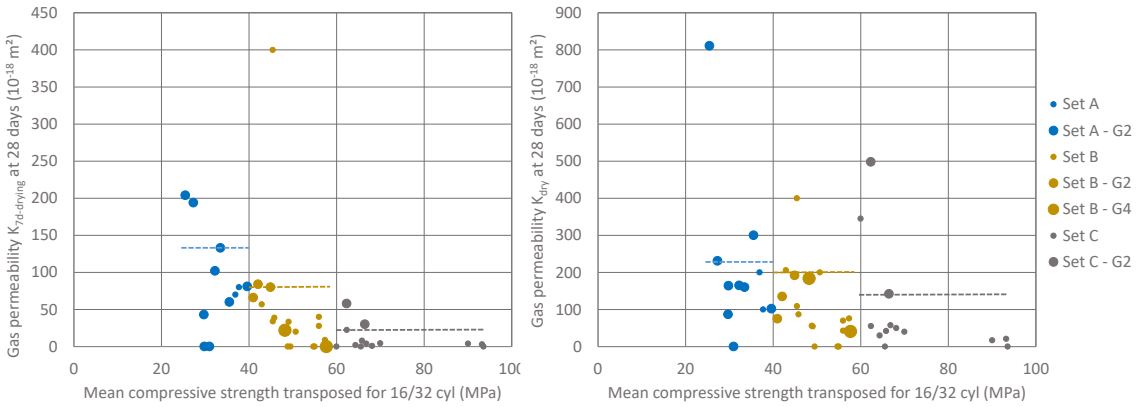

Figure 3.25. Apparent permeability k_7 (left) and k_{dry} (right) as a function of compressive strength

The apparent gas permeability was measured after 28 and 90 days of wet curing (Figure 3.26). As hydration reactions generally induce a decrease in porosity and a refinement of the porous network of cement-based materials, the permeability could be expected to decrease between 28 and 90 days. This was not observed here, as most of concretes had the same values, and the three groups were concerned. Several concretes with very low permeability at 28 days even showed higher values at 90 days. Longer hydration time actually induces an increase in Young's modulus. Stiffer cement paste is thus more vulnerable to restrained shrinkage when exposed to drying, with a probably more significant influence of micro- cracking on concrete microstructure.

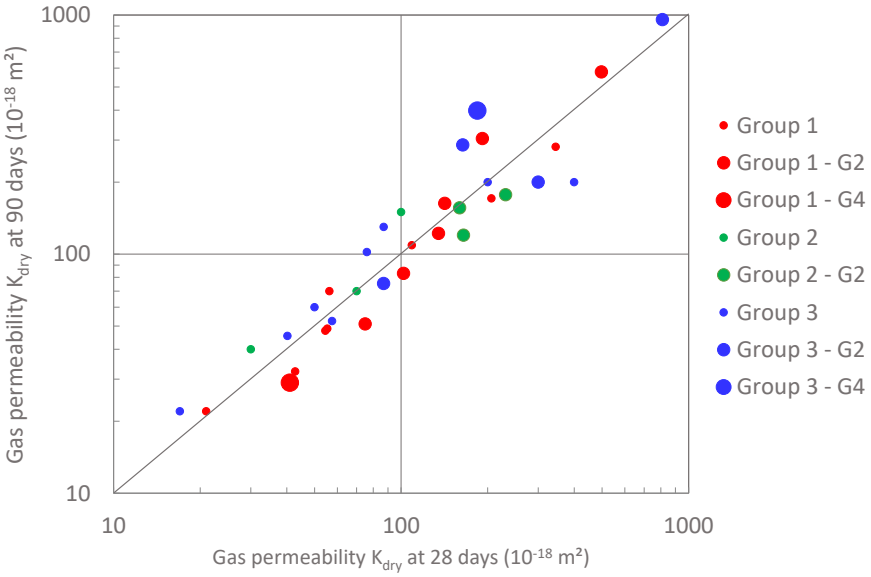

Figure 3.26. Apparent permeability after 28 and 90 days

5.4 Link between gas permeability values and prescriptive approach

The maximum permeability increased with water-to-binder ratio. However, for a given water-to-binder ratio, the permeability was distributed over several orders of magnitude, and a given permeability value could be reached for significantly different concrete mixtures in terms of binder type, water-to-binder ratio and aggregates properties.

For a given water-to-binder ratio, the increase in aggregates water absorption did not necessarily lead to an increase in permeability (Figure 3.27). Aggregates are likely to induce differences in the microstructure of concrete due to their own porosity and the properties of interfacial transition zone or ITZ (Ollivier et al. 1995, Scrivener et al., 2004). This more porous zone with different proportions of hydration products is formed at the interface between cement paste and aggregates due to wall effect and possible water release or uptake by porous aggregates. In this study aggregates were pre-saturated to minimize the variations of effective water content. Moreover, the locally higher porosity of aggregates and ITZ do not induce an increase in permeability as long as these zones are not fully connected.

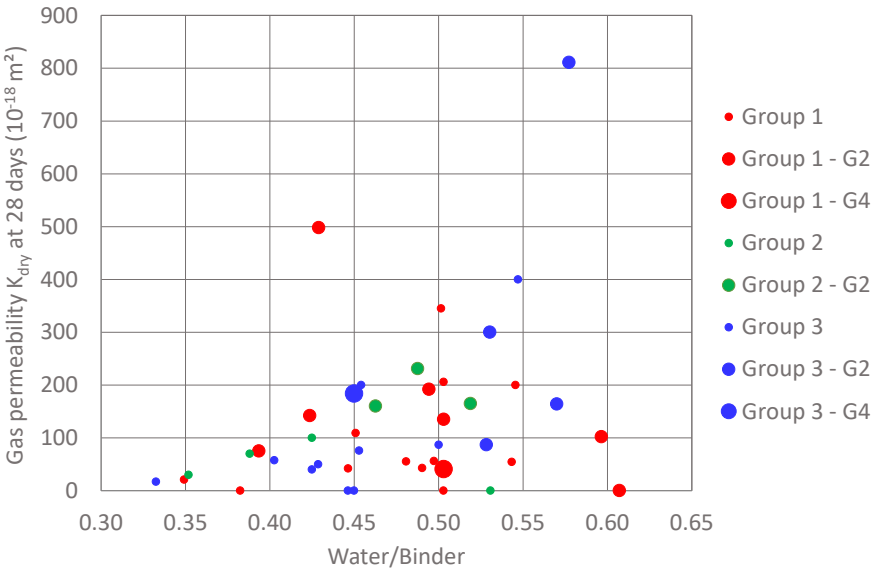

Figure 3.27. Gas permeability at dry state as a function of water-to-binder ratio

5.5 Link between gas permeability values and other durability properties

5.5.1 Porosity

On the graphs of Figure 3.28, 28-day and 90-day permeability k_{dry} have been plotted as a function of porosity at the same age.

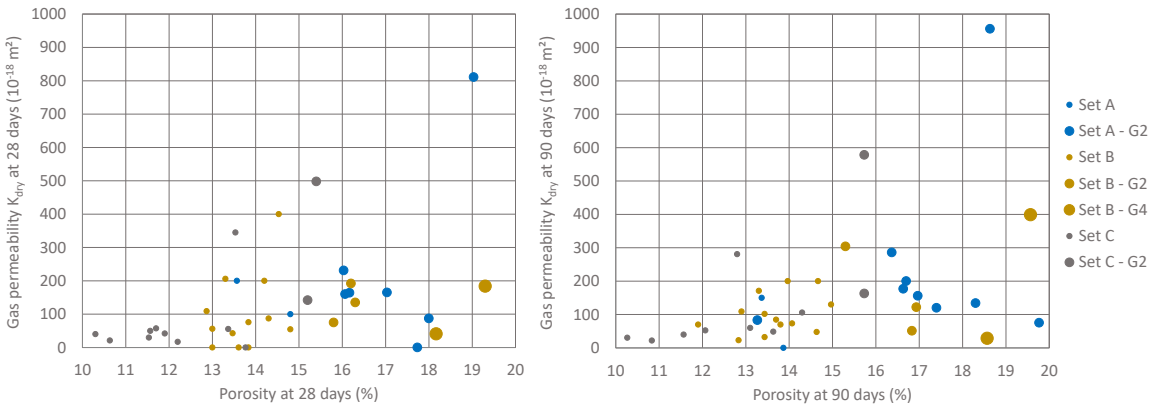

Figure 3.28. Gas permeability at dry state and porosity at 28 and 90 days

The maximum permeability increased with porosity, but there was not a clear correlation between both properties. Permeability is actually estimated from the gas flux through connected porosity in steady state, thus permeability depends on the size of pores more than the porous volume. The influence of aggregates water absorption on porosity can be clearly observed, as pointed out in section 3. It is noteworthy that all the increase in porosity cannot be attributed to aggregates water absorption, as aggregates G2 were used in concrete mixtures with high water-to-binder ratio thus higher porosity of cement paste, for instance. The highest porosity values, related to aggregates with relatively high-water absorption, did not necessarily resulted in high permeability. As mentioned in previous section, the local variations of porosity do not induce an increase in permeability unless they are connected.

5.5.2 Accelerated and natural carbonation

The permeability at dry state is compared with the accelerated and natural carbonation rates in Figure 3.29. The dotted line represents the highest carbonation rate for a given permeability, on a logarithmic scale. An increase of k_{dry} by one order of magnitude resulted in twice higher maximum carbonation rate, but there was not a clear correlation between both properties.

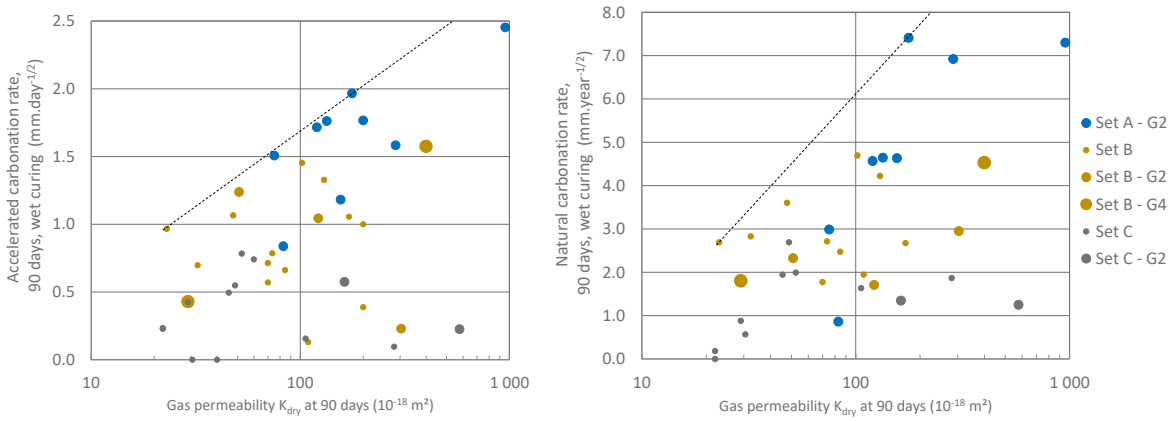

Figure 3.29. Accelerated (left) and natural carbonation (right) rates after wet curing and permeability at dry state.
The dotted line represents the highest carbonation rate for a given permeability, on a logarithmic scale

Carbonation does not only depend on the diffusivity of CO_2 but also on the content of carbonatable material (Papadakis et al., 1991). The permeability was thus compared with the permeability to CaO content ratio (Figure 3.30). This allows taking into account the gas transport in porosity as well as the chemical vulnerability of cement paste. The CaO content was estimated from the chemical compositions of cement and mineral additions, as a first estimation of carbonatable content. CaO can be found in hydrated forms in products vulnerable to carbonation: portlandite, C-(A-) S-H, calcium aluminates.

Figure 3.30 shows the same trends as Figure 3.29, with an increase in maximum carbonation rate for a given permeability. However, both results are not strongly correlated, due to several reasons.

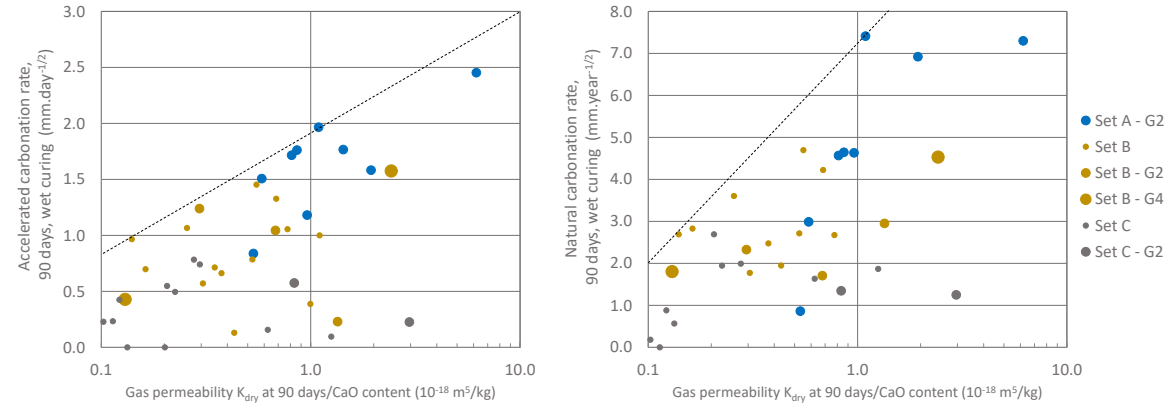

Figure 3.30. Accelerated (left) and natural (right) carbonation rate and permeability to CaO content ratio

First, all carbonation rates have been taken into account, including the values associated with lower coefficients of determination. Moreover, permeability and carbonation rate were associated to different microstructures. Permeability was measured after oven-drying at 80 °C

then 105 °C until constant mass. It is known that this pre-conditioning modifies the microstructure of cement paste and the structure of hydration products. The specimens were exposed to carbonation at 20 °C after drying at 45 °C. Carbonation also induces changes in microstructure and the carbonation of hydration products, coupled with drying and possible micro-cracking due to drying shrinkage and carbonation shrinkage. These microstructural changes depend on binder type. For instance, the diffusivity of carbonated paste can be higher or lower than non-carbonated paste. Permeability corresponds to non-reactive transport in steady state, whereas carbonation is reactive transport in non-steady state.

As a consequence, it would seem questionable to base recommendations on permeability values all on it. However, as the lowest permeability values ($k_{dry} < 30.10^{-18}$ m²) were associated to low carbonation rates (1 mm/day$^{1/2}$ and 3 mm/year$^{1/2}$ in natural and accelerated conditions respectively), low permeability could be suggested as sufficient (but not necessary) condition to mitigate carbonation.

The very poor correlation between carbonation and permeability has been pointed out in previous studies (Roziere et al., 2009). The data presented in Figure 3.31 correspond to concretes with different binders, aggregates, and curing conditions. The test emphasized the properties of the surface concrete layer exposed to early drying (dry curing conditions), which is also the first layer exposed to carbonation. This could explain previous attempts to use gas permeability as an indicator for carbonation behaviour.

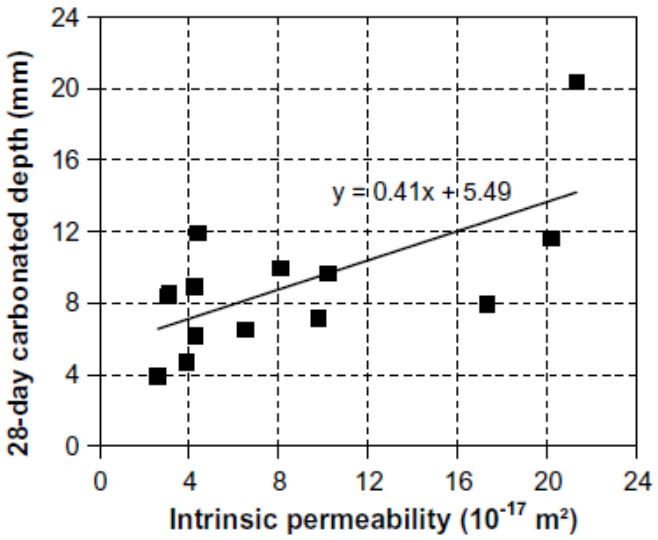

Figure 3.31. 28-day carbonated depth and intrinsic permeability at dry state (Roziere et al., 2009)

5.5.3 Torrent's air permeability

Ages of testing, values of moisture content, concrete surface temperature, and air permeability are given in Table 3.8. B5 and B7 concretes were tested at 18 and 55 days instead of 28 days, and B32 concrete at 127 days instead of 90 days.

Table 3.8. Moisture contents and air permeabilities

		Unit	B2	B5	B7	B6	B39	B23	B32
Theoritical 28 days	Curing time	(d)	28	18	55	28	26	28	24
	RH*	(%)	3.4	3.0	4.2	3.2	3.2	3.7	3.9
	RH std deviation	(%)	0.1	0.1	0.3	0.1	0.1	0.1	0.2
	Temperature**	(°C)	24.1	24.7	23.1	22.9	21.9	22.7	23.2
	k_T	(10^{-16} m²)	0.280	0.437	0.162	0.575	0.043	0.140	0.007
	k_T std deviation	(10^{-16} m²)	0.090	0.382	0.047	0.08	0.033	0.074	0.003
	$k_{T,cor}$***	(10^{-16} m²)	0.247	0.345	0.154	0.536	0.042	0.129	0.009
	$k_{T,cor}$ std deviation	(10^{-16} m²)	0.079	0.302	0.045	0.074	0.032	0.068	0.004
Theoritical 90 days	Curing time	(d)	89	90	88	98	89	90	127
	RH*	(%)	3.4	3.4	4.0	3.0	3.7	3.4	4.2
	RH std deviation	(%)	0.1	0.1	0.2	0.2	0.1	0.1	0.1
	Temperature**	(°C)	22.6	22.8	23.0	23.0	21.7	22.9	25.0
	k_T	(10^{-16} m²)	0.175	0.525	0.253	1.110	0.059	0.220	0.0015
	k_T std deviation	(10^{-16} m²)	0.076	0.576	0.064	0.209	0.047	0.138	0.0004
	$k_{T,cor}$***	(10^{-16} m²)	0.150	0.424	0.226	-	0.056	0.215	-
	$k_{T,cor}$ std deviation	(10^{-16} m²)	0.065	0.464	0.057	-	0.045	0.135	-

** Relative humidity on the concrete surface measured by the Tramex capacitive hydrometer*
*** Temperature on the concrete surface given by the PermeaTorr*
**** $k_{T,cor}$ corresponds to the air permeability corrected with the water porosity measured*

The difference between k_T and $k_{T,cor}$ values remained relatively low excepted for high permeability (0.25 . 10^{-16} m² and above).

The permeability at 90 days is higher than the 28-day values, excepted for B2 and B32 concretes. Hydration usually results in a refinement of the porosity thus lower permeability. The increase observed here could be due to micro-cracking from the surface due the drying of preconditioning stage (Bisschop et al., 2002, Samouh et al., 2017). The cracks induced by 28-day measurement were not (or not totally) healed by water curing and 90-day preconditioning increased the cracking density.

The gas permeability test performed on cores is a destructive and relatively expensive laboratory test, thus it would be useful to correlate these results with a non-destructive and/or cheaper transportable test. The values from gas permeability test k and Torrent's test k_T are compared on Figure 3.32 with a logarithmic graph. k_T is generally lower than k and there is not a strong correlation. The Torrent's permeability is globally consistent with 7-day gas

permeability. These values actually correspond to partially saturated material. The gas permeability test implies 80 °C oven drying, which allows reaching lower relative humidity thus drying finer pores than 50 °C drying recommended by Torrent's test, according to Kelvin-Laplace equation. The final drying at 105 °C recommended by gas permeability test results in the lowest water saturation thus the higher permeability. Note that different concretes can show a different cracking sensitivity during oven drying.

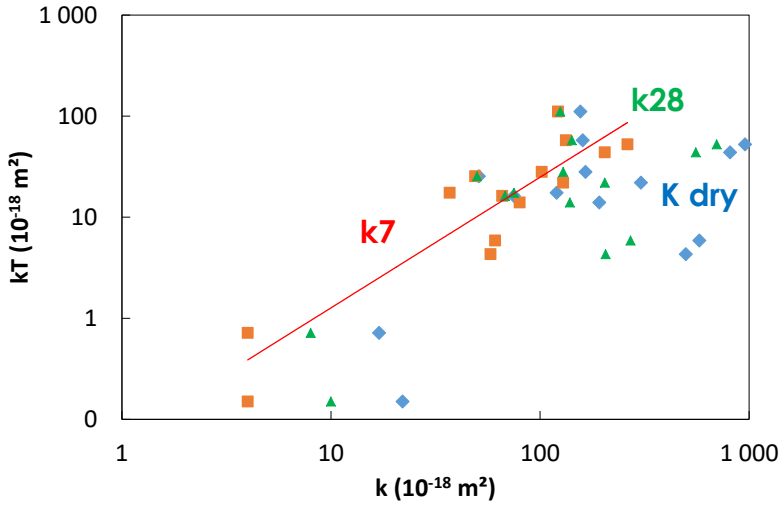

Figure 3.32. Torrent's permeability results function of gas permeability

Carbonation takes place at the surface of concrete structures. The correlation with Torrent's permeability would allow a more convenient and faster determination of the resistance to carbonation than other laboratory tests. Torrent's permeability has been compared with carbonation rate from French accelerated carbonation tests (XP P18-458 see section 7) in Figure 3.33.

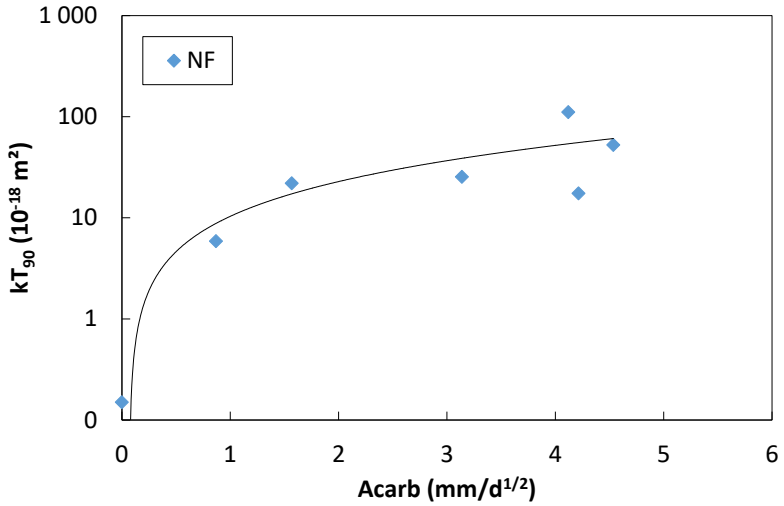

Figure 3.33. Results of Torrent's tests[1] and NF carbonation rates[2]

[1] Samples are preconditioned at 50°C during 7 days and 1h at 20°C before measurement
[2] NF carbonation rate are measured in accordance with The French standard XP P18-458

The highest carbonation rates (higher than 2 mm/d$^{1/2}$) correspond to the same order of magnitude of air permeability. The sensitivity of air permeability is much higher for lower carbonation rates. The resistance of these concretes to carbonation is actually provided by denser microstructure, thus slower CO_2 diffusion. For higher CO_2 diffusivities, the resistance to carbonation is also due to the composition of cement paste.

The highest carbonation kinetics (greater than 2 mm/day$^{0.5}$) correspond to the same order of magnitude of air permeability. Sensitivity is much higher for low carbonation kinetics. The resistance of these concretes to carbonation is effectively conferred by a denser microstructure, and therefore slower diffusion of CO_2. For more rapid diffusion, resistance to carbonation also depends more closely on the composition of the binder.

Accelerated and natural carbonation kinetics as a function of the permeability/initial CaO content ratio are also shown in Figure 3.34 for permeability after 7 days drying at 80 °C and Figure 3.35 for carbonation kinetics with a determination coefficient $R^2 > 0.95$.

There is no correlation between apparent permeability and other properties related to hardness, such as porosity and carbonation kinetics, under natural and accelerated conditions.

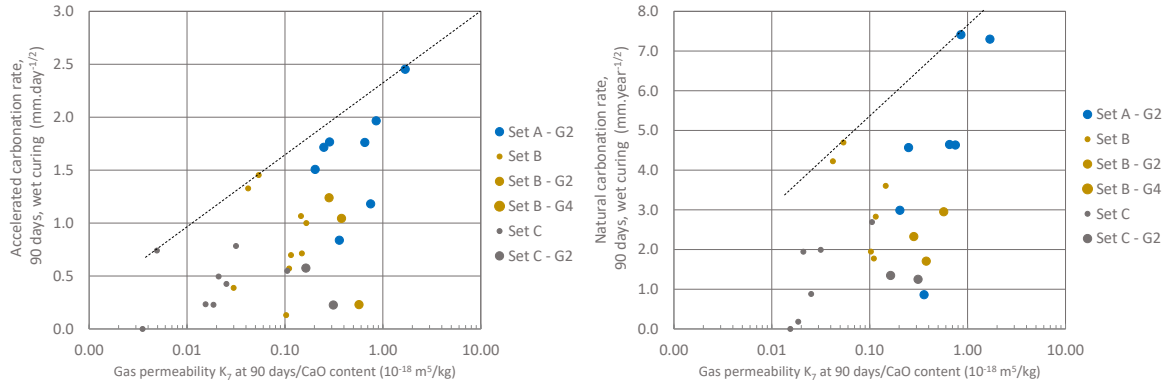

Figure 3.34. Accelerated (left) and natural carbonation (right) rates and permeability to CaO content ratio – permeability after 7-day drying

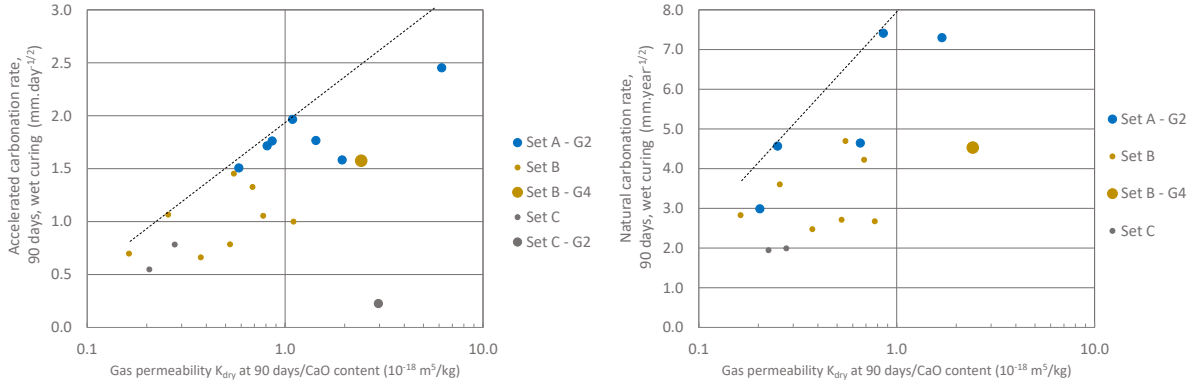

Figure 3.35. Accelerated (left) and natural (right) carbonation rate and permeability to CaO content ratio – carbonation rates with a coefficient of determination $R^2 > 0.95$

5.6 Conclusion and proposals

The apparent permeability measurements confirm that there is not a straightforward relationship between composition parameters (i.e. prescriptive approach) and the actual performance of concrete. The increase in strength class was observed to be consistent with lower permeability values, but the relative differences were not so high; the maximum value of

set C (C50/60 to C70/85) was higher than 50 % of the maximum value of set A (C20/25 to C30/37). The preconditioning of specimens induces a drying at 80 °C then 105 °C, which is known to induce significant changes at the level of the microstructure of cement-based materials. This could also explain why the values after 28 and 90 days of curing were close for most of studied concretes.

The apparent permeability values did not show any strong correlation with other durability properties, such as porosity and carbonation rate, in natural or accelerated conditions (Figures 3.33, 3.34 and 3.35). Each durability property describes concrete from a specific point of view. The permeability characterizes the connected porosity; thus it is less sensitive to variations in porous volumes that could be due to aggregates with higher absorption for example. The apparent permeability does not take into account chemical reactions that affect the phases of hydrated cement paste, such as chloride ingress and carbonation. The studied durability properties are actually associated with different phenomena and microstructures of tested specimens. The lack of correlation in experimental data leads to the conclusion that it does not seem possible to base threshold values for carbonation exposure classes on gas permeability values, as pointed out in previous studies (Figure 3.31).

Torrent's permeability test is relatively convenient and easy to perform in laboratory conditions. The results are sensitive to concrete composition. However there is not a strong correlation with gas permeability CEMBUREAU and carbonation rate obtained in laboratory. The Torrent's air permeability is consistent with gas permeability measured after 7-day drying. A decrease in air permeability of one order of magnitude (or more) can be associated to significantly lower carbonation rate. Note that Torrent's test was performed on a limited number of concretes.

Torrent's permeability and the apparent permeability after 7-day drying present the advantage of evaluating the performances of concrete within a relatively short preconditioning and testing time. As a consequence they could be used in a conservative and simple performance-based approach that would consist in targeting low permeability values.

6 Oxygen diffusivity

Authors: Gabriel Pham

6.1 Introduction - Operating mode

This section deals with the oxygen diffusion coefficient measured on the 42 concretes. The operating mode is described in the end of section.

6.2 Cartography

Oxygen diffusivities after 90 days of wet curing of 42 concretes at dry state are summarized in Table 3.9. Measurements are realized on one 5 cm thick disc except for concretes 6, 15, 17, 19, 21, 23, 25, 26, 27, 33, 37, 39b, 40 for which oxygen diffusivity is determined on three different discs. The covariance (CoV) is then calculated for these concretes.

Table 3.9. Oxygen diffusivity of concrete at dry state (90 days of wet curing)

N° concrete	D_{O2} (10^{-7} m².s^{-1}) 90d (dry state)		N° concrete	D_{O2} (10^{-7} m².s^{-1}) 90d (dry state)	
	Value	CoV (%)		Value	CoV (%)
1	1.9	-	22	1.6	-
2	2.4	-	23	2.8	4
3	3.0	-	24	2.3	-
4	1.4	-	25	1.8	5
5	2.1	-	26	2.3	6
6	4.6	10	27	0.7	16
7	2.2	-	28	1.5	-
8	2.0	-	29	0.5	-
9	2.0	-	30	0.9	-
10	4.7	-	31	0.5	-
11	2.4	-	32	-	-
12	0.7	-	33	2.5	59
13	-	-	34	1.0	-
14	-	-	35	0.7	-
15	2.0	3	36	1.2	-
16	1.3	-	37	1.3	11
17	1.8	11	38	0.5	-
18	0.7	-	39	2.6	-
19	1.9	33	39b	2.8	5
20	-	-	40	4.8	11
21	2.4	18	41	-	-

Variations in the oxygen diffusion coefficient as a function of the effective water/total binder ratio are shown in Figure 3.36.

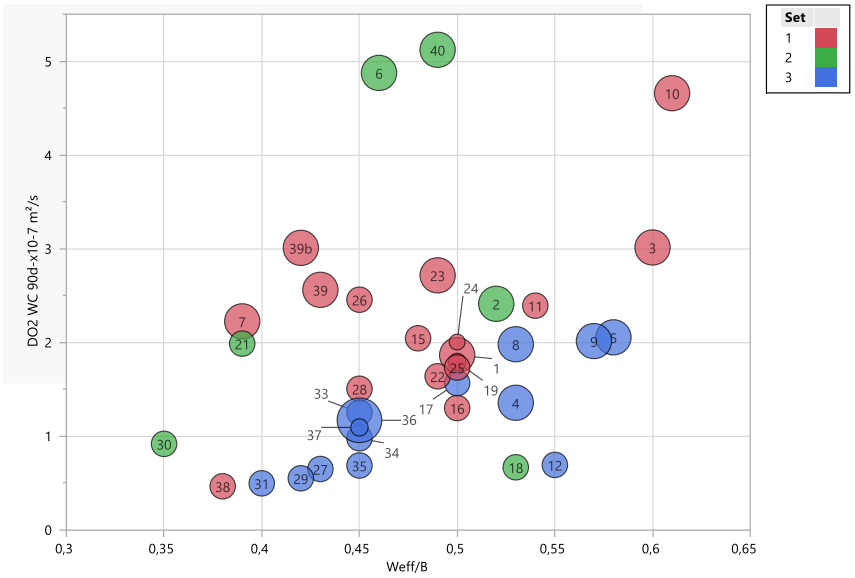

Figure 3.36. Oxygen diffusion coefficient (90d wet curing) vs efficient water to total binder ratio. The sizes of the points correspond to the water absorption of aggregates used (smallest size: lowest water absorption / largest size: highest water absorption)

The measured values of oxygen diffusivity vary between 0.5 and 5.10^{-7} m²/s. The diffusion coefficient of oxygen in air is ~1.10^{-5} m²/s.

For the same concrete set:

- no link between the oxygen diffusion coefficient and the W/B ratio is observed;
- for a given W_{eff}/B, concrete containing aggregates with high water absorption (G2) give the highest oxygen diffusivities.

Figure 3.37 shows the variations in the oxygen diffusion coefficient (90j wet cure) as a function of the quantity of total binder.

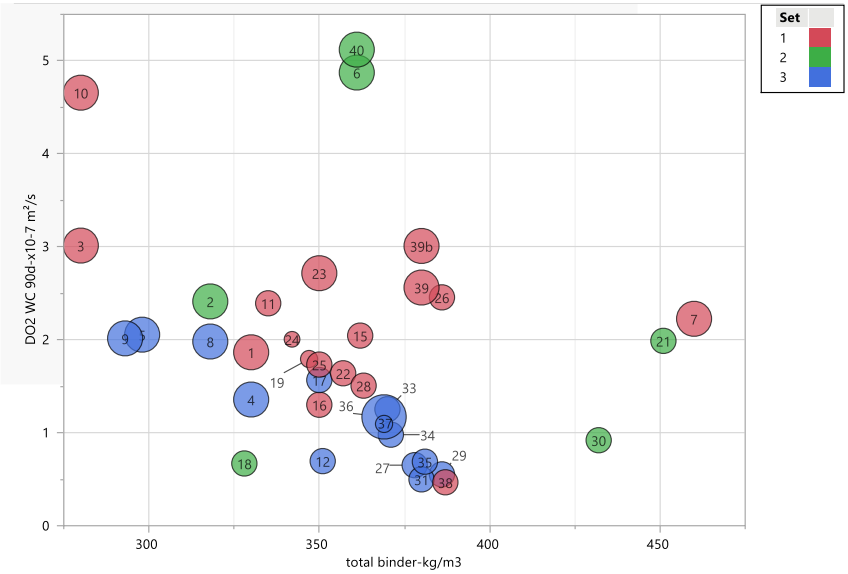

Figure 3.37. Oxygen diffusion coefficient (90d wet curing) vs total binder. The sizes of the points correspond to the water absorption of aggregates used (smallest size: lowest water absorption / largest size: highest water absorption)

For the concrete set 1 and 2, no link between the oxygen diffusion coefficient and the total binder content.

For concrete set 3, the oxygen diffusion coefficient seems to decrease with the total binder content.

6.3 Link between oxygen diffusivity values and prescriptive approach

Oxygen diffusion coefficient as a function of efficient water to total binder ratio and total binder are plotted complying with prescriptive approach according to NF EN 206/CN (Figure 3.38) and Fascicule 65 (Figure 3.39). The solid circles correspond to the concretes compliant with the “Fascicule 65” specification for the given class exposure in terms of mix design and the empty points to the non-compliant concretes.

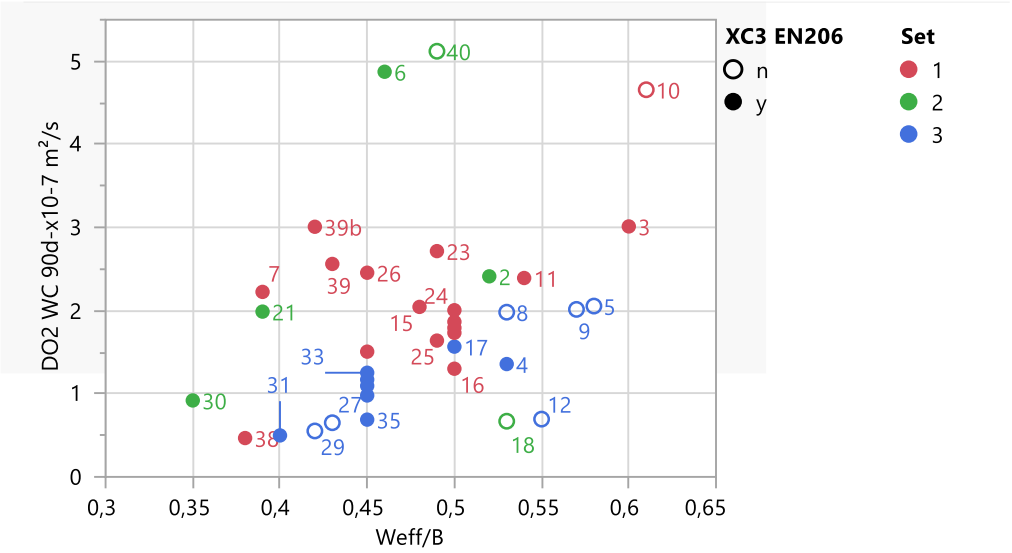

Figure 3.38. Oxygen diffusion coefficient (90d wet curing) vs efficient water to total binder ratio according to NF EN 206/CN mix design compliance for XC3 and XC4

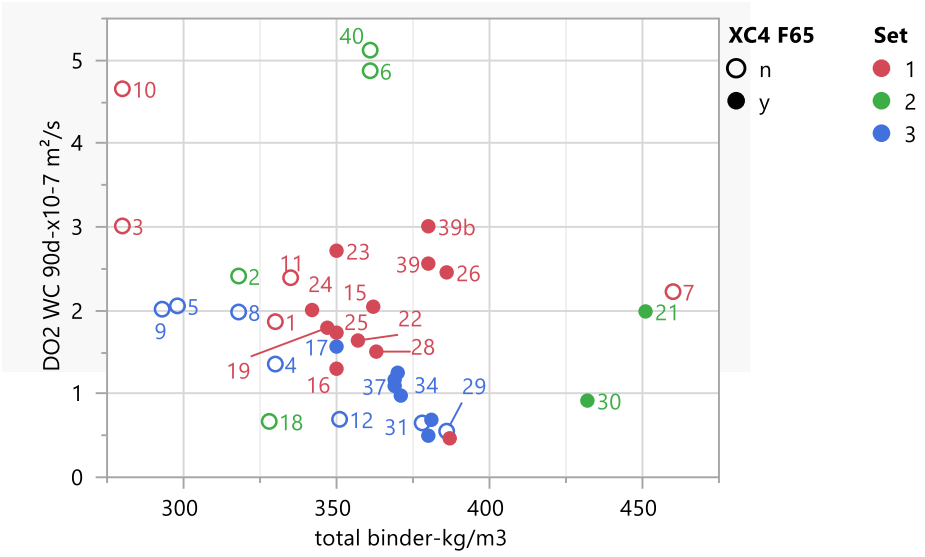

Figure 3.39. Oxygen diffusion coefficient (90d wet curing) vs total binder according to Fascicule 65 mix design compliance for XC4

The same colour code of the 3 sets defined previously is used. The labels in or close to the points represent the concrete number. In this paragraph, no codification is made to differentiate the type of aggregates. To do so, please refer to Figure 3.36 and Figure 3.37.

Whatever the class exposure (XC2 to XC4) no visible link is noticed in the whole data set between the oxygen diffusion coefficients and the compliance / non-compliance of the concrete formulas. Indeed, a concrete which does not comply with NF EN 206/CN or Fascicule 65 can give a low diffusivity and a concrete compliant with NF EN 206/CN a high diffusivity.

Based on this observation, it is difficult to define a threshold value on the oxygen diffusion coefficient in relation to the concrete mix design compliance for a given exposure class

Characteristic value of oxygen diffusivity

The characteristic value is defined as 90 % of concretes in compliance with standard NF EN 206/CN (50 years) or Fascicule 65 (100 years) considering concretes which have a compressive strength in accordance with the minimum resistance class corresponding to exposure class + 2 resistance classes above for EN 206 (or 3 resistance classes above for Fascicule 65). Concretes of higher strength are not included in the analysis.

The following equation is used:

$$DO_{2\ dur,k} = DO_{2\ dur,m} + 1.28\ \sigma \qquad \text{(Equ. 3.3)}$$

With $DO_{2\ dur,k}$ the characteristic value of oxygen diffusivity, $DO_{2\ dur,m}$ the mean value of oxygen diffusivity and σ the standard deviation.

Table 3.10 summarizes the characteristic values calculated according to the equation above.

Table 3.10. Thresholds calculated according to equation 3.3

	EN 206 (50 years of Design Service Life)				**Fascicule 65 (100 years of Design Service Life)**			
	XC1	**XC2**	**XC3**	**XC4**	**XC1**	**XC2**	**XC3**	**XC4**
Nb concretes fulfilling criterion	5	5	10	10	15	15	13	12
Mean	3.2	3.2	2.5	2.5	2.3	2.3	1.9	1.9
Std deviation	1.5	1.5	0.9	0.9	0.8	0.8	0.6	0.6
$DO_{2\ dur,k}$ ($10^{-7}m^2.s^{-1}$) 90d (dry state)	5.1	5.1	3.6	3.6	3.3	3.3	2.7	2.6

The slight gap on characteristic values of oxygen diffusivity between XC1/XC2 and XC3/XC4 is mainly due to the mix design of concretes tested. Effectively the XC1/XC2 concretes are not representative to this dedicated exposure class with lower water to binder ratio (<0.60).

6.4 Link between oxygen diffusivity permeability values and other durability properties

A pair plot graph is determined between the following durability parameters to evaluate the direct correlation with the oxygen diffusivity at same conditions (WC):

- compressive strength, f_c at 28d and 90d (WC);
- water porosity, Poro H_2O at 28d and 90d (WC);
- chloride diffusion coefficient, D_{rcm} at 28d and 90d (WC);

- electrical resistivity, Resistivity at 28d and 90d (WC);
- oxygen permeability at 7 days of drying, k_7, at 28d and 90d (WC);
- oxygen permeability at 28 days of drying, k_{28}, at 28d and 90d (WC);
- oxygen permeability at dry state, k_{dry}, at 28d and 90d (WC);
- water absorption coefficient, water abs coef, at 28d and 90d (WC);
- accelerated carbonation rate according to NF test protocol, rate NF (WC);
- accelerated carbonation rate according to EN test protocol, rate EN (WC);
- natural carbonation rate, rate NAT (WC).

The correlation coefficients with oxygen diffusivity are in Table 3.11.

Table 3.11. Correlation coefficients with oxygen diffusivity

	D_{O2} WC 90d-x10^{-7} m²/s
D_{O2} WC 90d (x10^{-7} m²/s)	1
f_c WC 28d (MPa)	-0.57
f_c WC 90d (MPa)	-0.60
Poro H_2O WC 28d (%)	0.54
Poro H_2O WC 90d (%)	0.47
D_{rcm} WC 28d (x10^{-12} m²/s)	0.70
D_{rcm} WC 90d (x10^{-12} m²/s)	0.61
Resistivity WC 28d (Ω.m)	-0.53
Resistivity WC 90d (Ω.m)	-0.52
k_{gas} k_7 28d (x10^{-18} m²)	0.19
k_{gas} k_{28} 28d (x10^{-18} m²)	0.126
k_{gaz} k_{dry} 28d (x10^{-18} m²)	0.06
k_{gas} k_7 90d (x10^{-18} m²)	0.58
k_{gas} k_{28} 90d (x10^{-18} m²)	0.21
k_{gas} k_{dry} 90d (x10^{-18} m²)	0.11
Water abs coef WC 28d (%)	0.51
Water abs coef WC 90d (%)	0.52
Rate NF WC (mm/day^{0,5})	0.55
Rate EN WC (mm/day^{0,5})	0.39
Rate NAT WC (mm/day^{0,5})	0.47

By focusing on parameters with correlation coefficients higher than 0.54 (in absolute value and arbitrarily set) the pair plot graph obtained is as follows (Figure 3.40).

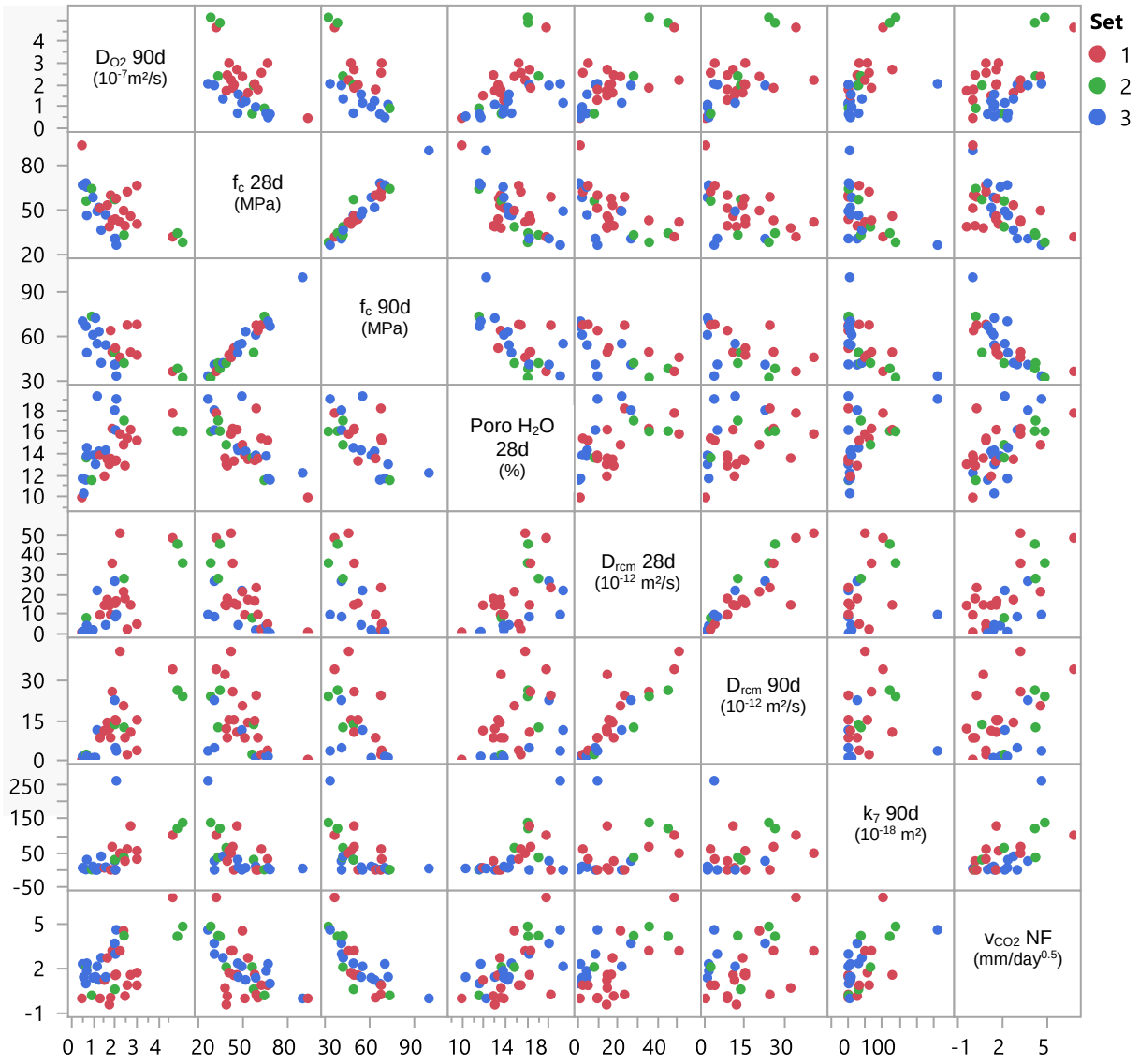

Figure 3.40. Pair plot graph with correlation coefficients compared to oxygen diffusivity higher than 0.54

6.4.1 Oxygen diffusivity (90d of wet curing) vs chloride diffusion coefficient (28d of wet curing)

The variation in oxygen diffusivity (wet cure 90j) as a function of the chloride ion diffusion coefficient is shown in Figure 3.41.

The best correlation with oxygen diffusivity after 90 days of wet curing and at dry state is obtained by considering the chloride diffusion after a wet curing of 28 days. The correlation coefficient R, gives 0.70 (i.e. coefficient of determination $R^2 = 0.49$).

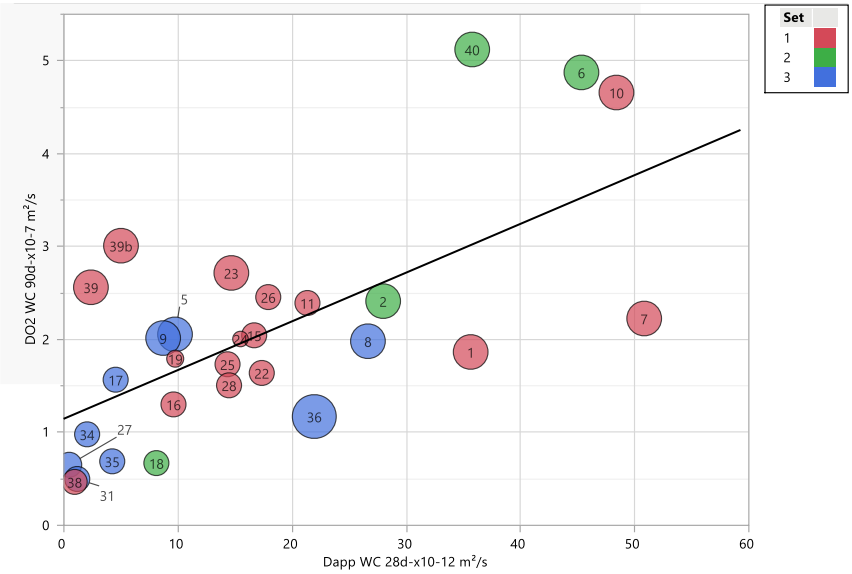

Figure 3.41. Oxygen diffusivity (90d wet curing) vs Chloride diffusion coefficient (28d wet curing). Black solid line represents the trend line of whole data

6.4.2 Oxygen diffusivity vs carbonation rate

(Papadakis et al, 1989) developed an analytical model based on the physicochemical processes of the carbonation. The model assumptions imply the formation of a sharp carbonation front and consider the cementitious material homogeneous, fully hydrated and in hydric equilibrium with the ambient environment.

The model predicts the carbonation depth x_c (m) according to the square root of time, the CO_2 concentration at the surface of the sample $[CO_2]$ ($mol.m^{-3}$), the effective diffusion coefficient of CO_2 $D_{e,CO2}$ ($m^2.s^{-1}$), the exposure time to carbonation t (s), and the amount of carbonatable products ($mol.m^{-3}$).

$$x_c = \sqrt{\frac{2\, D_{e,CO2}\, [CO_2]}{[Ca]}\, t} \qquad \text{(Equ. 3.4)}$$

As shown in this equation, the carbonation rate is directly linked to the square root of the CO_2 diffusivity divided by the carbonatable products. The latter can be estimated knowing the calcium content of each binder and its hydration degree at a given time.

According to the product datasheets and the following assumed hydration degree at 90 days of binders: 100 % for CEM I, 30 % for fly-ash, 50 % for slag, the total carbonatable products expressed here as mass of CaO (kg/m^3) are summarized in Table 3.12.

The oxygen diffusivity coefficient can be estimated from the carbon-dioxide diffusion coefficient using Graham's law with the following equation:

$$D_{e,CO2} = D_{e,O2}\sqrt{\frac{M_{O2}}{M_{CO2}}} \qquad \text{(Eq 3.5)}$$

where M_{O2} and M_{CO2} are the molar mass of oxygen and carbon dioxide respectively.

Thus, from Equation 3.4 and Equation 3.5 a linear correlation between $\sqrt{\frac{D_{e,O2}}{[Ca]}}$ and $\frac{x_c}{\sqrt{t}}$ (i.e. carbonation rate) can be deduced.

Table 3.12. Total carbonatable products at 90 days expressed as mass of CaO (kg/m^3)

N° Concrete	m_{CaO} tot 90d (kg/m^3)	N° Concrete	m_{CaO} tot 90d (kg/m^3)	N° Concrete	m_{CaO} tot 90d (kg/m^3)
1	179.5	15	231.7	29	149.3
2	144.4	16	207.8	30	195.2
3	154.1	17	153.8	31	140.7
4	103.7	18	135.1	32	171.7
5	115.4	19	206.0	33	162.6
6	162.2	20	205.4	34	137.4
7	173.1	21	202.2	35	156.1
8	124.2	22	196.5	36	151.2
9	117.5	23	207.8	37	151.2
10	154.1	24	203.0	38	228.8
11	184.4	25	224.0	39	194.9
12	135.7	26	247.0	39b	194.9
13	190.7	27	162.3	40	162.2
14	211.2	28	232.3		

Figures 3.42, 3.43 and 3.44 illustrate this correlation for accelerated carbonation according to French test protocol, accelerated carbonation according to EN test protocol and natural carbonation respectively (wet curing).

The carbonation rates are measured with the 4 points including the initial carbonation depth measurement.

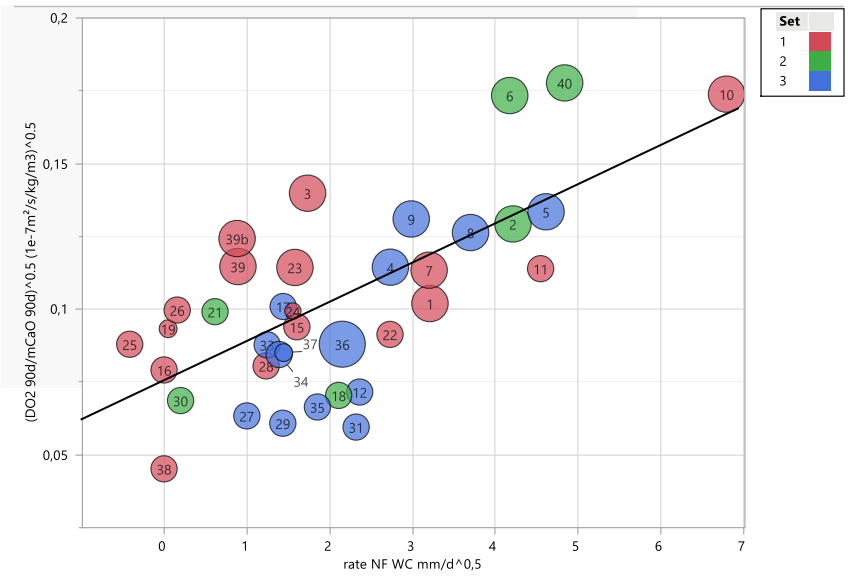

Figure 3.42. Square root of oxygen diffusivity to estimated carbonatable products ratio vs accelerated carbonation rate according to French test protocol (wet curing). Black solid line represents the trend line of whole data

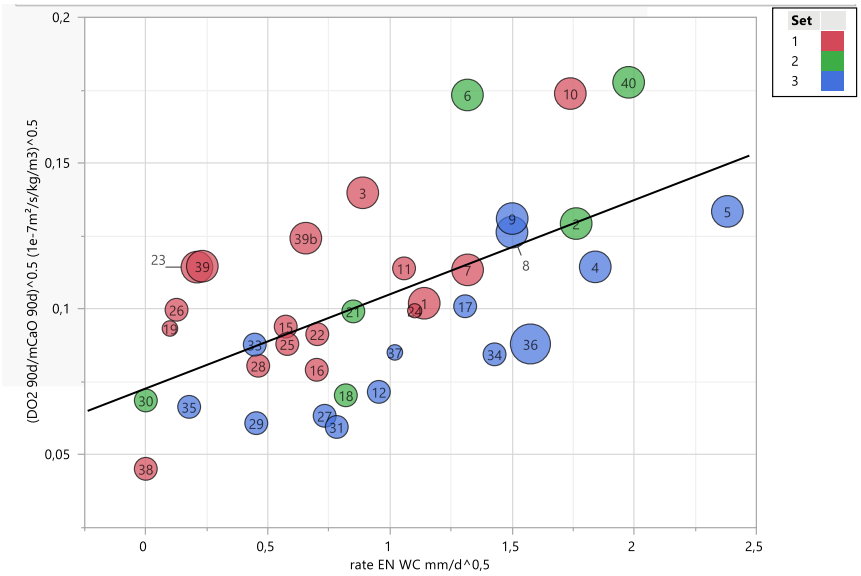

Figure 3.43. Square root of oxygen diffusivity to estimated carbonatable products ratio vs accelerated carbonation rate according to EN test protocol (wet curing). Black solid line represents the trend line of whole data

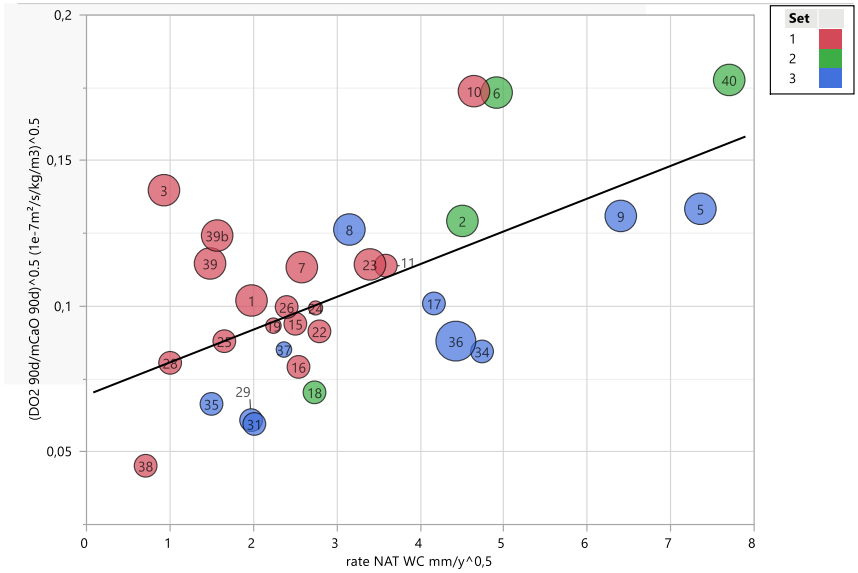

Figure 3.44. Square root of oxygen diffusivity to estimated carbonatable products ratio vs natural carbonation rate (wet curing). Black solid line represents the trend line of whole data

The coefficients of determination R² are summarized in Table 3.13.

Table 3.13. Coefficient of determination between $\sqrt{\frac{D_{e,O2}}{[Ca]}}$ and carbonation rates

	Coefficient of determination R² (on whole data)	Coefficient of determination R² (for each set)		
		Set 1	***Set 2***	***Set 3***
Accelerated carbonation FR	0.48	0.46	0.74	0.55
Accelerated carbonation EN	0.37	0.39	0.67	0.65
Natural carbonation	0.38	0.27	0.72	0.64

A trend is observed with a non-clear correlation.

However, for the accelerated carbonation EN, each set of concrete (1, 2 and 3) seems to follow a different trend regardless of aggregate.

The highest coefficient of determination is obtained with accelerated carbonation rate according to French test protocol.

Based on this observation, assuming that a threshold has been determined for the carbonation rate then it is difficult to define a corresponding threshold value for the oxygen diffusion coefficient to carbonatable products ratio.

6.5 Conclusion and proposals

The measured values of oxygen diffusivity vary between 0.5 and 5.10^{-7} m²/s.

Based on the approach defined in this core project i.e. 90 % of concretes in accordance with standard NF EN 206 (50 years) or Fascicule 65 (100 years) considering concretes which have a compressive strength in accordance with the minimum resistance class corresponding to exposure class + 2 or 3 resistance classes above, the following characteristic values can be deduced based on the calculation of the mean and 1.28*standard deviation:

- in compliance with EN206, $5.1.10^{-7}$ m²/s and $3.6.10^{-7}$ m²/s for XC1/XC2 and XC3/XC4 respectively;
- in compliance with Fascicule 65, $3.3.10^{-7}$ m²/s and $2.6.10^{-7}$ m²/s for XC1/XC2 and XC3/XC4 respectively.

However, it is difficult to define a threshold value on the oxygen diffusion coefficient in relation to the concrete mix design compliance for a given exposure class.

If a threshold can be determined for the carbonation rate, it will be difficult to define a corresponding threshold value for the oxygen diffusion coefficient to carbonatable products ratio. Therefore, under these testing conditions, it is difficult to propose the oxygen diffusivity as the main indicator describing the resistance to carbonation.

The non-clear correlation observed between oxygen diffusivity and carbonation rate (accelerated or natural) can be explained by:

- the difference on liquid saturation of samples measured in oxygen diffusion (dry state at 105 °C) and accelerated carbonation tests (at 65 % RH);
- the difference on carbonation degree of samples during the oxygen diffusion (samples non/slightly carbonated) and accelerated carbonation (samples partially carbonated) tests;
- the carbonation degree varies according to the type of binder and the relative humidity.

6.6 Appendix

6.6.1 Operating mode (Boumaaza, 2020)

6.6.1.1 Principle

The experimental method adopted to determine oxygen effective diffusion coefficient through cement-based samples, is based on the direct measurement of oxygen concentration diffusing through the sample inside a cell under constant temperature (20 °C) and pressure (1 atm).

The main element of the experimental set is the diffusion cell that is referred to as “downstream chamber”, it consists of a High-density polyethylene, gastight cell, separated from the ambient air of the climate chamber “called upstream chamber” by the sample.

Oxygen diffuses successively through the sample into the cell filled with nitrogen, where O_2 concentration is measured by the gas sensor.

When the steady state is reached the experiment is stopped and a diffusion curve (O_2 concentration- time) is collected.

Equipment was developed to allow the continuous readings of the concentration of oxygen that diffuses through the samples (cement pastes and concrete discs).

6.6.1.2 Characteristics of sample

Concrete samples are discs of 11 cm diameter and a thickness of 5 cm that were equilibrated at dry state in an oven at 105 °C. The equilibrium is considered reached when the mass variation does not exceed 0.05 % / day.

Concrete samples are prepared by covering its edges with an epoxy resin to ensure unidirectional diffusion flow during the tests.

6.6.1.3 Equipment

The climate chamber used during the test is a temperature, pressure and relative humidity-controlled chamber with the following conditions:

- the RH is regulated with silica gel placed in the chamber to reach the lowest RH in the chamber;
- at a temperature of 20 °C;
- at atmospheric pressure.

The diffusion cell consists of a High-density polyethylene, gastight cell, separated from the ambient air of the climate chamber by the sample. The dimensions of concrete cell are described in Table 3.14.

Table 3.14. Dimensions of concrete cell

Internal diameter (mm)	Internal length (mm)	Total volume (ml)
110	**22**	**209**

Geometry of the cell was determined so as to minimize as possible the total volume (Figure 3.45). An important diffusion volume may cause drying of the preconditioned samples.

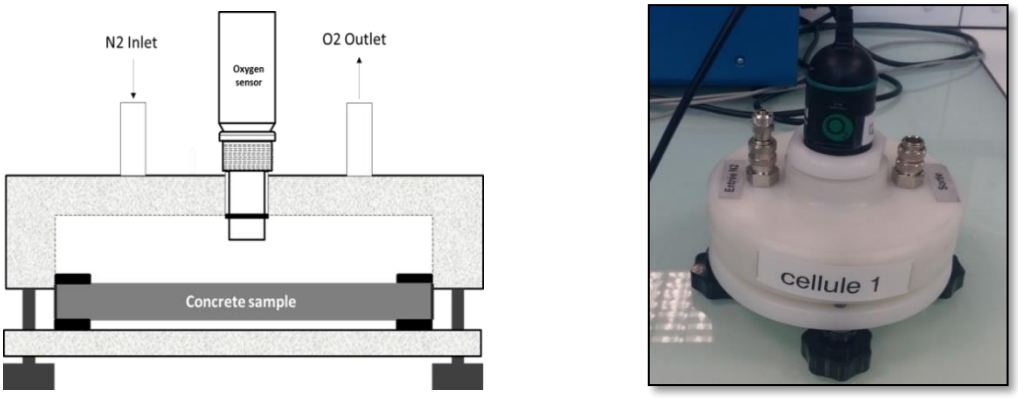

Figure 3.45. Concrete sample cell

The sensor used to measure the amount of gaseous oxygen diffusing through the sample inside the cell (Figure 3.46) has the following specifications:

- measurement Range: 0–27 %;
- pressure range: 0.5 atm to 1.5 atm;
- normal Operating Temperature Range: 25 °C (± 5 °C);
- operating Temperature Range: 5 to 40 °C (with calibration);
- operating Humidity Range: 0 to 95 % RH.

Figure 3.46. Oxygen gas sensor

6.6.1.4 Concrete sample conditioning before measurement

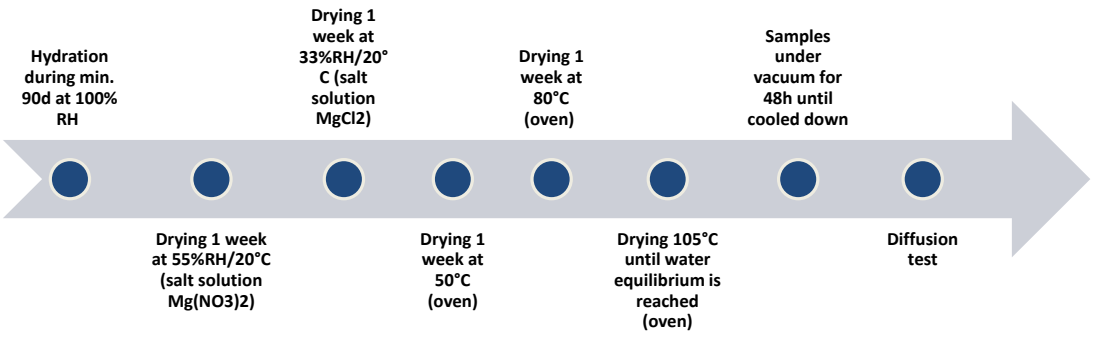

6.6.1.5 Measurement

The experimental set up is schematically shown in the Figure 3.47 hereafter.

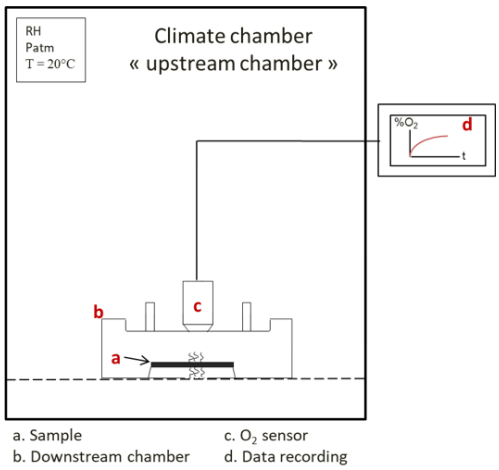

Figure 3.47. Experimental set up: concrete sample diffusion cell

The tested concrete sample is placed between two rubber joints and placed in the down part of the diffusion cell. At the beginning of test, the diffusion cell is flushed with nitrogen test for a short period of 30 seconds with a slow rate and placed inside a relative humidity-controlled chamber. One face of the sample is then exposed to the internal volume of the cell filled with nitrogen and the other face to the relative humidity-controlled air of the upstream chamber which creates the concentration gradient of oxygen. Therefore, oxygen diffuses successively through the sample into the cell where O_2 concentration is monitored by the gas sensor. When the steady state is reached (i.e. when O_2 concentration reaches 20 %), the experiment is stopped and an accumulation curve (O_2 concentration vs time) is collected.

O_2 effective diffusion coefficient ($D_{e,O2}$) is determined by fitting Fick's second law of diffusion to the data of the accumulation curve by least square method.

$$\phi(1 - S_l)\frac{\partial C}{\partial t} = \frac{\partial}{\partial x}\left(D_{e,O2}\frac{\partial C}{\partial x}\right) \quad \text{(Equ. 3.6)}$$

Where $D_{e,O2}$ is the oxygen-effective diffusion coefficient, C the oxygen concentration, ϕ the total porosity and S_l the water saturation degree of the sample.

The equation is solved in the inside volume of the cell to account for transient diffusion; for this volume we have porosity = 1, water saturation = 0 and $D_{O2\text{-}N2} = 10^{-5}$ m²/s.

Table 3.15 gives information about the reliability, measurement range, time and conditions of the test method.

Table 3.15. Summary of the main information about the O_2 diffusion test method on concrete samples

Repeatability coefficient	7 % to 10 %*
Coefficient of variation	8 % for dry state sample
Testing time	30 min to 3 days
Preconditioning time	2 months minimum
Measurements conditions	Ambient temperature and pressure, relative humidity level controlled with silica gel in the climatic chamber
Measurement range	10^{-6} to 10^{-11} m²/s

** Performed on hardened cement paste*

6.6.2 Link between oxygen diffusivity values and prescriptive approach

6.6.2.1 Complying with prescriptive approach XC1/XC2 according to NF EN 206/CN

Figures 3.48 and 3.49 show the oxygen diffusion coefficients function the efficient water to total binder ratio and total binder content for concrete complying (or not) with XC1/XC2 NF EN 206/CN. No clear correlation appears.

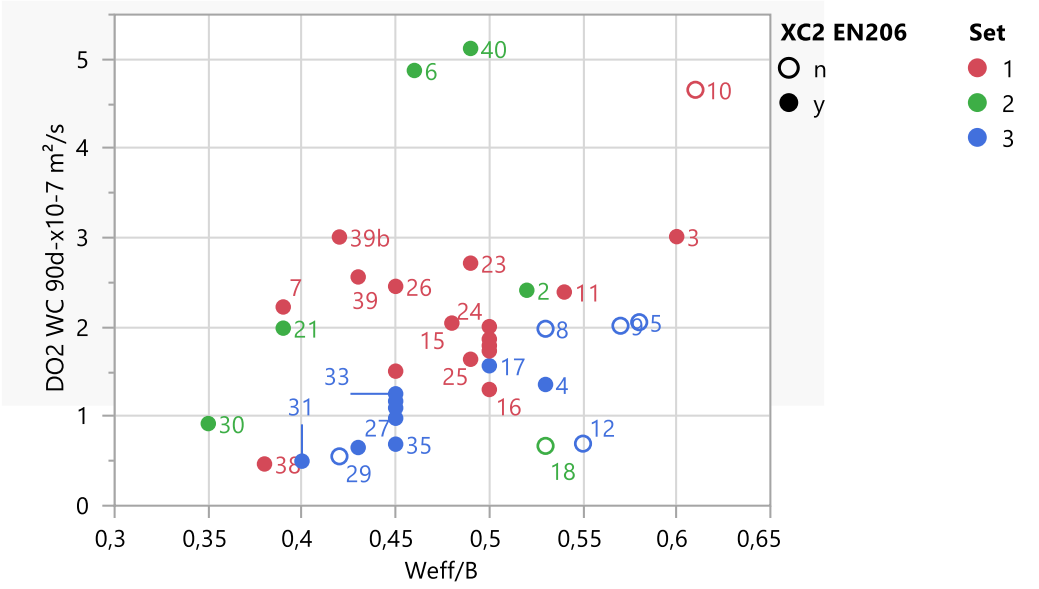

Figure 3.48. Oxygen diffusion coefficient (90d wet curing) vs efficient water to total binder ratio according to NF EN 206/CN mix design compliance for XC1 and XC2

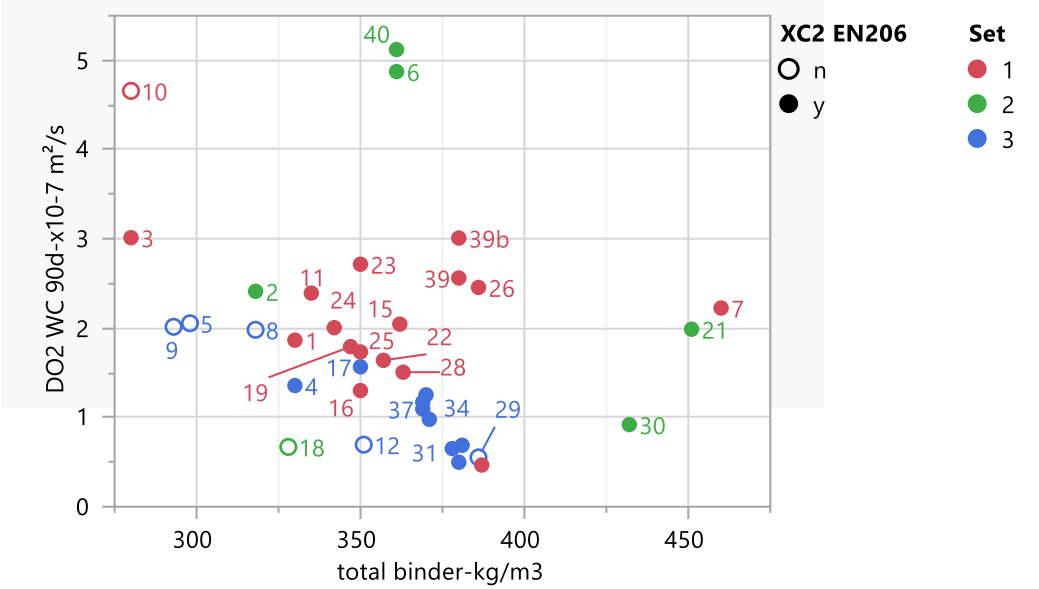

Figure 3.49. Oxygen diffusion coefficient (90d wet curing) vs total binder according to NF EN 206/CN mix design compliance for XC1 and XC2

6.6.2.2 Complying with prescriptive approach XC3/XC4 according to NF EN 206/CN

Figure 3.50 shows the oxygen diffusion coefficients function to the total binder content for concrete complying (or not) with XC3/XC4 NF EN 206/CN. No clear correlation appears.

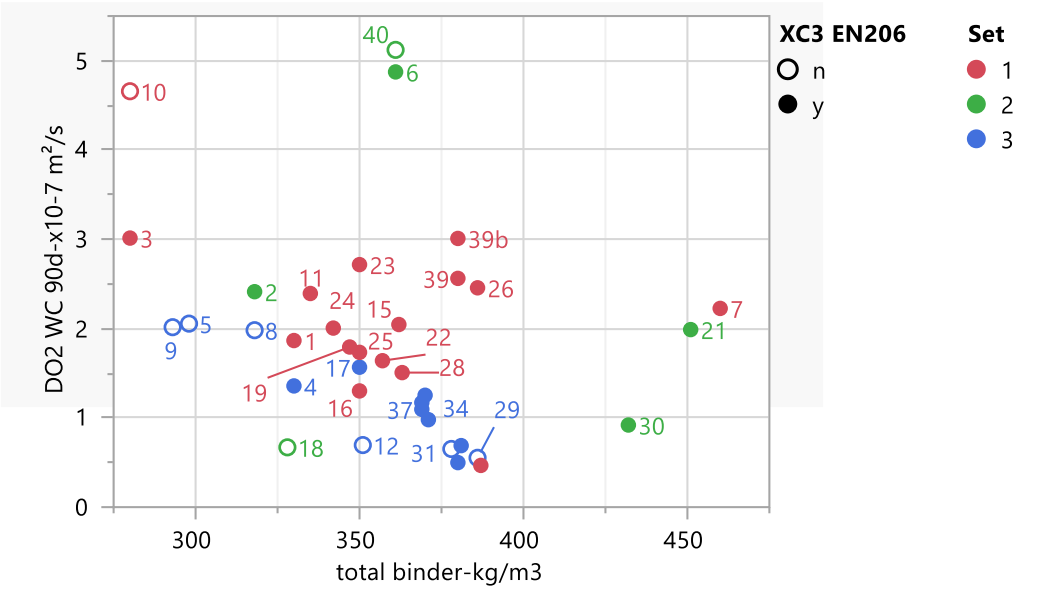

Figure 3.50. Oxygen diffusion coefficient (90d wet curing) vs total binder according to NF EN 206/CN mix design compliance for XC3 and XC4

6.6.2.3 Complying with prescriptive approach XC2 according to Fascicule 65

Figures 3.51 and 3.52 show the oxygen diffusion coefficients function the efficient water to total binder ratio and total binder content for concrete complying (or not) with XC2 Fascicule 65. No clear correlation appears.

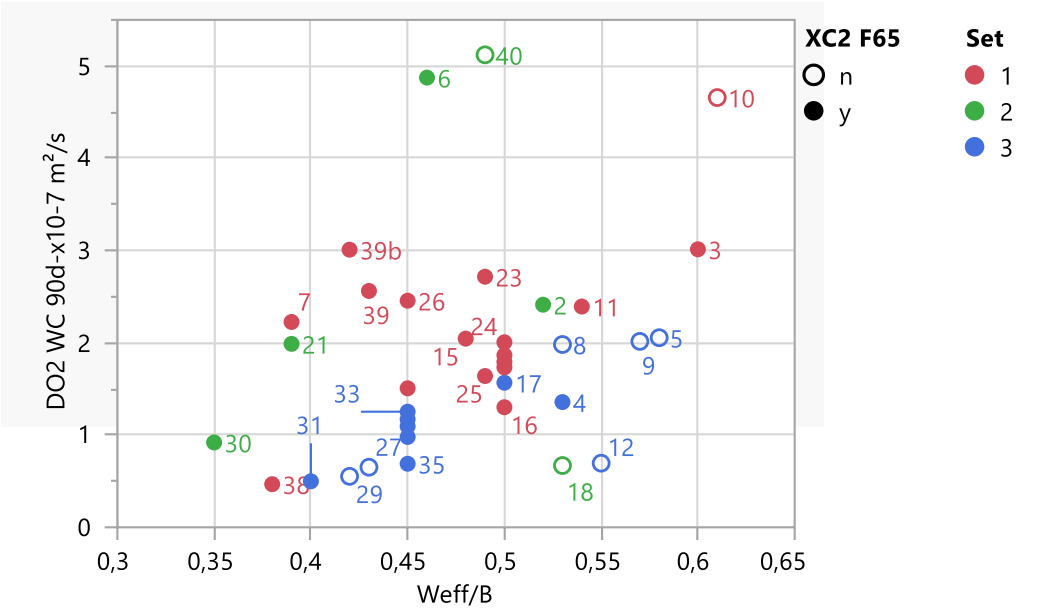

Figure 3.51. Oxygen diffusion coefficient (90d wet curing) vs efficient water to total binder ratio according to Fascicule 65 mix design compliance for XC2

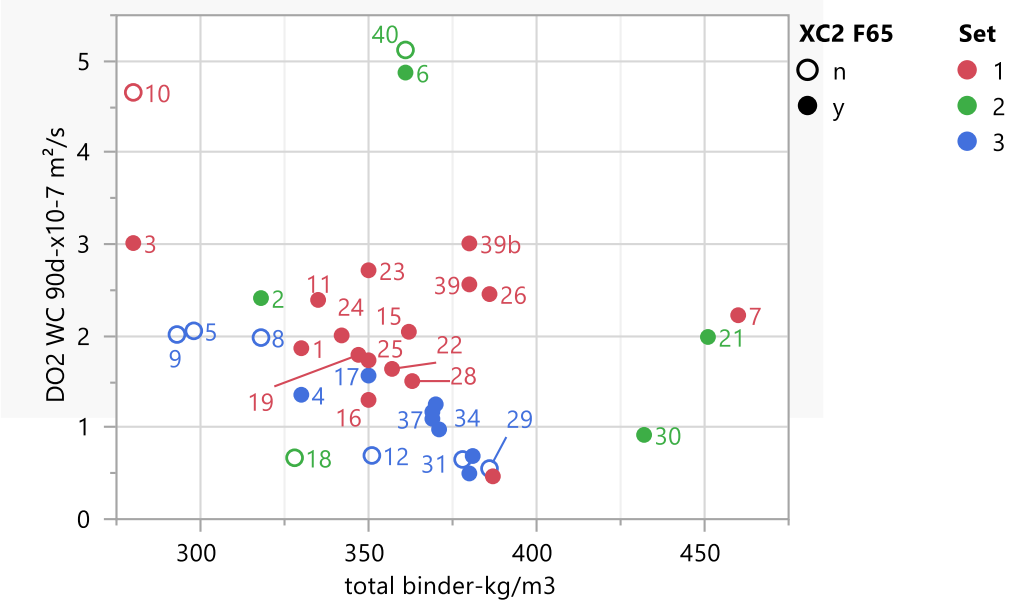

Figure 3.52. Oxygen diffusion coefficient (90d wet curing) vs total binder according to Fascicule 65 mix design compliance for XC2

6.6.2.4 Complying with prescriptive approach XC3 according to Fascicule 65

Figures 3.53 and 3.54 show the oxygen diffusion coefficients function the efficient water to total binder ratio and total binder content for concrete complying (or not) with XC3 Fascicule 65. No clear correlation appears.

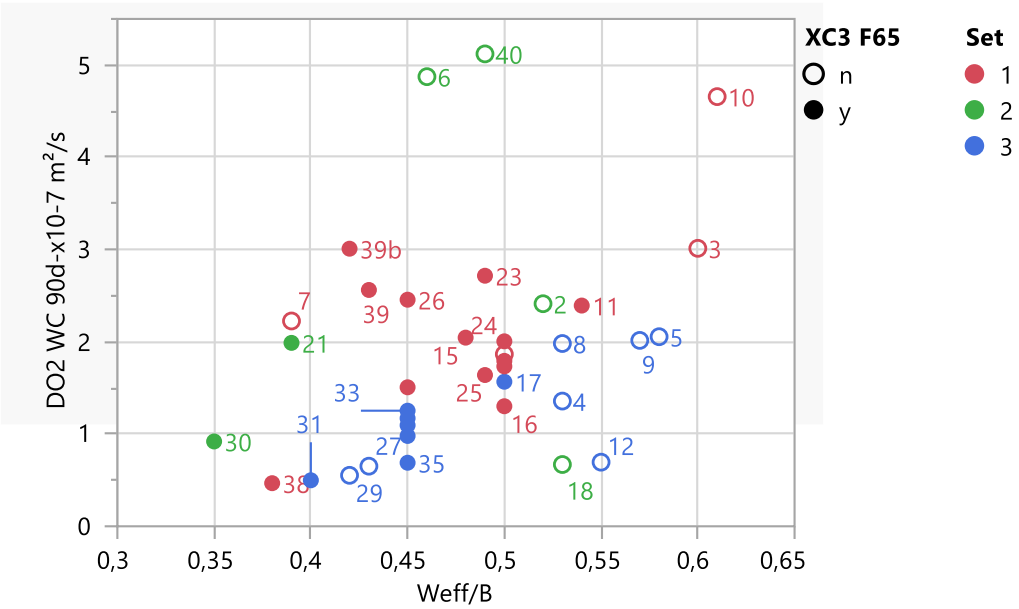

Figure 3.53. Oxygen diffusion coefficient (90d wet curing) vs efficient water to total binder ratio according to Fascicule 65 mix design compliance for XC3

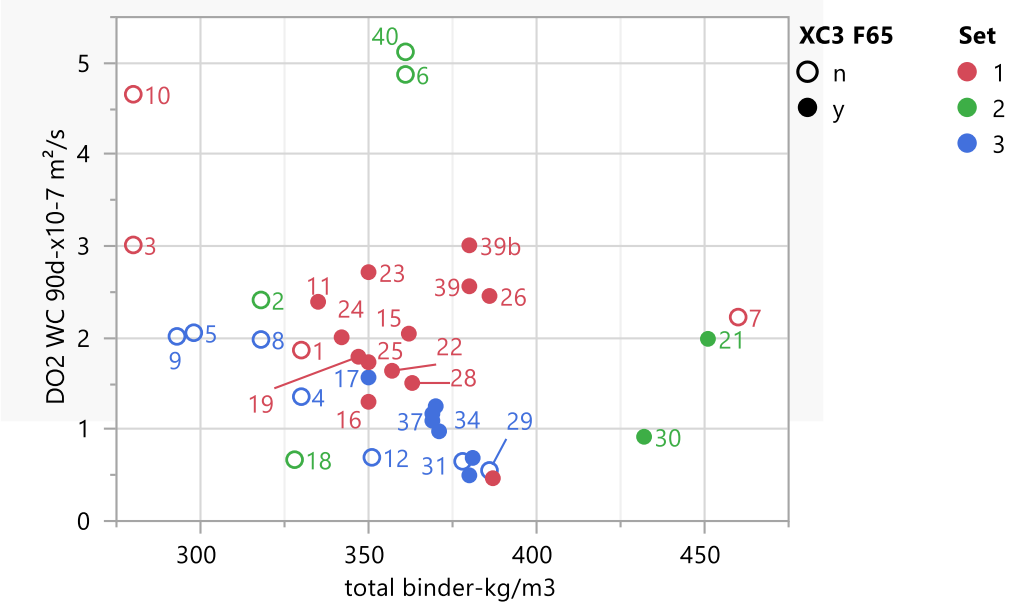

Figure 3.54. Oxygen diffusion coefficient (90d wet curing) vs total binder according to Fascicule 65 mix design compliance for XC3

6.6.2.5 Complying with prescriptive approach XC4 according to Fascicule 65

Figure 3.55 shows the oxygen diffusion coefficients as a function of the effective water/total binder ratio for concrete conforming (or not) to class XC4 according to fascicule 65.No clear correlation appears.

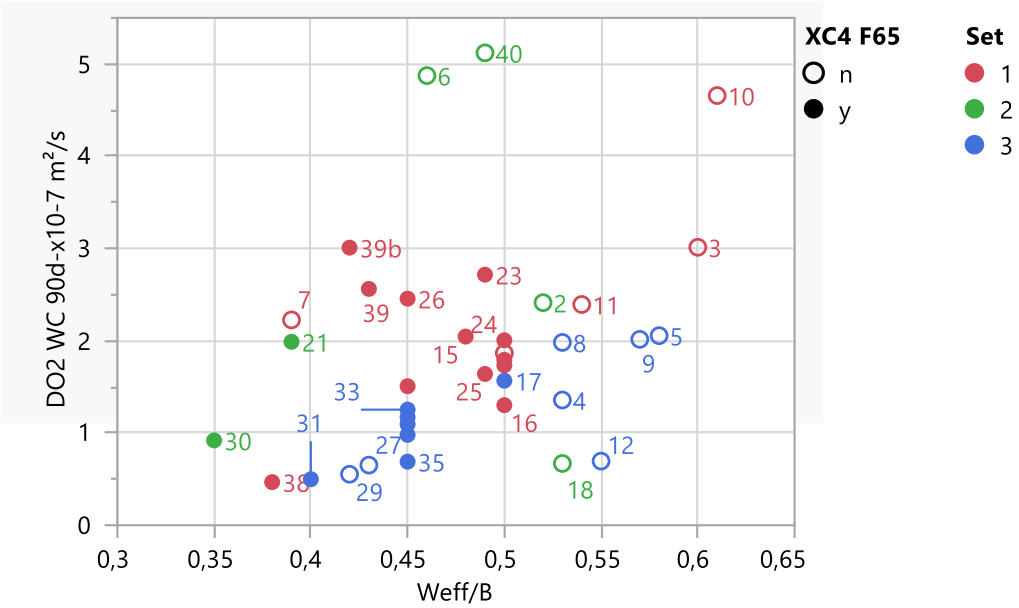

Figure 3.55. Oxygen diffusion coefficient (90d wet curing) vs efficient water to total binder ratio according to Fascicule 65 mix design compliance for XC4

7 Resistance to carbonation

Author: Philippe Turcry

7.1 Introduction

This section focuses on the results of the carbonation tests obtained during the experimental program on 42 concretes complying or not with the prescriptive approach of the current regulations for XC exposure classes. The objective is to obtain a mapping of concrete performance based on current prescriptive and performance specifications.

The 42 concretes were characterized using the accelerated carbonation test, established thanks to the work of the GT1A working group. The operating mode of this test was obtained by modifications of two operating modes existing at the start of the project, i.e., the European test “FprCEN/TS 12390-1” and the French test NF “XP P18-458 (2008)”. The natural carbonation of the concrete was also monitored over two years under controlled ambient conditions (20 ± 2 °C and 50 ± 5 % of relative humidity).

For each of the concretes characterized, carbonation depths were determined. The database so obtained is used first in the present report to propose a method for determining the rate of accelerated carbonation. This property is used as a performance indicator with respect to the risk of carbonation.

In a second part of the section, the rates of carbonation are compared with the mix parameters of concrete and their properties (e.g., durability indicators). Some correlations are thus highlighted, such as the correlation between accelerated carbonation rates and natural carbonation rates.

In a final section, the carbonation rate database is compared to the requirements of the regulations (EN 206 and Fascicle 65).

7.2 Operating mode

The 42 concretes were tested with an accelerated carbonation test developed during the PerfDuB project. This operating mode results from modifications of the European test from FprCEN/TS 12390-1. These modifications are based on results in the preliminary round robin tests in PN PerfDuB (see Chapter 1, WG1 report). The main specifications of the test are given in Table 3.16.

Table 3.16. Main steps of the accelerated carbonation test

Specimen	**Geometry**	10 Cylinders ∅ 11 cm x H 11 cm (sawn in 5 cylinders ∅ 11 cm x H 22 cm after curing)
Preconditioning phase	**Drying face**	Cylinder perimeter
	Total duration	≥ (14 + 7) days
	First phase	Oven-drying at 45 °C with the stopping criteria: duration ≥ 14 days and mass loss of mortar prisms ≥ 5.5 %
	Second phase	7 days at 20 °C and 65 % RH
Carbonation phase	**Faces in contact with CO_2**	Cylinder perimeter
	Conditions	20 ± 2 °C and 65 ± 5 % HR
	CO_2 concentration	3 ± 0.5 %
	Testing times	t_0, 28, 56 and 70 days

7.3 Determination of the carbonation rate

7.3.1 Different methods of determination by linear regression

The results of a carbonation accelerated test are four carbonation depths determined at t_0 (initial depth), 28, 56 and 70 days (in the final version of the operating mode, the third testing time is 42 days and not 56 days). From these depths expressed as a function of the squared root of time, a carbonation rate in mm/d$^{0.5}$ can be assessed by linear regression. The so-obtained carbonation rate gives an indication of the carbonation resistance. The following methods can be used for this purpose:

- "3 points": the linear regression is done only with the three accelerated carbonation depths, i.e., depths determined at 28, 56 and 70 days;
- "4 points": the linear regression is done with the four depths;
- "4 points F": the linear regression is done with the three accelerated carbonation depths and a fictive t_0 value equal to 0 mm (this method could be used when the initial carbonation depth is not determined);
- "EN 12390": the linear regression is done with the three accelerated carbonation depths and with a fixed intercept equal to the initial carbonation depth (or 0 if the initial carbonation depth was not measured) (method proposed in EN 12390-12 Standard).

Figure 3.56 gives an example of using these four regression methods. The carbonation rate is the slope of the regression line.

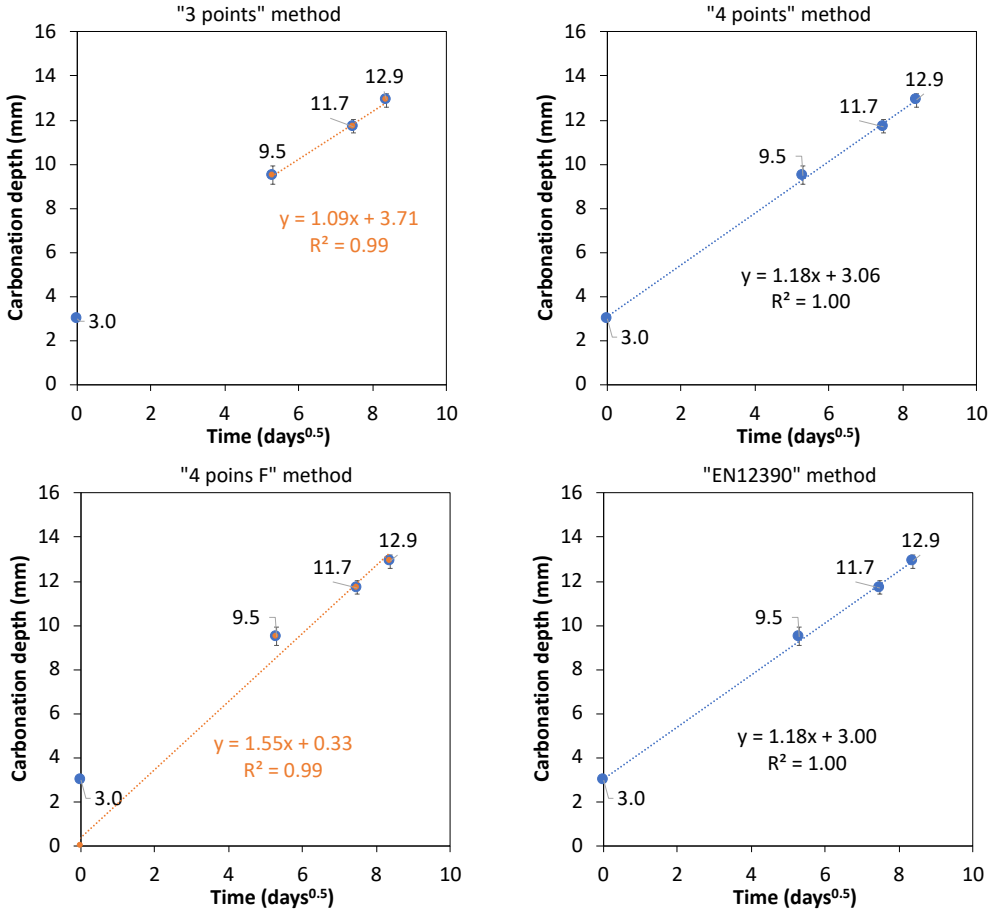

Figure 3.56. Examples of use of the linear regression methods for determining of the carbonation rate (dry-cured concrete 10 – EN operating mode)

In the case of natural conditions, carbonation rate in mm/year$^{0.5}$ was also deduced by linear regression from the depths expressed as a function of square root of time, as proposed in the NF EN 12390-12 Standard. The initial carbonation depth was taken equal to zero. Note that the time corresponds to the exposure time (which is not equal to the concrete age in the case of the water-curing).

7.3.2 Coefficient of determination

The coefficient of determination (R^2) was used as a simple indicator to assess the goodness of fit the linear regressions (despite the theoretical limitations of this approach). Using the methods described previously, a carbonation rate and a R^2 were determined for each concrete mixture of the PerfDuB database.

Figure 3.57 gives the so-obtained coefficient of determination as a function of the corresponding carbonation rate. R^2 tend to increase with carbonation rate. For concrete with high carbonation resistance, i.e., low carbonation rate, the time-evolution of the carbonation depth is not fully linear with the square root of time and the measurements are more scattered.

We note also the influence of the curing method: higher coefficients of regression are obtained in the case of dry-curing. This difference is mainly due to the influence on the carbonation rate.

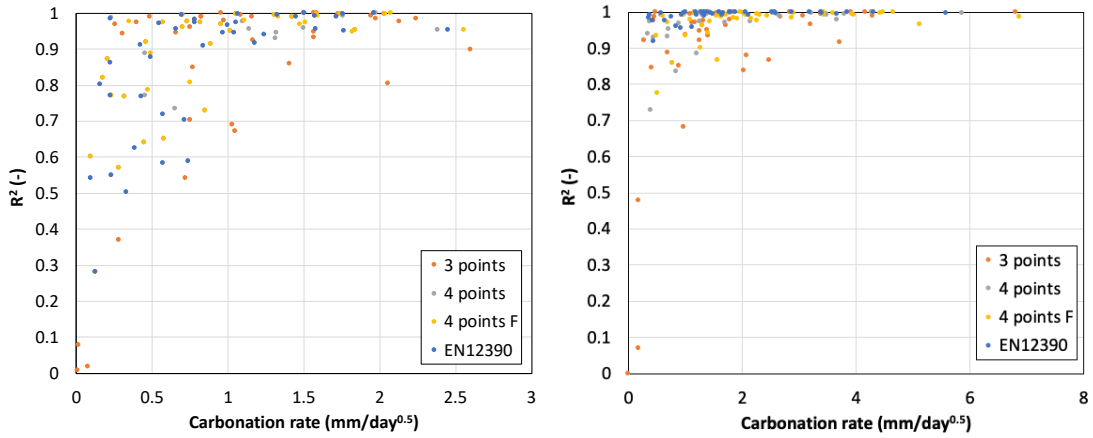

Figure 3.57. R^2 versus accelerated carbonation rates determined by the four regression methods in the case of wet-curing (left) and dry-curing (right)

7.3.3 Correlation between accelerated carbonation rate and natural carbonation rate

In Figures 3.58 and 3.59, the accelerated carbonation rates determined with the four methods are plotted versus the natural carbonation rates for all mixtures complying the previous criteria.

In the case of the “3 points” method, no clear correlation can be seen between natural rate and accelerated rate in the case of water-curing (Figure 3.58). The rate obtained with this method is not a relevant indicator of the natural carbonation resistance, and therefore it cannot be chosen as the method of determination.

The correlation is clearer for the three other methods, although data are scattered (especially for the dry-curing). This data spread may be partly due to the low accuracy of the natural carbonation rate since carbonation depths were determined only between 1 and 2 years. The best goodness-of-fit is obtained for the “EN12390” method. One can also note that the rate from this method is close to the one obtained with the “4 points” method.

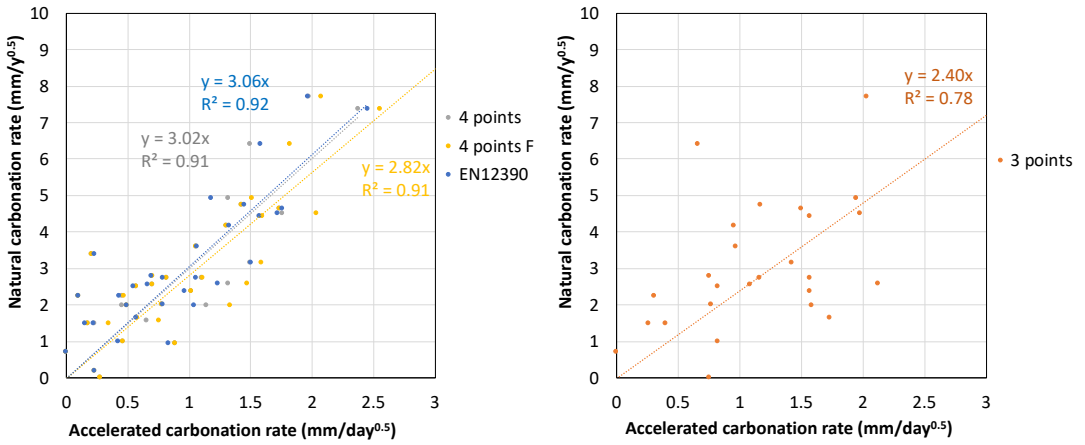

Figure 3.58. Natural carbonation rate versus accelerated carbonation rate (EN wet-curing)

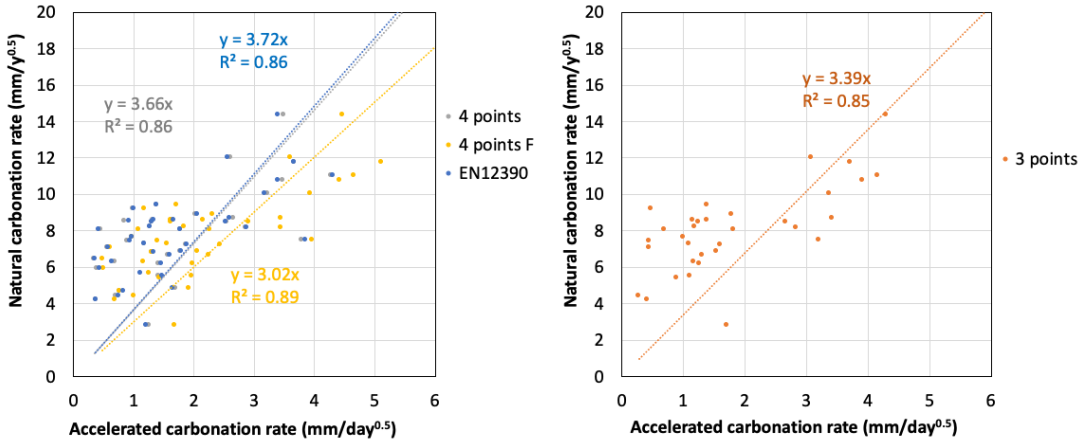

Figure 3.59. Natural carbonation rate versus accelerated carbonation rate (EN dry-curing)

7.3.4 Choice of a determination method of the carbonation rate

Based on the previous observations, it seems appropriate to define thresholds of R^2 used to assess the goodness of the linear regression as a function of the level of carbonation rate. Such an approach will maximize the number of concrete mixes complying with the criterium. Consequently, we proposed to define two ranges of carbonation rates associated with specific threshold of R^2 as follows:

- rate lower than 1 mm/day$^{0.5}$: $R^2 \geq 0.9$;
- rate higher than 1 mm/day$^{0.5}$: $R^2 \geq 0.95$.

The carbonation rate used are those complying with these criteria. The higher the carbonation rate is, the higher is the threshold that must be satisfied. This validation method is deemed to be safe since concrete, whose carbonation rate is difficult to determine even with an accelerated test (i.e., low and scattered carbonation depths, so low R^2), has a priori a higher resistance to carbonation.

Moreover, the method “EN 12390” and “4 points” give the best correlation between natural rate and accelerated one. As shown in Figure 3.60, both methods give almost the same carbonation rate.

In the light of this analysis, the “EN 12390” method seems to be the more relevant one for the determination of the carbonation rate from the accelerated test results. Thus, it was chosen for

the rest of the exploitation of PerfDuB database. In the following, data analysis is done for concretes complying with this validation method of the carbonation rate.

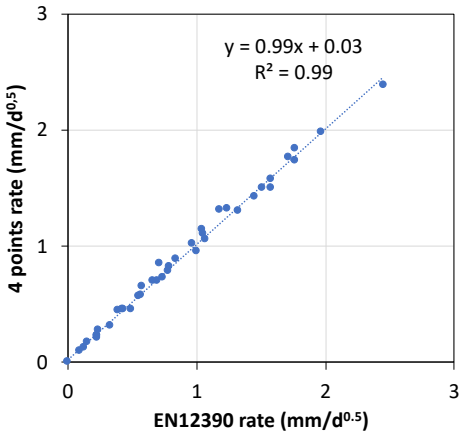

Figure 3.60. Comparison of the carbonation rates determined by the “4 points” and the “EN12390” method

7.4 Cartography

7.4.1 Main data

The carbonation rates determined for the 42 tested concretes are given in Table 3.17.

It should be kept in mind that the carbonation rates used to investigate correlations are only those complying the criteria on R² defined previously. This method of validation is supposed to guarantee the accuracy of the carbonation rates.

Table 3.17. Used database. The accelerated carbonation rates not complying with the criterion of R² are shown in red

Concrete number	Accelerated carbonation				Natural carbonation	
	Wet-cure		Dry-cure		Wet-cure	Dry-cure
	Rate (mm/d$^{0.5}$)	R²	Rate (mm/d$^{0.5}$)	R²	Rate (mm/y$^{0.5}$)	Rate (mm/y$^{0.5}$)
1	1.04	0.95	2.87	1.00	1.70	8.20
2	1.72	0.99	3.39	1.00	4.57	10.79
3	0.84	0.91	1.78	1.00	0.86	8.10
4	1.77	0.95	2.11	0.99	-	-
5	2.45	0.95	3.66	0.99	7.30	11.77
6	1.18	0.92	3.18	1.00	4.63	10.06
7	1.24	0.94	2.59	1.00	2.33	8.69
8	1.51	1.00	2.57	1.00	2.99	12.04
9	1.58	0.95	5.57	1.00	6.92	20.12
10	1.76	1.00	3.40	1.00	4.64	14.36
11	1.07	1.00	1.67	1.00	3.61	8.60
12	1.00	0.97	0.93	0.95	-	7.86
13	-	-	0.42	0.98	-	7.02

14	0.33	0.50	0.97	1.00	-	6.82
15	0.55	0.97	1.18	1.00	2.69	7.30
16	0.66	0.96	1.20	0.99	2.47	2.80
17	1.33	0.99	1.88	1.00	4.22	5.97
18	0.79	0.97	1.39	1.00	2.71	9.40
19	0.10	0.54	1.66	0.99	1.87	4.87
20	0.43	0.77	2.53	1.00	1.81	8.47
21	0.71	0.70	0.65	0.98	-	5.63
22	0.70	0.99	1.33	1.00	2.83	8.60
23	0.23	0.86	0.44	0.92	2.95	5.92
24	1.06	0.97	1.80	1.00	2.67	6.88
25	0.57	0.58	1.00	1.00	1.77	9.20
26	0.13	0.28	0.36	0.98	1.95	6.44
27	0.74	0.59	1.12	0.96	-	5.53
28	0.42	0.91	0.58	1.00	0.88	7.08
29	0.49	0.88	0.76	0.99	1.94	4.42
30	-	-	0.83	0.96	-	4.92
31	0.78	0.98	1.28	1.00	1.99	8.22
32	0.23	0.77	-	-	0.18	4.95
33	0.39	0.62	1.33	0.99	-	6.11
34	1.45	0.99	1.60	1.00	4.70	6.69
35	0.16	0.80	1.30	1.00	1.63	8.50
36	1.58	0.99	3.85	1.00	4.53	7.52
37	0.97	0.94	2.06	1.00	2.69	8.89
38	0.00	-	0.37	0.99	0.57	4.20
39	0.23	0.98	1.46	1.00	1.25	6.20
39b	0.57	0.72	1.48	0.99	1.35	5.53
40	1.97	1.00	4.30	1.00	7.41	11.02
41	0.23	0.55	0.94	0.99	0.00	7.43

7.4.2 Analysis background

To fully understand the influence of the studied parameters on the carbonation rate, it is necessary to keep in mind the phenomena controlling the carbonation of concrete. Carbonation is a reactive transfer controlled by two phenomena: the diffusion of gaseous CO_2 and the chemical reactions in the interstitial solution (dissolution of cement hydrates, reactions of dissolved CO_2 with calcium ions in solutions from the cement matrix, etc.)

Diffusion depends on the gas diffusion coefficient of the material and therefore on the properties of the microstructure and its degree of water saturation. The chemical reactions depend on the amount of calcium that can be mobilized from the calcium oxides of the binder. Their rates depend especially on the degree of water saturation and the degree of carbonation of the carbonatable elements.

The chemical rates are usually assumed to be much higher than the diffusion rate. This assumption is mainly true for water saturation degree higher than about 0.5. In this case, chemical reactions are assumed to be instantaneous. Two zones can be distinguished: a fully carbonated zone and a non-carbonated one. The progression of the carbonation depth, i.e., the front separating the two zones, can be written as function of the square root of time (Papadakis et al., 1991):

$$x_c = \mathrm{v}\sqrt{\mathrm{t}} \qquad \text{(Equ.3.7)}$$

where v is the carbonation rate (m/s$^{0.5}$).

The rate v can be written as follows:

$$\mathrm{v} = \sqrt{\frac{2\mathrm{D}}{\mathrm{n_c}}[CO_2]} \qquad \text{(Equ.3.8)}$$

where D is the gas diffusion coefficient of the carbonated material (m²/s), n_c the CO_2 binding capacity (mol/m^3) and $[CO_2]$ the ambient concentration of CO_2 (mol/m^3).

D is linked especially to the porosity and n_c is linked to the CaO content of the binder. Classically, concrete with low clinker content is less resistant to carbonation than concrete made with Portland cement of the same porosity. This tendency is usually explained by the lower CaO content of low clinker content binders (Younsi et al., 2011). Some studies show however that the gas diffusion coefficient is also higher for carbonated concrete made with low clinker content binder, such as slag cement (Gendron, 2019).

7.4.3 Correlations between accelerated carbonation rate and composition parameters

We first investigate the correlation between the carbonation rate and a key-parameter of the concrete mix-design, i.e., the ratio W/B (B is total cement + total additions). This parameter controls the mechanical performance. In Figure 3.61, the compressive strength determined at the age of 90 days is plotted as a function of the W_{eff}/B (left) and as a function of the W_{eff}/B^*, with B* the content of hydraulic or pozzolanic binders, i.e., all binder types except limestone and siliceous fillers. A far better correlation is observed for the W_{eff}/B^* than for the W_{eff}/B. In the following, the parameter W_{eff}/B^* was chosen to analyze the database.

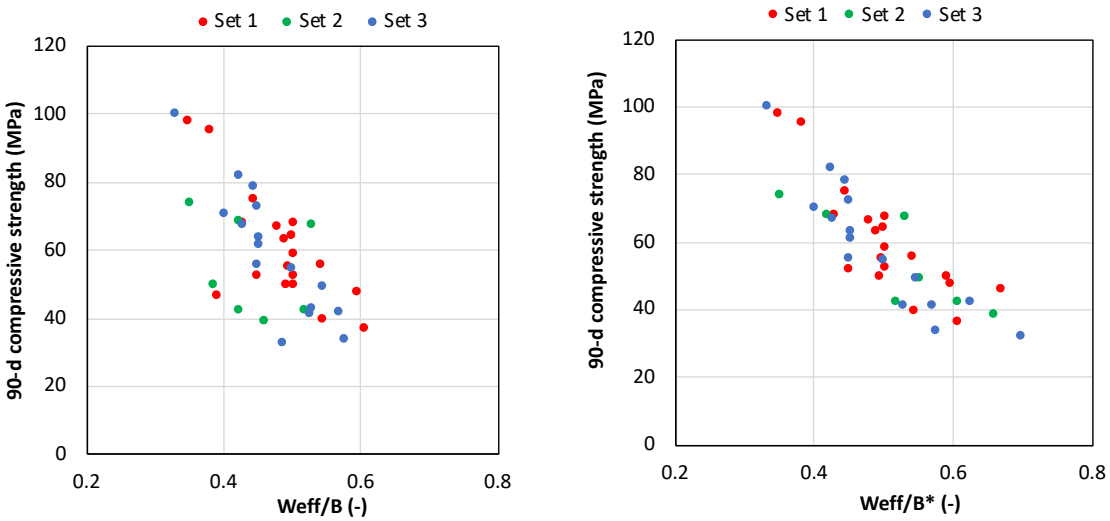

Figure 3.61. 90-day compressive strength versus W_{eff}/B (left) and W_{eff}/B^* (right) – wet-curing

In Figure 3.62(a), the correlation between the carbonation rate and the W_{eff}/B^* ratio is low

whatever curing type. However, we note that the carbonation rate is more correlated to the W_{eff}/B^* for the water-cured mixtures with high clinker content (set 1). For such concretes, the carbonation resistance becomes very high when the W_{eff}/B^* is lower than 0.4, and the accelerated carbonation rate is hardly measurable under this value. Water-cured concretes with low clinker content (set 3) carbonate faster than concretes of set 1 with the same W_{eff}/B^*. The trend lines given in Figure 3.62(b) indicate that the carbonation rate of set 3 concrete is roughly equal to the rate of set 1 concrete plus 0.7 mm/d$^{0/5}$ for a given W_{eff}/B^*.

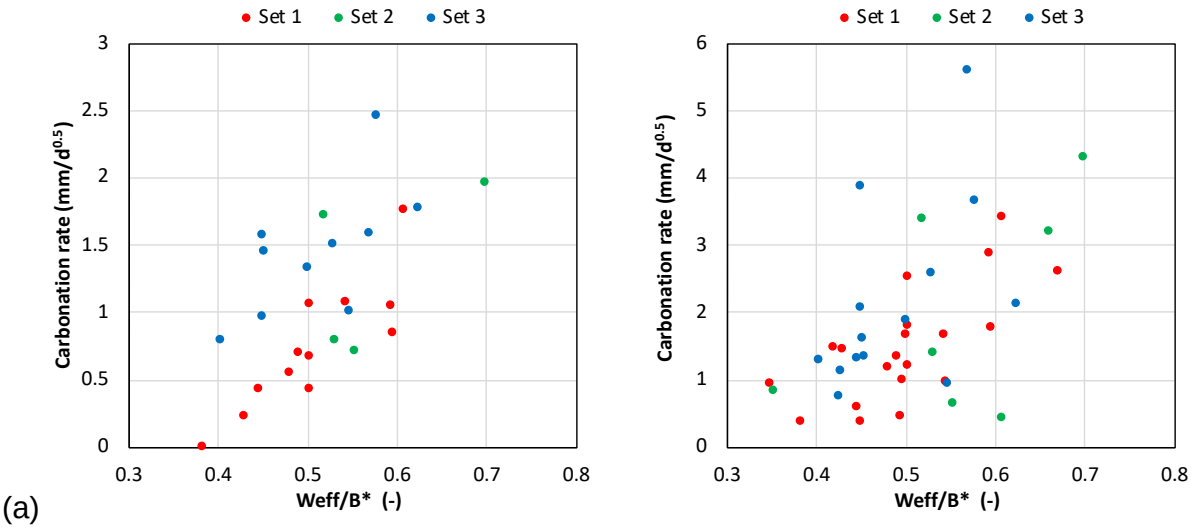

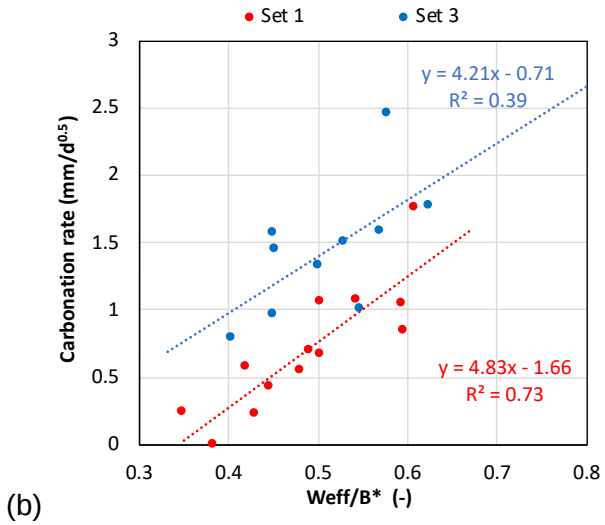

Figure 3.62. (a) Accelerated carbonation rate versus W_{eff}/B^* – wet-curing (left) and dry-curing (right) – (b) Accelerated carbonation rate versus W_{eff}/B^* – wet-curing, sets 1 and 3

Carbonation rate should be linked to the CO_2 binding capacity of the cementitious fraction, i.e., to the content of carbonatable elements, as recalled in section 7.4.2. From this principle, (Leemann and Moro, 2017) proposed to correlate the carbonation rate to the ratio W_{eff}/CaO with CaO the content of carbonatable calcium oxide in the binder. In this ratio, the water content W_{eff} is a mix-design parameter controlling the porosity and thus the gas diffusivity. Thus, the ratio W_{eff}/CaO should give global information about the carbonation rate.

As shown in Figure 3.63, the correlation is slightly better than for the W_{eff}/B^* in the case of wet-curing. Note that the points furthest from the trend line correspond to concretes made with fly ash. The W_{eff}/CaO gives only an overall tendency for the carbonation resistance. One limit of

such an approach is the CaO content. In fact, a part of calcium oxide may be not carbonatable. Lots of literature results show for instance that the degree of carbonation of portlandite remains lower than 50 % even in accelerated carbonation, e.g. (Thiery, 2005; Boumaaza et al., 2020; Steiner et al., 2020).

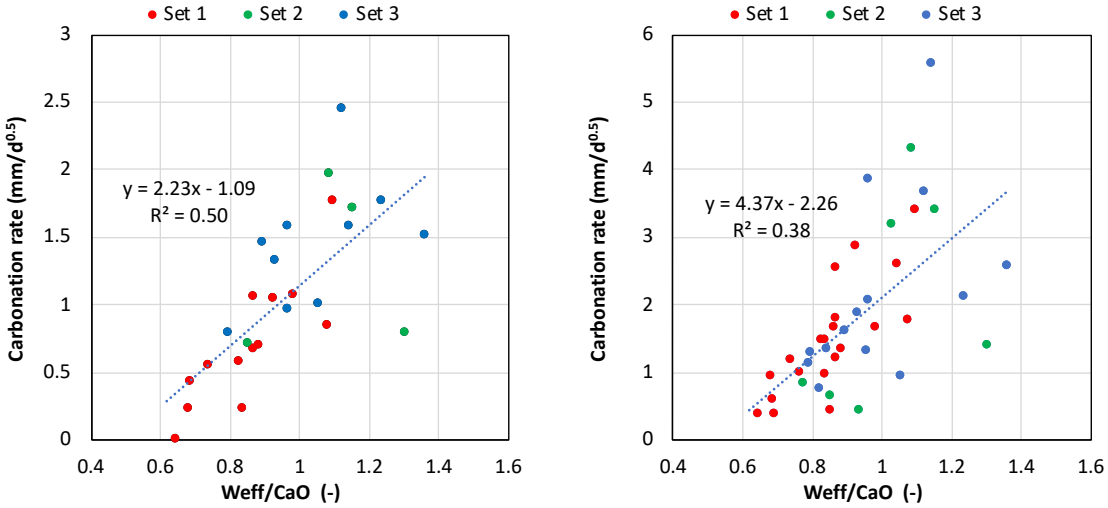

Figure 3.63. Accelerated carbonation rate versus Weff/CaO content – wet-curing (left) and dry-curing (right). The trend lines are calculated for all points

Figure 3.64 gives the correlation between carbonation rate and W_{eff}/CaO for the different aggregate types. The aggregates G2 and G4 are the most porous (absorption higher than 2.5 %), while the aggregates G1, G3 and G5 are dense (absorption lower than 1 %). The concretes containing aggregates G2 and G4 are also concretes made with the highest W_{eff}/CaO. Thus, it is difficult to separate the influence of the aggregate type from that of the W_{eff}/CaO. In the common range of W_{eff}/CaO (i.e., between 0.8 and 1), no clear influence of the aggregate can be observed.

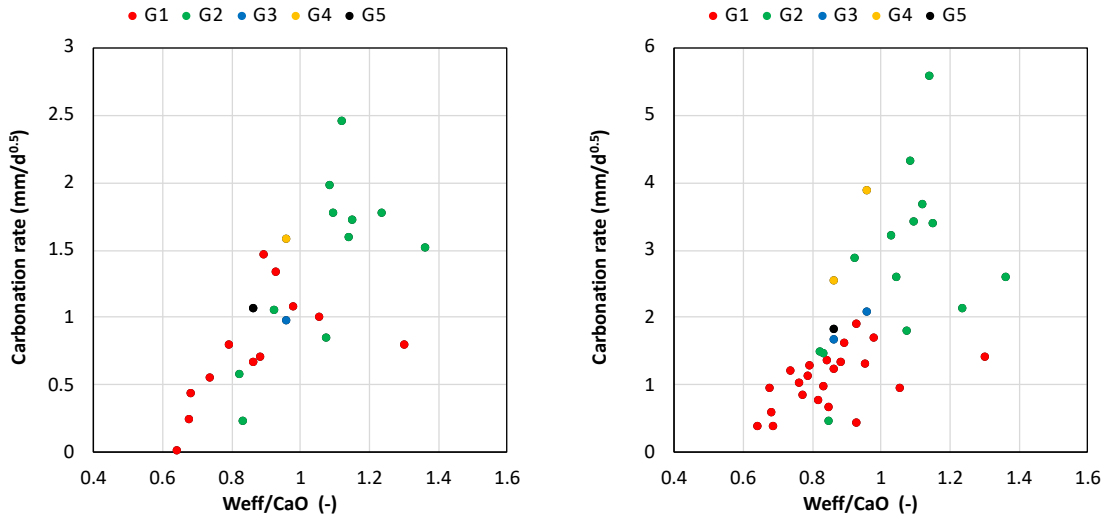

Figure 3.64. Accelerated carbonation rate versus Weff/CaO content – wet-curing (left) and dry-curing (right). The series Gi correspond to the aggregate types

The concretes 36 and 37 were made with the same paste composition and the same volume fraction of aggregates but different aggregate natures, i.e., G4 and G3 for 36 and 37

respectively. G3 is a dense limestone aggregate with absorption of 0.6 %, while G4 is a porous limestone aggregate with absorption higher than 4 %.

The porosity of aggregates affects both concrete porosity and carbonation resistance, as shown in Figure 3.65. The carbonation rate of the concrete made with G4 is 1.5 times higher the rate of the concrete made with G3. This is an evidence of the non-negligible effect of the nature of aggregates on concrete performance.

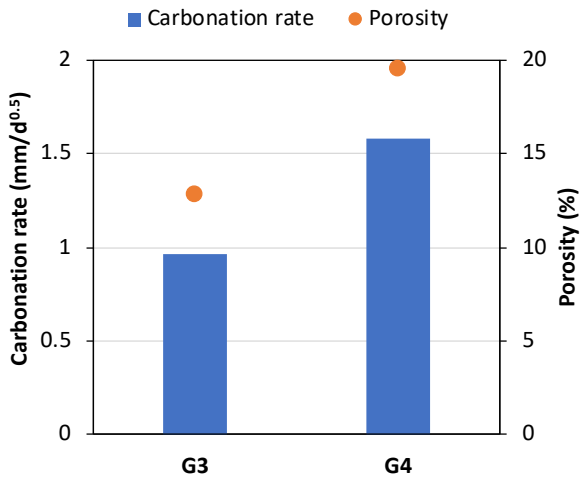

Figure 3.65. Accelerated carbonation rate and porosity of two concretes made with the same paste but different aggregates, namely G3 (absorption = 0.3 %) and G4 (absorption = 4 %)

In Figure 3.66, carbonation rate determined for dry-curing is plotted versus carbonation rate for wet-curing. The obtained correlation is rather poor (especially for the set 3). We note that the dry-curing rate deduced from the linear regression for a null wet-curing rate is non-null (y-intercept of 0.32 mm/day$^{0.5}$).

In fact, the impact of a dry-curing results in a given concrete thickness of poorer quality with respect to the transfer properties and the content carbonatable elements. We could therefore consider taking into account the effect of curing through an additive rather than a multiplicative term. This hypothesis is not clearly highlighted in these figures and a more detailed determination of this value would require additional investigations.

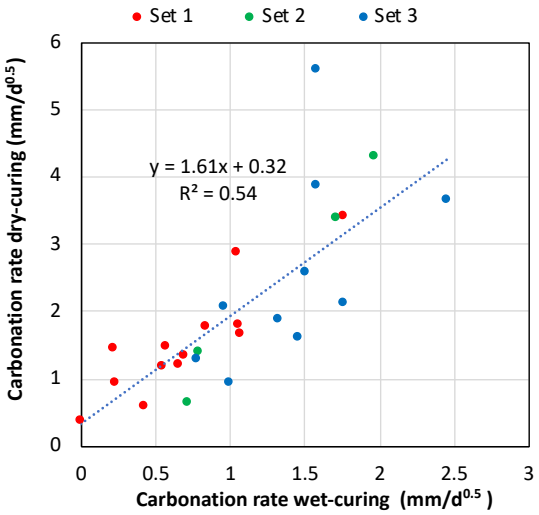

Figure 3.66. Accelerated carbonation rate determined for dry-curing versus rate for wet-curing

7.4.4 Correlations between accelerated carbonation rate and other properties

Compressive strength is the main property usually used to design the concrete mixture. Good correlations are observed between the compressive strength determined at the age of 90 days and the carbonation rate, especially in the case of wet-curing (Figure 3.67).

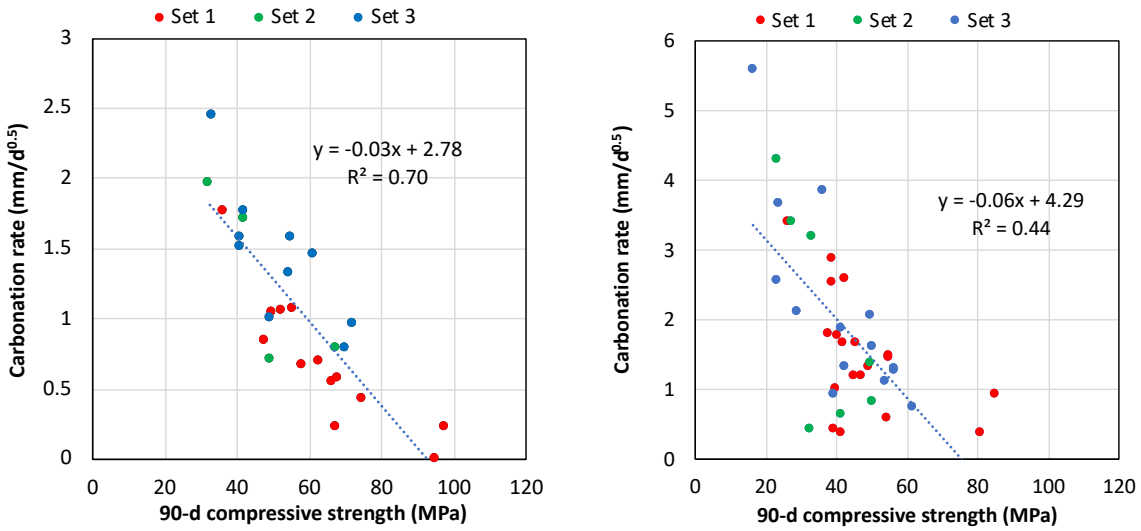

Figure 3.67. Accelerated carbonation rate versus 90d compressive strength – wet-curing (left) and dry-curing (right)

Correlations even better are obtained when only one set of concrete is considered for the linear regression (Figure 3.68). Several explanations can be provided. First, compressive strength is maybe the most reproducible concrete property (laboratories have a lot of experience for this testing method). Secondly, among a set of concrete, i.e., a set of clinker contents, the mechanical strength should mainly depend on the porosity, which should be also the case for the resistance to carbonation.

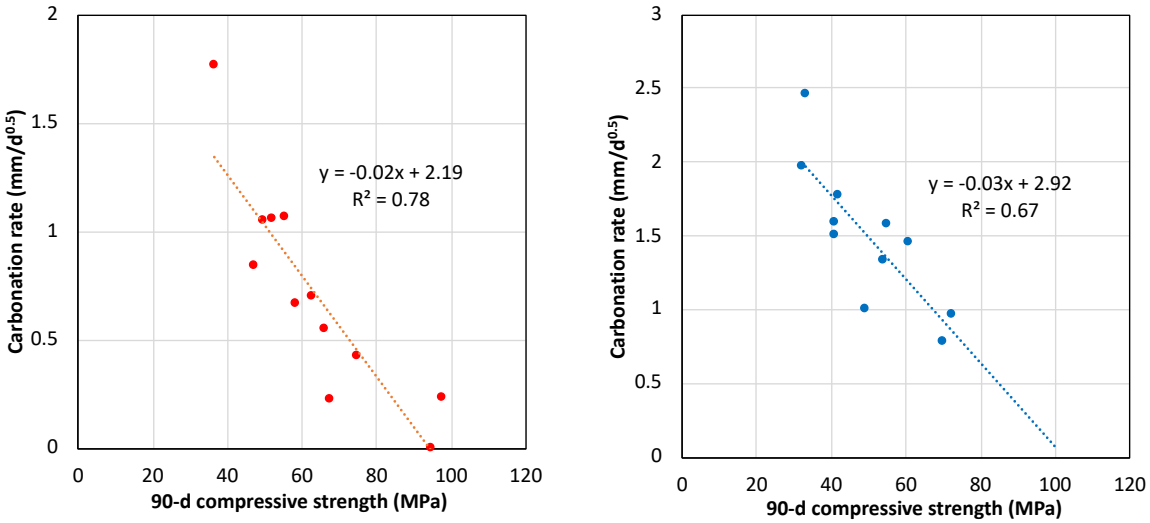

Figure 3.68. Accelerated carbonation rate versus 90d compressive strength for set 1 (left) and set 2 (right) – wet-curing.

Surprisingly, the carbonation rate is better correlated with compressive strength determined at the age of 90 days than with the water porosity (Figure 3.69). The porosity was only determined for the wet-curing (the correlation between the carbonation rate for the dry-curing and porosity are not investigated here).

The correlation is a little better when the porosity is related to the CaO content (Figure 3.70). The ratio porosity/CaO is assumed to give information of the rate V defined in section 7.4.2, i.e., the ratio of the gas diffusivity and the CO_2 binding capacity. Note, however, that the gas diffusivity controlling the carbonation rate is the gas diffusivity of the carbonated material. The porosity used here was determined for a sound material. The gas diffusivity is also related to the water saturation degree. Moreover, as discussed in section 7.4.3, the content of CaO provides only a rough estimation of the CO_2 binding capacity.

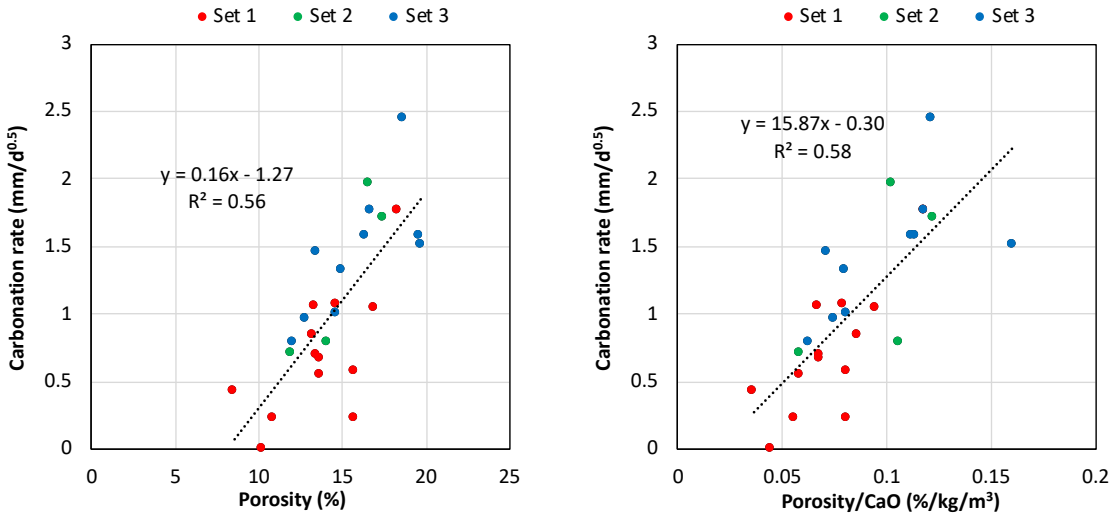

Figure 3.69. Accelerated carbonation rate versus porosity (left) and versus the ratio porosity/CaO content (right) – wet-curing

As proposed in section 4, the porosity can be corrected by the volume fraction of paste (i.e., the paste including water and all solid particles lower than 63 µm). In the case of non-porous aggregates, the ratio “porosity / paste fraction” corresponds to the porosity of the paste. As observed previously, when the parameter is divided by the content of CaO, the correlations are slightly better. The correction of the porosity with the paste fraction did not improve the correlation with the carbonation rate.

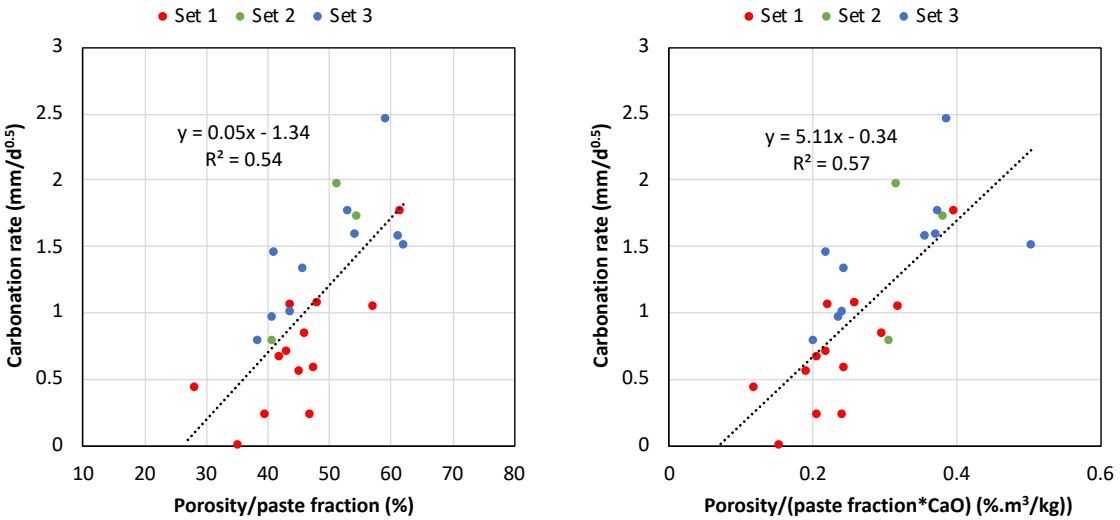

Figure 3.70. Accelerated carbonation rate versus the ratio porosity/paste fraction (left) and versus the ratio porosity / (paste fraction*CaO) (right) – wet-curing

The chloride diffusivity is a property which could provide indication on the gas diffusivity. (Rozière et al., 2009) found a good correlation between the accelerated carbonation rate (determined with the AFPC-AFREM procedure) and the ratio D_e/CaO with D_e the effective chloride diffusion coefficient (determined from a steady state migration test). The studied concretes were made with two binders: a CEM I cement and a mix of 70 % CEM I cement and 30 % fly ash). They correspond to concretes from set 1 and set 2 of the PerfDuB project.

In Figure 3.71, the carbonation rate is plotted as a function of the ratio D_{rcm}/CaO, with D_{rcm} the chloride migration coefficient. The latter was determined for all PerfDuB concretes from migration tests (see section 8). Globally, no correlation emerges from this figure. However, a strong correlation appears for the set 1, i.e., concretes made with high clinker content binders.

Moreover, linking the carbonation rate to the D_{rcm}/CaO suggests that the relation between these two parameters depends on the binder nature. Indeed, the clustering of concretes in 3 sets depending only on the clinker content is not relevant enough.

In Figure 3.71, three zones were drawing according to binder type: in red, zone with mainly binders with high clinker content (i.e., set 1), in blue, zone with mainly binders with clinker and slag (i.e., K-S from set 3), and in between, an intermediate zone with binders containing clinker, fly ash or siliceous filler (i.e., K-S or-Qz from sets 2 and 3).

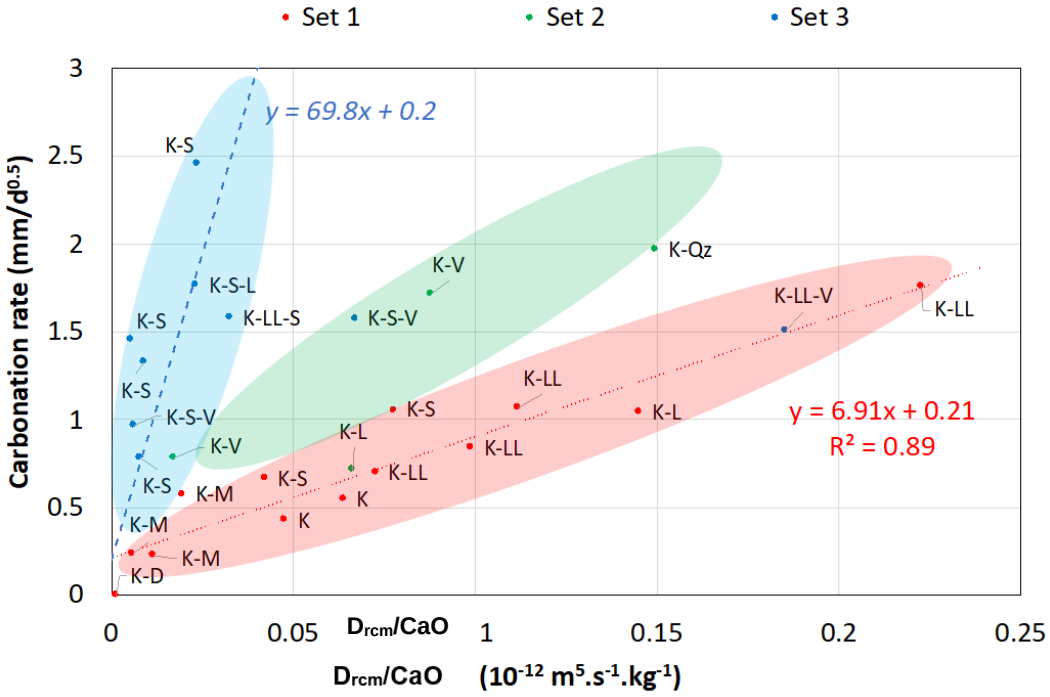

Figure 3.71. Accelerated carbonation rate versus the ratio D_{rcm}/CaO – wet-curing. "K-X" are related to the mineral admixtures' "X" with clinker "K"

The difference in the relation between the carbonation and the D_{rcm}/CaO due to the binder nature could first be a consequence of the use of a apparent chloride diffusion coefficient and not the effective one. It should be recalled that D_{rcm} is related to D_e and the chloride binding capacity of the binder. The latter is higher in the case of slag binder concrete and, as a result, the D_{rcm} should be lower for slag concretes that have the same D_e than Porltand cement concretes.

However, lot of literature results show that the chloride binding is negligeable during a migration test: the lower D_{rcm} and D_e of slag concretes are rather due to their finer pore network, e.g. (Baroghel-Bouny et al., 2013). Another explanation can be put forward with regard to

recent results from the literature (Dutzer et al., 2019). During carbonation, materials with high content of C-S-H, such as slag concretes, are submitted to high carbonation shrinkage and thus to micro-cracking which strongly increases the gas diffusion coefficient. For a cement paste containing mainly C-S-H, (Kangni-Foli et al., 2021) found that the gas diffusion coefficient increased by an order of magnitude after an accelerated carbonation at 3 % CO_2. Note that the slope of the blue zone axis in Figure 3.71 is approximately 10 times higher than the linear regression obtained from data of set 1 (i.e., red zone).

In the section 6, the link between the carbonation rate and the O_2 diffusion coefficient related to the content of CaO was investigated. The main trends depend to the concrete set (and undoubtedly to the binder nature). For a given ratio D_{O2}/CaO, the carbonation rate of set 3 is higher than that of set 1. That highlights that the more relevant indicator should be the gas diffusion determined after carbonation.

Figure 3.72 confirms this assertion. Indeed, concretes of set 3 that have the same resistivity than concretes of set 1 have also much lower carbonation resistance. Resistivity is a transfer property determined here for non-carbonated materials.

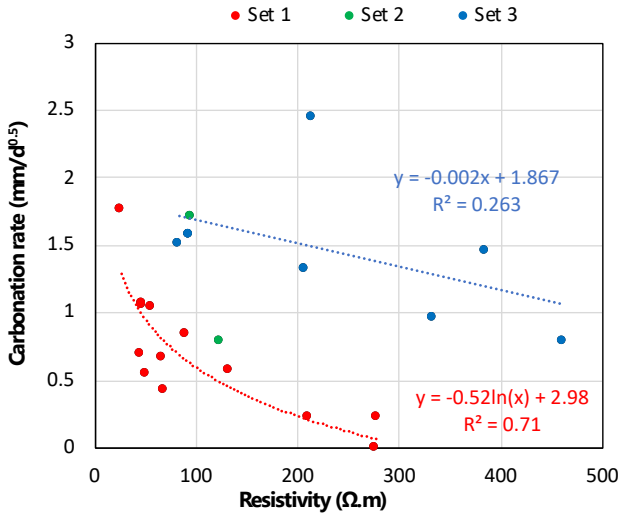

Figure 3.72. Accelerated carbonation rate versus the resistivity – wet-curing

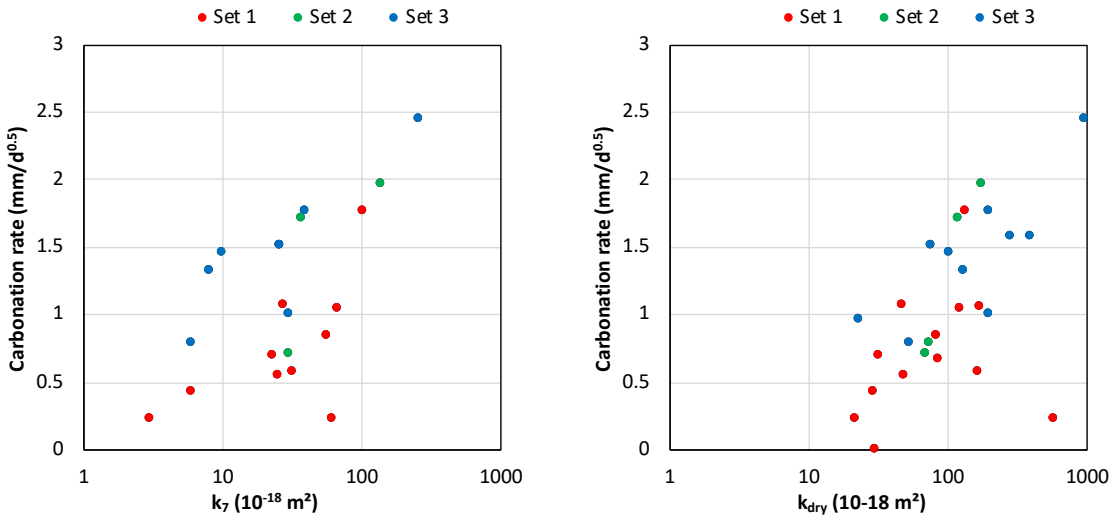

Figure 3.73. Accelerated carbonation rate versus apparent gas permeability (in log scale), k_7 determined after oven-drying at 80 °C for 7 days (left), and k_{dry} determined after drying of test specimen at 105 °C up to constant mass (right) – wet-curing

Again, as shown in Figure 3.73 (left), trends observed for the apparent gas permeability k_7 (determined after a 7-day oven-drying at 80°C) are different regarding the set: concretes of set 3 that have the same k_7 than concretes of set 1 have higher carbonation rate. Although data are scattered, the trends are closer for k_{dry}, i.e., the gas permeability determined after an oven-drying at 105 °C up to constant mass. That could be explained by the cracking of the specimens after this oven-drying. The gas permeability k_{dry} could be more representative of the gas diffusion coefficient at the carbonated state (gas diffusion of a damage concrete).

7.4.5 Correlations between natural carbonation rate and composition / properties

In the following, we investigate the correlations between natural carbonation rate and concrete mix-design parameters. The same parameters are used than in the case of accelerated carbonation, i.e., composition parameters (W_{eff}/B^*, W_{eff}/CaO) and properties (90-d compressive strength, porosity, porosity/CaO, D_{rcm}/CaO).

Globally speaking, the correlations between the carbonation rate and the investigated parameters are low, although the expected tendencies are obtained (for instance, the rate tends to increase with the W_{eff}/B^* and the W_{eff}/CaO, as shown in Figures 3.74 and 3.75 respectively).

Several explanations can be proposed:

- at the time of writing of this report, the carbonation rates were calculated from depths determined after 2 years of atmospheric carbonation. For some concretes, especially the wet-cured ones, the carbonation depths were low. In this case, the carbonation rate is more the rate of the specimen skin than that of the plain concrete;
- only one cylindrical specimen for each concrete was used for the natural carbonation test;
- the reproducibility of the natural carbonation test was not investigated during the PerfDuB project. Although the test is carried in rooms with controlled conditions (i.e., temperature of 20 ± 2 °C and relative humidity of 50 ± 5 %), differences of ambient conditions between laboratories (especially difference of relative humidity) could result in differences in carbonation rate.

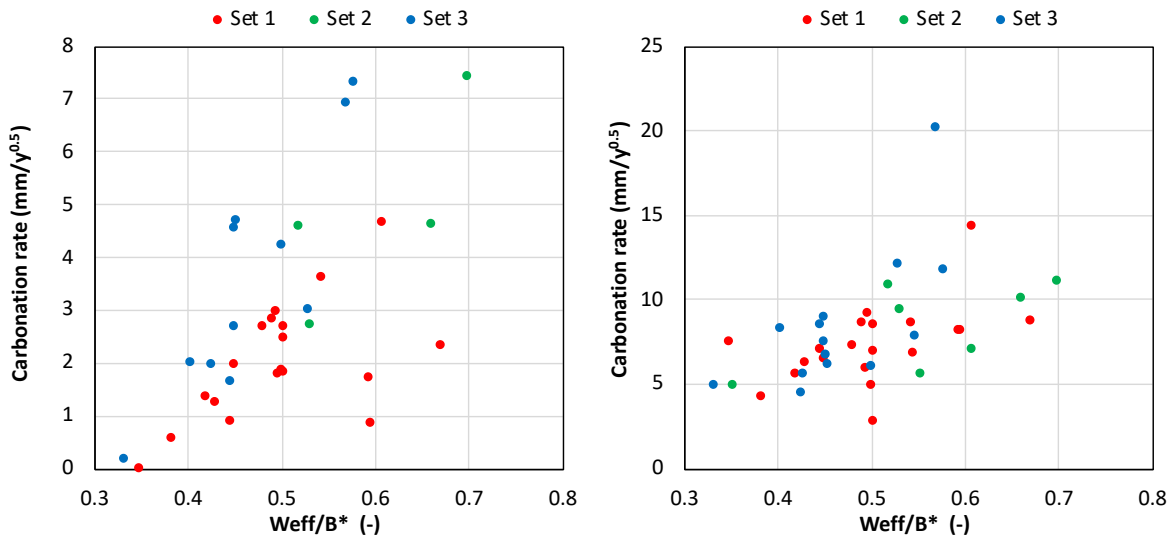

Figure 3.74. Natural carbonation rate versus W_{eff}/B^* – wet-curing (left) and dry-curing (right)

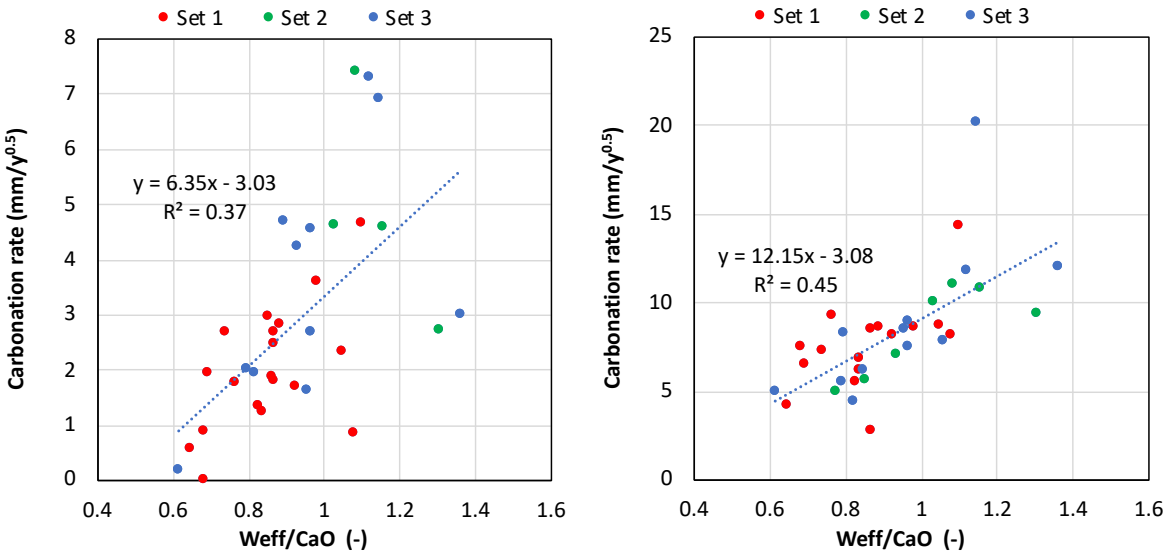

Figure 3.75. Natural carbonation rate versus W_{eff}/CaO – wet-curing (left) and dry-curing (right)

As shown in Figure 3.76, the natural carbonation rate tends to decrease with compressive strength, whether in wet or dry cure, always with a low correlation.

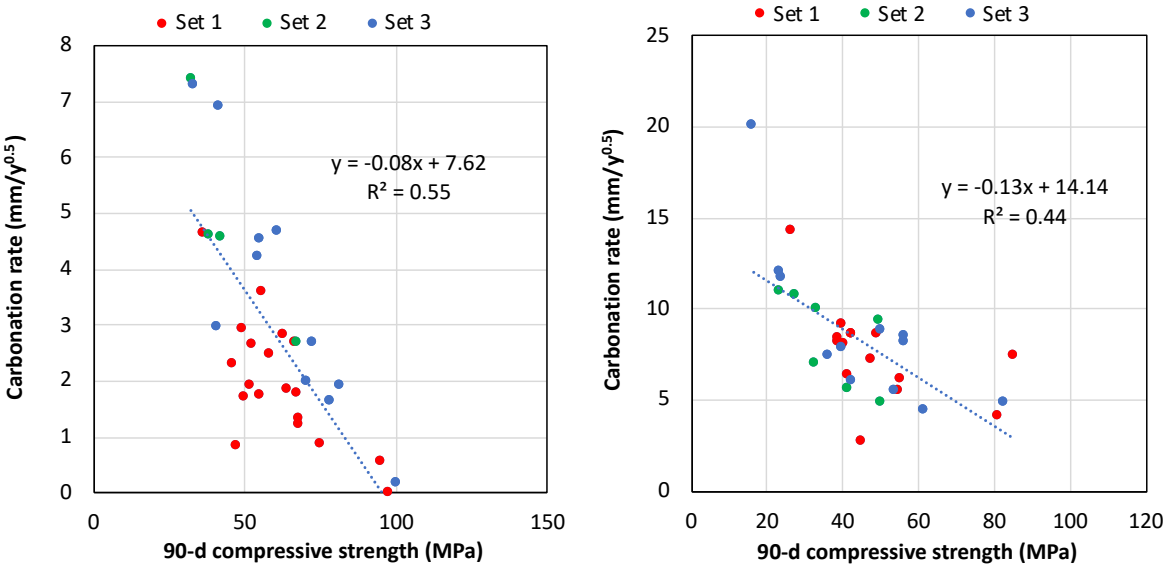

Figure 3.76. Natural carbonation rate versus 90d compressive strength – wet-curing (left) and dry-curing (right)

Figure 3.77 shows that the rate of carbonation tends to increase with the porosity of the concrete or with the porosity divided by the CaO content, but always with a weak correlation.

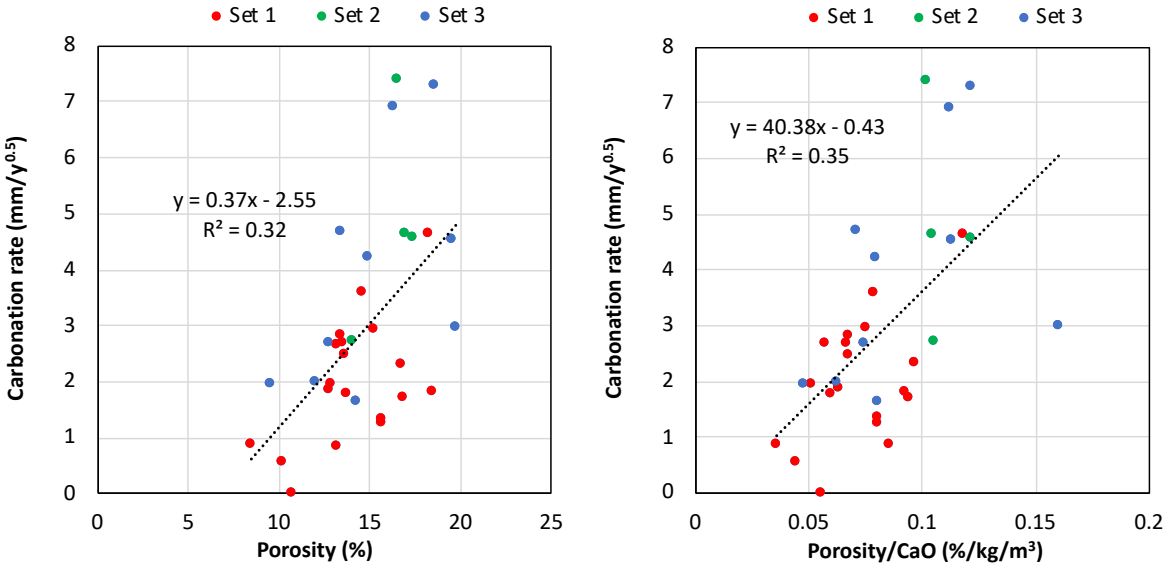

Figure 3.77. Natural carbonation rate versus porosity (left) measured at 90 days and versus the ratio porosity/CaO content (right) – wet-curing

The Figure 3.78 showing the natural carbonation rate versus the D_{rcm}/CaO content reveals 3 zones depending mainly on the binder nature, as observed for the accelerated carbonation (although data are here much more scattered, especially in the red zone). Again, the main axis of the blue zone has a slope roughly 10 times higher than that of the red zone.

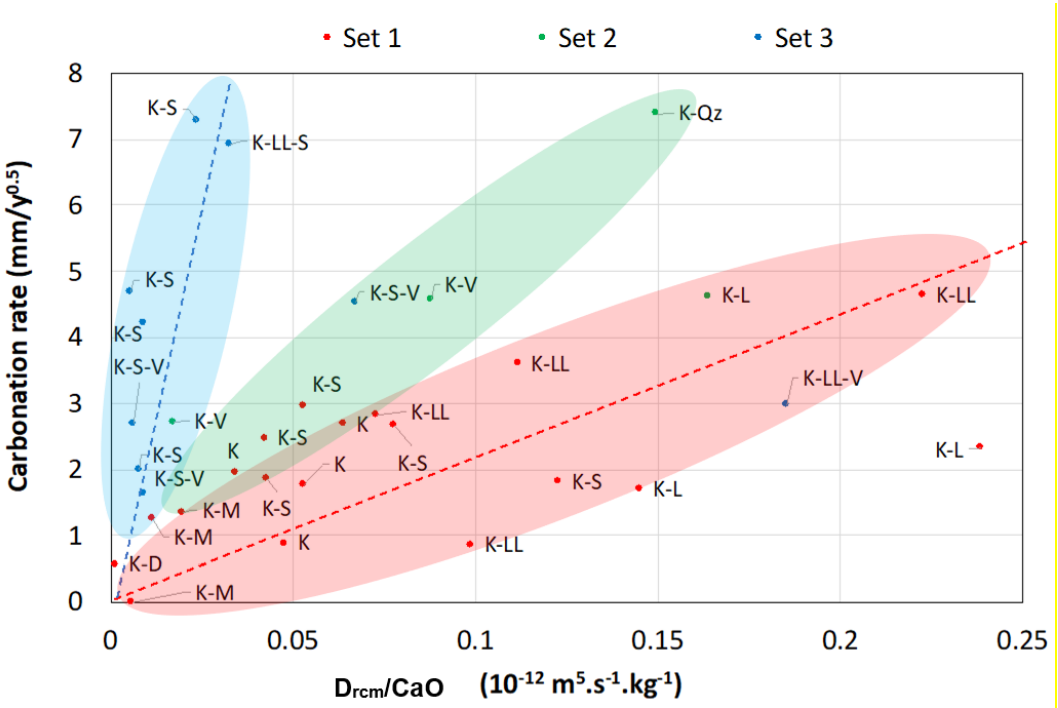

Figure 3.78. Natural carbonation rate versus the ratio D_{rcm}/CaO – wet-curing (90 days)

7.5 Correlation between natural rate and accelerated rate

In Figure 3.79, the natural carbonation rates are plotted versus the accelerated carbonation rates in the case of the wet-curing. Note that only the carbonation rates with R^2 higher or equal to 0.95 were used. The correlation between both rates is rather good. The correlation coefficient is found equal to 3. From this linear regression, the natural carbonation rate can be estimated from the rates determined with accelerated carbonation test.

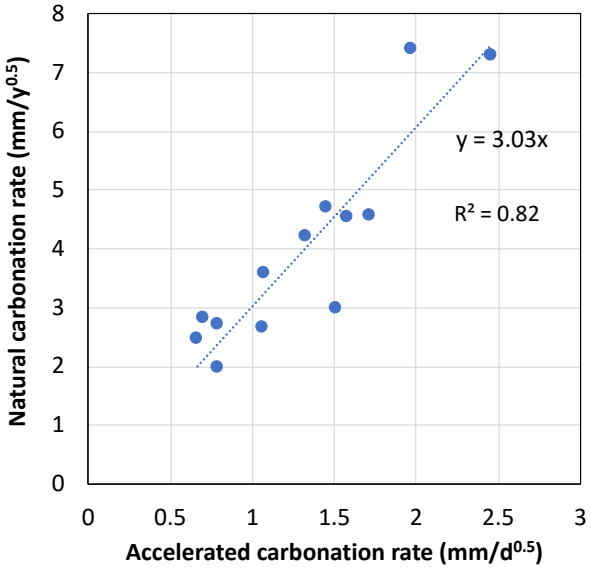

Figure 3.79. Natural carbonation rate versus accelerated carbonation rate (wet-curing)

If the only difference between natural and accelerated carbonation is the CO_2 concentration, the natural rate expressed in mm/year$^{1/2}$ could be calculated from the accelerated rate in mm/day$^{1/2}$, using the following equation:

$$v_{nat} = \sqrt{365}\sqrt{\frac{C_{nat}}{C_{acc}}}v_{acc} \qquad \text{(Equ. 3.9)}$$

Where: C_{nat} is the CO_2 concentration in the atmosphere and C_{acc} is the concentration in the accelerated test chamber (i.e., 3 %).

The theoretical ratio between v_{acc} and v_{nat} is equal to around 2.5, with C_{nat} taken equal to 0.05 %. We choose the latter value because the CO_2 concentration inside the testing room is usually higher than the outdoor CO_2 concentration of 0.045 %. The obtained ratio of 2.5 is rather closed to the correlation coefficient of 3.1 found with the PerfDuB data.

Of course, the CO_2 concentration is not the only difference between the two carbonation conditions. In fact, the hydric state is not the same since the specimens are oven-dried before the accelerated carbonation while drying and carbonation are concomitant phenomena in natural condition.

Moreover, during carbonation, the relative humidity (RH) is of 65 % for the accelerated test, while it is equal to 50 $\pm$ 5 % for the natural carbonatation. Thus, we could assume that the v_{nat} calculated with v_{acc} according to equation 3.9 is a natural rate for a RH of 65 %. An empirical model to evaluate the influence of RH on carbonation rate was proposed during the MODEVIE project (Figure 3.80). According to this model, the ratio between the rate at 50 % RH and the rate at 65 % RH is equal to 1.1. The theoretical ratio of 2.5 from equation 3.9 should be multiplied by 1.1, what brings it closer to the experimental coefficient of 3.0.

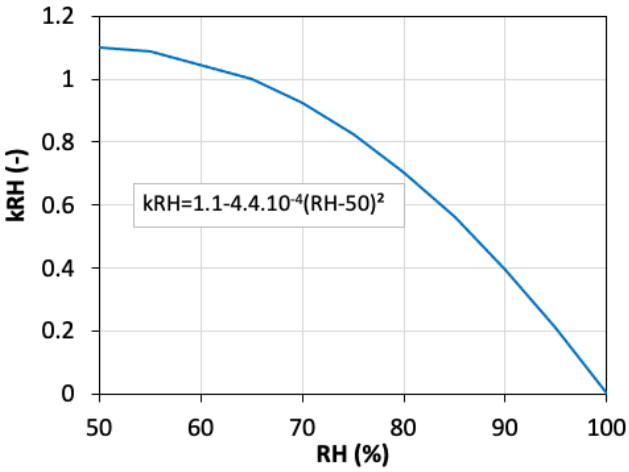

Figure 3.80. Empirical model to evaluate the influence of RH on the carbonation rate

Note that, in the Swiss standard SIA 262-1, a coefficient equal to 2.6 is proposed to convert the accelerated carbonation rate into natural rate. This test is carried out with a CO_2 concentration of 4 % after a preconditioning from the age of 72h to 28 days (drying in ambient conditions). According to Equation 3.9, the coefficient should be of around 2.

7.6 Accelerated carbonation rates and prescriptive approach

7.6.1 Fascicule n°65 of the CCTG (general technical clauses for public contracts) – design service life of 100 years

The Fascicule 65 specifies maximal values of two durability indicators, i.e., porosity and gas permeability (k_{dry}), for the exposure classes related to corrosion risk due to carbonation, i.e., XC classes. The maximal values found in Table 8.D are the following:

- classes XC1 and XC2: porosity = 15.5 %;
- class XC3: porosity = 15 % and k_{dry} = 200.10^{-18} m²;
- class XC4: porosity = 14.5 % and k_{dry} = 200.10^{-18} m².

In Figure 3.81, porosity of wet-cured concrete is plotted as a function of k_{dry}. Four sets of accelerated carbonation rate in mm/$d^{0.5}$ are given, namely: [0; 0.5[, [0.5; 1[, [1; 1.5[, [1.5; ∞[. In this figure, the concretes not complying with the specifications for mix-design from Table 8.B of the Fascicule 65 are also highlighted (crossed dots). Labels give resistivity of the concretes.

Whatever the exposure class, concretes with carbonation rate higher than 1.5 mm/$day^{0.5}$ do not comply with the specifications of the Fascicule 65 with respect to the durability indicators. For a design service life of 100 years, 1.5 mm/$day^{0.5}$ is an obvious threshold not to be exceeded.

For the exposure classes XC3 and XC4, concretes with a porosity lower than the limit specified by the Fascicule 65 have also a gas permeability lower than the specified value (200.10^{-18} m²). Most of these concretes have permeability even lower than 100.10^{-18} m². For the PerfDuB concretes, the use of a maximal k_{dry} from the Fascicule 65 is not relevant. On the contrary, some concretes whose composition does not comply with Table 8.B have porosity and k_{dry} both lower than the specified values (mainly concretes with rate between 0.5 and 1 mm/$d^{0.5}$):

- for XC3-XC4: concretes n°3, 12 and 18;
- for XC4: concretes n°16 and 21.

For such a concrete, with high content of mineral additions, the performance-based approach seems to me more appropriate.

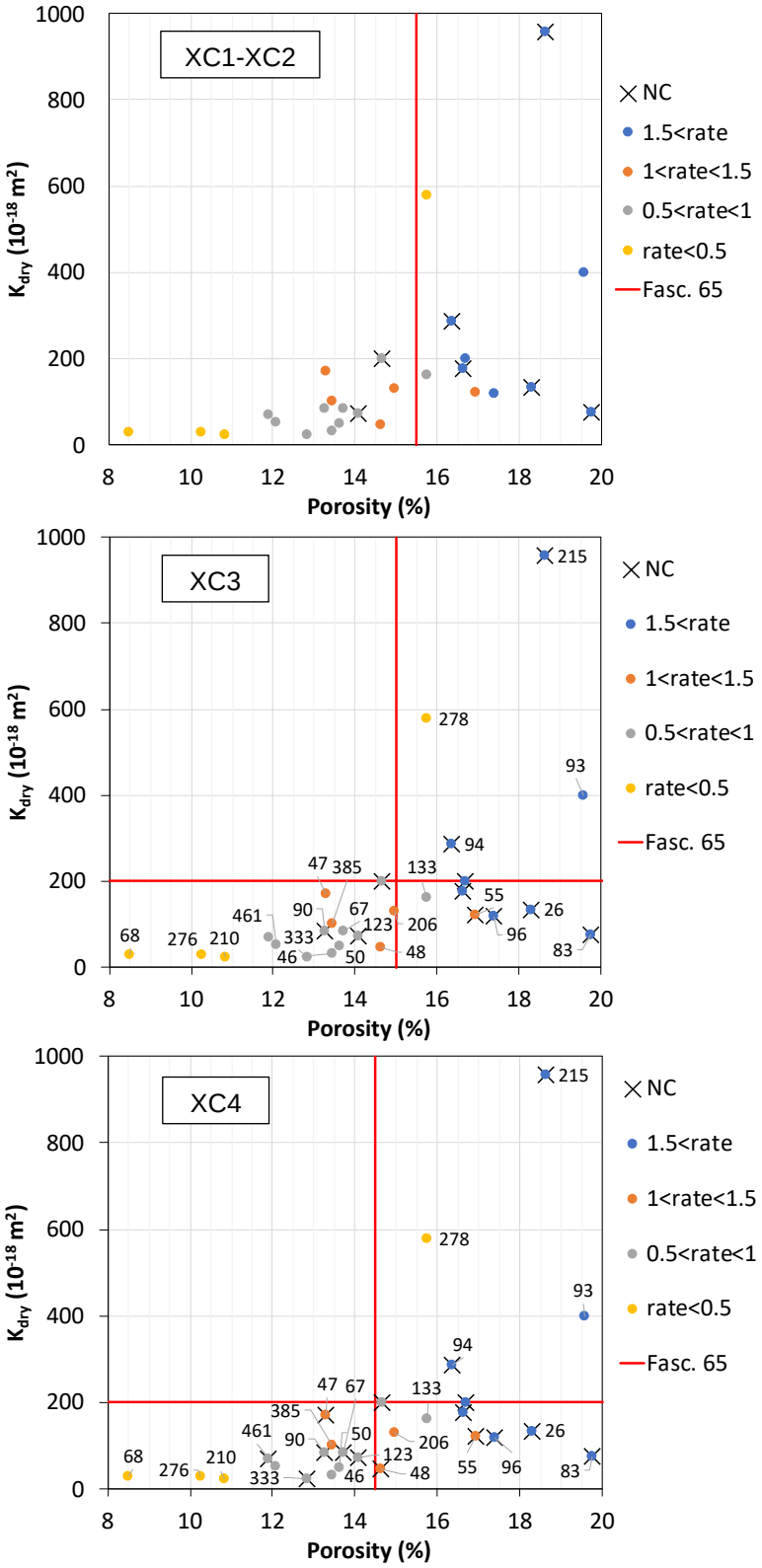

Figure 3.81. Gas permeability versus porosity for 4 accelerated carbonation rate ranges (in mm/d$^{0.5}$).
"NC" indicates concrete not complying with the Fascicule 65 (Table 8.B).
The red lines give the maximal porosity and k_{dry} specified by the Fascicule 65.
The labels give the resistivities in Ω.m. (90 days)

7.6.2 NF EN 206/CN (design service life of 50 years)

The NF EN 206/CN standard specifies limit values for composition parameters and strength for the exposure classes related to corrosion risk due to carbonation, i.e., XC classes. Figure 3.82 shows the accelerated carbonation rate as a function of the mean compressive strength determined at 28 days. The ranges of $f_{cm,28d}$ correspond to the strength classes required for each exposure class plus two strength classes, that is:

- XC1 and XC2: C20/25, C25/30 and C30/37;
- XC3 and XC4: C25/30, C30/37 and C35/45.

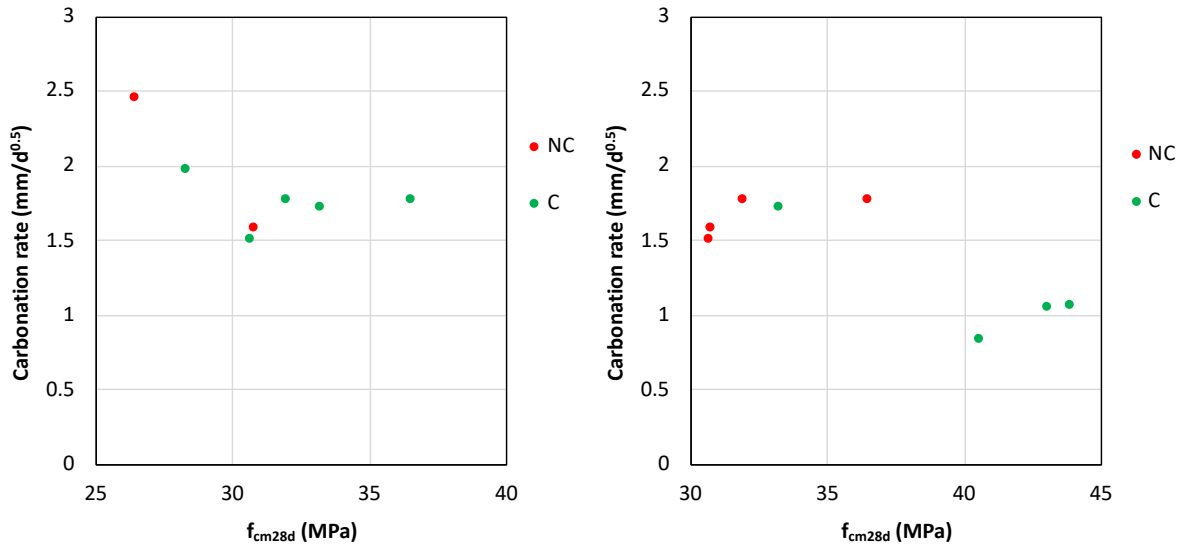

Figure 3.82. Accelerated carbonation rate versus compressive strength at 28 days for concretes complying or not (NC) with the specifications of the EN206 standard for XC1-XC2 classes (left) and XC3-XC4 classes (right) – wet-curing.

7.7 Conclusion and proposals

This section focused on the performance of 42 concretes with respect to the risk of carbonation. All analyses were performed using the database of carbonation depths determined for each of these concrete during the characterization campaign of the national project PerfDuB.

First, different methods to determine carbonation rate were compared using the database. **From this comparison, it was proposed to use the method of the EN 12390 standard for the determination of the rate**. With this method, the rate is determined from a linear regression carried out using the four carbonation depths resulting from the accelerated carbonation test. **In addition, two criteria on the coefficient of determination R^2 of the linear regression were proposed to valid or not the calculated carbonation rate.**

For each concrete, carbonation rates were determined for both curing conditions, i.e., dry-curing and wet-curing. Carbonation rate is an indicator of performance for the exposure classes XC. **This indicator was compared to various parameters: mix composition parameters and other properties, such as strength and durability indicators.** Three sets of concretes were defined to facilitate analysis. The sets depend on the clinker content of the binder: set 1 for clinker content higher than 78 % and 99 %, set 2 for clinker content bet between 60 % and 70 %, and set 3 for clinker content lower than 60 %. The main conclusions of the correlation investigation in the case of accelerated carbonation are the following:

- the best correlation between carbonation rate and mix parameters were obtained for the ratio of effective water and CaO (in binder) content. Note that this approach has its limits since the CaO content may not correspond to the carbonatable phases only;
- a rather good correlation was obtained between carbonation rate and the compressive strength. The correlations are even better for a given set of clinker content;
- the correlation between rate and porosity is lower than that obtained for strength. When porosity is related to the CaO content, the correlation is better;
- the rate was compared to the ratio of a transfer property and the CaO content. This approach corresponds to the classic link between carbonation rate and the ratio of the CO_2 diffusion coefficient and the CaO content. The transfer property used for this investigation was the chloride diffusion coefficient determined from migration test (see section 8). No correlation between this ratio and the carbonation rate was found. However, for a given set of clinker content, the correlation is good or very good. From recent literature results, this result could be explained by the fact that diffusion coefficient of low clinker content concrete (such as slag concrete) is affected by carbonation (due to microcracking). Thus, a better ratio should be the ratio of a transfer property determined on carbonated concrete and its CaO content.

A relation between the natural carbonation rate and the accelerated one using the results with the highest coefficients of determination was proposed. The accelerated carbonation test can thus provide an entry parameter of models to predict natural carbonation.

8 Chloride migration

Author: Michaël Dierkens

8.1 Operating modes

The operating mode used for the measurement of the chloride migration coefficient is that of PerfDuB National Project (V2). This operating mode is now the French experimental standard XP P 18-462.

8.2 Cartography

The data obtained from the 42 concretes tested are summarised in Table 3.18.

Table 1.18. Synthesis of experimental results

N° Concrete	Exposition Class		D_{rcm} (10^{-12} $m^2.s^{-1}$)			ρ (Ω.m)		
	NF EN 206/CN	fasc. 65	28d	90d	365d	28d	90d	365d
1	XD1	-	35.6	26.0	-	53	55	-
2	XD1	-	28.0	12.5	-	-	96	-
3	XD1	-		15.3	-	-	90	-
5	-	-	9.7	3.6	-	129	215	-
6	XD1	-	45.3	26.5	-	33	42	-
7	XD1	-	50.8	41.2	-	29	45	-

N° Concrete	Exposition Class		D_{rcm} (10^{-12} m².s^{-1})			ρ (Ω.m)		
	NF EN 206/CN	fasc. 65	28d	90d	365d	28d	90d	365d
8	-	-	26.6	22.8	-	57	83	-
9	-	-	8.7	4.8	-	123	94	-
10	-	-	48.4	34.5	-	40	26	-
11	XS1, XD2	-	21.3	20.7	17.7	40	48	71
14	XS2, XD2	-	32.5	14.7	-	-	-	-
15	XS2, XD2	XS2, XD2	16.7	15.0	13.7	45	50	61
16	XS2, XD2	XS2, XD2	9.6	8.5	6.1	54	67	105
17	XS3, XD3	XS2, XD2	4.5	1.7	2.8	134	206	335
18	-	-	8.1	2.3	0.6	77	123	367
19	XS2, XD2	XS2, XD2	9.8	8.6	-	53	46	-
20	XS2, XD2	XS2, XD2	23.4	24.6	20.7	26	32	36
21	XD1	-		13.6				
22	XS1, XD3	XS1, XD2	17.3	14.3	13.3	48	46	63
23	XS3, XD3	XS2, XD2	14.7	10.7	7.9	43	67	116
24	XS2, XD2	XS2, XD2	15.5	15.3	14.1	57	47	60
25	XS3, XD3, XF2	XS2, XD2	14.3	12.0	-	54	63	-
26	XS3, XD3, XF4	XS3, XD3, XF4	17.9	8.6	-	59	83	-
27	-	-	0.5		-	352		-
28	XS3, XD3	XS3, XD3	14.5	11.3	-	57	68	-
31	XS3, XD3	XS3, XD3	1.2	1.5	-	347	461	-
32	XD1	-	0.4		-	315	-	-
34	XS3, XD3	XS3, XD3	2.0	1.0	-	276	385	-
35	XS3, XD3	XS3, XD3	4.2	1.6	-	139	249	-
36	XS3, XD3	XS3, XD3	21.9	11.5	-	47	93	-
37	XS3, XD3	XS3, XD3	4.5	1.1	-	190	333	-
38	XS1, XD3	XS1, XD3	0.9	0.3	-	302	276	-
39	XS1, XD3	XS1, XD2	2.4	2.2	-	217	278	-
39b	XS1, XD3	XS1, XD3	5.0	3.8	-	111	133	-
40	-	-	35.8	24.2	-	29	-	-
41	XS3, XD3, XF2	XS3, XD3, XF2	1.1	1.1	-	217	210	-

Values of chloride migration coefficient and resistivity are presented at three ages of maturation as a function of water / binder ratio (Figure 3.83) and resistivity measurements (Figure 3.84).

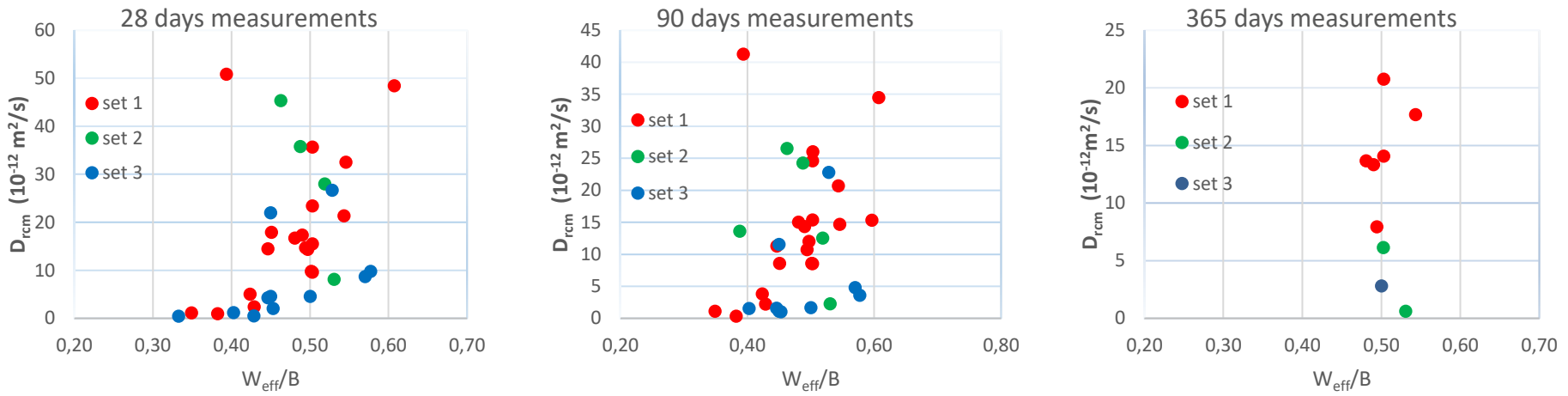

Figure 3.83. Values of the chloride migration coefficient expressed as a function of content effective water / binder ratio. Measurements at 28, 90 and 365 days

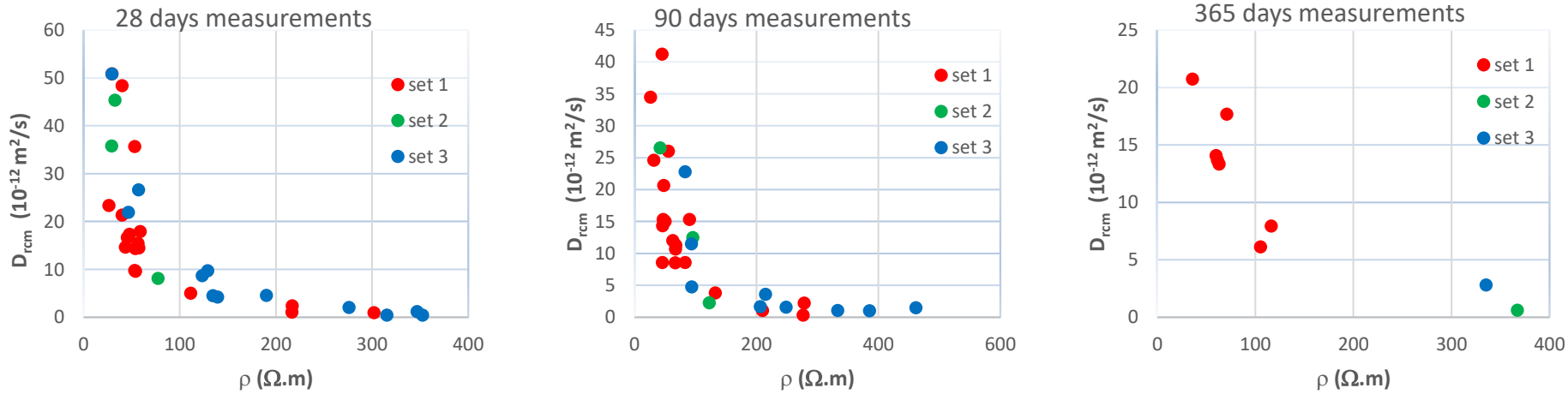

Figure 3.84. Values of the chloride migration coefficient (D_{rcm}) expressed as a function of the resistivity. Measurements at 28, 90 and 365 days

8.3 Ageing factor

The temporal evolution of the value of the chloride migration coefficient (D_{rcm}) is assumed to follow a power law in $t^{-\alpha}$ where α represents the "ageing factor". The value of α can be obtained by calculating a linear regression curve in a logarithmic graph (Figure 3.85).

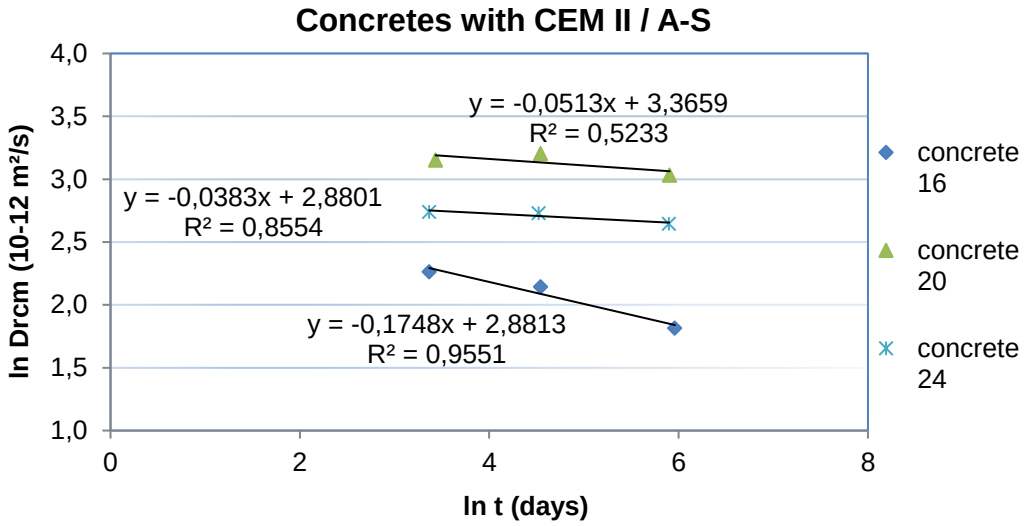

Figure 3.85. Examples of determinations of ageing factor.
a = 0.17 for concrete 16; 0.05 for concrete 20 and 0.04 for concrete 24

The accuracy on α is obtained as follow:

With $Y = \ln D_{rcm}$; $X = \ln t$; $Y = \alpha \,.\, X + b$; X' = mean value of X; Y' = mean value of Y; d: derivative

$\alpha = [\Sigma(X-X')(Y-Y')] / [\Sigma(X-X')^2]$

$\rightarrow \ln(\alpha) = \ln [\Sigma |X-X'| \,.\, |Y-Y'|\,] - \ln [\Sigma(X-X')^2]$

$\rightarrow d\alpha/\alpha = d[\Sigma |X-X'| \,.\, |Y-Y'|\,] / [\Sigma |X-X'| \,.\, |Y-Y'|\,] - d[\Sigma(X-X')^2] / [\Sigma(X-X')^2]$

$\rightarrow d\alpha/\alpha = [\Sigma\,(\,|X-X'|.d|Y-Y'| + d|X-X'|\,.\,|Y-Y'|\,)\,] / [\Sigma |X-X'| \,.\, |Y-Y'|\,] - [2.\Sigma\, d(X-X')] / [\Sigma(X-X')^2]$

$\rightarrow d\alpha/\alpha = [\Sigma\,(\,|X-X'|.dY + |Y-Y'|.dX\,)\,] / [\Sigma |X-X'| \,.\, |Y-Y'|\,] - [2.\Sigma\, dX] / [\Sigma(X-X')^2]$

with $dX = 0$: $d\alpha/\alpha = [\Sigma |X-X'|.dY\,|\,] / [\,\Sigma |X-X'| \,.\, |Y-Y'|\,]$

$d\alpha = \alpha \,.\, dY \,.\, [\Sigma |X-X'| / [\,\Sigma |X-X'\,| \,.\, |Y-Y'|\,]\,]$

Calculation are made with $dY = dD_{rcm} / D_{rcm} = (25\,\% \,.\, D_{rcm}) / D_{ecm} = 0.25$

The measurements obtained from the 42 concretes tested are summarised in Table 3.19.

Table 3.19. Calculation of ageing factor for chloride migration coefficient (D_{rcm})
Nomenclature: concrete number_cement type_addition type and content_effective water / binder ratio_compressive strength. Binder = total binder = cement + addition

				D_{rcm} (10^{-12} m².s^{-1})		
N° concrete	Exposition class		nomenclature	ageing factor α	nb of values	Accuracy
	NF EN 206/CN	fasc. 65				
1	XD1	-	1_CEM I_ 0,5_43	0.34	2	0.54
2	XD1	-	2_CEM I_V30_0,52_33	0.95	2	0.59
5	-	-	5_CEM I_S60_0,58_26	1.11	2	0.56
6	XD1	-	6_CEM I_L30_0,46_34	0.61	2	0.57
7	XD1	-	7_CEM I_L41_0,39_42	0.18	2	0.43
8	-	-	8_CEM II/A-LL_V30_0,53_31	0.32	2	1.04
9	-	-	9_CEM II/A-LL_S45_0,57_31	0.66	2	0.55
10	-	-	10_CEM II/A-LL_0,61_32	0.36	2	0.53
11	XS1, XD2	-	11_CEM II/A-LL_0,54_50	0.08	3	0.22
14	XS2, XD2	-	14_CEM I_0,55_38	0.68	2	0.43
15	XS2, XD2	XS2, XD2	15_CEM I_0,48_58	0.07	3	0.18
16	XS2, XD2	XS2, XD2	16_CEM II/A-S_0,5_51	0.17	3	0.19
17	XS3, XD3	XS2, XD2	17_CEM III/A_0,5_47	0.12	3	0.12
18	-	-	18_CEM I_V37_0,53_56	1.05	3	0.21
19	XS2, XD2	XS2, XD2	19_CEM II/A-S_0,5_60	0.11	2	0.42
20	XS2, XD2	XS2, XD2	20_CEM II/A-S_0,5_59	0.05	3	0.20
22	XS1, XD3	XS1, XD2	22_CEM II/A-LL_0,49_53	0.10	3	0.20
23	XS3, XD3	XS2, XD2	23_CEM II/A-S_0,49_46	0.26	3	0.22
24	XS2, XD2	XS2, XD2	24_CEM II/A-S_0,5_44	0.04	3	0.21
25	XS3, XD3, XF2	XS2, XD2	25_CEM I_0,5_39	0.13	2	0.37
26	XS3, XD3, XF4	XS3, XD3, XF4	26_CEM I_0,45_39	0.63	2	0.43
27	-	-	27_CEM I_S50_0,43_68	-	-	-
28	XS3, XD3	XS3, XD3	28_CEM I_0,45_NM	0.20	2	0.40
34	XS3, XD3	XS3, XD3	34_CEM III/A_0,45_59	0.56	2	0.40
35	XS3, XD3	XS3, XD3	35_CEM V/A (S-V)_0,45_66	0.75	2	0.39
36	XS3, XD3	XS3, XD3	36_CEM V/A (S-V)_0,45_49	0.56	2	0.43
37	XS3, XD3	XS3, XD3	37_CEM V/A (S-V)_0,45_56	1.28	2	0.45
38	XS1, XD3	XS1, XD3	38_CEM I_D8_0,38_94	1.17	2	0.53
39	XS1, XD3	XS1, XD2	39_CEM I_M20_0,43_62	0.07	2	0.40
39b	XS1, XD3	XS1, XD3	39b_CEM I_M20_0,42_66	0.24	2	0.44
40	-	-	40_CEM I_Qz30_0,49_28	0.38	2	0.49
41	XS3, XD3, XF2	XS3, XD3, XF2	41_CEM I_M20_0,35_93	-	-	-

The values of accuracy obtained with this method are too high. This approach is not conclusive.

The temporal evolution between 28 and 90 days for resistivity is expressed as a function of the temporal evolution of chloride migration coefficient (Figure 3.86). The graphic does not show any clear relation between those two temporal evolutions.

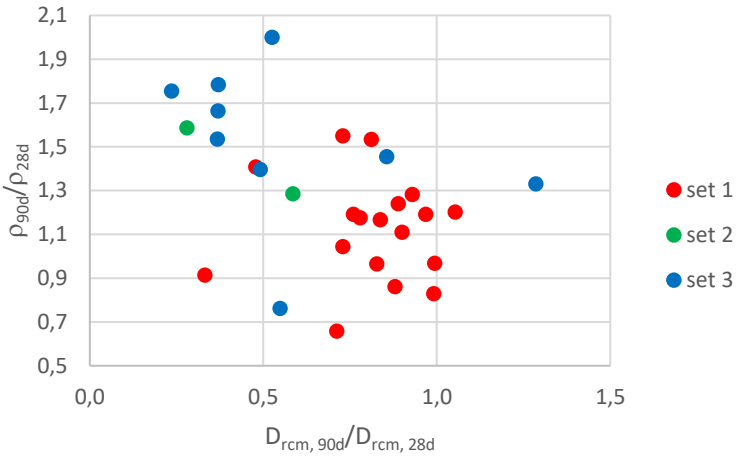

Figure 3.86. Time variation ratio of resistivity expressed as a function of time variation ratio of the chloride migration coefficient (D_{rcm}).

8.4 Link between chloride migration coefficient values and prescriptive approach

The values of the chloride migration coefficient D_{rcm} at 90 days are presented for each concrete as a function of the effective water / binder ratio in Figures 3.87 to 3.94. For each exposure class linked to the presence of chlorides, specific symbols are used to indicate if the formulation complies with the requirements of fascicule 65 (full circle), NF EN 206/CN standard (empty circle) or none of them (empty square). A red line is added to indicate the threshold specified in the Fascicule 65 for the measurement of the chloride migration coefficient.

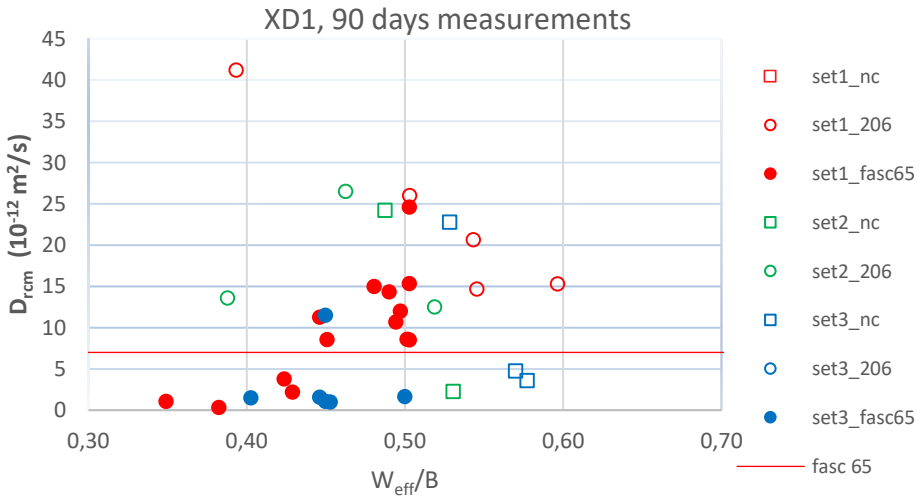

Figure 3.87. Chloride migration coefficient as a function of W_{eff}/B (XD1), 90d

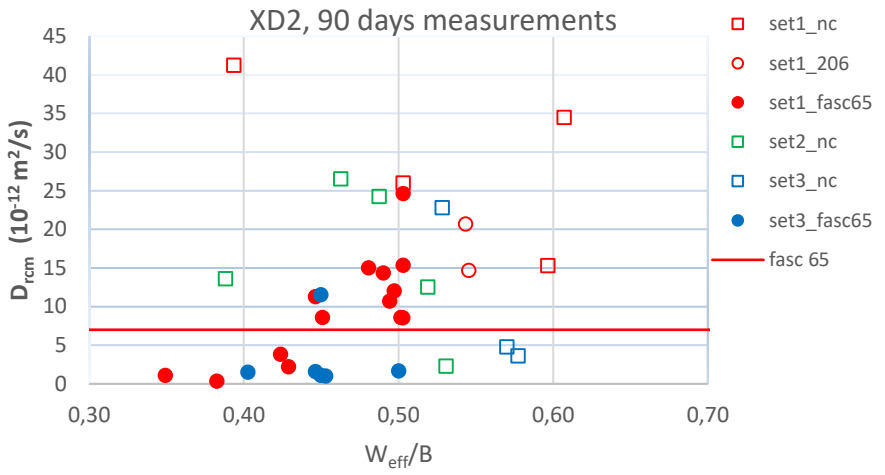

Figure 3.88. Chloride migration coefficient as a function of W_{eff}/B (XD2), 90d

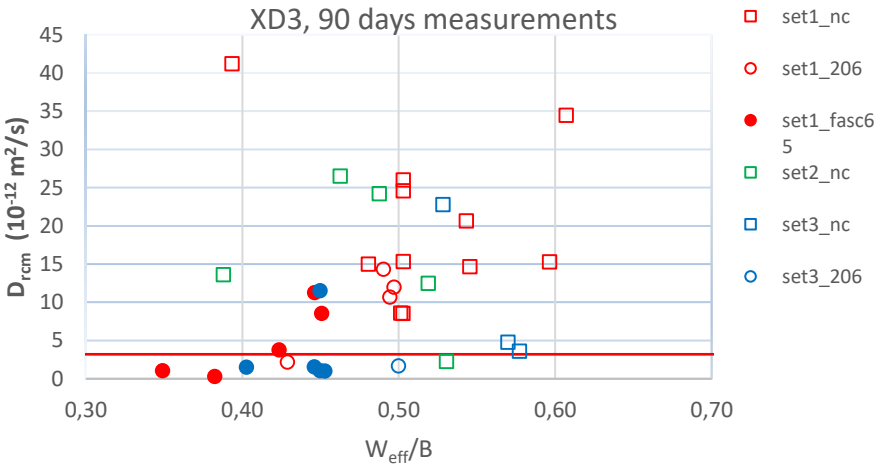

Figure 3.89. Chloride migration coefficient as a function of W_{eff}/B (XD3), 90d

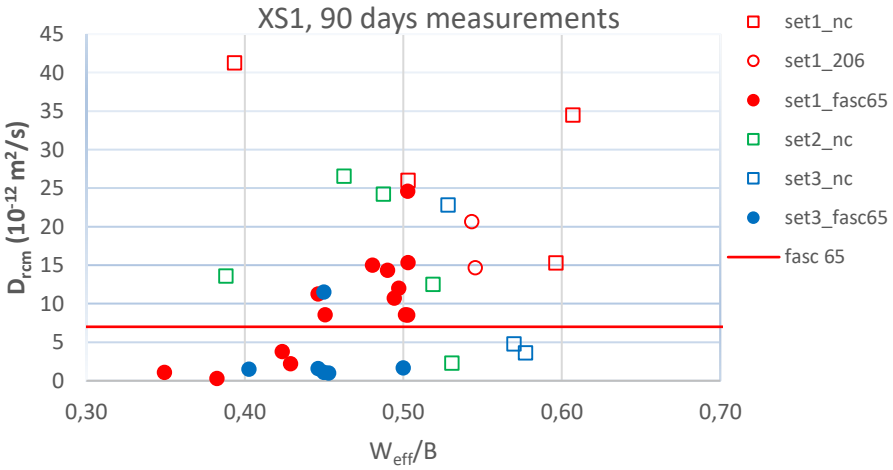

Figure 3.90. Chloride migration coefficient as a function of W_{eff}/B (XS1), 90d

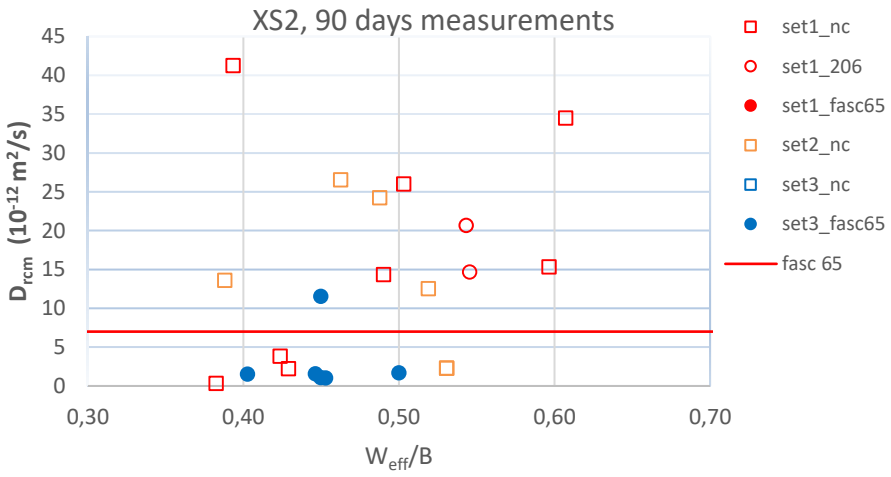

Figure 3.91. Chloride migration coefficient as a function of W_{eff}/B (XS2), 90d

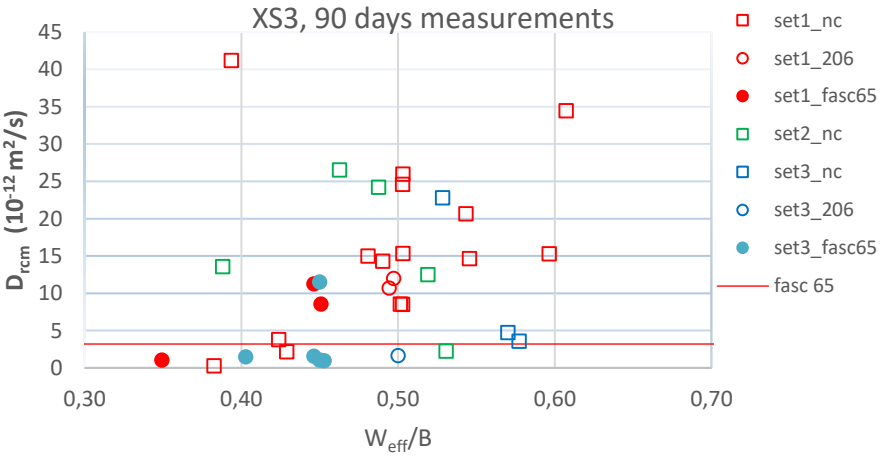

Figure 3.92. Chloride migration coefficient as a function of W_{eff}/B (XS3), 90d

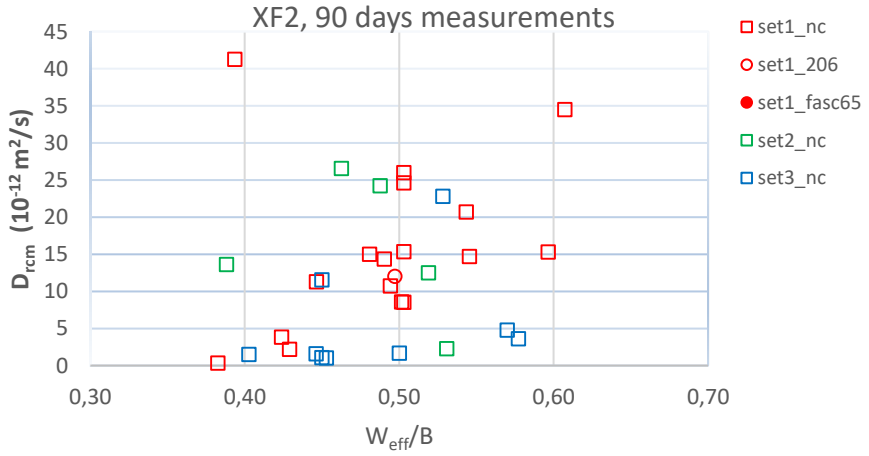

Figure 3.93. Chloride migration coefficient as a function of W_{eff}/B (XF2), 90d

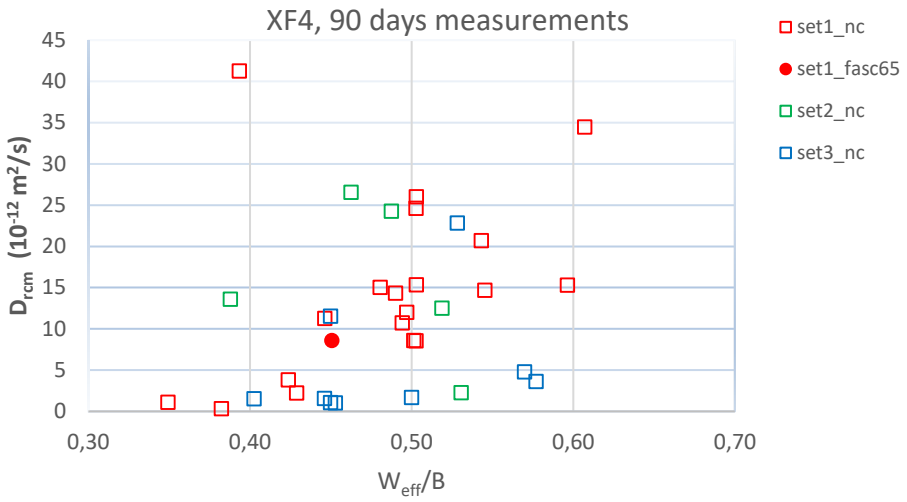

Figure 3.94. Chloride migration coefficient as a function of W_{eff}/B (XF4), 90d

Chloride migration coefficients are identified for each exposure class of concretes whose composition is compliant with EN 206 standard or fascicule 65. To avoid taking in consideration too performant concretes, strength class of the tested concretes considered is limited to:

- 2 classes higher than the minimal resistance class specified by EN 206 standard for 50 years duration structure;
- 3 classes higher than the minimal resistance class specified by fascicule 65 for 100 years duration structure.

The values of the chloride migration coefficient (D_{rcm}) which are consistent with 90 % of those concretes are then calculated and exposed in Table 3.20 (see section 10 for detailed calculations).

Table 3.20. Criteria for performantial qualification, with a characteristic value of 90 % obtained for the database

Exposure class	$D_{rcm, 90d}$ (10^{-12} m²/s)	
	50 years duration structure	100 years duration structure
XS1	33	18
XS2	33	18
XS3	17	10
XD1	46	18
XD2	33	18
XD3	17	10

Those values appear to be significantly higher than values usually taken in consideration.

8.5 Link between chloride migration coefficient values and electrical resistivity

Correlation between D_{rcm} and resistivity are presented in Figures 3.95 to 3.97.

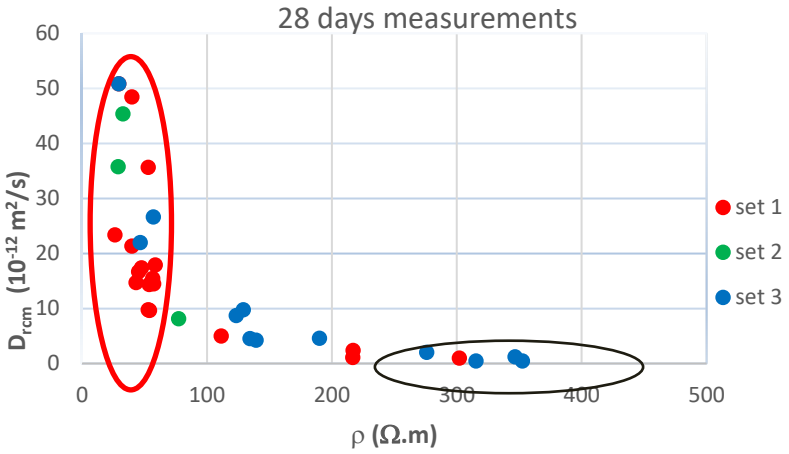

Figure 3.95. Link between D_{rcm} and resistivity, 28d

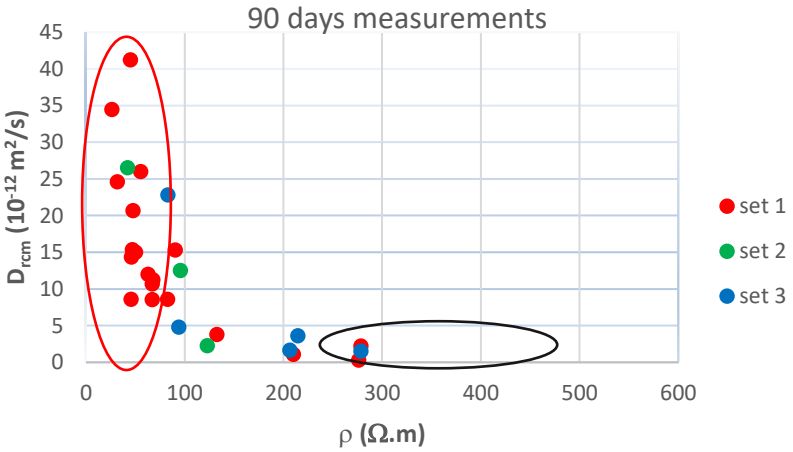

Figure 3.96. Link between D_{rcm} and resistivity, 90d

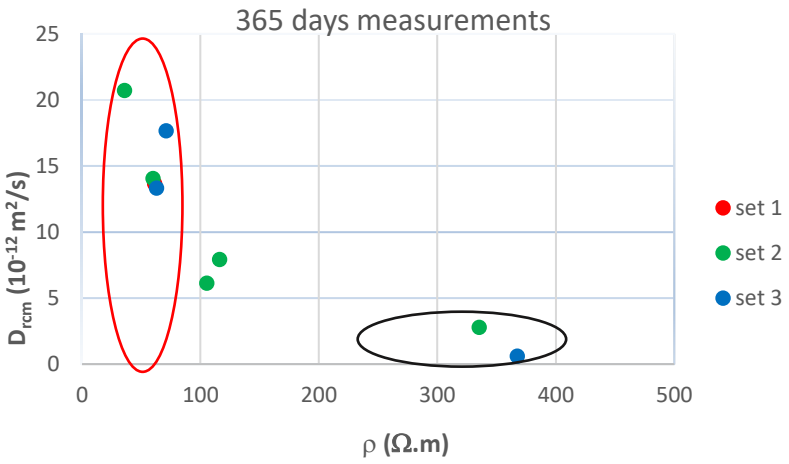

Figure 3.97. Link between D_{rcm} and resistivity, 365d

Three area can be defined:

- red area ($\rho < 60$ Ω.m): poor interest (values not differentiating);

- intermediate area: area where the use of a relation between ρ and D_{rcm} is useful;
- black area: if $\rho \geq 250$ Ω.m, then $D_{rcm} \leq 2.10^{-12}$ m²/s.

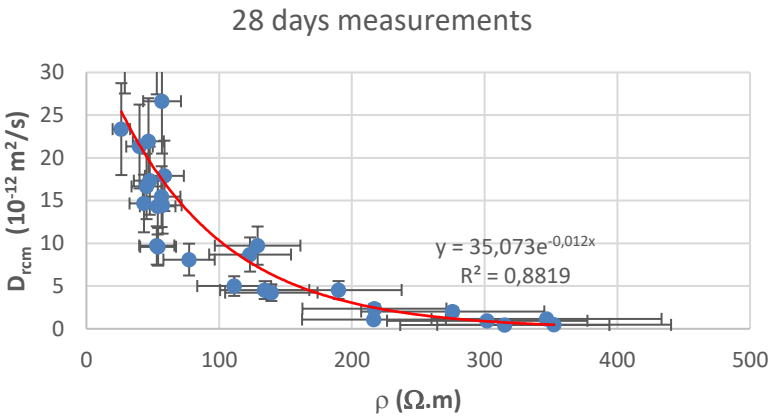

Figure 3.98. Link between D_{rcm} and resistivity, 28d

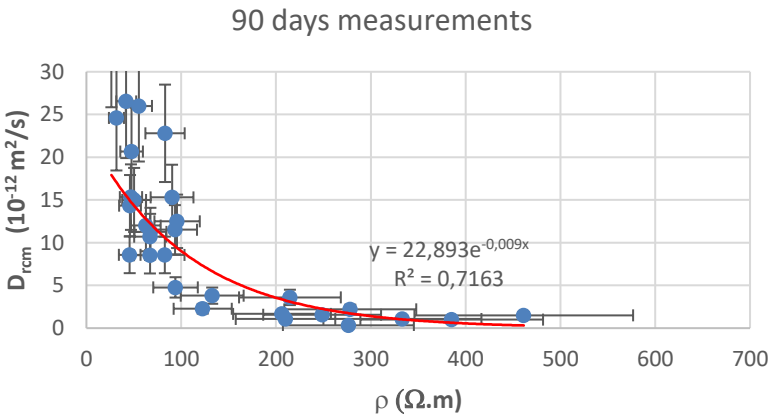

Figure 3.99. Link between D_{rcm} and resistivity, 90d

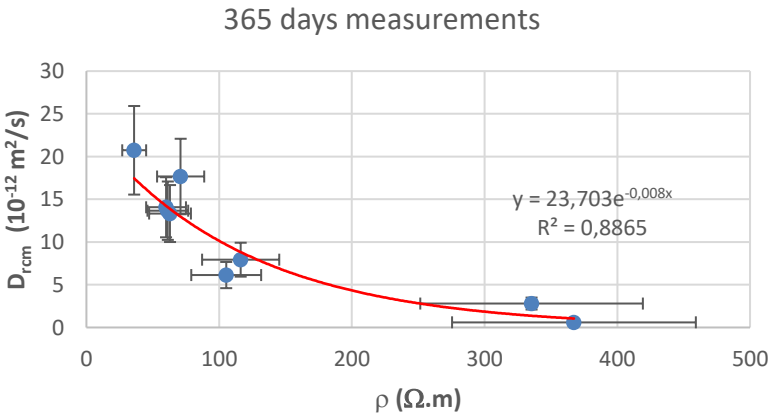

Figure 3.100. Link between D_{rcm} and resistivity, 365d

8.6 Conclusions and proposals

Values of chloride migration coefficient have been obtained for a large panel of concretes.

The attempt to obtain Deemed-to-Satisfy criteria from this data base failed. The values measured are assumed been too high compared to typical admitted ones and would be at risk being unsafe. For chloride migration coefficient, the approach should be more appropriately based on modelling and feedback from old structures.

Chloride migration coefficient expressed as a function of resistivity show that:

- when $60\ \Omega.m \leq \rho < 250\ \Omega.m$, a useful bijective relation between ρ and D_{rcm} can be obtained;
- if $\rho \geq 250\ \Omega.m$, then $D_{rcm} \leq 2.10^{-12}$ m²/s.

9 Study of variability

Authors: Sandrine Chanut, François Cussigh, Faber Fabbris, Lionel Linger, Jean Marc Potier

9.1 Introduction

The scope of work provided by PerfDuB GT3B “Study of the variability of durability indicators” was divided in the following three parts:

- a parametric survey, performed in laboratory (compositional parameters variation);
- a 1-year temporal variability survey of batching plant production (material-environmental parameters variation);
- a curing and spatial variability survey on specific mock-up (curing and geometric parameters variation on testing wall).

According to the PerfDuB project, this approach concerns two concrete mixtures developed for the construction of the Offshore Viaduct in La Réunion Island and one ready-mix concrete mixture (a typical one used in France for building purposes – Doubs department).

In order to complete this scope, the results obtained during the APPLET project have been included (two concretes).

The Table 3.21 summarizes the main properties of the 5 concretes observed in the variability survey.

Table 3.21 Main properties of the 5 concretes

Project	Strength class	Main exposure class	Nature of binder	Plant	Studies
Offshore Viaduct La Réunion Island Slab Pier PerfDuB	C40/50	XS2	CEM III/A 42,5 N CE PM-ES NF	On site	- Laboratory assessment - Temporal variability survey - In-situ variability survey
Offshore Viaduct La Réunion Island Segment PerfDuB	C45/55	XS3	CEM II/A-P 42,5 N CE PM NF + silica fume	On site	- Laboratory assessment - Temporal variability survey - In-situ variability survey
Ready-mix concrete PerfDuB	C30/37	XF1	CEM II/A-L 42,5R CE CP2 NF	Ready mix plant	- Laboratory assessment - Temporal variability survey - In-situ variability survey
A86 APPLET	C50/60		CEM I + fly ash	On site	- Temporal variability survey
Compiègne Viaduct APPLET	C35/45		CEM III/A	Ready mix plant	- Temporal variability survey

9.2 Laboratory assessment

The objective of parametric study is to analyse the variability of concrete properties on few batches performed in laboratory conditions. These batches are:

- three “nominal” batches;
- two water derivatives (+/- 10 L / m^3);
- two sand derivatives (+/- 10 % on the S/(S+G) ratio; S is sand and G is gravel weights).

For each batch, the following properties have been measured: consistency, concrete and air temperatures, compressive strength, water porosity, gas permeability, chloride diffusion and electrical resistivity.

For each durability parameter, the results have been presented according to the following types of graphic. The error bars correspond to the value issue of the calculation: (maximal value obtained for the “nominal” batches – minimal value obtained for the “nominal” batches) divided by 2.

In this part, only the results of water porosity have been described (Figures 3.101 to 3.103). The other characteristics have been compiled in Appendix A.

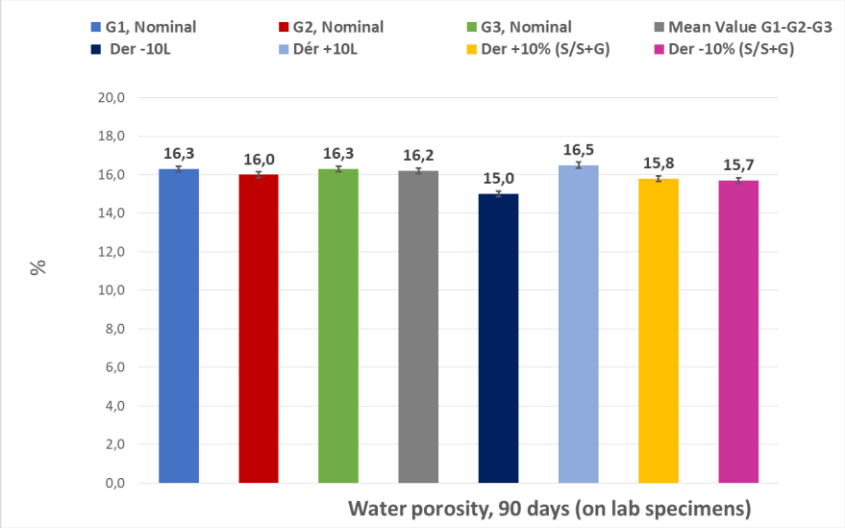

Figure 3.101. Water porosity **C30/37 ready mix concrete** (laboratory assessment)

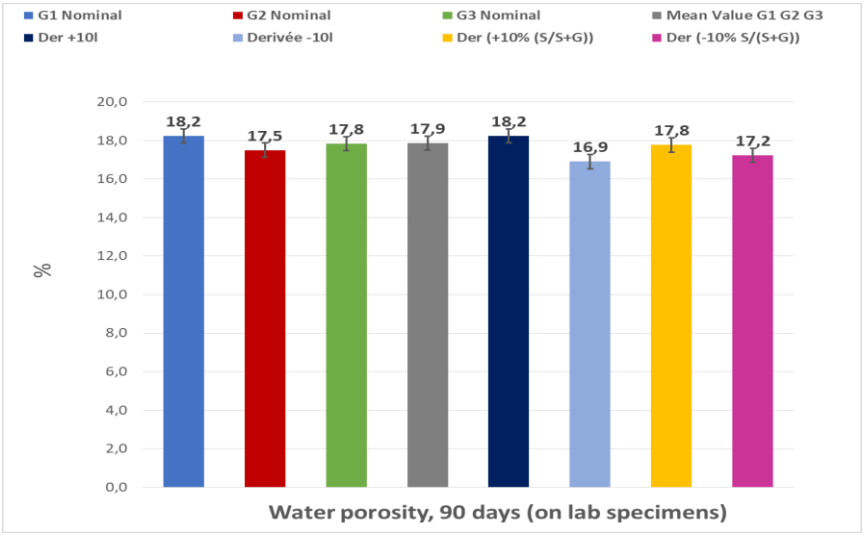

Figure 3.102. Water porosity **C40/50 viaduct La Reunion** (laboratory assessment)

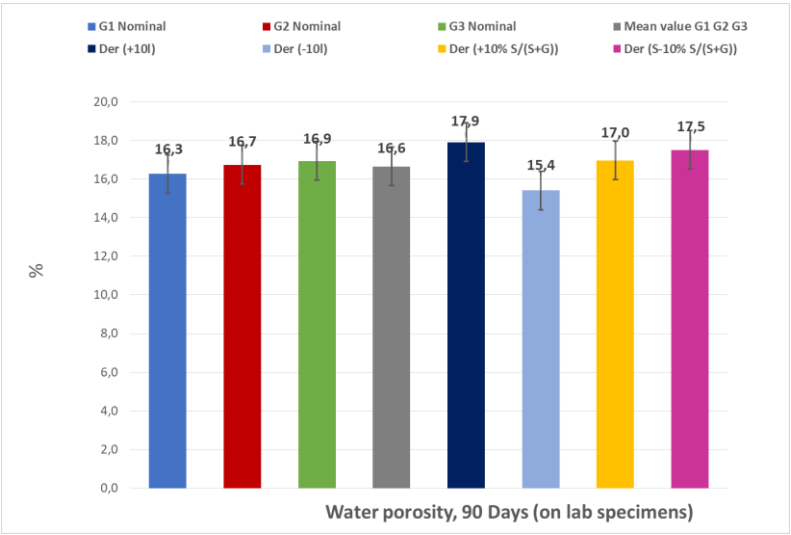

Figure 3.103. Water porosity **C45/55 viaduct La Reunion** (laboratory assessment)

With all the results obtained for the durability indicators during the laboratory assessment, a methodology for variability durability property will be proposed at the paragraph 9.4.

9.3 Temporal variability

The goal of this temporal variability study is to measure several parameters including fresh properties, compressive strength and durability indicators on concrete mixes used during project completion or mixes produced all along a whole year of production on a Ready-Mix Concrete plant. Temporal variability study requested by PerfDuB scope of work required to analyse at least 15 samples during one year in site conditions (Table 3.22).

Table 3.22. Number of samples corresponding to each concrete formula

Project	Number of samples / 1 year
Offshore Viaduct La Réunion Island Slab Pier PerfDuB	16 (17 including testing wall sampling)
Offshore Viaduct La Réunion Island Segment PerfDuB	34 (35 including testing wall sampling)
Ready-mix concrete PerfDuB	14 (15 including testing wall sampling)
A86 APPLET	40
Compiègne Viaduct APPLET	20

For each project, a specific report details the testing program and provides a synthesis of gathered results performed.

For the temporal variability with all the results and for each indicator of durability, the following data have been compiled:

- number of results;
- minimum value;
- maximum value;
- average;
- standard deviation;
- coefficient of variation.

A method to handle the variations associated to temporal variability and the way to estimate them is presented in the following paragraph.

9.4 Proposal/methodology for variability durability properties

The definition of acceptance criterion of a durability indicator is derived from the spirit of EN 206 for mechanical strength on the basis of a statistical normal distribution of results (average, standard deviation/coefficient of variation, minimum/maximum).

According to Eurocode 2 ongoing revision ERC definition, specified limits are given in terms of characteristic values (90 %). Gauss (normal) distribution is considered. Analogy with compressive strength initial assessment is looked after (as far as possible, because range of values is much larger).

The methodology for variability durability property is divided in two steps.

STEP 1: laboratory assessment / Parametric study (= initial test)

- **1.1** Coefficient of variation *estimated* by factual experience gathered on previous production data
- **1.2** Mean value obtained (with 3 batches « nominal »)
- **1.3** Standard deviation calculation on the basis of estimated coefficient of variation (point 1.1)
- **1.4** Margin of α = 1,5 × standard deviation (for 10 % fractile)

Note: The rounded value of 1.5 (= 2.0 x 1.28 / 1.64) is derived in the spirit of Annex A of EN 206 considering a 10 % fractile for durability indicators instead of 5 % assumed for compressive strength (leading to a recommended value of 2.0 x standard deviation for initial test compliance assessment).

- **1.5** Calculation of the characteristic value

STEP 2: temporal variation (= production)

- **2.1** With the mean value and the standard deviation obtained, calculation of the coefficient of variation
- **2.2** Margin of of α = 1,28 × standard deviation (for 10 % fractile)
- **2.3** Calculation of the characteristic value.

The estimated coefficients of variation for the laboratory study have been fixed in such a way that the *estimated characteristic value (*average + 1,5σ or – 1,5σ, depending on each durability parameter) would in any case be fulfilled, when considering the actual values in the temporal series - including the uncertainty associated to +/- 1,28 σ.

A graphical illustration of the proposed criterion is illustrated Figure 3.104 with an example (Water porosity, 90 days (%) - C30/37 Ready mix concrete).

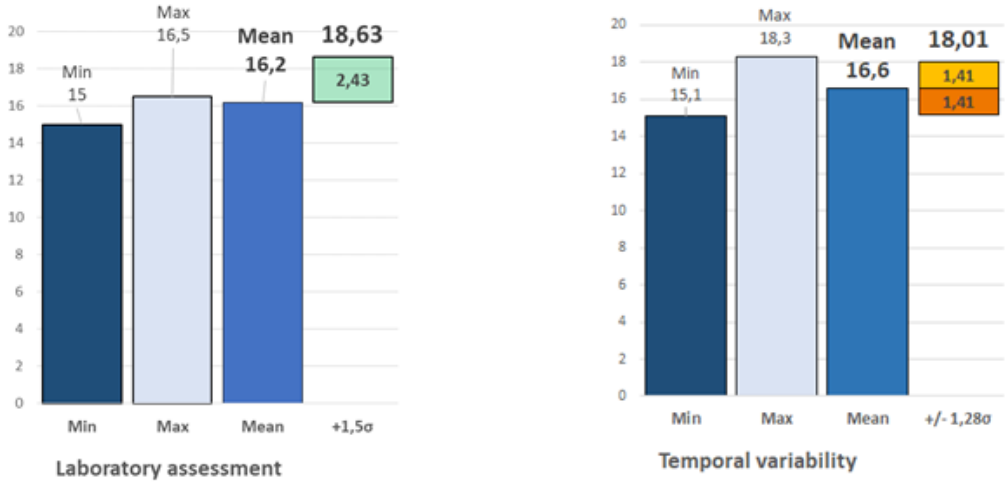

Figure 3.104. Graphical illustration of temporal variability estimation on the basis of laboratory results

In this figure (left side), the minimum, maximum and average values **from parametric study** are presented, as well as the margin corresponding to 1,5 σ (light green bar).

Here, the σ is estimated as described in step 1.

On the right side, the minimum, maximum and average values **from the temporal variability survey** are presented, as well the actual +/- 1,28 σ values.

In this case, obviously, the σ is calculated on the basis of experimental data (as described in step 2).

In the next pages, the complete results are presented (Tables 3.23 to 3.26).

Table 3.23. **C30/37** ready mix concrete initial test (STEP 1) / temporal variation (STEP 2)

	Initial test (STEP 1)											Temporal Variation (STEP 2)			
	Nom1	Nom2	Nom3	+10l water	-10l water	+10%S	-10%S	MIN	170			MIN	*190*		
Slump (mm) t0	190	200	210	220	170	210	230	MAX	230			MAX	*230*		
								MEAN nom	200,0						
Rc28 (MPa)	44,4	41,3	41,4	**40,5**	46,6	42,9	41,4	MIN	40,5	-4,4%		MIN	28,3		
		42,4						MAX	47	10,0%		MAX	42,5		
Estimated COV								MEAN nom	42,4			MEAN	35,4		
16%								Estimated standard deviation	6,78			Standard deviation	4,06	COV	11,5%
								Coeff	2,0			Coeff	1,64		
								Estimated characterictic value	**28,8**			Characteristic value	**28,7**		
Water porosity (%) 90j	16,3	16,0	16,3	**16,5**	15,0	15,8	15,7	MIN	15	-7,4%		MIN	15,1		
		16,2						MAX	17	1,9%		MAX	18,3		
								MEAN nom	16,2			MEAN	16,6		
Estimated COV								Estimated standard deviation	1,62			Standard deviation	1,1	COV	6,6%
10%								Coeff	1,5			Coeff	1,28		
								Estimated characterictic value	**18,6**			Characteristic value	**18,0**		
Mrcm (10^{-12} m²/s) 90j	16,0	19,0	14,7	15,3	12,7	**15,0**	14,0	MIN	12,7	-23,3%		MIN	9,3		
		16,6						MAX	19,0	14,7%		MAX	26,7		
Estimated COV								MEAN nom	16,6			MEAN	18,1		
30%								Estimated standard deviation	4,97			Standard deviation	4,54	COV	25,1%
								Coeff	1,5			Coeff	1,28		
								Estimated characterictic value	**24,0**			Characteristic value	**23,9**		
Resistivity (Ohm.m) 90j	44,0	41,5	39,8	**38,7**	46,8	36,3	38,5	MIN	36,3	-13,1%		MIN	32,9		
		41,8						MAX	47	12,1%		MAX	43,1		
Estimated COV								MEAN nom	41,8			MEAN	36,1		
20%								Estimated standard deviation	8,4			Standard deviation	2,9	COV	8,0%
								Coeff	1,5			Coeff	1,28		
								Estimated characterictic value	**29,2**			Characteristic value	**32,4**		
Gas permeability (10-18 m²)	65,2	85,3	74,2	58,2	37,2	49,3	56,4	MIN	37,2	-50,3%		MIN	50,9		
		74,9						MAX	85	13,9%		MAX	255		
Estimated COV								MEAN nom	74,9			MEAN	127		
50%								Estimated standard deviation	37,5			Standard deviation	64,5	COV	50,8%
								Coeff	1,5			Coeff	1,28		
								Estimated characterictic value	**131,1**			Characteristic value	209,6		
Capillary absorption (g/m²)	6389		6001	4019	4605	3325	4432	MIN	3325	-46,3%		MIN	3773		
		6195,0						MAX	6389	3,1%		MAX	7985		
Estimated COV								MEAN nom	6195,0			MEAN	6072		
20%								Estimated standard deviation	1239,0			Standard deviation	1297	COV	21,4%
								Coeff	1,5			Coeff	1,28		
								Estimated characterictic value	**8053,5**			Characteristic value	**7732,2**		

Table 3.24. C40/50 viaduct La Reunion initial test (STEP 1) / temporal variation (STEP 2)

	Initial test (STEP 1)											Temporal variation (STEP 2)			
	Nom1	Nom2	Nom3	+10l water	-10l water	+10%S	-10%S	MIN	150			MIN	*190*		
Slump (mm)	220	200	210	240	150	160	200	MAX	240			MAX	*230*		
								MEAN nom	210,0						
Rc28 (MPa)	49,5	57,7	51,2	**45,5**	59,2	51,7	48,7	MIN	45,5	-13,8%		MIN	47,2		
								MAX	59	12,1%		MAX	59,7		
Estimated COV								MEAN nom	52,8			MEAN	53,5		
8%								Estimated standard deviation	4,22			Standard deviation	3,6	COV	6,7%
								Coeff	2,0			Coeff	1,64		
								Estimated characterictic value	**44,4**			Characteristic value	**47,6**		
Water porosity (%) 90j	18,2	17,5	17,8	**18,2**	16,9	17,8	17,2	MIN	16,9	-5,4%		MIN	16,3		
								MAX	18	2,1%		MAX	18,1		
								MEAN nom	17,9			MEAN	17,3		
Estimated COV								Estimated standard deviation	0,89			Standard deviation	0,4	COV	2,3%
5%								Coeff	1,5			Coeff	1,28		
								Estimated characterictic value	**19,2**			Characteristic value	**17,8**		
Mrcm (10^{-12} m^2/s) 90j	3,1	3,5	3,2	3,1	3,1	**3,4**	3,0	MIN	3,0	-8,5%		MIN	2,5		
								MAX	3,5	5,8%		MAX	4,4		
Estimated COV								MEAN nom	3,3			MEAN	3,2		
25%								Estimated standard deviation	0,82			Standard deviation	0,6	COV	18,8%
								Coeff	1,5			Coeff	1,28		
								Estimated characterictic value	**4,5**			Characteristic value	**4,0**		
Resistivity (Ohm.m) 90j	150,0	140,0	150,0	**145,0**	167,0	156,0	176,0	MIN	140	-4,5%		MIN	129,6		
								MAX	176	20,0%		MAX	233,1		
Estimated COV								MEAN nom	146,7			MEAN	165		
20%								Estimated standard deviation	29,3			Standard deviation	27,5	COV	16,7%
								Coeff	1,5			Coeff	1,28		
								Estimated characterictic value	**102,7**			Characteristic value	**129,8**		
Gas permeability (10-18 m^2) 90j	95	96	210	**666**	54	196	141	MIN	54	-59,6%		MIN	35		
								MAX	666	398,3%		MAX	216		
Estimated COV								MEAN nom	133,7			MEAN	145		
30%								Estimated standard deviation	40,1			Standard deviation	49	COV	33,8%
								Coeff	1,5			Coeff	1,28		
								Estimated characterictic value	**193,8**			Characteristic value	**207,7**		
Capillary absorption (g/m^2)								MIN				MIN	2775		
								MAX				MAX	3280		
								MEAN nom				MEAN	2513		
								Estimated standard deviation				Standard deviation	463	COV	18,4%
								Coeff				Coeff	1,28		
								Estimated characterictic value				Characteristic value	**3105,6**		
Accelerated carbonation rate (mm/j^0,5)								MIN				MIN	0,48		
								MAX				MAX	1,14		
								MEAN nom				MEAN	0,79		
								Estimated standard deviation				Standard deviation	0,18	COV	22,8%
								Coeff				Coeff	1,28		
								Estimated characterictic value				Characteristic value	**1,02**		

Table 3.25. C45/55 viaduct La Reunion initial test (STEP 1) / temporal variation (STEP 2)

	Initial test (STEP 1)										Temporal variation (STEP 2)			
	Nom1	Nom2	Nom3	+10l water	-10l water	+10%S	-10%S	MIN	140					
Slump (mm)	210	200	210	220	140	190	210	MAX	220					
								MEAN nom	206,7					
Rc28 (MPa)	68,8	74,4	72,1	**67,7**	81,8	69,2	67,9	MIN	67,7	-5,7%	MIN	64,2		
								MAX	82	14,0%	MAX	83,2		
Estimated COV								MEAN nom	71,8		MEAN	77,5		
8%								Estimated standard deviation	5,74		Standard deviation	3,7	COV	4,8%
								Coeff	2,0		Coeff	1,64		
								Estimated characterictic value	**60,3**		Characteristic value	**71,4**		
Water porosity (%) 90j	16,3	16,7	16,9	**17,9**	15,4	17,0	17,5	MIN	15,4	-7,4%	MIN	14,4		
								MAX	18	7,6%	MAX	18,3		
								MEAN nom	16,6		MEAN	16,4		
Estimated COV								Estimated standard deviation	0,83		Standard deviation	1	COV	6,1%
5%								Coeff	1,5		Coeff	1,28		
								Estimated characterictic value	**17,9**		Characteristic value	**17,7**		
Mrcm (10^{-12} m²/s) 90j	3,7	4,3	3,7	4,6	3,2	4,2	**4,8**	MIN	3,2	-17,3%	MIN	2,3		
								MAX	4,8	22,7%	MAX	4,5		
Estimated COV								MEAN nom	3,9		MEAN	3,2		
25%								Estimated standard deviation	0,98		Standard deviation	0,6	COV	18,8%
								Coeff	1,5		Coeff	1,28		
								Estimated characterictic value	**5,4**		Characteristic value	**4,0**		
Resistivity (Ohm.m) 90j	193,4	167,6	182,1	152,6	176,1	149,3	**130,2**	MIN	130,2	-28,1%	MIN	143		
								MAX	193	6,8%	MAX	266		
Estimated COV								MEAN nom	181,0		MEAN	196		
20%								Estimated standard deviation	36,2		Standard deviation	27	COV	13,8%
								Coeff	1,5		Coeff	1,28		
								Estimated characterictic value	**126,7**		Characteristic value	**161,4**		
Gas permeability (10-18 m²) 90j	248	149	123	169	64	158	168	MIN	64	-63,1%	MIN	42		
		173,3						MAX	248	43,1%	MAX	455		
Estimated COV								MEAN nom	173,3		MEAN	123		
30%								Estimated standard deviation	52,0		Standard deviation	85	COV	69,1%
								Coeff	1,5		Coeff	1,28		
								Estimated characterictic value	**251,3**		Characteristic value	**231,8**		
Capillary absorption (g/m²)								MIN			MIN	1526		
								MAX			MAX	3483		
								MEAN nom			MEAN	2361		
								Estimated standard deviation			Standard deviation	481	COV	20,4%
								Coeff			Coeff	1,28		
								Estimated characterictic value			Characteristic value	**2976,7**		

Table 3.26. Summary of the coefficient of variation for each variability parameter

	C30/37 ready mix concrete PerfDuB		C40/50 Viaduct La Reunion PerfDuB		C45/55 Viaduct La Reunion PerfDuB		C50/60 A86 APPLET	C35/45 Viaduct APPLET	*COV % lowest admissible value (****) GT4*
	Coefficient Of Variation (COV) (%)								
	Step 1 (*)	Step 2 (**)	Step 1	Step 2	Step 1	Step 2	Step 2	Step 2	
Water porosity	10	6.6	5	2.3	5	6.1	6.5	3.5	*3*
Chloride migration	30	25.1	25	18.8	25	18.8	12.9	19.4	*20*
Electrical resistivity	20	8	20	16.7	20	13.8	17.6	18.2	*15*
Gas permeability	50	50.8	30	33.8	30	69.1	12 (***)	14 (***)	*35*
Capillary absorption	20	21.4	-	18.4	-	20.4	-	-	*20*
Accelerated carbonation rate	-	-	25	22.8	-	-	-	-	*25*

Minimal value for COV STEP2 for each property of durability

Maximal value for COV STEP2 for each property of durability

(*) COV STEP 1: Coefficient of variation estimated by factual experience on previous production data
(**) COV STEP 2: Coefficient of variation calculated with the mean value and the standard deviation obtained
(***): estimated with very limited number of values
(****): The estimated coefficients of variation for the laboratory study have been fixed in such a way that the estimated characteristic value (average + 1,5 σ or – 1,5 σ, depending on each durability parameter) would in any case be respected, when considering the actual values in the temporal series - including the uncertainty associated to +/- 1,28 σ
These values are included in the recommendations established by GT4 concerning the application of the performance-based approach.

9.5 *In situ* variability

9.5.1 Characteristics of the testing walls

The goal of the testing walls study is to analyse both curing and spatial impact on 90-day durability indicators. Then, three testing walls (2.5 m X 2.5 m x 0.3 m) have been built on site (one for each concrete mix) especially for this study:

- C30/37 ready mix concrete: testing wall: 22/6/2018;
- C40/50 viaduct La Reunion: testing wall: 15/5/2017;
- C45/55 viaduct La Reunion: testing wall: 10/5/2017.

For spatial study, it has been decided to measure chloride migration coefficient, water porosity, capillary water absorption and gas permeability on various cores cored at various three area on the testing wall as detailed into Figures 3.105 and 3.106 (spatial up, spatial middle and spatial down).

For curing study, it has been decided to measure chloride migration diffusion coefficient, water porosity, capillary water absorption and accelerated carbonation (on two core samples located in the surface and in the heart of the testing wall and extracted from same cores as detailed into Figures 3.105 and 3.106 (curing surface – core and curing heart – core).

In this part, only the results of water porosity have been described. The other characteristics have been compiled in Appendix B.

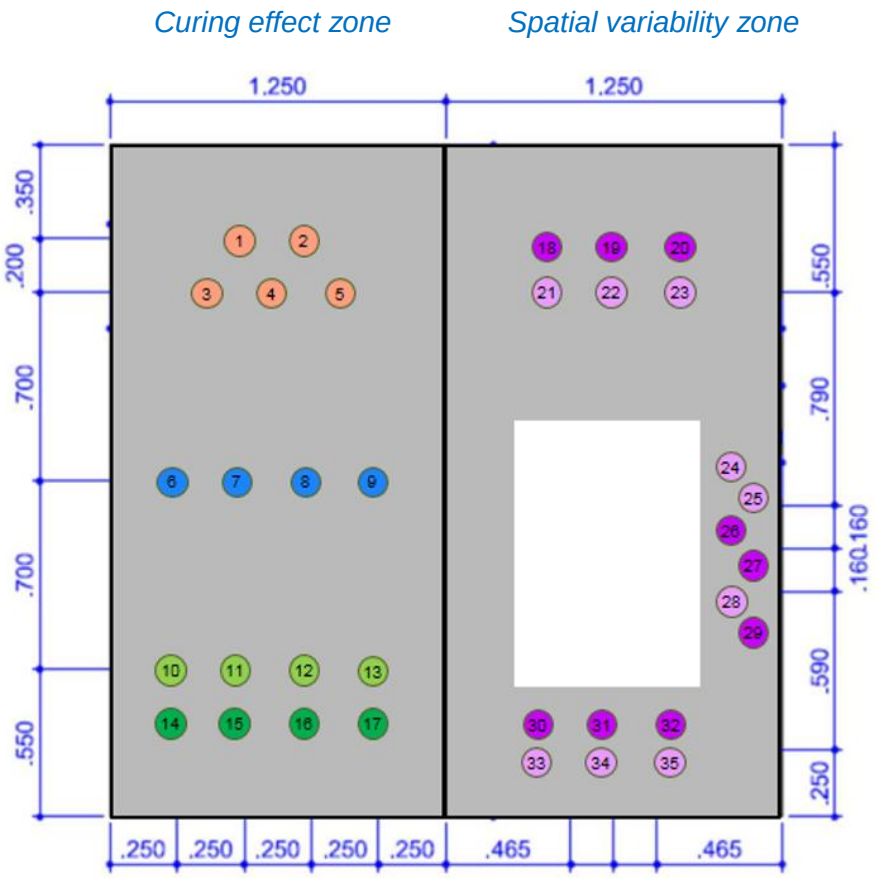

Figure 3.105. Testing wall

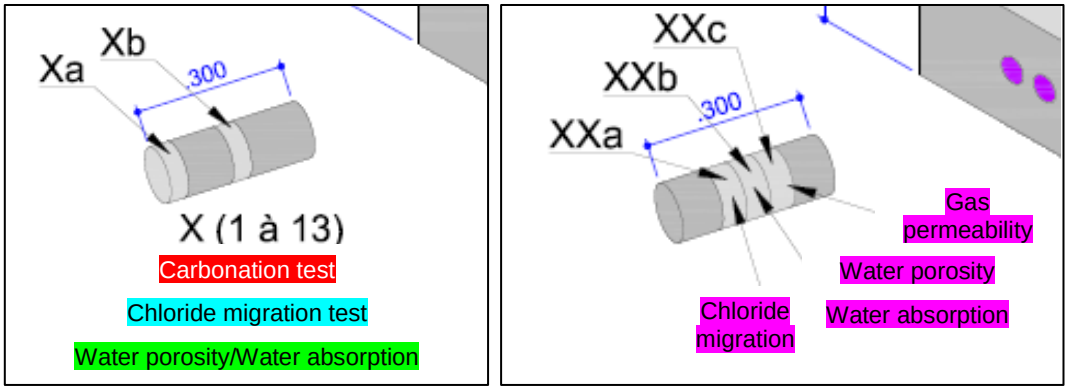

Figure 3.106. Details of core samples

Durability indicators have been measured on samples sawed into extracted 113 mm diameter cores and on concrete samples made during control of fresh concrete in order to compare values obtained on molded samples and on core samples.

Figure 3.107. C30/37 ready mix concrete - the testing wall before and after the core sampling session

As an example, the results of *in situ* variability for water porosity (spatial variability and curing effect survey) are presented in the following paragraph.

9.5.2 Spatial variability

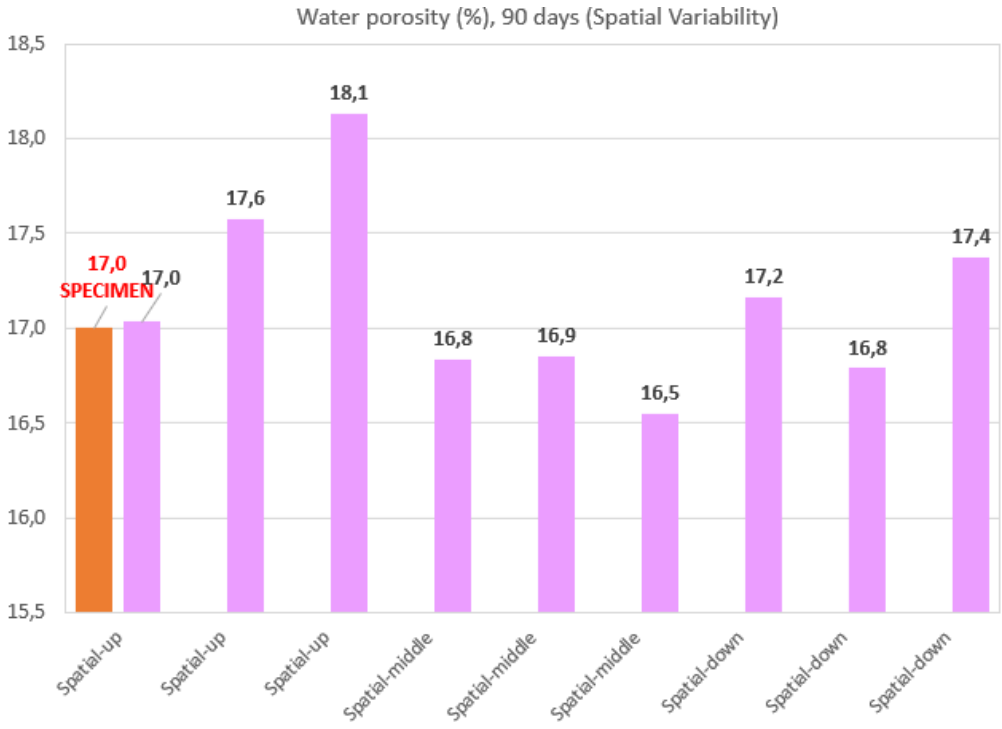

Figure 3.108. Water porosity C30/37 ready mix concrete (spatial study)

Table 3.27. Water porosity C30/37 ready mix concrete (spatial study)

	Localisation	Mean value (%)	Min value (%)	Max value (%)	Number of measurements
Water porosity, 90 days	Spatial up core	17.6	17.0	18.1	3
	Spatial middle core	16.7	16.5	16.9	3
	Spatial down core	17.1	16.8	17.4	3
		Mean value (%)	Standard deviation (%)	Coefficient of variation (%)	Number of measurements
	Spatial cores	17.1	0.5	3	9
	Molded sample specimen	17.0	0.5	3	3

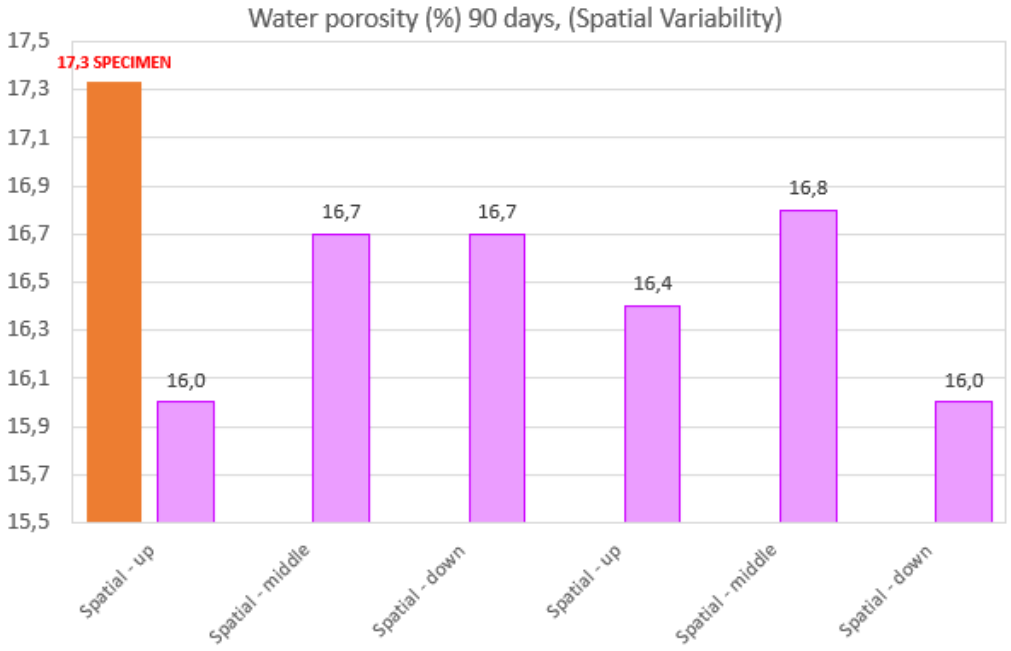

Figure 3.109. Water porosity **C40/50 viaduct La Reunion** (spatial study)

Table 3.28. Water porosity C40/50 viaduct La Reunion (spatial study)

	Localisation	Mean value (%)	Min value (%)	Max value (%)	Number of measurements
Water porosity, 90 days	Spatial up core	16.2	16.0	16.4	2
	Spatial middle core	16.8	16.7	16.8	2
	Spatial down core	16.4	16.0	16.7	2
		Mean value (%)	Standard deviation (%)	Coefficient of variation (%)	Number of measurements
	Spatial cores	16.4	0.4	2	6
	Molded sample specimen	17.3	0.3	1	3

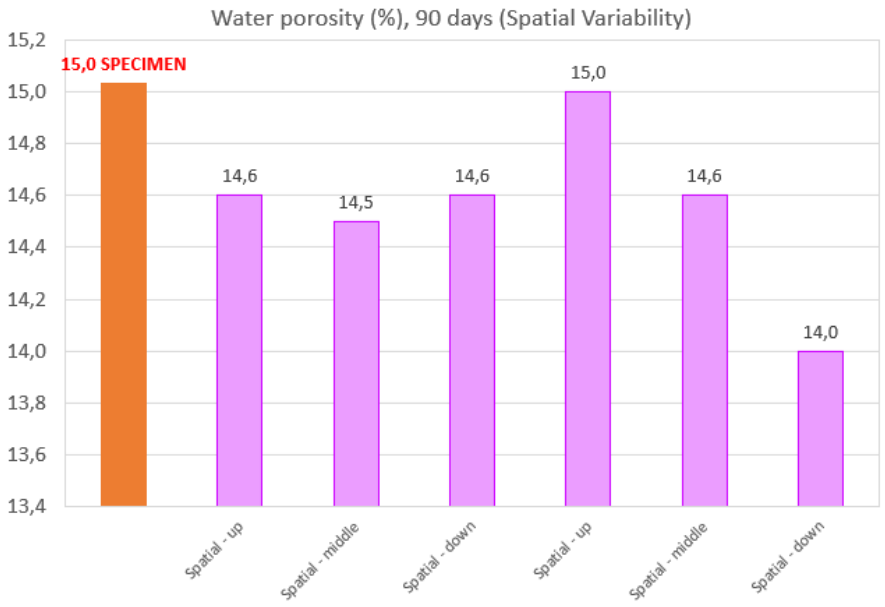

Figure 3.110. Water porosity **C45/55 viaduct La Reunion** (spatial study)

Table 3.29. Water porosity C45/55 viaduct La Reunion (spatial study)

	Localisation	Mean value (%)	Min value (%)	Max value (%)	Number of measurements
Water porosity, 90 days	**Spatial up core**	14.8	14.6	15.0	2
	Spatial middle core	14.6	14.5	14.6	2
	Spatial down core	14.3	14.0	14.6	2
		Mean value (%)	**Standard deviation (%)**	**Coefficient of variation (%)**	**Number of measurements**
	Spatial cores	14.6	0.3	2	6
	Molded sample specimen	15.0	0.2	1	3

Results obtained on core samples are slightly better than those from molded samples.

9.5.3 Curing study

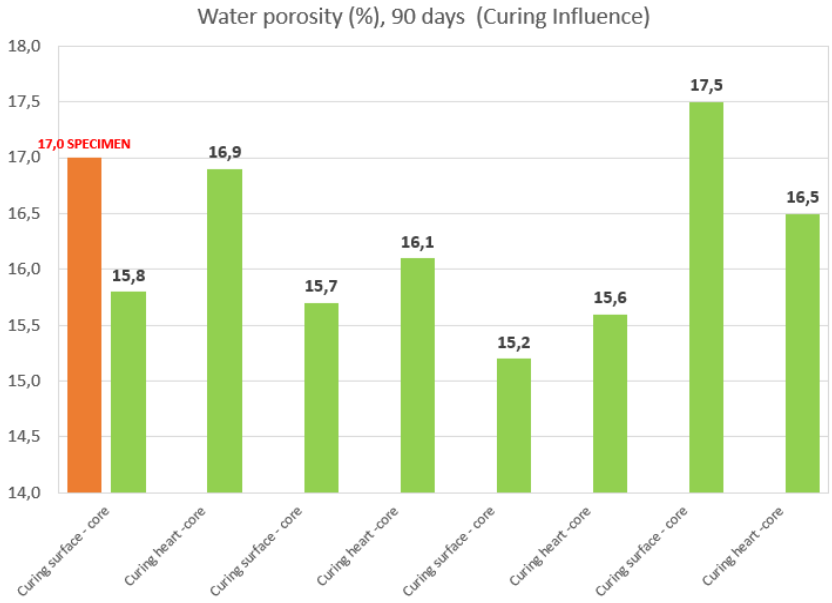

Figure 3.111. Water porosity C30/37 ready mix concrete (curing effect)

Table 3.30. Water porosity **C30/37 ready mix concrete** (curing effect)

Water porosity, 90 days	**Localisation**	**Mean value (%)**	**Min value (%)**	**Max value (%)**	**Number of measurements**
	Curing surface core	16.1	15.2	17.5	4
	Curing heart core	16.3	15.6	16.9	4
		Mean value (%)	**Standard deviation (%)**	**Coefficient of Variation (%)**	**Number of measurements**
	Curing cores	16.2	0.8	5	8
	Molded sample specimen	17.0	0.5	3	3

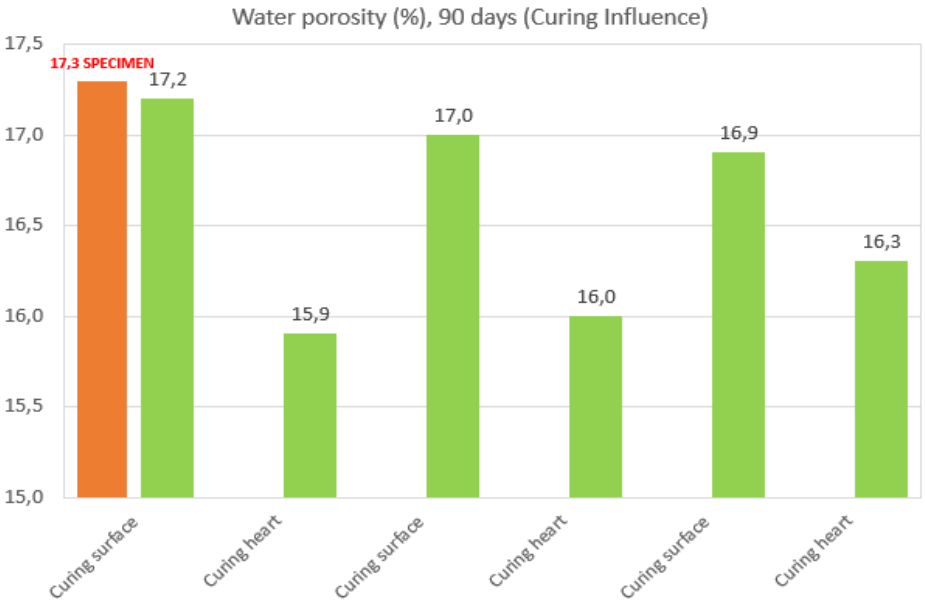

Figure 3.112. Water porosity **C40/50 viaduct La Reunion** (curing study)

Table 3.31. Water porosity **C40/50 viaduct La Reunion** (curing study)

	Localisation	Mean value (%)	Min value (%)	Max value (%)	Number of measurements
Water porosity, 90 days	**Curing surface core**	17.0	16.9	17.2	3
	Curing heart core	16.1	15.9	16.3	3
		Mean value (%)	**Standard deviation (%)**	**Coefficient of variation (%)**	**Number of measurements**
	Curing cores	16.6	0.6	3	6
	Molded sample specimen	17.3	0.3	1	3

Results obtained on core samples are slightly better than those from molded samples.

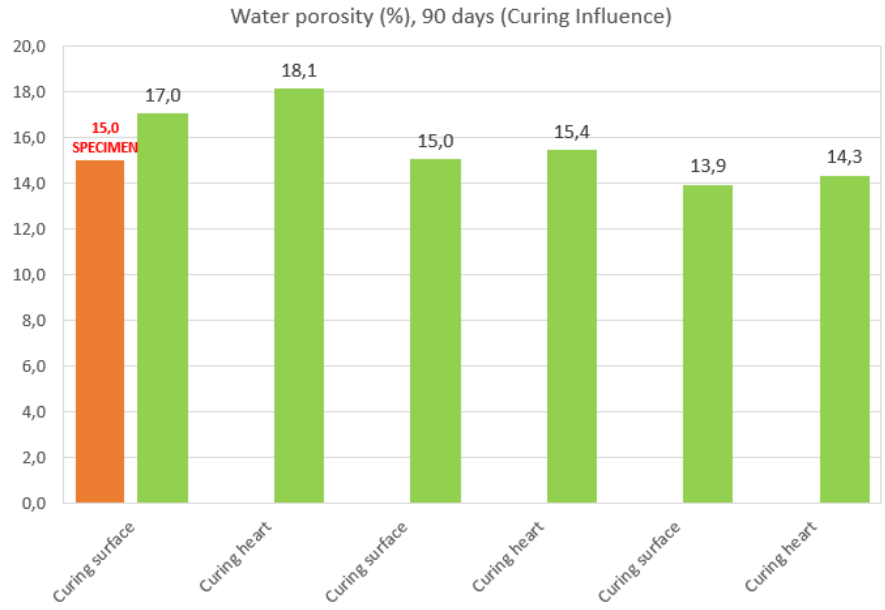

Figure 3.113. water porosity **C45/55 viaduct La Reunio**n (curing study)

Table 3.32. water porosity C45/55 viaduct La Reunion (curing study)

	Localisation	Mean value (%)	Min value (%)	Max value (%)	Number of measurements
Water porosity, 90 days	**Curing surface core**	15.3	13.9	17.0	3
	Curing heart core	15.9	14.3	18.1	3
		Mean value (%)	**Standard deviation (%)**	**Coefficient of variation (%)**	**Number of measurements**
	Curing cores	15.6	1.6	10 %	6
	Molded sample specimen	15.0	0.2	1 %	3

Note: for the viaduct project concrete mixtures, achieved water porosity are significantly higher than recommended values from Fascicule 65 due to intrinsic quality of local aggregates (around 2,5 % of conventional water absorption (24h) (chap 9.5.3)).

9.6 Temporal variability

In this paragraph, the graphs display both the temporal variability (blue squares and continuous line) as well the in-situ variability (green and orange circles; all coming from the cores on the mock-up, and corresponding to the day production of testing wall).

The dotted yellow lines, corresponding to the minimum and maximum in situ values (cores) aim just to easily visualize the in-situ variation; they are not intended to be extended over the time series (they concern just the day production of testing wall).

- C30/37 ready mix concrete: testing wall: 22/6/2018;
- C40/50 viaduct La Reunion: testing wall: 15/5/2017;
- C45/55 viaduct La Reunion: testing wall: 10/5/2017.

In this part, only the results of water porosity have been described. The other characteristics have been compiled in Appendix B.

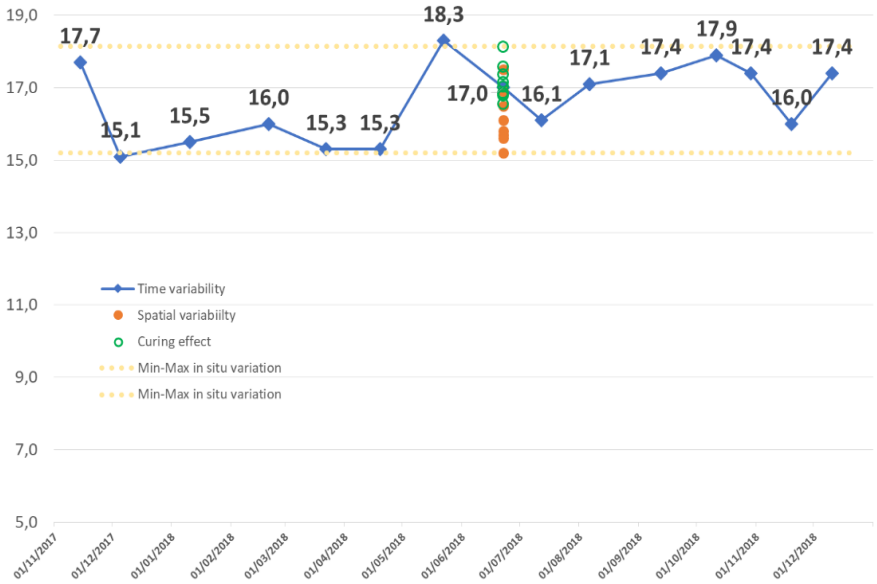

Figure 3.114. Water porosity **C30/37 ready mix concrete** (temporal/in situ variability)

Table 3.33. Water porosity C30/37 ready mix concrete (temporal/in situ variability)

Water porosity, 90 days	**Temporal variability (on sample)**	
	Mean value (%)	16.6
	Standard deviation (%)	1.1
	Coefficient of variation (%)	6
	Min value (%)	15.1
	Max value (%)	18.3
	Mean value (on sample – day of testing wall) (%)	17.0
	In-situ variability (on core)	
	Mean value In-situ variability (%)	16.7
	Min value In-situ variability (%)	15.2
	Max value In-situ variability (%)	18.1

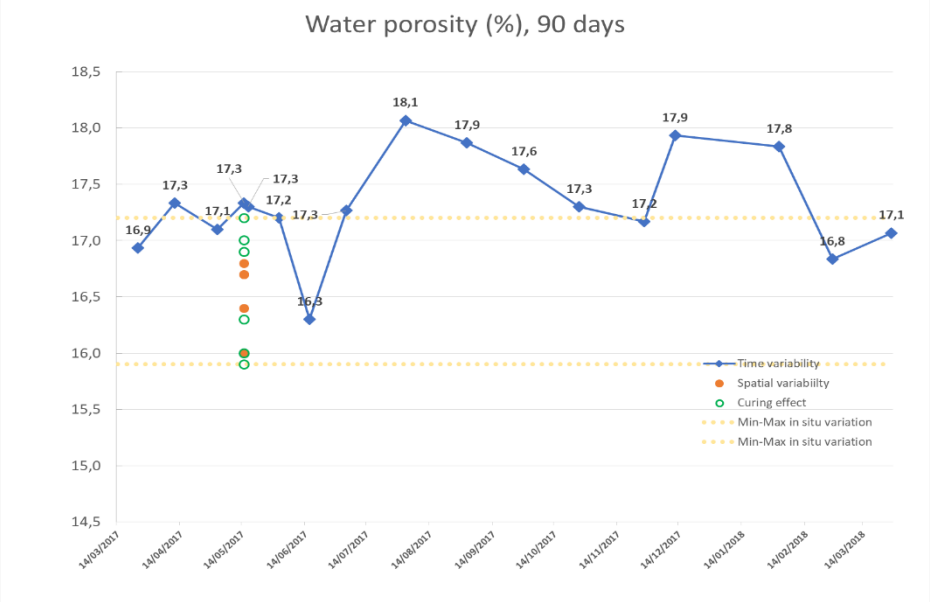

Figure 3.115. Water porosity C40/50 viaduct La Reunion (temporal/in situ variability)

Table 3.34. Water porosity C40/50 viaduct La Reunion (temporal/in situ variability)

Water porosity, 90 days	**Temporal variability (on sample)**	
	Mean value (%)	17.3
	Standard deviation (%)	0.4
	Coefficient of variation (%)	3
	Min value (%)	16.3
	Max value (%)	18.1
	Mean value (on sample – day of testing wall) (%)	17.3
	In-situ variability (on core)	
	Mean value In-situ variability (%)	16.5
	Min value In-situ variability (%)	15.9
	Max value In-situ variability (%)	17.2

The values of water porosity for the ready mix concrete C30/37 are as expected for the aggregates being used (limestone quarries); the values are moreover close to those of segment mix concrete in the La Réunion jobsite, showing an average compressive strength of 77.5 MPa at 28d.

Water porosity all along the production year is quite stable, with a low coefficient of variation.

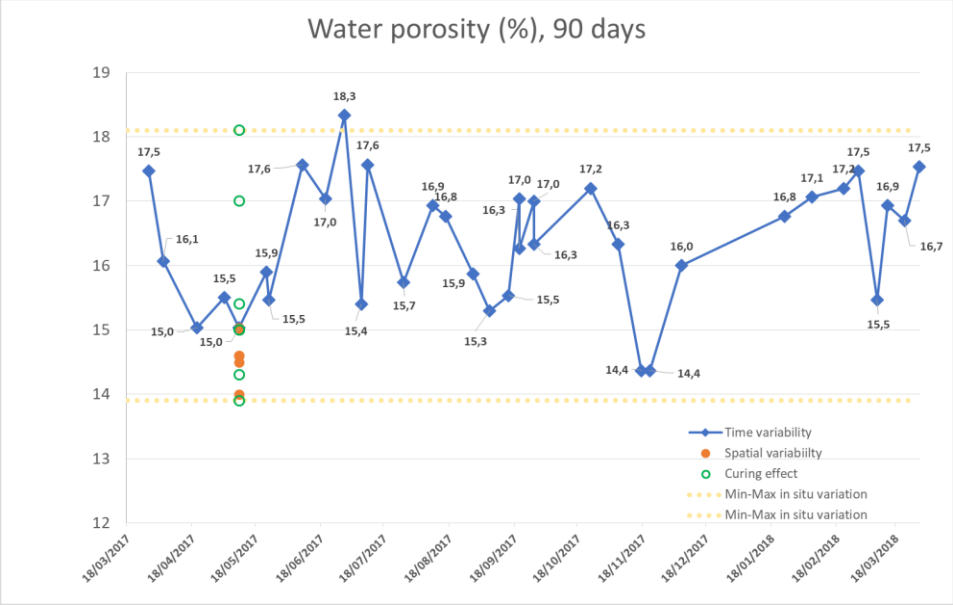

Figure 3.116. Water porosity **C45/55 viaduct La Reunion** (temporal/in situ variability)

Table 3.35. Water porosity **C45/55 viaduct La Reunion** (temporal/in situ variability)

Water porosity, 90 days	**Temporal variability (on sample)**	
	Mean value (%)	16.4
	Standard deviation (%)	1
	Coefficient of variation (%)	6
	Min value (%)	14.4
	Max value (%)	18.3
	Mean value (on sample – day of testing wall) (%)	15.0
	In-situ variability (on core)	
	Mean value In-situ variability (%)	15.1
	Min value In-situ variability (%)	13.9
	Max value In-situ variability (%)	18.1

9.7 Curing study – Additional studies

9.7.1 Introduction

For the slab pier concrete (type of cement: CEM III/A 42,5 N CE PM-ES NF) of La Reunion Island project, the highest recorded chloride migration coefficients at 90 days are related to cured surface. Additional measurement performed at 180 days do not confirm this trend. It is to be reminded that concrete demolding was carried out before achieving 35 % fcm_{28d} (15 MPa at 38 hours for slab pier concrete mix (≈28 % of fcm_{28d})).

According to the first results obtained at 90 days, additional tests have been carried out in order to characterize the impact of the curing conditions on their gas permeability and on their resistance to chlorides ingress (D_{rcm}) of four different concretes.

The Table 3.36 summarizes the main characteristics of these four concretes (among the 42 concretes of the PerFDuB national project).

Table 3.36. Main properties of the 4 concretes

Concrete reference	Unit	B15	B16	B17	B22
Strength class	(-)	C35/45	C35/45	C35/45	C35/45
Cement PerfDuB Code	(-)	CEM I 52,5N SR3	CEM II/A-S 52,5 N PM CP2 PM	CEM III/A 42,5 N	CEM II/A- LL 42,5 R
Main constituent other than clinker (%)	(-)	(-)	Slag (11 %)	Slag (43 %)	Limestone (14 %)
Total cement	(kg/m^3)	350	350	350	350
W_{eff}/B_{eq}	(-)	0.50	0.50	0.50	0.50
Aggregates	(-)	Agg1	Agg1	Agg1	Agg1

9.7.2 Curing study – Additional studies – Gas permeability

The curing conditions includes two cases: wet curing (ideal conditions in the laboratory) and dry curing (corresponding to site conditions from the point of obtaining the strength of 35 % fcm_{28d}).

- dry curing: k_{90d} B15 < k_{90d} B22 < k_{90d} B16 < k_{90d} B17;
- wet curing: k_{90d} B22 < k_{90d} B15 < k_{90d} B17 < k_{90d} B16.

The gas permeability test is suitable for revealing the effects of the curing conditions (impact of hydration, distribution of the porous network and wall effect). The latter are, as expected, most marked for concrete based on CEM III (concrete B17), for which hydration is far being completed at 35 % f $f_{cm,28d}$ and exchanges with the dry environment (artificial 50 % moisture content in laboratory) drastically emphasize the effect of drying on immature concrete. The other concretes are basically less impacted by limited curing time. However, and in any case, gas permeability remains of the same order of magnitude.

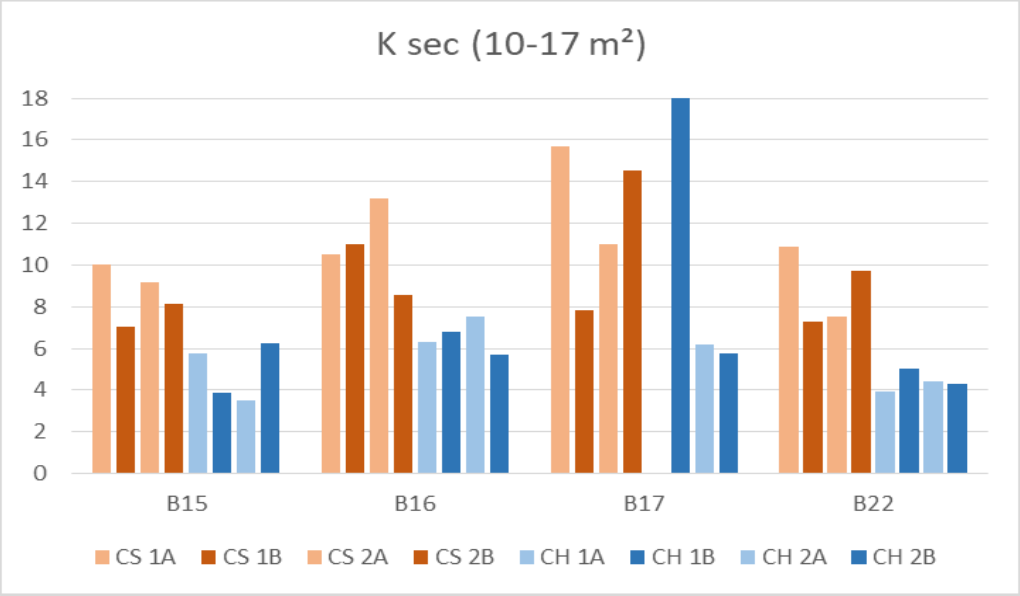

Figure 3.117. Gas permeability for 4 concretes under dry curing (=CS) and under wet curing (=CH)

9.7.3 Curing study – Additional studies – Chlorides ingress

The samples (cylinders) were cured until 35 % of 28-day compressive strength before being stored at 50 % RH and 20 °C, with only top and bottom sides exposed to desiccation (lateral sides have been coated with resin just after demolding). The D_{rcm} was then measured at 90 days on faces situated at different depths and compared with result obtained with wet curing. For concrete B15 with cement CEM I, it has been shown that the curing time has no impact on the D_{ecm}. For other concretes with additions, the curing time impacts on the D_{rcm}. The higher the substitution rate of additions, the higher the degree of impact. This is valid for both the D_{rcm} and the depth of concrete impacted. For concrete B17 with 43 % slag, the depth of concrete impacted remains lower than 2 cm.

Table 3.37. Chloride migration coefficient for 4 concretes under wet curing and under dry curing with removal of different depth of surface area

Concrete	Curing condition	D_{rcm} (10^{-12} m²/s)
B15	Water curing	16.5
	Dry curing with 3 cm depth removed	17.7
	Dry curing with 2 cm depth removed	17.5
	Dry curing with 1 cm depth removed	18.7
	Dry curing with 0 cm depth removed	19.0
B16	Water curing	12.0
	Dry curing with 3 cm depth removed	13.3
	Dry curing with 2 cm depth removed	15.4
	Dry curing with 1 cm depth removed	15.2
	Dry curing with 0 cm depth removed	18.4
B17	Water curing	3.2
	Dry curing with 3 cm depth removed	4.1
	Dry curing with 2 cm depth removed	3.7
	Dry curing with 1 cm depth removed	4.9
	Dry curing with 0 cm depth removed	5.9
B22	Water curing	14.9
	Dry curing with 3 cm depth removed	18.3
	Dry curing with 2 cm depth removed	18.5
	Dry curing with 1 cm depth removed	18.4
	Dry curing with 0 cm depth removed	21.2

However, and in any case, chloride migration coefficient remains of the same order of magnitude for a given concrete and seems to be also influenced by hydration conditions of lateral sides of the cylinders (even if they have been protected from drying by coating with resin). Furthermore, curing conditions after demolding (50 % relative humidity) are not representative at all of real structure conditions exposed to chlorides, for which relative humidity is high (most of the time, chloride migration coefficient is used for modelling considering a fully saturated conditions) and effect of curing duration limitation is much weaker.

9.8 Synthesis

This graphic synthesis concerns all the results and associated variability obtained on two concretes formulation developed for the construction of the Offshore Viaduct in La Réunion Island (C40/50 and C45/55) and one ready-mix concrete formulation (C30/37 : a typical one used in France for building purposes – Doubs department) during :

- A laboratory assessment,
- A 1-year temporal variability study of batching plant production,
- A curing and spatial variability (= In situ variability) study on specific mock-up.

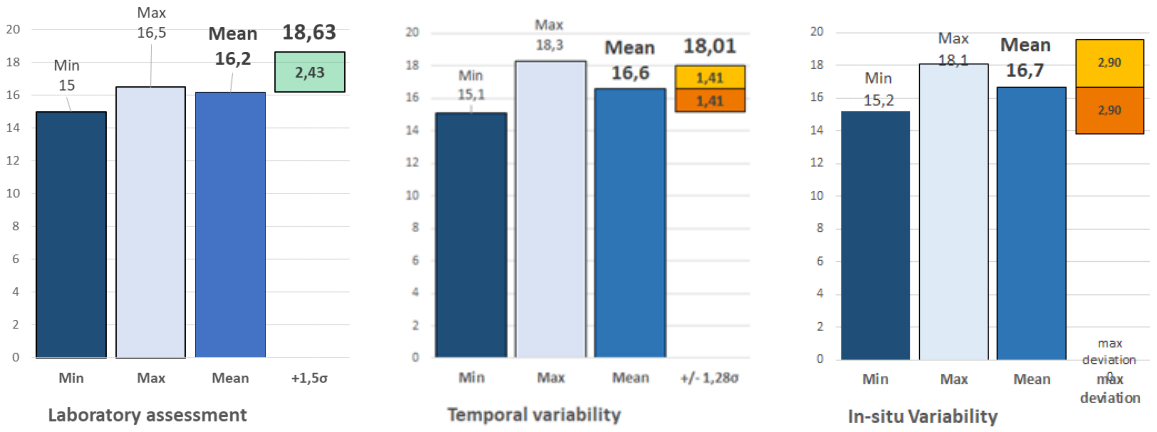

Figure 3.118. Water porosity, 90 days (%) - C30/37 Ready mix concrete

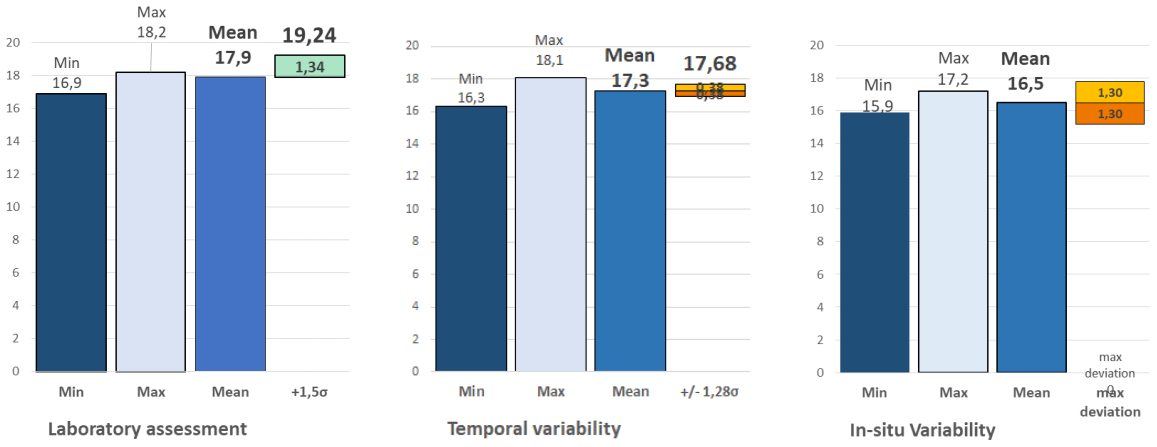

Figure 3.119. Water porosity, 90 days (%) - C40/50 Viaduct La Reunion

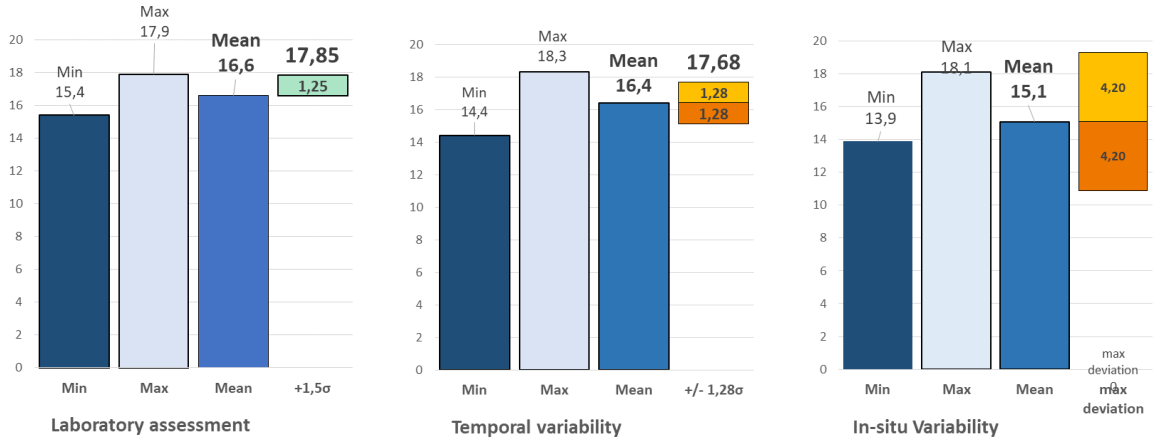

Figure 3.120. Water porosity, 90 days (%) - C45/55 Viaduct La Reunion

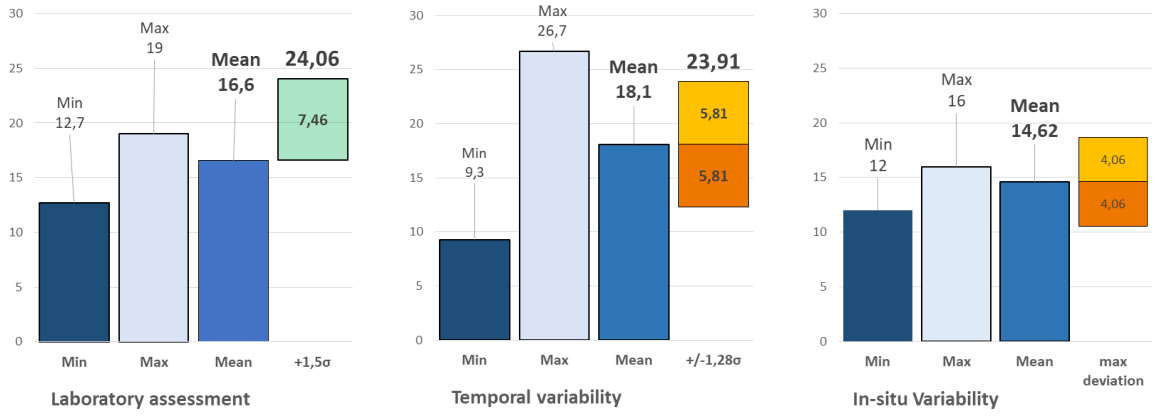

Figure 3.121. Chloride migration D_{rcm} 90 days (10^{-12} m²/s) - C30/37 Ready mix concrete

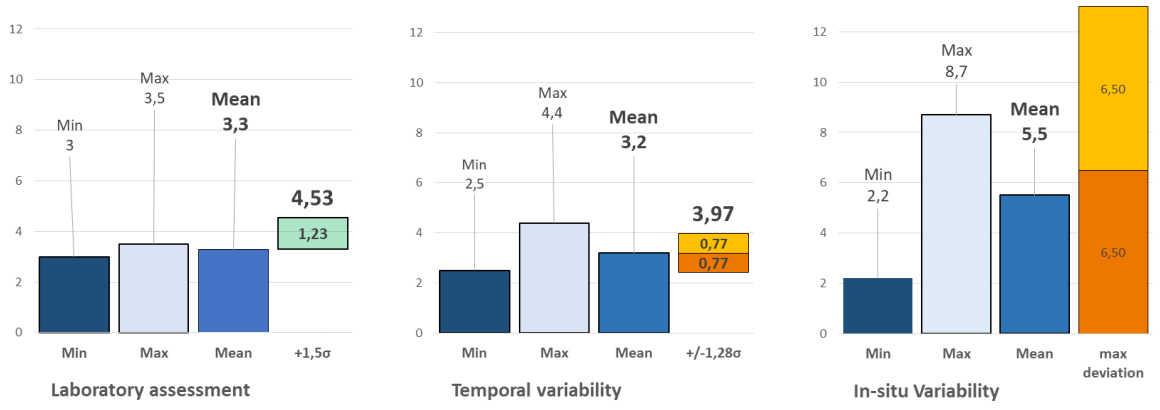

Figure 3.122. Chloride migration D_{rcm} 90 days (10^{-12} m²/s) - C40/50 Viaduct La Reunion

The highest recorded chloride migration coefficients at 90 days are corresponding to curing surface and much lesser for molded specimens compared to slices extracted at the core of the wall. At 180 days, all trends are broadly similar. It is to be reminded that concrete demolding was carried out before achieving the 35% of fcm_{28d}.

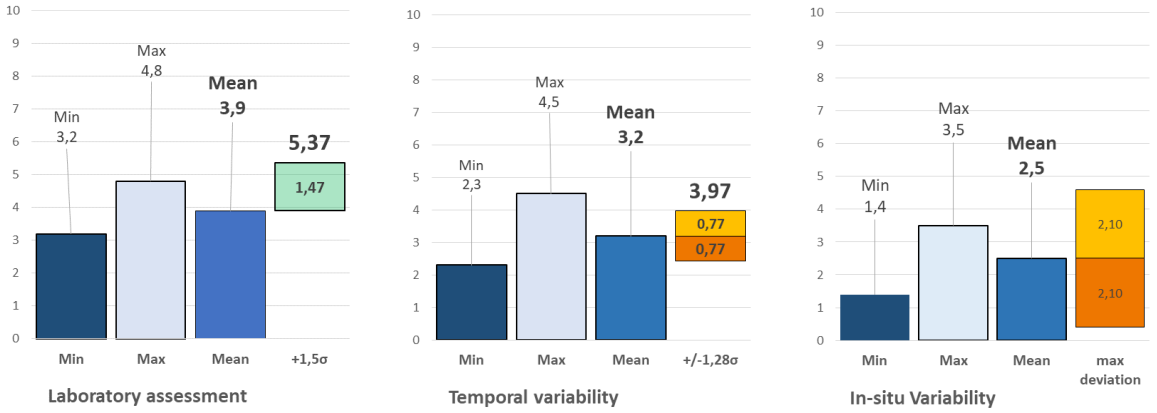

Figure 3.123. Chloride migration D_{rcm} 90 days (10^{-12} m²/s) - C45/55 Viaduct La Reunion

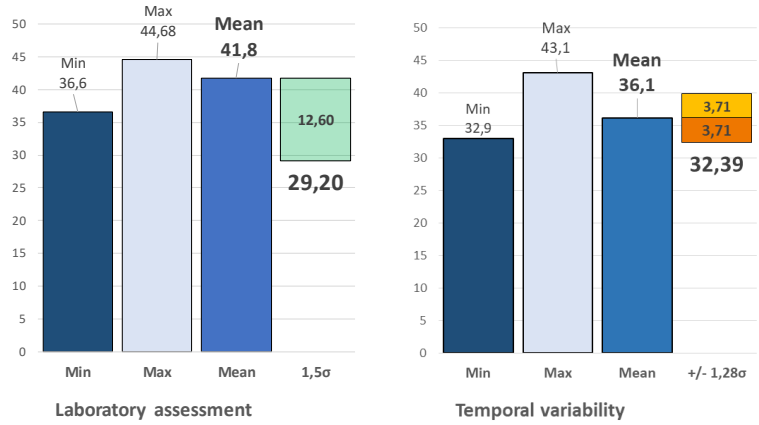

Figure 3.124. Resistivity 90 days (Ω.m) - C30/37 Ready mix concrete

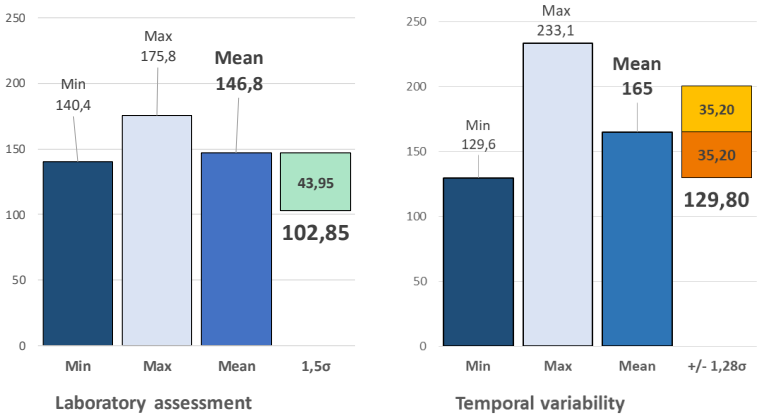

Figure 3.125. Resistivity 90 days (Ω.m) - C40/50 Viaduct La Reunion

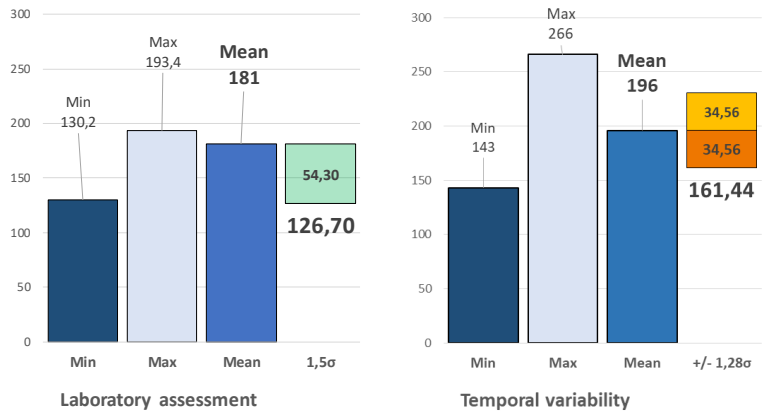

Figure 3.126. Resistivity 90 days (Ω.m) - C45/55 Viaduct La Reunion

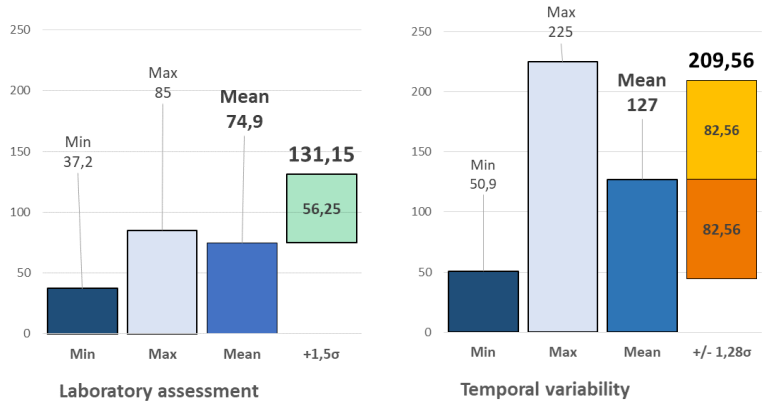

Figure 3.127. Gas permeability 90 days (10^{-18} m²) - C30/37 Ready mix concrete

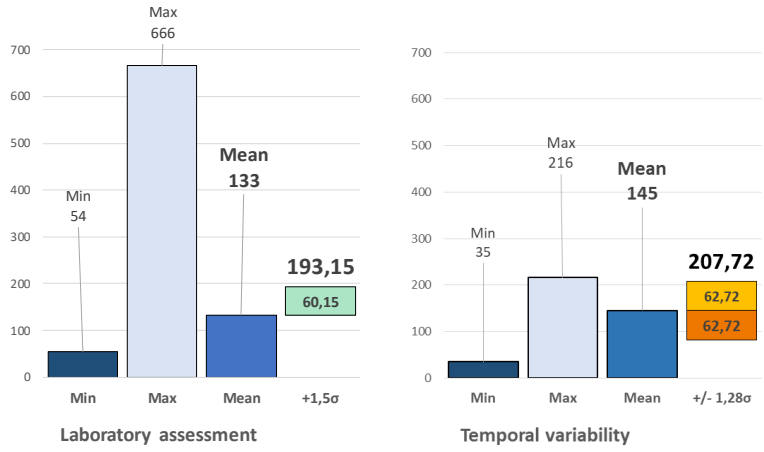

Figure 3.128. Gas permeability 90 days (10^{-18} m²) - C40/50 Viaduct La Reunion

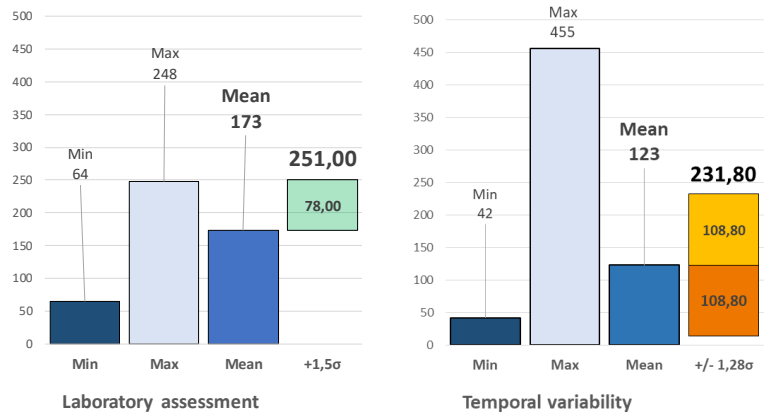

Figure 3.129. Gas permeability 90 days (10^{-18} m²) - C45/55 Viaduct La Reunion

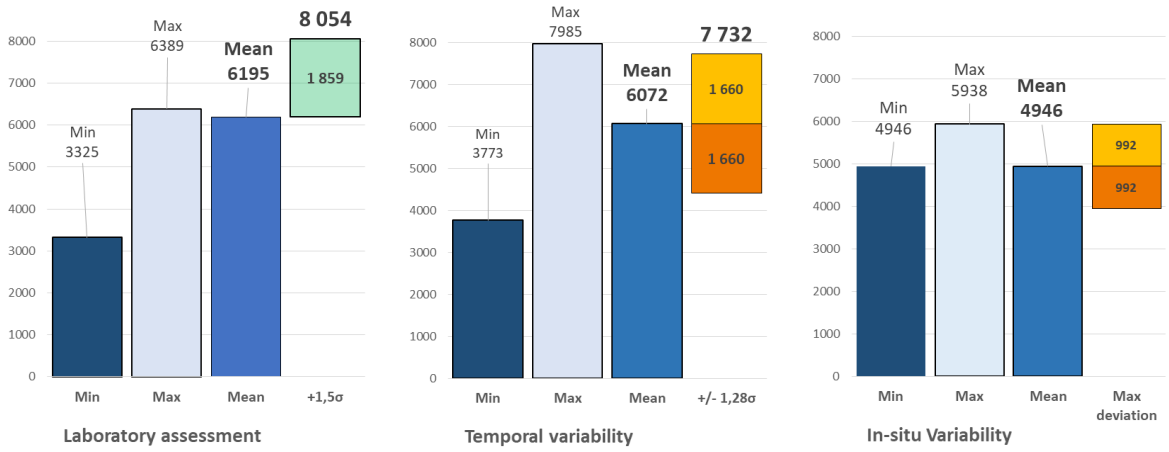

Figure 3.130. Capillary absorption coefficient 90 days (g/m²) - C30/37 Ready mix concrete

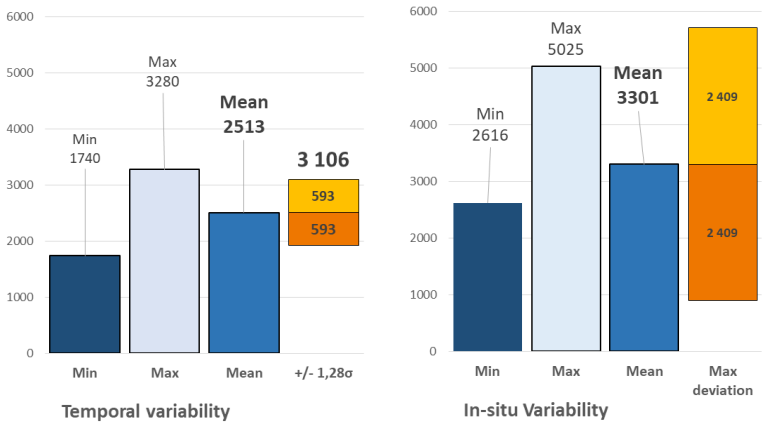

Figure 3.131. Capillary absorption coefficient 90 days (g/m²) - C40/50 Viaduct La Reunion

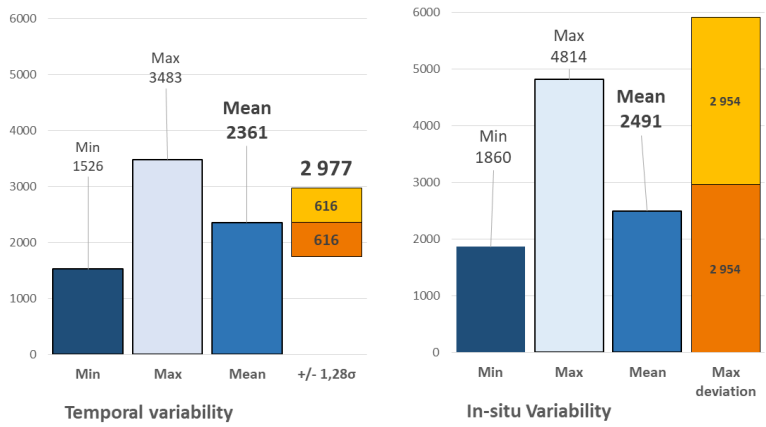

Figure 3.132. Capillary absorption coefficient 90 days (g/m²) - C45/55 Viaduct La Reunion

10 Elements for Performance-Based Approach implementation

Authors: François Cussigh, Jonathan Mai-Nhu, Patrick Rougeau, François Toutlemonde

10.1 Introduction

This section deals with the contribution of the National Project PerfDuB to implement the Performance-Based Approach at two levels:

- French national level: the goal is to define a Fascicule of Documentation referenced in NF EN 206/CN;
- European level in the field of ERC “Exposure Resistance Classes” system.

10.2 Methodology for the definition of threshold values for the durability properties considered in the Performance-Based Approach at the French national level

10.2.1 Context

One of the objectives of the National Project PerfDuB is to define performance criteria to justify the durability of concrete according to the exposure classes considered. One of the methodologies used to define these performance criteria is the analysis of the durability properties of the 42 concretes. The other methodologies concern on the one hand the use of the design service life modelling developed in the ANR project Modevie, and on the other hand the analysis of field experience based on detailed investigations of 19 old structures (bridges, quays, historic monuments, dams) for which the general durability properties were measured (water porosity, chloride diffusion, gas permeability, carbonation, etc.) and the durability indicators were evaluated (chloride penetration profiles, carbonation depths, electrode potentials, resistivity, presence of disorders, etc.). The last two methodologies are covered in other reports of PN PerfDuB, GT2b and GT2a respectively.

This section deals with the methodology for using the feedback from results of the database for the definition of performance criteria according to the exposure classes, considering the concretes complying with the prescriptive approach. This methodology was applied to determine the threshold value for the accelerated carbonation rate for XC classes and for chloride migration coefficient for XS and XD classes. The criteria are based on 90 days measurement and correspond to characteristic values with 90 % fractile.

The determination of alternative criteria such as the porosity divided by the paste volume content is defined in the section 4.

10.2.2 Definition of concretes for each exposure class

The first step is to define the representative concretes to be considered in the analysis for each exposure class. It was decided to consider concretes complying with the composition prescriptive rules for each exposure class and whose compressive strength class is greater than the minimum required class of:

- 2 classes for concretes complying with the requirements of NF EN 206/CN (design service life: 50 years);
- 3 classes for concretes complying with the requirements of Fascicule 65 (design service life: 100 years).

For example, considering XC2 and design service life 50 years, the Table 3.38 is an extract from NA.F1 Table of NF EN 206/CN.

Table 3.38. Extract from NA.F1 Table of NF EN 206/CN

	X0	XC1	XC2
Rapport E_{eff}/liant éq maximal [c)]	–	0,65	0,65
Classe de résistance minimale	–	C20/25	C20/25
Teneur mini en liant éq (kg/m^3) [c)] d)	150	260	260
Teneur minimale en air (%)	–	–	–
Essai(s) de performances [m)]	–	–	–

The concretes to be considered in the analysis are all the concretes which are complying with DTS requirements and whose compressive strength class are C20/25 or C25/30 or C30/37.

The following Tables summarize all the study concretes selected for each exposure class according to this procedure.

Table 3.39. Summary of all the concretes considered for the definition of performance criteria a: XC classes

Exposure class	Design service life 50 years	Design service life 100 years
XC1	2_CEM I_V30_0,52_33 3_CEM II/A-LL_0,6_41 4_CEM III/A_ 0,53_37 6_CEM I_L30_0,46_34 10_CEM II/A-LL_0,61_32 13_CEM I_L30_0,42_39 40_CEM I_Qz30_0,49_28 8_CEM II/A-LL_V30_0,53_31 14_CEM I_0,55_38	1_CEM I_ 0,5_43 2_CEM I_V30_0,52_33 3_CEM II/A-LL_0,6_41 6_CEM I_L30_0,46_34 7_CEM I_L41_0,39_42 11_CEM II/A-LL_0,54_50 13_CEM I_L30_0,42_39 14_CEM I_0,55_38 16_CEM II/A-S_0,5_50 17_CEM III/A_0,5_47 23_CEM II/A-S_0,49_46 24_CEM II/A-S_0,5_44 25_CEM I_0,5_50 26_CEM I_0,45_46 33_CEM III/A_0,45_52
XC2		
XC3	1_CEM I_ 0,5_43 2_CEM I_V30_0,52_33 3_CEM II/A-LL_0,6_41 6_CEM I_L30_0,46_34 7_CEM I_L41_0,39_42 13_CEM I_L30_0,42_39 14_CEM I_0,55_38 17_CEM III/A_0,5_47 23_CEM II/A-S_0,49_46 24_CEM II/A-S_0,5_44 26_CEM I_0,45_46	11_CEM II/A-LL_0,54_50 13_CEM I_L30_0,42_39 14_CEM I_0,55_38 16_CEM II/A-S_0,5_50 17_CEM III/A_0,5_47 21_CEM I_L30_0,39_57 22_CEM II/A-LL_0,49_57 23_CEM II/A-S_0,49_46 24_CEM II/A-S_0,5_44 25_CEM I_0,5_50 26_CEM I_0,45_46 33_CEM III/A_0,45_52 34_CEM III/A_0,45_59 37_CEM V/A (S-V)_0,45_56
XC4		17_CEM III/A_0,5_47 22_CEM II/A-LL_0,49_57 23_CEM II/A-S_0,49_46 25_CEM I_0,5_50 26_CEM I_0,45_46 33_CEM III/A_0,45_52 34_CEM III/A_0,45_59 37_CEM V/A (S-V)_0,45_56

b: XD classes

Exposure class	Design service life 50 years	Design service life 100 years
XD1	1_CEM I_ 0,5_43 2_CEM I_V30_0,52_33 3_CEM II/A-LL_0,6_41 6_CEM I_L30_0,46_34 7_CEM I_L41_0,39_42 13_CEM I_L30_0,42_39 14_CEM I_0,55_38 17_CEM III/A_0,5_47 23_CEM II/A-S_0,49_46 24_CEM II/A-S_0,5_44 26_CEM I_0,45_46	17_CEM III/A_0,5_47 22_CEM II/A-LL_0,49_57 23_CEM II/A-S_0,49_46 25_CEM I_0,5_50 26_CEM I_0,45_46 33_CEM III/A_0,45_52 34_CEM III/A_0,45_59 37_CEM V/A (S-V)_0,45_56
XD2	11_CEM II/A-LL_0,54_50 14_CEM I_0,55_38 16_CEM II/A-S_0,5_50 17_CEM III/A_0,5_47 23_CEM II/A-S_0,49_46 24_CEM II/A-S_0,5_44 25_CEM I_0,5_50 26_CEM I_0,45_46 33_CEM III/A_0,45_52	
XD3	17_CEM III/A_0,5_47 22_CEM II/A-LL_0,49_57 23_CEM II/A-S_0,49_46 25_CEM I_0,5_50 26_CEM I_0,45_46 33_CEM III/A_0,45_52 34_CEM III/A_0,45_59 37_CEM V/A (S-V)_0,45_56	30_CEM I_V30_0,35_64 26_CEM I_0,45_46 33_CEM III/A_0,45_52 34_CEM III/A_0,45_59 35_CEM V/A (S-V)_0,45_66 37_CEM V/A (S-V)_0,45_56

c: XS classes

Exposure class	Design service life 50 years	Design service life 100 years
XS1 **XS2**	11_CEM II/A-LL_0,54_50 14_CEM I_0,55_38 16_CEM II/A-S_0,5_50 17_CEM III/A_0,5_47 23_CEM II/A-S_0,49_46 24_CEM II/A-S_0,5_44 25_CEM I_0,5_50 26_CEM I_0,45_46 33_CEM III/A_0,45_52	17_CEM III/A_0,5_47 22_CEM II/A-LL_0,49_57 23_CEM II/A-S_0,49_46 25_CEM I_0,5_50 26_CEM I_0,45_46 33_CEM III/A_0,45_52 34_CEM III/A_0,45_59 37_CEM V/A (S-V)_0,45_56
XS3	17_CEM III/A_0,5_47 22_CEM II/A-LL_0,49_57 23_CEM II/A-S_0,49_46 25_CEM I_0,5_50 26_CEM I_0,45_46 33_CEM III/A_0,45_52 34_CEM III/A_0,45_59 37_CEM V/A (S-V)_0,45_56	30_CEM I_V30_0,35_64 26_CEM I_0,45_46 33_CEM III/A_0,45_52 34_CEM III/A_0,45_59 35_CEM V/A (S-V)_0,45_66 37_CEM V/A (S-V)_0,45_56

It should be remembered that the concretes cover a wide range and the database was built with concretes which voluntarily deviate from the prescriptive requirements of some exposure classes to study the impact of the composition parameters according to the exposure classes. These database construction rules have led to the production of few concretes which comply with exposure classes XC1 and XC2 only.

10.2.3 Methodology for the definition of mean threshold value

For each exposure class, a threshold mean value is determined from mean results obtained for each from the set of concretes and is then noted $P_{dur,threshold\ DDB}$ (DDB stands for "Durability DataBase")

$P_{dur,threshold\ DDB}$ is determined in such a way that 90 % of the concretes in the database (which correspond to concretes complying with the prescriptive approach) are retained by the performance-based approach. The Figure 3.133 gives an example for the determination of $D_{rcm,threshold\ DDB}$.

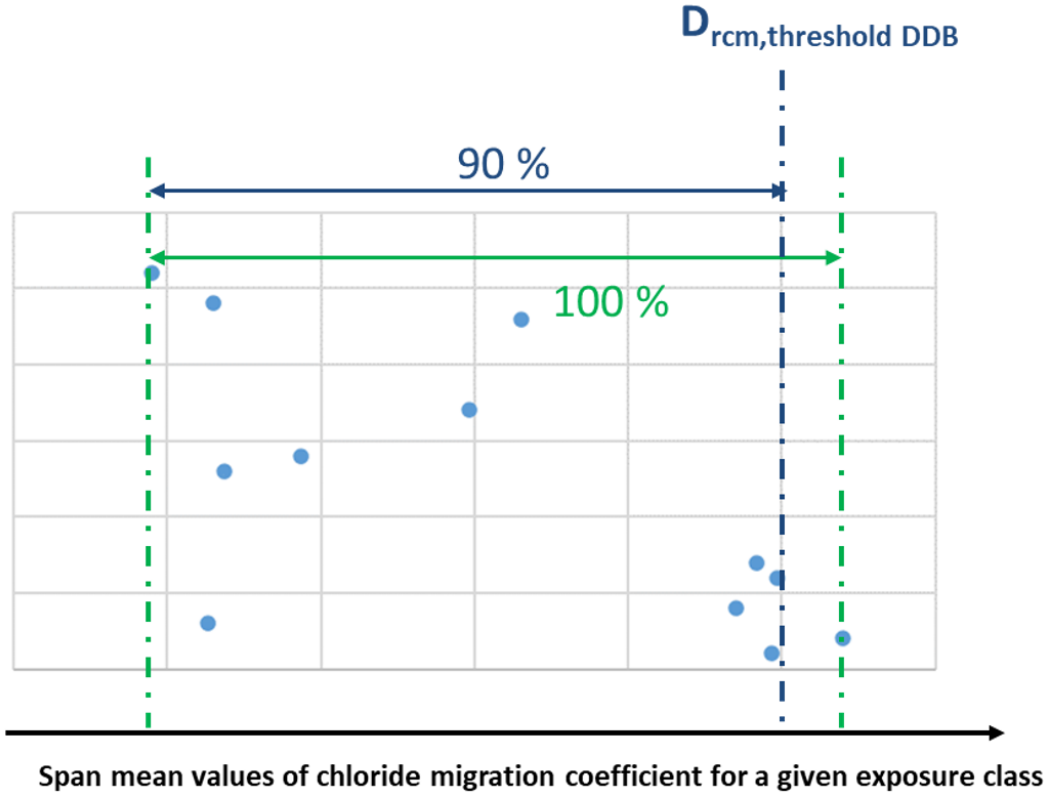

Figure 3.133. Example of the determination of $D_{rcm,threshold\ DDB}$

10.2.4 Methodology for the definition of characteristic threshold values

For each exposure class, the characteristic threshold value is then determined from the mean value by using the following hypotheses:

- the statistical distributions of the durability properties follow normal probability density functions (Aït-Mokhtar *et al*, 2013) even it is questionable for carbonation rate;
- the associated coefficient of variation for each durability property is equal to fixed value determined from several investigations on real structures (concretes with diverse compressive strength from C30/37 to C50/60), see Table 3.40.

Table 3.40. Fixed values for coefficient of variation of the durability properties, based on field experience in several projects (Offshore Viaduct in La Réunion Island, ready-mix concrete in PerfDuB, A86 tunnel, Compiègne Viaduct) with concretes C30/37, C35/45, C40/50, C45/55 and C50/60

Tests	Proposed fixed value for coefficient of variation (%)	Minimum value to consider for each indicator in application of performance-based approach (%)
Compressive strength (for reference value)	10	-
Porosity	6	3
Chloride migration D_{rcm}	25	20
Electrical resistivity	20	15
Gas permeability	30	-
Accelerated carbonation rate	25	25

The characteristic value is calculated with 90 % fractile as following:

$$P_{dur,k} = P_{dur,threshold\ DBB} + 1.28\ \sigma \qquad \text{(Equ. 3.10)}$$

Where 1.28 is the Student factor corresponding to 90 % fractile and σ is the standard deviation of the durability property determined from the fixed values of coefficient of determination (Table 3.40). These coefficients of variation are discussed in section 9.

The Figure 3.134 gives a schematic representation of the characteristic threshold value determined from the mean value of the durability properties. For some durability indicators the threshold values are “min values” (e.g. resistivity) similarly with compressive strength when others are “max values” (e.g. D_{rcm}).

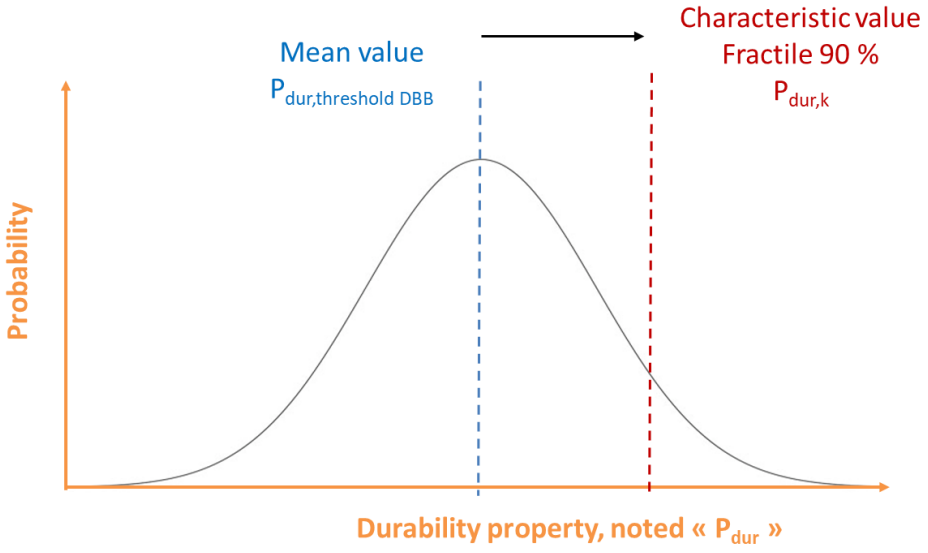

Figure 3.134. Schematic representation of characteristic value determined from mean value for the durability properties

10.2.5 Performance criteria for durability properties

Tables 3.41 and 3.42 present the performance criteria for the accelerated carbonation rate and the chloride migration coefficient for both design service life 50 and 100 years.

Table 3.41. Performance criteria for accelerated carbonation rate (after 90 days of wet curing)

Exposure class XC	Performance criteria (characteristic value 90 % fractile) Accelerated carbonation rate (V_{acc}, mm/day$^{0.5}$)	
	50 years	100 years
XC1	2.3	1.8
XC2	2.3	1.8
XC3	2.0	1.6
XC4	2.0	1.7

Table 3.42. Performance criteria for chloride migration (after 90 days of wet curing)

Exposure class XS/XD	Performance criteria (characteristic value 90 % fractile) Chloride migration coefficient (D_{rcm}, 10^{-12} m²/s)	
	50 years	100 years
XS1	33	18
XS2	33	18
XS3	17	10
XD1	46	18
XD2	33	18
XD3	17	10

10.3 ERC presentation

10.3.1 ERCs concept

The concept of ERCs, currently under development in European standardization bodies, corresponds to a global approach to ensure durability and has a number of purposes:

- introduce for the durability of structures and rigorously the concepts of reliability until then reserved for the mechanical behaviour of concrete;
- translate a performance requirement at the level of the structure into performance to be obtained at the material level;
- using predictive models and field experience, link resistance classes in durability to exposure classes, to reinforcement covers and to the design service life of the structure (50 or 100 years);
- integrate the variability of the durability properties of concrete;
- define the relevant test protocoles for carbonation and chloride migration;
- set up to specify a concrete mixture a performance-based approach of durability as an alternative to the obligation of means.

For all concrete structures, controlling durability requires being able to establish links between a target service life, the environment in which the structure will be and the characteristics of the structure. The Eurocodes thus provide rules for determining the concrete cover. The EN 206 standard is responsible for specifying the characteristics of the concrete to be used. The EN 13670 and EN 13369 standards are concerned with the implementation of concrete and the construction of parts of the structure, whether they are made with concrete cast on site or in a prefabrication plant.

In the system prior to ERCs, the relationship between design service life, structure exposure class, reinforcement cover and concrete characteristics is primarily based on compressive strength. The ERC concept aims to better take into account the durability mechanisms and is based on properties that are much more decisive for the aging of concrete: the rate of CO_2 penetration and chloride migration for marine environments (Figure 3.135).

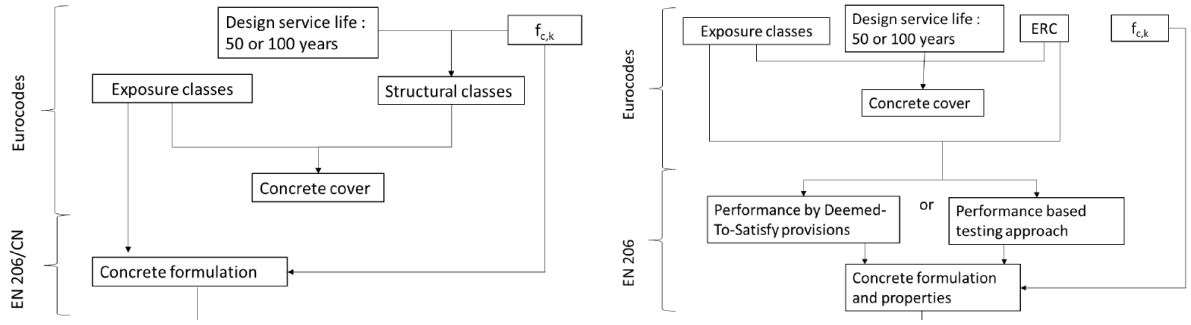

Figure 3.135. ERC concept

10.3.2 General benefits

The ERC-concept is innovative because it sets up for now and the future a new process for the way to consider concrete durability in the normative process. Main contribution of ERC concept is the fact that the methodology developed creates for the first time in concrete sector a coherent link between:

- ***field experience and practicioners feedback*****,** as it is traditionally the case in normative work;
- ***limit values for the definition of concrete mixes*** considering two options: prescriptive approach or performance-based approach;
- ***modelling of concrete durability properties***, especially the risks of corrosion due to carbonation and chlorides migration. This last point, the introduction of modelling in discussions between experts, constitutes a determinant new step and takes into account the results of scientific work carried out in recent decades and combine it with comprehensive field studies and practical experience.

Previously the limit values for the definition of concrete mixes were based solely on consideration of the field experience and experimental studies in laboratory. The limit states for durability mechanisms were considered implicitly without a precise definition. Now, due to the use of modelling to determine ERC classes, the limit states will be defined explicitly and precisely. This point has been addressed and developed in particular in the definitions of ERC for carbonation and chlorides exposition.

The introduction of the ERC-concept leads also to a more exhaustive consideration of the probabilistics and statistical issues of concrete durability properties and mechanisms. As for the mechanical properties, the limit values of concrete durability will be determined by considering their variability and with reference to a fractile and not only to a mean value.

By considering modelling and its necessary calibration based on field data, ERC concept leads to a better understanding and consideration of the durability mechanisms. Thus, the contribution of ERC is not just a matter of implementing the performance-based approach, but also leads to a much more precise and reliable prescriptive approach of the concrete real properties.

Often neglected in the scientific literature, industrial processes nevertheless have a great influence on the final properties of the material, including the mechanical properties, durability, aesthetic aspects or even environmental impact and in particular CO_2 emissions.

The final performance of concrete certainly depends on the characteristics and proportions of the constituents, but also on the industrial process specificities: mixer, system for concrete placing, compacting equipment, heat treatment, curing, which constitute as many possible variables in the industrial process.

Particularly, the following issues which characterize the industrial plants are key-points:

- the high compactness of the concrete due to the efficient vibro-compacting equipment for the concrete casting
- the low variability of the concrete characteristics because of the transport which is limited to the plant;
- the efficient control of reinforcement positioning and the control of concrete curing conditions.

By focusing more on the physico-chemical mechanisms which are key factors for the durability of the structures and the real performance of concrete at the scale of the structure and by introducing the probabilistic and statistical issues, ERC concept will make possible to better integrate the contribution of industrial processes in addition with the material issues.

10.3.3 The contribution of PN PerfDuB to ERC concept

The contribution of PN PerfDuB to ERC concept adresses several issues and particularly:

- the way to model design service life when the concrete structure is exposed to carbonation or chloride migration;
- concrete cover determination;
- threshold values definition for each ERC;
- statistical data in order to determine for example the standard deviation to be used;
- consideration to calculate the ageing factor when using cementitious mineral additions.

11 Conclusion

PerfDuB National Project leads a large survey on 42 concretes representative to the French experience and practice. These concretes have been fully investigated using of highly validated test protocols for durability properties.

The investigations carried out the correlation, and the absence of correlation which is finally also useful, between the durability properties themselves and between durability properties and concrete mix characteristics.

The threshold values proposed by the PerfDuB National Project for the durability properties have been used as a basis to produce the project of FD P 18-480, the French standard for performance-based approach in the field of NF EN 206/CN. These threshold values are based on three complementary approaches:

- the cartography of the properties measured for the 42 concretes presented in the present report;
- the design service life modelling developed in the ANR project Modevie;
- and the data coming from the field experience on old structures.

A large and representative data base, as it has been done in Perfdub National Project, is a necessary tool in the methodology to determine threshold for performance-based approach. The making, characterising, and analysing of the 42 concretes contribute to determine robust threshold values for each durability indicator. These results combined with those coming from modelling and the feedback coming from old structures are the basis for the implementation of the performance-based approach in NF EN 206/CN.

This data base provides a major contribution to the concrete sector for both French and European levels. It will be useful to implement the performance-based approach in EN 206 and NF EN 206/CN standards.

References

(Aït-Mokhtar et al., 2013) Aït-Mokhtar A. et al. (2013), “Experimental investigation of the variability of concrete durability properties”, Cement and Concrete Research, Elsevier, vol.45, n°1, p.21–36 (APPLET project).

(Andrade et al., 2014) Andrade C., d’Andrea R. & Rebolledo N. (2014), “Chloride ion penetration in concrete: The reaction factor in the electrical resistivity model”, Cement and Concrete Composites, Elsevier, vol.47, p.41–46.

(Baroghel-Bouny et al., 2013) Baroghel-Bouny V., Dierkens M., Wang X., Soive A., Saillio M., Thiery M. & Thauvin B. (2013), “Ageing and durability of concrete in lab and in field conditions: investigation of chloride penetration”, Journal of Sustainable Cement-Based Materials, Taylor & Francis, vol.2, n°2, p.67–110.

(Bisschop et van Mier, 2002) Bisschop J. & van Mier J.G.M. (2002), “How to study drying shrinkage microcracking in cement-based materials using optical and scanning electron microscopy?”, Cem. Concr. Res., vol.32, n°2, p.279–287.

(Boumaaza, 2020) Boumaaza M. (2020), “Experimental investigation of gas diffusivity and CO2-binding capacity of cementitous materials”, thèse, Université de La Rochelle.

(Denis et al., 2018) Denis P.-E., Linger L., Aït Alaïwa A., Ben Attaya S., Hoarau G., Caro J. & Cussigh F. (2018), “Use of resistivity as a routine concrete quality control tool. Outcomes of

records gathered during 2-year for the New Coastal Road on Reunion Island (France) offshore viaduct", fib 5th Congress, 2018, Melbourne.

(Dutzer et al., 2018) Dutzer V., Dridi W., Poyet S., Le Bescop P. & Bourbon X. (2019), "The link between gas diffusion and carbonation in hardened cement pastes", Cem. Concr. Res., vol.123, p.105795.

(Gendron, 2019) Gendron F. (2019), « Carbonatation des matériaux cimentaires: étude de la diffusion du CO2», thèse de doctorat en Génie civil, Université de La Rochelle.

(Kangni-Foli et al., 2021) Kangni-Foli E., Poyet S., Le Bescop P., Charpentier T., Bernachy-Barbé F., Dauzères A., L'Hôpital E. & d'Espinose de Lacaillerie J.-B. (2021), "Carbonation of model cement pastes: The mineralogical origin of microstructural changes and shrinkage", Cem. Concr. Res., vol.144, p.106446.

(Leemann et Moro, 2017) Leemann A. & Moro F. (2017), "Carbonation of concrete: the role of CO2 concentration, relative humidity and CO2 buffer capacity", Materials and Structures, Springer, vol.50, n°1, 30 (14 p.).

(Linger et al., 2018) Linger L., Carcassès M., Cassagnabère F., Cussigh F., Rougeau P., Mai-Nhu J. & Denis P.E. (2018), "Influence of aggregates porosity on concrete overall durability – Outcomes of investigations carried out for the New Coastal Road on La Reunion Island major project", in Hordijk D.A. & Luković M. (dir.), High Tech Concrete: Where Technology and Engineering Meet, Proceedings of the 2017 fib Symposium, Springer.

(Liu et al., 2015) Liu Y., Presuel-Moreno F.J. & Paredes M.A. (2015), "Determination of chloride diffusion coefficients in concrete by electrical resistivity method", ACI Materials Journal, American Concrete Institute (ACI), vol.112, n°5, p.631–340.

(Ollivier et al., 1995) Ollivier J.P., Maso J.C. & Bourdette B. (1995), "Interfacial transition zone in concrete", Advanced Cement Based Materials, Elsevier, vol.2, n°1, p.30–38.

(Papadakis et al., 1989) Papadakis V.G., Vayenas C.G. & Fardis M.N. (1989), "A reaction engineering approach to the problem of concrete carbonation", AIChE Journal, American Institute of Chemical Ingineers, vol.35, n°10, p.1639–1650.

(Papadakis et al., 1991) Papadakis V.G., Vayenas C.G. & Fardis M.N. (1991), "Fundamental modeling and experimental investigation of concrete carbonation", ACI Materials Journal, vol.88, n°4, p.363–373.

(Rozière, 2007) Rozière E. (2007), "Étude de la durabilité des bétons par une approche performantielle", thèse de doctorat en Génie civil, École Centrale de Nantes.

(Rozière et al., 2009) Rozière E., Loukili A. & Cussigh F. (2009), "A performance based approach for durability of concrete exposed to carbonation", Construction and Building Materials, Elsevier, vol.23, n°1, p.190–199.

(Samouh et al., 2017) Samouh H., Rozière E. & Loukili A. (2017), "The differential drying shrinkage effect on the concrete surface damage: Experimental and numerical study", Cem. Concr. Res., vol.102, p.212–224.

(Scrivener et al., 2004) Scrivener K.L., Crumbie A. & Laugesen P. (2004), "The interfacial transition zone (ITZ) between cement paste and aggregate in concrete", Interface Science, Springer, vol.12, n°4, p.411–421.

(Steiner et al., 2020) Steiner S., Lothenbach B., Proske T., Borgschulte A. & Winnefeld F. (2020), "Effect of relative humidity on the carbonation rate of portlandite, calcium silicate hydrates and ettringite", Cem. Concr. Res., vol.135, p.106116.

(Thiery, 2005) Thiery M. (2005), "Modélisation de la carbonatation atmosphérique des matériaux cimentaires: prise en compte des effets cinétiques et des modifications microstructurales et hydriques", thèse de doctorat en Matériaux et structures, ENPC.

(Torrent, 1992) Torrent R.J. (1992), “A two-chamber vacuum cell for measuring the coefficient of permeability to air of the concrete cover on site”, Materials and Structures, vol.25, p.358–365.

(Younsi et al., 2011) Younsi A., Turcry P., Rozière E., Aït-Mokhtar A. & Loukili A. (2011), “Performancebased design and carbonation of concrete with high fly ash content”, Cem. Concr. Comp., vol.33, n°10, p.993–1000.

Appendix A: Mix proportion of the 42 concretes (section 3)

Name of the concrete		1_CEM I_ 0,5_43	2_CEM I_V30_0,52_33	3_CEM II/A-LL_0,6_41	4_CEM III/A_ 0,53_37	5_CEM I_S60_0,58_26
Cement	Type	CEM I	CEM I	CEM II/A-LL	CEM III/A	CEM I
	Content (kg/m³)	280	223	280	280	119
Addition	Type	Limestone addition	Fly ash	-	Limestone addition	Slag
	Content (kg/m³)	50	95	-	50	179
Sand (0/4)	Type (5)	S2	S2	S2	S2	S2
	Content (kg/m³)	830	782	894	832	798
Coarse aggregate 1	Type (5)	G2 (6/20)	G2 (6/20)	G2 (6/20)	G2 (6/20)	G2 (6/20)
	Content (kg/m³)	906	946	914	908	940
Coarse aggregate 2	Type (5)	-	-	-	-	-
	Content (kg/m³)	-	-	-	-	-
Admixture 1	Type	Water-Reducing Admixture	Water-Reducing Admixture	Water-Reducing Admixture	Water-Reducing Admixture	Water-Reducing Admixture
	Content (kg/m³)	4.6	2.2	1.8	2.1	1,0
Admixture 2	Type	-	-	-	-	-
	Content (kg/m³)	-	-	-	-	-
Water content (W_{eff}) (l)		166	165	167	175	172
W_{eff}/C		0.59	0.74	0.60	0.63	1.45
W_{eff}/B		0.50	0.52	0.60	0.53	0.58
Density at the fresh state (kg/m³)		2322	2270	2306	2312	2125
Air (%)		1.3	1.9	1.0	1.4	1.5
Compressive strength class (4)		C35/45	C25/30	C30/37	C30/37	C20/25

Name of the concrete		6_CEM I_L30_0,46_34	7_CEM I_L41_0,39_42 (2)	8_CEM II/A-LL_V30_0,53_31	9_CEM II/A-LL_S45_0,57_31	10_CEM II/A-LL_0,61_32
Cement	Type	CEM I	CEM I	CEM II/A-LL	CEM II/A-LL	CEM II/A-LL
	Content (kg/m³)	253	270	223	161	280
Addition	Type	Limestone addition	Limestone addition	Fly ash	Slag	-
	Content (kg/m³)	108	190	95	132	-
Sand (0/4)	Type (5)	S2	S2	S2	S2	S2
	Content (kg/m³)	820	831	836	869	897
Coarse aggregate 1	Type (5)	G2 (6/20)	G2 (6/20)	G2 (6/20)	G2 (6/20)	G2bis (6/12)
	Content (kg/m³)	891	761	895	904	904
Coarse aggregate 2	Type (5)	-	-	-	-	-
	Content (kg/m³)	-	-	-	-	-
Admixture 1	Type	Water-Reducing Admixture	Water-Reducing Admixture	Water-Reducing Admixture	Water-Reducing Admixture	Water-Reducing Admixture
	Content (kg/m³)	1.8	6.5	3.0	1.8	2,9
Admixture 2	Type	-	Collaxim XR	-	-	-
	Content (kg/m³)	-	1.61	-	-	-
Water content (W_{eff}) (l)		167	181	168	167	170
W_{eff}/C		0.66	0.67	0.75	1.04	0.61
W_{eff}/B		0.46	0.39	0.53	0.57	0.61
Density at the fresh state (kg/m³)		2284	2312	2302	2280	2324
Air (%)		2.4	1.5	1.3	1.8	1.5
Compressive strength class (4)		C25/30	C35/45	C25/30	C25/30	C25/30

Name of the concrete		11_CEM II/A-LL_0,54_50	12_CEM I_S60_0,55_46	13_CEM I_L30_0,42_39	14_CEM I_0,55_38	15_CEM I_0,48_58
Cement	Type	CEM II/A-LL	CEM I	CEM I	CEM I	CEM I
	Content (kg/m³)	335	140	298	330	362
Addition	Type	-	Slag	Limestone addition	-	-
	Content (kg/m³)	-	211	128	-	-
Sand (0/4)	Type (5)	S1	S1	S1	S1	S1
	Content (kg/m³)	832	806	776	820	832
Coarse aggregate 1	Type (5)	G1 (4/11)	G1 (4/11)	G1 (4/11)	G1 (4/11)	G1 (4/11)
	Content (kg/m³)	402	300	289	305	408
Coarse aggregate 2	Type (5)	G1 (11/22)	G1 (11/22)	G1 (11/22)	G1 (11/22)	G1 (11/22)
	Content (kg/m³)	626	673	648	685	625
Admixture 1	Type	Water-Reducing Admixture	Water-Reducing Admixture	Water-Reducing Admixture	Water-Reducing Admixture	Water-Reducing Admixture
	Content (kg/m³)	2.6	6.2	3.0	2.1	2,8
Admixture 2	Type	-	-	-	-	-
	Content (kg/m³)	-	-	-	-	-
Water content (W_{eff}) (l)		182	192	181	180	174
W_{eff}/C		0.54	1.37	0.61	0.55	0.48
W_{eff}/B		0.54	0.55	0.42	0.55	0.48
Density at the fresh state (kg/m³)		2370	NM (1)	NM (1)	NM (1)	2410
Air (%)		1.3	NM(1)	NM (1)	NM (1)	1.4
Compressive strength class (4)		C40/50	C35/45	C30/37	C30/37	C50/60

Name of the concrete		16_CEM II/A-S_0,5_51	17_CEM III/A_0,5_47	18_CEM I_V37_0,53_56	19_CEM II/A-S_0,5_60	20_CEM II/A-S_0,5_59
Cement	Type	CEM II/A-S	CEM III/A	CEM I	CEM II/A-S	CEM II/A-S
	Content (kg/m³)	350	350	208	347	346
Addition	Type	-	-	Fly ash	-	-
	Content (kg/m³)	-	-	120	-	-
Sand (0/4)	Type (5)	S1	S1	S1	S3	S4
	Content (kg/m³)	804	815	781	847	763
Coarse aggregate 1	Type (5)	G1 (4/11)	G1 (4/11)	G1 (4/11)	G3 (4/12)	G4 (4/10)
	Content (kg/m³)	395	303	378	358	208
Coarse aggregate 2	Type (5)	G1 (11/22)	G1 (11/22)	G1 (11/22)	G3 (12/20)	G4 (10/20)
	Content (kg/m³)	604	680	590	678	763
Admixture 1	Type	Water-Reducing Admixture	Water-Reducing Admixture	Water-Reducing Admixture	Water-Reducing Admixture	Water-Reducing Admixture
	Content (kg/m³)	3.1	3.0	3.5	0.8	1,8
Admixture 2	Type	-	-	-	-	-
	Content (kg/m³)	-	-	-	-	-
Water content (W_{eff}) (l)		176	175	174	174	174
W_{eff}/C		0.50	0.50	0.84	0.50	0.50
W_{eff}/B		0.50	0.50	0.53	0.50	0.50
Density at the fresh state (kg/m³)		2340	2363	2340	2415	2326
Air (%)		2.4	1.8	1.5	1.1	2.0
Compressive strength class (4)		C40/50	C35/45	C45/55	C50/60	C45/55

Name of the concrete		21_CEM I_L30_0,39_57	22_CEM II/A-LL_0,49_53	23_CEM II/A-S_0,49_46	24_CEM II/A-S_0,5_44	25_CEM I_0,5_39
Cement	Type	CEM I	CEM II/A-LL	CEM II/A-S	CEM II/A-S	CEM I
	Content (kg/m³)	316	357	350	342	350
Addition	Type	Limestone addition	-	-	-	-
	Content (kg/m³)	135	-	-	-	-
Sand (0/4)	Type (5)	S1	S1	S2	S5	S1
	Content (kg/m³)	774	820	810	786	791
Coarse aggregate 1	Type (5)	G1 (4/11)	G1 (4/11)	G2 (6/20)	G5 (4/14)	G1 (4/11)
	Content (kg/m³)	288	403	907	379	381
Coarse aggregate 2	Type (5)	G1 (11/22)	G1 (11/22)	-	G5 (11/22)	G1 (11/22)
	Content (kg/m³)	646	617	-	642	576
Admixture 1	Type	Water-Reducing Admixture	Water-Reducing Admixture	Water-Reducing Admixture	Water-Reducing Admixture	Water-Reducing Admixture
	Content (kg/m³)	3.0	3.6	2.3	0.7	3,5
Admixture 2	Type	-	-	-	-	Air entrained Agent
	Content (kg/m³)	-	-	-	-	0,84
Water content (W_{eff}) (l)		175	175	173	172	174
W_{eff}/C		0.55	0.49	0.49	0.50	0.50
W_{eff}/B		0.39	0.49	0.49	0.50	0.50
Density at the fresh state (kg/m³)		2351	2390	2246	2330	2260
Air (%)		2.0	1.0	1.2	2.3	5.6
Compressive strength class (4)		C45/55	C45/55	C35/45	C35/45	C40/50

Name of the concrete		26_CEM I_0,45_39	27_CEM I_S50_0,43_68	28_CEM I_0,45_66	29_CEM I_S60_0,42_70	30_CEM I_V30_0,35_64
Cement	Type	CEM I	CEM I	CEM I	CEM I	CEM I
	Content (kg/m³)	386	189	363	154	302
Addition	Type	-	slag	-	slag	Fly ash
	Content (kg/m³)	-	189	-	232	130
Sand (0/4)	Type (5)	S1	S1	S1	S1	S1
	Content (kg/m³)	789	820	832	812	796
Coarse aggregate 1	Type (5)	G1 (4/11)	G1 (4/11)	G1 (4/11)	G1 (4/11)	G1 (4/11)
	Content (kg/m³)	376	305	409	399	296
Coarse aggregate 2	Type (5)	G1 (11/22)	G1 (11/22)	G1 (11/22)	G1 (11/22)	G1 (11/22)
	Content (kg/m³)	561	685	626	611	665
Admixture 1	Type	Water-Reducing Admixture	Water-Reducing Admixture	Water-Reducing Admixture	Water-Reducing Admixture	Water-Reducing Admixture
	Content (kg/m³)	2,8	2,7	5,5	4,5	8,1
Admixture 2	Type	Air entrained agent	-	-	-	-
	Content (kg/m³)	1.38	-	-	-	-
Water content (W_{eff}) (l)		174	162	162	164	152
W_{eff}/C		0.45	0.86	0.45	1.06	0.50
W_{eff}/B		0.45	0.43	0.45	0.42	0.35
Density at the fresh state (kg/m³)		2260	NM (1)	2410	2390	NM (1)
Air (%)		6.8	NM (1)	1.6	1.3	NM (1)
Compressive strength class (4)		C35/45	C55/67	C55/67	C55/67	C50/60

Name of the concrete		31_CEM III/A_0,4_67	32_CEM I_S50_0,33_90	33_CEM III/A_0,45_52	34_CEM III/A_0,45_59	35_CEM V/A (S-V)_0,45_66
Cement	Type	CEM III/A	CEM I	CEM III/A	CEM III/A	CEM V/A (S-V)
	Content (kg/m³)	380	200	370	371	381
Addition	Type	-	Slag	-	-	-
	Content (kg/m³)	-	200	-	-	-
Sand (0/4)	Type (5)	S1	S1	S1	S1	S1
	Content (kg/m³)	830	845	817	815	808
Coarse aggregate 1	Type (5)	G1 (4/11)	G1 (4/11)	G1 (4/11)	G1 (4/11)	G1 (4/11)
	Content (kg/m³)	309	314	304	303	396
Coarse aggregate 2	Type (5)	G1 (11/22)	G1 (11/22)	G1 (11/22)	G1 (11/22)	G1 (11/22)
	Content (kg/m³)	696	706	682	680	607
Admixture 1	Type	Water-Reducing Admixture	Water-Reducing Admixture	Water-Reducing Admixture	Water-Reducing Admixture	Water-Reducing Admixture
	Content (kg/m³)	2.9	9.2	4.0	4.5	5,5
Admixture 2	Type	-	-	-	-	-
	Content (kg/m³)	-	-	-	-	-
Water content (W_{eff}) (l)		153	133	168	168	170
W_{eff}/C		0.40	0.67	0.45	0.45	0.45
W_{eff}/B		0.40	0.33	0.45	0.45	0.45
Density at the fresh state (kg/m³)		NM (1)	NM (1)	2363	2351	2385
Air (%)		NM (1)	NM (1)	1.5	1.2	1.1
Compressive strength class (4)		C55/67	C70/85	C40/50	C45/55	C50/60

Name of the concrete		36_CEM V/A (S-V)_0,45_49	37_CEM V/A (S-V)_0,45_56	38_CEM I_D8_0,38_94	39_CEM I_M20_0,43_62	39b_CEM I_M20_0,42_66
Cement	Type	CEM V/A (S-V)	CEM V/A (S-V)	CEM I	CEM I	CEM I
	Content (kg/m³)	369	369	357	304	304
Addition	Type	-	-	Silica fume	Metakaolin	Metakaolin
	Content (kg/m³)	-	-	30	76	76
Sand (0/4)	Type (5)	S4	S3	S1	S2	S2
	Content (kg/m³)	746	826	858	786	791
Coarse aggregate 1	Type (5)	G4 (4/10)	G3 (4/12)	G1 (4/11)	G2 (6/20)	G2 (6/20)
	Content (kg/m³)	208	375	319	916	921
Coarse aggregate 2	Type (5)	G4 (10/20)	G3 (12/20)	G1 (11/22)	-	-
	Content (kg/m³)	780	676	720	-	-
Admixture 1	Type	Water-Reducing Admixture	Water-Reducing Admixture	Water-Reducing Admixture	Water-Reducing Admixture	Water-Reducing Admixture
	Content (kg/m³)	1.2	1.0	8.5	5.5	5,5
Admixture 2	Type	-	-	-	-	-
	Content (kg/m³)	-	-	-	-	-
Water content (W_{eff}) (l)		166	166	148	163	161
W_{eff}/C		0.45	0.45	0.41	0.54	0.53
W_{eff}/B		0.45	0.45	0.38	0.43	0.42
Density at the fresh state (kg/m³)		2340	2424	2450	2270	2303
Air (%)		0.8	1.0	1.5	2.5	1.9
Compressive strength class (4)		C40/50	C45/55	C70/85	C50/60	C55/67

Name of the concrete		40_CEM I_Qz30_0,49_28	41_CEM I_M20_0,35_93
Cement	Type	CEM I	CEM I
	Content (kg/m³)	253	302
Addition	Type	Siliceous addition	Metakaolin
	Content (kg/m³)	108	76
Sand (0/4)	Type (5)	S2	S1
	Content (kg/m³)	789	793
Coarse aggregate 1	Type (5)	G2 (6/20)	G1 (4/11)
	Content (kg/m³)	897	550
Coarse aggregate 2	Type (5)	-	G1 (11/22)
	Content (kg/m³)	-	540
Admixture 1	Type	Water-Reducing Admixture	Water-Reducing Admixture
	Content (kg/m³)	2.2	18,9
Admixture 2	Type	-	-
	Content (kg/m³)	-	-
Water content (W_{eff}) (l)		176	132
W_{eff}/C		0.70	0.44
W_{eff}/B		0.49	0.35
Density at the fresh state (kg/m³)		2202	2426
Air (%)		5.9	1.3
Compressive strength class (4)		C20/25	C70/85

Comments:

(1) NM: not measured.

(2): Concrete 7 is a SCC (Slump flow measured at 5 min equals 610 mm).

(3): XA classes are not studied. Compliance with classes XS2 and XS3 is established without taking into account the PM nature of the binder.

(4): The compressive strength class is calculated by taking into account the value measured after 28 days of wet curing and by reducing a coefficient of variation of 10 % and a coefficient k equal to 1.48.

(5) S1/G1 aggregates are semi-crushed alluvial aggregates (water absorption around 1 %).
S2/G2/G2bis aggregates are rolled alluvial sand-limestone aggregates (water absorption greater than 2.5 %).
S3/G3 aggregates are crushed limestone aggregates (water absorption around 0.5 %).
S4/G4 aggregates are crushed limestone aggregates (water absorption around 4 %).
S5 sand is a rolled marine aggregate (water absorption around 0.8 %).
G5 gravels are crushed gneiss gravels (water absorption around 0.5 %).

- The concrete nomenclature is described in section 4 of the GT3 deliverable.
- The slumps measured after 5 min are (200 ± 10) mm, except for SCC (Concrete n°7).
- The cement content, addition content, sand content, coarse aggregate content and admixtures are given in kg/m³.

Appendix B: Additional data on variability study (section 9)

3.B.1 Appendix paragraph 9.2

3.B.1.1 Laboratory assessment / Capillary absorption coefficient (on lab specimens)

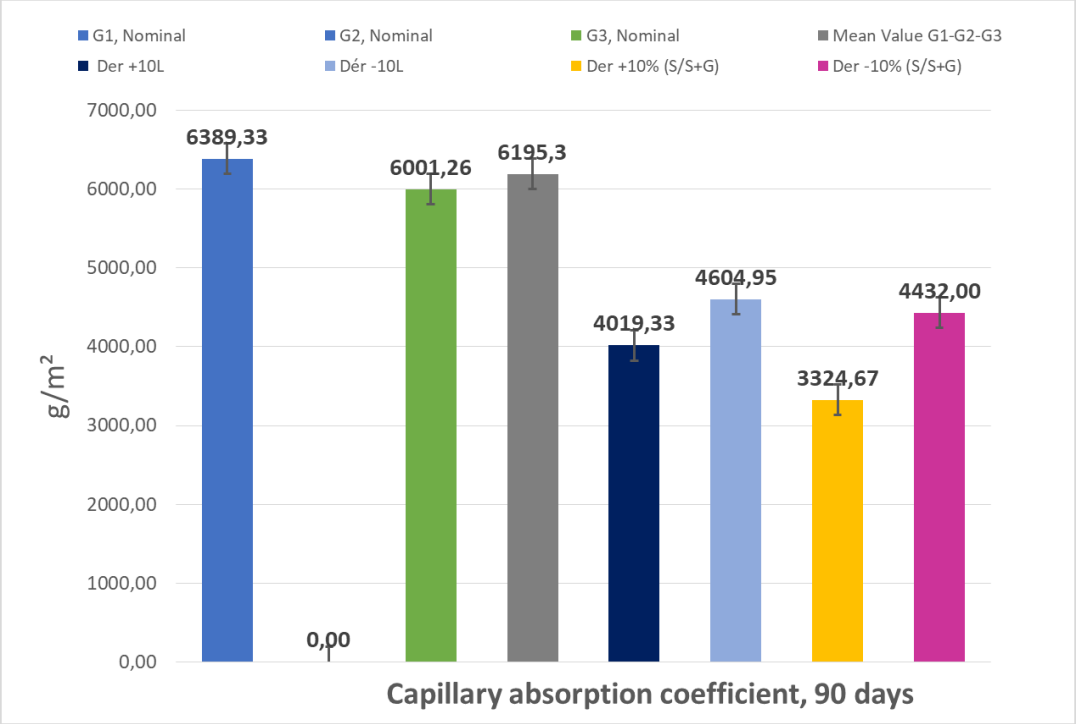

Figure 3.B.1. Capillary absorption coefficient C30/37 ready mix concrete (laboratory assessment)

3.B.1.2 Laboratory assessment / Carbonation (on lab specimens)

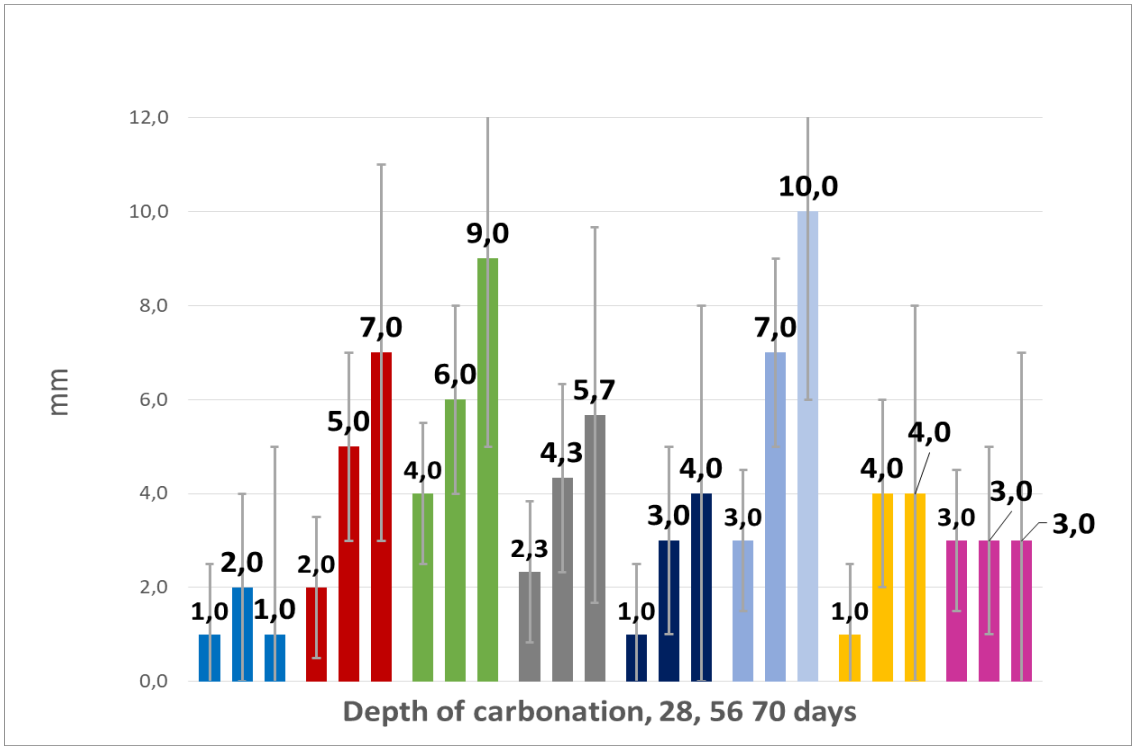

Figure 3.B.2. Depth of carbonation C30/37 ready mix concrete (laboratory assessment)

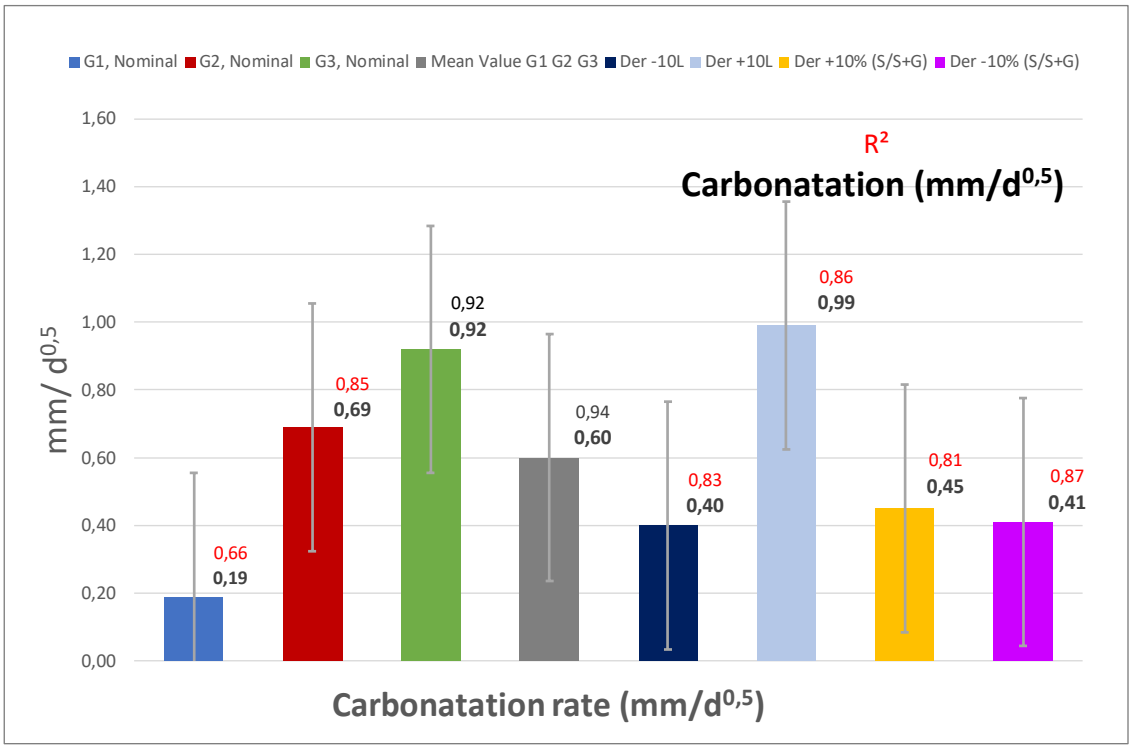

Figure 3.B.3. Carbonation rate C30/37 ready mix concrete (laboratory assessment)

3.B.1.3 Laboratory assessment / Chloride migration D_{rcm} (on lab specimens)

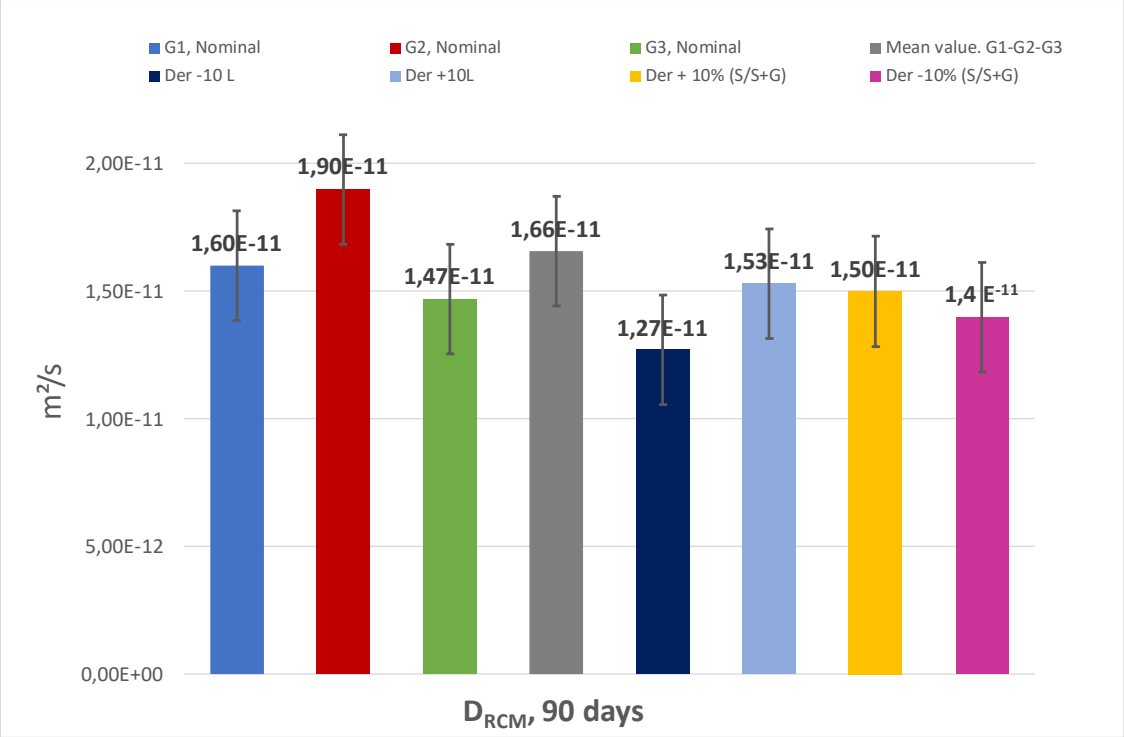

Figure 3.B.4. D_{rcm} C30/37 ready mix concrete (laboratory assessment)

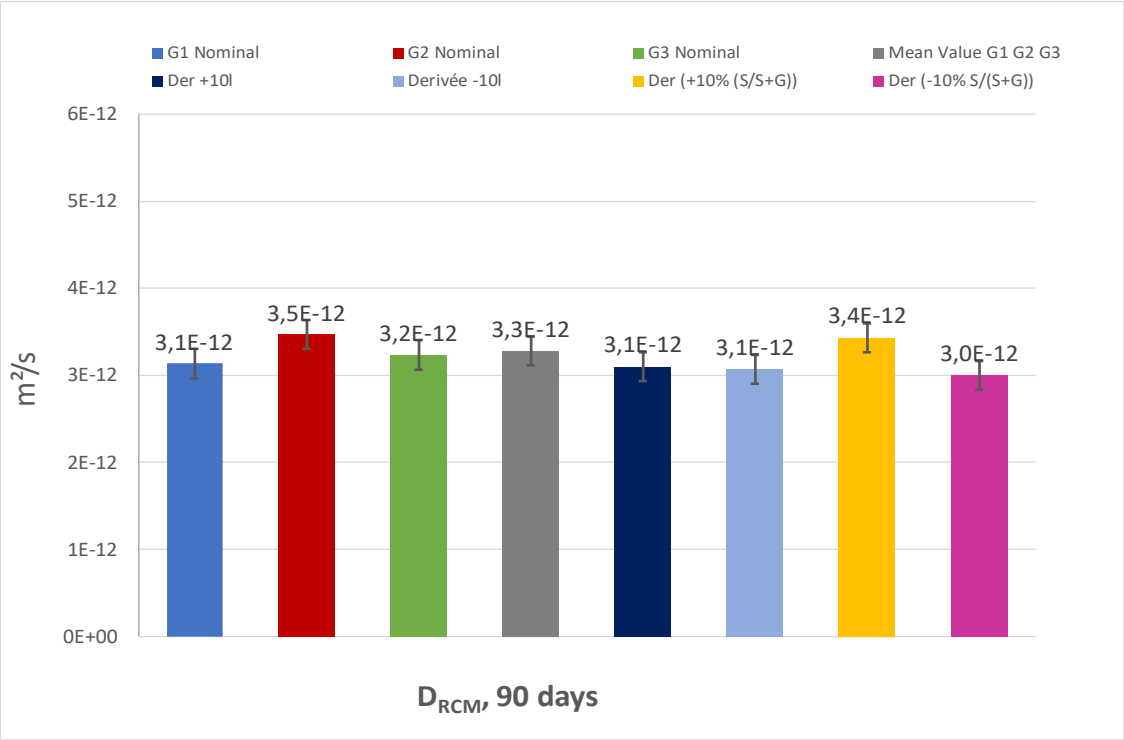

Figure 3.B.5. D_{rcm} C40/50 viaduct La Réunion (laboratory assessment)

3.B.1.4 Laboratory assessment / Resistivity (on lab specimens)

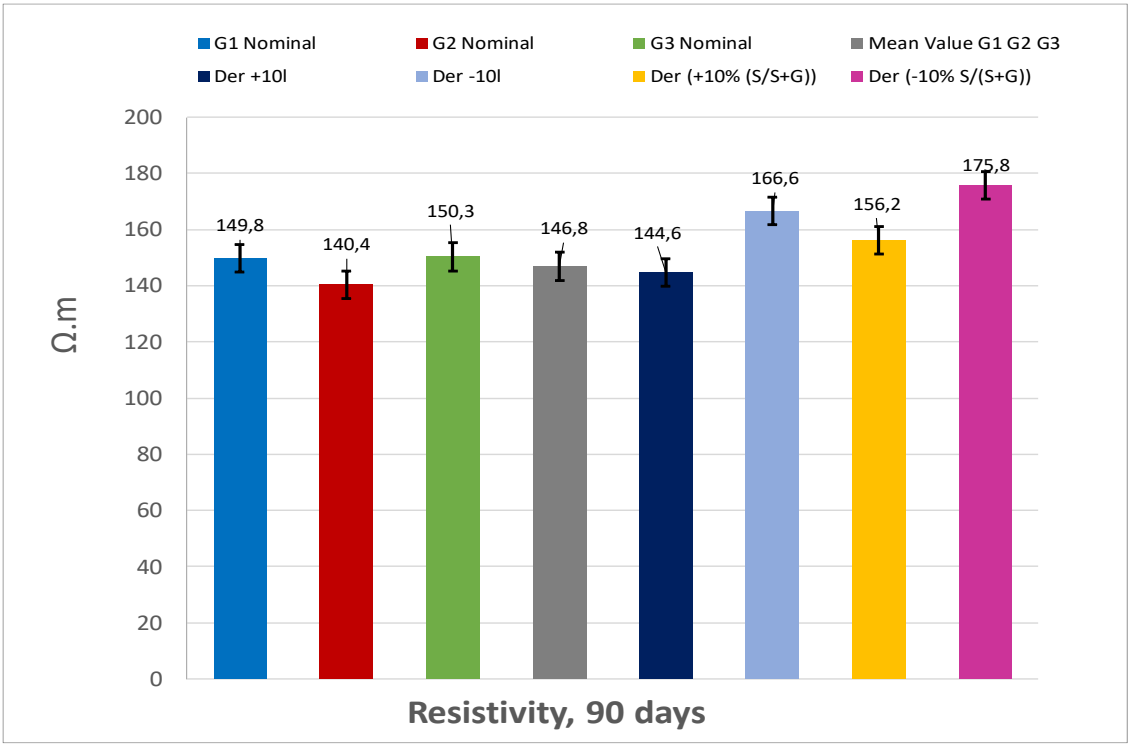

Figure 3.B.6. Resistivity C40/50 viaduct La Reunion (laboratory assessment)

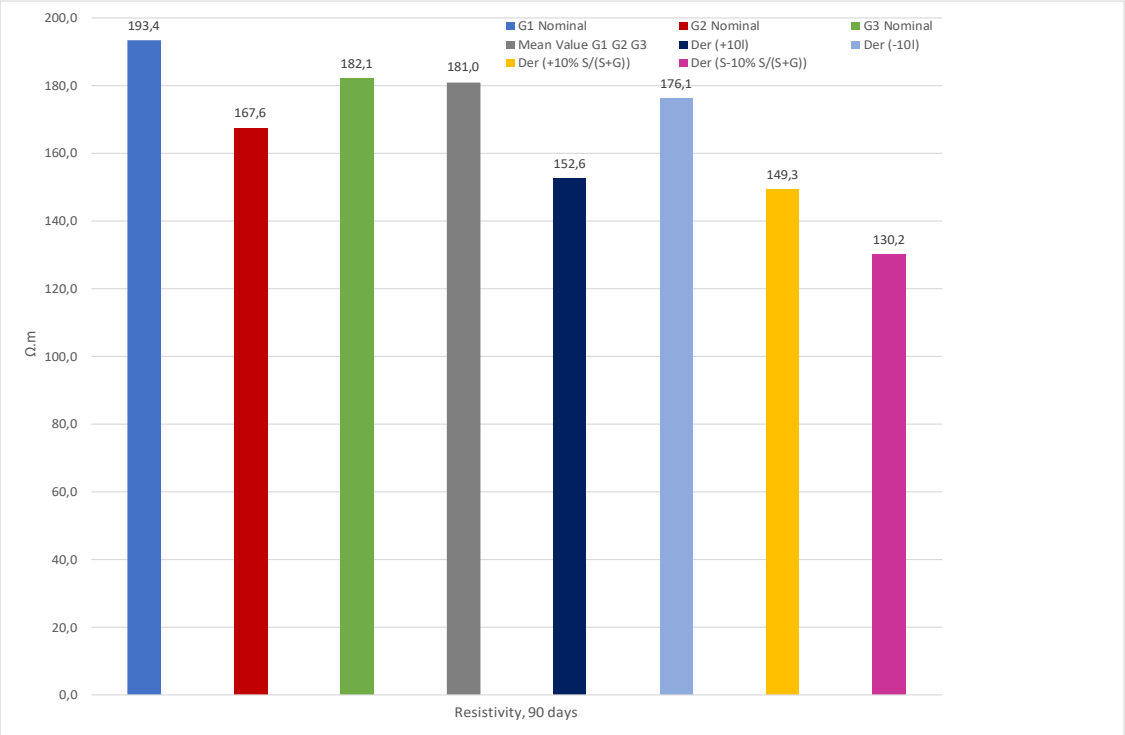

Figure 3.B.7. Resistivity C45/55 viaduct La Reunion (laboratory assessment)

3.B.1.5 Laboratory assessment / Gas permeability (on lab specimens)

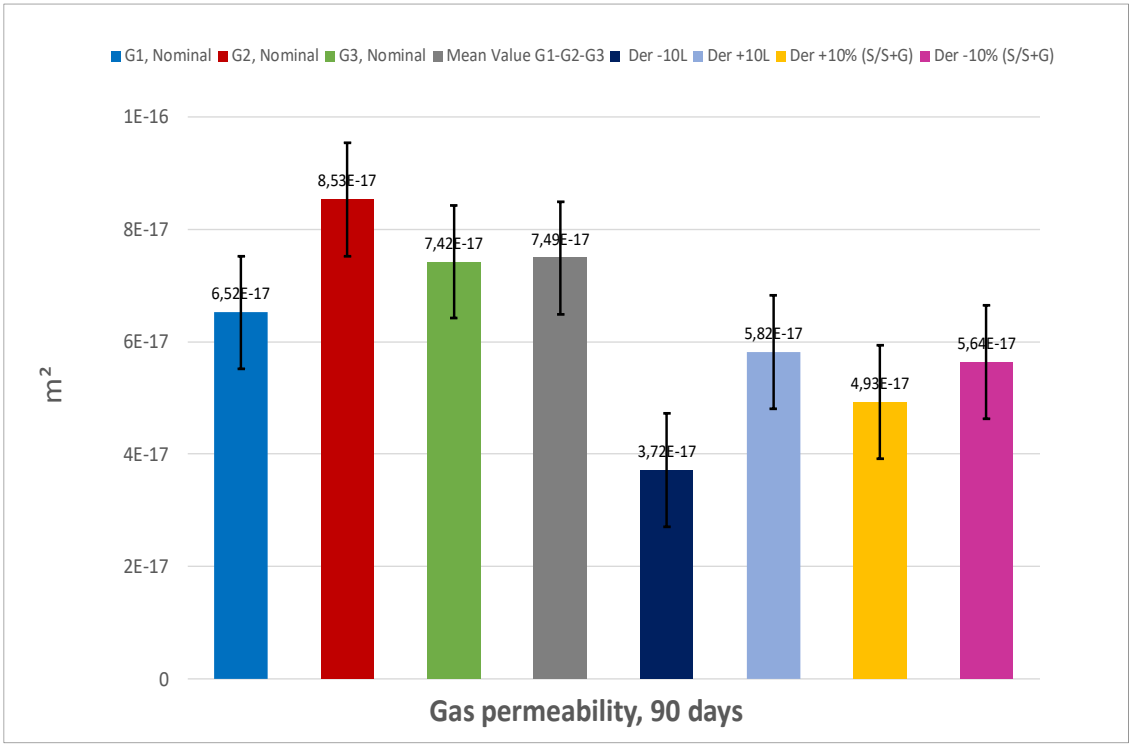

Figure 3.B.8. Gas permeability C30/37 ready mix concrete (laboratory assessment)

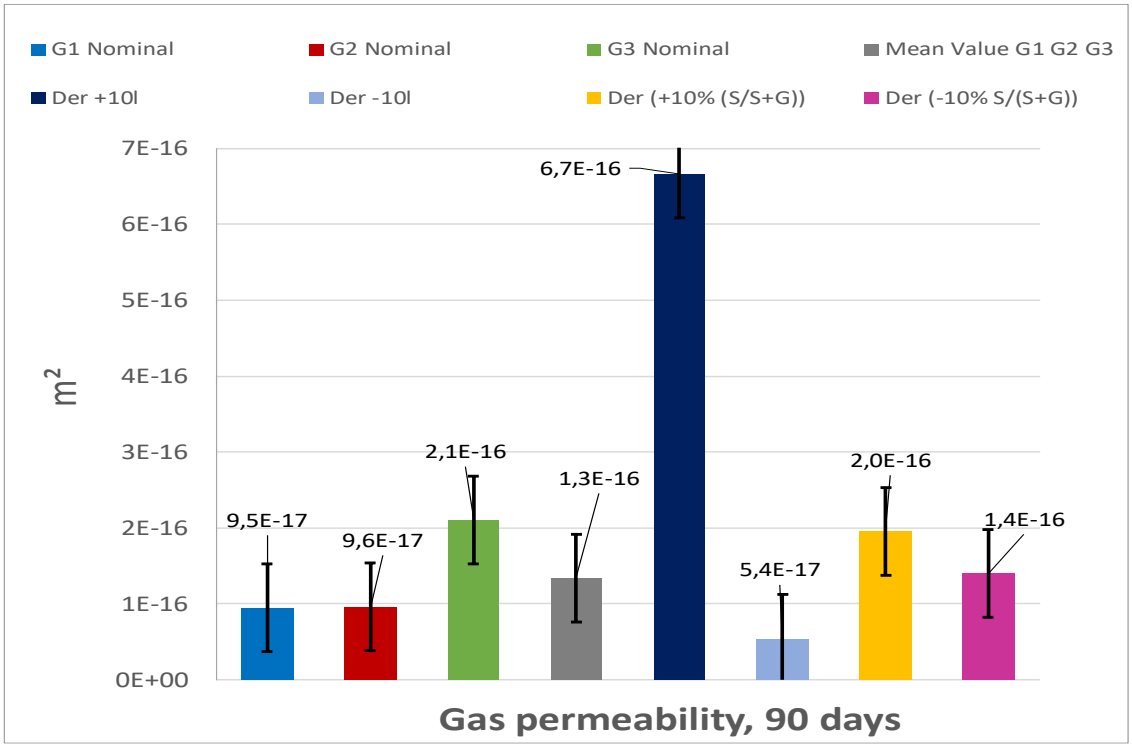

Figure 3.B.9. Gas permeability C40/50 viaduct La Reunion (laboratory assessment)

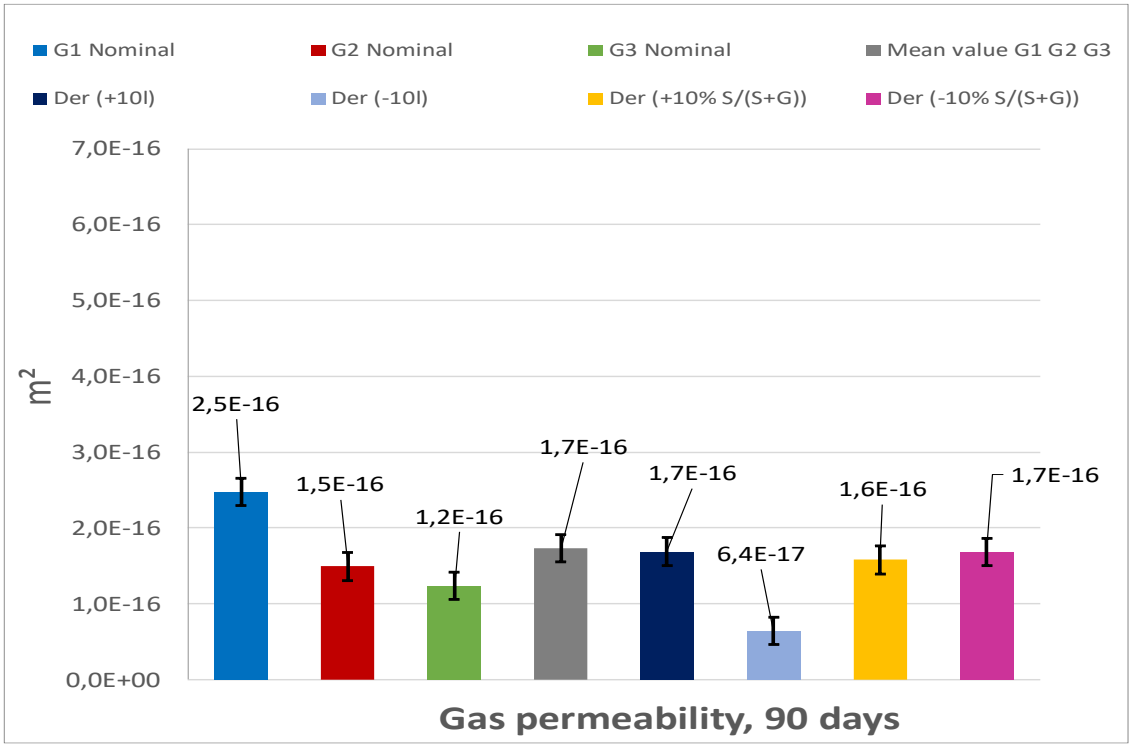

Figure 3.B.10. Gas permeability C45/55 viaduct La Reunion (laboratory assessment)

3.B.1.6 Laboratory assessment / Torrent permeability (on lab specimens)

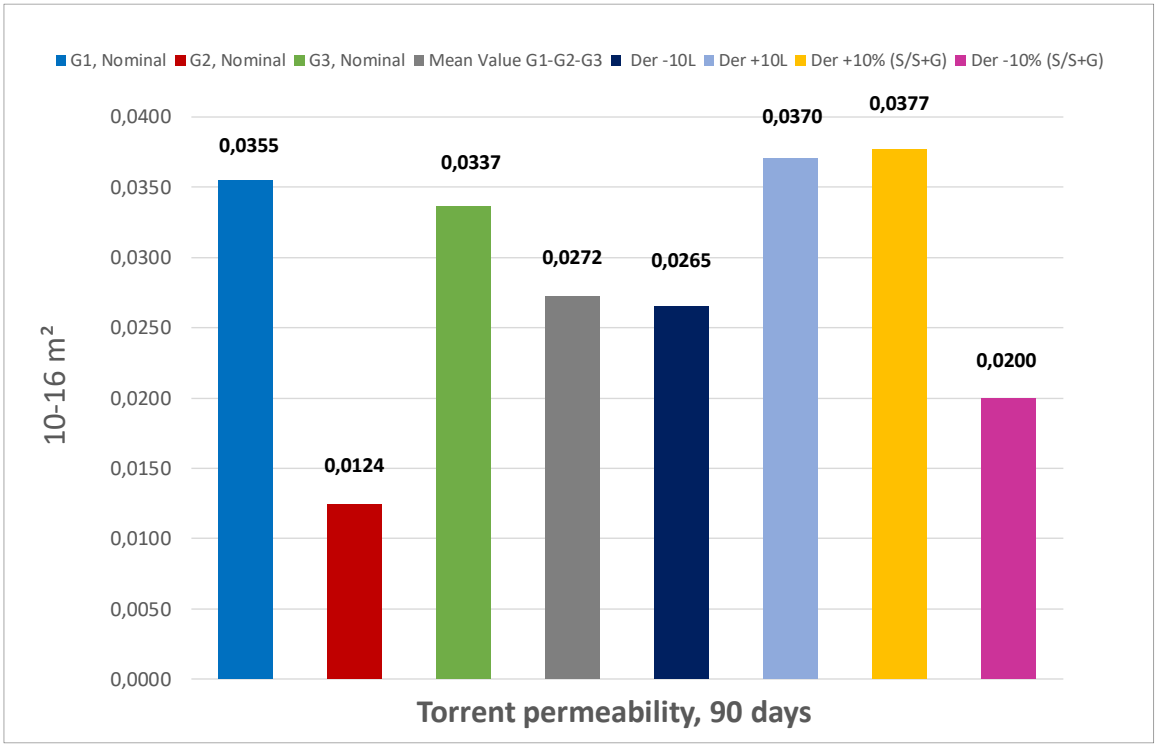

Figure 3.B.11. Torrent permeability C30/37 ready mix concrete (laboratory assessment)

3.B.2 Appendix paragraph 9.5.2

3.B.2.1 Spatial variability / Capillary absorption coefficient

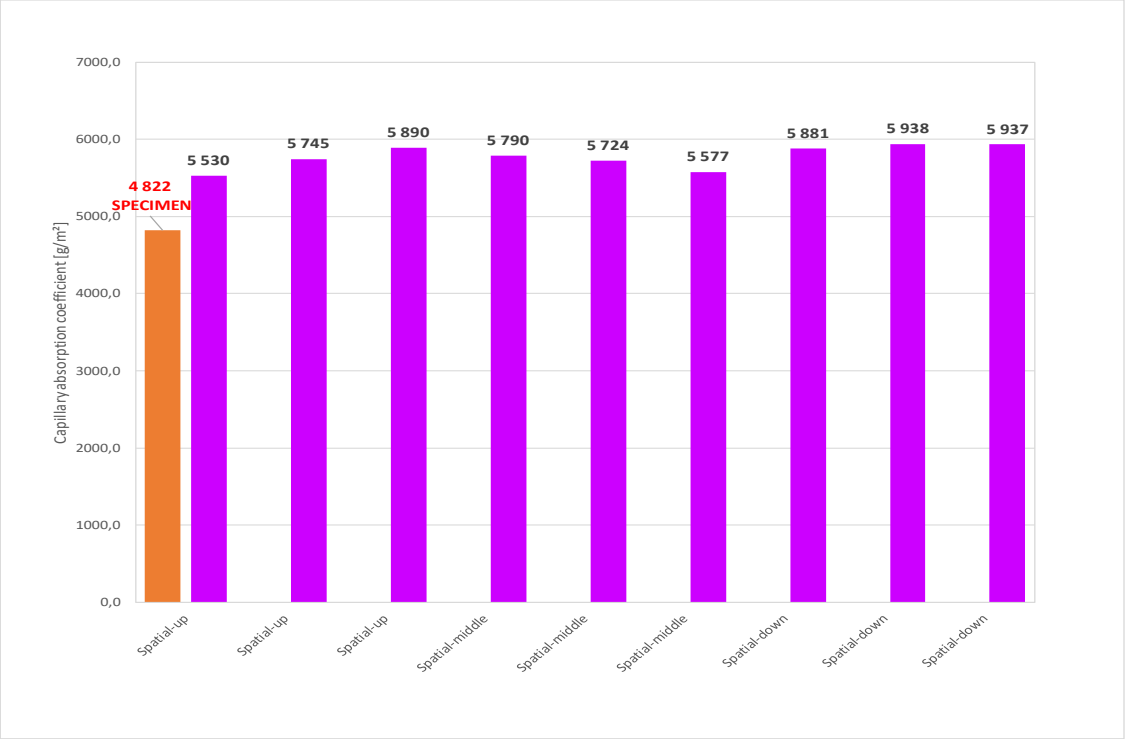

Figure 3.B.12. Capillary absorption coefficient C30/37 ready mix concrete (spatial study)

Table 3.B.1. Capillary absorption coefficient C30/37 ready mix concrete (spatial study)

	Localisation	Mean value	Min value	Max value	Number of measurements
Capillary absorption coefficient, 90 days (g/m²)	Spatial up core	5722	5530	5890	3
	Spatial middle core	5697	5577	5790	3
	Spatial down core	5919	5881	5938	3
		Mean value	**Standard deviation**	**Coefficient of variation**	**Number of measurements**
	Spatial cores	5779	150	3 %	9
	Molded sample specimen	4822	-	-	-

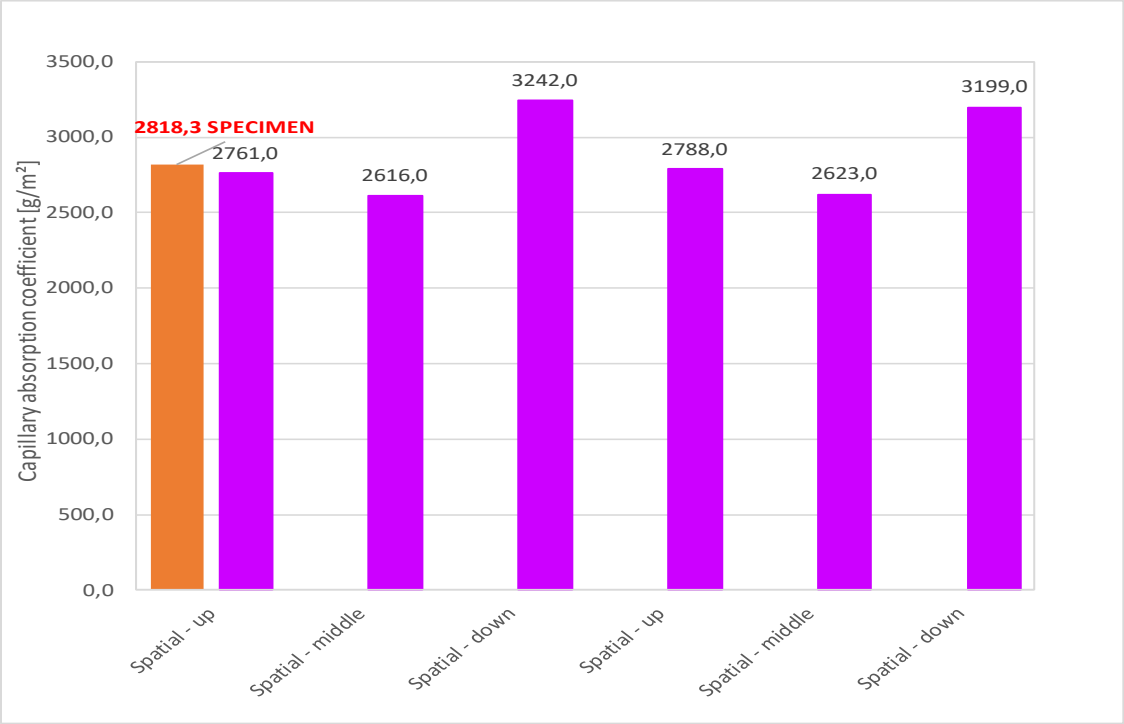

Figure 3.B.13. Capillary absorption coefficient C40/50 viaduct La Reunion (spatial study)

Table 3.B.2. Capillary absorption coefficient C40/50 viaduct La Reunion (spatial study)

	Localisation	Mean value	Min value	Max value	Number of measurements
Capillary absorption coefficient, 90 days (g/m²)	Spatial up core	2775	2761	2788	2
	Spatial middle core	2620	2616	2623	2
	Spatial down core	3221	3199	3242	2
		Mean value	**Standard deviation**	**Coefficient of variation**	**Number of measurements**
	Spatial cores	2872	280	10 %	6
	Molded sample specimen	2818	79	3 %	3

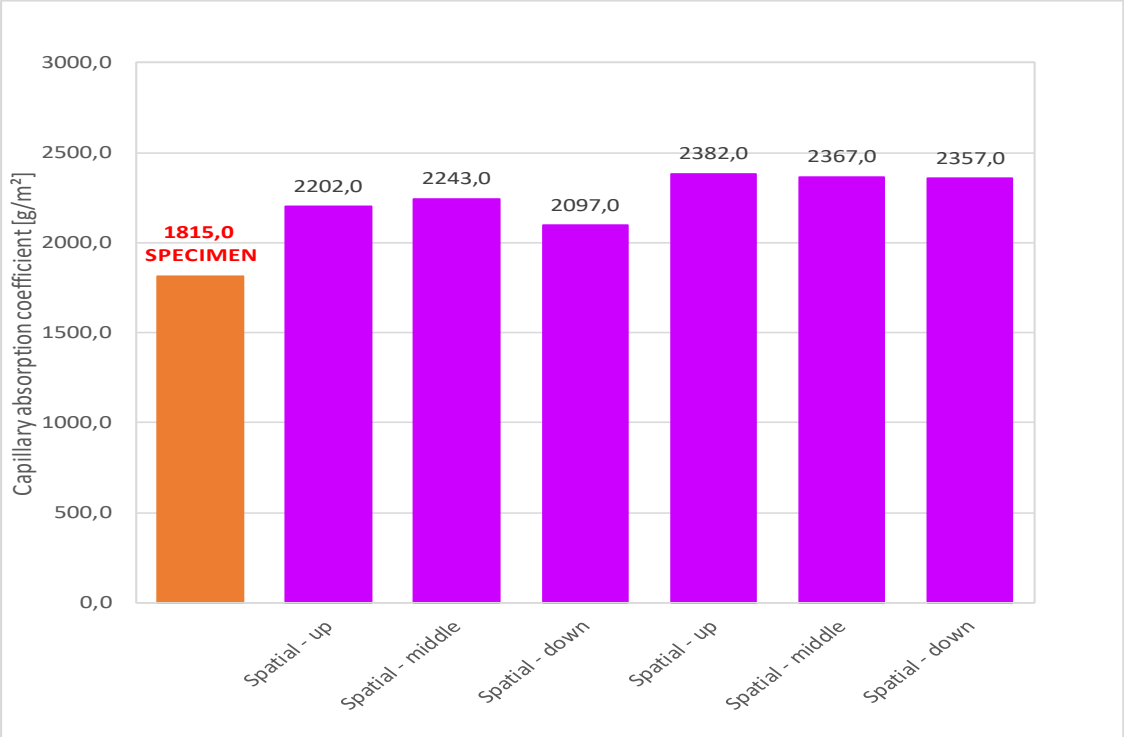

Figure 3.B.14. Capillary absorption coefficient C45/55 viaduct La Reunion (spatial study)

Table 3.B.3. Capillary absorption coefficient C45/55 viaduct La Reunion (spatial study)

	Localisation	Mean value	Min value	Max value	Number of measurements
Capillary absorption coefficient, 90 days (g/m²)	Spatial up core	2292	2202	2382	2
	Spatial middle core	2305	2243	2367	2
	Spatial down core	2227	2097	2357	2
		Mean value	**Standard deviation**	**Coefficient of variation**	**Number of measurements**
	Spatial cores	2275	114	5 %	6
	Molded sample specimen	1815	100	6 %	3

3.B.2.2 Spatial variability / Chloride migration D_{rcm}

Figure 3.B.15. Chloride migration D_{rcm} C30/37 ready mix concrete (spatial study)

Table 3.B.4. Chloride migration D_{rcm} C30/37 ready mix concrete (spatial study)

	Localisation	Mean value	Min value	Max value	Number of measurements
Chloride migration D_{rcm}, 90 days (10^{-12}.m²/s)	Spatial up core	13.5	12.4	14.2	3
	Spatial middle core	13.1	12.7	13.3	3
	Spatial down core	13.9	12.3	15.4	3
		Mean value	**Standard deviation**	**Coefficient of variation**	**Number of measurements**
	Spatial cores	13.5	1.0	7 %	9
	Molded sample specimen	20.7	-	-	-

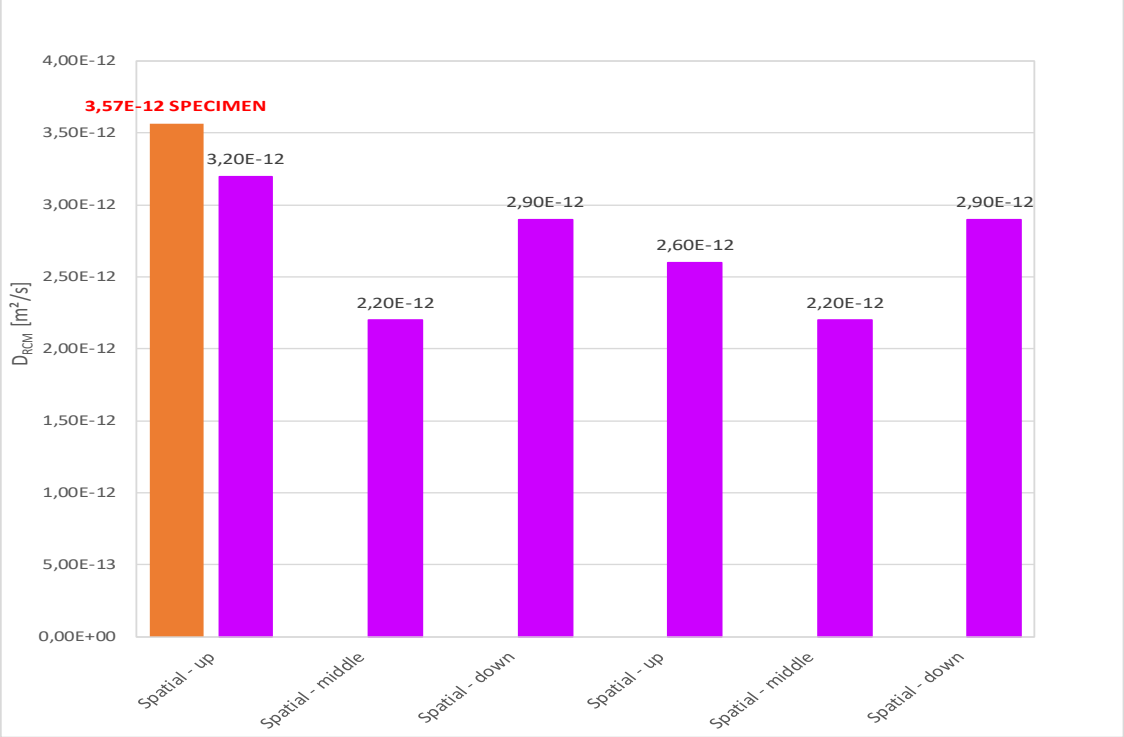

Figure 3.B.16. Chloride migration D_{rcm} C40/50 viaduct La Reunion (spatial study)

Table 3.B.5. Chloride migration D_{rcm} C40/50 viaduct La Reunion (spatial study)

	Localisation	Mean value	Min value	Max value	Number of measurements
Chloride migration D_{rcm}, 90 days (10^{-12}.m²/s)	Spatial up core	2.9	2.6	3.2	2
	Spatial middle core	2.2	2.2	2.2	2
	Spatial down core	2.9	2.9	2.9	2
		Mean value	**Standard deviation**	**Coefficient of variation)**	**Number of measurements**
	Spatial cores	2.7	0.4	15 %	6
	Molded sample specimen	3.6	0.4	11 %	3

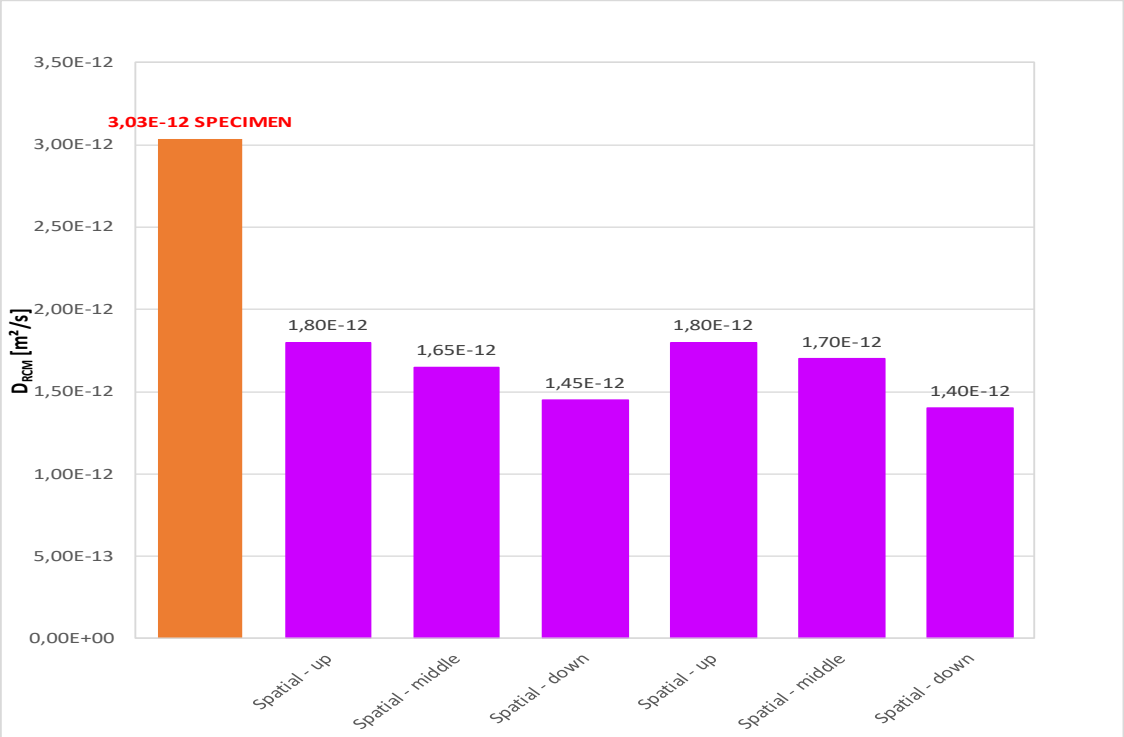

Figure 3.B.17: Chloride migration D_{rcm} C45/55 viaduct La Reunion (spatial study)

Table 3.B.6. Chloride migration D_{rcm} C45/55 viaduct La Reunion (spatial study)

	Localisation	Mean value	Min value	Max value	Number of measurements
Chloride migration D_{rcm}, 90 days (10^{-12}.m²/s)	Spatial up core	1.8	1.8	1.8	2
	Spatial middle core	1.7	1.6	1.7	2
	Spatial down core	1.4	1.4	1.5	2
		Mean value	**Standard deviation**	**Coefficient of variation**	**Number of measurements**
	Spatial cores	1.6	0.2	11 %	6
	Molded sample specimen	3.0	0.2	8 %	3

3.B.2.3 Spatial variability / Gas permeability k_{gas}

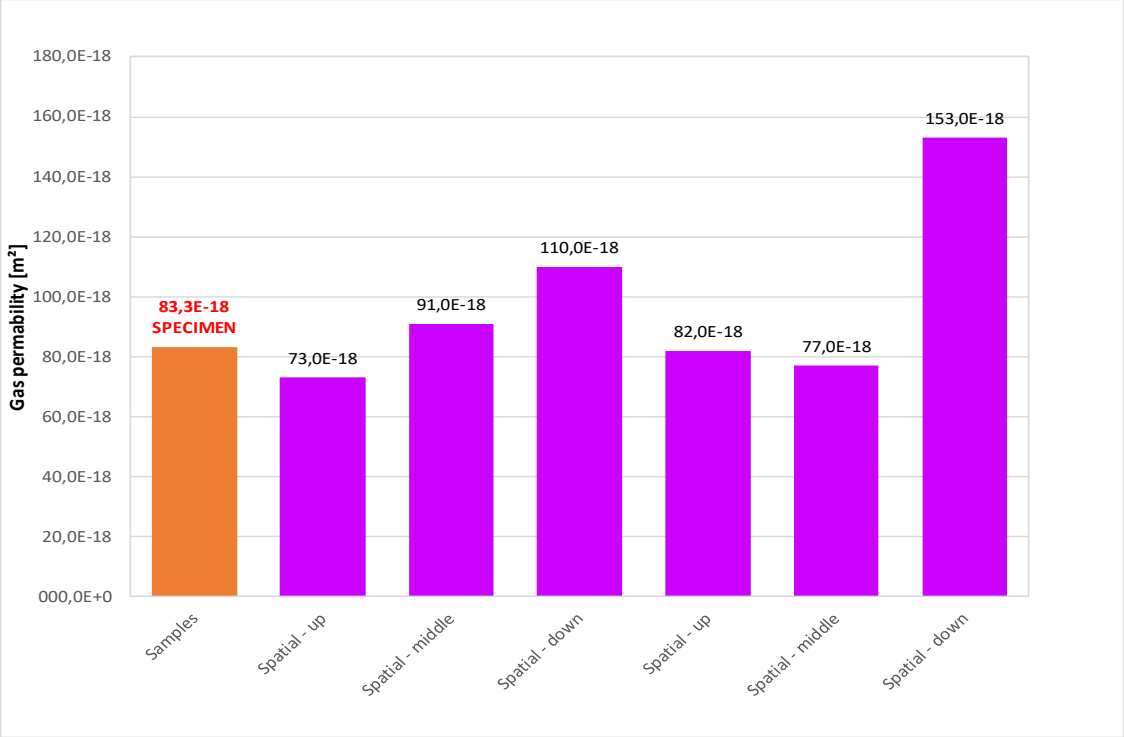

Figure 3.B.18. Gas permeability C40/50 viaduct La Reunion (spatial study)

Table 3.B.7. Gas permeability C40/50 viaduct La Reunion (spatial study)

	Localisation	Mean value	Min value	Max value	Number of measurements
Gas permeability, 90 days (10^{-18} m²)	Spatial up core	78	73	82	2
	Spatial middle core	84	77	91	2
	Spatial down core	132	110	153	2
		Mean value	**Standard deviation**	**Coefficient of variation**	**Number of measurements**
	Spatial cores	98	30	31 %	6
	Molded sample specimen	83	27	32 %	3

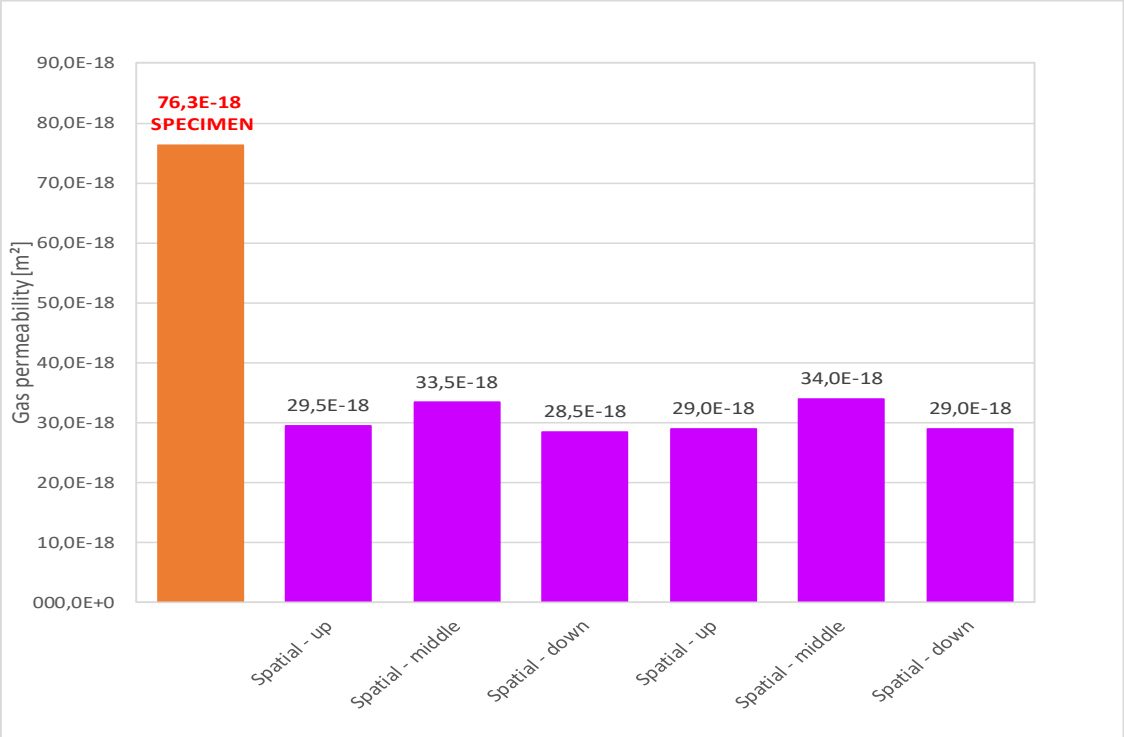

Figure 3.B.19. Gas permeability C45/55 viaduct La Reunion (spatial study)

Table 3.B.8. Gas permeability C45/55 viaduct La Reunion (spatial study)

	Localisation	Mean value	Min value	Max value	Number of measurements
Gas permeability, 90 days (10^{-18} m²)	Spatial up core	29	29	29	2
	Spatial middle core	34	33	34	2
	Spatial down core	29	29	29	2
		Mean value	**Standard deviation**	**Coefficient of variation**	**Number of measurements**
	Spatial cores	31	2	8 %	6
	Molded sample specimen	76	15	19 %	3

3.B.3 Appendix paragraph 9.5.3

3.B.3.1 Curing study / Capillary absorption coefficient

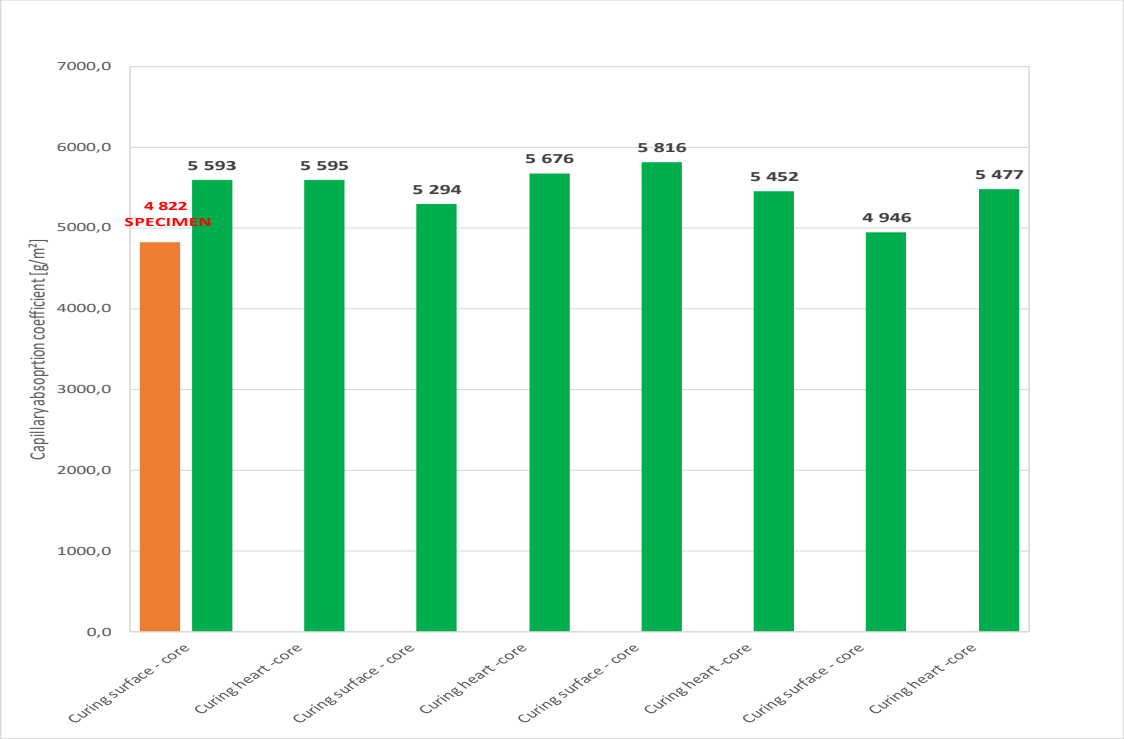

Figure 3.B.20. Capillary absorption coefficient C30/37 ready mix concrete (curing study)

Table 3.B.9. Capillary absorption coefficient C30/37 ready mix concrete (curing study)

	Localisation	Mean value	Min value	Max value	Number of measurements
Capillary absorption coefficient, 90 days (g/m²)	Curing surface core	5412	4946	5816	4
	Curing heart core	5550	5452	5676	4
		Mean value	**Standard deviation**	**Coefficient of variation**	**Number of measurements**
	Curing cores	5481	267	5 %	8
	Molded sample specimen	4822	-	-	-

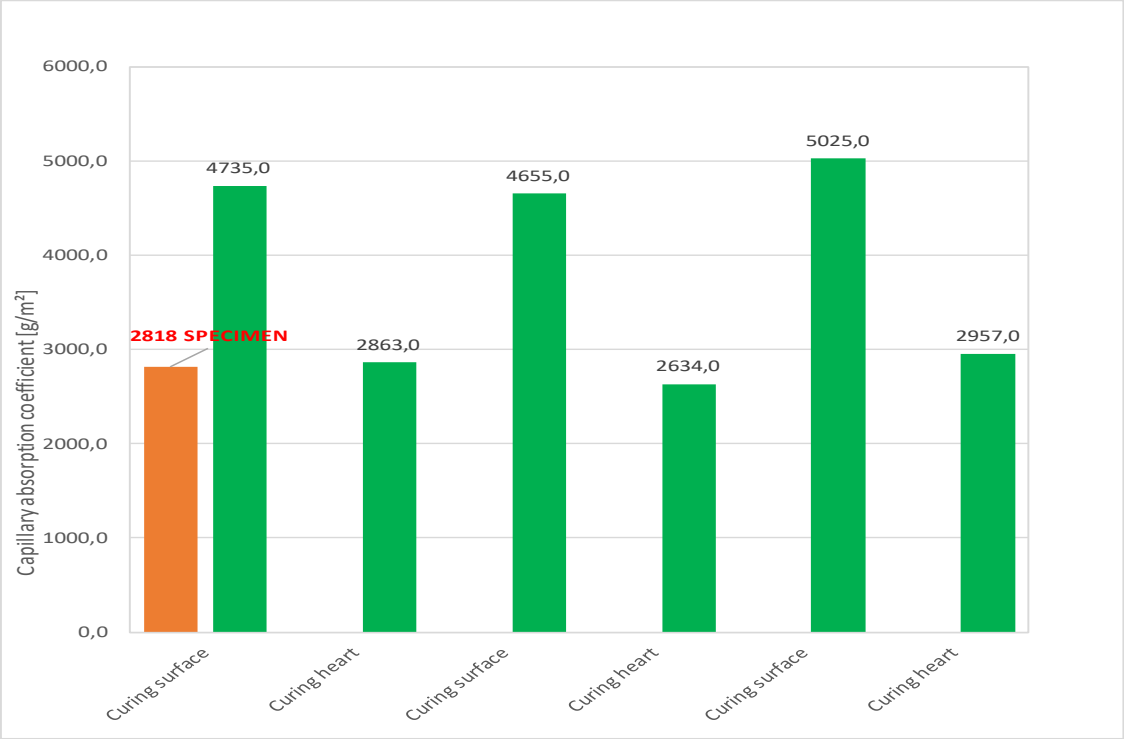

Figure 3.B.21. Capillary absorption coefficient C40/50 viaduct La Reunion (curing study)

Table 3.B.10. Capillary absorption coefficient C40/50 viaduct La Reunion (curing study)

	Localisation	Mean value	Min value	Max value	Number of measurements
Capillary absorption coefficient, 90 days (g/m²)	Curing surface core	4805	4655	5025	3
	Curing heart core	2818	2634	2957	3
		Mean value	**Standard deviation**	**Coefficient of variation**	**Number of measurements**
	Curing cores	3811	1100	29 %	6
	Molded sample specimen	2818	79	3 %	3

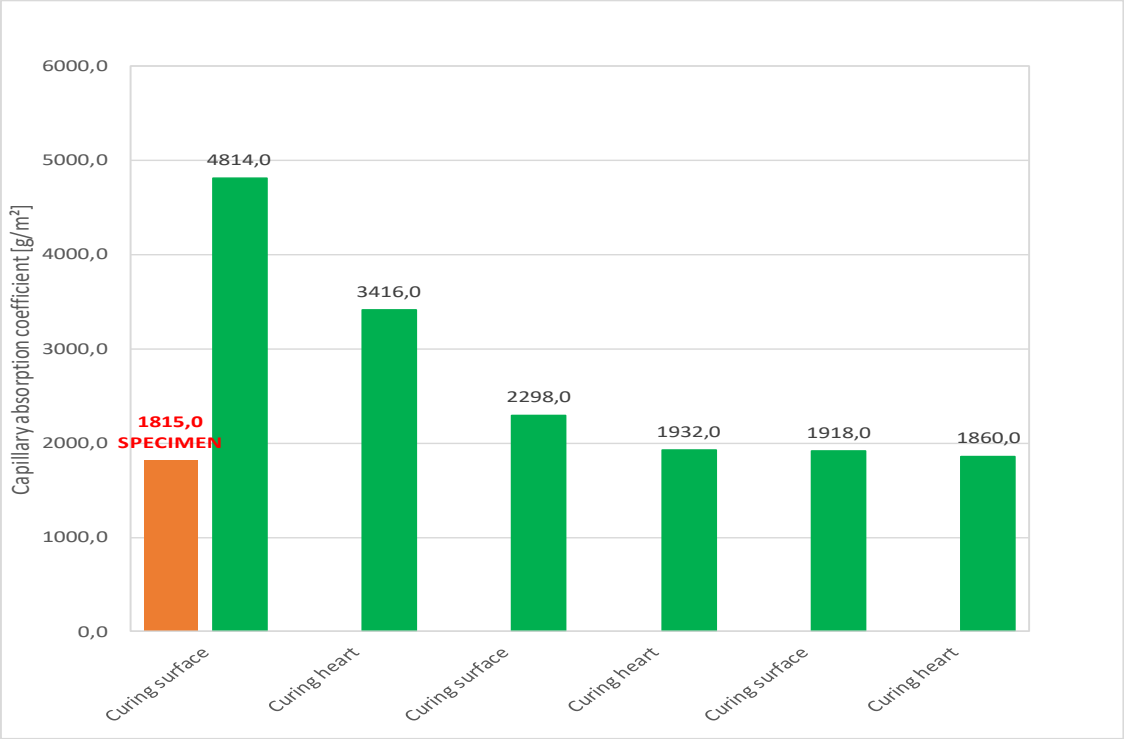

Figure 3.B.22. Capillary absorption coefficient C45/55 viaduct La Reunion (curing study)

Table 3.B.11. Capillary absorption coefficient C45/55 viaduct La Reunion (curing study)

	Localisation	Mean value	Min value	Max value	Number of measurements
Capillary absorption coefficient, 90 days (g/m²)	Curing surface core	3010	1918	4814	3
	Curing heart core	2403	1860	3416	3
		Mean value	**Standard deviation**	**Coefficient of variation**	**Number of measurements**
	Curing cores	2706	1187	44 %	6
	Molded sample specimen	1815	100	6 %	3

3.B.3.2 Curing study / Chloride migration D_{rcm}

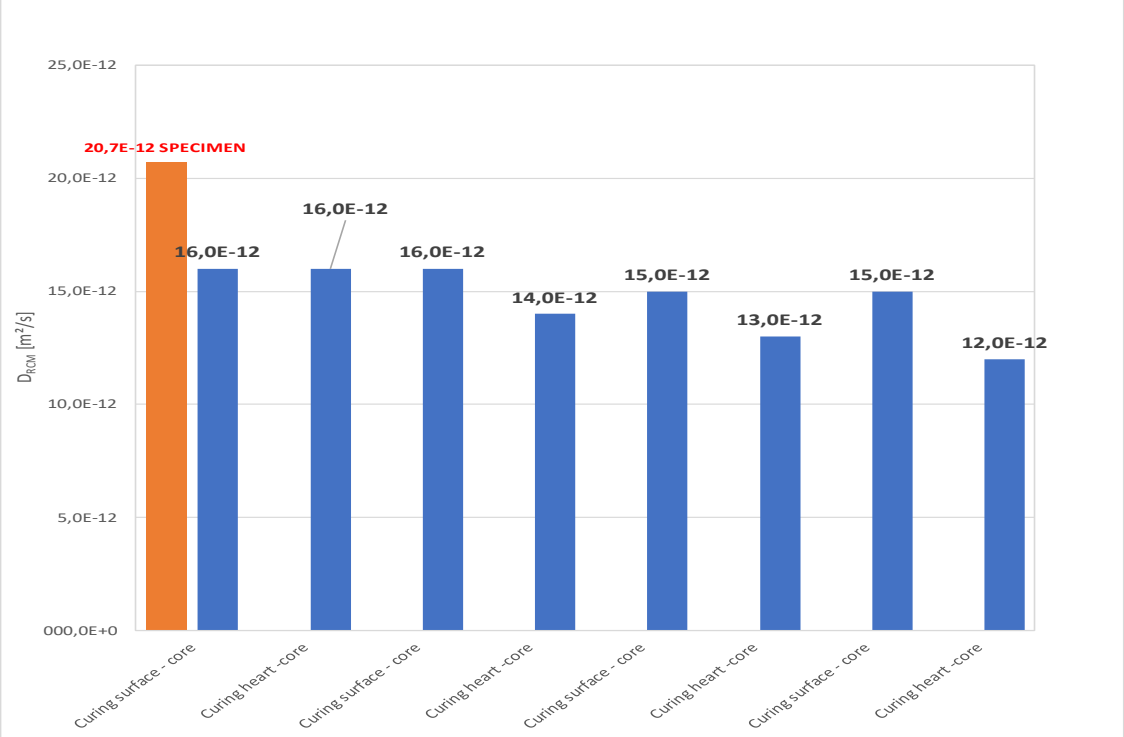

Figure 3.B.23. Chloride migration D_{rcm} C30/37 ready mix concrete (curing study)

Table 3.B.12. Chloride migration D_{rcm} C30/37 ready mix concrete (curing study)

Chloride migration D_{rcm}, 90 days (10^{-12} m²/s)	**Localisation**	**Mean value**	**Min value**	**Max value**	**Number of measurements**
	Curing surface core	15.5	15.0	16.0	4
	Curing heart core	13.8	12.0	16.0	4
		Mean value	**Standard deviation**	**Coefficient of variation**	**Number of measurements**
	Curing cores	14.6	1.5	10 %	8
	Molded sample specimen	20.7	-	-	-

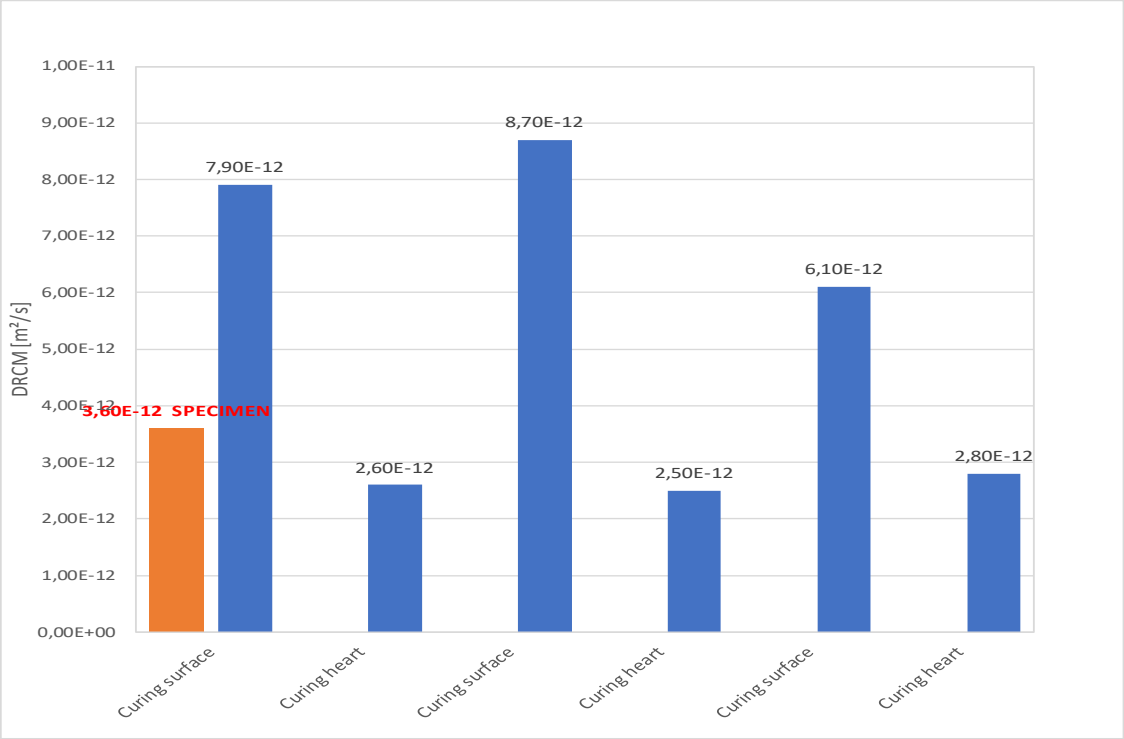

Figure 3.B.24. Chloride migration D_{rcm} C40/50 viaduct La Reunion (curing study)

Table 3.B.13. Chloride migration D_{rcm} C40/50 viaduct La Reunion (curing study)

	Localisation	Mean value	Min value	Max value	Number of measurements
Chloride migration D_{rcm}, 90 days (10^{-12} m²/s)	Curing surface core	7.6	6.1	8.7	3
	Curing heart core	2.6	2.5	2.8	3
		Mean value	**Standard deviation**	**Coefficient of variation**	**Number of measurements**
	Curing cores	5.1	2.8	56 %	6
	Molded sample specimen	3.6	0.4	11 %	3

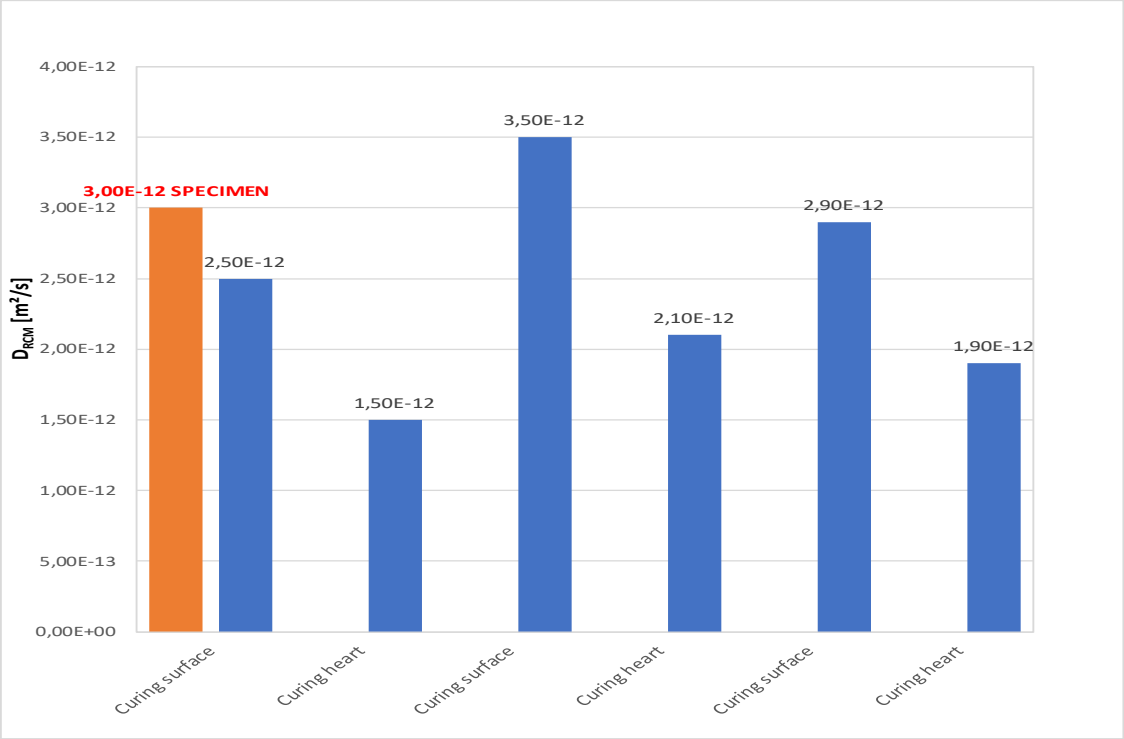

Figure 3.B.25. Chloride migration D_{rcm} C45/55 viaduct La Reunion (curing study)

Table 3.B.14. Chloride migration D_{rcm} C45/55 viaduct La Reunion (curing study)

	Localisation	Mean value	Min value	Max value	Number of measurements
Chloride migration D_{rcm} 90 days (10^{-12} m²/s)	Curing surface core	3.0	2.5	3.5	3
	Curing heart core	1.8	1.5	2.1	3
		Mean value	**Standard deviation**	**Coefficient of variation**	**Number of measurements**
	Curing cores	2.4	0.7	30 %	6
	Molded sample specimen	3.0	0.2	8 %	3

3.B.4 Appendix paragraph 9.6

3.B.4.1 Capillary absorption coefficient

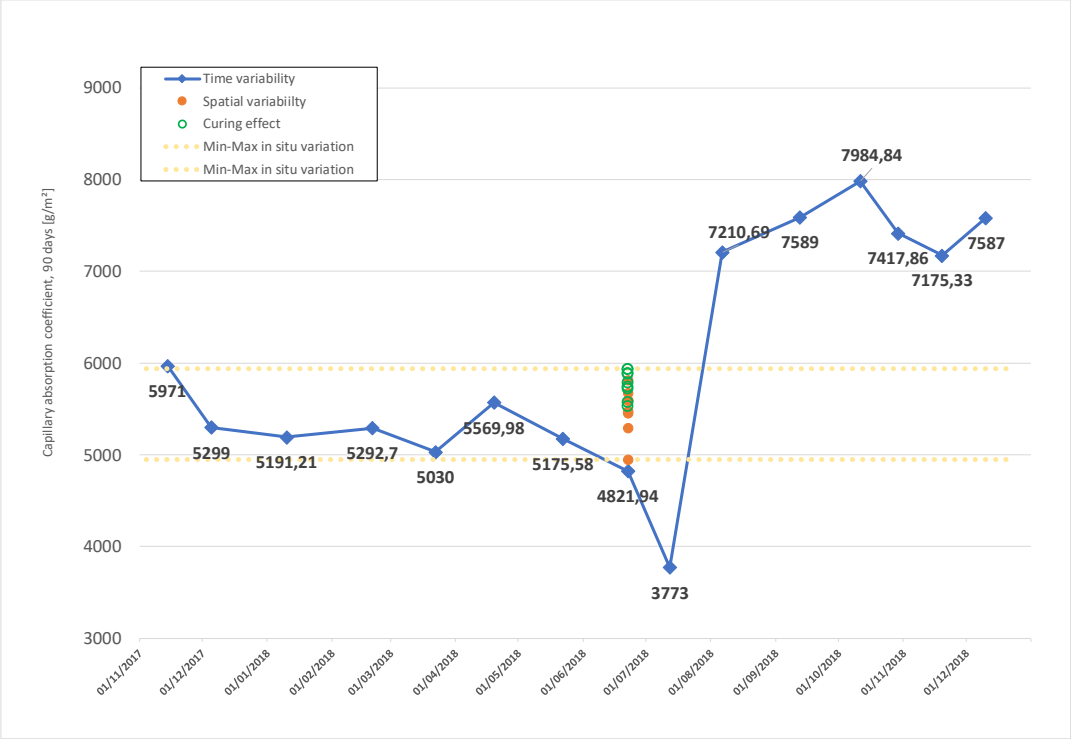

Figure 3.B.26. Capillary absorption coefficient C30/37 ready mix concrete (temporal/in situ variability)

Table 3.B.15. Capillary absorption coefficient C30/37 ready mix concrete (temporal/in situ variability)

Capillary absorption coefficient, 90 days (g/m²)	**Temporal variability (on sample)**	
	Mean value	6073
	Standard deviation	1297
	Coefficient of variation	21 %
	Min value	3773
	Max value	7985
	Mean value (on sample – day of testing wall)	4822
	In-situ variability (on core)	
	Mean value In-situ variability	5630
	Min value In-situ variability	4946
	Max value In-situ variability	5938

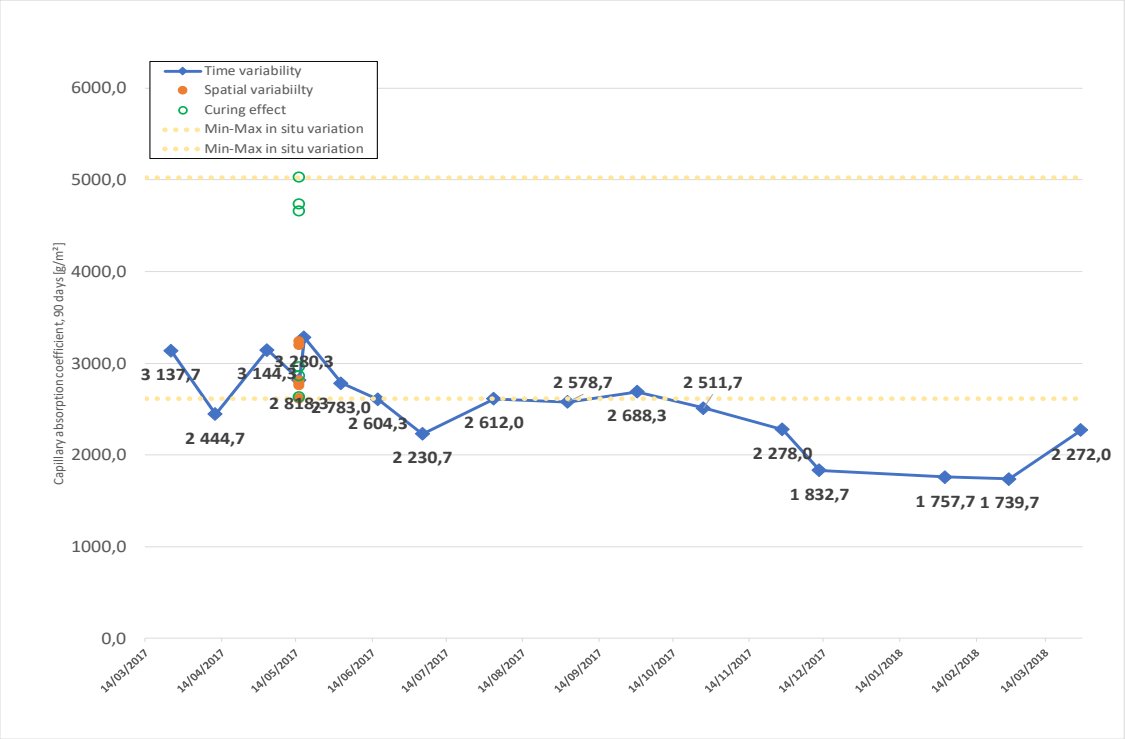

Figure 3.B.27. Capillary absorption coefficient C40/50 viaduct La Reunion (temporal/in situ variability)

Table 3.B.16. Capillary absorption coefficient C40/50 viaduct La Reunion (temporal/in situ variability)

Capillary absorption coefficient, 90 days (g/m²)	**Temporal variability (on sample)**	
	Mean value	2513
	Standard deviation	463
	Coefficient of variation	18 %
	Min value	1740
	Max value	3280
	Mean value (on sample – day of testing wall)	2818
	In-situ variability (on core)	
	Mean value In-situ variability	3301
	Min value In-situ variability	2616
	Max value In-situ variability	5025

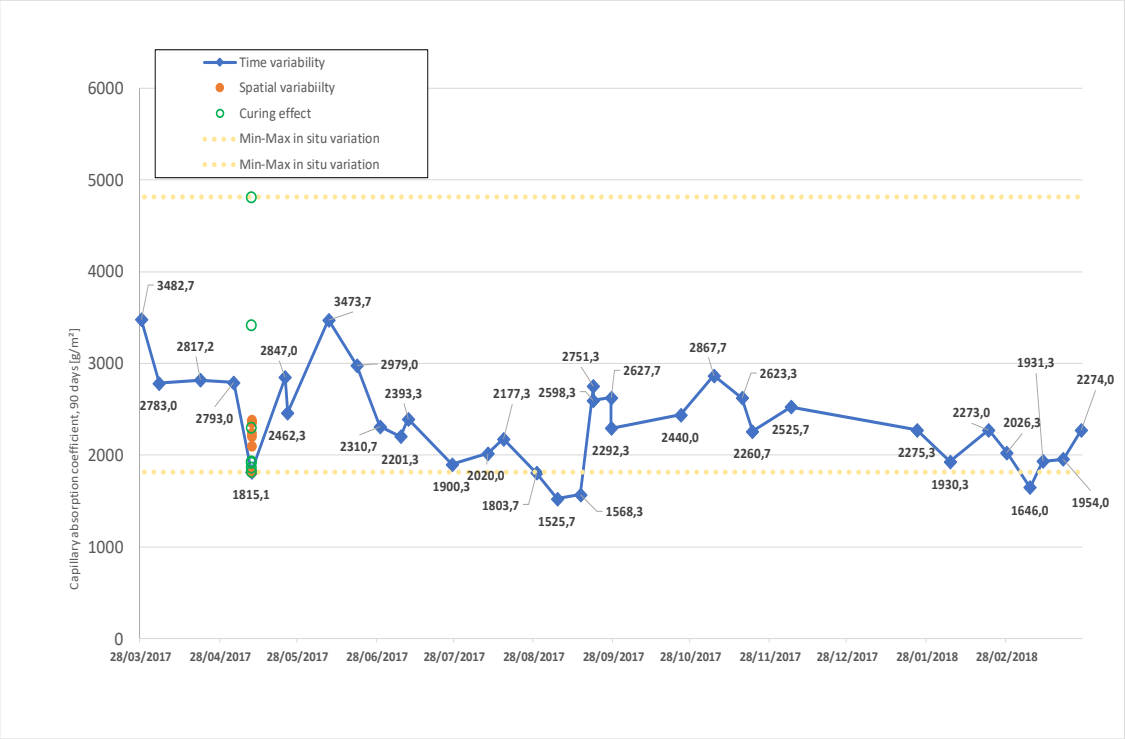

Figure 3.B.28. Capillary absorption coefficient C45/55 viaduct La Reunion (temporal/in situ variability)

Table 3.B.17. Capillary absorption coefficient C45/55 viaduct La Reunion (temporal/in situ variability)

Capillary absorption coefficient, 90 days (g/m²)	**Temporal variability (on sample)**	
	Mean value	2361
	Standard deviation	481
	Coefficient of variation	20 %
	Min value	1526
	Max value	3483
	Mean value (on sample – day of testing wall)	1815
	In-situ variability (on core)	
	Mean value In-situ variability	2491
	Min value In-situ variability	1860
	Max value In-situ variability	4814

Capillary water absorption in the RMC series shows a **net gap** between a first group of results (November 2017- July 2018, average **5125 g/m²**) and a second one (August 2018-December 2018, average **7494 g/m²**) whose cause has not been identified.
The overall coefficient of variation (21 %) is moreover the same as in La Réunion measurements (even if the results are not clearly separated in that case).
We quote from that report: *High dispersion between individual findings with sometimes a difference of around 600 g/m² between minimum and maximum value of a same concrete sample raising the question of reliability of testing protocol".*

3.B.4.2 Chloride migration D_{rcm}

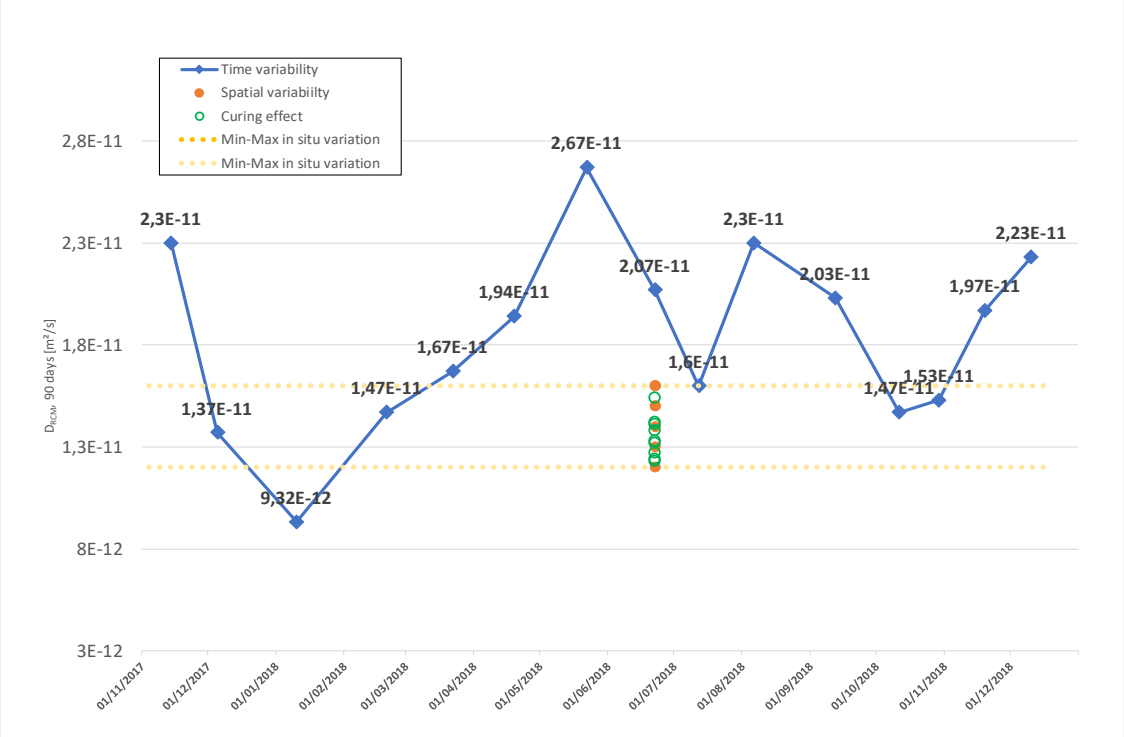

Figure 3.B.29. D_{rcm} C30/37 ready mix concrete (temporal/in situ variability)

Table 3.B.18. D_{rcm} C30/37 ready mix concrete (temporal/in situ variability)

Chloride migration D_{rcm}, 90 days (10^{-12} m²/s)	**Temporal variability (on sample)**	
	Mean value (10^{-12} m²/s)	18.0
	Standard deviation	5.0
	Coefficient of variation	25 %
	Min value	9.3
	Max value	27
	Mean value (on sample – day of testing wall)	20.7
	In-situ variability (on core)	
	Mean value In-situ variability	14.1
	Min value In-situ variability	12.0
	Max value In-situ variability	16.0

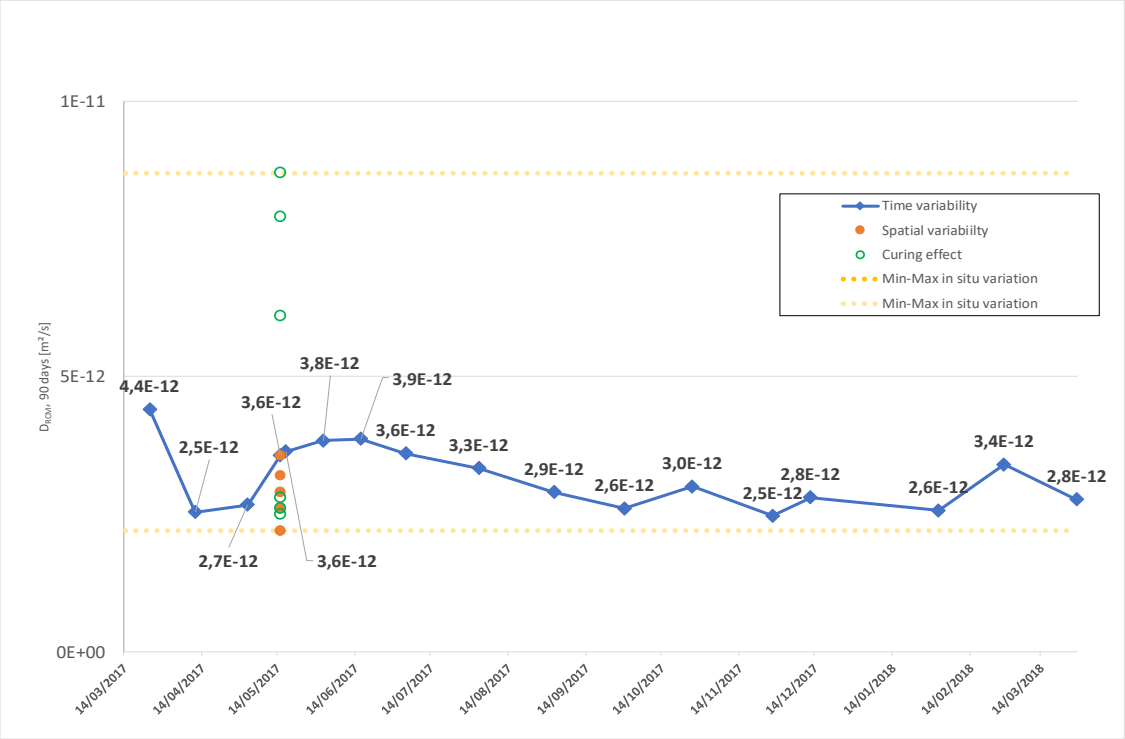

Figure 3.B.30. D_{rcm} C40/50 viaduct La Reunion (temporal/in situ variability)

Table 3.B.19. D_{rcm} C40/50 viaduct La Reunion (temporal/in situ variability)

Chloride migration D_{rcm}, 90 days (10^{-12} m²/s)	**Temporal variability (on sample)**	
	Mean value	3.2
	Standard deviation	0.6
	Coefficient of variation	18 %
	Min value	2.5
	Max value	4.4
	Mean value (on sample – day of testing wall)	3.6
	In-situ variability (on core)	
	Mean value In-situ variability	5.5
	Min value In-situ variability	2.2
	Max value In-situ variability	8.7

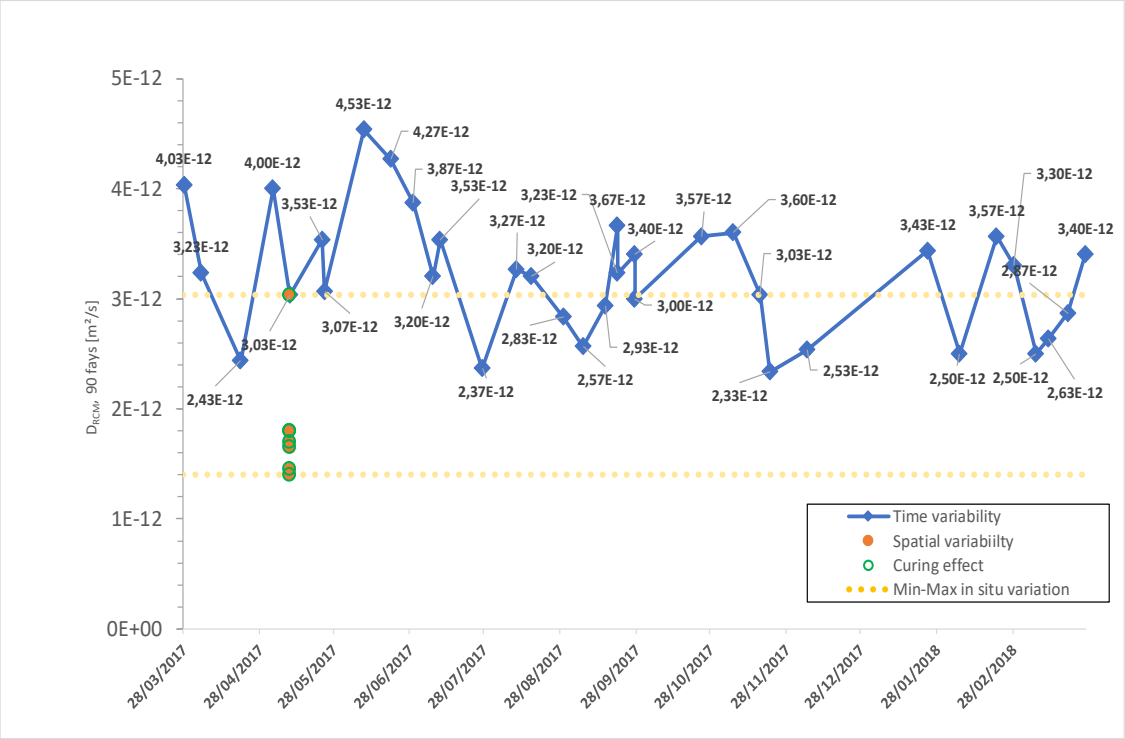

Figure 3.B.31. D_{rcm} C45/55 viaduct La Reunion (temporal/in situ variability)

Table 3.B.20. D_{rcm} C45/55 viaduct La Reunion (temporal/in situ variability)

Chloride migration D_{rcm}, 90 days (10^{-12} m²/s)	**Temporal variability (on sample)**	
	Mean value	3.2
	Standard deviation	0.6
	Coefficient of variation	17 %
	Min value	2.3
	Max value	4.5
	Mean value (on sample – day of testing wall)	3.0
	In-situ variability (on core)	
	Mean value In-situ variability	2.5
	Min value In-situ variability	1.4
	Max value In-situ variability	3.5

Chloride migration coefficient (90d) is varying during the whole year; no seasonal sensitivity seems to be traceable.

The difference on D_{rcm} between Ready Mix Concrete and La Réunion is linked to the cementitious materials types (to less extent to lower W/C ratio).

3.B.4.3 Gas Permeability

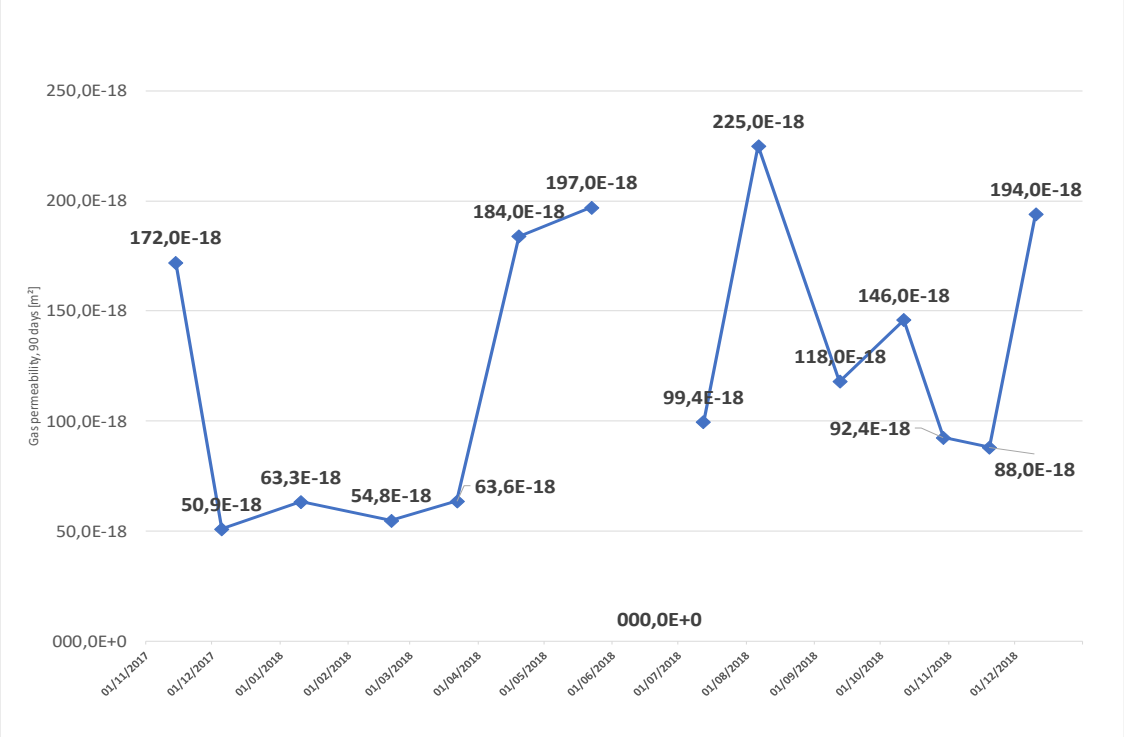

Figure 3.B.32. Gas permeability C30/37 ready mix concrete (temporal/in situ variability)

Table 3.B.21. Gas permeability C30/37 ready mix concrete (temporal/in situ variability)

Gas permeability, 90 days (10^{-18} m²)	**Temporal variability (on sample)**	
	Mean value	128
	Standard deviation	65
	Coefficient of variation	51 %
	Min value	51
	Max value	225
	Mean value (on sample – day of testing wall)	-
	In-situ variability (on core)	
	Mean value In-situ variability	**-**
	Min value In-situ variability	**-**
	Max value In-situ variability	**-**

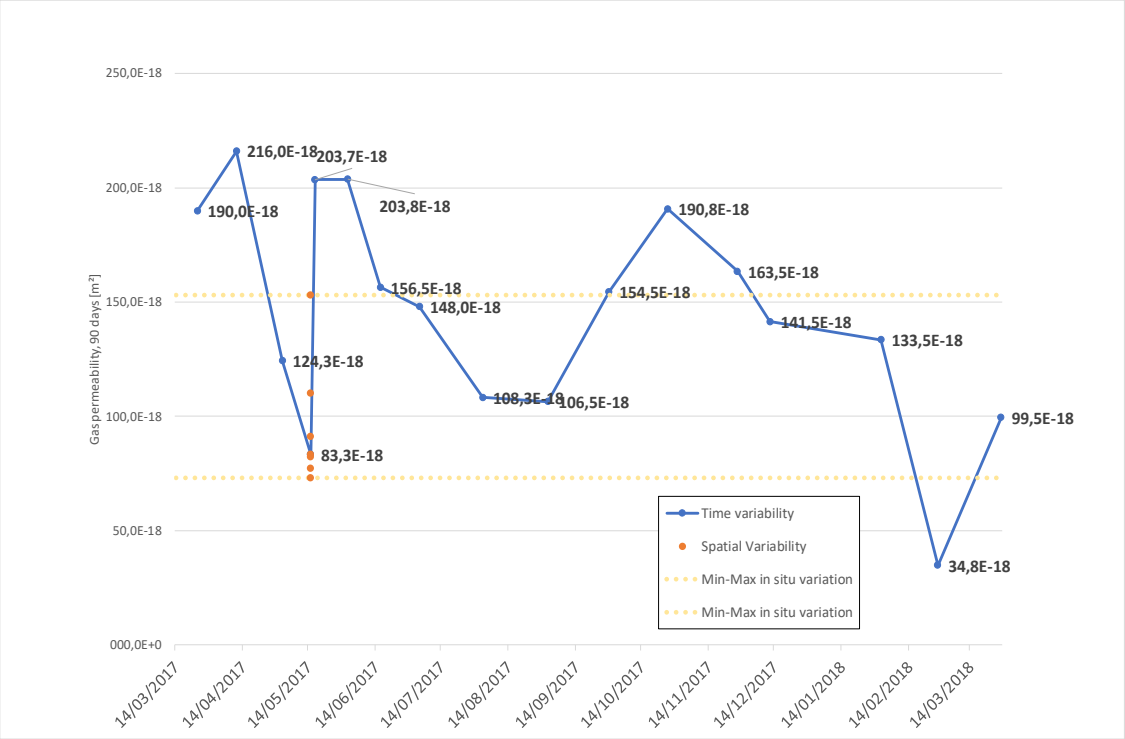

Figure 3.B.33. Gas permeability C40/50 viaduct La Reunion (temporal/in situ variability)

Table 3.B.22. Gas permeability C40/50 viaduct La Reunion (temporal/in situ variability)

Gas permeability, 90 days (10^{-18} m²)	**Temporal variability (on sample)**	
	Mean value	145
	Standard deviation	49
	Coefficient of variation	34 %
	Min value	35
	Max value	216
	Mean value (on sample – day of testing wall)	83
	In-situ variability (on core)	
	Mean value In-situ variability	98
	Min value In-situ variability	73
	Max value In-situ variability	153

For the Ready Mix Concrete C30/37 series, gas permeability coefficient (K_{gaz}), 90d, shows an significant variation all along the 1-year testing session, varying from a minimum value of $51 \cdot 10^{-18}$ m² to a maximum of $255 \cdot 10^{-18}$ m².

The average value is $127 \cdot 10^{-18}$ m², not far from the average value in La Réunion test session (segment mix), i.e. $123 \cdot 10^{-18}$ m² (but for a compressive strenght class of 45/55).

The standard deviation being of $65 \cdot 10^{-18}$ m², this leads to a variation coefficient of 0,51 (as a reminder, the same magnitude was associated to a 0.70 variation coefficient for the La Réunion test series).

For the La Réunion series, Gas permeability results highlight very high variability during the 1-year of measurement with important variation coefficients of 49 % and 34 % respectively for 28 and 90-day of concrete maturity. Moreover, there are a very high dispersion with sometimes between 200.10^{-18} m² and 400.10^{-18} m² between individual results of a same concrete sample. As a reminder, gas permeability criterion is ≤ 200.10^{-18} m² according to Fascicule 65 French recommendations for a XS3 exposure class.

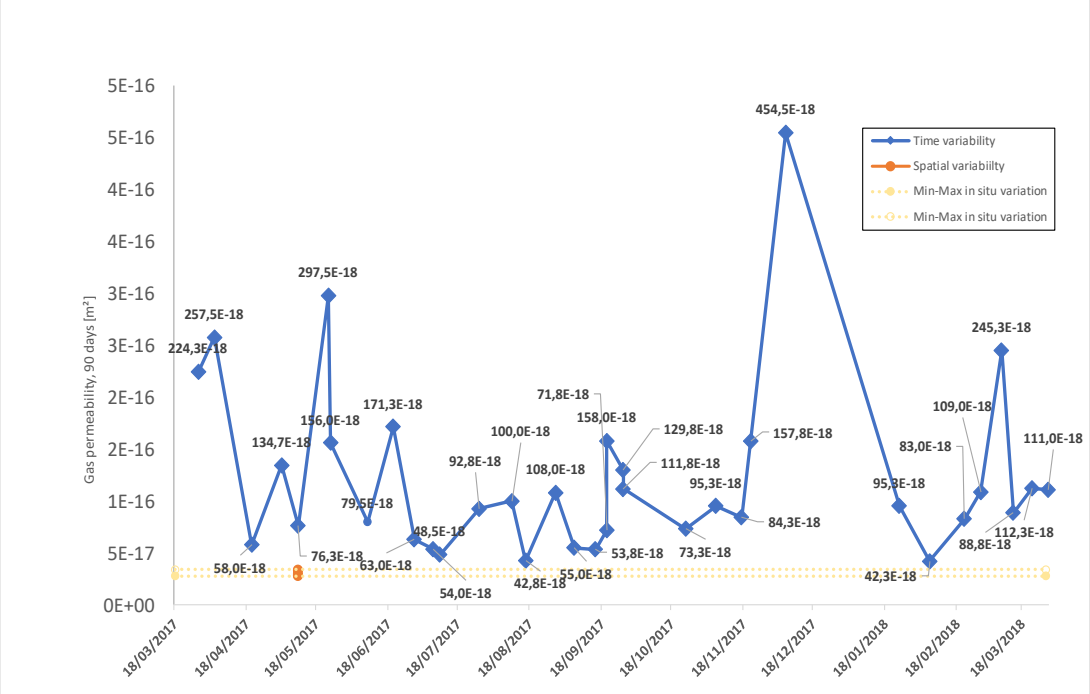

Figure 3.B.34. Gas permeability C45/55 viaduct La Reunion (temporal/in situ variability)

Table 3.B.23. Gas permeability C45/55 viaduct La Reunion (temporal/in situ variability)

Gas permeability, 90 days (10^{-18} m²)	**Temporal variability (on sample)**	
	Mean value	123
	Standard deviation	85
	Coefficient of variation	70 %
	Min value	42
	Max value	455
	Mean value (on sample – day of testing wall)	76
	In-situ variability (on core)	
	Mean value In-situ variability	31
	Min value In-situ variability	29
	Max value In-situ variability	34

Gas permeability results highlight very high variability during the 1-year of measurement with important variation coefficients of 70 % for 90-day of concrete maturity. Moreover, there are a very high dispersion with sometimes more than 400.10^{-18} m² between individual results of a same concrete sample. As a reminder, gas permeability criterion is ≤ 200.10^{-18} m² according to Fascicule 65 French recommendations for a XS3 exposure class.

CHAPTER 4

Definition of performance thresholds according to exposure classes

Authors *(Organisations)*

Myriam Carcassès *(LMDC, Université de Toulouse)*

François Cussigh *(VINCI Construction France)*

François Toutlemonde (Appendix) *(Université Gustave Eiffel)*

Work Group: WG2B

Summary

1 Introduction

The purpose of this report is to explain the sources of the performance threshold values defined to ensure compliance with a satisfactory design service life (50 years or 100 years) for the exposure classes related to the reinforcement corrosion issue (XC, XS and XD).

It details the hypotheses adopted for the calculation of service life by modelling the initiation and corrosion phases, and then compares the results of the performance thresholds obtained with those observed on concretes complying with the usual prescriptive rules allowing the required durability to be obtained a priori.

Finally, following the convergence of the thresholds supervised by the Scientific Committee, it led to the definition of performance thresholds by exposure class and design service life.

2 Modelling contributions for the XC, XD and XS exposure classes

2.1 Introduction

The modelling part of the French national PerfDuB project aimed at setting up a methodology to justify the durability of concrete structures using a performance-based approach to durability. Based on available scientific models for the different phenomena involved (i.e. carbonation, chloride ion penetration and chloride ion- or carbonation-induced corrosion), the objective was to propose a global engineering model capable of providing a reliable assessment of the service life of reinforced concrete structures subject to corrosion risk. This service life (t_{final}) is defined by calculating the sum of the corrosion initiation period (t_{ini}) and the corrosion propagation period (t_{prop}):

$$t_{final} = t_{ini} + t_{prop} \qquad \text{(Equ. 4.1)}$$

It is indeed essential to take into account the corrosion propagation stage, whether during the design of the structure or during the re-evaluation of an existing structure with a view, for example, to planning a possible repair. As far as the design of a new structure is concerned, taking into account the propagation phase should allow the thickness of the cover to be optimised, as design based on the initiation time alone is excessively safe, particularly for carbonation.

The service limit criterion chosen in this project is the quantity of corrosion products assumed to be necessary for the appearance of the first corrosion-induced cracks: this is a safe approach linked to operational practice.

The work presented is the result of this modelling approach: it is a model that integrates different phenomenologies depending on the exposure class considered. All the input data for the model are characteristic values.

The originality of the model used, resulting from the French ANR MODEVIE project, is that it is based both on physico-chemical phenomena recognized as being of the first order for the risks of corrosion of reinforcement and on input parameters easily accessible to the engineer insofar as they are measurable using standardized operating procedures.

Concerning the robustness of the model, it is based on the consideration of:

- data from the literature on the different mechanisms related to CO_2 or chloride diffusion and reinforcement corrosion;

- experimental results from the French PerfDuB National Project database corresponding to 42 concretes;
- observations made on old structures exposed to different environmental conditions;
- the variability of the input parameters;
- and the comparison of the service lives calculated by the model with the service lives specified in the standards (50 or 100 years), for different concrete/cover combinations defined in standard NF EN 206/CN and Eurocode 2 according to the exposure classes.

First, the general principles of the model are presented and then performance thresholds are proposed.

2.2 Exposure classes XC

2.2.1 Modelling of the initiation time

As in most analytical carbonation models, such as the *fib* model-code 2010, we assume that the evolution of the carbonation depth (x_c) as a function of time is controlled by CO_2 diffusion. x_c (mm) is therefore written as a function of the square root of time (yr):

$$x_c(t) = v_{nat}\, k_{RH}\, k_c \sqrt{t_{eff}} \qquad \text{(Equ. 4.2)}$$

The rate of carbonation depends on both material properties and environmental conditions. To take account each of these parameters, the model is rewritten by decomposing each effect by independent empirical functions that were constructed from the French PerfDuB project database, as well as from data in the literature. These functions are described below.

- **v_{nat} (mm/year^{0,5}), the natural carbonation rate** is the carbonation rate under reference conditions of 20 °C, 65% relative humidity and 450 ppm CO_2. It is obtained for concrete subjected to carbonation under these conditions after a 90-day wet cure. Since atmospheric carbonation is a slow phenomenon, v_{nat} can be deduced from the results of an accelerated carbonation test. The latter is carried out according to a protocol defined during the French PerfDuB project, with a 3% CO_2 concentration and a preconditioning phase to obtain a sufficiently desaturated zone to facilitate gas diffusion (revised version of XP-P18-458 published in 2022). During this project, 42 concrete mixes were tested under natural and accelerated conditions to determine a correlation between v_{nat} (mm/year^{0,5}) and v_{acc} (mm/day^{0,5}), the accelerated carbonation rate. The regression parameter (α) of the following linear relationship is determined from the figure below (Figure 4.1) for which only those accelerated carbonation results are retained that lead to an acceptable coefficient of determination in accordance with the test method used.

  $$v_{nat} = \alpha\, v_{acc} \qquad \text{(Equ. 4.3)}$$

  The results obtained on existing structures (GT2a, chapter 2) seem consistent with this correlation.

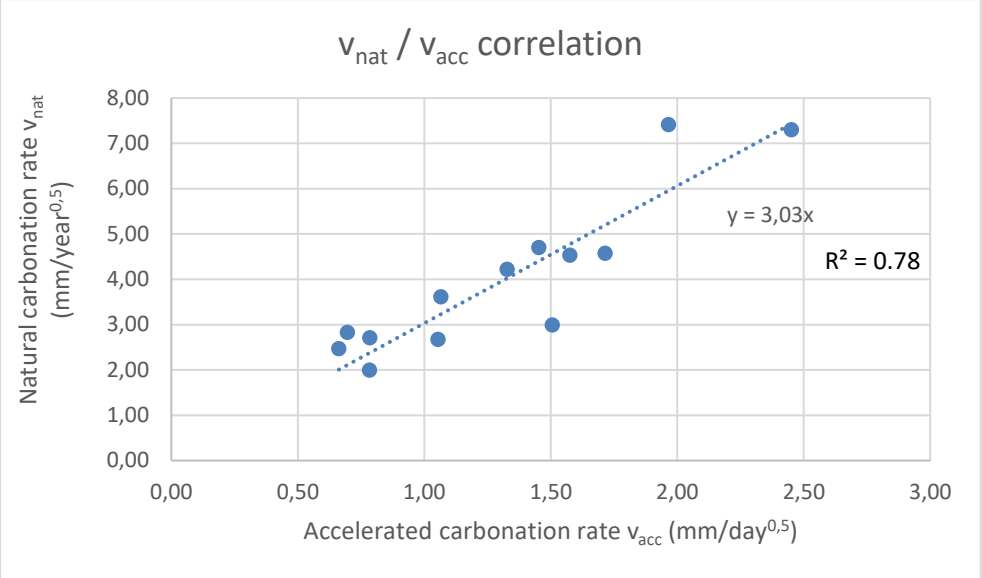

Figure 4.1. Correlation between v_{nat} and v_{acc} deduced from the results obtained on PerfDuB concretes

- **t_{eff} (year), the time of effective carbonation:** the humidification/drying cycles due to rain strongly influence the progression of the carbonation front. x_c no longer progresses as soon as the surface of the material is saturated with rainwater. A drying period is then necessary so that the "drying front" exceeds x_c to allow CO_2 diffusion and carbonation to progress further downstream (Bakker, 1993). From this observation, an effective carbonation time is defined as follows:

$$t_{eff} = t - (t_w + t_d) = (1 - (1 + \beta_w)\, ToW)\, .\, t \qquad \text{(Equ. 4.4)}$$

where t is the total exposure time, t_w is the total humidification time and t_d is the time required for the "drying front" to reach the carbonation front. To simplify this equation, it is assumed that the relationship between t_d and t_w is linear. Indeed, these two times are essentially related to the pore distribution. This rather safe approach leads to introduce two parameters: a constant β_w and T_0W the proportion of the number of rainy days per year.

To define the number of rainy days, we choose to use a daily precipitation threshold of 10 mm (which is a high enough value to remain safe). The latter data comes from the study detailed in (Vu *et al.*, 2019) on 45 concretes subjected to natural carbonation, sheltered or not from rain, for 5 years in different countries. From these data, β_w was found to be at least equal to 1.5: this is the value retained. T_0W is determined from the exposure class: it is taken as 0 for classes XC1 to XC3 and 0.05 for class XC4. This value is retained for France and corresponds to a national minimum value, which remains on the safe side. It is possible to retrieve weather data for a longer return period and a wider area of investigation (including France) on CLIMDEX: https://www.climdex.org.

- **k_{RH} (unitless), influence of ambient relative humidity on the initiation phase:** the carbonation rate is generally maximum for a relative humidity (RH) of about 60%. For high RH, the carbonation rate is controlled by the diffusion of CO_2, while for low RH, it is mainly controlled by the kinetics of chemical reactions. The proposed carbonation model is based on the assumption that carbonation is controlled by gas diffusion. Strictly speaking, the effect of low RH cannot be taken into account with this model. However, in a phenomenological approach, we propose an empirical function to model the influence of RH over the whole range (0 to 100%):

$$k_{RH} = 1.1\left(1 - \left(\frac{(RH - 50)}{50}\right)^2\right) \quad \text{(Equ. 4.5)}$$

The Figure 4.2 compares this k_{RH}-function to the *fib* model and to data from the literature.

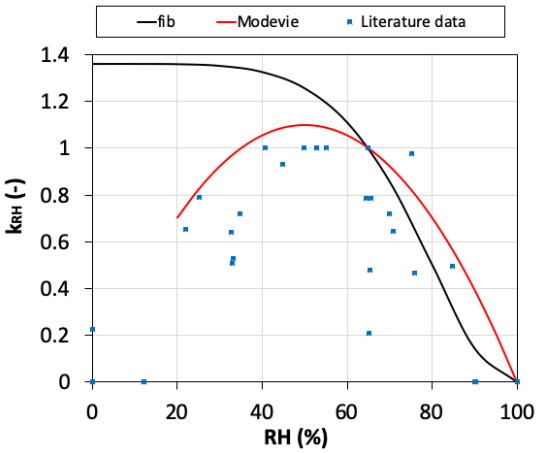

Figure 4.2. Comparison of literature data with the fib model and the Modevie model of relative humidity (RH) on the carbonation rate

The RH value thus corresponds to the ambient relative humidity value in France and is determined from the exposure class according to Table 4.1.

Table 4.1. Carbonation model data

Exposure class	RH relative humidity (%)
XC1	50
XC2	90
XC3	75
XC4	65

- **k_c (unitless), influence of the cure:** In our model, $\underline{k_c}$ is considered as a constant equal to 1. This approach is based on the following considerations:
  - the relationship 4.3 between v_{nat} and v_{acc} is established for a wet cure of 90 days. In the case of a short curing period ("dry curing") corresponding to a demoulding when the compressive strength is equal to 35 % of f_{c28d}, the results obtained from the PerfDuB database show an apparent carbonation rate multiplied by 2 when using the first measurement periods (up to 2 years) but with a strong inflection towards lower rates after 1 year tending towards the rates measured in wet curing conditions;
  - the choice of a $\underline{k_c} = 1$ is consistent with the results obtained on old structures (GT2a: chapter 2) where the real carbonation measured after several decades is found from the carbonation rate measured in wet curing and without taking into account a factor k_c (it is likely that the effect of curing is covered by taking into account an exponent of 0.5, whereas for the XC3 and XC4 classes, current experience tends towards exponents of 0.45 and 0.40 respectively (Hunkeler F., von Greve-Dierfeld S., 2019) - the difference over 50 years corresponds to an increase of up to 50%);

- on the other hand, and from a purely physical point of view, the lack of curing leads to a given thickness of concrete of lesser quality with respect to transfer properties (which depends a priori on the compactness of the concrete) and beyond this thickness we find the wet cure type concrete: we could therefore consider taking into account the effect of cure through an additive term rather than a multiplicative one. A more precise determination of this value would require additional investigations and it was decided to keep an exponent 0.5 on the progression of carbonation as a function of time, which allows to cover this indeterminacy without taking into account an additive term.

- t_{ini} (year) is then determined so that the carbonation front reaches the reinforcement. For this purpose, a characteristic cover corresponding to a fractile of 10% C_{char}(mm) is used, such as:

$$C_{char} = C_{min} + (2.33 - 1.28)\,\sigma \qquad \text{(Equ. 4.6)}$$

Where C_{min} = minimum cover thickness in mm (EC2) for 50 or 100 years design service lives (see Table 4.2).

With ΔC_{dev} = 10 mm = 2.33 σ (2.33 corresponds to the 1% fractile), we obtain $C_{char} = C_{min}$ + 4,5 mm.

Table 4.2. Minimum cover (EC2)

Exposure class	Minimum cover (mm) at 50 years (structural class S4)	Minimum cover (mm) at 100 years (structural class S6)
XC1	15	25
XC2	25	35
XC3	25	35
XC4	30	40

2.2.2 Propagation time modelling

t_{prop} (year) is determined from the following relationship:

$$t_{prop} = \frac{X_{crit}}{V_{corr}} \qquad \text{(Equ. 4.7)}$$

where x_{crit} is the critical diameter loss for a crack opening of 0.1 mm and v_{corr} is the corrosion rate. x_{crit} (µm) is taken from the work of (Torres-Acosta and Sagues, 2004).

$$x_{crit} = 11\left(\frac{C_{char}}{D}\right)\left(\frac{C_{char}}{L} + 1\right)^2 \qquad \text{(Equ. 4.8)}$$

with: C_{char} = characteristic cover (mm); D = reinforcement diameter, i.e. 20 mm in a first approach; L = length of the anodic area (mm).

In the case of carbonation, we will consider a uniform corrosion and thus a ratio $\frac{C_{char}}{L}$ close to 0.

- v_{corr} is calculated as a function of the corrosion current density i_{corr} (Equ. 4.9) by a relation deduced from Faraday's law (valid for uniform corrosion).

$$v_{corr} = \frac{\Delta s}{\Delta t} = \frac{MFe}{\rho s.F.za} i_{corr} = 11.61\, i_{corr} \qquad \text{(Equ. 4.9)}$$

With: v_{corr} (µm/s) the corrosion rate; Δs (µm) the diameter loss; Δt (s) the time; M_{Fe} (56 g/mol) the molar mass of iron; ρ_s (g/m³) the density of steel; F the Faraday constant (96500 C); Za the number of electrons exchanged at the anode and i_{corr} (µA/cm²) the corrosion current density.

- the corrosion current density is determined by an empirical formula obtained from the thesis work of A. El Farissi (2020) based on a large literature review.

$$i_{corr} = V_0 \cdot \frac{k_{corr} \cdot k_T}{\rho_0} \qquad \text{(Equ. 4.10)}$$

with: V_0 (168.9 µA.Ωm.cm^{-2}) obtained from the exploitation of literature data, constant that reflects the corrosion potential;

k_{corr} (-) parameter that expresses the influence of relative humidity on the propagation phase,

k_T (-) parameter that reflects the influence of temperature,

ρ_0 (Ω.m) the electrical resistivity of concrete under saturated conditions: for class XC1, this value is corrected with a k'_{RH} factor to take into account the case of permanently dry environments, leading to a 10-fold increase in resistivity (Lifecon p.118, 2004) according to following Figure 4.3.

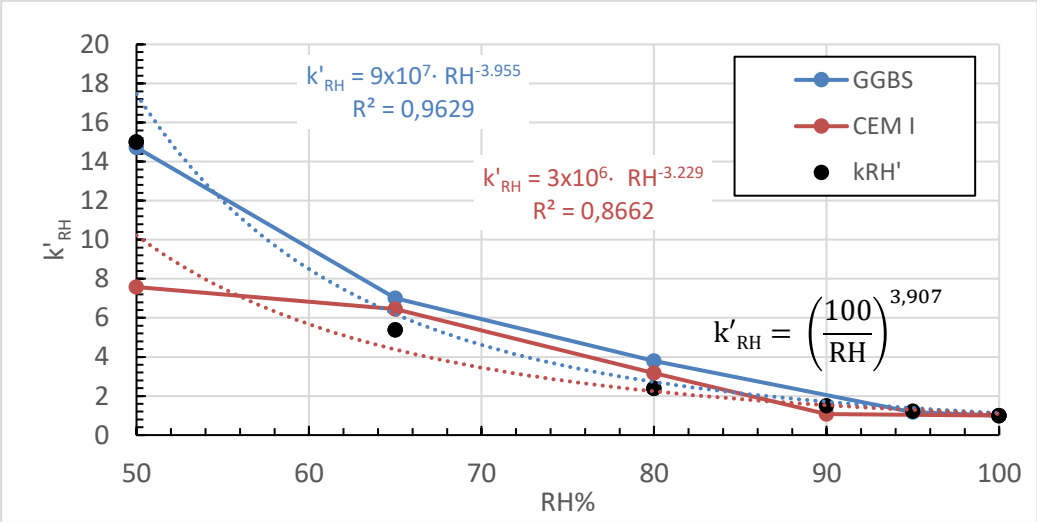

Figure 4.3. Determination of k'_{RH} for resistivity determination (Lifecon 2004 pp 108)

- The effect of temperature is taken into account from an Arrhenius law where T is the ambient temperature equal to the annual average temperature for a given environment (K), T_0 the reference temperature (293 K) and b, the regression constant taken equal to 4220 K (A. El Farissi, 2020).

$$k_T = e^{-4220\left(\frac{1}{T} - \frac{1}{T_0}\right)} \qquad \text{(Equ. 4.11)}$$

For the relative humidity, it is considered that the corrosion process in the case of carbonation presents an optimum that corresponds to RH_{crit} for which the corrosion current density is maximum. Given the lack of consensus in the literature on the influence of relative humidity on the corrosion process and after exploitation of a large number of data from the literature (see thesis Anass El Farissi, 2020), we end up with a RH_{crit} = 95% and a regression parameter c

equal to 6. The ambient relative humidity is determined, as for t_{ini}, from the exposure class concerned.

$$k_{corr} = \frac{1}{\left(\frac{RH - RH_{crit}}{c}\right)^2 + 1} \quad \text{(Equ. 4.12)}$$

2.2.3 Proposed performance thresholds

The use of the model we have just described makes it possible to define performance thresholds expressed in terms of maximum accelerated carbonation speed for a given environment for design service lives (DSL) of 50 and 100 years. A modulation according to 3 resistivity classes corresponding to the performance ranges observed on the 42 PerfDuB concretes, the value of which directly influences the propagation time, makes it possible to scan all the families of concrete available.

The results are presented in the Table 4.3. Values allowing for one or two structural class reductions in cover were also calculated and are shown in Appendices B and C.

Table 4.3. Performance qualification criteria (characteristic values at 90%)
Classes XC - DSL 50 years and 100 years

Exposure class	Modulation according to resistivity class at 90 d (Ω.m)	Accelerated carbonation rate (mm/day^{0,5})	
		Modelling 50 years	Modelling 100 years
XC1	< 100	4	4
	100 à 175	4	4
	> 175	4	4
XC2	< 100	3.5	3.3
	100 à 175	3.5	3.3
	> 175	3.6	3.3
XC3	< 100	1.7	1.6
	100 à 175	1.8	1.7
	> 175	2	1.8
XC4	< 100	2	1.7
	100 à 175	2.4	1.9
	> 175	4	2.4

It can be seen that the severity of the v_{acc} thresholds obtained by the modelling is in line with that of the prescriptive approach: the level of requirement generally increases in the same way as in the prescriptive approach. For class XC1, the risk of carbonation corrosion is almost zero. In fact, we obtain a threshold for v_{acc} higher than the maximum value obtained for all 42 PerfDuB concretes.

When comparing the thresholds for 50 and 100 years of design service life, we observe almost the same values for the same exposure class: this result is in conformity with the rules of the art (EC2) which recommend for the same exposure class to keep the same quality of concrete and to increase the cover.

2.3 Exposure classes XS and XD

2.3.1 Preamble

The model allows the calculation of the project use duration t_{final} (year) as defined in the introduction 2.1, for the XS classes and for XD2 and XD3. Class XD1 has not been implemented due to lack of reliable input data to model the transfer properties in this environment.

2.3.2 Modelling of the initiation time

As shown in Equation 4.13, the proposed model is constructed from an analytical solution of Fick's second law expressing the chloride concentration profile (g/L) at a given time t (El Farissi and al, 2018). The *fib* model has the same overall form (*fib* Model code Bulletin 34, 2006). This model has been modified to make it compatible with a performantial approach to durability based on laboratory tests.

$$C(x,t) = C_0 + (C_{s,\Delta x} - C_0)\left[1 - \mathrm{erf}\left(\frac{x - \Delta x}{2.\sqrt{D_m(t).t}}\right)\right] \qquad \text{(Equ. 4.13)}$$

With: C(x, t) (% mass binder), the chloride concentration at depth x (mm) and time t (s); C_0 (% mass binder), the initial chloride concentration; $C_{s,\Delta x}$ (% mass binder), the maximum surface concentration at depth x (m); $D_m(t)$ (m^2/s) the average diffusion coefficient over the entire exposure time and up to time t (s), which is a mathematically correct solution.

Equation 4.13 is used to calculate the corrosion initiation time which corresponds to the time when the concentration C(x, t) at the reinforcement is equal to the critical chloride concentration C_{crit}. The latter is expressed as free chloride and taken as 0.6% per mass of binder, which is a conservative approach and is consistent with the definitions of the ERC classes. We have chosen to work with free chlorides in the above equation because these are the ones involved in the corrosion process and we assume that the initial concentration C_0 is negligible as long as the specifications given in the concrete standard EN 206 are complied with (considering that the initial chlorides are mostly fixed to the cementitious matrix).

We therefore look for t_{ini} such that C(x,t) = 0.6% with x = C_{char}, C_{char} being the characteristic cover as defined in the previous section from the minimum cover: $C_{char} = C_{min} + 4.5$ mm. One can find in the Table 4.4 the values of C_{min} defined in EC2 in the case of classes XS and XD.

Table 4.4. Minimum cover values - Classes XS-XD - DSL 50 years and 100 years

Corrosion class	Minimum cover (mm) at 50 years (class S4)	Minimum cover (mm) at 100 years (class S6)
XS1	35	45
XS2	40	50
XS3	45	55
XD3	45	55
XD2	40	50

- **Depth x (mm):** it is known that the chloride concentration is maximum at a certain depth with a value higher than that of the environmental content. This phenomenon is generally explained by an accumulation of chlorides due to capillary suction in the area subjected to wetting/drying cycles i.e. in classes XS3 and XD3. In the proposed model, it is assumed that x remains constant after a long period of exposure. The following

empirical model was derived from literature data (Baroghel-Bouny *et al.*, 2013; Lindvall, 2003; Gao *et al.*, 2017; Wang *et al.*, 2018) (Figure 4.4 left).

$$\Delta x = 0{,}45\left(\frac{\varphi}{\varphi_s}\right)^5 \Delta x_0 \qquad \text{(Equ. 4.14)}$$

where: φ (%) is the water accessible porosity of the concrete; φ_s is a porosity threshold equal to 11.5%; Δx_0 is the reference depth equal to 10 mm. Equation 4.14 allows to calculate Δx in class XS3/XD3 from a material durability indicator, whereas it is considered constant (10 mm) in the *fib* model, independently of the concrete mix. For the other exposure classes, Δx is taken as 0.

- **$C_{s,\Delta x}$ (% binder by mass), the chloride concentration at depth Δx:** this concentration is determined from an enrichment coefficient E (-) multiplied by the free chloride concentration in the water-saturated porosity C_{sat} (Equ. 4.15).

$$C_{s,\Delta x} = E * C_{sat} \quad \text{with} \quad C_{sat} = \varphi \frac{C_{env}}{M_b} \qquad \text{(Equ. 4.15)}$$

with: C_{env} (g/l) the chloride concentration in the environment and M_b the binder dosage expressed in kg/m³ of concrete. A linear relationship between E and the water-accessible porosity of concrete is obtained from literature data (Figure 4.4 right).

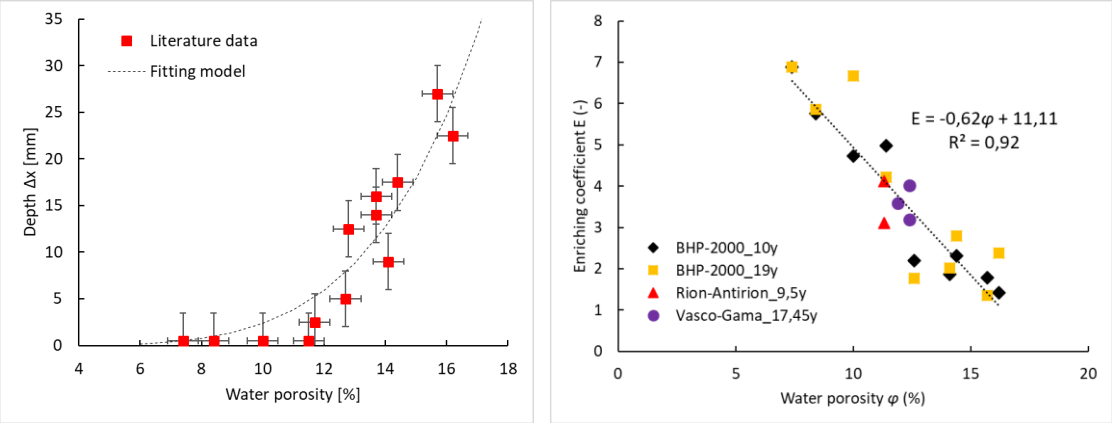

Figure 4.4. Correlations between depth of maximum chloride concentration ($C_{s,\Delta x}$) and porosity (left) and enrichment coefficient (E) and porosity (right).

This relation is used for exposure class XS3, i.e. E_{XS3} = - 0.62φ + 11.11. In exposure class XS1, it is observed from the available feedback, in particular in the analysis of old structures (GT2a of the PerfDuB project: chapter 2) that there is no surface enrichment: E_{XS1} = 1. In class XS2/XD2, a constant enrichment is assumed, calculated for a porosity of 15%: we obtain $E_{XS2/XD2}$ = 1.81, which is consistent with the results obtained on structures. In class XD3, the feedback from BHP 2000 on the specimens preserved in the Maurienne valley shows a lower enrichment than that obtained on the La Rochelle specimens, which is about 2/3 lower: the same relationship is therefore maintained, i.e. E_{XD3} = 0.33 E_{XS3}.

$C_{s,\Delta x}$ can thus be determined directly from the exposure conditions (C_{env}) and a durability indicator (φ). On this calculated value, we apply a partial safety coefficient (obtained from a standard CoV of 45% and 90% reliability level) whose value depends on the variability of the environmental conditions defined in *fib* bulletin 76. Considering on the one hand the variability attributed to the material and on the other hand the variability attributed to the environment, we can deconvolute the above expression in order to remove the part of the variability brought by the material and estimated at 6%

for the porosity. We then obtain the safety coefficients defined in Table 4.5. In the case of XS2, a constant enrichment independent of the porosity is assumed, so the CoV given by the *fib* bulletin 76 is kept.

Table 4.5. Safety factor applied to $C_{s,\Delta x}$ and environmental chloride concentration C_{env}

Exposure class	Safety coefficient	C_{env} chloride concentration (g/l)
XS1	1.3	22
XS2	1.3	22
XS3	1.5	22
XD3	1.9	22
XD2	1.9	10

Environmental concentration C_{env} is determined from the exposure class according to the Table 4.5. For classes XS, the average concentration of sea water is used. For class XD3 corresponding to areas in contact with de-icing salts (pavements, roads, etc.), it is difficult to know this concentration precisely, as it depends on the salting practices adopted. We have chosen to keep the same concentration as for the XS3 class: indeed, the prescriptive approach imposes the same level of severity for these two classes. In the case of class XD2 (e.g. swimming pools or industrial environments), again it may be complicated to estimate C_{env} but the use of sodium hypochlorite type products at 6 g/l chlorine equivalent produced on site by electrochlorination is common in water treatment facilities. To provide a safety margin, we have set C_{env} for class XD2 at 10 g/l.

We have chosen to integrate a dissociation of the XS3 exposure class, which due to surface enrichment phenomena leads to high risks of corrosion.

We therefore consider the following subclasses:

- XS3m: tidal or splash zone
- XS3e: area exposed to sea spray

The XS3m class incorporates submerged parts that are close to aerated areas (typically up to 5 m below the lowest water level) and splash zones (typically up to 10 m above the highest water level).

For the XS3e class we considered a surface concentration of chloride ions twice as low as that adopted in the XS3m class, based in particular on the multiple readings taken on the Gimsøystraumen Bridge and 35 other bridges in the marine environment (data provided by S. Helland, registered under CEN-TC104-SC1-WG1-N0223).

- **Average diffusion coefficient D_m (t) (m²/s):** the model is based on the chloride diffusion coefficient determined by a migration test, usually performed at 90 days of age (D_{rcm}). Knowing that the diffusion coefficient will decrease with time, an aging function is used to correct D_{rcm}. The mathematical solution of Fick's law can then be written as equation 4.13 where the average diffusion coefficient D_m is expressed as follows.

$$D_m(t) = k_T \left(\frac{t_0}{t_{th}}\right)^{\alpha_M} \left[\frac{(1-\alpha_M)t + \alpha_M t_{th}}{(1-\alpha_M)t}\right] D_{rcm}(t_0) \qquad \text{(Equ. 4.16)}$$

In equation 4.16, D_{rcm} (m²/s) is the migration coefficient determined at age t_0 (day). The time t_{th} (day) is the threshold at which the diffusion coefficient is assumed to become

constant. This is taken as 50 years by default (in the context of the use of the ageing factor values recommended by the *fib*). α_M is the ageing factor.

- k_T takes into account the influence of temperature in the form of an Arrhenius law.

  For classes XS2-XS3 and XD3, in order to take into account the real conditions of exposure, an ambient temperature of 15 °C (288 K) shall be taken as opposed to 20 °C (293 K) for XS1 and XD2.

When comparing equation 4.16 with the *fib* model equation (Equ. 4.17: Bulletin 34 - Fib) where there is no threshold value for D_{app} (t) and for which the integration of Fick's law does not take into account the time dependence of the diffusion coefficient, a relationship between α_A and α_M can be established (Equ. 4.18).

$$D_{app}(t) = k_e . k_t . D_{rcm}(t_0) . \left(\frac{t_0}{t}\right)^{\alpha_A} \quad \text{(Equ. 4.17)}$$

$$\left[\frac{t_0}{t}\right]^{(\alpha_M - \alpha_A)} = 1 - \alpha_M \quad \text{(Equ. 4.18)}$$

There is no analytical solution to this equation, so we approach it α_M from a polynomial of degree 4 (Equ. 4.19).

$$\alpha_M = 8.7773 . \alpha_A^4 - 8.2618 . \alpha_A^3 + 2.6738 . \alpha_A^2 + 0.9129 . \alpha_A + 0.0033 \quad \text{(Equ. 4.19)}$$

The values of the ageing coefficient α_A can be found in (Bulletin fib 34) in a tabular form that does not cover all possible concrete mix designs. Empirical relationships are also available in the literature, for example the Life-365 model (LIFE-365, 2008). Finally, the coefficient α_M can be obtained from experimental data from at least 3 measurements spread over 1 year. But most of the time only one value of D_{rcm} is available at a young age (usually 90 days). It is then necessary to determine this coefficient from empirical relationships.

We propose a relationship from the fib table and the Life-365 relationships to calculate α_A as a function of the binder composition entered as the respective mass % of blast furnace slag, fly ash, silica fume and metakaolin expressed in relation to the binder. The relationship is a linear combination of these % with the coefficients of Table 4.6.

We then calculate α_A= 0.3 + (%additions) x (addition coefficient Table 4.6) with an upper limit corresponding to the maximum increase in ageing factor provided for in bulletin fib 76.

Table 4.6. Weighting coefficient for calculating the ageing factor according to the composition of the binder

CEM I	0.3		Upper limit
Slag coefficient	0.2	Max for slag	0.15
Fly ash coefficient	1.1	Max for fly ash	0.3
Silica fume coefficient	1.1	Max for silica fume	0.1

Note: at this time, lack of data does not allow other additions or major constituents of cement to be included in the calculation of the aging factor.

2.3.3 Propagation time modelling

This section deals with the prediction of the duration of the corrosion propagation phase up to the production of a quantity of corrosion products related to the presence of chlorides that is supposed to lead to the appearance of the first crack. We are therefore interested in the localized corrosion related to the macropile process. The first step consisted in developing a model to evaluate the corrosion current density. The proposed model takes into account the impact of parameters related to:

- the anodic behaviour such as the concentration of free chlorides and the steel/concrete interface;
- the cathodic behaviour such as oxygen availability;
- the ohmic interaction between the anodic and cathodic zones, in particular, the electrical resistivity of the concrete which depends on the relative humidity, the type of binder, the surface ratio between the cathode and the anode (very high in real structures), and the distance between the aerated cathode and the anode (important parameter for XS2 type exposures);
- the influence of temperature.

The relationship between local cross-sectional loss and the development of corrosion cracking has been deduced from other studies in the literature and has been updated to account for the fact that, in submerged areas, corrosion products are more mobile and are likely to fill the porosity of the surrounding concrete before inducing swelling pressures that cause concrete cracking.

The corrosion current density is only partially taken into account to obtain a local reduction of the steel section; the other part of the current density is used for the extension of the anodic zones in their length.

After determining the corrosion current density and the cross-sectional area loss of the steel initiating the cracking in the concrete, it is possible to calculate the duration of the propagation phase before the first corrosion cracks appear using Faraday's law.

2.3.3.1 Corrosion current density model

The developed model predicts the maximum corrosion density (directly after initiation) and is based on experimental results obtained from an experimental test developed by Chalhoub *et al.* (2019a). The latter is built on the galvanic coupling between a chloride-free cathode sample representing passive steel and an anode sample that is oven-dried (40 °C) and then saturated in sodium chloride solutions at different concentrations from 12 to 280 g/L. The galvanic current density i_{corr} between the active and passive corroding steel is expressed in A/m^2 in Equation 4.20. The corrosion current density parameters are presented in Table 4.7 and the input data required to calculate these parameters are summarized in Table 4.8.

$$i_{corr} = \gamma_{Cl} \frac{k_{Cl}\ k_{C/A}\ k_T\ k_{O_2}\ k_f}{\rho} \qquad \text{(Equ. 4.20)}$$

Table 4.7. Corrosion propagation model factors

Factor	Definition	Value or expression
γ_{Cl}	Calibration constant	0.173 A.Ω/m
k_{Cl}	Parameter related to free chloride contamination	$\frac{(\lvert Cl\text{-}C_{crit}\rvert + Cl - C_{crit})^{0.89}}{0.08}$ with Cl the final chloride concentration at the end of the DSL and C_{crit} = 0.6%.
$k_{C/A}$	Parameter related to the C/A ratio	4 (Chalhoub *et al.*, 2020)
k_T	Temperature-related parameter	$k_T = e^{4220\left(\frac{1}{293} - \frac{1}{T}\right)}$
k_{O_2}	Parameter corresponding to oxygen availability	1 except for XS2 to be determined according to the immersed steel part and the length of mobilizable cathode: -0.0055. ρ_0+10.262
ρ	Electrical resistivity of concrete (Ω)	$\rho=\rho_0\ k'_{RH}$
k'_{RH}	Factor related to the impact of relative humidity on electrical resistivity	$K'_{RH} = \left(\left(\frac{100}{RH}\right)^4\right)^d$ (S. Lay, 2003 and C. Chaloub, 2019b)
k_f	Parameter corresponding to an interface default (Zhang *et al.*, 2020)	1 (effect not taken into account)

Table 4.8. Input parameters of the corrosion propagation model and their corresponding data source

Input parameter	Definition	Origin of the data	Unit
C_{crit}	Critical value expressed as free chloride	Cl = 0,6% (safety value)	%/m binder
Cl	Free Cl rate	Cl=Cf (value at the end of the design service life)	%/m binder
T	Temperature	Determined from a weather station near the structure	kelvin
ρ_0	Electrical resistivity under saturated conditions performed at 20°C	Laboratory measurement according to CEM RILEM TC-154 techniques	Ω.m
RH	Relative humidity at the steel/concrete interface	100% except for XS1 where RH = 75%.	%
d	Factor related to drying periods	$d=\begin{cases} 0 \rightarrow \text{Wet concrete} \\ 1 \rightarrow \text{Dry concrete} \end{cases}$	-

2.3.3.2 Loss of steel section causing the appearance of corrosion cracks

Many predictive models are based on a uniform steel section loss. This approach does not represent the localized aspect of chloride-induced corrosion in concrete. In recent years, for a better consideration of corrosion-induced cracking, some researchers have been interested in the actual distribution of corrosion products at the steel/concrete interface hence their expansion (Oh *et al.*, 2003; Malumbela *et al.*, 2011; Loukil *et al.*, 2017). In order to determine the crack opening (whether average or maximum) or the loss of steel section initiating corrosion, an empirical or analytical relationship may be satisfactory taking into account some physical and geometrical parameters.

The proposed approach (Alonso et al,1998, modified by Vidal et al, 2004) is a possible solution that we have used as a first approach.

$$S_a = A_s \left[1-\left[1-\frac{2\,Pr_{O_2}\,pf_g}{D}\left(7.53+9.32\frac{c}{D}\right)10^{-3}\right]^2\right] \qquad \text{(Equ. 4.21)}$$

With: S_a is the local area loss leading to the initiation of corrosion cracking (m^2);

D is the nominal diameter of the steel bar (m);

A_s is the cross-sectional area of the reinforcement which is equal to $\frac{\pi D^2}{4}$ (m^2);

c is the cover thickness (m);

p_{fg} is the geometric pitting factor and is taken to be equal to 4;

Pr_{O_2} is the parameter that takes into account the pressure of the corrosion products as a function of the availability of oxygen with 1 for exposure classes XS1 and XS3 and 2.5 for class XS2 (this hypothesis requires comparison with experimental data). If oxygen is available, then the pressure of the products formed increases and less products are needed to crack the concrete.

2.3.3.3 Prediction of corrosion propagation time

The corrosion current density predicted by the model can then be used to calculate the duration of the propagation phase before the first corrosion cracks appear. The total anodic corrosion current contributes to the depth penetration and also to the lateral extension of the anodic zone(s). Therefore, only part of the total current density will be used to calculate the section mass loss. The corrosion propagation time t_{prop} corresponding to the appearance of the first corrosion crack can be calculated using the Faraday relation. The equation relating the propagation period to the corrosion rate can therefore be expressed in years as follows:

$$t_{prop} = \mu\left(\frac{S_a}{D}\right)\left(\frac{1}{k\,i_{corr}}\right) \qquad \text{(Equ. 4.22)}$$

The first term is a constant ($\mu=\frac{\rho_s\,Z\,F}{2\,M\tan(\varphi)} = 5.07^{10}$ A.s/m^3 = 1629 A.yr/m^3). The second term depends on the concrete structure (reinforcement diameter and cover) with S_a in m^2 and D in m, with a lump-sum value of 0.02m. In the third term related to the corrosion density, k is the factor corresponding to the part of the current leading to the loss of section of the steel which is taken in first approach equal to 0.5.

2.3.4 Proposed performance thresholds

The use of the model we have just described makes it possible to define performance thresholds expressed in terms of maximum migration coefficients for a given environment, for design service lives of 50 and 100 years. A modulation according to 4 ageing factor classes allows to scan all the available concrete families. The resistivity is fixed at 50 Ω.m, which is safe. The thresholds are calculated for two porosity values: 15% and 13.5%.

The results are presented in Table 4.9. Values allowing for one or two structural class reductions in cover were also calculated and are shown in Appendices B and C.

Table 4.9. Performance qualification criteria (90% characteristic values)
Classes XS-XD - DSL 50 years and 100 years

Exposure class	Modulation according to ageing factor class	$D_{rcm\ 90d}$ (10^{-12}m²/s)	
		Modelling 50 years	Modelling 100 years
XS1	0.30 à 0.39	19 (26*)	16 (22*)
	0.40 à 0.49	30	28 (36*)
	0.50 à 0.59	50	50
	0.60 and above	90	90
XS2	0.30 à 0.39	6 (7*)	4 (5*)
	0.40 à 0.49	8.5	7.5 (8*)
	0.50 à 0.59	14 (16*)	13 (14*)
	0.60 and above	27 (30*)	28 (31*)
XS3e	0.30 à 0.39	5	4
	0.40 à 0.49	7	7.5
	0.50 à 0.59	12	13
	0.60 and above	22	28
XS3m	0.30 à 0.39	2	2
	0.40 à 0.49	3	3
	0.50 à 0.59	5	5
	0.60 and above	10	13
XD2	0.30 à 0.39	9	6
	0.40 à 0.49	13	12
	0.50 à 0.59	22	19
	0.60 and above	42	40
XD3	0.30 à 0.39	11	9
	0.40 à 0.49	17	15
	0.50 à 0.59	27	27
	0.60 and above	53	60

**: values with an asterisk are applicable for concrete whose water porosity measured at 90 days is less than or equal to 13,5%*

It can be seen that the severity of the D_{rcm} thresholds obtained by the modelling is in line with that of the prescriptive approach: the level of requirement increases in the same way as in the prescriptive approach.

When comparing the thresholds for 50 and 100 years of DSL (Design Service Life), we observe almost the same values for the same exposure class: this result is in conformity with the rules of the art (EC2) which recommend for the same exposure class to keep the same quality of concrete and to increase the cover. The reduction in porosity leads to a reduction in the concentration of surface chlorides and thus allows a relaxation of the migration coefficient for certain exposure classes.

2.4 Comparison of the proposed thresholds with the cover values according to the European ERC class approach

The proposed thresholds for the exposure classes related to reinforcement corrosion risks were compared to those resulting from the modelling carried out by France in the context of the preparation of the revision of Eurocode 2 by the European group TC250/WG1/TG10 between 2018 and 2020. These models were used to define the recommended covers according to ERC classes and exposure classes, the mandate of the European group being in particular to introduce the concept of exposure resistance class (ERC) in substitution of the structural class for the determination of the reinforcement cover.

The corresponding models are analytical models, simpler than those developed within the framework of MODEVIE and PerfDuB, taking into account at the beginning of the project fixed propagation times per exposure class independently of the characteristics of the concrete. They have been adapted to introduce a modulation linked to the electrical resistivity in the XC classes and to consider a diffusion of chloride ions in an unsaturated environment in the XD1 and XS1 classes.

The principles of these models are given in Appendix A and the corresponding results are entitled "XRC model" and "XRDS model" in the following chapter. The evaluation of the thresholds finally retained and presented in the following chapter is also presented in Appendix A.

3 Definition of performance thresholds for classes XC, XS and XD

3.1 Introduction

The performance thresholds used in the French National PerfDuB Project are based on three approaches:

- lifetime t_{final} calculations according to the models described in section 2;
- mapping of the 42 concretes characterized in the framework of the PerfDuB WG3 work;
- lifetime calculations according to the principles of the European work on ERC (Exposure Resistance Classes).

The feedback on old structures was taken into account within the framework of the appropriation of the MODEVIE engineering model by the PerfDuB project. This allowed to reduce the differences between the current prescriptive impositions and those resulting from the modelling, thus authorising a work of convergence of the thresholds allowing to reach values consolidated by the multiplicity of the approaches.

In each of the following sub-paragraphs, per type of exposure class, the thresholds resulting from the three approaches are compared and the finally deduced values are defined. In these sub-paragraphs, the thresholds obtained for mixes complying with Eurocode NF EN 1992-1-1 for structural classes S4 (50-year design life) and S6 (100-year design life) are presented. Thresholds for reductions of one structural class (respectively two structural classes) are given in Annex B (respectively Annex C).

The thresholds selected were chosen from predefined series covering the range of performance sought and incorporating a difference between successive values within the same series of between 2 and 3 times the standard deviation of the test reproducibility

determined during the final cross-testing campaign of WG1 of the PerfDuB project. These runs are as follows:

- accelerated characteristic carbonation rate (in mm/day$^{0.5}$) measured at 28 days:

  1 - 1.4 - 1.8 - 2.2 - 2.6 - 3 - 3.5 - 4

- chloride migration coefficient (in 10^{-12} m²/s) measured at 90 days:

  1 – 1.5 - 2 - 3 - 5 - 9 - 16 - 22 - 28

3.2 Performance thresholds for XC classes

For the XC classes, the different approaches give similar values which are expressed in terms of characteristic values (with a 90% fractile) for 50-year (Table 4.10) and 100-year (Table 4.11) design service lives.

Table 4.10. Performance thresholds (characteristic values at 90%) - Classes XC - DSL 50 years

	Performance qualification criteria				
	Modulation according to resistivity class at 90d (Ω.m)	Characteristic accelerated carbonation rate (in mm/day$^{0.5}$) for 50-year durability			
Exposure class		Data base	Modevie Modelling	Model XRC	Thresholds retained
XC1	< 100	2.3	4	4	4
	100 à 175		4		
	> 175		4		
XC2	< 100	2.3	3.5	3	3
	100 à 175		3.5	3	3.5
	> 175		3.6	3.5	
XC3	< 100	2.0	1.7	1.8	1.8
	100 à 175		1.8	2.2	2.2
	> 175		2.0	2.2	
XC4	< 100	2.0	2.0	2.2	1.8
	100 à 175		2.4	2.6	2.2
	> 175		4	2.6	3

The thresholds used are slightly more severe than those in the database, except for classes XC1 and XC2 for which the database contains few concretes corresponding to these classes (most are XC3/XC4). When the PerfDuB and XRC models diverged slightly, the arbitration was made in the direction of safety.

Table 4.11. Performance thresholds (characteristic values at 90%) - Classes XC - DSL 100 years

	Performance qualification criteria				
	Modulation according to resistivity class at 90d (Ω.m)	Characteristic accelerated carbonation rate (in mm/day$^{0.5}$) for 100-year durability			
Exposure class		Data base	Modevie Modelling	Model XRC	Thresholds retained
XC1	< 100	1.8	4	4	4
	100 à 175				
	> 175				
XC2	< 100	1.8	3.3	2.6	2.6
	100 à 175			3	3
	> 175				
XC3	< 100	1.6	1.6	1.8	1.8
	100 à 175		1.7		
	> 175		1.8		
XC4	< 100	1.7	1.7	1.8	1.8
	100 à 175		1.9	2.2	
	> 175		2.4		2.2

The thresholds used are close to those in the database except for classes XC1 and XC2 for which the database contains few concretes corresponding to these classes (most are XC3/XC4). When the PerfDuB and XRC models diverged slightly, the arbitration was made in the direction of safety.

3.3 Performance thresholds for XS classes

For the XS classes, the different approaches give the following values which are expressed in terms of characteristic values (with a 90% fractile) for 50-year (Table 4.12) and 100-year (Table 4.13) design service lives.

Table 4.12. Performance thresholds (characteristic values at 90%) - Classes XS - DSL 50 years

	Performance qualification criteria				
	Modulation according to ageing factor class	Chloride ion migration coefficient (in 10^{-12} m²/s) for 50-year durability			
Exposure class		Data base	PerfDuB Modelling	Model XRDS	Thresholds retained
XS1	0.30 à 0.39	34	19 (26*)	11	16 (28*)
	0.40 à 0.49		30	19	28
	0.50 à 0.59		50	33	
	0.60 and above		90	56	
XS2	0.30 à 0.39	34	6 (7*)	2.4	5 (9*)
	0.40 à 0.49		8.5	4.1	9
	0.50 à 0.59		14	6.9	16
	0.60 and above		27	11.8	
XS3e	0.30 à 0.39	17	5	5	5
	0.40 à 0.49		7	9	9
	0.50 à 0.59		12	16	16
	0.60 and above		22	22	22
XS3m	0.30 à 0.39	17	2	1.6	2
	0.40 à 0.49		3	2.7	3
	0.50 à 0.59		5	4.6	5
	0.60 and above		10	7.8	9

**: values with an asterisk are applicable for concrete whose water porosity measured at 90 days is less than or equal to 13.5%.*

There is a large discrepancy between the values from the database and those from the modelling. Insofar as experience feedback on old structures has shown weaknesses in the current prescriptive system concerning some of these classes (XS3 in particular, with structures designed for a design service life of 100 years that show visible signs of corrosion after 30 years of service despite compliant covers), the safety choice was made to take into account mainly the modelled values.

Table 4.13. Performance thresholds (characteristic values at 90%) - Classes XS - DSL 100 years

Exposure class	Performance qualification criteria				
	Modulation according to ageing factor class	Chloride ion migration coefficient (in 10^{-12} m²/s) for 100-year durability			
		Data base	PerfDuB Modelling	Model XRDS	Thresholds retained
XS1	0.30 à 0.39	17	16 (22*)	11	9 (16*)
	0.40 à 0.49		28	19	22
	0.50 à 0.59		50	33	
	0.60 and above		90	56	
XS2	0.30 à 0.39	17	4 (5*)	2.4	3 (5*)
	0.40 à 0.49		7.5	4.1	5
	0.50 à 0.59		13	6.9	9
	0.60 and above		28	11.8	
XS3e	0.30 à 0.39	10	4	5	5
	0.40 à 0.49		7	9	9
	0.50 à 0.59		13	16	16
	0.60 and above		26	22	22
XS3m	0.30 à 0.39	10	2	1.6	2
	0.40 à 0.49		3	2.7	3
	0.50 à 0.59		5	4.6	5
	0.60 and above		13	7.8	9

**: the values with an asterisk are applicable for concretes whose water porosity measured at 90 days is less than or equal to 13.5%.*

As for 50 years, there is a large discrepancy between some values from the database and those from the modelling, particularly for the XS2 and XS3 classes. The same safety choice was therefore made to take into account mainly the modelled values.

3.4 Performance thresholds for XD classes

For the XD classes, the different approaches give the following values which are expressed in terms of characteristic values (with a 90% fractile) for 50-year (Table 4.14) and 100-year (Table 4.15) design service lives.

Table 4.14. Performance thresholds (characteristic values at 90%) - Classes XD - DSL 50 years

	Performance qualification criteria				
	Modulation according to ageing factor class	Chloride ion migration coefficient (in 10^{-12} m²/s) for 50-year durability			
Exposure class		Data base	Modelling PerfDuB	Model XRDS	Thresholds retained
XD1	0.30 à 0.39	46		19	16 (28*)
	0.40 à 0.49			31	28
	0.50 à 0.59			53	
	0.60 and above			91	
XD2	0.30 à 0.39	34	9	8	9
	0.40 à 0.49		13	13.5	16
	0.50 à 0.59		22	23	22
	0.60 and above		42	29	
XD3 frequent salting	0.30 à 0.39	17	11		9
	0.40 à 0.49		17		16
	0.50 à 0.59		27		22
	0.60 and above		53		
XD3 Very frequent salting	0.30 à 0.39	17		4.8	5
	0.40 à 0.49			8.1	9
	0.50 à 0.59			13.7	16
	0.60 and above			23.3	

** values with an asterisk are applicable for concrete with a water porosity measured at 90 days lower than or equal to 13.5%.*

As before for the XS classes, the discrepancies between the database and the models led to the use of the values from the latter.

For the XD3 class, it was decided to retain stricter values in case of very frequent salting, based on the XRDS model, than those derived from the PerfDuB model. For the XD1 class, which is considered less severe than the XS1 class, the thresholds defined for the XS1 class were retained for safety reasons.

Table 4.15. Performance thresholds (characteristic values at 90%) - Classes XD - DSL 100 years

Exposure class	Performance qualification criteria				
	Modulation according to ageing factor class	Chloride ion migration coefficient (in 10^{-12} m²/s) for 100-year durability			
		Data base	Modelling PerfDuB	Model XRDS	Thresholds retained
XD1	0.30 à 0.39	17		19	16 (22*)
	0.40 à 0.49			31	28
	0.50 à 0.59			53	
	0.60 and above			91	
XD2	0.30 à 0.39	17	9	8	9
	0.40 à 0.49		12	13.5	16
	0.50 à 0.59		19	23	22
	0.60 and above		40	39	
XD3 frequent salting	0.30 à 0.39	10	9		9
	0.40 à 0.49		15		16
	0.50 à 0.59		27		22
	0.60 and above		60		
XD3 Very frequent salting	0.30 à 0.39	10		4.8	5
	0.40 à 0.49			8.1	9
	0.50 à 0.59			13.7	16
	0.60 and above			23.3	

**: values with an asterisk are applicable for concrete with a water porosity measured at 90 days lower than or equal to 13.5%.*

The same safety principles were applied as for a 50-year project operating life.

References

(Alonso *et al.*, 1998) Alonso C., Andrade C., Rodriguez J. & Diez J.M. (1998), "Factors controlling cracking of concrete affected by reinforcement corrosion", Materials and Structures, Springer, n°31, p.435–441.

(Bakker, 1993) Bakker R.F.M. (1993), Model to calculate the rate of carbonation in concrete under different climatic conditions, Rapport CEMIJ bv Laboratorium.

(Baroghel-Bouny *et al.*, 2013) Baroghel-Bouny V., Dierkens M., Wang X., Soive A., Saillio M., Thiery M. & Thauvin B. (2013), "Ageing and durability of concrete in lab and in field conditions: investigation of chloride penetration", *Journal of Sustainable Cement-Based Materials*, Taylor & Francis, vol.2, n°2, p.67–110.

fib Model code:

- *Bulletin* 34 (2006), "Model code for Design Service Life", 116 p.
- *Bulletin* 65 (2012), "fib: Model Code 2010 – Volume 1", 357 p.
- *Bulletin* 66 (2012), "fib: Model Code 2010 – Volume 2", 377 p.
- *Bulletin* 76 (2015), "*fib*: Benchmarking of deemed-to-satisfy provisions in standards: Durability of reinforced concrete structures exposed to chlorides", 204 p.

(Chalhoub *et al.*, 2019a) Chalhoub C., François R. & Carcassès M. (2019a), "Determination of chloride threshold initiating corrosion: A new set-up taking the localized aspect of corrosion into account", Cement and Concrete Research, Elsevier, vol.124, p.105825.

(Chalhoub, 2019b) Chalhoub C. (2019b), Study of the initiation and propagation phases of chloride induced corrosion in reinforced concrete structures, PhD, Université de Toulouse.

(Chalhoub *et al.*, 2020) Chalhoub C., François R. & Carcassès M. (2020), "Effect of Cathode-Anode distance and electrical resistivity on macrocell corrosion currents and cathodic response in cases of chloride induced corrosion in reinforced concrete structures", Construction and Building Materials, Elsevier, vol.245, p.118337.

(El Farissi *et al.*, 2018) El Farissi A., Turcry P., Younsi A., Ait-Mokhtar A., Ait-Alaiwa A. & Gotteland P. (2018), "Analysis of the influence of chloride exposure conditions and material properties on the convection zone depth and the corresponding chloride content", 12th *fib* International PhD Symposium in Civil Engineering, august 2018, Prague.

(El Farissi, 2020) El Farissi A. (2020), Prédiction de la durée d'utilisation des ouvrages en béton armé par une approche performantielle dans le cas de la corrosion induite par la carbonatation ou l'attaque des ions chlorure, PhD Thesis, Université de La Rochelle.

(Gao *et al.*, 2017) Gao Y., Zhang J., Zhang S. & Zhang Y. (2017), "Probability distribution of convection zone depth of chloride in concrete in a marine tidal environment", *Constr. Build. Mater.*, vol.140, p.485–495.

Fascicule n°65 (2017), *Exécution des ouvrages de génie civil en béton*, Cahier des clauses techniques générales applicables aux marchés publics de travaux de génie civil.

(Hunkeler et von Greve-Dierfeld, 2019) Hunkeler F. & von Greve-Dierfeld S. (2019), "Karbonatisierung von Beton und Korrosionsgeschwindigkeit der Bewehrung im karbonatisierten Beton", Forschungsprojekt AGB 2013/005 auf Antrag der AGB Bruckenforschung, final Report.

(Lay *et al.*, 2003) Lay S., Schiesl P. & Cairns J. (2003), "Lifecon deliverable D 3.2 Service Life Models. Instructions on methodology and application of models for the prediction of the residual service life for classified environmental loads and types of structures in Europe", Technical research center of Finland.

LIFE-365 (2008), Life-365 Service Life Prediction Model.

(Lindvall, 2003) Lindvall A. (2003), Environmental actions on concrete exposed in marine and road environments and its response. Consequences for the initiation of chloride induced reinforcement corrosion, PhD Thesis, Chalmers University of Technology.

(Loukil et Feki, 2017) Loukil N. & Feki M. (2017), “Zn–Mn alloy coatings from acidic chloride bath: Effect of deposition conditions on the Zn–Mn electrodeposition-morphological and structural characterization”, *Applied Surface Science*, Elsevier, vol.410, p.574–584.

(Malumbela *et al.*, 2011) Malumbela G., Alexander M. & Moyob P. (2011), “Model for cover cracking of RC beams due to partial surface steel corrosion”, *Constr. Build. Mater.*, vol.25, n°2, p.987–991.

(Oh e*t al.*, 2003) Oh B., Jang S. & Shin Y. (2003), “Experimental investigation of the threshold chloride- concentration for corrosion initiation in reinforced concrete structures”, *Magazine of Concrete Research*, Institution of Civil Engineers (ICE), vol.55, n°2, p.117–124.

(Torres-Acosta et Sagues, 2004) Torres-Acosta A. & Sagues A. (2004), “Concrete cracking by localized steel corrosion – Geometric effects”, *ACI Materials Journal*, American Concrete Institute (ACI), vol.101, p.501–507.

(Vidal *et al.*, 2004) Vidal T., Castel A. & Francois R. (2004), “Analyzing crack width to predict corrosion in reinforced concrete”, *Cement and Concrete Research*, vol.34, n°1, p.165–174.

(Vu *et al.*, 2019) Vu Q.H., Pham G., Chonier A., Brouard E., Rathnarajan S., Pillai R., Gettu R., Santhanam M., Aguayo F., Folliard K.J. *et al.* (2019), “Impact of different climates on the resistance of concrete to natural carbonation”, *Constr. Build. Mater.*, vol.216, p.450–467.

(Wang *et al.*, 2018) Wang Y., Wu L., Wang Y., Li Q. & Xiao Z. (2018), “Prediction model of long-term chloride diffusion into plain concrete considering the effect of the heterogeneity of materials exposed to marine tidal zone”, *Constr. Build. Mater.*, vol.159, p.297–315.

(Zhang *et al.*, 2020) Zhang W., Francois R. & Yu L. (2020), “Influence of load-induced cracks coupled or not with top-casting-induced defects on the corrosion of the longitudinal tensile reinforcement of naturally corroded beams exposed to chloride environment under sustained loading”, *Cement and Concrete Research*, vol.129, article 105972.

APPENDIX A: Principles of the models from the "ERC" work

A.1 Risk of carbonation-induced corrosion - XC

A.1.1 Definition of Carbonation Resistance Classes XRC

The definition of exposure resistance classes (ERC) with respect to the risk of carbonation-induced corrosion (XRC) is obtained from the depth of carbonation in mm (characteristic value associated with a 90% non-exceedance fractile) assumed to be reached after 50 years under reference conditions (CO_2 content of 400 ppm in an atmosphere maintained at a constant 20 °C and 65% relative humidity). XRC has the dimension of a carbonation rate, expressed in mm per square root of years.

EN 206 and EN 1992-1-1 have chosen to associate the numerical value designating the XRC class with the quotient by 7 of the depth of carbonation expected at 50 years under the reference conditions described above. Although 7 is an approximate value of the square root of 50, this designation is conventional and does not imply that the rate of carbonation is constant with time.

The recommended values of XRC classes retained at European level include the value XRC0,5 and values staggered by one unit between XRC1 and XRC7.

A.1.2 Summary of modelling assumptions ("XRC model")

The model adopted by the French approach within TC250/SC2/WG1/TG10 to express the depth of carbonation as a function of time can be summarized by the following equation:

$$x_c(t) / x_{c0} = k \cdot k_e \, (t / t_0)^{alpha\_e} \qquad x_{c0} = 1 \text{ mm} \qquad t_0 = 1 \text{ year} \qquad \text{(Equ. 4.A.1)}$$

With: k is the "nominal average" carbonation rate derived from the correspondence with the XRC class. Assuming that the transfer properties of the concrete do not change at the long term times corresponding to the design service life, k was taken as constant in the application of the equation for all times corresponding to the end of the initiation period $t_{SL} - t_{prop}$ and t_{SL} is the design service life (50 or 100 years)

t_{prop}: time allowed for corrosion propagation (within an acceptable limit typically associated with a corrosion-induced crack opening limited to 50 µm)

alpha_e: exponent associated with the kinetics of the progression of the carbonation front, depending on the humidity conditions associated with the exposure class

k_e: modulation coefficient of the carbonation rate, depending on the humidity conditions associated with the exposure class

From the depth of carbonation reached, the minimum cover for durability ($c_{min,dur}$ according to the notation of EN 1992-1-1) is obtained from the following equation:

$$c_{min,dur} = \Delta c_\beta + x_c(t_{SL} - t_{prop}) = \Delta c_\beta + k \cdot k_e \cdot (t_{SL} - t_{prop})^{alpha\_e} \qquad \text{(Equ. 4.A.2)}$$

to ensure a probability of non-exceedance compatible with a target reliability index equal to 1.5: $P(c_{min,dur} < x_c(t_{SL} - t_{prop})) < 7\%$

Thus, based on carbonation depth distributions measured on structures and in order to respect this target of $\beta = 1.5$, we integrate a value of Δc_β equal to 3 mm for $t_{SL} = 50$ years and to 7 mm for $t_{SL} = 100$ years.

For the determination of the cover depths, the values in the table 4.A.1 were adopted.

Table 4.A.1. Parameters adopted for the calculation of recommended cover depths - Model proposed by France in TC250/SC2/WG1/TG10

		t_{prop} (year)			
Reference	**Resistivity (Ω.m)**	**XC1**	**XC2**	**XC3**	**XC4**
Low	< 100	45/48 - 90/96	10	20	5
Intermediate	100 - 175	45/48 - 90/96	15	25	20
High	> 175	45/48 - 90/96	20	30	30
		XC1	**XC2**	**XC3**	**XC4**
Alpha_e		0.5	0.4	0.45	0.4
k_e		1	0.5	0.87	0.83

Finally, the relationships between XRC class, characteristic value of natural carbonation rate, accelerated carbonation rate and threshold of specification of this value, were established on the following basis:

- Factor 3 between the natural carbonation rate in mm/year$^{0.5}$ and the accelerated carbonation rate in mm/day$^{1/2}$, based on the results of PerfDuB supported by the results of F. Hunkeler's team (taking into account the test protocols EN 12390-12 and EN 12390-10 modified according to the preconditioning provisions developed in PerfDuB);
- Factor 1.1 corresponding to the ratio of carbonation rates at constant relative humidity of 50% (PerfDuB test conditions) to 65% (XRC definition);
- Exponent alpha_e equal to 0.45 for the calculation of the depth of carbonation under the reference conditions of definition of the XRC classes, i.e. stationary relative humidity conditions equal to 65 % over 50 years.

The correspondence between the thresholds proposed by PerfDuB for the performance approach and the XRC classes is summarized in the table 4.A.2 below.

Table 4.A.2. Thresholds associated with XRC classes and link with PerfDuB specifications

$k_{acc\ 90}$ PerfDuB 50% RH (mm/day$^{0.5}$)	**$k_{nat\ 90}$ 65%RH (mm/year$^{0.5}$)**	**Carbo depth (90%) at 50 years (ref) (mm)**	**XRC**	**XRC (rounded)**	**$k_{acc\ 90}$ specific (65%RH) (mm/day$^{0.5}$)**
0.2	0.545	3.171	0.45		0.18
0.6	1.636	9.515	1.36		0.54
1	2.727	15.859	2.27		0.91
1.4	3.818	22.202	3.17	3	1.27
1.8	4.909	28.545	4.08	4	1.63
2.2	6	34.889	4.98	5	1.99
2.6	7.090	41.232	5.89	6	2.36
3	8.181	47.576	6.80	7	2.72
3.5	9.545	55.505	7.93	8	3.17
4	10.909	63.434	9.06	9	3.62

A.1.3 Recommended cover depths calculations based on XRC classes

Table 4.A.3. Recommended cover depths $c_{min,dur}$ (XRC format) - Reference resistivity (< 100 Ω.m)

XRC	XC1		XC2		XC3		XC4	
	50 years	100 years	50 years	100 years	50 years	100 years	50 years	100 years
0.5	10	10	10	10	10	10	10	10
1	10	10	10	15	10	20	10	20
2	10	10	10	20	**15**	**25**	15	25
3	10	15	15	20	**20**	**30**	**20**	**30**
4	10	**15**	**15**	**25**	**25**	**40**	**25**	**40**
5	10	20	**20**	**30**	30	45	**30**	45
6	**10**	20	25	**35**	30	50	35	50
7	15	**20**	**25**	40	35	60	40	60
8	15	25	30	45	40	70	50	70
9	**15**	**25**	35	50	50	75	55	75

Table 4.A.4. Recommended cover depths - Medium resistivity (100 to 175 Ω.m)

XRC	XC1		XC2		XC3		XC4	
	50 years	100 years	50 years	100 years	50 years	100 years	50 years	100 years
0.5	10	10	10	10	10	10	10	10
1	10	10	10	15	10	20	10	20
2	10	10	10	20	**15**	**25**	15	25
3	10	15	15	20	20	**30**	**20**	**30**
4	10	**15**	**15**	**25**	**20**	**35**	**25**	**35**
5	10	20	20	**30**	**25**	45	30	**40**
6	**10**	20	**20**	35	30	50	**30**	50
7	15	**20**	**25**	**35**	35	60	35	55
8	15	25	30	40	40	65	40	65
9	**15**	**25**	30	45	45	75	45	70

Table 4.A.5. Recommended cover depths - High resistivity (> 175 Ω.m)

XRC	XC1		XC2		XC3		XC4	
	50 years	100 years	50 years	100 years	50 years	100 years	50 years	100 years
0.5	10	10	10	10	10	10	10	10
1	10	10	10	15	10	20	10	15
2	10	10	10	20	15	25	15	25
3	10	15	15	20	15	30	15	30
4	10	15	15	25	20	35	20	35
5	10	20	20	30	25	45	25	40
6	10	20	20	35	30	50	30	45
7	15	20	25	35	30	60	30	55
8	15	25	25	40	35	65	35	60
9	15	25	30	45	40	70	40	70

The above tables were obtained by postulating the values of k associated to classification in the XRC classes, and rounding the obtained value of $c_{min,dur} = \Delta c_{\beta} + k \cdot k_e \cdot (t_{SL} - t_{prop})^{alpha\_e}$ according to the following rule: rounding to the equal or higher value, unless this rounding corresponds to an increase of + 4 mm (in which case the rounding is to the lower value, with a deviation of - 1 mm).

The tables show in red the values corresponding to the current "pivot" mixes (recommended values for structural classes S4 for a 50-year design service life and S6 for a 100-year design service life); in blue and green, respectively, the values corresponding to the one and two-class modulations.

These values were compared with the results of the modelling carried out within the framework of MODEVIE, and with the performances measured on the concretes characterized within the framework of PerfDuB, and made it possible to arrive at the threshold values of performance finally proposed.

A.1.4 Assessment of recommended performance thresholds

The recommended thresholds correspond to accelerated carbonation rates of 4; 3.5; 3; 2.6; 2.2; 1.8; 1.4 and 1 mm/day$^{0.5}$ fairly close to the XRC9, XRC8, XRC7, XRC6, XRC5, XRC4, XRC3 and XRC2 classes. They are shown in the tables 4.A1.6 to 4.A1.9 below.

It appeared important to evaluate a posteriori the margin associated with the combination of thresholds and cover depths associated with the current use of structural classes, taking into account a potentially significant impact of rounding. This margin is assessed by comparing the $c_{min,dur}$ cover deduced from the structural class, hereafter noted $c_{min,dur}$ PerfDuB, and the cover calculated according to the modelling, noted $c_{min,dur}$ EU calculation gross.

Table 4.A.6. Recommended performance thresholds (90% characteristic values) - XC classes - DUP 50 and 100 years

Exposure class	Performance qualification criteria (90% characteristic values)		
	Modulation according to resistivity class at 90 d (Ω.m)	50 years	100 years
		PerfDuB proposal (S4 - S3 - S2)	PerfDuB proposal (S6 - S5 - S4)
XC1	< 100	4 - 3 - 2.2	4 - 3 - 1.8
	100 à 175		
	> 175		
XC2	< 100	3 - 2.6 - 2.2	2.6 - 2.2 - 1.8
	100 à 175	3.5 - 3 - 2.2	3 - 2.6 - 1.8
	> 175		
XC3	< 100	1.8 - 1.4 - 1	1.8 - 1.4 - 1
	100 à 175	2.2 - 1.8 - 1.4	
	> 175		
XC4	< 100	1.8 - 1.4 - 1	1.8 - 1.4 - 1
	100 à 175	2.2 - 1.8 - 1.4	
	> 175	3 - 2.6 - 1.8	2.2 - 1.8 - 1.4

Table 4.A.7. Cover values without modulation (pivot classes S4 - S6)

Exposure class	t_{SL}	Resistivity at 90 d (Ω.m)	k_{acc} threshold (mm/day$^{0.5}$)	$c_{min.dur}$ PerfDuB (mm)	$c_{min.dur}$ calculation EU gross (mm)
XC1	50 years	-	4	15	16
	100 years	-	4	25	25
XC2	50 years	< 100	3	25	25
		≥ 100	3.5	25	27
	100 years	< 100	2.6	35	33
		≥ 100	3	35	36
XC3	50 years	< 100	1.8	25	23
		≥ 100	2.2	25	25
	100 years	-	1.8	35	38
XC4	50 years	< 100	1.8	30	26
		100 à 175	2.2	30	27
		> 175	3	30	30
	100 years	≤ 175	1.8	40	38
		> 175	2.2	40	40

In almost all situations the comparison is safe and well adjusted, or the deviation is limited to 2 mm.

In the case of XC3 - 100 years without modulation, the deviation is 3 mm and the compensatory margins are to be found in a low occurrence of prescription and a real level of humidity (inside the cells of bow-girder bridges or hollow piles) or protection conditions (slabs under waterproofing) limiting the effective penetration of the carbon dioxide more than taken into account in the calculations.

Table 4.A.8. Cover values with one class modulation (classes S3 - S5)

Exposure class	t_{SL}	Resistivity at 90 d (Ω.m)	k_{acc} threshold (mm/day$^{0.5}$)	$c_{min.dur}$ PerfDuB (mm)	$c_{min.dur}$ calculation EU gross (mm)
XC1	50 years	-	3	10	13
	100 years	-	3	20	20
XC2	50 years	< 100	2.6	20	22
		≥ 100	3	20	24
	100 years	< 100	2.2	30	29
		≥ 100	2.6	30	32
XC3	50 years	< 100	1.4	20	18
		≥ 100	1.8	20	21
	100 years	-	1.4	30	31
XC4	50 years	< 100	1.4	25	21
		100 à 175	1.8	25	22
		> 175	2.6	25	27
	100 years	≤ 175	1.4	35	31
		> 175	1.8	35	34

In almost all situations the comparison is safe and well adjusted, or the deviation is limited to 2 mm.

The only residual deviations exceeding 3 mm concern the application of the modulation of one class in the case XC1 - 50 years and XC2 - 50 years (threshold of 3 for resistivity > 100 Ω.m).

For the XC1 environment, the modelling adopted is rather irrelevant given the duration of propagation time that can be accepted in an environment where the risk of corrosion is not proven by experience. The adopted threshold of 2 classes above the value not allowing modulation is consistent with the current resistance-based modulation provisions.

For the XC2 environment, the "hidden" margins lie in a pessimistic estimate of the permissible duration of corrosion propagation (particularly for medium to high resistivity) and a fairly safe consideration of the effect of the humidity of the surrounding environment.

Table 4.A.9. Cover depths values with two class modulation (classes S2 - S4)

Exposure class	t_{SL}	Resistivity at 90 d (Ω.m)	k_{acc} threshold (mm/day$^{0.5}$)	$c_{min.dur}$ PerfDuB (mm)	$c_{min.dur}$ calculation EU gross (mm)
XC1 (Prestressed concrete)	50 years	-	2.2	15	20
	100 years	-	1.8	25	25
XC2	50 years	< 100	2.2	15	19
		≥ 100	2.2	15	18
	100 years	< 100	1.8	25	25
		≥ 100	1.8	25	25
XC3	50 years	< 100	1	15	14
		≥ 100	1.4	15	17
	100 years	-	1	25	24
XC4	50 years	< 100	1	20	16
		100 à 175	1.4	20	18
		> 175	1.8	20	19
	100 years	≤ 175	1	30	24
		> 175	1.4	30	28

It should be noted that in order for the comparison of recommended cover depths to remain relevant with a modulation of 2 classes, it was carried out in XC1 for the cover depths of prestressing reinforcements.

In almost all situations the comparison is safe and well adjusted, or the deviation is limited to 2 mm.

The only residual deviations exceeding 3 mm concern the application of a two-class modulation in the XC1 - 50 years and XC2 - 50 years cases (for a threshold of 2.2 regardless of resistivity).

For the XC1 environment, the modelling adopted is rather irrelevant considering the importance of the propagation time that can be admitted in an environment where the risk of corrosion is not proven by experience. The threshold adopted for a modulation of 2 structural classes remains consistent with the current modulation provisions based on a performance similar to the pivot class in XC4.

In the case of the XC2 environment, the "hidden" margins lie in a pessimistic estimate of the permissible duration of corrosion propagation (in the calculation, 10 to 20 years depending on the resistivity) and a safe consideration of the effect of the humidity of the surrounding environment.

A.2 Chloride-induced corrosion risk - XD / XS

A.2.1 Definition of the XRDS chloride penetration resistance classes

The definition of the exposure resistance classes (ERC) with respect to the risk of corrosion induced by chloride penetration (XRDS) is obtained from the depth (in mm) reached by the chlorides (characteristic value associated with a 90% non-exceedance fractile) at which it is assumed to be reached after 50 years under reference conditions (penetration by a face exposed to reference seawater with a concentration of 30 g/l of sodium chloride NaCl at 20 °C), a chloride concentration equal to 0.6% of the binder mass (cement + type II additions). It was chosen to express XRDS as a diffusion coefficient, expressed in 10^{-13} m²/s.

By noting d_{Cl} the reference depth corresponding to reaching a chlorides mass content of 0.6% with respect to the binder content, standards EN 206 and EN 1992-1-1 have chosen to associate the numerical value designating the XRDS class with a quarter of the quotient of the square of d_{Cl} (expressed in mm), by the duration of 50 years (expressed in seconds), which amounts to XRDS = $d_{Cl}^2/631$. By this choice, XRDS can for example be interpreted as the characteristic value (90% fractile of non-exceedance) of the apparent diffusion coefficient at 50 years of the concrete considered $D_{app}(t_{50})$, assuming that the reference conditions associated with the XRDS definition correspond to an initial chloride concentration of zero (reasoning in free chlorides) and a surface concentration of 3.81% (without taking into account the fixation of these chlorides).

The recommended values of XRDS classes retained at the European level correspond to values of d_{Cl} typically ranging from 15 mm (very high performance concretes) to more than 80 mm (in particular in less aggressive environments), hence XRDS classes ranging from 0.5 to 10. The consideration of a diffusion mechanism in an unsaturated environment for exposure classes XD1 and XS1 leads to extend this range with classes XRDS15, XRDS20, XRDS25 and XRDS30.

A.2.2 Summary of modelling assumptions ("XRDS model")

The model adopted by the French approach in TC250/SC2/WG1/TG10 to express chloride concentration as a function of depth x and time t is summarized by the following equation.

$$C(x,t) = C_i + (C_s - C_i)\left[\operatorname{erfc}\left(\frac{x - \Delta x}{2\sqrt{Dapp(t).t}}\right)\right] \qquad \text{(Equ. 4.A.3)}$$

In this equation erfc represents the complementary error function, D_{app} (t) is the apparent chloride diffusion coefficient, Δx is the thickness of the "convection zone" where water cycles disrupt the mechanism of chloride progression by diffusion, C_i is the initial chloride content (taken to be zero in a reasoning where it is assumed that the chlorides initially present are bound and do not participate in diffusion) and C_s is the so-called "surface" concentration, in fact its maximum value governing the diffusion mechanism (where a concomitant mechanism of possible fixation is not considered). C_s is calculated as the product of the concentration of the liquid on the surface, supposed to fill entirely the porosity of the concrete accessible to water, by an enrichment factor E typically between 2 and 3.5 and higher for concretes of low porosity. The value of D_{app} (t_{50}) is considered constant for calculations associated with a 50-year design service life, given the relatively low values of corrosion propagation times accepted in chloride environments. For calculations associated with a 100-year design life, a conservative value of the aging factor α equal to 0.2 was used to extrapolate D_{app} according to the commonly accepted empirical equation:

$$D_{app} = D_0(t_0/t)^{\alpha} \qquad \text{(Equ. 4.A.4)}$$

The threshold concentration corresponding to the beginning of the corrosion propagation phase is still under discussion in the scientific community. A value decreasing with the porosity of the material was chosen, varying between 0.4 and 0.8%, higher in unsaturated conditions (XD1 and XS1). The depth Xc corresponding to having reached this concentration can be directly deduced from D_{app} in the saturated reference environment. Depending on the exposure class, account is taken of an apparent diffusion affected by the average temperature and, where appropriate, by a reduction coefficient reflecting the unsaturated nature of the environment, as well as a surface concentration modulated in relation to the reference saturated conditions.

Finally, the minimum cover with respect to durability is obtained from equation:

$$c_{min,dur} = \Delta c_{\beta} + x_c(t_{SL} - t_{prop}) \qquad \text{(Equ. 4.A.5)}$$

to ensure a probability of non-exceedance compatible with a target reliability index equal to 1.5: $P(c_{min,dur} < x_c(t_{SL} - t_{prop})) < 7\%$.

The margin Δc_{β} was modulated according to the porosity, and takes into account a higher dispersion in case of concomitant carbonation. All the parameters associated with the modelling assumptions (boundary conditions of the diffusion calculation) are summarised below. For safety reasons, for the calculation of Cs, the concentration of chloride ions in seawater was taken to be 24 g/l.

Table 4.A.10. Parameters associated with the calculations according to the different exposure classes

Expo class	$[Cl^-]$ peak	T° effect (15 °C)	Diff. not sat. + variable salting	Thickness Convection area		t_{prop} (year)	Δc_{β} margin + carbo (mm)	$[Cl^-]_{crit}$
				Δx 50 years (mm)	Δx 100 years (mm)			
XS2	C_s	$D_{(20°C)}$ x 0.75		0	0	10	poro² x 0.02	0.44 to 0.7%
XS1	0.5 x*C_s	$D_{(20°C)}$ x 0.75	D x 0.85[6]	0	0	10	poro² x 0.04	0.54 to 0.8%
XS3	1.25 x C_s	$D_{(20°C)}$ x 0.75		poro² x 0.03	poro² x 0.04	2	poro² x 0.02	0.44 to 0.7%
XD2	0.5 x C_s	$D_{(20°C)}$ x 0.75		0	0	5	poro² x 0.03	0.44 to 0.7%
XD1	0.5 x C_s	$D_{(20°C)}$ x 0.75	D x 0.85[6] x 0.75	0	0	15	poro² x 0.04	0.54 to 0.8%
XD3	0.75 x C_s	$D_{(20°C)}$ x 0.75	D x 0.75	poro² x 0.04	poro² x 0.05	5	poro² x 0.02	0.44 to 0.7%

In addition to these assumptions, the correspondence between the XRDS class and the value of the apparent diffusion coefficient is conditioned by assumptions on the binder content, porosity, enrichment factor, and the coefficient of variation resulting from the local variability of the material acting on both diffusivity and surface concentration. On the other hand, the dispersion on the ageing factor and the local variability of the exposure have not been included in this term because the influence of these parameters occurs separately. The table below summarizes the assumptions on the material associated with the XRDS classes taken into account in the simulations, which take into account the thresholds currently fixed by the NF EN 206/CN standard and fascicule 65.

Table 4.A.11. Parameters associated with the calculations according to the different classes of resistance to exposure to chlorides

XRDS	d_{Cl}	Hypotheses			Consequences			Hyp Variab CoV
		Binder content	Poro	Enrichment factor	C_s (XS2)	C_s (XS2)	D_{app} (50) (charac 90%)	
	(mm)	(kg/m^3)	(%)	30/poro	(kg/m^3)	(% Binder)	(10^{-13} mm^2/s)	(%)
0.5	17.8	450	11.8	3.232	9.15	2.0	0.913	64.7
1	25.1	440	12.0	3.125	9.00	2.0	1.811	62.5
1.5	30.8	430	12.2	3.023	8.85	2.1	2.695	60.5
2	35.5	420	12.4	2.927	8.71	2.1	3.556	58.5
3	43.5	410	12.6	2.834	8.57	2.1	5.291	56.7
4	50.2	400	12.8	2.747	8.44	2.1	6.980	54.9
5	56.2	385	13.0	2.663	8.31	2.2	8.521	53.3
6	61.5	370	13.3	2.544	8.12	2.2	10.015	50.9
8	71.1	360	13.5	2.47	8.00	2.2	13.149	49.4
10	79.4	350	13.8	2.36	7.83	2.2	16.311	47.3
15	97.3	330	13.9	2.33	7.77	2.4	23.147	46.6
20	112	320	14.0	2.30	7.71	2.4	30.110	45.9
25	126	300	14.5	2.14	7.45	2.5	36.642	42.8
30	138	280	15.0	2.00	7.20	2.6	42.215	40.0

The correspondence between XRDS, the characteristic value of the apparent diffusion coefficient at 50 years, the average value of this coefficient, and the threshold value specified for the chloride migration coefficient measured at 90 days (as practiced in France and according to the protocol improved and justified within the framework of PerfDuB, in particular with regard to the preconditioning of the samples) corresponds to the formula:

$$D_{app}(t) = k.\ D_{rcm}\,(t_0).A\,(t) \qquad \text{(Equ. 4.A.6)}$$

with $A(t) = (t_0/t)^{\alpha}$, t_0 = 90 days, t = 50 years and k = 1 which is a safe choice neglecting the interactions of chlorides with the cement matrix.

In this context, a flat-rate coefficient of variation of 47% was taken into account, i.e. a ratio of 1.6 between the specified characteristic value and the average value.

This correspondence is given in the table 4.A2.12 below, for four discrete values of the aging factor α.

Table 4.A.12. Migration coefficient thresholds calculated for the different classes of resistance to chloride exposure

Exposure class	d_{Cl} (mm)	D_{app} (50 year) charac. (10^{-13} m²/s)	D_{app} (50 year) average (10^{-13} m²/s)	$D_{rcm\ 90d}$ charac. (in 10^{-12} m²/s)			
				α = 0.3	α = 0.4	α = 0.5	α = 0.6
XRDS0.5	17.8	0.913	0.499	0.4	0.7	1.1	1.9
XRDS1	25.1	1.811	1.005	0.8	1.3	2.3	3.9
XRDS1.5	30.8	2.695	1.518	1.2	2.0	3.4	5.8
XRDS2	35.5	3.556	2.032	1.6	2.7	4.6	7.8
XRDS3	43.5	5.291	3.064	2.4	4.1	6.9	11.8
XRDS4	50.2	6.980	4.096	3.2	5.5	9.3	15.7
XRDS5	56.2	8.521	5.064	4.0	6.8	11.5	19.5
XRDS6	61.5	10.015	6.061	4.8	8.1	13.7	23.3
XRDS8	71.1	13.149	8.052	6.3	10.7	18.2	30.9
XRDS10	79.4	16.311	10.157	8.0	13.5	23.0	39.0
XRDS15	97.3	23.147	14.492	11.4	19.3	32.8	55.7
XRDS20	112.4	30.110	18.953	14.9	25.2	42.9	72.8
XRDS25	125.6	36.642	23.659	18.6	31.5	53.5	90.9
XRDS30	137.6	42.215	27.905	21.9	37.2	63.1	107.2

A.2.3 Recommended cover depth calculations based on XRDS classes

Table 4.A.13. Recommended cover depths $C_{min,dur}$

XRDS	XS1		XS2		XS3		XD1		XD2		XD3	
	50 yr	100 yr	50 yr	100 yr	50 yr	100 yr	50 yr	100 yr	50 yr	100 yr	50 yr	100 yr
0.5	10	10	15	20	25	30	10	10	10	15	20	20
1	15	20	20	30	**35**	**40**	10	15	15	15	20	25
1.5	20	20	25	35	**40**	**50**	10	15	15	20	25	30
2	20	25	**30**	**40**	**45**	**55**	15	15	20	20	30	35
3	20	25	**40**	**50**	**55**	70	15	20	20	25	**35**	40
4	25	30	45	60	60	80	15	20	25	30	40	**45**
5	25	30	**50**	65	70	90	20	25	25	35	**40**	**50**
6	**25**	**35**	55	75	80	100	20	25	**30**	**35**	**45**	**55**
8	30	40	65	85	90	115	20	30	**35**	**45**	**50**	65
10	**30**	**40**	70	100	100	130	**25**	30	**40**	**50**	60	75
15	**35**	**45**	90	120	125	160	30	**35**	45	60	70	90
20	40	**55**	105	140	145	185	**30**	**40**	**50**	65	80	105
25	45	60	120	160	165	210	**35**	**45**	60	75	90	115
30	50	65	130	180	180	235	**40**	**50**	65	85	100	130

The table 4.A2.13 was obtained by assuming the values of D_{app} corresponding to classification in XRDS classes, as specified above, and rounding the obtained value of the recommended minimum cover depth $C_{min,dur} = \Delta c_\beta + x_c(t_{SL} - t_{prop})$ to the nearest 5 mm according to the following rule: rounding up to the equal or higher value, unless this rounding corresponds to an increase of + 4 mm (in which case the rounding is to the lower value, with a deviation of - 1 mm).

The table shows the values for the current "pivot" mixes in red (recommended values for structural classes S4 for a 50-year design life and S6 for a 100-year design life); the values for the one and two-class modulations in blue and green, respectively. In particular, the following "pivot" classes, which are identical for the 50 and 100-year design service lives, emerge:

Exposure class	50 years	100 years
XD1	XRDS25	XRDS25
XS1	XRDS15	XRDS15
XD2	XRDS10	XRDS10
XS2	XRDS3	XRDS3
XD3	XRDS6	XRDS6
XS3	XRDS2	XRDS2

Table 4.A.14. Classes of resistance to chloride exposure: pivot classes and associated thresholds

Exposure class	Expo	Design service life	Poro (%)	$D_{rcm\ 90d}$ threshold (in 10^{12} m²/s)			
				α = 0.3	α = 0.4	α = 0.5	α = 0.6
XRDS2	XS3	50 years / 100 years	12.4	1.6	2.7	4.6	7.8
XRDS3	XS2	50 years / 100 years	12.6	2.4	4.1	6.9	11.8
XRDS6	XD3	50 years / 100 years	13.3	4.8	8.1	13.7	23.3
XRDS10	XD2	50 years / 100 years	13.8	8	13.5	23	39
XRDS15	XS1	50 years / 100 years	13.9	11.4	19.3	32.8	55.7
XRDS25	XD1	50 years / 100 years	14.5	18.6	31.5	53.5	90.9

The threshold values of the diffusion coefficients derived from these classes were compared with the results of the modelling carried out within the framework of MODEVIE, and with the performances measured on the concretes characterised within the framework of PerfDuB, and made it possible to arrive at the performance threshold values finally proposed, by re-examining the modelling hypotheses if necessary: distinction of tidal and sprayed areas from areas subject to spray in class XS3; distinction of areas subject to frequent or very frequent salting in classes XD3; taking into account a significantly longer propagation time in classes XS2 insofar as the levels presenting a risk of dissolved oxygen and electrical continuity with tidal areas are excluded.

A.2.4 Assessment of recommended performance thresholds

The recommended thresholds, listed below, correspond to discrete values of the apparent chloride diffusion coefficient identified by the 90-day non-steady-state (accelerated) migration test. The values retained (expressed in 10^{-12} m²/s) are 28, 22, 16, 9, 5, 3, 2, 1.5 and 1. The scaling of these values is compatible, to the nearest rounding, with an approximate correspondence with the XRDS20, XRDS10, XRDS6, XRDS4, XRDS2 and XRDS1.5 classes.

Table 4.A.15. Recommended cover depths corresponding to the reference structural classes XS

Exposure class	Performance qualification criteria, $D_{rcm\ 90d}$ (in 10^{-12} m²/s) (90% characteristic values)		
	Aging factor	50 years	100 years
		PerfDuB proposal (S4)	PerfDuB proposal (S6)
XS1	0.30 à 0.39	16 (28 if poro < 13.5%)	9 (16 if poro < 13.5%)
	0.40 and above	28	22
XS2	0.30 à 0.39	5 (9 if poro < 13.5%)	3 (5 if poro < 13.5%)
	0.40 à 0.49	9	5
	0.50 and above	16	9
XS3e (Sea spray)	0.30 à 0.39	5	5
	0.40 à 0.49	9	9
	0.50 à 0.59	16	16
	0.60 and above	22	22
XS3m (Splash and tidal zone)	0.30 à 0.39	2	2
	0.40 à 0.49	3	3
	0.50 à 0.59	5	5
	0.60 and above	9	9

For the XS exposure classes detailed above as well as for the XD classes in the table below, the modulation of one structural class / 2 classes is to be associated with the shift of one step (resp. 2 steps) of the threshold of the chloride diffusion coefficient (result of the 90 days test in 10^{-12} m²/s), to the right, in the following list:

28 - 22 - 16 - 9 - 5 - 3 - 2 – 1.5 – 1

Table 4.A.16. Recommended cover depths corresponding to the reference structural classes XD

Exposure class	Performance qualification criteria ($D_{rcm\ 90d}$ in 10^{-12}m²/s) (90% characteristic values)		
	Ageing factor	50 years	100 years
		PerfDuB proposal (S4)	PerfDuB proposal (S6)
XD1	0.30 à 0.39	16 (28 if poro < 13.5%)	16 (22 if poro < 13.5%)
	0.40 and above	28	28
XD2	0.30 à 0.39	9	9
	0.40 à 0.49	16	16
	0.50 and above	22	22
XD3f (Frequent salting)	0.30 à 0.39	9	9
	0.40 à 0.49	16	16
	0.50 and above	22	22
XD3tf (Very frequent salting)	0.30 à 0.39	5	5
	0.40 à 0.49	9	9
	0.50 and above	16	16

It appeared important to evaluate a posteriori the margin associated with the combination of these thresholds and the covers associated with the current use of structural classes, taking into account a potentially significant impact of rounding. This margin is assessed by comparing the $c_{min,dur}$ cover deduced from the structural class, hereafter noted $c_{min,dur}$ PerfDuB, and the cover calculated according to the modelling, noted $c_{min,dur}$ XRDS gross.

The calculations were carried out with the adjusted assumptions presented below. The effect of an average temperature of 15°C was systematically taken into account, introducing a coefficient of 0.75 with respect to the value determined at 20°C. Cs was assumed to be equal to 6.6 kg/m^3 regardless of the porosity of the material, consistent with a seawater salinity corresponding to 22 g/l of chlorides. The binder content assumptions were based on the requirements of fascicule 65 of the CCTG for the 100-year design service life and on those of standard NF EN 206/CN for the 50-year design service life. For the simulations corresponding to a porosity lower than the threshold of 13.5%, it was possible to consider a higher binder content.

Table 4.A.17. Simulations used to validate thresholds - associated parameters

Exposure class	Surface / peak concentration	Diff. not sat. + variable salting	Convection zone depth in mm (50 years)	Convection zone depth in mm (100 years)	t_{prop} (year)	Margin Δc_β incl. carbonation (mm)
XS2	Cs		0	0	30	poro² x 0.02
XS1	0.5 x Cs	D x 0.85^6	0	0	10	poro² x 0.04
XS3e	0.65 x Cs		poro² x 0.03	poro² x 0.04	2	poro² x 0.02
XS3m	1.25 x Cs		poro² x 0.03	poro² x 0.04	2	poro² x 0.02
XD2	0.5 x Cs		0	0	5	poro² x 0.03
XD1	0.5 x Cs	D x 0.85^6 x 0.75	0	0	15	poro² x 0.04
XD3f	0.6 x Cs	D x 0.75	poro² x 0.04	poro² x 0.05	5	poro² x 0.02
XD3tf	0.75 x Cs	D x 0.75	poro² x 0.04	poro² x 0.05	5	poro² x 0.02

Table 4.A.18. Validation of thresholds by comparison of recommended cover depths - XS-base thresholds (pivot classes S4-S6)

$D_{rcm\ 90}$ spec (10^{-12} m²/s)	Ageing Fact. α	Exposure class.	Service life (year)	Poro. (%)	Binder content (kg/m³)	D_{app} μ (50) (10^{-13} m²/s)	CoV (%)	D_{app} (50) char. (10^{-13} m²/s)	Enrich. 30/poro	C crit (% binder)	$c_{min.dur}$ XRDS gross (mm)	$c_{min.dur}$ PerfDuB (mm)
9	0.3	**XS1**	100	14	330	11.48	45.9	18.24	2.14	0.60	34.2	45
16	0.3	**XS1**	50	14.5	330	20.4	42.8	31.59	2.07	0.55	34.9	35
16	0.3	**XS1**	100	13.5	330	20.4	49.4	33.32	2.22	0.65	41.2	45
28	0.3	**XS1**	50	13.5	330	35.71	49.4	58.33	2.22	0.65	39.7	35
22	0.4	**XS1**	100	14	330	16.52	45.9	26.24	2.14	0.60	39.5	45
28	0.4	**XS1**	50	14.5	330	21.02	42.8	32.55	2.07	0.55	35.3	35
3	0.3	**XS2**	100	14	330	3.83	45.9	6.08	2.14	0.60	48.8	50
5	0.3	**XS2**	50	14.5	330	6.38	42.8	9.88	2.07	0.55	40.8	40
5	0.3	**XS2**	100	13.5	380	6.38	49.4	10.42	2.22	0.65	52.6	50
9	0.3	**XS2**	50	13.5	330	11.48	49.4	18.75	2.22	0.65	44.1	40
5	0.4	**XS2**	100	14	330	3.75	45.9	5.96	2.14	0.60	47.1	50
9	0.4	**XS2**	50	14.5	330	6.76	42.8	10.47	2.07	0.55	41.9	40
9	0.5	**XS2**	100	14	330	3.98	45.9	6.32	2.14	0.60	48.4	50
16	0.5	**XS2**	50	14.5	330	7.07	42.8	10.95	2.07	0.55	42.7	40
5	0.3	**XS3e**	100	13	350	6.38	53.3	10.74	2.31	0.60	52.9	55
5	0.3	**XS3e**	50	13.5	350	6.38	49.4	10.42	2.22	0.55	42.5	45
9	0.4	**XS3e**	100	13	350	6.76	53.3	11.38	2.31	0.6	54.1	55
9	0.4	**XS3e**	50	13.5	350	6.76	49.4	11.04	2.22	0.55	43.5	45
16	0.5	**XS3e**	100	13	350	7.07	53.3	11.90	2.31	0.60	55.2	55
16	0.5	**XS3e**	50	13.5	350	7.07	49.4	11.55	2.22	0.55	44.3	45
22	0.6	**XS3e**	100	13	350	5.72	53.3	9.63	2.31	0.60	50.7	55
22	0.6	**XS3e**	50	13.5	350	5.72	49.4	9.34	2.22	0.55	40.7	45
2	0.3	**XS3m**	100	13	**400**	2.55	53.3	4.29	2.31	0.60	57.5	55
2	0.3	**XS3m**	50	13.5	350	2.55	49.4	4.16	2.22	0.55	49.7	45
3	0.4	**XS3m**	100	13	350	2.25	53.3	3.79	2.31	0.60	59.0	55
3	0.4	**XS3m**	50	13.5	350	2.25	49.4	3.67	2.22	0.55	47.2	45
5	0.5	**XS3m**	100	13	350	2.21	53.3	3.72	2.31	0.60	58.6	55
5	0.5	**XS3m**	50	13.5	350	2.21	49.4	3.61	2.22	0.55	46.9	45
9	0.6	**XS3m**	100	13	350	2.34	53.3	3.94	2.31	0.60	60.0	55
9	0.6	**XS3m**	50	13.5	350	2.34	49.4	3.82	2.22	0.55	48.0	45

Table 4.A.19. Validation of thresholds by comparison of recommended cover depths - XS-modulation of one class (S3-S5)

$D_{rcm\ 90}$ spec (10^{-12} m²/s)	Ageing Fact. α	Exposure class.	Service life (year)	Poro. (%)	Binder content (kg/m³)	D_{app} (50) avg (10^{-13} m²/s)	CoV (%)	D_{app} (50) char. (10^{-13} m²/s)	Enrich. 30/poro	C_{crit} (% binder)	$c_{min.dur}$ XRDS gross (mm)	$c_{min.dur}$ PerfDuB (mm)
5	0.3	**XS1**	100	14	330	6.38	45.9	10.13	2.14	0.60	27.5	40
9	0.3	**XS1**	50	14.5	330	11.48	42.8	17.78	2.07	0.55	28.3	30
9	0.3	**XS1**	100	13.5	330	11.48	49.4	18.75	2.22	0.65	32.7	40
22	0.3	**XS1**	50	13.5	**350**	28.05	49.4	45.81	2.22	0.65	34.9	30
16	0.4	**XS1**	100	14	330	12.01	45.9	19.08	2.14	0.60	34.9	40
22	0.4	**XS1**	50	14.5	330	16.52	42.8	25.58	2.07	0.55	32.3	30
2	0.3	**XS2**	100	14	330	2.55	45.9	4.05	2.14	0.60	40.6	45
3	0.3	**XS2**	50	14.5	330	3.83	42.8	5.93	2.07	0.55	32.5	35
3	0.3	**XS2**	100	13.5	**380**	3.83	49.4	6.26	2.22	0.65	41.6	45
5	0.3	**XS2**	50	13.5	330	6.38	49.4	10.42	2.22	0.65	33.8	35
3	0.4	**XS2**	100	14	330	2.25	45.9	3.57	2.14	0.60	37.3	45
5	0.4	**XS2**	50	14.5	330	3.75	42.8	5.81	2.07	0.55	32.2	35
5	0.5	**XS2**	100	14	330	2.21	45.9	3.51	2.14	0.60	37.1	45
9	0.5	**XS2**	50	14.5	330	3.98	42.8	6.16	2.07	0.55	33.1	35
3	0.3	**XS3e**	100	13	350	3.83	53.3	6.45	2.31	0.60	45.8	50
3	0.3	**XS3e**	50	13.5	350	3.83	49.4	6.26	2.22	0.55	35.0	40
5	0.4	**XS3e**	100	13	350	3.75	53.3	6.31	2.31	0.60	42.9	50
5	0.4	**XS3e**	50	13.5	350	3.75	49.4	6.12	2.22	0.55	34.7	40
9	0.5	**XS3e**	100	13	350	3.98	53.3	6.70	2.31	0.60	43.9	50
9	0.5	**XS3e**	50	13.5	350	3.98	49.4	6.50	2.22	0.55	35.5	40
16	0.6	**XS3e**	100	13	350	4.16	53.3	7.00	2.31	0.60	44.7	50
16	0.6	**XS3e**	50	13.5	350	4.16	49.4	6.79	2.22	0.55	36.1	40
1.5	0.3	**XS3m**	100	13	**400**	1.91	53.3	3.22	2.31	0.60	51.1	50
1.5	0.3	**XS3m**	50	13.5	350	1.91	49.4	3.12	2.22	0.55	44.3	40
2	0.4	**XS3m**	100	13	350	1.50	53.3	2.52	2.31	0.60	50.0	50
2	0.4	**XS3m**	50	13.5	350	1.50	49.4	2.45	2.22	0.55	40.3	40
3	0.5	**XS3m**	100	13	350	1.33	53.3	2.24	2.31	0.60	47.7	50
3	0.5	**XS3m**	50	13.5	350	1.33	49.4	2.17	2.22	0.55	38.4	40
5	0.6	**XS3m**	100	13	350	1.30	53.3	2.19	2.31	0.60	47.3	50
5	0.6	**XS3m**	50	13.5	350	1.30	49.4	2.12	2.22	0.55	38.1	40

Table 4.A.20. Validation of thresholds by comparison of recommended cover depths - XS-modulation of two classes (S2-S4)

$D_{rcm\ 90}$ spec (10^{-12} m²/s)	Ageing Fact. α	Exposure class.	Service life (year)	Poro. (%)	Binder content (kg/m³)	D_{app} (50) avg (10^{-13} m²/s)	CoV (%)	D_{app} (50) char. (10^{-13} m²/s)	Enrich. 30/poro	Ccrit (% binder)	$c_{min.dur}$ XRDS gross (mm)	$c_{min.dur}$ PerfDuB (mm)
3	0.3	**XS1**	100	14	330	3.83	45.9	6.08	2.14	0.60	23.1	35
5	0.3	**XS1**	50	14.5	330	6.38	42.8	9.88	2.07	0.55	23.2	25
5	0.3	**XS1**	100	13.5	330	6.38	49.4	10.42	2.22	0.65	26.3	35
16	0.3	**XS1**	50	13.5	**370**	20.4	49.4	33.32	2.22	0.65	29.9	25
9	0.4	**XS1**	100	14	330	6.76	45.9	10.74	2.14	0.60	28.1	35
16	0.4	**XS1**	50	14.5	330	12.01	42.8	18.60	2.07	0.55	28.7	25
1.5	0.3	**XS2**	100	14	330	1.91	45.9	3.03	2.14	0.60	35.6	40
2	0.3	**XS2**	50	14.5	330	2.55	42.8	3.95	2.07	0.55	27.3	30
2	0.3	**XS2**	100	13.5	**380**	2.55	49.4	4.16	2.22	0.65	34.6	40
3	0.3	**XS2**	50	13.5	330	3.83	49.4	6.26	2.22	0.65	27.0	30
2	0.4	**XS2**	100	14	330	1.50	45.9	2.38	2.14	0.60	31.2	40
3	0.4	**XS2**	50	14.5	330	2.25	42.8	3.48	2.07	0.55	25.9	30
3	0.5	**XS2**	100	14	330	1.33	45.9	2.11	2.14	0.60	29.6	40
5	0.5	**XS2**	50	14.5	330	2.21	42.8	3.42	2.07	0.55	25.8	30
2	0.3	**XS3e**	100	13	350	2.55	53.3	4.29	2.31	0.60	39.2	45
2	0.3	**XS3e**	50	13.5	350	2.55	49.4	4.16	2.22	0.55	30.2	35
3	0.4	**XS3e**	100	13	350	2.25	53.3	3.79	2.31	0.60	35.6	45
3	0.4	**XS3e**	50	13.5	350	2.25	49.4	3.67	2.22	0.55	28.9	35
5	0.5	**XS3e**	100	13	350	2.21	53.3	3.72	2.31	0.60	35.3	45
5	0.5	**XS3e**	50	13.5	350	2.21	49.4	3.61	2.22	0.55	28.8	35
9	0.6	**XS3e**	100	13	350	2.34	53.3	3.94	2.31	0.60	36.1	45
9	0.6	**XS3e**	50	13.5	350	2.34	49.4	3.82	2.22	0.55	29.3	35
1	0.3	**XS3m**	100	13	**400**	1.28	53.3	2.15	2.31	0.6	43.6	45
1	0.3	**XS3m**	50	13.5	350	1.28	49.4	2.09	2.22	0.55	37.9	35
1.5	0.4	**XS3m**	100	13	350	1.13	53.3	1.90	2.31	0.60	44.7	45
1.5	0.4	**XS3m**	50	13.5	350	1.13	49.4	1.85	2.22	0.55	36.2	35
2	0.5	**XS3m**	100	13	350	0.88	53.3	1.48	2.31	0.60	40.6	45
2	0.5	**XS3m**	50	13.5	350	0.88	49.4	1.44	2.22	0.55	33.0	35
3	0.6	**XS3m**	100	13	350	0.78	53.3	1.31	2.31	0.60	38.9	45
3	0.6	**XS3m**	50	13.5	350	0.78	49.4	1.27	2.22	0.55	31.6	35

The tables 4.A2.18 to 4.A2.20 show on a green background the cases where the provisions are estimated to be safe by calculation. On the yellow background, the necessary mix estimated by the calculation does not exceed the value resulting from the application of the Eurocode model by more than 5 mm, which can be considered as a margin covered by the difference between nominal and minimum mix (execution-related tolerance). With some plausible adjustments to the binder content assumptions, no situation appears where the mix is more than 5 mm below the calculated value. The number of cases where the calculated cover is less than the required value increases for the tables corresponding to a cover modulation, which is satisfactory.

Table 4.A.21. Validation of thresholds by comparison of recommended cover depths - XD-base thresholds (pivot classes S4-S6)

$D_{rcm\ 90}$ spec (10^{-12} m²/s)	Ageing Fact. α	Exposure class.	Service life (year)	Porosity (%)	Binder content (kg/m³)	D_{app} (50) avg (10^{-13} m²/s)	CoV (%)	D_{app} (50) char. (10^{-13} m²/s)	Enrich. 30/poro	Ccrit (% binder)	$c_{min.dur}$ XRDS gross (mm)	$c_{min.dur}$ PerfDuB (mm)
16	0.3	**XD1**	100	14	330	20.4	45.9	32.4	2.14	0.6	42.3	45
16	0.3	**XD1**	50	15	280	20.4	40.0	30.86	2.00	0.5	37.4	35
22	0.3	**XD1**	100	13.5	330	28.05	49.4	45.81	2.22	0.65	46.2	45
28	0.3	**XD1**	50	13.5	330	35.71	49.4	58.33	2.22	0.65	38.0	35
28	0.4	**XD1**	100	14	330	21.02	45.9	33.39	2.14	0.60	42.8	45
28	0.4	**XD1**	50	15	280	21.02	40.0	31.8	2.00	0.50	37.8	35
9	0.3	**XD2**	100	14	330	11.48	45.9	18.24	2.14	0.50	54.7	50
9	0.3	**XD2**	50	14.5	330	11.48	42.8	17.78	2.07	0.45	44.0	40
16	0.4	**XD2**	100	14	**350**	12.01	45.9	19.08	2.14	0.50	54.3	50
16	0.4	**XD2**	50	14.5	330	12.01	42.8	18.6	2.07	0.45	44.9	40
22	0.5	**XD2**	100	14	330	9.72	45.9	15.44	2.14	0.50	50.8	50
22	0.5	**XD2**	50	14.5	330	9.72	42.8	15.05	2.07	0.45	41.0	40
9	0.3	**XD3F**	100	13	350	11.48	53.3	19.32	2.31	0.60	55.7	55
9	0.3	**XD3F**	50	13.5	350	11.48	49.4	18.75	2.22	0.55	43.9	45
16	0.4	**XD3F**	100	13	350	12.01	53.3	20.22	2.31	0.60	56.8	55
16	0.4	**XD3F**	50	13.5	350	12.01	49.4	19.62	2.22	0.55	44.9	45
22	0.5	**XD3F**	100	13	350	9.72	53.3	16.36	2.31	0.60	51.5	55
22	0.5	**XD3F**	50	13.5	350	9.72	49.4	15.88	2.22	0.55	40.8	45
5	0.3	**XD3TF**	100	13	385	6.38	53.3	10.74	2.31	0.60	57.4	55
5	0.3	**XD3TF**	50	13	350	6.38	53.3	10.74	2.31	0.60	46.3	45
9	0.4	**XD3TF**	100	13	385	6.76	53.3	11.38	2.31	0.60	58.8	55
9	0.4	**XD3TF**	50	13	350	6.76	53.3	11.38	2.31	0.60	47.3	45
16	0.5	**XD3TF**	100	13	385	7.07	53.3	11.9	2.31	0.60	59.9	55
16	0.5	**XD3TF**	50	13	350	7.07	53.3	11.9	2.31	0.60	48.2	45

Table 4.A.22. Validation of thresholds by comparison of recommended cover depths - XD-modulation of one class (S3-S5)

$D_{rcm\ 90}$ spec (10^{-12} m²/s)	Ageing Fact. α	Exposure class	Service life (year)	Poro. (%)	Binder content (kg/m³)	D_{app} (50) avg (10^{-13} m²/s)	CoV (%)	D_{app} (50) char. (10^{-13} m²/s)	Enrich. 30/poro	Ccrit (% binder)	$c_{min.dur}$ XRDS gross (mm)	$c_{min.dur}$ PerfDuB (mm)
9	0.3	**XD1**	100	14	330	11.48	45.9	18.24	2.14	0.60	33.7	40
9	0.3	**XD1**	50	15	280	11.48	40.0	17.37	2.00	0.50	30.3	30
16	0.3	**XD1**	100	13.5	330	20.4	49.4	33.32	2.22	0.65	40.4	40
22	0.3	**XD1**	50	13.5	330	28.05	49.4	45.81	2.22	0.65	34.5	30
22	0.4	**XD1**	100	14	330	16.52	45.9	26.24	2.14	0.60	38.8	40
22	0.4	**XD1**	50	15	280	16.52	40.0	24.99	2.00	0.50	34.5	30
5	0.3	**XD2**	100	14	330	6.38	45.9	10.13	2.14	0.50	42.3	45
5	0.3	**XD2**	50	14.5	330	6.38	42.8	9.88	2.07	0.45	34.5	35
9	0.4	**XD2**	100	14	330	6.76	45.9	10.74	2.14	0.50	43.3	45
9	0.4	**XD2**	50	14.5	330	6.76	42.8	10.47	2.07	0.45	35.2	35
16	0.5	**XD2**	100	14	330	7.07	45.9	11.23	2.14	0.5	44.2	45
16	0.5	**XD2**	50	14.5	330	7.07	42.8	10.95	2.07	0.45	35.9	35
5	0.3	**XD3F**	100	13	350	6.38	53.3	10.74	2.31	0.60	42.3	50
5	0.3	**XD3F**	50	13.5	350	6.38	49.4	10.42	2.22	0.55	33.7	40
9	0.4	**XD3F**	100	13	350	6.76	53.3	11.38	2.31	0.60	43.5	50
9	0.4	**XD3F**	50	13.5	350	6.76	49.4	11.04	2.22	0.55	34.6	40
16	0.5	**XD3F**	100	13	350	7.07	53.3	11.90	2.31	0.60	44.4	50
16	0.5	**XD3F**	50	13.5	350	7.07	49.4	11.55	2.22	0.55	35.3	40
3	0.3	**XD3TF**	100	13	385	3.83	53.3	6.45	2.31	0.60	47.2	50
3	0.3	**XD3TF**	50	13	350	3.83	53.3	6.45	2.31	0.60	38.2	40
5	0.4	**XD3TF**	100	13	385	3.75	53.3	6.31	2.31	0.60	46.8	50
5	0.4	**XD3TF**	50	13	350	3.75	53.3	6.31	2.31	0.60	37.9	40
9	0.5	**XD3TF**	100	13	385	3.98	53.3	6.70	2.31	0.60	47.9	50
9	0.5	**XD3TF**	50	13	350	3.98	53.3	6.70	2.31	0.60	38.7	40

As for the XS classes, the XD class tables show on a green background the cases where the provisions are estimated safe by the calculation. The yellow background shows that the required mix estimated by the calculation does not exceed the value derived from the application of the Eurocode by more than 5 mm, which can be considered as a margin covered by the deviation between nominal and minimum mix (execution-related tolerance). With a very limited number of plausible adjustments to the binder content assumptions, there is no situation where the mix is more than 5 mm below the calculated value. The number of cases where the calculated mix is less than the required value increases for the tables corresponding to a mix modulation, which is satisfactory as there is less feedback.

Table 4.A.23. Validation of thresholds by comparison of recommended cover depths - XD-modulation of two classes (S2-S4)

$D_{rcm\ 90}$ spec (10^{-12} m²/s)	Ageing Fact. α	Exposure class	Service life (year)	Poro. (%)	Binder content (kg/m³)	D_{app} (50) avg (10^{-13} m²/s)	CoV (%)	D_{app} (50) char. (10^{-13} m²/s)	Enrich. 30/poro	Ccrit (% binder)	$c_{min.dur}$ XRDS gross (mm)	$c_{min.dur}$ PerfDuB (mm)
5	0.3	**XD1**	100	14	330	6.38	45.9	10.13	2.14	0.60	27.1	35
5	0.3	**XD1**	50	15	280	6.38	40.0	9.65	2.00	0.50	24.9	25
9	0.3	**XD1**	100	13.5	330	11.48	49.4	18.75	2.22	0.65	32.1	35
16	0.3	**XD1**	50	13.5	**350**	20.4	49.4	33.32	2.22	0.65	29.6	25
16	0.4	**XD1**	100	14	330	12.01	45.9	19.08	2.14	0.60	34.2	35
16	0.4	**XD1**	50	15	**320**	12.01	40.0	18.17	2.00	0.50	29.4	25
3	0.3	**XD2**	100	14	330	3.83	45.9	6.08	2.14	0.50	34.1	40
3	0.3	**XD2**	50	14.5	330	3.83	42.8	5.93	2.07	0.45	28.1	30
5	0.4	**XD2**	100	14	330	3.75	45.9	5.96	2.14	0.50	33.8	40
5	0.4	**XD2**	50	14.5	330	3.75	42.8	5.81	2.07	0.45	27.9	30
9	0.5	**XD2**	100	14	330	3.98	45.9	6.32	2.14	0.50	34.6	40
9	0.5	**XD2**	50	14.5	330	3.98	42.8	6.16	2.07	0.45	28.5	30
3	0.3	**XD3F**	100	13	350	3.83	53.3	6.45	2.31	0.60	33.6	45
3	0.3	**XD3F**	50	13.5	350	3.83	49.4	6.26	2.22	0.55	27.0	35
5	0.4	**XD3F**	100	13	350	3.75	53.3	6.31	2.31	0.60	33.3	45
5	0.4	**XD3F**	50	13.5	350	3.75	49.4	6.12	2.22	0.55	26.7	35
9	0.5	**XD3F**	100	13	350	3.98	53.3	6.70	2.31	0.60	34.1	45
9	0.5	**XD3F**	50	13.5	350	3.98	49.4	6.50	2.22	0.55	27.4	35
2	0.3	**XD3TF**	100	13	385	2.55	53.3	4.29	2.31	0.60	40.6	45
2	0.3	**XD3TF**	50	13	350	2.55	53.3	4.29	2.31	0.60	33.0	35
3	0.4	**XD3TF**	100	13	385	2.25	53.3	3.79	2.31	0.60	39.0	45
3	0.4	**XD3TF**	50	13	350	2.25	53.3	3.79	2.31	0.60	31.6	35
5	0.5	**XD3TF**	100	13	385	2.21	53.3	3.72	2.31	0.60	38.7	45
5	0.5	**XD3TF**	50	13	350	2.21	53.3	3.72	2.31	0.60	31.4	35

APPENDIX B: Performance thresholds for a single structural class reduction

Table 4.B.1. Performance thresholds for reduction of one structural class expressed in terms of characteristic values (with a fractile of 90%) - Exposure classes XC for a 50-year design service life

	Performance qualification criteria				
	Modulation according to resistivity class at 90d (Ω.m)	Characteristic accelerated carbonation rate (in mm/day$^{0.5}$) for 50-year design service life			
Exposure class		Data base	Modevie Modelling	Model XRC	Thresholds retained
XC1	< 100	/	4	2.6	**3**
	100 à 175		4		
	> 175		4		
XC2	< 100	/	2.9	2.2	**2.6**
	100 à 175		2.9	2.6	**3**
	> 175		2.9	2.6	
XC3	< 100	/	1.4	1.4	**1.4**
	100 à 175		1.5	1.8	**1.8**
	> 175		1.6	1.8	
XC4	< 100	/	1.7	1.8	**1.4**
	100 à 175		2	1.8	**1.8**
	> 175		3	2.2	**2.6**

Table 4.B.2. Performance thresholds for reduction of one structural class expressed in terms of characteristic values (with a 90% fractile) - exposure classes XC for a 100-year design service life

	Performance qualification criteria				
	Modulation according to resistivity class at 90d (Ω.m)	Characteristic accelerated carbonation rate (in mm/day$^{0.5}$) for 100-year design service life			
Exposure class		**Data base**	**Modevie Modelling**	**Model XRC**	**Thresholds retained**
XC1	< 100	/	4	3	**3**
	100 à 175				
	> 175				
XC2	< 100	/	2.9	2.2	**2.2**
	100 à 175			2.2	**2.6**
	> 175				
XC3	< 100	/	1.4	1.4	**1.4**
	100 à 175		1.4		
	> 175		1.5		
XC4	< 100	/	1.5	1.4	**1.4**
	100 à 175		1.6	1.8	**1.8**
	> 175		2		

Table 4.B.3. Performance thresholds for reduction of one structural class expressed in terms of characteristic values (with a 90% fractile) - XS exposure classes for a 50-year design service life

	Performance qualification criteria				
	Modulation according to ageing factor class	Chloride ion migration coefficient (in 10^{-12} m²/s) for 50-year design service life			
Exposure class		**Data base**	**PerfDuB Modelling**	**Model XRDS**	**Thresholds retained**
XS1	0.30 à 0.39	/	14 (19*)		**9 (22*)**
	0.40 à 0.49		22		**22**
	0.50 à 0.59		36		
	0.60 and above				
XS2	0.30 à 0.39	/	4		**3 (5*)**
	0.40 à 0.49		7		**5**
	0.50 à 0.59		11		**9**
	0.60 and above		20		
XS3e	0.30 à 0.39	/	3		**3**
	0.40 à 0.49		5		**5**
	0.50 à 0.59		8		**9**
	0.60 and above		16		**16**
XS3m	0.30 à 0.39	/	1.3		**1.5**
	0.40 à 0.49		2.2		**2**
	0.50 à 0.59		3.5		**3**
	0.60 and above		7		**5**

**: values with an asterisk are applicable for concretes whose water porosity measured at 90 days is less than or equal to 13.5%*

For the XS classes, the thresholds resulting from the XRDS modelling were not calculated but the covers deduced from the values retained were checked for consistency with the targeted cover reduction (see appendix A).

Table 4.B.4. Performance thresholds for reduction of one structural class expressed in terms of characteristic values (with a 90% fractile) - XS exposure classes for a 100-year design service life

	Performance qualification criteria				
	Modulation according to ageing factor class	Chloride ion migration coefficient (in 10^{-12} m²/s) for 100-year design service life			
Exposure class		Data base	PerfDuB Modelling	Model XRDS	Thresholds retained
XS1	0.30 à 0.39	/	13 (17*)		**5 (9*)**
	0.40 à 0.49		22		**16**
	0.50 à 0.59		40		
	0.60 and above				
XS2	0.30 à 0.39	/	3		**2 (3*)**
	0.40 à 0.49		6		**3**
	0.50 à 0.59		10		**5**
	0.60 and above		22		
XS3e	0.30 à 0.39	/	3		**3**
	0.40 à 0.49		5		**5**
	0.50 à 0.59		9		**9**
	0.60 and above		22		**16**
XS3m	0.30 à 0.39	/	1.4		**1.5**
	0.40 à 0.49		2.4		**2**
	0.50 à 0.59		4.5		**3**
	0.60 and above		10		**5**

**: values with an asterisk are applicable for concrete whose water porosity measured at 90 days is less than or equal to 13.5%*

For the XS classes, the thresholds resulting from the XRDS modelling were not calculated but the covers deduced from the values retained were checked for consistency with the targeted cover reduction (see Appendix A).

Table 4.B.5. Performance thresholds for reduction of one structural class expressed in terms of characteristic values (with a 90% fractile) - XD exposure classes for a 50-year design service life

	Performance qualification criteria				
	Modulation according to ageing factor class	Chloride ion migration coefficient (in 10^{-12} m²/s) for 50-year design service life			
Exposure class		Data base	PerfDuB Modelling	Model XRDS	Thresholds retained
XD1	0.30 à 0.39	/			**9 (22*)**
	0.40 à 0.49				**22**
	0.50 à 0.59				
	0.60 and above				
XD2	0.30 à 0.39	/	6		**5**
	0.40 à 0.49		10		**9**
	0.50 à 0.59		16		**16**
	0.60 and above		31		
XD3 Frequent salting	0.30 à 0.39	/	7		**5**
	0.40 à 0.49		11		**9**
	0.50 à 0.59		19		**16**
	0.60 and above		36		
XD3 Very frequent salting	0.30 à 0.39	/			**3**
	0.40 à 0.49				**5**
	0.50 à 0.59				**9**
	0.60 and above				

**: values with an asterisk are applicable for concretes whose water porosity measured at 90 days is less than or equal to 13.5%*

For the XD classes, the thresholds resulting from the XRDS modelling were not calculated, but the covers deduced from the values retained were checked for consistency with the targeted cover reduction (see Appendix A).

Table 4.B.6. Performance thresholds for reduction of one structural class expressed in terms of characteristic values (with a 90% fractile) - XD exposure classes for a 100-year design service life

	Performance qualification criteria				
	Modulation according to ageing factor class	Chloride ion migration coefficient (in 10^{-12} m²/s) for 100-year design service life			
Exposure class		Data base	Modelling PerfDuB	Model XRDS	Thresholds retained
XD1	0.30 à 0.39	/			9 (16*)
	0.40 à 0.49				22
	0.50 à 0.59				
	0.60 and above				
XD2	0.30 à 0.39	/	5		5
	0.40 à 0.49		8		9
	0.50 à 0.59		15		16
	0.60 and above		33		
XD3 Frequent salting	0.30 à 0.39	/	7		5
	0.40 à 0.49		12		9
	0.50 à 0.59		21		16
	0.60 and above		46		
XD3 Very frequent salting	0.30 à 0.39	/			3
	0.40 à 0.49				5
	0.50 à 0.59				9
	0.60 and above				

**: values with an asterisk are applicable for concretes whose water porosity measured at 90 days is less than or equal to 13.5%*

For the XD classes, the thresholds resulting from the XRDS modelling were not calculated, but the covers deduced from the values retained were checked for consistency with the targeted cover reduction (see Appendix A).

APPENDIX C: Performance thresholds for reduction of 2 structural classes

Table 4.C.1. Performance thresholds for reduction of two structural classes expressed in terms of characteristic values (with a 90% fractile) - Exposure classes XC for a 50-year design service life

	Performance qualification criteria				
	Modulation according to resistivity class at 90d (Ω.m)	Characteristic accelerated carbonation rate (in mm/day$^{0.5}$) for 50-year design service life			
Exposure class		Data base	Modevie Modelling	Model XRC	Thresholds retained
XC1	< 100	/	4	1.4	**2.2**
	100 à 175		4		
	> 175		4		
XC2	< 100	/	2.3	1.8	**2.2**
	100 à 175		2.3	1.8	
	> 175		2.3	1.8	
XC3	< 100	2.0	1.1	1	**1**
	100 à 175		1.2	1	**1.4**
	> 175		1.2	1.4	
XC4	< 100	2.0	1.3	1.4	**1**
	100 à 175		1.5	1.4	**1.4**
	> 175		2	1.8	**1.8**

Table 4.C.2. Performance thresholds for reduction of two structural classes expressed in terms of characteristic values (with a 90% fractile) - Exposure classes XC for a 100-year design service life

	Performance qualification criteria				
	Modulation according to resistivity class at 90d (Ω.m)	Characteristic accelerated carbonation rate (in mm/day$^{0.5}$) for 100-year design service life			
Exposure class		**Data base**	**Modevie Modelling**	**Model XRC**	**Thresholds retained**
XC1	< 100	/	4	1.8	**1.8**
	100 à 175		4		
	> 175		4		
XC2	< 100	/	2.4	1.8	**1.8**
	100 à 175		2.4	1.8	
	> 175		2.4	1.8	
XC3	< 100	/	1.2	1	**1**
	100 à 175		1.2		
	> 175		1.3		
XC4	< 100	/	1.3	1	**1**
	100 à 175		1.4	1.4	
	> 175		1.6		**1.4**

Table 4.C.3 - Performance thresholds for reduction of two structural classes expressed in terms of characteristic values (with a 90% fractile) - exposure classes XS for a 50-year design service life

	Performance qualification criteria				
	Modulation according to ageing factor class	Chloride ion migration coefficient (in 10^{-12} m²/s) for 50-year design service life			
Exposure class		**Data base**	**PerfDuB Modelling**	**Model XRDS**	**Thresholds retained**
XS1	0.30 à 0.39	34	10 (14*)		**5 (16*)**
	0.40 à 0.49		16		**16**
	0.50 à 0.59		26		
	0.60 and above				
XS2	0.30 à 0.39	34	3		**2 (3*)**
	0.40 à 0.49		5		**3**
	0.50 à 0.59		8		**5**
	0.60 and above		16		
XS3e	0.30 à 0.39	17	2		**2**
	0.40 à 0.49		3		**3**
	0.50 à 0.59		5		**5**
	0.60 and above		10		**9**
XS3m	0.30 à 0.39	17	0.9		**1**
	0.40 à 0.49		1.5		**1.5**
	0.50 à 0.59		2.4		**2**
	0.60 and above		4.5		**3**

**: values with an asterisk are applicable for concrete whose water porosity measured at 90 days is less than or equal to 13.5%*

For the XS classes, the thresholds resulting from the XRDS modelling were not calculated but the covers deduced from the values retained were checked for consistency with the targeted cover reduction (see Appendix A).

Table 4.C.4 - Performance thresholds for reduction of two structural classes expressed in terms of characteristic values (with a 90% fractile) - exposure classes XS for a 100-year design service life

	Performance qualification criteria				
	Modulation according to ageing factor class	Chloride ion migration coefficient (in 10^{-12} m²/s) for 100-year design service life			
Exposure class		Data base	PerfDuB Modelling	Model XRDS	Thresholds retained
XS1	0.30 à 0.39	/	10 (13*)		**3 (5*)**
	0.40 à 0.49		17		**9**
	0.50 à 0.59		30		
	0.60 and above		90		
XS2	0.30 à 0.39	/	2.5		**1.5 (2*)**
	0.40 à 0.49		4		**2**
	0.50 à 0.59		8		**3**
	0.60 and above		18		
XS3e	0.30 à 0.39	/	2.4		**2**
	0.40 à 0.49		4		**3**
	0.50 à 0.59		7		**5**
	0.60 and above		16		**9**
XS3m	0.30 à 0.39	/	1		**1**
	0.40 à 0.49		1.8		**1.5**
	0.50 à 0.59		3		**2**
	0.60 and above		7		**3**

**: values with an asterisk are applicable for concretes whose water porosity measured at 90 days is less than or equal to 13.5%*

For the XS classes, the thresholds resulting from the XRDS modelling were not calculated, but the covers deduced from the values retained were checked for consistency with the targeted cover reduction (see Appendix A).

Table 4.C.5 - Performance thresholds for reduction of two structural classes expressed in terms of characteristic values (with a fractile of 90%) - XD exposure classes for a 50-year design service life

	Performance qualification criteria				
	Modulation according to ageing factor class	Chloride ion migration coefficient (in 10^{-12} m²/s) for 50-year design service life			
Exposure class		**Data base**	**PerfDuB Modelling**	**Model XRDS**	**Thresholds retained**
XD1	0.30 à 0.39	/			**5 (16*)**
	0.40 à 0.49				**16**
	0.50 à 0.59				
	0.60 and above				
XD2	0.30 à 0.39	/	4		**3**
	0.40 à 0.49		7		**5**
	0.50 à 0.59		12		**9**
	0.60 and above		23		
XD3 Frequent salting	0.30 à 0.39	/	4		**3**
	0.40 à 0.49		7		**5**
	0.50 à 0.59		12		**9**
	0.60 and above		23		
XD3 Very frequent salting	0.30 à 0.39	/			**2**
	0.40 à 0.49				**3**
	0.50 à 0.59				**5**
	0.60 and above				

**: values with an asterisk are applicable for concrete whose water porosity measured at 90 days is less than or equal to 13.5%*

For the XD classes, the thresholds resulting from the XRDS modelling were not calculated, but the covers deduced from the values retained were checked for consistency with the targeted cover reduction (see Appendix A).

Table 4.C.6 - Performance thresholds for reduction of two structural classes expressed in terms of characteristic values (with a fractile of 90%) - XD exposure classes for a 100-year design service life

	Performance qualification criteria				
	Modulation according to ageing factor class	Chloride ion migration coefficient (in 10^{-12} m²/s) for 100-year design service life			
Exposure class		**Data base**	**PerfDuB Modelling**	**Model XRDS**	**Thresholds retained**
XD1	0.30 à 0.39	/			**5 (9*)**
	0.40 à 0.49				**16**
	0.50 à 0.59				
	0.60 and above				
XD2	0.30 à 0.39	/	4		**3**
	0.40 à 0.49		7		**5**
	0.50 à 0.59		12		**9**
	0.60 and above		26		
XD3 Frequent salting	0.30 à 0.39	/	5		**3**
	0.40 à 0.49		9		**5**
	0.50 à 0.59		16		**9**
	0.60 and above		35		
XD3 Very frequent salting	0.30 à 0.39	/			**2**
	0.40 à 0.49				**3**
	0.50 à 0.59				**5**
	0.60 and above				

**: values with an asterisk are applicable for concrete whose water porosity measured at 90 days is less than or equal to 13.5%*

For the XD classes, the thresholds resulting from the XRDS modelling were not calculated, but the covers deduced from the values retained were checked for consistency with the targeted cover reduction (see Appendix A).

Conclusion

The PerfDuB National Project is an important step in the development of our knowledge of the ageing of reinforced concrete structures and the technical specification of concretes. It follows on from collaborative research projects conducted in France over the last few decades, the results of which have enabled the construction industry to make progress thanks to a scientific approach to the phenomena involved, whereas the rules of the art were originally essentially empirical.

Controlling the longevity of concrete structures is essential for a construction material whose main virtue is its great potential durability without major maintenance. Maintaining this technical quality while optimising formulations in terms of their environmental impact, particularly low-carbon concretes, is a major challenge for the construction industry. Thanks to a large number of experimental and modelling results, combined with extensive and unprecedented feedback on old structures, the PerfDub National Project has succeeded in putting forward consensual proposals, both in terms of operating methods and the normative application of the performance-based approach. Fascicule FD P18-480, which explains the application methods, and the new concrete standard NF EN 206/CN, which refers to it, were published in October 2022, which means that standardised performance concretes can now be used, opening the door to the democratisation of these concretes. So, while we obviously hope that these proposals will quickly be put to use by the profession, we can consider that the main objectives set at the start of the project have been achieved.

However, much remains to be done. The case of attack on concrete by chemically aggressive media, which is currently mainly dealt with using a comparative approach, needs to be fed by a database of accelerated ageing test results with the aim of defining absolute criteria. As regards the corrosion propagation phase, which is a new element of the PerfDuB National Project, the understanding of the mechanisms and the corresponding modelling need to be refined.

It is with this aim in mind in particular that test bodies, i.e. twenty-eight reinforced concrete walls, have been made and installed at ageing sites (in La Rochelle and the Paris region): like those carried out at the end of the 1990s as part of the BHP 2000 National Project, they will make it possible to carry out in situ measurements and further improve our knowledge of the durability of reinforced concrete and our ability to optimise its use.

François Cussigh

Director of the project

Gilles Escadeillas

Scientific Director of the project

Acknowledgements

The challenges of the PerfDuB National Research Project "Performantial Approach to the Durability of Concrete Structures", launched in 2015, were to define a nationwide methodology for justifying the durability of concrete (and concrete structures) using a performantial approach, including the "absolute" method and the "comparative" method. The aim was to aggregate knowledge and experience feedback, and to fill in the gaps, in a framework that brought together the vast majority of stakeholders. The aim of the project was to make the performance-based approach operational and widely used.

The PerfDuB National Project was managed and administered by IREX, the Institute for Applied Research and Experimentation in Civil Engineering (www.irex.asso.fr), whose main mission is to set up and monitor collective research initiatives, including National Projects approved by the Steering Committee for Applied Research in Civil Engineering of the French Ministry for Ecological Transition and Territorial Cohesion. I would like to take this opportunity to thank the entire IREX team, which helped to make the work of the partners as smooth and efficient as possible over the period of the project.

The project brought together more than 50 partners over the period 2015-2022. We would like to thank them all for their investment, the time they devoted to the substantial work carried out to achieve the results developed.

The general objectives and scope of the research were to:

- develop a real engineering of the concrete material through the study of 42 concretes and the drafting of test procedures;
- enable the prescription of standardised concretes incorporating recycled or low environmental impact aggregates;
- optimise the overall cost and durability of new structures;
- know how to requalify old structures and optimise maintenance management;
- prepare a methodology that can be transposed to the European level, which would enhance the value of French expertise in concrete structures.

This book, the collective work of most of the partners, brings together in the chapters that follow the major conclusions of this work.

Philippe Gotteland

General Delegate of IREX

PerfDuB Working Group leaders

The PerfDuB research programme is divided into different areas, each of which is led by a pair of representatives from industry and academia to ensure a good balance between theoretical and pragmatic approaches.

Theme	Coordinators
Durability testing (WG1)	B. Thauvin (Cerema) C. Clergue (Sigma Béton) D. Rogat (Sigma Béton)
• Sub-group 1: carbonation/chlorides (WG1A)	P. Turcry (Université de La Rochelle) E. Rozière (GeM Nantes) J. Mai-Nhu (CERIB)
• Sub-group 2: freezing/chipping (WG1B)	C. Clergue (Sigma Béton) D. Rogat (Sigma Béton) L. Izoret (ATILH)
• Sub-group 3: external attack (WG1C)	M. Guéguen-Minerbe (IFSTTAR-UGE) F. Cassagnabère (LMDC Toulouse)
Permissible performance thresholds (WG2)	M. Carcassès (LMDC Toulouse) E. Brouard (Lafarge) F. Moro (Lafarge)
• Sub-group 1: old structures (WG2A)	B. Godart (IFSTTAR-UGE)
• Sub-group 2: modelling (WG2B))	V. Baroghel-Bouny (IFSTTAR-UGE)
Choice of reference concretes and consideration of variability (WG3)	E. Rozière (GeM Nantes) P. Rougeau (CERIB)
• Sub-group 1: reference concretes (WG3A)	O. Collin (Lafarge Bétons) J.-M. Laye (Lafarge)
• Sub-group 2: variability (WG3B)	P. Gegout (Bouygues TP) S. Chanut (Eiffage Génie Civil)
Contractualisation of the approach (WG4)	L. Linger (Vinci Construction Grands Projets) P. Gegout (Bouygues TP) P. Fonollosa (Bouygues TP) J.-M. Potier (SNBPE)
Valorisation (WG5)	S. Mansoutre (Vicat) P. Brédy-Tuffé (Vicat) C. Clergue (Eiffage Génie Civil) S. Chanut (Eiffage Génie Civil)

Participants in the CSI International Scientific Committee

From October 2016 to October 2021, 6 CSIs (face-to-face and distance learning) will be offered to our foreign scientific colleagues, mainly from Europe, in the form of an International Monitoring Committee.

The PerfDuB National Project was presented to them, from the state of the art of a performance-based approach to contractualisation and French standardisation based on the results of the PN.

The aim of these meetings was twofold: to compare and adapt the research program to the opinion of international sustainability experts, and to prepare for the subsequent dissemination of this performance-based approach at an international level.

We would therefore like to extend our warmest thanks to the following people for their participation and their contribution to our National Project.

Name	Country
Mark Alexander	South Africa
Rolf Breitenbuecher Lars Meyer Udo Wiens	Germany
Geert De Schutter	Belgium
Arezki Tagnit-Hamou	Canada
Carmen Andrade	Spain
Véronique Baroghel-Bouny François Toutlemonde	France
Stefano Cangiano Roberto Cucitore	Italy
Steinar Helland Steinar Leivestad	Norway
Joost Gulikers	Netherlands
Arlindo Goncalvez	Portugal
Tom Harrison †	United Kingdom
Mikael Hallgren	Sweden
Fritz Hunkeler Karen Scrivener	Switzerland

PerfDuB partners

Typology	Partners
Research centres	CERIB
Construction companies	BOUYGUES TP EIFFAGE Infrastructures FFB FNTP VINCI Construction France VINCI Construction Grands Projets
Manufacturers / Trade associations	ARGECO CEMEX CHRYSO CIMENTS CALCIA CONDENSIL ECOCEM EQIOM IMERYS LafargeHolcim France MBSF OMYA SFIC SIBELCO SIKA SNBPE SURSCHISTE UNPG VICAT

Typology	Partners
Engineering / Design offices	CONCRETE GEOS Laboratories GINGER CEBTP LERM RINCENT BTP SIGMA BETON SITES TECHNICONCRETE
Public authorities	ANDRA DGITM EDF
Research organisations	C2MA CEA Saclay CEREMA ECL ENS Cachan ESTP GeM ICUBE INSA de Rennes L2MGC LASIE LGCgE LMDC LRMH Université Gustave-Eiffel
Insurers	SOCABAT

List of PerfDuB internal study reports

Working Group 1: Durability tests

PERF/R/005 - Etude préliminaire : Essais croisés de carbonatation accélérée, P. Turcry (LaSIE, Université de La Rochelle)

PERF/R/006 - Etude préliminaire : Essais paramétriques de carbonatation accélérée, A.Chonier et G. Pham (LafargeHolcim)

PERF/R/010 - Étude préliminaire : Essais croisés de migration des chlorures et résistivité, L. Schmitt et J. Mai-Nhu (CERIB)

PERF/R/011 - Etude préliminaire : Essais croisés de perméabilité aux gaz, J.-L. Dupuy et E. Perin (LERM)

PERF/R/012 - Etude préliminaire : Essais croisés de perméabilité aux gaz, G. Pham et T. Parment (LafargeHolcim)

PERF/R/013 - Etude préliminaire : Essais croisés de carbonatation accélérée, E. Rozière (GeM, Centrale Nantes)

PERF/R/014 - Essai de porosité accessible à l'eau et d'absorption d'eau par capillarité dans le cadre de la campagne d'essais croisés du PN Perfdub (Tranche 1) (selon la version V1 de la norme NF P 18-459 - mars 2010), L. Schmitt (CERIB)

PERF/R/015 - Etude préliminaire : Essais croisés de perméabilité aux gaz, L. Schmitt et J. Mai-Nhu (CERIB)

PERF/R/016 - Etude préliminaire : Etude paramétrique relative à la perméabilité aux gaz, F. Agostini (Centrale Lille)

PERF/R/017 - Concretes Designs, mixing, placing and maturation, M. Gueguen (IFSTTAR), F. Jacquemot (CERIB), F. Cassagnabère (LMDC, Université de Toulouse)

PERF/R/018 - Etude préliminaire : Essais croisés de porosité accessible à l'eau et absorption capillaire, J.-L. Dupuy et E. Perin (LERM)

PERF/R/019 - Etude préliminaire : Essais croisés de migration des chlorures et résistivité, Stéphanie BONNET (Laboratoire GeM, UMR CNRS 6183, équipe IEG)

PERF/R/021 - Etude préliminaire fabrication des éprouvettes (bétons n°1, 4, 7, 31, 38), S. Delair (GINGER CEBTP)

PERF/R/022 - Etude préliminaire : Essais croisés de migration des chlorures et résistivité électrique, J-L. Dupuy, E. Perin, A. Ammouche (LERM)

PERF/R/023 - Etude préliminaire : Essais croisés de perméabilité aux gaz, B. Boulet et V. Garde (Cerema Clermont-Ferrand)

PERF/R/024 - Étude préliminaire : Essais croisés de carbonatation accélérée, L. Schmitt et J. Mai-Nhu (CERIB)

PERF/R/025 - Étude préliminaire : Essais paramétriques de carbonatation accélérée, L. Schmitt et J. Mai-Nhu (CERIB)

PERF/R/026 - Etude préliminaire : Essais croisés de migration des chlorures et résistivité, B. Thauvin et M. Menguy (Cerema St Brieuc), M. Dierkens et C. Merzejewski (Cerema Lyon)

PERF/R/027 - Essai accéléré de lixiviation par la méthode du LEACHCRETE, L. Bessette et E. Schmitt (VICAT)

PERF/R/028 - Etude préliminaire RSE : Perfectionnement de l'essai RSE. Essai alternatif en laboratoire, E. Rozière et S. Boudache (GeM, Centrale Nantes), F. Cassagnabère (LMDC, Université de Toulouse)

PERF/R/029 - Etude préliminaire RSE : Perfectionnement de l'essai RSE. Essai alternatif en laboratoire, O. Omikrine Metalssi et M. Jabbour (IFSTTAR)

PERF/R/030 - Diffusion des chlorures sur 5 bétons, A. Bauland et G. Pham (LafargeHolcim)

PERF/R/031 - Essai de porosité accessible à l'eau et d'absorption d'eau par capillarité. Etude paramétrique, P. Paya (Cerema Aix-en-Provence), G. Pham (LafargeHolcim), T. Fanget (Cerema Autun)

PERF/R/033 - Etudes préliminaires : Essais croisés de carbonatation accélérée, S. Kamali-Bernard, Y. Muy et J.-Y Brossault (LGCGM Rennes)

PERF/R/034 - Etude préliminaire : Essai de porosité accessible à l'eau et d'absorption d'eau par capillarité dans le cadre de la campagne d'essais croisés du PN Perfdub (Tranche 1) (selon la version V1 de la norme NF P 18-459 - mars 2010), R. Dutruel (EDF CEIDRE/TEGG/laboratoire béton)

PERF/R/035 - Etude préliminaire : Etude paramétrique relative à la carbonatation accélérée, S. Kamali-Bernard, Y. Muy et J.-Y Brossault (LGCGM Rennes)

PERF/R/036 - Perfectionnement de l'essai de Lixiviation à pH constant - Travaux de la tranche 1, F. Jacquemot (CERIB), A. Bertron, M. Berthomier et V. Mazars (LMDC, Université de Toulouse), P. Le Bescop (CEA), R. Dutruel et G. Zammout (EDF), A. Ammouche (LERM), M. Salgues et D. Bulteel (ARMINES)

PERF/R/037 - Etude préliminaire RSE : Essai alternatif en laboratoire selon la norme SIA 262/1 :2013-ANNEXE D, S. Meulenyzer (Lafargeholcim Centre de Recherche)

PERF/R/038 - Etude préliminaire RSE : Perfectionnement de l'essai RSE. Essai alternatif en laboratoire, F. Cassagnabère (LMDC, Université de Toulouse)

PERF/R/039 - Perméabilité aux gaz sur les bétons d'un des 5 lots, G. Pham et T. Parment (LafargeHolcim)

PERF/R/040 - Etude préliminaire : Biodégradation, M. Guéguen Minerbe et T. Chaussadent (IFSTTAR), M. Peyre Lavigne et A. Bertron (INSA Toulouse)

PERF/R/042 - Essai accéléré de lixiviation (eau pure acide) – Leachcrete - Tranche 1, E. Moudilou (Ciments CALCIA)

PERF/R/047 - Essais de carbonatation accélérée EN sur 8 bétons (lot 1), A. Chonier et G. Pham (LafargeHolcim)

PERF/R/048 - Étude préliminaire : Exploitation statistique des résultats des essais croisés, S. Delair (GINGER CEBTP)

PERF/R/049 - Essai de biodégradation : Exposition in situ de mortiers en présence d'H_2S, M. Guéguen Minerbe et T. Chaussadent (IFSTTAR), M. Peyre Lavigne et A. Bertron (INSA Toulouse)

PERF/R/050 - Caractérisation d'un échantillon de béton prélevé sur un ouvrage d'assainissement (biodétérioration en présence d'H_2S) et essai accéléré sur un échantillon prélevé dans une zone saine de cet ouvrage, M. Guéguen Minerbe et T. Chaussadent (IFSTTAR)

PERF/R/053 - Essais de carbonatation accélérée NF sur 9 formules béton, S. Delair (GINGER CEBTP)

PERF/R/054 - Résistivité, migration des chlorures en régime non stationnaire sur les bétons d'un des 5 lots, P.-A Franco et J. Semenadisse (Vinci Construction France)

PERF/R/062 - Migration des ions chlorure et résistivité sur les bétons d'un des 5 lots, G. Martin, B. Loiseau et L. Schmitt (CERIB)

PERF/R/063 - Porosité accessible à l'eau, absorption capillaire et absorption d'eau sur les bétons d'un des 5 lots, G. Martin, B. Loiseau et L. Schmitt (CERIB)

PERF/R/064 - Perméabilité aux gaz sur les bétons d'un des 5 lots, G. Martin, B. Loiseau et L. Schmitt (CERIB)

PERF/R/066 - Carbonatation accélérée selon le mode opératoire français sur 8 bétons, E. Rozière, F. Kaddah, M. Marcel, M. Michaut et Vincent Wisniewski (GeM, Centrale Nantes)

PERF/R/067 - Sulfate resistance test - Part 2: Test on GT3 concretes, F. Cassagnabère et D.L. Tran (LMDC, Université de Toulouse)

PERF/R/068 - Carbonatation accélérée selon le mode opératoire français et carbonatation naturelle sur un lot de 8 bétons, P. Turcry, A. El Farissi, J.D. Lau Hiu Hoong, Y. Hou, P-Y. Mahieux et A. Younsi (LaSIE, UMR 7356 CNRS, La Rochelle Université)

PERF/R/069 - Carbonatation accélérée selon le mode opératoire européen sur un lot de 8 bétons, P. Turcry, A. El Farissi, J.D. Lau Hiu Hoong, Y. Hou, P-Y. Mahieux et A. Younsi (LaSIE, UMR 7356 CNRS, La Rochelle Université)

PERF/R/071 - Essais de perméabilité aux gaz sur carottes de bétons de diamètre 50 mm, E. Perin, A. Ammouche et J.-L. Dupuy (LERM SETEC)

PERF/R/072 - Essais de porosité accessible, d'absorption capillaire et d'absorption d'eau, J.-L. Dupuy, M. Bonnet, E. Perin et A. Ammouche (LERM SETEC)

PERF/R/073 - Essais de résistivité électrique et de migration des chlorures en régime non stationnaire sur un lot de 8 bétons, M. Bonnet, E. Perin, J.-L. Dupuy et A. Ammouche (LERM SETEC)

PERF/R/076 - Essais de perméabilité au gaz - Tranche 2, E. Perin, M. Bonnet, J.-L. Dupuy et A. Ammouche (LERM SETEC)

PERF/R/081 - Etude préliminaire : Essais croisés de perméabilité aux gaz, M. Choinska et Y. Aidi (GeM, Centrale Nantes)

PERF/R/082 - Carbonatation accélérée selon le mode opératoire français sur 8 bétons, L. Schmitt (CERIB)

PERF/R/083 - Carbonatation accélérée selon le mode opératoire européen sur 8 bétons, L. Schmitt (CERIB)

PERF/R/084 - Impact of sample size on chloride migration coefficient, P. Nicot et F. Cassagnabère (LMDC, Université de Toulouse)

PERF/R/085 - Essai de biodégradation, M. Guéguen Minerbe et T. Chaussadent (Université Gustave Eiffel), M. Peyre Lavigne et A. Bertron (INSA Toulouse)

PERF/R/086 - Etude préliminaire : Etude paramétrique relative à la perméabilité aux gaz, M. Choinska et D. Niknezhad (GeM, Centrale Nantes)

PERF/R/087 - Caractérisation de 5 mortiers (CEM I faible teneur en C_3A, CEM I, CEM III, CEM V et CAC) par les tests de biodétérioration, M. Guéguen Minerbe et T. Chaussadent (Université Gustave Eiffel)

PERF/R/088 - Etude préliminaire : Etude de l'essai de perméabilité Torrent, M. Choinska, D. Niknezhad et M. Achour (GeM, Centrale Nantes)

PERF/R/089 - Essai accéléré de lixiviation par la méthode du LEACHCRETE, L. Bessette et E. Schmitt (VICAT)

PERF/R/090 - Essai accéléré de lixiviation par la méthode du LEACHCRETE, L. Bessette et E. Schmitt (VICAT)

PERF/R/092 - Etude préliminaire RSE : Perfectionnement de l'essai RSE. Essai alternatif en laboratoire, M. Salgues et D. Bulteel (ARMINES), F. Cassagnabère (LMDC, Université de Toulouse)

PERF/R/093 - Exploitation statistique des résultats des essais interlaboratoires, C. Mary-Dippe et F. Costanzi (GINGER CEBTP)

PERF/R/094 - Lixiviation à pH constant - Travaux de la tranche 2, F. Jacquemot (CERIB), A. Bertron, V. Mazars et M. Schiettekatte (LMDC, Université de Toulouse), P. Le Bescop (CEA), J. Philippot, R. Dutruel et G. Zammout (EDF), A. Ammouche (LERM), M. Salgues et D. Bulteel (ARMINES)

PERF/R/095 - Round robin tests - Analysis of the European results, J. Mai-Nhu (CERIB)

PERF/R/096 - Lixiviation à pH constant - Travaux de la tranche 4, P. Barthelemy et F. Jacquemot (CERIB)

PERF/R/097 - Carbonatation naturelle et carbonatation accélérée selon le mode opératoire européen d'un lot de 4 bétons, S. Kamali-Bernard, Y. Muy, E. Piolet et J.-Y. Brossault (LGCGM Rennes)

PERF/R/100 - Mesure de la perméabilité à l'air Torrent sur 8 bétons, G. Pham (LafargeHolcim)

PERF/R/103 - Perméabilité aux gaz sur les bétons d'un des 5 lots, M. Choinska (GeM – UMR CNRS 6183), L. Guiheneuf (CAPACITES, Université de Nantes)

PERF/R/104 - Etude préliminaire RSE :- Perfectionnement de l'essai RSE - Essai alternatif en laboratoire, O. Omikrine Metalssi et M. Jabbour (Université Gustave Eiffel)

PERF/R/105 - Suivi de dégradation en site réel de bétons afin d'apprécier l'augmentation de cinétique générée par l'essai accéléré développé : RSE, E. Rozière, S. Boudache et A. Loukili (GeM, Centrale Nantes), H. Colina et L. Izoret (ATILH)

PERF/R/106 - Etude préliminaire : Essais croisés de carbonatation accélérée, P. Fonollosa (Bouygues TP – PIM)

PERF/R/107 - Etude préliminaire : Essais croisés de porosité accessible à l'eau et d'absorption d'eau par capillarité, P. Fonollosa (Bouygues TP – PIM)

PERF/R/108 - Etude préliminaire : Essais croisés de migration des chlorures et résistivité, P. Fonollosa (Bouygues TP – PIM)

PERF/R/109 - Essais de porosité accessible à l'eau, d'absorption capillaire et d'absorption d'eau, P. Fonollosa (Bouygues TP – PIM)

PERF/R/110 - Carbonatation accélérée selon le mode opératoire français sur 8 bétons, P. Fonollosa (Bouygues TP – PIM)

PERF/R/111 - Carbonatation accélérée selon le mode opératoire européen sur 8 bétons, P. Fonollosa (Bouygues TP – PIM)

PERF/R/113 - Influence de la cure sur la perméabilité aux gaz - Tranche 3, M. Choinska (GeM – UMR CNRS 6183), L. Guiheneuf (CAPACITES, Université de Nantes)

Working Group 2: Permissible performance thresholds

PERF/R/001 - Procédures d'auscultation des ouvrages - Compilation des résultats disponibles sur corps d'épreuve du PN BHP 2000, V. Baroghel-Bouny et B. Godart (IFSTTAR)

PERF/R/002 - Pont Rion-Antirion - Synthèse des données de durabilité, A. Ammouche et C. Carde (LERM SETEC)

PERF/R/003 - Pont Vasco de Gama - Synthèse des données de durabilité, A. Ammouche et C. Carde (LERM SETEC)

PERF/R/004 - Etude de l'évolution des indicateurs de durabilité des ouvrages en béton dans leur environnement - Rapport de synthèse intermédiaire, B. Godart (IFSTTAR)

PERF/R/007 - Ouvrage sur la Bruche de la RD2420 à La Broque, A. Campaner (Cerema Est, Laboratoire de Strasbourg)

PERF/R/008 - Quai des TCD sur le Scorff à Lorient - Diagnostic, R. Quéguiner et B. Thauvin (Cerema Saint-Brieuc)

PERF/R/009 - Doublement du viaduc de Volesvres, T. Fanget et C. Aubagnac (Cerema Centre-Est, DL Autun)

PERF/R/020 - Déviation Nord de Loudéac, RN164 - Passage Inférieur n°1 - Diagnostic, R. Quéguiner et B. Thauvin (Cerema Saint-Brieuc)

PERF/R/032 - Auscultation d'ouvrages anciens de moins de 20 ans déjà expertisés (expertise partielle ou complète), V. Baroghel-Bouny (IFSTTAR)

PERF/R/041 - RN 176 - Pont Chateaubriand - Piles P11 et P12 - Diagnostic, R. Quéguiner et B. Thauvin (Cerema Saint-Brieuc)

PERF/R/043A - Caractérisation physico-chimique du béton de l'ouvrage de la RD 2420 sur la Bruche à la Broque, M. Saillio (IFSTTAR)

PERF/R/043B - Caractérisation physico-chimique des bétons du tunnel PI/SNCF/Blondel, M. Saillio (IFSTTAR)

PERF/R/043C - Caractérisation physico-chimique de la carotte n°6 intrados quai TCD, M. Saillio (IFSTTAR)

PERF/R/044 - Pont Vasco de Gama - Synthèse des données de durabilité, A. Ammouche et C. Carde (LERM SETEC)

PERF/R/045 - Pont Rion-Antirion - Synthèse des données de durabilité, A. Ammouche et C. Carde (LERM SETEC)

PERF/R/046 - PI SNCF/Blondel Ste Musse - Toulon, N. Cordier (Cerema Méditerranée, Laboratoire d'Aix-en-Provence)

PERF/R/051 - Investigations sur OA entre 20 et 50 ans en classe d'exposition XF : Piles du PS de St-Poncy sur A75 (XF4, XD3) - Essai L-barre, M. Neang et S. Delair (GINGER CEBTP)

PERF/R/052 - Investigations sur OA entre 20 et 50 ans en classe d'exposition XF : Piles du PS du Pirou sur A75 (XF4, XD3) - Essai L-barre sur béton de pile, M. Neang et S. Delair (GINGER CEBTP)

PERF/R/055 - Caractérisation d'échantillons de bétons anciens issus du palais d'Iéna à Paris, A. Bresson et A. Ammouche (LERM SETEC)

PERF/R/056 - Caractérisation d'échantillons de bétons anciens issus de la Bourse du travail à Bordeaux, A. Bresson et A. Ammouche (LERM SETEC)

PERF/R/058 - RN94 --Pont de la Vachette, N. Cordier et B. Berenger (Cerema Méditerranée, Laboratoire d'Aix-en-Provence)

PERF/R/059 - Arc du Pont X - Diagnostic, B. Thauvin (Cerema Saint-Brieuc)

PERF/R/070 - RD28 - Pont des Vallières, N. Cordier et B. Berenger (Cerema Méditerranée, Laboratoire d'Aix-en-Provence)

PERF/R/074 - Rapport de présentation du Palais d'Iéna, H. Jourdan et M. Bouichou (LRMH)

PERF/R/075 - Rapport de présentation de la Bourse du Travail de Bordeaux, H. Jourdan et M. Bouichou (LRMH)

PERF/R/077 - Reconstitution de la formule d'un béton ancien issu de l'arc du Pont Boutiron sur l'Allier, A. Bresson (LERM SETEC)

PERF/R/078 - Caractérisation des bétons de culée et de corniche du pont de la Vachette sur RN94, T. Lenormand et A. Ammouche (LERM SETEC)

PERF/R/079 - Reconstitution de la formule du béton de l'arc du pont sur le ravin des Vallières sur RD28 (06), T. Lenormand et A. Ammouche (LERM SETEC)

PERF/R/080 - Ouvrage maritime X, N. Cordier et B. Berenger (Cerema Méditerranée, Laboratoire d'Aix-en-Provence)

PERF/R/098 - Pont Rion-Antirion - Synthèse des données de durabilité – Rapport final, A. Ammouche et C. Carde (LERM SETEC)

PERF/R/101 - Implementation of an accelerated method by thermomaturation to quantify the aging factor, M. Carcassès, F. Cassagnabère, N. Zarbita, L. Boix et V. Mazars (LMDC, Université de Toulouse)

PERF/R/102 - Densité de courant de corrosion induite par la carbonatation ou les chlorures en fonction du type de ciment, R. François et M. Carcasses (LMDC, Université de Toulouse)

Working Group 3: Design concretes and variability

PERF/R/057 - Fabrication des éprouvettes (bétons n°19, 20, 24, 36 et 37), G. Martin (CERIB)

PERF/R/060 - Etude de la vitesse de corrosion en fonction de la formulation du béton et son environnement – fabrication des éprouvettes, P.-A. Franco (Vinci Construction France)

PERF/R/061 - Fabrication de 11 bétons avec granulats G1 au laboratoire de Vinci Construction France (bétons n°11, 15, 16, 18, 22, 25, 26, 28, 29, 35 et 38), I. El Khadiri (Vinci Construction France)

PERF/R/065 - Fabrication des bétons et confection des éprouvettes pour les essais interlaboratoires du GT1A, S. Delair, C. Mary-Dippe et F. Costanzi (GINGER CEBTP)

PERF/R/091 - Offshore Viaduct in La Reunion Island, P.-E. Denis (Vinci Construction Grands Projets)

PERF/R/099 - Influence de la cure sur la résistance à la pénétration des chlorures - Fabrication de 4 bétons, P.-A. Franco (Vinci Construction France)

PERF/R/112 - Fabrication de 11 bétons avec granulats G2, P. Fonollosa (Bouygues TP – PIM)